

THÈSE POUR OBTENIR LE GRADE DE DOCTEUR DE L'UNIVERSITÉ DE MONTPELLIER

En Génétique et Génomique

École doctorale GAIA - Biodiversité, Agriculture, Alimentation, Environnement, Terre, Eau

Unité de recherche UMR 5554 - ISEM - Institut des Sciences de l'Evolution de Montpellier

Evolution et prévalence de l'hybridogénèse sociale chez les fourmis (Formicidae)

Présentée par Arthur Weyna
Le 13 décembre 2021

Sous la direction de Nicolas Galtier
et Jonathan Romiguier

Devant le jury composé de

Tatiana Giraud, Directrice de recherche CNRS, Université Paris-Saclay

Serge Aron, Directeur de recherche FRS-FNRS, Université Libre de Bruxelles

Mathilde Dufay, Professeur des Universités, Université de Montpellier

Thomas Guillemaud, Directeur de recherche INRAE, Sophia Agrobiotech, Nice

rapporteuse

rapporteur



UNIVERSITÉ
DE MONTPELLIER

Acknowledgements

I first thank my two supervisors, Jonathan Romiguier and Nicolas Galtier, for their invaluable scientific and personal support throughout these three years. Thank you Jonathan for your contagious enthusiasm about both ants and computers. I am forever grateful for the time you invested in patiently transmitting your knowledge and ideas. Thank you Nicolas for your remarkable ability to put yourself in your students' shoes, and to give credits even to their most ridiculous ideas.

I would also like to thank the members of the jury, who kindly accepted to evaluate my work, Tatiana Giraud, Serge Aaron, Mathilde Dufay and Thomas Guillemaud.

I thank my friends and all members of my family for their unconditional support, especially in darker times. My mother and father for understanding and encouraging me in all aspects of life. Nathan Mazet, Maurine Hammel, Léo-Paul Dagallier and Salma el Yammouni for sharing their home and putting up with me for the last two years.

My warmer thoughts go to Taïna Lemoine, for sharing my life and for bringing joy in all its aspects.

I would like to thank all my past scientific supervisors, Julien Foucaud, Jerome Orivel and Julien Claude for their guidance. I would not be here without the professional experience they provided.

I would finally like to express my gratitude to various people from ISEM and beyond, who helped me in the course of this thesis. Charles Mullon for introducing me to the world of modelling, with infinite patience and great pedagogy. Rumsaïs Blatrix for sharing his love for ants, and for overseeing this thesis. Bernard Kaufmann for his benevolence and guidance. Astrid Cruaud, Jean-Yves Rasplus and Sabine Nidelet for their crucial technical support. Birgit Schlick-Steiner and Florian Steiner for providing key insights and samples. Claude Lebas for his invaluable field work and knowledge. Celine Devaux for always having an open ear. Elodie Lauroua for her life-saving lab skills. Hugo Darras for fruitful discussions and insightful remarks. Suzanne Ryder and Agnèle Touret-Alby for their trust and help with museum samples.

Abstract

Hybridization is a fundamental process of biological evolution, which participates in determining the pace of speciation and represents a major source of genetic diversity for many organisms. In ants, hybridization has a special status because its interplay with colonial life has led to the evolution of spectacular reproductive systems, that incorporate inter-specific mating as an integral part of colonial life. In particular, a few ant species have developed social hybridogenesis, a reproductive system where workers can only develop from hybrid larvae, while queens are still produced via regular mating. In this thesis, three separate research projects were undertaken to gain better knowledge about the first steps of the evolution of social hybridogenesis, and about its prevalence within ants.

Several hypotheses and verbal models have been proposed in previous literature to explain how eusocial species can transition from regular reproductive systems to social hybridogenesis. In the first project of this thesis, I present the first in-depth mathematical treatment of the question, and describe a new potential evolutionary pathway to social hybridogenesis. I show that this reproductive system could be the ending-point of an arms-race between non-hybrid ant larvae, which seek access to the reproductive caste, and their mother, which resorts to hybridization to supplement its workforce. I also use this model to investigate the effects of several key parameters on the evolution of social hybridogenesis, such as the efficiency of hybrid workers, or multiple matings and clonal reproduction by queens.

While the number of documented hybridogenetic systems has been growing significantly in the last few years, the actual prevalence of this reproductive system in ants remains unknown. In the second project of this thesis, I develop a statistical method which allows for the detection of hybrid workers from single individual data. I then apply this method to existing genome sequencing data in several hundreds of ant species. I show that hybrids are more commonly detected in Hymenoptera, and particularly ants, than in other groups of arthropods. I present a list of candidate ant species which could reveal to reproduce via social hybridogenesis.

One promising model for future studies of social hybridogenesis is the harvester ant genus *Messor*, where three species were recently shown to display this mode of reproduction. In the last project of this thesis, I engage key preliminary analyses in *Messor*. I first construct the first phylogeny of the group, including about half of known *Messor* species, using non-destructive genome sequencing of museum specimens. I also use hybrid detection to ask whether some of this species might be good candidates for social hybridogenesis. Second, I lean on the special case of the *Messor structor* group, a European species complex in which social hybridogenesis has been detected before, but was never described in depth. I show that only one species in this group, *M. ibericus*, reproduces via social hybridogenesis, and present evidence suggesting that this system may involve a form of male clonality.

Résumé

L'hybridation est un processus fondamental de la biologie évolutive, qui participe à déterminer le rythme de la spéciation et représente une source majeure de diversité génétique pour de nombreux organismes. Chez les fourmis, l'hybridation a un statut particulier car son interaction avec l'eusocialité a mené à l'évolution d'intrigants systèmes de reproduction, qui incorporent les accouplements inter-spécifiques en tant que part intégrante de la vie en colonie. En particulier, certaines espèces de fourmis ont développé l'hybridogénèse sociale, un mode de reproduction dans lequel les ouvrières ne peuvent se développer qu'à partir de larves hybrides, mais où les reines sont toujours produites à travers des accouplements intra-spécifiques. Dans cette thèse, trois projets de recherche ont été menés avec pour objectifs de mieux comprendre les premières étapes de la mise en place de l'hybridogénèse sociale, et d'évaluer sa prévalence parmi les fourmis.

Plusieurs hypothèses et modèles verbaux ont été proposés pour tenter d'expliquer comment l'hybridogénèse sociale peut émerger à partir de systèmes de reproduction plus standards. Dans le premier projet de cette thèse, je présente le premier traitement mathématique détaillé de cette question, et décris un nouveau chemin évolutif vers l'hybridogénèse sociale. Je montre qu'elle peut être l'issue d'une course aux armements entre les larves en développement, qui cherchent à accéder à la caste reproductrice, et leur reine, qui utilise l'hybridation pour produire plus d'ouvrières. J'utilise également ce modèle afin d'étudier les effets de plusieurs paramètres clefs, comme l'efficacité des ouvrières hybrides, le nombre d'accouplements effectués par les reines, ou la possibilité pour elles de produire de nouvelles reines par clonage.

Si le nombre de cas décrits d'hybridogénèse sociale a augmenté significativement dans les dernières années, sa vraie prévalence au sein des fourmis reste inconnue. Dans le second projet de cette thèse, je développe une méthode statistique qui permet la détection d'ouvrières hybrides à partir de données génomiques individuelles. J'applique ensuite cette méthode à des données génétiques existantes pour plusieurs centaines d'espèces de fourmis. Je montre que les hybrides sont plus souvent détectés chez les Hyménoptères, et particulièrement chez les fourmis, que dans d'autres groupes d'Arthropodes. Je présente une liste d'espèces de fourmis candidates qui pourraient être impliquées dans des systèmes hybridogénétiques.

Un modèle prometteur pour l'étude de l'hybridogénèse est le genre de fourmis moissonneuses *Messor*, dans lequel trois cas indépendants de ce système de reproduction ont été décrits. Dans le dernier projet de cette thèse, j'engage des analyses clefs au sein du genre *Messor*. Je reconstruis la première phylogénie du groupe, incluant la moitié des espèces connues du groupe, en utilisant une méthode de séquençage non-destructive sur des spécimens de musée. J'utilise également la méthode développée précédemment pour identifier d'éventuels nouveaux systèmes hybridogénétiques parmi ces espèces. En parallèle, je me penche sur le cas particulier du groupe *Messor structor*, un complexe d'espèces européen chez lequel l'hybridogénèse sociale a été détectée précédemment, mais n'a jamais été décrite en détails. Je montre que l'hybridogénèse sociale n'est présente que chez une seule des cinq espèces de ce groupe, *M. ibericus*. Je présente également des résultats semblant suggérer que ce système repose sur une forme de clonalité mâle.

Contents

Introduction	1
Hybridization as a major evolutionary process	1
Hybridization in ants	4
Social hybridogenesis	6
Evolution of social hybridogenesis	12
Thesis objectives and overview	16
Chapter 1 - Deterministic evolution of social hybridogenesis from intra-colonial conflicts: A model	19
Article: Hybridization enables the fixation of selfish queen genotype in eusocial colonies. <i>Evolution Letters</i> (2021).	20
Appendix: Mathematical derivations and additional analyses.	33
Chapter 2 - Genomic evidence for the prevalence of social hybridogenesis in ants	53
Article: Detection of F1 hybrids from single genomes reveals frequent hybridization in Hymenoptera and particularly ants. Under revision in <i>Molecular Biology and Evolution</i>	54
Chapter 3 - Social hybridogenesis in <i>Messor</i> harvester ants	79
Article: A phylogenetic study of <i>Messor</i> harvester ants from museum specimens: implications for the study of social hybridogenesis. <i>Unpublished</i>	80
Article: Distribution and characteristics of social hybridogenesis within the <i>Messor structor</i> species group. <i>Unpublished</i>	97
Discussion	113
A general evolutionary path towards social hybridogenesis ?	113
Insights into the determinants of social hybridogenesis	116
Are Hybridogenetic systems doomed to disappear ?	118
Conclusion and perspectives	120
Appendices	131
Other Scientific projects	131
Résumé détaillé	224

Introduction

Hybridization as a major evolutionary process

Hybridization can be defined as a process in which members of genetically distinct populations mate and produce viable offspring of mixed ancestry (Abbott et al., 2013; Barton & Hewitt, 1985). Instances of hybridization and the new forms that they produce have long caught the attention of biologists (Stebbins, 1959), and have provided key insights throughout history. Darwin and other early evolutionary biologists, for instance, spent a great deal of time studying hybrids and their fitness (Pickersgill, 2009; Roberts, 1919). Part of their work was obviously motivated by the potential of hybridization as a source of new economically important phenotypes, especially in domesticated plants. But less practically, they also recognized that hybridization was a useful challenge to a discrete definition of species (Mallet, 1995) and to the concept of gradual evolution, from which an understanding of the mechanisms of heredity could be obtained. Of course, once such understanding was obtained in the following decades, the role of hybridization as a model of study was not diminished. Instead, the development of genetics and molecular biology only emphasized that hybridization plays a key role in several aspects of biological evolution (Abbott et al., 2013; Barton, 2001; Barton, 2020; Stebbins, 1959). In this section, the main causes and consequences of hybridization in natural population are broadly summarized.

Through a body of seminal theoretical work by geneticists (Dobzhansky, 1940; Mayr, 1942), it was first understood that depending on hybrid fitness, hybridization events can drive speciation in natural populations. Consider a zone of contact between two divergent parental populations that can produce hybrids (i.e., hybrid zone). In the absence of strong disruptive selection, and if hybrids can survive and reproduce, successive generations of hybridization and back-crossing can be expected to progressively blend the genetic material of both parental populations (i.e., gene flow), leading to population homogenization and to the slow-down of speciation (see Abbott et al., 2013; Feder et al., 2012; Pinho & Hey, 2010; Smadja & Butlin, 2011 or Barton, 2020 for useful reviews of speciation with gene flow). In the most extreme cases, genetic mixing between hybridizing species may even counterbalance neutral divergence and disruptive selection, leading to a reduction of species richness via the genetic assimilation of rare species (Levin et al., 1996). This is especially likely when hybrids are fitter than their parent (i.e., hybrid vigor or heterosis), in which case active hybridization can represent an advantageous reproductive strategy that will be selected for, thus further enhancing gene-flow. While the possible determinants of heterosis in natural populations are still debated, an advantage to hybrids may arise in several configurations (see Birchler et al., 2010 for a short and general review). First, hybrids may display new intermediary phenotypes that are more effective in marginal environments. For instance, females of the American spadefoot toad *Spea bombifrons* were shown to actively seek inter-specific mates in ephemeral ponds, where hybrid tadpoles perform better due to faster development (Pfennig, 2007). Alternatively, hybrid genotypes may profit from increased heterozygosity and from new and more efficient allele combinations at specific genetic loci (i.e., overdominance; Semel et

al., 2006), or from the genetic complementation of deleterious variants fixed in each parental population (Charlesworth & Willis, 2009). It was also shown that hybrids can sometimes profit from increased genome size and functional capabilities, through the cumulation of genes that are unique to each of their parental populations (Fu & Dooner, 2002).

But the consequence of hybridization on speciation can be opposite when hybrids are less fit than their purebred parents (i.e., hybrid depression). In general, hybrid depression may result from strictly ecological processes (e.g., if hybrids display unfit phenotypes relative to their purebred parents), but is more often the consequence of intrinsic incompatibilities between hybridizing lineages (i.e., hybrid incompatibilities; Abbott et al., 2013; Barton, 2020; Pinho & Hey, 2010; Smadja & Butlin, 2011). Such incompatibilities, or post-zygotic barriers, are usually considered to be very likely in recent hybrid zones, because the vast array of new combinations that result from hybridization has never been exposed to selection. As a result, hybrid depression is expected to be more frequent than heterosis in natural population (Barton, 2001). This is the rationale behind the notorious Bateson-Dobzhansky-Muller (BDM) model for genetic incompatibilities (Bateson, 1909; Dobzhansky, 1940; Muller, 1942). The BDM model posits that reduced fitness in hybrids may result from negative epistatic interactions between pairs of alleles exclusive to each hybridizing lineage. While this simple model of genetic incompatibilities has received much support and remains dominant in the literature (see Welch, 2004 for an overview), hybrid incompatibilities have been shown to result from a variety of other mechanisms including immune response (Bombliès et al., 2007), cytoplasmic incompatibilities (Bordenstein et al., 2001), gene duplication and pseudogenization (Lynch & Force, 2000) or epigenetic mechanisms (Vrana et al., 2000). It was also demonstrated that hybrid depression can result from chromosome rearrangements, which by breaking synteny between hybridizing lineages can impair major cytological mechanisms such as mitosis or meiosis, leading to hybrid unviability or hybrid sterility (Bhattacharyya et al., 2013; Dion-Coté et al., 2015). Independently of their proximal causes, hybrid incompatibilities and postzygotic barriers usually result in an advantage to hybridization avoidance, and thus to the rapid and adaptive evolution of phenotypes that prevent successful mating between divergent populations (i.e., the evolution of prezygotic reproductive barriers via reinforcement; Abbott et al., 2013; Barton, 2020; Smadja & Butlin, 2011). These reproductive barriers will in turn prevent genetic mixing and promote further divergence, thus accelerating speciation.

Beyond its major effects on speciation, genetic studies also revealed that genetic exchange through hybridization plays an important role as a source of genetic variation across the tree of life (Anderson, 1949; Barton, 2001; Moran et al., 2021). Even when hybridization is rare, exchanged genetic material can remain in recipient species on the long-term (i.e., genetic introgression), sometimes even reaching fixation (Abbott et al., 2013; Barton, 2020; Feder et al., 2012; Moran et al., 2021). In some instances, the fixation of introgressed elements has been shown to provide key adaptation to recipient species. Perhaps the most iconic example of such adaptive introgression can be found in the human lineage. Some extant populations of modern humans carry alleles that are believed to originate from other extinct hominins such as Neanderthals or

Denisovans, and that would provide advantageous functions related to pigmentation, immunity or metabolism (reviewed in Racimo et al., 2015). Not unrelatedly, adaptive introgression has been argued to play a major role in the adaptation of invasive species to their invasive range, by providing key genetic material and adaptations from related local species (Fournier & Aron, 2021; Smith et al., 2020). In fact, some authors have argued that through introgression, hybridization could be the most widespread and dominant source of genetic variation in multicellular sexual organisms (Barton, 2020; Mallet, 2005; Moran et al., 2021). Introgressed elements can indeed provide entirely new genes, new genotypic combinations, or even new organelles (e.g. mitochondrial introgression; Darras & Aron, 2015; Seixas et al., 2018) and endosymbionts (e.g. hybrid transmission of *Wolbachia*; Raychoudhury et al., 2009), which cannot arise from mutation alone. But just as mutation, most of the new genetic variation brought by hybridization is expected to be neutral or harmful, because they were never exposed to selection in their new ecological and genomic context (Barton, 2001; Martin & Jiggins, 2017; Moran et al., 2021). Accordingly, many introgressed elements have been found to be deleterious, and to increase genetic load (i.e., average fitness reduction due to unfavorable genetic material) in recipient species (Martin & Jiggins, 2017; Moran et al., 2021). This is especially likely when recipient population are small relative to donor species, leading to asymmetrical gene-flow, and to the fixation of introgressed material via genetic drift (Pfennig, 2021).

Realizing the potentially far-reaching consequences of hybridization on speciation and adaptation has left researchers to wonder about the actual prevalence of this process in extant organisms (Barton, 2001; Mallet, 2005; Stebbins, 1959). Historically, two more or less opposed lines of thoughts seem to have dominated this debate. Many biologists, and especially botanists, were confronted to many direct examples of natural hybrids (which are abundant in plants; Pickersgill, 2009; Stebbins, 1959), and readily saw hybridization as a common process. They were also the first to suggest that hybridization could lead to the formation of new species via the process of hybrid speciation (i.e., the birth of new species following the reproductive isolation of hybrid lineage; Mallet, 2007). On the other hand, many zoologists did not see such abundance of hybrids, and continued for a long time to see hybridization as a rare oddity usually prevented by strong reproductive barriers (Barton, 2001; Mallet, 2005; Mallet, 2007). The advent of genetics and molecular data would eventually prove the latter wrong, by uncovering several examples of species born through hybrid speciation (e.g. 2 to 4% of speciation events in flowering plants may be associated with polyploidization following hybridization; Otto & Whitton, 2000), and by providing accumulating evidence for the pervasiveness of hybridization in many taxa, including animals (Mallet, 2005). Genetic analyses however, also confirmed the old intuition that taxa can differ drastically in their propensity to hybridize (e.g., Mallet, 2005 estimates that 10% of animals and 25% of plants often hybridize), leading to new question and hypotheses regarding the determinants of such heterogeneity. It is recognized that hybridization rates within taxa strongly depend on biogeography and historical contingencies. Diverse taxa with many young species that are recurrently put into contact by environmental change and frequent migration are mechanically expected to display more hybridization (Edmands, 2002). But hybridization is also

dependent on a variety of other factors that modulate the strength of prezygotic and postzygotic reproductive barriers (Mallet, 2005; Smadja & Butlin, 2011). For instance, mating can involve complex phenotypes (e.g, pheromonal signaling, courtship behavior, sexual selection, lock and key mechanisms in genitalia) that can evolve quickly and reduce hybridization opportunities (Löfstedt et al., 1991; Mallet, 2005; Safran et al., 2013; West & Kodric-Brown, 2015; Wojcieszek & Simmons, 2013). Hybridization rates can also be modulated by demographic parameters, with some locally rare species using interspecific mating as a coping strategy when more suitable conspecific mates are absent (Toews et al., 2018). Overall, a very wide array of biotic and abiotic factors have the potential to modulate hybridization rates (Mallet, 2005). Their study is an active field in biology, with many ramifications and models of study.

Hybridization in ants

One particularly important taxon for the evolutionary studies of hybridization is ants (Formicidae). Ants have long been known to display comparatively high hybridization rates on the basis of both morphological and molecular data (e.g., Hung & Vinson, 1977; Seifert & Goropashnaya, 2004; Seifert, 1999; Steiner et al., 2011; Umphrey & Danzmann, 1998; Van Der Have et al., 2011; reviewed at length by Feldhaar et al., 2008). In his useful review, Feldhaar et al. (2008) compiled experimental evidence showing frequent hybridization in 22 species, for only 6 represented genera. One iconic example involves Palearctic mount-building red wood ants (*Formica rufa* group), where evidence for complex reticulated evolution indicates frequent gene-flow via multi-directional hybridization (Seifert, 2021). In fact, Seifert (2021) estimates that about half of the 13 recognized species of the *F. rufa* group hybridize, and that hybridization frequencies are above 20% in three species. Another striking example is that of European *Leptothorax*. In some parts of Central Europe, data suggest that almost half the females of these discrete generalist ants hybridize (Douwes & Stille, 1991; Seifert, 1999), indicating low to nonexistent reproductive barriers. In this section, the peculiarities of the tight relationship that ants maintain with hybridization are presented.

While they remain largely untested, several hypothesis have been formulated to explain frequent hybridization in ants. Some authors proposed that this propensity may be linked to haplodiploidy, the reproductive system ancestral to ants and other Hymenoptera (figure 1a). In Hymenoptera, females are diploid, usually produced via sex, while males are haploid produced through arrhenotokous parthenogenesis (i.e., development of unfertilized eggs). It was suggested that such reproductive system could reduce direct selection against hybridization, because queens mated to allospecific males can still produce non-hybrid males, thus retaining non-null fitness even in the face of strong hybrid depression (Nonacs, 2006; Umphrey, 2006). Another complementary hypothesis is that eusociality, whereby reproductive females (i.e., queens) produce a large number of sterile helper individuals (i.e., workers) to form colonies, may explain increased hybridization rates. Specifically, it was suggested that selection against hybridization could be weaker in eusocial species because the fitness cost of hybrid sterility should be minimal in species producing a large majority of sterile individuals (Nonacs, 2006; Umphrey, 2006). If

these hypotheses were echoed by several authors (e.g., Cordonnier et al., 2020; Feldhaar et al., 2008; Kronauer et al., 2011; Kulmuni et al., 2010), it is important to note that they could apply to social bees and wasps as well. In these groups however, evidence for natural hybridization is comparatively scarce (Feldhaar et al., 2008; Fournier & Aron, 2021). While this might be the result of wild bees and wasps being largely understudied when compared to ants, it might also indicate that ants possess additional characteristics relevant to frequent hybridization. The most obvious of such characteristics is probably species richness. Ants count more than 13 964 valid species worldwide (according to AntCat; Bolton, 2021), with much cryptic diversity left to be described, while social bees and wasps have less than a thousand species each (according to a broad search on the Catalogue of Life; (Cachuela-Palacio, 2006)). This diversity is thought to be linked to the loss of flight in workers, which enabled ants to colonize a variety of terrestrial micro-habitats (Peeters & Ito, 2015). The resulting small-scale diversification, when coupled with the large dispersion range of winged queens and males, may have participated in creating propitious conditions for contact between species (Feldhaar et al., 2008). Additionally, the extreme functional simplification of workers (Peeters & Ito, 2015) could have favored hybridization by making hybrid individuals less affected by developmental defects linked to hybrid incompatibilities (e.g., fluctuating asymmetry; Ross & Robertson, 1990). Finally, it was proposed that the typically low morphological and behavioral divergence observed between males of related ant species participates in reducing prezygotic barriers to hybridization in this group (Feldhaar et al., 2008).

Besides the reasons behind its relatively high frequency, hybridization in ants also has some important, and sometimes unsuspected, consequences. Similarly to others groups, hybridization in ants was sometimes found to lead to genetic introgression (Feldhaar et al., 2008; Fournier & Aron, 2021; Van Der Have et al., 2011). For instance, clear mitochondrial introgressions were observed in *Tetramorium* (Cordonnier et al., 2019) and *Cataglyphis* (Darras & Aron, 2015; Eyer et al., 2016). Yet, the majority of described hybrid system in ants seem to display very clear species boundaries, and little to no gene flow. This has been interpreted as evidence that first-generation (F1) hybrid queens are often absent or unviable, thus limiting opportunities for back-crossing and genetic introgression (Feldhaar et al., 2008). Alternatively, limited back-crossing and introgression might be caused by reduced viability in sons of hybrid queens (Cordonnier et al., 2020). Under standard meiosis expectations in haplodiploids, hybrid queens produce sons that carry only one recombinant haplome. Extending Haldane's rule (usually applied to sexual chromosomes; Haldane, 1924; Turelli, 1998) to their whole genome, these sons are expected to suffer from every epistatic genetic incompatibilities they carry, both dominant and recessive. This is nicely exemplified by an unusual hybrid system that was described in Finnish *Formica* ants (*Formica aquilonia* x *polycтена*). In this system, recurrent hybridization between two lineages has led to substantial introgression, but introgressed elements are surprisingly confined to female genomes, with males being consistently found to be purebred (Kulmuni et al., 2010; Kulmuni & Pamilo, 2014). This configuration has been shown to result from the systematic unviability of males that carry introgressed alleles (i.e., only the few males that are lucky enough

to be born without them survive), presumably due to strong BDM incompatibilities exposed in their haploid genome.

But the most peculiar consequence of frequent hybridization in ants is probably the emergence of new traits and organizations that let them play around hybrids and their characteristics. In two separate hybrid zones involving the same genus (*Lasius claviger* x *latipes* in northeastern USA and *Lasius niger* x *alienus* in England), morphological and allozyme studies (Pearson, 1983; Umphrey & Danzmann, 1998; Wing, 1968; reviewed in details in Umphrey, 2006) have revealed that queens from one species (*L. latipes* and *L. alienus*, respectively) very frequently reproduce with allospecific males (49% and 16% of inter-specifically mated queens, respectively), leading to the production of F1 hybrid workers and queens (figure 1b). In both cases, the high number of produced hybrids contrasted deeply with a total absence of mature nests headed by hybrid queens, suggesting that these queens suffer from severe hybrid depression. Yet, the stability of the involved population also suggested that the resulting cost of hybridization in these system had to be compensated somehow. Two non-exclusive hypotheses were then proposed to explain an advantage to hybridization in these ants. First, it was suggested that queens use hybridization only when suitable conspecific mates are absent (i.e., as a “best of bad situations”; Umphrey, 2006), in order to ensure sperm acquisition and colony foundation. Such inter-specifically mated queens would then produce colonies composed of hybrid workers, and retain some reproductive ability via the production of sons. Alternatively, it was argued that an advantage to hybridization in *Lasius* may lie directly in having a hybrid workforce. While empirical evidence of heterosis in ants is scarce at best (Feldhaar et al., 2008; James et al., 2002; Julian & Cahan, 2006; Ross & Robertson, 1990), several authors suggested that hybrid workers could provide enhanced colony productivity or better pathogen resistance (Anderson et al., 2008; Feldhaar et al., 2008; Julian & Cahan, 2006; Schwander et al., 2010; Umphrey, 2006). In any case, because these strategies would take advantage of the allospecific males whose sperm is used (i.e., which will sire only sterile workers), they were readily referred to as sperm parasitism (Umphrey, 2006) or as cleptogamy (Seifert, 1999). In a theoretical point of view, the finding that some ants may benefit from hybridization via sperm parasitism suggest one radical change in the life-history of involved species. Specifically, these hybridizing species shift from a situation where they profit from caste plasticity in regular larvae (i.e., usually necessary to produce both workers and queens) to a situation where they suffer from it because it leads to the costly production of essentially useless hybrid queens. In idealized conditions, it would be more optimal for such species to entirely funnel hybrid larvae towards the worker caste, thus theoretically avoiding the costs of hybridization. In fact, this is what is found in some ant species that have committed to hybridization to the point that it has become an integral part of their life-cycle.

Social hybridogenesis

Hybridization-dependent reproductive systems are found in several distantly related species of ants. Many of these systems differ from each other in some ecological or life-history aspects, but they do share a common feature: the production of workers has become possible only via

hybridization with another species or lineage, as regular (i.e., non-hybrid) larvae have seemingly become genetically destined to develop into queens (i.e., lost their developmental plasticity almost entirely; Darras et al., 2014a; Helms Cahan et al., 2004). Because the resulting association between female caste and hybrid status is nearly perfect, caste determination in hybridization-dependent reproductive systems has often been referred to as strong genetic caste determination (strong GCD), in opposition to weak GCD (i.e., where genotypes have a marginal impact on development; see Hughes et al., 2008 for an example in leaf-cutting ants), and environmental caste determination or ECD (i.e., the ancestral caste determination system in Hymenoptera, where caste is determined by environmental conditions; see Schwander et al., 2010 for a review on ECD and GCD). In species with strong GCD, hybrid queens are usually absent or very rare, which strongly reduces opportunities for gene flow and maintains the genetic integrity of involved lineage on the long-term. As such, strong GCD allows for the stable production of a hybrid workforce by successive generations of purebred queens. This particular fact has inspired early discoverers of strong GCD (Helms Cahan et al., 2002) to draw parallels between their model and hybridogenesis (Schultz, 1969), a hemiclinal mode of reproduction found in the stick insect *Bacillus rossius-grandis* (chapter 16 of Schön et al., 2009), the Teleost genera *Hypseleotris* and *Poeciliopsis* (chapter 19 of Schön et al., 2009), and the water frog *Pelophylax esculenta* (chapter 20 of Schön et al., 2009). In hybridogenesis, entire populations of F1 hybrids (usually all-female populations, but see chapters 19 and 20 of Schön et al., 2009) are maintained across generations because they selectively transmit only one parental genome, while the second is renewed by mating with the corresponding parental species (figure 1c; reviewed in Beukeboom & Vrijenhoek, 1998 and Lavanchy & Schwander, 2019). Driven by the analogy between multicellular organisms and eusocial colonies (i.e., the infamous “super-organism”; Wheeler, 1911), Helms Cahan et al. (2002) have coined the term “social hybridogenesis” to refer to strong GCD systems in ants. While this term was not always employed (e.g., Fournier et al., 2005; Rey et al., 2013), it is now widely used to refer to all types of strong GCD in ants (Lavanchy & Schwander, 2019). In this section, known hybridogenetic systems in ants are described, focusing on the ecological and life-history particularities of each system.

Historically, the first case of social hybridogenesis was discovered in *Solenopsis* fire ants. Studying hybrid nests from a Texan hybrid zone between *S. geminata* and *S. xyloni* using isozymes, Hung & Vinson (1977) found that workers always produced protein variants from both parental species, while queens only produced the *S. xyloni* variant. This was first interpreted as genomic elimination or imprinting in the supposedly hybrid queens. But later genetic studies would reveal that queens of these hybrid queens are in fact purebred *S. xyloni* females that reproduce through social hybridogenesis (Helms Cahan & Vinson, 2003). While reproduction in *S. xyloni* outside the Texan hybrid zone usually involves standard ECD, *S. xyloni* within said hybrid zone has evolved strong GCD and relies on inter-specific mating for worker production. Interestingly, although the hybrid zone between both species could appear quite symmetrical at first sight, social hybridogenesis was found only in *S. xyloni*, with no production of F1 hybrids by *S. geminata* queens (Helms Cahan & Vinson, 2003; Hung & Vinson, 1977). Hypotheses involving

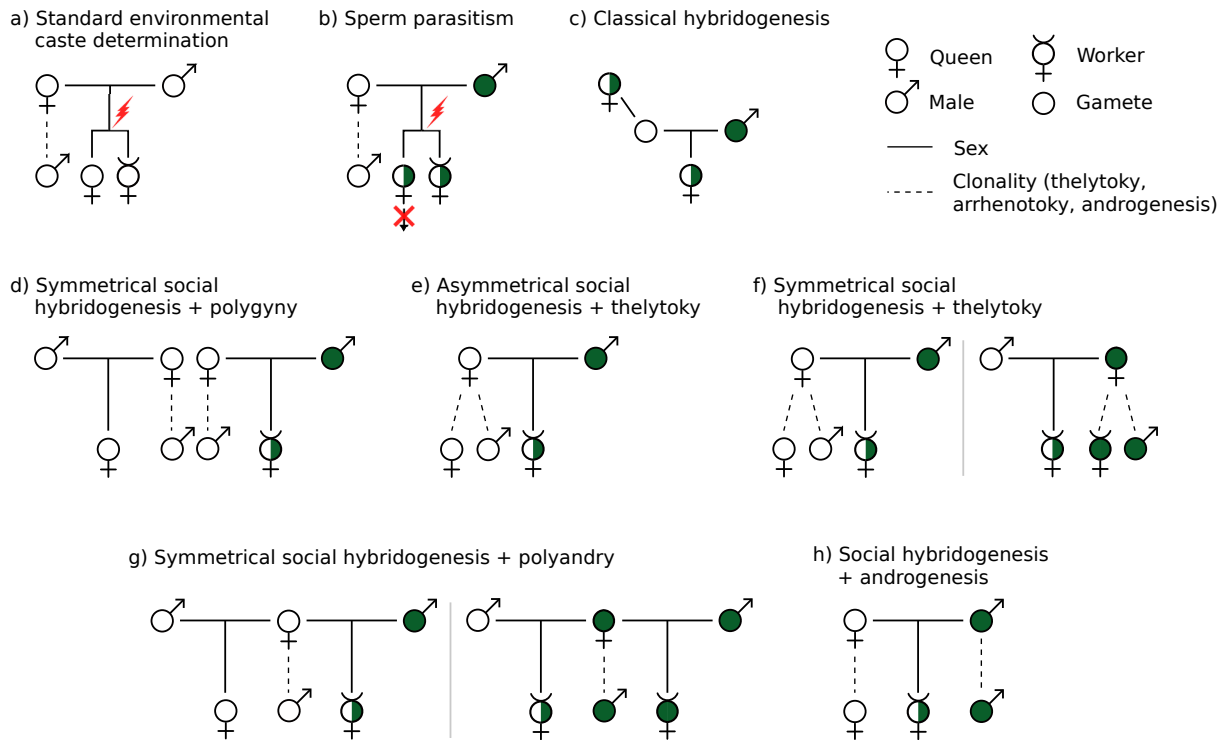


Figure 1: The many forms of hybridization-dependent reproductive systems. Empty and green symbols represent individuals from genetically distinct lineages, that can hybridize to form hybrids (half-green symbols). Red sparks represent environmental effects on caste determination. The red cross indicates a lack of access to reproduction. The represented reproductive systems are found in **a)** most ants and other social Hymenoptera, **b)** *Lasius latipes* and *L. alienus*, **c)** *Bacillus* stick-insects, *Hypseleotris* and *Poeciliopsis* fishes and *Pelophylax* water frogs, **d)** *Solenopsis xyloni*, **e)** *Solenopsis geminata*, **f)** 8 species of *Cataglyphis* desert ants, **g)** *Pogonomyrmex* and *Messor barbarus*, **h)** *Wasmannia auropunctata*, *Vollenhovia emeryi*, *Paratrechina longicornis* and *Cardiocondyla kagutsuchi*.

competition between males and biased sex-ratio have been raised to explain this fact (Hung & Vinson, 1977), but the reasons behind such an asymmetry are still unknown. Another interesting characteristic of *S. xyloni* is that its queens are monandrous (i.e., they mate with only one male each). To achieve both the production of hybrid workers and non-hybrid queens, *S. xyloni* colonies must be polygynous and contain at least two queens, each mated to one type of male (figure 1d; Helms Cahan & Vinson, 2003). This particular fact has led to the conclusion that polygyny must have been a prerequisite to the evolution of social hybridogenesis in this species.

Possible links between polygyny and social hybridogenesis may be further suggested by the recent discovery of two separate hybridogenetic systems involving Floridan populations of *S. geminata* (Lacy et al., 2019). In these populations, social hybridogenesis is combined with polygyny, while neighboring non-hybridogenetic populations (whose males are used by hybridogenetic queens for worker production) are monogynic. However polygyny in these systems cannot easily be interpreted as a precondition to social hybridogenesis because as opposed to

S. xyloni queens, hybridogenetic *S. geminata* queens do not mate with males from their own population for queens production. Instead, they produce their reproductive daughters via thelytokous parthenogenesis (i.e., female clonality; figure 1e). In this particular instance, it is more likely that polygyny is a consequence of clonality, which would have reduced genetic variance between queens and homogenized their cuticular semiochemical profile to the point that individual recognition became impaired (Lacy et al., 2019).

Many other instances of social hybridogenesis that involve thelytokous parthenogenesis are found in *Cataglyphis* desert ants. Successive genetic studies in this genus (Aron et al., 2016; Darras et al., 2014a; Darras et al., 2014b; Darras et al., 2019; Eyer et al., 2016; Kuhn et al., 2017; Kuhn et al., 2020; Leniaud et al., 2012), spanning over most of the Mediterranean Basin and the Middle East, have revealed that 8 *Cataglyphis* species (among 16 investigated) display social hybridogenesis. As a result, *Cataglyphis* is the one single genus that counts the most known cases of social hybridogenesis, making it a key model for understanding the evolution and ecology of this reproductive system (Aron et al., 2016; Doums & Monnin, 2020). Unlike in *Solenopsis*, social hybridogenesis in *Cataglyphis* is always symmetrical (figure 1f; Kuhn et al., 2020). Hybridogenetic *Cataglyphis* queens do not mate with males from another non-hybridogenetic species or lineage, but with males from another hybridogenetic lineage that mirrors this behavior. This results in the coexistence of pairs of divergent but ecologically inter-dependent lineages, that rely on each other's males for worker production (Darras et al., 2019; Kuhn et al., 2017; Kuhn et al., 2020). Beyond this symmetry, perhaps the most important particularity of hybridogenetic *Cataglyphis* is that they combine social hybridogenesis with a conditional use of sex (Doums et al., 2013a). Similarly to *S. geminata*, queens of hybridogenetic *Cataglyphis* outbreed for worker production but usually produce their reproductive daughter via thelytokous parthenogenesis (Aron et al., 2016; Doums & Monnin, 2020; Kuhn et al., 2020). This is thought to have played a significant role in the success of social hybridogenesis in the group, because it removes the strict obligation for queens to mate with conspecific males, effectively halving the cost of mate searching. This particular combination may also be a successful strategy because parthenogenesis allows queens to profit from a two-fold increase in their reproductive output, while social hybridogenesis maintains genetic diversity in the workforce. But such use of parthenogenesis also raises new questions regarding the maintenance of social hybridogenesis on the long term. Besides increased homozygosity in queens (Doums et al., 2013a) and the costly production of diploid males (Doums et al., 2013b), parthenogenesis entails that males rarely partake in effective mating (i.e., they mostly sire sterile workers). It could thus be predicted that males in hybridogenetic *Cataglyphis* should eventually stop being produced, as they represent a genetic dead-end, which would lead to the collapse of dependent lineages (Darras et al., 2014b; Schwander & Keller, 2012). Yet, males are still found in natural conditions, and the multiplicity and range of hybridogenetic systems in *Cataglyphis* suggests that they are fairly stable (Darras et al., 2014b; Kuhn et al., 2020). The key to this conundrum may lie in sporadic intra-lineage matings, evidenced by both rare occurrences of hybrid queens (Darras et al., 2019) and mitochondrial introgression (Darras & Aron, 2015; Eyer et al., 2016) across lineage pairs, or in rare

reproduction by hybrid workers (Aron et al., 2016; Kuhn et al., 2020).

Another very well studied example of social hybridogenesis is found in the harvester ant genus *Pogonomyrmex* in Southern USA (Helms Cahan et al., 2002; Volny & Gordon, 2002). In this genus, ancestral hybridization events between two related species (*P. barbatus* and *P. rugosus*) have led to the independent evolution of several (at least two; Anderson et al., 2006; Mott et al., 2015; Sirviö et al., 2011; but see Schwander et al., 2007) dependent lineages pairs, that co-occur with their parental species and reproduce via symmetrical social hybridogenesis. Unlike in *Cataglyphis*, social hybridogenesis in *Pogonomyrmex* does not involve thelytokous parthenogenesis. Here, hybridogenetic queens mate with both con- and allo-specific males to produce queens and workers, respectively (i.e., queens are polyandrous; figure 1g). In fact, high levels of polyandry were observed in both hybridogenetic (more than 3 mates per queen; Helms Cahan et al., 2002) and non-hybridogenetic (up to more than 10 mates per queen in *P. badius*; Rheindt et al., 2004) *Pogonomyrmex* species, and were suggested to have been a prerequisite to the emergence of social hybridogenesis. But beyond the ability to mate multiply, social hybridogenesis in *Pogonomyrmex* also requires that each type of males is available to queens. This entails that phenology and mate-finding strategies are shared within dependent lineage pairs. In *Pogonomyrmex*, this is achieved through the synchronization and blending of nuptial flights between lineages, which are triggered by the same climatic events (Helms Cahan et al., 2004; Schwander et al., 2006). Interestingly, mixed mating swarms in *Pogonomyrmex* have been shown to be associated with some level of mate choice behavior by queens (Herrmann & Cahan, 2014) which could increase the odds for queens to mate with both types of males. It remains unclear however if such mechanisms are effective, as a close match between sperm frequency in queens spermathecae (i.e., an organ specialized in storing sperm) and male frequency within swarms suggests that mating is effectively random (Schwander et al., 2006). Such random mating was shown to impose fitness costs upon hybridogenetic queens, by making them ultimately unable to control the proportion of hybrid and non-hybrid eggs they lay (Schwander et al., 2006). Because of strong GCD, this translates into the continuous production of queen-destined non-hybrid larvae that will often abort due to resource limitations and phenological constraints (i.e., queens can be raised only in mature colonies and at the right season). Interestingly, random mating also has some other, perhaps more fortunate, consequences. In particular, it was shown to lead to a negative frequency-dependent selection pressure which favors the rarest lineage. Because queens that belong to a locally rare lineage are more likely to encounter inter-specific mates, they are more likely to found viable colony. They also produce less aborting non-hybrid larvae, which can be a critical advantage in the early stage of colony foundation (Helms Cahan et al., 2004; Schwander et al., 2006). Such evolutionary pattern is thought to participate in the maintenance of dependent lineages pairs (Helms Cahan & Julian, 2010; Kuhn et al., 2017; Yamauchi & Yamamura, 2006).

A very similar case of social hybridogenesis was later discovered in harvester ant genus *Messor*, from the Palearctic region. *Messor* ants share many ecological traits with *Pogonomyrmex*. They are specialized granivores that thrive in arid to semi-arid environments by collecting and storing

large amount of seeds (Branstetter et al., 2016; Steiner et al., 2011). Within *Messor*, *M. barbarus* was the first species shown to display social hybridogenesis (Norman et al., 2016; Romiguier et al., 2017). Similarly to *Pogonomyrmex*, social hybridogenesis in *M. barbarus* consists of inter-dependent lineages that reproduce via symmetrical social hybridogenesis with polyandry (figure 1g). Also like *Pogonomyrmex*, colonies of both lineages co-occur in the field, and share all aspects of phenology and mating strategy. But *M. barbarus* does display a few key differences with *Pogonomyrmex*. First, *M. barbarus* does not co-occur with identified parental species. Instead, *M. barbarus* is an ecologically dominant species that displays social hybridogenesis across all investigated parts of its range (Spain, France, Italy and Morocco; Romiguier et al., 2017). Additionally, *M. barbarus* displays only one inter-dependent lineage pair, which can be found across its whole range. This suggests that the evolution of social hybridogenesis in *M. barbarus* happened once, and was followed by a shared range expansion of both inter-dependent lineages. If this is the case, it may represent evidence for an ecological advantage to social hybridogenesis in *Messor*, which could help explain why multiple convergent evolutions towards this reproductive system occurred in the genus. While less studied and understood, two more instances of social hybridogenesis were uncovered in *Messor* (in *M. ebeninus* from Israel, and in french populations of *M. structor*; Romiguier et al., 2017). It is currently unknown however if social hybridogenesis is found across the whole range of these species. It is also unknown which form of social hybridogenesis these two species display.

Finally, the last known form of social hybridogenesis occurs in at least three species from unrelated genera, *Wasmannia auropunctata* (Foucaud et al., 2007; Fournier et al., 2005; Rey et al., 2013), *Vollenhovia emeryi* (Ohkawara et al., 2006), *Paratrechina longicornis* (Pearcy et al., 2011) and *Cardiocondyla kagutsuchi* (Okita & Tsuchida, 2016). In these species, as in hybridogenetic *S. geminata* and *Cataglyphis*, queens and workers are produced via thelytokous parthenogenesis and outbreeding, respectively. One very significant difference however, is that the lineage that provides males for worker production is an all-male lineage maintained via male clonality (i.e., androgenesis; figure 1h). Androgenesis is a very rare phenomenon overall, reported only in a handful of animal and plant species (reviewed in Schwander & Oldroyd, 2016). In hybridogenetic ants, the mechanisms that underlie androgenesis are unknown, but two hypotheses have nonetheless been proposed (Foucaud et al., 2007; Fournier et al., 2005; Rey et al., 2013). It is a possibility that male clonality is the result of maternal genome elimination following fecundation. Alternatively, it could be the result of the fecundation of anucleate eggs, produced directly by queens. In both cases, this would result in a haploid egg which would automatically develop as a clone of its father, with the exception of cytoplasmic elements (e.g., mitochondria) which would still be of maternal origin. Interestingly, although androgenesis could be interpreted as a form of sexual parasitism by males (i.e., hijacking eggs; Schwander & Oldroyd, 2016), it was shown that it is most likely not the case in *W. auropunctata* (Rey et al., 2013). In this invasive species, the combination of parthenogenesis and social hybridogenesis is found only in some populations (i.e., especially in its invasive range), and non-hybridogenetic populations with sexual reproductive systems can still be found. This has allowed for controlled crosses between individual from

both types of populations, and for an investigation of the genetic determinants of clonality and social hybridogenesis. Surprisingly, it would appear from these crosses that androgenesis in *W. auropunctata* is a maternal trait, observed only when crosses involve females of parthenogenetic and hybridogenetic populations (Rey et al., 2013). This has been interpreted as evidence that androgenesis is in fact a by-product of thelytokous parthenogenesis, which in this case would lead to the production of anucleate eggs. It is highly suspected that the resulting hybridogenetic system, that effectively maintains a genetically diverse F1 hybrid workforce without any need for “true” outcrossing (i.e., mates can originate from the same nest) has been and will be responsible for the strong invasive capabilities of these ants (Foucaud et al., 2007; Fournier et al., 2005; Rey et al., 2013).

Evolution of social hybridogenesis

The evolution of social hybridogenesis is far from a marginal fact. Instead, it is important to recognize it as a game-changing innovation with many theoretical and ecological implications. Theoretically, strong GCD appears as a challenge to formal theories for the evolution of eusociality (see box 1). On a more ecological point of view, social hybridogenesis as a partial hybridization avoidance mechanism represents a key innovation that allows ants to integrate hybridization as a part of their life-history (Schwander & Keller, 2012). The significance of this transition, together with the growing number of alternative forms social hybridogenesis may take, has led to many interrogations regarding the conditions that can trigger its evolution and favor its maintenance (e.g., Anderson et al., 2008; Sirviö et al., 2011). In this section, the different verbal models proposed to explain the evolution and maintenance of social hybridogenesis are presented.

Historically, three main models have been invoked to explain the evolution of strong GCD and social hybridogenesis (reviewed in Sirviö et al., 2011 and Anderson et al., 2008), and were developed almost exclusively through the study of *Pogonomyrmex* dependent lineages. Because at least three of the four hybridogenetic lineages known in *Pogonomyrmex* have been shown to be of hybrid origin (i.e., their nuclear genome contains elements of the two parental species, *P. barbatus* and *P. rugosus*, Anderson et al., 2008), ancestral hybridization is at the core of these models. The first and simplest model posits that social hybridogenesis could evolve through the appearance of a recessive mutation at a single locus with a major effect on caste (figure 2a; Anderson et al., 2006; Volny & Gordon, 2002). When exposed at the homozygous state, this mutant allele would have the effect of shunting larval development towards the queen caste. Such allele would thus act as a selfish genetic element, increasing its representation in the reproductive caste but reducing colonial productivity through impaired worker production. This would lead to increased selection for mechanisms that ensure the production of workers, one of which could be the restoration of heterozygous states via hybridization. In this scenario, the resulting episodes of hybridization would then lead to the introgression of the focal caste-biasing allele, eventually promoting the evolution of hybridogenetic lineage pairs. The second model is a two-locus model (figure 2b; Helms Cahan & Keller, 2003) which was developed on the idea

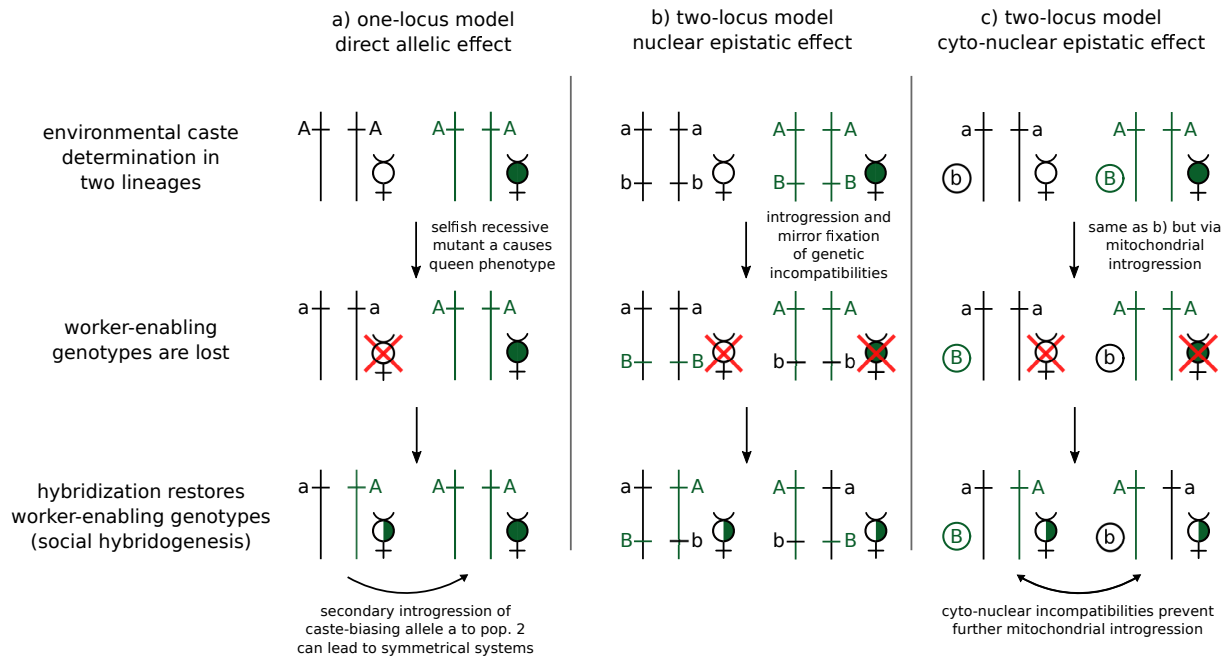


Figure 2: Three genetic models for the evolution of social hybridogenesis.

The figure represents worker genotypes in two interacting lineages at each step of three theoretical evolutionary scenarios. **a)** The first and simplest model posits that social hybridogenesis could evolve via the appearance of a recessive mutation at a single locus with a major effect on caste (Anderson et al., 2006; Volny & Gordon, 2002). **b)** The second model is based on the idea that lineage-specific combinations of co-adapted alleles must interact to elicit worker development. Following introgression and the fixation of incompatibilities, hybridization becomes necessary to restore worker-enabling combinations (Helms Cahan & Keller, 2003). **c)** The third model is similar to the second, but assumes that a mitochondrial locus is involved in worker development (Linksvayer et al., 2006).

that direct allelic effects on caste (as supposed in the first model) are incongruent with empirical evidence for a more dominant effect of epistasis (i.e. interaction between loci; Libbrecht et al., 2011; Schwander & Keller, 2008). In this model, two initial lineages possess different co-adapted alleles at both loci that must interact to elicit worker development. Following hybridization and introgression between these lineages, genetic drift would lead to the simultaneous fixation of mirror incompatibilities in both lineages. In turn, this would result in the necessity for both lineages to hybridize in order to restore compatible combinations and maintain worker production. The third and last model is in essence very similar to the second (figure 2c; Linksvayer et al., 2006). It assumes the exact same evolutionary scenario, but differs in that one of the two interacting loci is assumed to be a mitochondrial locus. The motivation behind this variant was to explain the absence of mitochondrial introgression between dependent lineages of *Pogonomyrmex*. Under this model, mitochondrial incompatibilities would lead to strong selection against mitochondrial introgression.

These three presented models were discussed and debated at length (Anderson et al., 2008; Sirviö et al., 2011), but no consensus has been reached. In fact, each of these models presents

strengths and weaknesses when confronted to experimental data from both *Pogonomyrmex* and other species. The first one-locus model is perhaps the most parsimonious of the three, and successfully explains both asymmetrical and symmetrical (i.e., via the introgression of a caste-biasing allele) cases of social hybridogenesis. It also fits nicely with intriguing experimental data from *Messor*, where one single nucleotide was found to be at the heterozygous state in each and every hybrid worker sampled across three hybridogenetic systems, while being at the homogeneous state in non-hybrid queens of both hybridogenetic and non-hybridogenetic species (Romiguier et al., 2017). This model however, clashes with the view that epistatic effects dominate caste determination in *Pogonomyrmex* (Helms Cahan & Vinson, 2003; Libbrecht et al., 2011; Schwander & Keller, 2008; Sirviö et al., 2011). It also fits poorly with further empirical evidence from quantitative genetics (Linksvayer, 2006) and developmental studies (Trible & Kronauer, 2017), that do prove the existence of direct genetic effects on caste, but which also suggest that caste is a complex trait under the control of many genes with small effect. The two epistatic models are obviously more compatible with the epistatic view. However, these models require that ancestral hybridization occurred to explain the appearance of strong GCD. If this is consistent with empirical data about *Pogonomyrmex*, other hybridogenetic systems have yet to yield evidence for such population history (e.g., *Messor*; Romiguier et al., 2017). These models also require that two lineages simultaneously fix specific alleles combinations. It is thus unclear how these models account for the evolution of asymmetrical social hybridogenesis. Finally, and perhaps most importantly, these models assume that these fixations happened by chance (i.e., via genetic drift). While small effective population size and strong genetic drift seem to be the norm in ants (Barth et al., 2014; Romiguier et al., 2014; Weyna & Romiguier, 2021 in Appendix), it remains very unlikely that such random happenings are at the basis of the increasing number of known cases of social hybridogenesis.

In explaining multiple convergent evolution towards social hybridogenesis, purely adaptive hypothesis such as that employed in the first one-locus model possess a natural advantage. It is indeed tempting to ask whether multiple examples of transitions towards strong GCD and social hybridogenesis could be driven by the same deterministic mechanism. As often mentioned in the literature, an obvious potential advantage to social hybridogenesis, and that could explain its evolution, is heterosis in workers (e.g., Anderson et al., 2008; Feldhaar et al., 2008; Kuhn et al., 2020; Lavanchy & Schwander, 2019; Schwander et al., 2006; Umphrey, 2006). If F1 hybrid workers are more efficient than regular workers, then hybridization could be gradually adopted by queens as a way to enhance colony productivity. The following evolutionary scenario would then primarily depend on whether fertile queens can also arise from F1 hybrid larvae. If such hybrid queens are frequently produced, the resulting gene flow may lead to introgression or genetic assimilation, potentially reducing the advantages of hybrid workers (as their heterozygosity is reduced). If, however, F1 hybrid queens are absent or non-fertile, divergence and genetic differences between lineages will be maintained despite increasingly frequent hybridization. In such case, hybridization may represent a stable and reliable source of over-efficient workers. In turn, this would gradually remove the selective pressure that maintains developmental plasticity in

Box 1: social hybridogenesis as a (major?) evolutionary transition

Eusociality is often presented as a major evolutionary transition (Maynard Smith & Szathmáry, 1995), where smaller entities (individuals) have come together and specialized to form larger reproductive entities (colonies) with new functions. Eusociality is accepted by most biologists to have evolved via kin selection (Birch & Okasha, 2015; Hamilton, 1964; Queller & Strassmann, 1998; but see Nowak, 2010 for hotly refuted critics). At its core, kin selection theory explains how genes responsible for the worker phenotype could propagate despite causing sterility. These genes are selected for because sterility in helper workers greatly increases the reproductive output of related queens, which have high probability to carry the same genes (see Frank, 2013 for a full theoretical overview). In this context, the evolution and maintenance of eusociality is highly dependent on high relatedness between individuals and developmental plasticity (i.e., the same genotypes must be able to produce both workers and queens; Schwander et al., 2010). In the same context, social hybridogenesis appears as an entirely new and puzzling way to achieve eusociality and colonial life, where developmental plasticity is abandoned in favor of a genetic control on caste, and where more unrelated individuals (i.e., hybrid workers) are involved in reproduction. This last fact is important because in the language of evolutionary transitions, reliance on hybrid individuals could be seen as the integration of a new entity (i.e., a second species) into reproductive units (figure 3). Although this analogy has obvious limits (e.g., absence of new function, the second species does not directly profit from its participation), understanding the evolutionary mechanisms underlying transitions towards social hybridogenesis may provide invaluable retrospective insights into the evolution of eusociality.

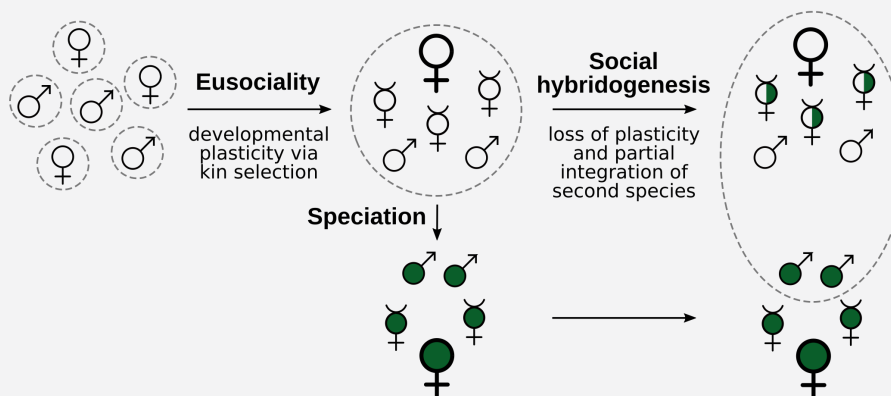


Figure 3: Eusociality and social hybridogenesis: towards complex reproductive units.

non-hybrid larvae, and could eventually lead to a complete loss of the ability to produce workers from such larvae, locking involved lineages into systems corresponding to social hybridogenesis. While such evolutionary path appears credible, heterosis in workers cannot easily be considered as the primary mechanism driving the evolution of social hybridogenesis. The main reason for this is the scarcity of empirical evidence supporting heterosis in ants (Feldhaar et al., 2008; James et al., 2002; Julian & Cahan, 2006; Ross & Robertson, 1990). An other, less evident

reason is that it is somewhat hard to envision a situation where hybrids show both heterosis and decreased probability to develop into queens. In ancestral ECD, the probability for a given larvae to develop into a queen is known to depend in part upon its size (Trible & Kronauer, 2017), and thus upon the general quality of its development. Naively, if heterosis implies improved somatic functions, it could be more expected to promote the queen developmental pathway.

Thesis objectives and overview

The repeated evolution of social hybridogenesis in various ants genera with variable ecology and histories hints towards the existence of a general and deterministic mechanism for such evolution. Yet, to this date, the only adaptive mechanisms proposed for the evolution of social hybridogenesis involve either worker heterosis or the evolution of a single mutation with major effect on caste, both of which conflict with experimental data.

In the first chapter of this thesis, my collaborators and I develop the first formal population genetic model that allows for a rigorous derivation of the conditions that could lead to an adaptive evolution of strong GCD and social hybridogenesis. This model is similar to the one-locus model presented above in that it assume that direct genetic effects on caste allow for the evolution of the probability for developing larvae to develop into either female caste (i.e., caste-ratio). It is different however in that it is not assumed that caste is acted upon by a single recessive mutant with major effect. Instead, the model treats caste as a quantitative trait that may depend on the the direct effects on many genes with small effect, and that may coevolve with hybridization by queens (which is also treated as a quantitative trait). This model allows for a mathematical investigation of the effects of several key parameters on the evolution of caste-ratio and hybridization, such as heterosis in workers, relatedness within colonies and polyandry, or the possibility for queens to reproduce through thelytokous parthenogenesis. Because the model also has several shortcomings (e.g., gene flow is assumed to be absent between interacting lineages), a significant effort was made to present and comment all mathematical details and results obtained in this project (see appendix of chapter 1). This was done with the hope that this first model may be refined and constructed upon in future work.

This modeling work has yielded results suggesting that strong GCD and hybridization may indeed coevolve adaptively, until social hybridogenesis is fixed within populations. But most interestingly, the uncovered underlying mechanism is more general than previously suspected. According to our model, transitions towards social hybridogenesis may be driven by inevitable intra-colonial conflicts between developing larvae and their mother, and could occur even when hybridization entails strong fitness costs (e.g., sterile queen production or hybrid depression in workers). One possible interpretation to this result is that known cases of social hybridogenesis are in fact only the tip of the iceberg, and that many instances of social hybridogenesis remain to be discovered.

In the second chapter of this thesis, my supervisors and I follow this line of thought, and develop a methodology that could eventually lead to the identification of new hybridogenetic systems. Social hybridogenesis is notoriously hard to uncover, because proving its presence requires genetic data for many individuals, ideally including both workers and queens. Such population-level data is costly to produce, and exists only for relatively few model species. The bulk of ant diversity (13 964 valid species according to Antcat; Bolton, 2021) was never investigated genetically, especially at the population level. But a glimmer of hope arises from the intensive work of several authors (Branstetter et al., 2017; Faircloth et al., 2012) who set out to study the phylogeny of ants at the largest scale possible. In the course of their still ongoing work, these authors have produced and published genome sequencing data for hundreds of ant species, including many non-model and taxonomically important species. As is usual in phylogenomic studies, most of these sequencing data were produced using only one individual (usually a worker) per species. While this is a serious limitation to their use in the search of new hybridogenetic systems, they can still be used to detect one of the hallmark of strong GCD: F1 hybrid workers. F1 hybrids carry two divergent parental haplotypes, which manifest as characteristic patterns in the distribution of their genome-wide heterozygosity. By developing a coalescent-based statistical description of expected heterozygosity patterns in F1 hybrids, their detection from single genomes was revealed both possible and accurate. Using this original approach on the available data allowed us to produce a list of candidate species that may reveal to display social hybridogenesis. More generally, by reproducing the same analysis on similar data for other groups of Arthropods, we produced new evidence supporting that hybridization is more frequent in ants.

The new methodology developed in chapter 2 was also useful in two other, more exploratory projects. Specifically, it allowed us to position instances of social hybridogenesis in *Messor* harvester ants, at two separate levels of focus. As mentioned in the introduction, the *Messor* genus was revealed before the start of this thesis to contain at least three independent instances of social hybridogenesis, among 9 investigated species, in *M. barbarus*, *M. ebeninus* and *M. structor* (Romiguier et al., 2017). Because *Messor* contains 126 valid species distributed across Africa and Eurasia (Bolton, 2021), it might yield many more instances of social hybridogenesis, and allow for powerful comparative studies with the potential to yield key insights about the genetic, demographic, biogeographic and ecological conditions that can lead to the evolution of social hybridogenesis. The two projects presented in chapter 3 are ongoing and exploratory projects that aim at gathering new data, and answering preliminary questions regarding social hybridogenesis in *Messor*, clearing the way for future studies.

In the first part of chapter 3, my collaborators and I focused on *Messor* at the large scale with two main objectives: producing the first phylogeny of the genus (which is still unknown) containing as much newly sampled species as possible, and finding out if any of these new species display F1 hybrid workers. Because the range of *Messor* is very wide, and spans many countries difficult to access, field sampling was not retained as a viable strategy in the context of this thesis. Instead, we chose to rely on species available from museum collections. After preliminary research, two

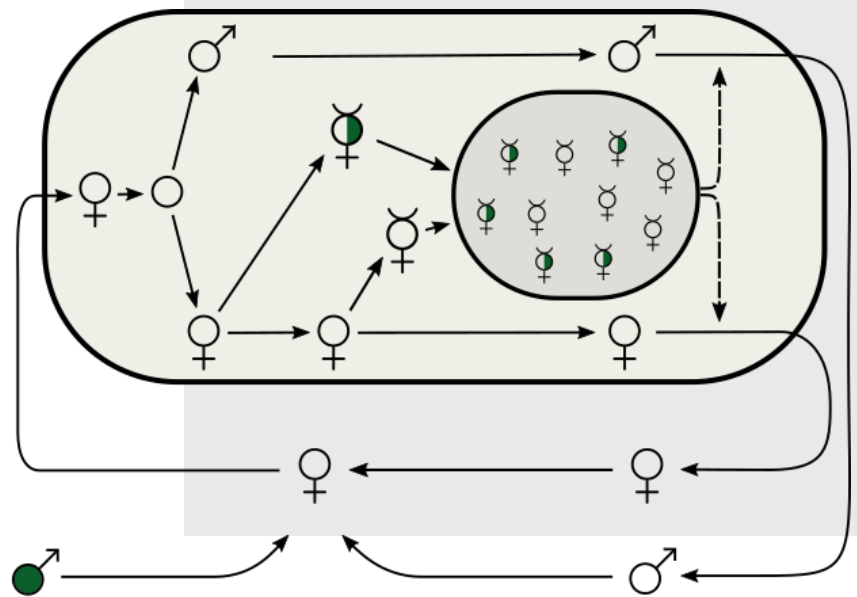
museums were found to possess pinned specimens of *Messor*, the Museum National d'Histoire Naturelle (MNHN) in Paris, and the Natural History Museum (NHM) in London. While the collaboration with MNHN was delayed due to unforeseen contingencies, the NHM accepted to lend us specimens for 54 identified species of *Messor*. Because many of these specimen are unique and valuable (i.e. historical specimens and types), a choice was made to process them using non-destructive DNA extraction methods (i.e., digesting and extracting soft tissues without specimen grinding). This was achieved through a fruitful collaboration with a team of skilled entomologists from the Centre de Biologie pour la Gestion des Populations (Astrid Cruaud, Jean-Yves Rasplus et Sabine Nidelet), who mastered these methods, and via the work of Elodie Lauroua, an intern under the supervision of Jonathan Romiguier and myself. With their help, we were able to assemble the first phylogenomic dataset of *Messor*, eventually yielding the first phylogeny of the group and preliminary insights about the frequency of social hybridogenesis within it.

In the second part of chapter 3, my collaborators and I focused more specifically on the the special case of *Messor structor*. Together with *M. barbarus*, *M. structor* is the only species of *Messor* than can be found in Europe and that is known to display social hybridogenesis (Romiguier et al., 2017). But unlike *M. barbarus*, the distribution and modalities of social hybridogenesis within *M. structor* were mostly unknown at the beginning of this thesis. This impeded comparative studies of these two species and called for an exploratory investigation of the latter. However, such a study of social hybridogenesis in *M. structor* also had to contend with recent taxonomic developments within the species. In 2018, a study by Steiner et al. revealed that the widely spread *M. structor* is in fact a species complex (which we refer to as *M. structor sensus lato* throughout this thesis) composed of at least 5 separate species with overlapping ranges. In this project, we constructed a genomic dataset containing samples of these five new species, and used it to determine which of these species are involved in hybridogenetic systems. This also yielded preliminary answers regarding the form of social hybridogenesis found in *M. structor s.l.*

Chapter 1

Deterministic evolution of social hybridogenesis from intra-colonial conflicts: A model

Arthur Weyna, Jonathan Romiguier & Charles Mullon



Hybridization enables the fixation of selfish queen genotypes in eusocial colonies

Arthur Weyna,¹ Jonathan Romiguier,^{1,2,*} and Charles Mullon^{3,4,*}

¹*Institut des Sciences de l'Evolution (UMR 5554), University of Montpellier, CNRS, Montpellier 34000, France*

²*E-mail: jonathan.romiguier@umontpellier.fr*

³*Department of Ecology and Evolution, University of Lausanne, Lausanne 1015, Switzerland*

⁴*E-mail: charles.mullon@unil.ch*

Received June 9, 2021

Accepted August 9, 2021

A eusocial colony typically consists of two main castes: queens that reproduce and sterile workers that help them. This division of labor, however, is vulnerable to genetic elements that favor the development of their carriers into queens. Several factors, such as intracolony relatedness, can modulate the spread of such caste-biasing genotypes. Here we investigate the effects of a notable yet understudied ecological setting: where larvae produced by hybridization develop into sterile workers. Using mathematical modeling, we show that the coevolution of hybridization with caste determination readily triggers an evolutionary arms race between nonhybrid larvae that increasingly develop into queens, and queens that increasingly hybridize to produce workers. Even where hybridization reduces worker function and colony fitness, this race can lead to the loss of developmental plasticity and to genetically hard-wired caste determination. Overall, our results may help understand the repeated evolution toward remarkable reproductive systems (e.g., social hybridogenesis) observed in several ant species.

KEY WORDS: Ant, caste determination, eusociality, genetic conflicts, hybridization, Hymenoptera, parasitism, reproductive system, social hybridogenesis.

Eusociality is characterized by a striking division of reproductive labor between two castes: queens and workers (Crespi and Yanega 1995). Queens monopolize reproduction, while typically sterile workers specialize on other colony tasks such as foraging and tending to the brood. The sterility of workers initially seemed so inconsistent with natural selection that Darwin referred to eusociality as his “one special difficulty” (Darwin 1859, ch. 7). This apparent paradox was resolved in the 1960s with Hamilton’s theory of kin selection (Hamilton 1964). Hamilton demonstrated that natural selection can favor eusociality when workers preferentially help relatives (who can transmit the same genetic material). In addition to laying the theoretical basis for the evolution of eusociality, Hamilton’s work led to the insight that caste determination should be plastic to allow identical gene copies to be in workers and in the queen they help (Seger 1981). In line with this notion, the developmental fate of female larvae in many eusocial insects depends on environmental factors (Trible and Kronauer

2017), such as food quantity and quality (Brian 1956, 1973), temperature and seasonality (Brian 1974; Schwander et al. 2008) or signals emitted by adults of the colony (Penick and Liebig 2012; Libbrecht et al. 2013). Probably the most iconic example of such plasticity is found in honeybees where queens arise only from larvae reared in royal cells and fed with royal jelly. For long, this and many other empirical findings strengthened the idea that caste determination is under strict environmental control and largely free from genetic effects.

More recently, however, substantial genetic variation for caste determination has been described across a number of eusocial species (Winter and Buschinger 1986; Moritz et al. 2005; Hartfelder et al. 2006; Linksvayer 2006; Schwander and Keller 2008; Smith et al. 2008; Frohshammer and Heinze 2009; Schwander et al. 2010). This variation is thought to derive from caste-biasing genotypes that bias the development of their carrier toward a particular caste (Moritz et al. 2005; Hughes and Boomsma 2008). Those genotypes that favor larval development toward the reproductive caste have sometimes been

*These authors share senior authorship.

referred to as “royal cheats” as they cause the individuals that carry them to increase their own direct reproduction at the expense of other colony members (e.g., Anderson et al. 2008; Hughes and Boomsma 2008). The segregation of such royal cheats should depend on a balance between: (1) direct benefits from increased representation in the reproductive caste; and (2) indirect costs due to reduced worker production and colony productivity (Hamilton 1964). As highlighted by abundant theory, several factors can influence these benefits and costs and thus tip the balance for or against the evolution of royal cheats. For instance, low relatedness between larvae due to polyandry (when queens mate with multiple males) or polygyny (when colonies have multiple queens) increases competition between genetic lineages within colonies and thereby favors royal cheating (e.g., Reuter and Keller 2001). Conversely, selection against cheats is bolstered by low dispersal abilities and high within-group relatedness (e.g., Hamilton 1964; Lehmann et al. 2008; Boomsma 2009), bivoltinism and asymmetrical sex-ratio (e.g., Trivers and Hare 1976; Seger 1983; Alpedrinha et al. 2014; González-Forero 2015; Quiñones and Pen 2017), coercion (i.e., policing; Wenseleers et al. 2004; Dobata 2012), queen longevity and competition between queens (e.g., Queller 1994; Bourke and Chan 1999; Avila and Fromhage 2015), or where workers reproduce following queen death (Field and Toyoizumi 2020).

One intriguing factor that has been proposed to influence the cost of royal cheating is sperm parasitism, a behavior consisting in queens using the sperm of another species or lineage to produce hybrid workers (Linksvayer 2006; Anderson et al. 2008). Both morphological and genetic data suggest that this behavior is common in many ant species (e.g., in multiple *Temnothorax* populations, the majority of queens were found to produce some hybrid workers; Douwes and Stille 1991; Umphrey 2006 and Feldhaar et al. 2008 for reviews). In these species, sperm parasitism results in hybrid larvae that rarely, if ever, develop as fertile queens and rather become sterile workers (presumably due to genetic incompatibilities between parental lineages; Feldhaar et al. 2008; Tribble and Kronauer 2017). Such hybrids should therefore be impervious to genetic caste-biasing effects and thus provide a reliable source of workers. In principle, this alternative supply of workers may reduce the indirect cost of royal cheats and hence favor their evolution (Anderson et al. 2008). But beyond these broad-brush predictions, the effect of sperm parasitism on the segregation of royal cheats remains poorly understood.

Here, we develop a mathematical model to explore the evolution of genetic caste determination via royal cheats when queens can hybridize to produce workers. In particular, we assess the effects of key factors on the evolutionary dynamics of caste determination, such as polyandry and queen parthenogenesis (when queens have the ability to produce daughters asexually), as well as their interactions with potential costs and benefits

of hybridization, for instance, owing to hybrid incompatibilities or hybrid vigor.

The Model

We consider a large population of annual eusocial haplodiploids with the following life-cycle (Fig. 1). First, virgin queens mate with a fixed number $m \in \{1, 2, \dots\}$ of males. Each of these mates can either be an allo- (with probability η) or a con-specific male (with complementary probability $1 - \eta$). Once mated, queens found monogynous colonies (i.e., one queen per colony) and lay a large number of eggs. A proportion f of these eggs are diploid (and develop into females) and $(1 - f)$ are haploid (and develop into males). Assuming random egg fertilization, a queen therefore produces on average $f\eta$ hybrid and $f(1 - \eta)$ nonhybrid females. We assume that a hybrid female can only develop as a worker, while a nonhybrid female can either develop as a worker (with probability ω) or as a queen (with complementary probability $1 - \omega$). Overall, a colony thus consists of $f\eta$ hybrid and $f(1 - \eta)\omega$ nonhybrid sterile workers, as well as $f(1 - \eta)(1 - \omega)$ virgin queens and $(1 - f)$ males that are available for reproduction at the next generation.

If only virgin queens and males can reproduce, their reproductive success depends on the workforce of their colony of origin. Specifically, we assume that the probability that a sexual reaches the mating pool increases linearly with the total number of workers in the colony, combining hybrid and nonhybrid workers (we show later that our results do not change qualitatively when the increase is nonlinear). We nonetheless allow for differential contribution to the workload between hybrid and nonhybrid workers, with the contribution of hybrid workers weighted by a parameter $e \geq 0$ (so that the effective workforce of a colony is $ef\eta + f(1 - \eta)\omega$). When $e = 1$, hybrid workers have the same working efficiency as nonhybrid workers. By contrast, when $e < 1$, hybrid workers are less efficient, for instance, due to outbreeding depression. This can also reflect other potential costs associated with hybridization, such as the production of sterile or nonviable hybrid queens (Feldhaar et al. 2008). Conversely, when $e > 1$, hybrid workers outperform regular workers, due, for example, to hybrid vigor (Umphrey 2006).

Results

HYBRIDIZATION AND SPERM PARASITISM, EVEN COSTLY, CAN LEAD TO THE FIXATION OF ROYAL CHEATS AND THE COMPLETE LOSS OF INTRASPECIFIC WORKERS

We first investigate the evolution of caste determination by allowing the probability ω that a larva develops as a worker to

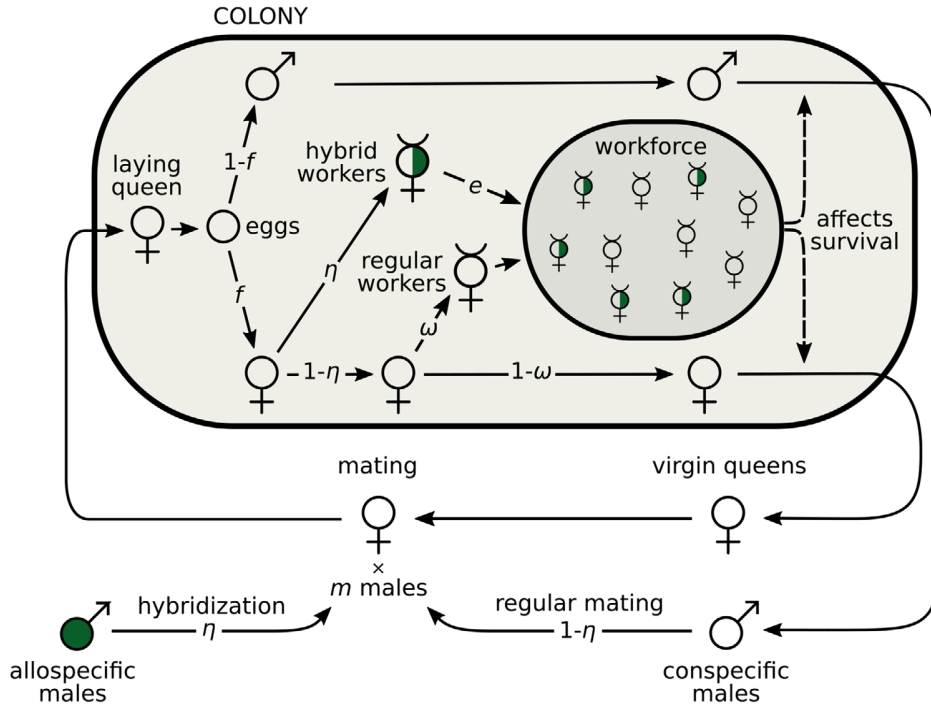


Figure 1. The life cycle of an annual eusocial with hybridization and sperm parasitism. At each generation, the life-cycle begins with virgin queens mating with m males, each of which has a probability η to be allo-specific and $1 - \eta$ to be conspecific. After mating, a queen founds a colony and starts producing eggs. Hybrid female eggs (with allo-specific paternal origin) all develop into workers. Regular female eggs (with conspecific paternal origin) develop into workers with probability ω and into queens otherwise. The variable η thus captures the tendency of queens to hybridize and parasitize sperm, while ω controls caste determination.

vary. We assume that this probability is under individual genetic control (i.e., the future caste of a female larva depends only on its own genotype) and that it evolves via random mutations with weak additive phenotypic effects (Appendix A for details on our methods). Mutational effects are unbiased so a new mutation is equally likely to increase or decrease the tendency ω of becoming a worker. Those mutations that decrease ω can be considered as more selfish as they increase the likelihood that their carriers develop into queens at the expense of other individuals of the same colony. Following the terminology of Hughes and Boomsma (2008), we thus refer to mutations decreasing ω as royal cheats. As a baseline, we consider the case where queens mate with a large number of males (i.e., $m \rightarrow \infty$) and where hybridization is fixed at a given level (e.g., η is the proportion of allo-specific males in the pool of mates from which females choose randomly).

Our analyses (Appendix B.1.1) reveal that the probability for a larva to develop as a worker evolves toward a unique and stable equilibrium,

$$\omega^* = \frac{1}{3} - e \frac{2\eta}{3(1-\eta)}. \quad (1)$$

To interpret this equation (1), consider first the case where hybridization is costless ($e = 1$). Equation (1) then tells that in the absence of hybridization ($\eta = 0$), a larva will develop into a worker with a probability of $1/3$ at equilibrium (in line with previous models that ignore hybridization, e.g., Reuter and Keller 2001, Appendix B.1.4 for connection). But as hybridization increases ($\eta > 0$), royal cheating is increasingly favored and larvae become increasingly likely to develop as queens rather than workers (i.e., $\omega^* < 1/3$, Fig. 2A). In fact past a threshold of hybridization ($\eta \geq 1/3$), the population evolves toward a complete loss of nonhybrid workers via the fixation of increasingly caste-biasing royal cheats alleles ($\omega \rightarrow 0$). In this case, nonhybrid females eventually all develop into queens that rely on sperm parasitism to produce workers.

Equation (1) also shows that the performance of hybrid workers relative to nonhybrids, e , modulates the effect of hybridization on the evolution of caste determination (Fig. 2B). As a result, royal cheating and worker-loss evolution are facilitated when hybrids outperform regular workers ($e > 1$) but hindered otherwise ($e < 1$). Nevertheless, even when hybridization is extremely costly ($0 < e \ll 1$), complete worker-loss can evolve (Fig. 2C).

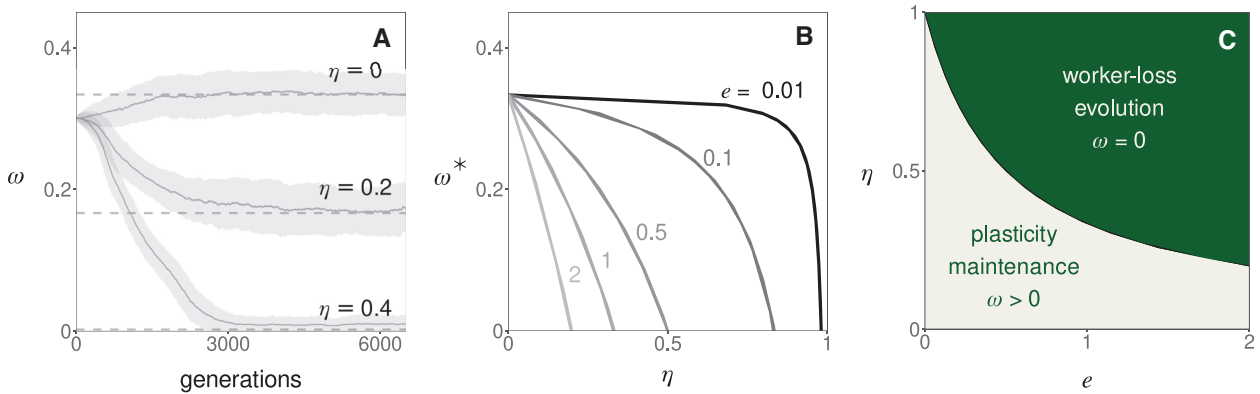


Figure 2. The fixation of royal cheats and evolution of intraspecific worker-loss. (A) Evolution of the probability ω that a female larva develops into a worker in a simulated population when queens mate with a large number of males (polyandry, $m \rightarrow \infty$) and the proportion of allospecific males η is fixed (top $\eta = 0$; middle $\eta = 0.2$, bottom $\eta = 0.4$; other parameters: $e = 1$, Appendix A.3 for details on simulations). Plain lines (and surrounding gray areas) show the population average ω (and its standard deviation). Dashed lines show the predicted equilibrium (from eq. 1). (B) Equilibrium of ω as a function of hybridization η and the efficiency of hybrid workers e (from eq. 1). (C) Parameter combinations leading to the evolution of complete worker-loss (i.e., $\omega \rightarrow 0$, in green, corresponding to $\eta \geq 1/(1 + 2e)$, which is found by substituting eq. 1 into $\omega^* \leq 0$).

WORKER-LOSS READILY EMERGES FROM THE COEVOLUTION OF GENETIC CASTE DETERMINATION AND SPERM PARASITISM, DRIVEN BY INTRACOLONIAL CONFLICT

The above analysis indicates that intraspecific worker-loss can evolve when queens have a sufficiently high tendency to hybridize. This raises the question of whether such tendency is also subject to selection. To answer this question, we allow the probability η that a queen's mate is allospecific to coevolve with caste determination (ω). We assume that this probability η is under individual queen control (i.e., it depends only on a queen's genotype) and like caste determination, evolves via rare mutations with weak additive phenotypic effects (Appendix A for details).

We find that depending on the efficiency e of hybrid workers, the coupled evolutionary dynamics of hybridization η and caste determination ω lead to an evolutionary arms race with one of two contrasted outcomes (Appendix B.1.2 for analysis). When e is small ($e \leq 1/4$, Fig. 3A gray region), the population evolves hybridization avoidance ($\eta \rightarrow 0$) while the probability ω to develop as a worker stabilizes for its baseline equilibrium ($\omega^* = 1/3$, Fig. 3B). By contrast, when hybrid workers are at least half as efficient as regular workers ($e \geq 1/2$, Fig. 3A, dark green region), intraspecific worker-loss evolves ($\omega \rightarrow 0$) and hybridization stabilizes at an intermediate equilibrium ($\eta^* = 2/3$, Fig. 3D). When hybrid worker efficiency is intermediate ($1/4 < e < 1/2$, Fig. 3A, light green region), the population evolves either hybridization avoidance or intraspecific worker-loss depending on initial conditions (Fig. 3C), with worker-loss favored by high initial tendency η of queens to hybridize. In sum, provided four hybrid workers are at least as good as one regular worker ($e > 1/4$),

the coevolution of genetic caste determination and hybridization can lead to worker-loss in our model.

To better understand the forces at play in the emergence of worker-loss, we further used a kin-selection approach to decompose the invasion fitness of mutant alleles into the sum of: (1) their direct fitness effects on the reproductive success of the individuals that express them; and (2) of their indirect fitness effects on other related individuals that can also transmit them (Taylor and Frank 1996, Appendix B.1.3 for details). Starting with a population at the baseline equilibrium in absence of hybridization ($\omega = 1/3$, $\eta = 0$), we tracked these different fitness effects along a typical evolutionary trajectory that leads to worker-loss (black arrow heads, Fig. 3D) for alleles that influence the tendency of a larva to develop as a worker (Fig. 3E) and of a queen to hybridize (Fig. 3F).

Our kin selection analysis reveals that alleles that increase hybridization in queens are selected because they allow queens to increase the number of sexuals produced by their colony (especially via males, blue curve, Fig. 3F). This is because the baseline tendency ω to develop as a worker that evolves is optimal from the point of view of a gene in a larvae, but sub-optimal from the point of view of a gene in a queen who would benefit from a larger workforce. Hybridization by queens evolves to rectify this and align colony composition with the interests of the queen. Simultaneously, as queens evolve greater hybridization and augment their workforce with hybrids, genes in nonhybrid larva have an increasing interest for their carriers to develop as queens rather than workers (Fig. 3E). These two selective processes via queens and larvae fuel one another in an evolutionary arms race whose endpoint is complete intraspecific

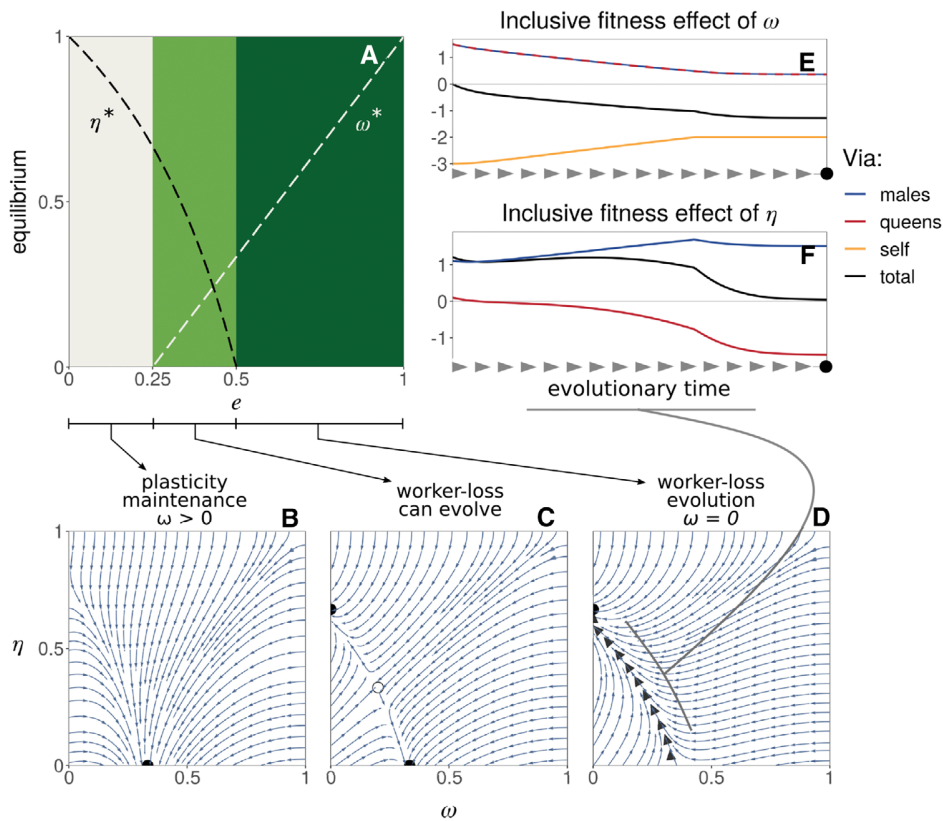


Figure 3. The coevolution of caste determination and sperm parasitism. (A) Evolutionary equilibria (for η in black and ω in white) as a function of hybrid worker efficiency e (eq. B6 in Appendix B.1.2 for details). These equilibria, however, are evolutionary repellers (eq. B7 in Appendix B.1.2). As a result, three types of coevolutionary dynamics are possible depending on e as illustrated in panels (B)–(D) (from eq. B5). These panels show examples of phenotypic trajectories when worker-loss: Panel (B) never evolves ($e = 0.1$); Panel (C) can evolve depending on initial conditions ($e = 0.4$); Panel (D) always evolves ($e = 0.7$). Black filled circles indicate the two evolutionary endpoints: hybridization avoidance with developmental plasticity ($\omega = 1/3$ and $\eta = 0$ in B and C) or worker-loss with hybridization ($\omega = 0$ and $\eta = 2/3$ in C and D). Empty circle in (C) shows the internal unstable equilibrium (eq. B6). Thick grey arrow heads in (D) represent the trajectory of a population starting from $\omega = 1/3$ and $\eta = 0$ and evolving to worker-loss. (E) Fitness effects of caste determination ω in a mutant larva via itself (in orange), related queens (red), and related males (blue) along the trajectory leading to worker-loss shown in panel (D) (total selection in black, Appendix B.1.3 for derivation). We see that negative fitness effects via self (orange line) lead to a total selection effect that is negative (black line). This indicates that mutant larvae with increasingly small values of ω are selected because these values increase larvae’s direct fitness (by increasing the probability that they develop into queens). (F) Fitness effects of hybridization η in a mutant queen, via its sons (blue) and daughter queens (red) along the trajectory leading to worker-loss shown in panel (D) (total selection in black). Positive total selection (in black) is mostly due to an increase of fitness via males (in blue). This says that mutant queens with increasingly large values of η are selected because this increases their reproduction, especially via males.

worker-loss. Our decomposition of fitness effects thus shows that the loss of nonhybrid workers evolves in our model due to within-colony conflicts over colony composition. In fact, our results suggests that worker-loss emerges because hybridization allows queens to control the production of workers in their colony, while nonhybrid larvae lose their tendency to develop as workers to promote their own reproduction via the fixation of royal cheats.

WORKER-LOSS IS IMPAIRED BY LOW POLYANDRY BUT FACILITATED BY ASEQUAL REPRODUCTION

So far, we have assumed that queens mate with a large, effectively infinite, number of males. By increasing relatedness within the brood, low polyandry ($2 \leq m \ll \infty$), and monandry ($m = 1$) mediate within-colony conflicts and therefore should be relevant to the evolutionary arms race leading to worker-loss (Anderson et al. 2008; Schwander et al. 2010). To test this, we

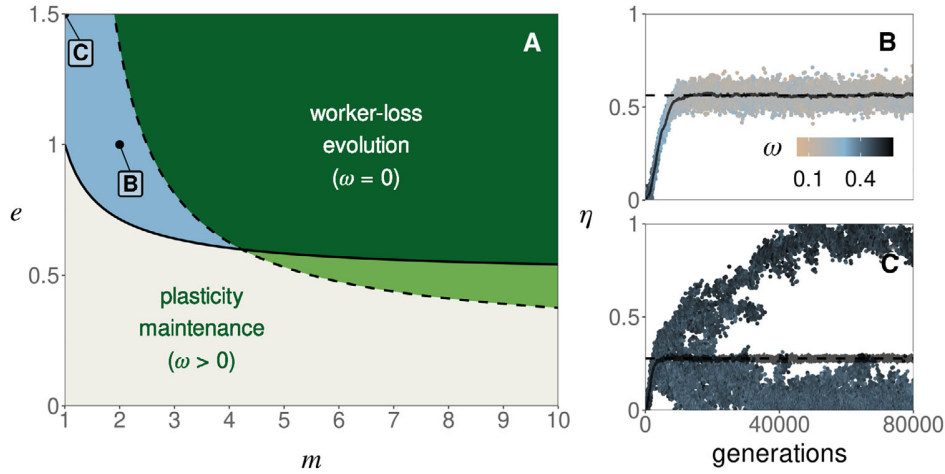


Figure 4. The effects of monandry and low polyandry. (A) Outcome of selection as a function of mate number m and hybrid worker efficiency e . Over the dashed line, worker-loss is a stable equilibrium (i.e., a population with traits $\omega = 0$ and $\eta = 2/3$ cannot be invaded, eq. B16 in Appendix B.2.1). Over the plain line, hybridization can invade when rare (i.e., $\eta = 0$ is unstable, eq. B18 in Appendix B.2.1). Below both lines (gray region), plasticity in caste determination is maintained (as in Fig. 3B). Over both lines (dark green region), hybridization and worker-loss evolve (as in Fig. 3D). In the light green region, worker-loss evolve for some initial conditions (as in Fig. 3C). In the blue region, there exists an internal attractor equilibrium (i.e., the population converges toward a phenotype $0 < \eta^* < 1$ and $0 < \omega^* < 1$) that is either uninvadable (for $2 \leq m \leq 4$, see, e.g., panel B) or invadable leading to polymorphism (for $m = 1$, see, e.g., panel C). (B) Evolution toward an uninvadable phenotype in a simulated population (when $e = 1$ and $m = 2$). Each dot represents the value of η of one of 20 haplotypes randomly sampled every 100 generation in a simulated population of 10,000 queens (Appendix A.3 for details on simulations). The color of each dot gives the value of ω of the associated haplotype (legend). The horizontal dashed line represents the predicted equilibrium (from Fig. S1). The gray line represents the mean value of η across the simulation. (C) Evolution toward an invadable phenotype and the emergence of polymorphism in a simulated population (when $e = 1.5$ and $m = 1$, other parameters and figure legend: same as B).

investigated the effect of mate number m on the coevolution of ω and η (Appendix B.2.1 for details).

We find that as the number m of mates decreases, the conditions for intraspecific worker-loss emergence become more restrictive. Specifically, the threshold of hybrid worker efficiency e above which worker-loss always evolves increases as polyandry decreases (as $m \rightarrow 1$, Fig. 4A, dark green region). In addition, when the number of mates is low ($m \leq 4$), evolutionary dynamics do not necessarily lead to either complete worker-loss or hybridization avoidance. For intermediate values of e (Fig. 4A, blue region) the population actually converges to an intermediate state where queens partially hybridize ($0 < \eta^* < 1$) and larvae retain developmental plasticity ($0 < \omega^* < 1$, Fig. 4B, Appendix B.2.1 and Fig. S1 for analysis). Under monandry ($m = 1$) the evolution toward such intermediate state always happens when hybrid workers outperform regular workers ($e > 1$, Fig. 4A, blue region).

In the special case of monandry and overperforming hybrid workers ($m = 1$ and $e > 1$), our mathematical analysis further shows that partial hybridization and larval plasticity is not evolutionary stable (Appendix B.2.1, Figs. S1 and S2). Rather, the population experiences disruptive selection that should favor the emergence of polymorphism. To test this, we performed

individual-based simulations under conditions predicted to lead to polymorphism (Fig. 4C). These show the emergence and long-term coexistence of two types of queens: one that hybridizes with low probability (and reproduces via both males and queens); and another that mates almost exclusively with allospecific males and thus reproduces mostly via males (because $m = 1$, these queens only produce hybrid workers and males). Beyond this special case, the evolution of worker-loss is impeded by low polyandry and impossible under monandry in our model. This is because with a low number of mates, a queen runs the risk of being fertilized by only one type of male. Under complete worker-loss (when the population is fixed for $\omega = 0$), a queen mated to only conspecific males produces only larvae destined to be queens but no workers to ensure their survival and thus has zero fitness.

Our finding that monandry inhibits the emergence of worker-loss contrasts with the observation that several ant species, notably of the genus *Cataglyphis*, lack nonhybrid workers and rely on sperm parasitism for workers in spite of being mostly monandrous (Kuhn et al. 2020). One potential mechanism that could have allowed such evolution is thelytokous parthenogenetic reproduction by queens, whereby queens can produce daughters clonally. This reproduction mode, which is common in eusocial Hymenoptera (Rabeling and Kronauer 2013) and in

particular in *Cataglyphis* (Kuhn et al. 2020), could allow queens fertilized exclusively by allospecific males to nevertheless produce queens via parthenogenesis. To investigate how thelytokous parthenogenesis influences the evolution of caste determination, we extend our model so that a fraction c of the female progeny of queens is produced parthenogenetically (Appendix B.2.2 for details). We assume that larvae produced in such a way are equivalent to nonhybrid larvae: they develop into workers with a probability ω determined by their own genotype (which in this case is the same as their mother's genotype) and if they develop into workers, they have the same working efficiency as nonhybrid workers (i.e., there is no direct cost or benefit to parthenogenesis).

The coevolutionary dynamics of caste determination and hybridization with parthenogenesis are in general too complicated to be tractable. We could nonetheless gain insights into worker-loss evolution by performing an invasion analysis, asking (1) when is worker-loss ($\omega = 0$) evolutionary stable (so that a population where intraspecific workers have been lost cannot be invaded by a genetic mutant with developmental plasticity)? And (2) when can hybridization evolve when absent in the population (i.e., when is $\eta = 0$ evolutionary unstable)? When these two conditions are met, evolution will tend to favor the emergence and maintenance of worker-loss (e.g., as in Fig. 3D). We thus studied when conditions (1) and (2) above are both true in terms of parthenogenesis c , as well as hybrid workers efficiency e and mate number m . This revealed that parthenogenesis has a nonmonotonic relationship with worker-loss evolution (Fig. 5A and B). As parthenogenesis increases from zero, worker-loss evolution is initially favored, especially under monandry (as expected; e.g., Fig. 5C; see eq. B26 in the Appendix for details). But past a threshold of parthenogenesis, the conditions leading to worker-loss become increasingly stringent until such evolution becomes impossible (see eq. B25 in the Appendix for details). This is because as parthenogenesis increases, the relatedness among a queen and larvae of the same colony also increases. The conflict between them, which fuels the evolution of worker-loss, therefore abates until it is no longer advantageous for a larva to preferentially develop as a queen.

We additionally computed the level of hybridization favored by selection when the population has evolved worker-loss (and this is an evolutionarily stable state). We find that hybridization increases as queens mate with fewer males and as parthenogenesis increases (Fig. 5D), so much so that selection can lead to complete hybridization ($\eta = 1$, e.g., Fig. 5C). As a result, there exists a range of intermediate values of parthenogenesis for which worker-loss evolves in association with a complete loss of intraspecific matings, that is, queens never mate with males of their own species or lineage. These males are nevertheless still

being produced in our model (as the primary sex ratio is such that $f < 1$).

Discussion

In sum, our analyses indicate that worker-loss readily evolves when queens can hybridize with a lineage of males by whom fertilization leads to the production of workers. This evolution in our model occurs through a sequence of substitutions of alleles that increasingly bias the development of their carrier toward the queen caste, that is, “royal cheats”. Hybridization, or sperm parasitism, allows royal cheats to fix in the population by providing a way for colonies to compensate for the reduced workforce. In fact, when queens are capable of recognizing genetic differences among males and when royal cheats are present in the population, selection favors hybridization by queens to regain control over caste allocation in their colony. This in turn promotes greater cheating by larvae, which favors greater hybridization by queens and so on. This evolutionary arms race, fueled by intracolony conflicts, eventually leads to complete intraspecific worker-loss: a state where larvae have lost their developmental plasticity and develop as workers or queens depending only on whether they are the product of hybridization or not, respectively.

MODEL LIMITATIONS

Of course, our analyses are based on several idealized assumptions. In particular, we assumed that the probability for larvae to develop as workers is under complete larval genetic control. Typically the developmental fate of female larvae also depends on various environmental factors created by adult colony members, such as food quality and quantity (Brian 1956; Tribble and Kronauer 2017), or mechanical (Penick and Liebig 2012) and chemical (Schwander et al. 2008; Penick et al. 2012) stimuli. The conclusions of our study apply as long as these environmental effects are held constant (or evolve more slowly than genetic caste determination). In this case, worker-loss would emerge via royal cheats that modify larval developmental reaction norm to environmental effects in such a way that their carriers are more likely to develop as queens (Hughes and Boomsma 2008; Wolf et al. 2018). We also assumed that caste determination and hybridization evolve via rare mutations with weak additive effects at a single locus. These assumptions, which are typical to adaptive dynamics and kin selection approaches, have been extensively discussed elsewhere in a general context (Frank 1998; Rousset 2004; Geritz and Gyllenberg 2005; Dercole and Rinaldi 2008). In particular, all our results extend to the case where traits are determined by many genes and/or many co-segregating alleles, provided genetic variance in the population remains small (e.g., Charlesworth 1990; Iwasa et al. 1991; Abrams et al. 1993; Mullon and Lehmann 2019). In cases where mutations have

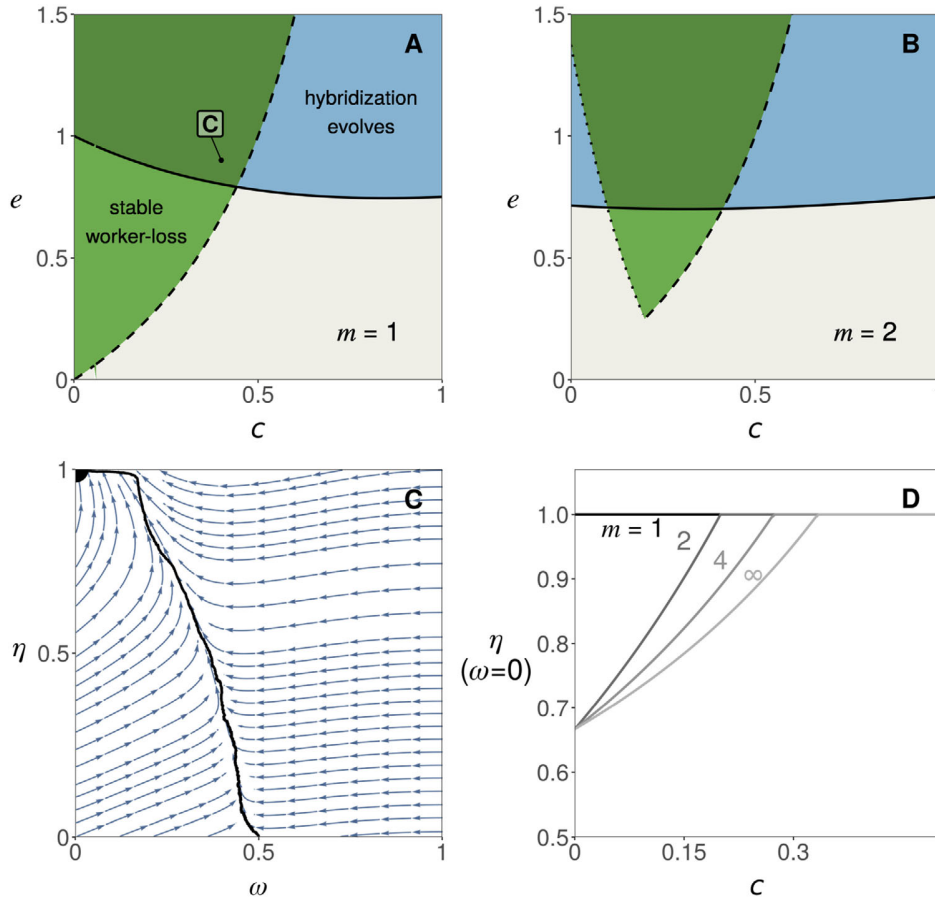


Figure 5. The influence of thelytokous parthenogenesis. (A) and (B) Invasion analysis as a function of parthenogenesis c and hybrid worker efficiency e (with $m = 1$ in A and $m = 2$ in B). In the region over the plain line, hybridization can invade when rare (i.e., $\eta = 0$ is unstable, eq. B23). In the region over the dashed line (in A) or framed by the dotted and dashed lines (in B), worker-loss is a stable equilibrium (i.e., a population at equilibrium for η and with $\omega = 0$ cannot be invaded, Appendix B.2.2, eqs. B25 and B26 for details). In the dark green region, selection thus favors both the evolution of hybridization and the maintenance of worker-loss (e.g., panel C). In the light green region, worker-loss can evolve only for some initial conditions (as in Fig. 3C). (C) Phenotypic trajectories leading to worker-loss (when $e = 0.9$, $c = 0.4$, and $m = 1$). Arrows show the direction of evolution favored by selection. Black filled circles indicate the evolutionary end-point. The black line shows the average trait values of a simulated population starting at $(\omega = 1/2, \eta = 0)$. In this example, selection leads to a state where worker-loss ($\omega = 0$) is coupled with complete hybridization ($\eta = 1$). (D) Level of hybridization η favored by selection when worker-loss has evolved ($\omega = 0$) as a function of parthenogenesis c . This shows that worker-loss is always associated to complete hybridization ($\eta = 1$) under monandry ($m = 1$) and if $c \geq (m - 1)/(3m - 1)$ under polyandry ($m > 1$) (Appendix B.2.2, eq. B24, for details).

large additive or dominance effects, we expect more complex evolutionary dynamics, such as genetic polymorphism. These dynamics can nonetheless be straightforwardly investigated with the recurrence equations we derived (eq. A4 in Appendix). However, our model cannot accommodate potential interaction effects among loci (i.e., epistasis). If a quantitative genetics analysis in *Temnothorax curvispinosus* supports that caste determination is influenced by additive effects in this species (Linksvayer 2006), only epistatic effects were found in *Pogonomyrmex rugosus* (Schwander and Keller 2008). It would therefore be relevant in the future to allow for a more complex genetic basis of caste determination, including epistasis (in particular, in the context of the

evolution of unorthodox reproductive systems, see next section). Another important assumption we made is that hybrid larvae do not develop into fertile queens, for instance owing to hybrid incompatibilities (Tribble and Kronauer 2017). If fertile hybrid queens are produced regularly, evolution toward worker-loss like in our model is less likely to happen as hybrids no longer make a reliable source of workers. In ants at least, the idea that hybrid queens are rarely fertile is supported by the contrast between high frequency of interspecific mating on one hand, and weak genetic signals of interspecific gene flow on the other (Umphrey 2006; Feldhaar et al. 2008). Finally, we focused in the main text on the case where colony productivity increases linearly with

workers (i.e., the probability that a sexual survives until reproduction increases linearly with the number of workers). More realistically, the gain in productivity brought by one additional worker is likely to decrease with increasing workforce (Nonacs and Tobin 1992; Reuter and Keller 2001). Such diminishing returns tend to favor cheating because the indirect benefit of developing into a worker gets smaller as colony size increases (e.g., Reuter and Keller 2001; Field and Toyoizumi 2020). In line with this, we find that worker-loss evolves even more easily under diminishing compared to linear returns (Appendix B.2.3 and fig. S3).

AN ADAPTIVE PATH TO UNORTHODOX REPRODUCTIVE SYSTEMS?

Our result that sperm parasitism favors the emergence of worker-loss via the fixation of royal cheats may be relevant to unorthodox reproductive systems found in ants. Of particular interest is social hybridogenesis, whereby females produced through regular intralinear mating or thelytokous parthenogenesis develop into queens, while workers emerge from eggs fertilized by allospecific males (Helms Cahan et al. 2002; Helms Cahan and Vinson 2003; Anderson et al. 2006; Romiguier et al. 2017; Lacy et al. 2019; Kuhn et al. 2020). Such a striking system was first described just two decades ago in *Pogonomyrmex* harvester ants (Helms Cahan et al. 2002), and has since been found in several species spread across four genera (Helms Cahan et al. 2002; Helms Cahan and Vinson 2003; Romiguier et al. 2017; Lacy et al. 2019; Kuhn et al. 2020). If these observations suggest that social hybridogenesis has evolved independently multiple times, the evolutionary origins of this complex system remain poorly understood (Anderson et al. 2008; Schwander et al. 2010; Lavanchy and Schwander 2019). One early suggestion is based on the hypothesis that worker development requires the combination of co-adapted alleles at key loci (i.e., requires epistatic interactions; Helms Cahan and Keller 2003). According to this theory, worker-loss in hybridogenetic lineages would have originated in the random loss of such combinations during episodes of ancestral hybridization. Present hybridization would then have evolved to restore genetic combinations and epistatic interactions in F1-hybrids allowing for worker development.

Here, we have shown mathematically that social hybridogenesis could also result from additive genetic effects on caste development and queen-larvae conflicts within colonies. This theory, previously described verbally in Anderson et al. (2006, 2008), may help explain the multiple convergence toward social hybridogenesis because virtually every sexual eusocial species should experience queen-larvae conflicts over caste investment. Furthermore, because this path to social hybridogenesis does not depend on changes in the sympatric species whose sperm is parasitized, our model is relevant to both cases of asymmetrical (where the sympatric species produces workers through

regular sex, as, e.g., in *Solenopsis xyloni*; Helms Cahan and Vinson 2003) and symmetrical social hybridogenesis (where the sympatric species also produces workers via hybridization, as, e.g., in *Pogonomyrmex* harvester ants; Anderson et al. 2006).

Our model may also be relevant to other unorthodox systems of reproduction such as those found in populations of *Wasmannia auropunctata* (Fournier et al. 2005), *Vollenhovia emeyri* (Ohkawara et al. 2006), or *Paratrechina longicornis* (Pearcy et al. 2011). As with some forms of social hybridogenesis, queens of these systems produce their reproductive daughters via female parthenogenesis and their workers via sex with genetically distant males. In contrast to social hybridogenesis, however, these males belong to a divergent all-male lineage maintained by male clonality. This is further accompanied with a complete absence of arrhenotokous males (i.e., queens never make hemiclinal haploid sons, as shown in *W. auropunctata*; Rey et al. 2013). When queens are able to produce daughters parthenogenetically in our model, evolution can lead to a state where worker-loss is coupled with a complete absence of intralinear mating (i.e., $\eta = 1$, Fig. 5C and D). In this state, arrhenotokous males represent a genetic dead-end, laying the basis for their disappearance. To investigate these systems in more detail, it would be interesting to extend our model to consider the evolution of female parthenogenesis and male clonality.

Our formal approach is especially useful in a context where hybrid vigor in workers has been raised to explain the evolutionary origin of social hybridogenesis and other hybridization-dependent systems (Julian and Cahan 2006; Umphrey 2006; Anderson et al. 2008; Feldhaar et al. 2008; Schwander et al. 2010). According to this argument, selection favored hybridization because hybrid workers are more efficient, more resilient, or better suited to exploit marginal habitats than regular workers. But in spite of much effort, empirical evidence supporting hybrid vigor in workers is still lacking (Ross and Robertson 1990; James et al. 2002; Julian and Cahan 2006; Feldhaar et al. 2008). Further challenging this view, we have shown here that hybrid vigor is not necessary to the evolution of hybridization-dependent reproductive systems. In fact, our results demonstrate that these systems can easily evolve even when hybridization is costly due to pre- and postzygotic barriers (i.e., when $e < 1$, e.g., because hybridization leads to an inefficient workforce due to hybrid incompatibilities in workers; or increased efforts in mate-finding and mating, Maroja et al. 2014; or the production of nonviable or infertile hybrid queens, Umphrey 2006; Feldhaar et al. 2008). In contrast to previous suggestions (Anderson et al. 2008), our model thus indicates that hybridization-dependent reproductive systems can emerge among species that have already substantially diverged, and can be maintained even with further accumulation of hybrid incompatibilities.

More generally, our results suggest that natural selection can lead to an association between hybridization and caste determination. To date, such associations have been reported in only 18 distinct ant species or populations (Helms Cahan et al. 2002; Helms Cahan and Vinson 2003; Fournier et al. 2005; Anderson et al. 2006; Ohkawara et al. 2006; Pearcy et al. 2011; Romiguier et al. 2017; Lacy et al. 2019; Kuhn et al. 2020). But this rarity may be due—at least partly—to the difficulty with describing these systems (which in particular requires sampling and genotyping both queens and workers of the same populations, Helms Cahan et al. 2002). For instance, studies specifically testing for social hybridogenesis discovered five new cases of this reproductive system in *Cataglyphis* (out of 11 species tested, Kuhn et al. 2020) and three in *Messor* (out of 9, Romiguier et al. 2017). These considerations, together with our results, support the notion that currently known cases likely represent only a small fraction of extant eusocial systems relying on hybridization (Helms Cahan et al. 2002; Lavanchy and Schwander 2019).

FACTORS PROMOTING THE EVOLUTION OF INTRASPECIFIC WORKER-LOSS

In addition to showing that hybrid vigor is not necessary for the emergence of intraspecific worker-loss, our model highlights several factors that can facilitate such evolution. The first of these is polyandry, which favors sperm parasitism and worker-loss by minimizing the risks associated with hybridization. Interestingly, even though polyandry is generally rare in social insects (Strassmann 2001; Hughes et al. 2008), meaningful exceptions are found in *Pogonomyrmex* (Rheindt et al. 2004) and *Messor* (Norman et al. 2016) harvester ants, two taxa where social hybridogenesis has evolved multiple times (Anderson et al. 2006; Romiguier et al. 2017). Although the number of males a queen mates with is fixed in our model, it is conceivable that this number also responds to hybridization, leading polyandry and hybridization to coevolve. Indeed as low levels of polyandry represent a risk for out-breeding queens, we can expect selection to favor queen behaviors that increase their number of mates. This would in turn allow for greater levels of hybridization, which would increase selection on polyandry and so on. We therefore expect that the coevolution between polyandry, hybridization, and caste determination further promotes the emergence of worker loss. For species that are fixed for strict (or close to) monandry, our model shows that worker-loss can evolve when queens have the ability to reproduce via thelytokous parthenogenesis as it allows interspecifically mated queens to nevertheless produce daughter queens. This supports the notion that thelytoky has been important for the convergent evolution of social hybridogenesis in the (mostly) monandrous *Cataglyphis* ants (Kuhn et al. 2020).

Although not considered in our study for simplicity, another factor that can minimize the risks associated with hybridization

in monandrous species is polygyny, whereby related queens form multi-queen nests. Such social organization allows both intra- and interspecifically mated queens to be part of the same colony, which can then produce both queens and workers. Polygyny should therefore further facilitate hybridization. Although this may have played a role in the evolution of social hybridogenesis in the polygynous *Solenopsis* species with this reproductive system (Helms Cahan and Vinson 2003; Lacy et al. 2019), we do not expect polygyny to be critical for the evolution of worker-loss as such loss has been described in both monogynic and polygynic species of the same genus (e.g., *Messor barbarus* and cf. *structor*; Romiguier et al. 2017). Beyond these considerations, any trait (e.g., polyandry, polygyny, or reproduction by workers) that influences kinship structure within colonies and thus modulates intracolony conflicts has the potential to play a role in the evolution of worker-loss. Studying the evolution of such traits and its feedback on hybridization and caste determination therefore represents an interesting avenue for future research.

More important for the evolution of worker-loss in our model is that queens hybridize often enough. This readily happens when the propensity of queens to mate with allo- versus conspecific males evolves (Fig. 3). In this case, sperm parasitism, worker-loss, and social hybridogenesis emerge even in species that initially do not hybridize. Such evolution of hybridization is especially likely to occur where queens are able to recognize differences among males and choose their mates accordingly. There is, however, currently little, if any, evidence for such direct mate or sperm choice in eusocial insects (Strassmann 2001; Schwander et al. 2006; Umphrey 2006; Feldhaar et al. 2008). Alternatively, queens may be able to modulate the degree of hybridization via more indirect mechanisms, such as mating flight synchronization (Kaspari et al. 2001). Under completely random mating, hybridization can reach sufficient levels for worker-loss to evolve in our model as long as allo-specific males are sufficiently abundant (Fig. 2), for instance, because phenology is shared with an ecologically dominant species (Klein et al. 2017). In intermediate situations where allo-specific males are available but scarce, the evolution of caste determination under random mating leads to a situation where queens produce both hybrid and nonhybrid workers (Fig. 2A and B). Such a scenario may be relevant to species of ants where hybrid workers has been reported but where worker-loss has not evolved (e.g., in some North American *Solenopsis* or European *Temnothorax*; Feldhaar et al. 2008).

Whether it occurs randomly or not, hybridization requires pre-zygotic barriers to be sufficiently low. Various mechanisms, such as secondary contacts or high dispersal ability, are known to lower these barriers (de Aguiar et al. 2009). In particular, it has been proposed that the typically low phenotypic variation among males of different ant species facilitates hybridization in this taxa (Feldhaar et al. 2008). With these considerations in mind, it is

noteworthy that all known cases of social hybridogenesis have been found in ants that live in dry climates (Helms Cahan et al. 2002; Helms Cahan and Vinson 2003; Romiguier et al. 2017; Lacy et al. 2019; Kuhn et al. 2020), where the synchronicity of mating flights between species is highest due to shared dependence on punctual climatic events (Hölldobler and Wilson 1990; Feldhaar et al. 2008).

At a broader level, our results suggest that worker-loss can readily evolve when a source of workers that is impervious to royal cheats can be exploited by queens. Besides sperm parasitism, other forms of parasitism can provide such a source of workers and have been associated with worker-loss (Nonacs and Tobin 1992). In inquiline ants such as *Teleutomyrmex schneideri*, for instance, queens do not themselves produce workers but rather infiltrate the colony of a host and trick host workers into caring for their progeny (Hölldobler and Wilson 1990; Buschinger 2009). Like in our model, such social parasitism could be the endpoint of an arms race between queens and larvae of the same lineage, whereby increasingly caste-biasing cheats reduce colony workforce leading queens to increasingly rely on host workers.

CONCLUSIONS

Intracolony conflicts are inevitably part of the social lives of nonclonal organisms. Here we have shown that such conflicts readily lead to an association between interspecific sperm parasitism and intraspecific worker-loss via the fixation of royal cheats. This association is especially relevant to the evolution of reproductive systems that like social hybridogenesis rely on hybridization. Beyond these unorthodox systems and sperm parasitism, the fixation of royal cheats and loss of intraspecific workers may be connected to other forms of antagonistic interspecific relationships such as social parasitism. More broadly, our model illustrates how the unique conflicts that are inherent to eusocial life can lead to evolutionary arms races, with implications for elaborate reproductive systems and novel ecological interactions between species.

ACKNOWLEDGMENTS

We thank Nicolas Galtier for useful discussions, Miya Qiaowei Pan, Laurent Keller, and Tanja Schwander for comments on an earlier version of our manuscript, the Swiss National Science Foundation (PCEFP3181243 to CM) and the french national research agency (ANR t-ERc RoyalMess) for funding.

AUTHOR CONTRIBUTIONS

AW, JR, and CM conceived the study. AW performed the analysis and wrote the first draft of the manuscript under the guidance of JR and CM. All authors contributed to the final version.

DATA ARCHIVING

A Mathematica notebook that reproduces our results and a R file implementing our simulations are available here: <https://zenodo.org/record/5167179>.

LITERATURE CITED

- Abrams, P. A., Y. Harada, and H. Matsuda. 1993. On the relationship between quantitative genetic and ESS models. *Evolution* 47:982–985.
- Alpedrinha, J., A. Gardner, and S. A. West. 2014. Haplodiploidy and the evolution of eusociality: worker revolution. *Am. Nat.* 184:303–317.
- Anderson, K. E., J. Gadau, B. M. Mott, R. A. Johnson, A. Altamirano, C. Strehl, et al. 2006. Distribution and evolution of genetic caste determination in *Pogonomyrmex* seed-harvester ants. *Ecology* 87:2171–2184.
- Anderson, K. E., T. A. Linksvayer, and C. R. Smith. 2008. The causes and consequences of genetic caste determination in ants (Hymenoptera: Formicidae). *Myrmecol. News* 11:119–132.
- Avila, P., and L. Fromhage. 2015. No synergy needed: ecological constraints favor the evolution of eusociality. *Am. Nat.* 186:31–40.
- J Boomsma, J. 2009. Lifetime monogamy and the evolution of eusociality. *Philos. Trans. R. Soc. B Biol. Sci.* 364:3191–3207.
- Bourke, A. F. G., and G. L. Chan. 1999. Queen-worker conflict over sexual production and colony maintenance in perennial social insects. *Am. Nat.* 154:417–426.
- Brännström, A., J. Johansson, and N. Von Festenberg. 2013. The hitchhiker's guide to adaptive dynamics. *Games* 4:304–328.
- V Brian, M. 1956. Studies of caste differentiation in *Myrmica Rubra* L. 4. Controlled larval nutrition. *Insect. Soc.* 3:369–394.
- . 1973. Temperature choice and its relevance to brood survival and caste determination in the ant *myrmica rubra* L. *Physiol. Zool.* 46:245–252.
- . 1974. Caste differentiation in *Myrmica rubra*: the role of hormones. *J. Insect Physiol.* 20:1351–1365.
- Buschinger, A. 2009. Social parasitism among ants: a review (Hymenoptera: Formicidae). *Myrmecol. News* 12:219–235.
- Caswell, H. 2000. *Matrix population models*. Sinauer Associates Inc, Sunderland, MA.
- Charlesworth, B. 1990. Optimization models, quantitative genetics, and mutation. *Evolution* 44:520–538.
- Crespi, B. J., and D. Yanega. 1995. The definition of eusociality. *Behav. Ecol.* 6:109–115.
- Darwin, C. 1859. *On the origin of species*. J. Murray, Lond., U.K.
- de Aguiar, M., M. Baranger, E. M. Baptestini, and L. Kaufman. 2009. Global patterns of speciation and diversity. *Nature* 460:384–387.
- Dercole, F., and S. Rinaldi. 2008. *Analysis of evolutionary processes: The adaptive dynamics approach and its applications*. Princeton Univ. Press, Princeton, NJ.
- Dobata, S. 2012. Arms race between selfishness and policing: two-trait quantitative genetic model for caste fate conflict in eusocial hymenoptera. *Evolution* 66:3754–3764.
- Douwes, P., and B. Stille. 1991. Hybridization and variation in the *Leptothorax tuberum* group (Hymenoptera: Formicidae). *Z. Zool. Syst. Evol.* 29:165–175.
- Feldhaar, H., S. Foitzik, and J. Heinze. 2008. Lifelong commitment to the wrong partner: hybridization in ants. *Philos. Trans. R. Soc. B Biol. Sci.* 363:2891–2899.
- Field, J., and H. Toyozumi. 2020. The evolution of eusociality: no risk-return tradeoff but the ecology matters. *Ecol. Lett.* 23:518–526.
- Fournier, D., A. Estoup, J. Orivel, J. Foucaud, H. Jourdan, J. Le Breton, et al. 2005. Clonal reproduction by males and females in the little fire ant. *Nature* 435:1230–1234.

- Frank, S. A. 1998. Foundations of social evolution. Princeton Univ. Press, Princeton, NJ.
- Frohschammer, S., and J. Heinze. 2009. A heritable component in sex ratio and caste determination in a *Cardiocondyla* ant. *Front. Zool.* 6:1–6.
- Geritz, S. A. H., and M. Gyllenberg. 2005. Seven answers from adaptive dynamics. *J. Evol. Biol.* 18:1174–1177.
- Geritz, S. A. H., E. Kisdi, G. Meszéna, and J. A. J. Metz. 1998. Evolutionarily singular strategies and the adaptive growth and branching of the evolutionary tree. *Evol. Ecol.* 12:35–57.
- Geritz, S. A. H., J. A. J. Metz, and C. Rueffler. 2016. Mutual invadability near evolutionarily singular strategies for multivariate traits, with special reference to the strongly convergence stable case. *J. Math. Biol.* 72:1081–1099.
- González-Forero, M. 2015. Stable eusociality via maternal manipulation when resistance is costless. *J. Evol. Biol.* 28:2208–2223.
- D Hamilton, W. 1964. The genetical evolution of social behaviour. I. *J. Theor. Biol.* 7:1–16.
- Hartfelder, K., G. R. Makert, C. C. Judice, G. A. G. Pereira, W. C. Santana, R. Dallacqua, et al. 2006. Physiological and genetic mechanisms underlying caste development, reproduction and division of labor in stingless bees. *Apidologie* 37:144–163.
- Helms Cahan, S., and L. Keller. 2003. Complex origin of a genetic system of caste determination in harvester ants. *Nature* 424:306–309.
- Helms Cahan, S., J. D. Parker, S. W. Rissing, R. A. Johnson, T. S. Polony, M. D. Weiser, et al. 2002. Extreme genetic differences between queens and workers in hybridizing *Pogonomyrmex* harvester ants. *Proc. R. Soc.* 269:1871–1877.
- Helms Cahan, S., and S. B. Vinson. 2003. Reproductive division of labor between hybrid and nonhybrid offspring in a fire ant hybrid zone. *Evolution* 57:1562–1570.
- Hölldobler, B., and E. Wilson. 1990. The ants. Harvard Univ. Press, Cambridge, MA.
- Hughes, W. H., B. P. Oldroyd, M. Beekman, and F. L. W. Ratnieks. 2008. Ancestral monogamy shows kin selection is key to the evolution of eusociality. *Science* 320:1213–1216.
- Hughes, W. O. H., and J. J. Boomsma. 2008. Genetic royal cheats in leaf-cutting ant societies. *Proc. Natl. Acad. Sci.* 105.
- Iwasa, Y., A. Pomiankowski, and S. Nee. 1991. The evolution of costly mate preferences. II. The handicap principle. *Evolution* 45:1431–1442.
- James, S. S., R. M. Pereira, K. M. Vail, and B. H. Ownley. 2002. Survival of imported fire ant (Hymenoptera: Formicidae) species subjected to freezing and near-freezing temperatures. *Environ. Entomol.* 31:127–133.
- Julian, G. E., and S. H. Cahan. 2006. Behavioral differences between *Pogonomyrmex rugosus* and dependent lineages (H1/H2) harvester ants. *Ecology* 87:2207–2214.
- Kaspari, M., J. Pickering, J. T. Longino, and D. Windsor. 2001. The phenology of a neotropical ant assemblage: evidence for continuous and overlapping reproduction. *Behav. Ecol. Sociobiol.* 50:382–390.
- Klein, E. K., L. Lagache-Navarro, and R. J. Petit. 2017. Demographic and spatial determinants of hybridization rate. *J. Ecol.* 105:29–38.
- Kuhn, A., H. Darras, O. Paknia, and S. Aron. 2020. Repeated evolution of queen parthenogenesis and social hybridogenesis in *Cataglyphis* desert ants. *Mol. Ecol.* 29:549–564.
- Lacy, K. D., D. Shoemaker, and K. G. Ross. 2019. Joint evolution of asexuality and queen number in an ant. *Curr. Biol.* 29:1394–1400.
- Lavanchy, G., and T. Schwander. 2019. Hybridogenesis. *Curr. Biol.* 29:R1–R15.
- Lehmann, L., C. Mullon, E. Akçay, and J. V. Cleve. 2016. Invasion fitness, inclusive fitness, and reproductive numbers in heterogeneous populations. *Evolution* 70:1689–1702.
- Lehmann, L., V. Ravigne, and L. Keller. 2008. Population viscosity can promote the evolution of altruistic sterile helpers and eusociality. *Proc. R. Soc. B Biol. Sci.* 275:1887–1895.
- Leimar, O. 2009. Multidimensional convergence stability. *Evol. Ecol. Res.* 11:191–208.
- Libbrecht, R., M. Corona, F. Wende, D. O. Azevedo, J. E. Serrão, and L. Keller. 2013. Interplay between insulin signaling, juvenile hormone, and vitellogenin regulates maternal effects on polyphenism in ants. *Proc. Natl. Acad. Sci.* 110:11050–11055.
- A Linksvayer, T. 2006. Direct, maternal and sibsocial genetic effects on individual and colony traits in an ant. *Evolution* 60:2552–2561.
- Maroja, L. S., Z. M. Mckenzie, E. Hart, J. Jing, E. L. Larson, and D. P. Richardson. 2014. Barriers to gene exchange in hybridizing field crickets: the role of male courtship effort and cuticular hydrocarbons. *BMC Evol. Biol.* 14:1–10.
- Moritz, R. F. A., H. M. G. Lattorff, P. Neumann, F. B. Kraus, S. E. Radloff, and H. R. Hepburn. 2005. Rare royal families in honeybees. *Apis mellifera*. *Naturwissenschaften* 92:488–491.
- Mullon, C., L. Keller, and L. Lehmann. 2018. Social polymorphism is favoured by the co-evolution of dispersal with social behaviour. *Nat. Ecol. Evol.* 2:132–140.
- Mullon, C., and L. Lehmann. 2019. An evolutionary quantitative genetics model for phenotypic (co)variances under limited dispersal, with an application to socially synergistic traits. *Evolution* 4:166–34.
- Nonacs, P., and J. E. Tobin. 1992. Selfish larvae: Development and the evolution of parasitic behavior in the Hymenoptera. *Evolution* 46:1605–1620.
- Norman, V., H. Darras, C. Tranter, S. Aron, and W. O. H. Hughes. 2016. Cryptic lineages hybridize for worker production in the harvester ant *Messor barbarus*. *Biol. Lett.* 12:1–5.
- Ohkawara, K., M. Nakayama, A. Satoh, A. Trindl, and J. Heinze. 2006. Clonal reproduction and genetic caste differences in a queen-polymorphic ant, *Vollenhovia emeryi*. *Biol. Lett.* 5:359–363.
- Parker, G. A., and J. Maynard Smith. 1990. Optimality theory in evolutionary biology. *Nature* 348:27–33.
- Pearcy, M., M. A. D. Goodisman, and L. Keller. 2011. Sib mating without inbreeding in the longhorn crazy ant. *Proc. R. Soc.* 278:2677–2681.
- Penick, C. A., and J. Liebig. 2012. Regulation of queen development through worker aggression in a predatory ant. *Behav. Ecol.* pp. 992–998.
- Penick, C. A., S. S. Prager, and J. Liebig. 2012. Juvenile hormone induces queen development in late-stage larvae of the ant *Harpegnathos saltator*. *J. Insect Physiol.* 58:1643–1649.
- Phillips, P., and S. J. Arnold. 1989. Visualizing multivariate selection. *Evolution* 43:1209–1222.
- C Queller, D. 1994. Extended parental care and the origin of eusociality. *Proc. R. Soc. B Biol. Sci.* 256:105–111.
- Quiñones, A. E., and I. Pen. 2017. A unified model of Hymenopteran preadaptations. *Nat. Commun.* 8:1–13.
- Rabeling, C., and D. J. C. Kronauer. 2013. Thelytokous parthenogenesis in eusocial hymenoptera. *Annu. Rev. Entomol.* 58:273–292.
- Reuter, M., and L. Keller. 2001. Sex ratio conflict and worker production in eusocial Hymenoptera. *Am. Nat.* 158:166–177.
- Rey, O., B. Facon, J. Foucaud, A. Loiseau, and A. Estoup. 2013. Androgenesis is a maternal trait in the invasive ant *Wasmannia auropunctata*. *Proc. R. Soc. B Biol. Sci.* 280:1–7.
- Rheindt, F. E., J. Gadau, C.-P. Strehl, and B. Hölldobler. 2004. Extremely high mating frequency in the Florida harvester ant (*Pogonomyrmex badius*). *Behav. Ecol. Sociobiol.* 56:472–481.
- Ross, K. G., and J. L. Robertson. 1990. Developmental stability, heterozygosity, and fitness in two introduced fire ants (*Solenopsis invicta* and *S. richteri*) and their hybrid. *Heredity* 64:93–103.

- Romiguier, J., A. Fournier, S. H. Yek, and L. Keller. 2017. Convergent evolution of social hybridogenesis in *Messor* harvester ants. *Mol. Ecol.* 26:1108–1117.
- Rousset, F. 2004. Genetic structure and selection in subdivided populations. Princeton Univ. Press, Princeton, NJ.
- Rousset, F., and O. Ronce. 2004. Inclusive fitness for traits affecting metapopulation demography. *Theoret. Popul. Biol.* 65:127–141.
- Schwander, T., S. H. Cahan, and L. Keller. 2006. Genetic caste determination in *Pogonomyrmex* harvester ants imposes costs during colony founding. *J. Evol. Biol.* 19:402–409.
- Schwander, T., J.-y. Humbert, C. S. Brent, S. H. Cahan, L. Chapuis, E. Renai, et al. 2008. Maternal effect on female caste determination in a social insect. *Curr. Biol.* 18:265–269.
- Schwander, T., and L. Keller. 2008. Genetic compatibility affects queen and worker caste determination. *Science* 322:552.
- Schwander, T., N. Lo, M. Beekman, B. P. Oldroyd, and L. Keller. 2010. Nature versus nurture in social insect caste differentiation. *Trends Ecol. Evol.* 25:275–282.
- Seger, J. 1981. Kinship and covariance. *J. Theor. Biol.* 91:191–213.
- . 1983. Partial bivoltinism may cause alternating sex-ratio biases that favour eusociality. *Nature* 301:59–62.
- Smith, C. R., K. E. Anderson, C. V. Tillberg, J. Gadau, and A. V. Suarez. 2008. Caste determination in a polymorphic social insect: nutritional, social, and genetic factors. *Am. Nat.* 172:497–507.
- Strassmann, J. 2001. The rarity of multiple mating by females in the social Hymenoptera. *Insect. Soc.* 48:1–13.
- Taylor, P. D., and S. A. Frank. 1996. How to make a kin selection model. *J. Theor. Biol.* 180:27–37.
- Tribble, W., and D. J. C. Kronauer. 2017. Caste development and evolution in ants: it's all about size. *J. Exp. Biol.* 53:53–62.
- Trivers, L. R., and H. Hare. 1976. Haplodiploidy and the evolution of the social insects. *Science* 191:249–263.
- J Umphrey, G. 2006. Sperm parasitism in ants: selection for interspecific mating and hybridization. *Ecology* 87:2148–2159.
- Wenseleers, T., A. G. Hart, and F. L. W. Ratnieks. 2004. When resistance is useless: policing and the evolution of reproductive acquiescence in insect societies. *Am. Nat.* 164:E154–E167.
- Winter, U., and A. Buschinger. 1986. Genetically mediated queen polymorphism and caste determination in the slave-making ant, *Harpagoxenus sublaevis* (Hymenoptera: Formicidae). *Entomol. Gen.* 11:125–137.
- Wolf, J. I., P. Punttila, and P. Seppä. 2018. Life-history trait variation in a queen-size dimorphic ant. *Ecol. Entomol.* 43(6): 763–773.
- Wolfram Research, Inc. 2020. Mathematica.

Associate Editor: C. Moreau

Supporting Information

Additional supporting information may be found online in the Supporting Information section at the end of the article.

Table S1: Colonial investment in males, queens and workers.

Figure S1: Properties of the internal singular strategy under monoandry and low polyandry.

Figure S2: Polymorphism under monandry is due to positive correlational selection. A.

Figure S3: Non-linear effects of investment in workers.

Appendix: Mathematical derivations and additional analyses

Methods

Here we describe our methods to investigate the evolutionary dynamics of: (1) the probability ω for a non-hybrid larvae to develop as a worker; and (2) the propensity η for queens to hybridize. These methods are organised as follows. First in section 4.4, we present a population genetics model that describes the change in allele frequencies at a biallelic locus that determines the value of ω in larvae and of η in queens. Second (in section 4.4), we obtain the invasion fitness of a mutant allele coding for deviant trait values in a population otherwise monomorphic for a resident allele. Then, we use this invasion fitness in section 4.4 as a platform to infer the long-term adaptive dynamics of both traits (i.e. their gradual evolution under the input of rare mutations with weak phenotypic effects). Specifically, we derive the joint evolutionary equilibria of ω and η (i.e. singular values), as well as their properties (i.e. convergence stability and evolutionary stability, Dercole & Rinaldi, 2008 for textbook treatment). Finally in section 4.4, we describe our individual-based simulations. A Mathematica notebook reproducing our analyses and figures is provided as a supplement here: <https://zenodo.org/record/4434257>.

Short term evolution: population genetics

Set-up

We consider a single locus with two alleles, a and b , that affect the expression of both ω and η in their carrier. Specifically, the probability for a larva with genotype $v \in \{aa, ab, bb\}$ to develop as a worker is ω_v , while each mate of a queen with genotype $v \in \{aa, ab, bb\}$ is allospecific with a probability η_v . To track the segregation of alleles a and b in the population, we let $p_{aa}^{\circ}(t)$, $p_{bb}^{\circ}(t)$, and $p_{ab}^{\circ}(t)$ respectively denote the proportion of queens with genotype aa , bb and ab before mating at generation t (with $p_{aa}^{\circ}(t) + p_{bb}^{\circ}(t) + p_{ab}^{\circ}(t) = 1$). Similarly, $p_a^{\delta}(t)$ and $p_b^{\delta}(t)$ respectively denote the proportion of conspecific males with haploid genotype a and b before mating at generation t (with $p_a^{\delta}(t) + p_b^{\delta}(t) = 1$).

Recurrence equations for the evolution of genotype frequencies

Our first goal is to develop recurrence equations for the frequencies of each genotype in males and females (i.e. express $p_u^{\delta}(t+1)$ and $p_v^{\circ}(t+1)$ in terms of $p_u^{\delta}(t)$ and $p_v^{\circ}(t)$ for $u \in \{a, b\}$ and

$v \in \{aa, ab, bb\}$). By definition, these frequencies can be written as

$$\begin{aligned} p_u^\sigma(t+1) &= \frac{n_u^\sigma(t+1)}{n_a^\sigma(t+1) + n_b^\sigma(t+1)} \\ p_v^\varphi(t+1) &= \frac{n_v^\varphi(t+1)}{n_{aa}^\varphi(t+1) + n_{ab}^\varphi(t+1) + n_{bb}^\varphi(t+1)}, \end{aligned} \quad (1)$$

where $n_u^\sigma(t+1)$ is the number of males of genotype $u \in \{a, b\}$ at generation $t+1$, and $n_v^\varphi(t+1)$ the number of queens of genotype $v \in \{aa, ab, bb\}$ at generation $t+1$ in the mating pool. Under our assumption that the probability for a sexual to reach the mating pool increases with the workforce of a colony (section 2 in main text), the numbers of males and females of each genotype can be expressed as:

$$\begin{aligned} n_v^\sigma(t+1) &= x_{aa \rightarrow v}^\sigma(t) n_{aa}^\varphi(t) p_{aa}^\varphi(t) + x_{ab \rightarrow v}^\sigma(t) n_{ab}^\varphi(t) p_{ab}^\varphi(t) + x_{bb \rightarrow v}^\sigma(t) n_{bb}^\varphi(t) p_{bb}^\varphi(t) \\ n_v^\varphi(t+1) &= x_{aa \rightarrow v}^\varphi(t) n_{aa}^\varphi(t) p_{aa}^\varphi(t) + x_{ab \rightarrow v}^\varphi(t) n_{ab}^\varphi(t) p_{ab}^\varphi(t) + x_{bb \rightarrow v}^\varphi(t) n_{bb}^\varphi(t) p_{bb}^\varphi(t), \end{aligned} \quad (2a)$$

where $x_{u \rightarrow v}^\sigma(t)$ is the number of males with genotype $v \in \{a, b\}$, and $x_{u \rightarrow v}^\varphi(t)$ the number of queens with genotype $v \in \{aa, ab, bb\}$, produced by a colony founded by a queen of genotype $u \in \{aa, ab, bb\}$ at generation t . Following Reuter & Keller (2001), we assume that these numbers are proportional to the energy invested into the production of sexuals. So instead of numbers, $x_{u \rightarrow v}^\sigma(t)$ can be viewed as the investment into the production of males (of genotype $v \in \{a, b\}$) and $x_{u \rightarrow v}^\varphi(t)$ into the production of queens (of genotype $v \in \{aa, ab, bb\}$) by a colony whose queen has genotype $u \in \{aa, ab, bb\}$. Finally, $n_u^\varphi(t)$ is the effective workforce of a colony whose queen has genotype $u \in \{aa, ab, bb\}$ at generation t . This effective workforce is given by the sum of all types of workers present in a colony, including hybrids (with the latter weighted by their efficiency e), i.e.

$$n_u^\varphi(t) = (x_{u \rightarrow aa}^\varphi(t) + x_{u \rightarrow ab}^\varphi(t) + x_{u \rightarrow bb}^\varphi(t) + e x_{u \rightarrow hyb}^\varphi(t))^\alpha \quad (2b)$$

where $x_{u \rightarrow v}^\varphi(t)$ is the investment into the production of workers of genotype $v \in \{aa, ab, bb, hyb\}$ (with hyb denoting hybrid genotype) made by a colony whose queen has genotype $u \in \{aa, ab, bb\}$ at generation t . The parameter $\alpha > 0$ determines the effect of the workforce on the probability for a sexual to reach the mating pool. When $\alpha = 1$, investment in workers affects the survival of queens and males linearly (i.e. one extra unit of workforce always increases survival by the same amount). By contrast when $\alpha < 1$, investment in workers show diminishing returns. Conversely when $\alpha > 1$, investment in workers show increasing returns. For most of our analyses, we assume linear effects of the workforce ($\alpha = 1$). We relax this assumption in section 4.4.

We specify the investments into males, $x_{u \rightarrow v}^\sigma(t)$, queens, $x_{u \rightarrow v}^\varphi(t)$, and workers, $x_{u \rightarrow v}^\varphi(t)$, in terms of model parameters in Table S1. For the sake of completeness, we do so for a model that encompasses all the effects explored sequentially in the main text, i.e. we allow for both traits ω and η to coevolve; for a finite number m of mates for each queen; and for a fraction c of a queen's brood to be produced via parthenogenesis. To read Table S1, note that the different

investments made by a colony with a queen of type $u \in \{aa, ab, bb\}$ (i.e. $x_{u \rightarrow v}^{\sigma}(t)$, $x_{u \rightarrow v}^{\rho}(t)$, and $x_{u \rightarrow v}^{\chi}(t)$) depend on the types of males she has mated with. To capture this, we let $M_{u,v}$ be the random number of males of genotype $v \in \{a, b, h\}$ (where h denotes allospecific type) that a queen of genotype $u \in \{aa, ab, bb\}$ mates with. Assuming that each mate is independent from one another, these random variables follow a multinomial distribution with parameters,

$$\mathbf{M}_u = (M_{u,a}, M_{u,b}, M_{u,h}) \sim \text{Multinomial} \left(m, (1 - \eta_u)p_a^{\sigma}(t), (1 - \eta_u)p_b^{\sigma}(t), \eta_u \right), \quad (3)$$

where m is the total number of mates; $(1 - \eta_u)p_v^{\sigma}(t)$ is the probability that in one mating event a queen of type u mates with a conspecific male of type $v \in \{a, b\}$ (which requires that this queen does not hybridize, with probability $(1 - \eta_u)$, and encounters a male of type v , with probability given by its proportion, $p_v^{\sigma}(t)$); and η_u is the probability that in one mating event a queen of type u mates with an allospecific male.

To get to the recurrence equations tracking the proportion of males and queens of each genotype, we first substitute the entries of Table S1 into eq. (2) (with $\alpha = 1$). Doing so we obtain polynomials for the numbers $n_v^{\sigma}(t + 1)$ (for $v \in \{a, b\}$) and $n_v^{\rho}(t + 1)$ (for $v \in \{aa, ab, bb\}$) in terms of the random variables $M_{u,a}$, $M_{u,b}$, and $M_{u,h}$ (with $u \in \{aa, ab, bb\}$). We marginalise (i.e. take the expectation of) these polynomials over the joint probability mass function of $M_{u,a}$, $M_{u,b}$, and $M_{u,h}$ for each $u \in \{aa, ab, bb\}$, which is given by eq. (3). Finally, the so-obtained numbers of different types of individuals (eq. 2) are substituted into eq. (1). From this operation and using the fact that $p_a^{\sigma}(t) = 1 - p_b^{\sigma}(t)$ and $p_{aa}^{\rho}(t) = 1 - p_{bb}^{\rho}(t) - p_{ab}^{\rho}(t)$, we obtain a recurrence equation,

$$\begin{pmatrix} p_b^{\sigma}(t + 1) \\ p_{ab}^{\rho}(t + 1) \\ p_{bb}^{\rho}(t + 1) \end{pmatrix} = \mathbf{F} \begin{pmatrix} p_b^{\sigma}(t) \\ p_{ab}^{\rho}(t) \\ p_{bb}^{\rho}(t) \end{pmatrix}, \quad (4)$$

that is characterised by a mapping $\mathbf{F} : [0, 1]^3 \rightarrow [0, 1]^3$. This recurrence is too complicated to be presented here for the general case but can straightforwardly be iterated numerically to track allelic frequency changes for given parameter values (see Mathematica notebook for e.g.).

Long-term evolution: adaptive dynamics

To gain more analytical insights, we use the recurrence eq. (4) to study the long term adaptive dynamics of both traits under the assumption that traits evolve via mutations that are rare and with weak additive phenotypic effects.

Invasion fitness of rare additive allele

An adaptive dynamics model is typically based on the invasion fitness of a mutant allele in a population that is otherwise fixed for a resident allele (i.e. the asymptotic growth rate of a mutant allele). To obtain this invasion fitness, we first introduce some notation. We denote the

Investment		Queen		
caste	type	aa	ab	bb
males	a	$x_{aa \rightarrow a}^{\sigma}(t) = (1-f)$	$x_{ab \rightarrow a}^{\sigma}(t) = \frac{1}{2}(1-f)$	$x_{bb \rightarrow a}^{\sigma}(t) = 0$
	b	$x_{aa \rightarrow b}^{\sigma}(t) = 0$	$x_{ab \rightarrow b}^{\sigma}(t) = \frac{1}{2}(1-f)$	$x_{bb \rightarrow b}^{\sigma}(t) = (1-f)$
queens	aa	$x_{aa \rightarrow aa}^{\sigma}(t) = f\left(c + (1-c)\frac{M_{aa,a}}{m}\right)(1 - \omega_{aa})$	$x_{ab \rightarrow aa}^{\sigma}(t) = f(1-c)\frac{1}{2}\frac{M_{ab,a}}{m}(1 - \omega_{aa})$	$x_{bb \rightarrow aa}^{\sigma}(t) = 0$
	ab	$x_{aa \rightarrow ab}^{\sigma}(t) = f(1-c)\frac{M_{aa,b}}{m}(1 - \omega_{ab})$	$x_{ab \rightarrow ab}^{\sigma}(t) = f\left(c + (1-c)\frac{1}{2}\frac{M_{ab,a} + M_{ab,b}}{m}\right)(1 - \omega_{ab})$	$x_{bb \rightarrow ab}^{\sigma}(t) = f(1-c)\frac{M_{bb,a}}{m}(1 - \omega_{ab})$
	bb	$x_{aa \rightarrow bb}^{\sigma}(t) = 0$	$x_{ab \rightarrow bb}^{\sigma}(t) = f(1-c)\frac{1}{2}\frac{M_{ab,b}}{m}(1 - \omega_{bb})$	$x_{bb \rightarrow bb}^{\sigma}(t) = f\left(c + (1-c)\frac{M_{bb,b}}{m}\right)(1 - \omega_{bb})$
sexs	aa	$x_{aa \rightarrow aa}^{\chi}(t) = f\left(c + (1-c)\frac{M_{aa,a}}{m}\right)\omega_{aa}$	$x_{ab \rightarrow aa}^{\chi}(t) = f(1-c)\frac{1}{2}\frac{M_{ab,a}\omega_{aa}}{m}$	$x_{bb \rightarrow aa}^{\chi}(t) = 0$
	ab	$x_{aa \rightarrow ab}^{\chi}(t) = f(1-c)\frac{M_{aa,b}}{m}\omega_{ab}$	$x_{ab \rightarrow ab}^{\chi}(t) = f\left(c + (1-c)\frac{1}{2}\frac{M_{ab,a} + M_{ab,b}}{m}\right)\omega_{ab}$	$x_{bb \rightarrow ab}^{\chi}(t) = f(1-c)\frac{M_{bb,a}\omega_{ab}}{m}$
	bb	$x_{aa \rightarrow bb}^{\chi}(t) = 0$	$x_{ab \rightarrow bb}^{\chi}(t) = f(1-c)\frac{1}{2}\frac{M_{ab,b}\omega_{bb}}{m}$	$x_{bb \rightarrow bb}^{\chi}(t) = f\left(c + (1-c)\frac{M_{bb,b}}{m}\right)\omega_{bb}$
	hyb	$x_{aa \rightarrow hyb}^{\chi}(t) = f(1-c)\frac{M_{aa,h}}{m}$	$x_{ab \rightarrow hyb}^{\chi}(t) = f(1-c)\frac{M_{ab,h}}{m}$	$x_{bb \rightarrow hyb}^{\chi}(t) = f(1-c)\frac{M_{bb,h}}{m}$

Table S1: Colonial investment in males, queens and workers. Each entry in the table gives the investment into one type of individuals (given caste/genotype combination; rows), in a colony led by a queen with a given genotype (columns). Each expression depends only on model parameters and genotypic values for each trait. Genotypic values for hybridization probability in queens of genotype u (η_u) do not appear explicitly but determine the distribution of the random variables $M_{u,a}$, $M_{u,b}$ and $M_{u,h}$ (eq. 3). To see how we constructed this table, consider for e.g. the investment in queens of genotype ab in a colony led by a queen of genotype ab (fourth row, second column). First, queens can arise only from the fraction f of the brood that is diploid. Next, as the laying queen is of genotype ab , the fraction c of diploid eggs that are produced through parthenogenesis will also be of genotype ab . The fraction $(1-c)$ of diploid eggs that are fertilised through regular sex is ab with a probability that depends on the queen's mates: $(M_{ab,a} + M_{ab,b})/(2m)$ (assuming random chromosomal segregation and fertilisation, e.g. because the amount of sperm provided by each male is the same and well-mixed within a queen's spermathecae). Finally, diploid ab eggs develop into queens with probability $1 - \omega_{ab}$. The other entries of the table are derived similarly.

resident allele by a vector $\mathbf{z} = (\omega, \eta)$ where ω is probability that a larva homozygote for the resident allele develops into a worker, and η is the probability that a mate of queen homozygote for the resident allele is allo-specific. Similarly, the mutant allele is described by a vector $\boldsymbol{\zeta} = (\omega + \delta_\omega, \eta + \delta_\eta)$ whose first entry gives the probability that a larva homozygote for the mutant allele develops into a worker, and whose second entry is the probability that a mate of a queen homozygote for the mutant allele is allo-specific (δ_ω and δ_η thus denote the mutant effect on trait values). Assuming additive genetic effects on phenotypes, a heterozygote then expresses phenotype $(\omega + \delta_\omega/2, \eta + \delta_\eta/2)$.

To use the recurrence equations developed in the previous section, we arbitrarily set allele a as the resident and b as the mutant. The allele specific trait values (appearing in table S1 and eq. 3) are then replaced by:

$$\begin{aligned} \omega_{aa} &= \omega & \eta_{aa} &= \eta \\ \omega_{ab} &= \omega + \frac{1}{2}\delta_\omega & \eta_{ab} &= \eta + \frac{1}{2}\delta_\eta \\ \omega_{bb} &= \omega + \delta_\omega & \eta_{bb} &= \eta + \delta_\eta. \end{aligned} \tag{5}$$

Next, we use the fact that the mutant is rare so that its frequency in the population is of the order of a small parameter denoted $0 < \epsilon \ll 1$. As a rare allele can only be found in heterozygous form in a large panmictic population, the initial dynamics of a mutant allele b can be described through linear approximations of $p_b^\sigma(t+1)$ and $p_{ab}^\sigma(t+1)$ at a near-zero frequency of b (e.g. Brännström et al., 2013). In other words, eq. (4) can be linearised to

$$\begin{pmatrix} p_b^\sigma(t+1) \\ p_{ab}^\sigma(t+1) \end{pmatrix} = \mathbf{A}(\boldsymbol{\zeta}, \mathbf{z}) \begin{pmatrix} p_b^\sigma(t) \\ p_{ab}^\sigma(t) \end{pmatrix} + \mathcal{O}(\epsilon^2), \tag{6}$$

where $\mathbf{A}(\boldsymbol{\zeta}, \mathbf{z})$ is a 2×2 matrix that depends on mutant and resident phenotypes, $\boldsymbol{\zeta}$ and \mathbf{z} , and ϵ is a small parameter of the order of the frequency of the mutant b in males and queens.

The invasion fitness of the mutant phenotype, which we write as $W(\boldsymbol{\zeta}, \mathbf{z})$, is then given by the leading eigenvalue of $\mathbf{A}(\boldsymbol{\zeta}, \mathbf{z})$ (e.g. Caswell, 2000), i.e.

$$W(\boldsymbol{\zeta}, \mathbf{z}) = \lambda_{\max}(\mathbf{A}(\boldsymbol{\zeta}, \mathbf{z})), \tag{7}$$

where $\lambda_{\max}(\mathbf{M})$ gives the leading eigenvalue of a matrix \mathbf{M} . In a large population, $W(\boldsymbol{\zeta}, \mathbf{z})$ tells the fate of the mutant allele. If $W(\boldsymbol{\zeta}, \mathbf{z}) \leq 1$, then the mutant allele is purged by selection and vanishes with probability one. Otherwise if $W(\boldsymbol{\zeta}, \mathbf{z}) > 1$, the mutant has a non zero probability of invading the population (e.g. Brännström et al., 2013).

Directional selection

When mutations are rare with weak phenotypic effects, the population first evolves under directional selection whereby an advantageous mutation fixes before a new mutation arises so that the population “jumps” from one monomorphic state to another (Dercole & Rinaldi, 2008). To study these dynamics, we use the selection gradient, $\mathbf{s}(\mathbf{z})$, which is a vector pointing in the direction favoured by selection at every point $\mathbf{z} \in [0, 1] \times [0, 1]$ of the phenotypic space (i.e., the space of all possible phenotypic combinations with ω and η both between 0 and 1 as they are both probabilities) . This vector is given by the marginal effect of each trait on invasion fitness, i.e.

$$\mathbf{s}(\mathbf{z}) = \begin{pmatrix} s_\omega(\mathbf{z}) \\ s_\eta(\mathbf{z}) \end{pmatrix} = \begin{pmatrix} \left. \frac{\partial W(\boldsymbol{\zeta}, \mathbf{z})}{\partial \delta_\omega} \right|_{\boldsymbol{\zeta}=\mathbf{z}} \\ \left. \frac{\partial W(\boldsymbol{\zeta}, \mathbf{z})}{\partial \delta_\eta} \right|_{\boldsymbol{\zeta}=\mathbf{z}} \end{pmatrix}, \quad (8)$$

where $s_\omega(\mathbf{z})$ and $s_\eta(\mathbf{z})$ give the direction of selection on ω and η respectively.

Singular strategies. A singular strategy, $\mathbf{z}^* = (\omega^*, \eta^*)$, is such that all selection gradients are equal to zero,

$$\mathbf{s}(\mathbf{z}^*) = \mathbf{0}. \quad (9)$$

A singular strategy therefore represents a potential equilibrium in the context of adaptive dynamics (Brännström et al., 2013).

Jacobian matrix and convergence stability. Whether the population evolves towards or away from a singular strategy \mathbf{z}^* depends on the Jacobian matrix,

$$\mathbf{J}(\mathbf{z}^*) = \begin{pmatrix} \left. \frac{\partial s_\omega(\mathbf{z})}{\partial \omega} \right|_{\mathbf{z}=\mathbf{z}^*} & \left. \frac{\partial s_\omega(\mathbf{z})}{\partial \eta} \right|_{\mathbf{z}=\mathbf{z}^*} \\ \left. \frac{\partial s_\eta(\mathbf{z})}{\partial \omega} \right|_{\mathbf{z}=\mathbf{z}^*} & \left. \frac{\partial s_\eta(\mathbf{z})}{\partial \eta} \right|_{\mathbf{z}=\mathbf{z}^*} \end{pmatrix}. \quad (10)$$

Specifically, one necessary condition for a singular strategy to be an evolutionary attractor is that the greatest real part of the eigenvalues of $\mathbf{J}(\mathbf{z}^*)$ is negative (Leimar, 2009). Such a singular strategy \mathbf{z}^* is said to be convergence stable. Otherwise, the population will be repelled away from \mathbf{z}^* . Even if \mathbf{z}^* is convergence stable, it is possible for the population to evolve away from \mathbf{z}^* when both evolving traits are genetically correlated (Leimar, 2009). A sufficient condition for a singular strategy to be an attractor is that the symmetric part of the Jacobian matrix, $(\mathbf{J}(\mathbf{z}^*) + \mathbf{J}(\mathbf{z}^*)^T)/2$, is negative-definite, in which case \mathbf{z}^* is said to be *strongly* convergence stable (Leimar, 2009). When this is true, the population evolves towards \mathbf{z}^* , whatever the genetic correlations between both traits (i.e. independently from the statistical distribution of mutational effects on both traits).

Stabilising/disruptive selection.

Once the population is at an equilibrium for directional selection (i.e. a convergence stable phenotype), it either remains monomorphic under stabilising selection (when the equilibrium is evolutionary stable or uninvadable, Parker & Maynard Smith, 1990) or becomes polymorphic due to disruptive selection (when the equilibrium is not evolutionary stable or invadable, Geritz et al., 1998). When two traits are coevolving, this depends on the Hessian matrix (Phillips & Arnold, 1989; Leimar, 2009; Geritz et al., 2016),

$$\mathbf{H}(\mathbf{z}^*) = \begin{pmatrix} h_{\omega\omega}(\mathbf{z}^*) & h_{\omega\eta}(\mathbf{z}^*) \\ h_{\omega\eta}(\mathbf{z}^*) & h_{\eta\eta}(\mathbf{z}^*) \end{pmatrix} = \begin{pmatrix} \left. \frac{\partial^2 W(\boldsymbol{\zeta}, \mathbf{z})}{\partial \delta_\omega^2} \right|_{\boldsymbol{\zeta}=\mathbf{z}=\mathbf{z}^*} & \left. \frac{\partial^2 W(\boldsymbol{\zeta}, \mathbf{z})}{\partial \delta_\omega \partial \delta_\eta} \right|_{\boldsymbol{\zeta}=\mathbf{z}=\mathbf{z}^*} \\ \left. \frac{\partial^2 W(\boldsymbol{\zeta}, \mathbf{z})}{\partial \delta_\omega \partial \delta_\eta} \right|_{\boldsymbol{\zeta}=\mathbf{z}=\mathbf{z}^*} & \left. \frac{\partial^2 W(\boldsymbol{\zeta}, \mathbf{z})}{\partial \delta_\eta^2} \right|_{\boldsymbol{\zeta}=\mathbf{z}=\mathbf{z}^*} \end{pmatrix}. \quad (11)$$

An equilibrium \mathbf{z}^* is uninvadable if $\mathbf{H}(\mathbf{z}^*)$ is negative-definite. Otherwise, selection may be disruptive and the population may experience evolutionary branching, whereby it splits among two diverging morphs (Geritz et al., 1998; Leimar, 2009; Geritz et al., 2016).

Individual-based simulations

To complement our mathematical analysis, we also performed individual based simulations (an R script implementing these is provided as a supplement here: <https://zenodo.org/record/4434257>). These simulations track a population of $N_q = 10000$ diploid queens (with $f = 0.5$, see figure legends for other parameters). Each queen is characterized by its genotype: a pair of haplotypes, each of which is given by the values of ω and η they code for (so four genotypic values in total). Simulations are initialized by setting both haplotypes of all N_q queens to the same arbitrary values (i.e. we start with a monomorphic population). Each generation of a simulation consists of the following steps:

1. **Mating.** First, queens mate. To model this process, we first compute the propensity η_i of each queen $i \in \{1, 2, \dots, N_q\}$ to hybridize as the mean of the two relevant alleles it is carrying. Then, each queen i is mated with a number m_i of conspecific haploid males. This number m_i is drawn from a binomial distribution with m trials and success probability $(1 - \eta_i)$ (in line with eq. 3). At the first generation, all males carry the same genetic values for ω and η as queens (i.e. the initial trait values). In subsequent generations, males are sampled (with replacement) as single haplotypes from the $2i$ haplotypes present in the laying queens of the previous generation. Following eq. (2a), the probability to sample a given haplotype is weighted by the investment in workers within its colony of origin (as the investment in workers increases the probability for males to reach the mating pool).
2. **Colony development.** Each queen i settles to form a colony. We characterise each colony in two steps. First, a list is constructed that contains the $2m_i$ non-hybrid diploid female genotypes produced within each colony (i.e. the combinations of the alleles of a queen and

of its conspecific mates). If thelytokous parthenogenesis is included ($c > 0$), the genotype of the queen itself is added to this list. Second, the investment in workers within each colony is calculated following equations in table S1 and eq. (2b). These calculations use the genetic value expressed by each of the $2m_i + 1$ non-hybrid genotype within the female progeny (characterised in the first step), as well as the proportion of the brood produced sexually and asexually (the parameter c), the proportion of conspecific and allospecific males the queen has mated with (i.e. m_i/m and $1 - m_i/m$), and the efficiency of hybrid workers (the parameter e).

3. **Next-generation queens.** To generate the next generation of queens, N_q new diploid female genotypes are sampled (with replacement) from all non-hybrid genotypes produced within each colony. Following table S1, the probability to sample a given genotype is weighted by its own genetic value of $(1 - \omega)$ and by the investment in workers within its colony of origin (as the investment in workers increases the probability for queens to reach the mating pool). Finally, each genotypic value independently mutates with probability 10^{-2} . Mutation effects are drawn independently from a normal distribution with mean 0 and standard deviation 10^{-2} . Mutated genetic values are capped between 0 and 1 to ensure that traits remain within their domain of definition.

Analyses

Here, we present the derivations of our results summarised in the main text. These derivations are organised in the same order as they appear in the main text. As a supplement, we also provide a Mathematica (Wolfram Research, 2020) notebook that allows to follow our analyses.

Baseline model

We first explore the baseline case where females mate with a large (effectively infinite) number of mates and there is no parthenogenesis (i.e. when $m \rightarrow \infty$ and $c = 0$).

Independent evolution of genetic caste determination

As presented in the main text, we initially assume that hybridization η is fixed and only caste determination ω evolves. Using eq. (8) with $m \rightarrow \infty$ and $c = 0$, we find that the selection gradient on genetic caste determination is,

$$s_\omega(\mathbf{z}) = \frac{1}{6} \left(\frac{1 - \eta}{\eta e + (1 - \eta)\omega} - \frac{2}{1 - \omega} \right). \quad (1)$$

Accordingly, there is a unique singular strategy ω^* for caste determination when hybridization η is fixed (i.e. ω^* such that $s_\omega((\omega^*, \eta)) = 0$),

$$\omega^* = \frac{1}{3} - e \frac{2\eta}{3(1 - \eta)}, \quad (2)$$

which is eq. 1 of the main text.

It is straightforward to show that with hybridization fixed, the singular strategy (eq. 2) is convergence stable (plugging eq. 2 into the Jacobian, that is eq. 10, for a single trait with $m \rightarrow \infty$ and $c = 0$),

$$\left. \frac{\partial s_\omega(\mathbf{z})}{\partial \omega} \right|_{\omega=\omega^*} = -\frac{9(1 - \eta)^2}{4(1 + \eta(e - 1))^2} < 0 \quad (3)$$

as well as uninvadable (plugging eq. 2 into the Hessian, that is eq. 11, for a single trait with $m \rightarrow \infty$ and $c = 0$),

$$\left. \frac{\partial^2 W(\boldsymbol{\zeta}, \mathbf{z})}{\partial \delta_\omega^2} \right|_{\omega=\omega^*} = -\frac{3(1 - \eta)^2}{4(1 + \eta(e - 1))^2} < 0. \quad (4)$$

Therefore, when hybridization is fixed, our analyses show that genetic caste determination will gradually evolve to the singular value eq. (2) and remain monomorphic for this value (which is what we observe when we simulate this scenario, fig. 2A).

Coevolution of genetic caste determination and hybridization

An unstable singularity. When both caste determination ω and hybridization η evolve, their trajectories under directional selection are given by the selection gradient vector,

$$\mathbf{s}(\mathbf{z}) = \begin{pmatrix} s_\omega(\mathbf{z}) \\ s_\eta(\mathbf{z}) \end{pmatrix} = \begin{pmatrix} \frac{1}{6} \left(\frac{1-\eta}{\eta e + (1-\eta)\omega} - \frac{2}{1-\omega} \right) \\ \frac{1}{1-\eta} \left(\frac{e}{3[\eta e + (1-\eta)\omega]} - \frac{1}{2} \right) \end{pmatrix} \quad (5)$$

(from eq. 8 with $m \rightarrow \infty$ and $c = 0$). Solving the above for $\mathbf{z}^* = (\omega^*, \eta^*)$ such that $\mathbf{s}(\mathbf{z}^*) = (0, 0)$ yields a single singular strategy in two dimensional trait space,

$$\mathbf{z}^* = \begin{pmatrix} \omega^* \\ \eta^* \end{pmatrix} = \begin{pmatrix} e + \frac{e-1}{3} \\ 2 + \frac{1}{e-1} \end{pmatrix}, \quad (6)$$

which is plotted in fig. 3A against e . However, when we look at the Jacobian matrix of the system eq. (5) at this singular value (i.e. substitute eqs. 5 and 6 into eq. 10),

$$\mathbf{J}(\mathbf{z}^*) = \begin{pmatrix} -\frac{9}{16(e-1)^2} & -\frac{3}{8e} \\ -\frac{3}{4e} & -\frac{(e-1)^2}{4e^2} \end{pmatrix}, \quad (7)$$

we see that this matrix has a negative determinant,

$$\det(\mathbf{J}(\mathbf{z}^*)) = -\frac{9}{64e^2} < 0 \quad (8)$$

so its eigenvalues cannot both be negative (since the product of the eigenvalues of a matrix is equal to its determinant). Hence the singular value \mathbf{z}^* eq. (6) is not convergence stable, but rather an evolutionary repeller.

Our result that evolutionary trajectories will be repelled away from the singular value eq. (6) tells us that adaptive dynamics will eventually get to the boundary of the trait space. This trait space consists of the square $[0, 1] \times [0, 1]$ (as both traits must be between zero and one). Two edges of this square (when $\omega = 1$ or $\eta = 1$) cannot be accessed by evolutionary dynamics as either of these trait values lead to zero fitness (as a population monomorphic for $\omega = 1$ or $\eta = 1$ produces no queen in our baseline model). We can therefore focus on dynamics along the edges $\eta = 0$ or $\omega = 0$ of the trait space, which respectively correspond to the case of hybridization avoidance and worker-loss.

Convergence to hybridization avoidance. Evolutionary dynamics will settle somewhere on the edge where hybridization is absent in the population ($\eta = 0$) only if: (1) selection on hybridization maintains it at zero (i.e. $s_\eta(\mathbf{z}) \leq 0$ when $\eta = 0$); and (2) selection on caste determination settles for an equilibrium ω^* (i.e. $s_\omega(\mathbf{z}) = 0$ for some ω^* when $\eta = 0$). From eq. (5), these two conditions are true when $e \leq 1/2$ and the equilibrium for caste determination is simply $\omega^* = 1/3$ (in line with eq. 2). As established in eq. (3), this equilibrium is convergence stable and evolutionary stable when η is fixed.

Convergence to worker-loss. Similarly, for adaptive dynamics to converge somewhere on the edge where workers are no longer produced from regular sex ($\omega = 0$), these two conditions are necessary: (1) selection on caste determination maintains $\omega = 0$ (i.e. $s_\omega(\mathbf{z}) \leq 0$ when $\omega = 0$); and (2) selection on hybridization favours an equilibrium η^* (i.e. $s_\eta(\mathbf{z}) = 0$ for some η^* when $\omega = 0$). Substituting eq. (5) into these conditions, they reduce to $e \geq 1/4$ and $\eta^* = 2/3$. In addition, we see from eq. (5) that when $\omega = 0$,

$$\left. \frac{\partial s_\eta(\mathbf{z})}{\partial \eta} \right|_{\eta=2/3} = -\frac{9}{4} < 0, \quad (9)$$

and we further find that

$$\left. \frac{\partial^2 W(\boldsymbol{\zeta}, \mathbf{z})}{\partial \delta_\eta^2} \right|_{\eta=2/3} = -\frac{3}{4} < 0. \quad (10)$$

This tells us that the population will converge towards and remain monomorphic for $\eta^* = 2/3$ when $\omega = 0$ is fixed.

Three phase portraits. Put together, the above observations allow us to deduce that depending on the parameter e , there are three possible types of phase portraits for the adaptive dynamics of both traits (fig. 3B-D). When $e \leq 1/4$, the singular value eq. (6) is outside of the trait space (or on its boundary when $e = 1/4$) and the point $(\omega = 1/3; \eta = 0)$ is an evolutionary stable attractor, meaning that the population will converge towards hybridization avoidance (fig. 3B). When $e \geq 1/2$, the singular value eq. (6) is also outside of the trait space (or on its boundary when $e = 1/2$) and the point $(\omega = 0; \eta = 2/3)$ is an evolutionary stable attractor, meaning that the population will converge towards worker-loss (fig. 3D). Finally when $1/4 < e < 1/2$, the singular value eq. (6) is a repeller that lies within the trait space (i.e. $0 < \omega^* < 1$ and $0 < \eta^* < 1$) and both points $(\omega = 1/3; \eta = 0)$ and $(\omega = 0; \eta = 2/3)$ are evolutionary stable attractors. In this case evolutionary dynamics will depend on initial values (fig. 3C).

Decomposition of directional selection in terms of inclusive fitness effects

The kin selection approach. In this section, we use the so-called "kin selection" or "inclusive fitness" approach to obtain the selection gradient eq. (5) (Taylor & Frank, 1996). This approach, which is based on invasion analyses of alleles in class-structured populations, gives the

same quantitative result about directional selection than other common methods in theoretical evolutionary biology such as adaptive dynamics, population or quantitative genetics (assuming genetic variance for traits is small, e.g. Taylor & Frank, 1996; Rousset, 2004; Lehmann et al., 2016). But one particular advantage of a kin selection approach is that it immediately decomposes directional selection on mutant alleles into the sum of: (1) their direct fitness effects on the reproductive success of the individuals that express them; and (2) of their indirect fitness effects on other related individuals that can also transmit them. This decomposition allows to delineate the various forces at play in the evolution of social behaviours (Hamilton, 1964). Here, we use it to better understand the evolution towards worker-loss (and obtain fig. 3E-F).

We follow Taylor & Frank (1996)'s general method. Consider a population with mean trait values ω and η . In this population, consider a focal colony that is home to a mutant allele that codes for deviant trait values η_\bullet in queens and ω_\bullet in larvae that carry this allele. Let ω_0 denote the mean trait value expressed by all larvae within this focal colony. Using this notation, the expected number of successful (i.e. that mate) males that are produced by the focal colony and that carry the mutant allele is given by,

$$w_\delta = \frac{(1-f)[f((1-\eta_\bullet)\omega_0 + \eta_\bullet e)]}{(1-f)[f((1-\eta)\omega + \eta e)]}, \quad (11)$$

where the numerator and denominator are the total number of males produced by the focal and a random colony, respectively. For the focal colony (the numerator), $(1-f)$ is the probability that an egg is haploid (i.e. male) while the term in square brackets is the colony's investment in workers (which in our model is also the probability that a sexual reaches maturity). The denominator follows the same logic for an average colony in the population.

Similarly, the expected number of successful queens that are produced by the focal colony that carry the mutant allele is,

$$w_\varphi = \frac{f(1-\eta_\bullet)(1-\omega_\bullet)[f((1-\eta_\bullet)\omega_0 + \eta_\bullet e)]}{f(1-\eta)(1-\omega)[f((1-\eta)\omega + \eta e)]}, \quad (12)$$

where $f(1-\eta_\bullet)(1-\omega_\bullet)$ is the number of queens produced in the focal colony and the term in square brackets is the probability that a queen survives till mating (i.e. the colony's investment in workers).

Fitness effects within a mutant colony. With the above notation, the selection gradient vector can then be computed as,

$$\mathbf{s}(\mathbf{z}) = \begin{pmatrix} s_\omega(\mathbf{z}) \\ s_\eta(\mathbf{z}) \end{pmatrix} \propto \begin{pmatrix} v_\varphi \frac{\partial w_\varphi}{\partial \omega_\bullet} + v_\delta \frac{\partial w_\delta}{\partial \omega_0} r_{1m} + v_\varphi \frac{\partial w_\delta}{\partial \omega_0} r_{1f} \\ v_\delta \frac{\partial w_\delta}{\partial \eta_\bullet} r_{qm} + v_\varphi \frac{\partial w_\delta}{\partial \eta_\bullet} r_{qf} \end{pmatrix}, \quad (13)$$

where all derivatives are evaluated at $\omega_{\bullet} = \omega_0 = \omega$ and $\eta_{\bullet} = \eta_0 = \eta$; r_{lm} is the relatedness of a female larva to a brother; r_{lf} is the relatedness of a female larva to a sister; r_{qm} is the relatedness of a queen to its sons; r_{qf} is the relatedness of a queen to its daughters; $v_{\text{♂}}$ is the reproductive value of males and $v_{\text{♀}}$ is the reproductive value of queens (all these relatedness coefficients and reproductive values are for a monomorphic population, Taylor & Frank, 1996; Rousset & Ronce, 2004; Lehmann et al., 2016). Plugging eqs. (11) and (12) into eq. (13) with relatedness coefficients and reproductive values corresponding to a haplodiploid system with infinite matings (i.e. $r_{\text{lm}} = 1/2$, $r_{\text{lf}} = 1/4$, $r_{\text{qm}} = 1$, $r_{\text{qf}} = 1/2$, $v_{\text{♂}} = 1/2$, $v_{\text{♀}} = 1$), we obtain expressions equivalent to eq. (5). But in contrast to eq. (5), the selection gradients in eq. (13) are expressed as a sum of fitness effects of a mutant allele via a given category of individual. More specifically, the gradient $s_{\omega}(\mathbf{z})$ in eq. (13) is decomposed as the fitness effects of an allele coding for a mutant value of ω in larvae: on the larvae that express this allele ($v_{\text{♀}} \frac{\partial w_{\text{♀}}}{\partial \omega_{\bullet}}$, yellow line in fig. 3E), on their brothers ($v_{\text{♂}} \frac{\partial w_{\text{♂}}}{\partial \omega_0} r_{\text{lm}}$, blue line in fig. 3E), and on their sisters (i.e. queens, $v_{\text{♀}} \frac{\partial w_{\text{♀}}}{\partial \omega_0} r_{\text{lf}}$, red line in fig. 3E) that can also transmit the allele. Similarly, the gradient $s_{\eta}(\mathbf{z})$ in eq. (13) is composed of the fitness effects of an allele coding for a mutant value of η in queens: via their sons ($v_{\text{♂}} \frac{\partial w_{\text{♂}}}{\partial \eta_{\bullet}} r_{\text{qm}}$, blue line in fig. 3F) and daughters (i.e. queens, $v_{\text{♀}} \frac{\partial w_{\text{♀}}}{\partial \eta_{\bullet}} r_{\text{qf}}$, red line in fig. 3F). To construct panels E and F of fig. 3, we evaluated these five terms outlined above at every step of an evolutionary trajectory from the baseline equilibrium in absence of hybridization ($\omega = 1/3, \eta = 0$) to complete worker-loss ($\omega = 0, \eta = 2/3$). The evolutionary trajectory was obtained by iteration, starting from the baseline equilibrium and taking steps of size 0.001 (in units of trait space) in the direction of the selection gradient (eq. 5).

Correspondence with Reuter and Keller (2001)

Here we connect our results to those of Reuter & Keller (2001), who used a kin selection approach to study the evolution of caste determination when under full queen, full larval, or mixed control (in the absence of hybridization). Our model corresponds to the case of full larval control (eq. 3 of Reuter & Keller, 2001). Our selection gradient $s_{\omega}(\mathbf{z})$, shown in eq. (1) with $\eta = 0$, reduces to eq. 3 of Reuter & Keller (2001) when we assume linear effects of investment in workers on colony productivity. More specifically, if we set their term $\Delta_c = \delta s / (\delta w) \times 1/f$ (their notation in their eq. 3, where Δ_c corresponds to the gain in sexual production brought by one additional worker) to

$$\Delta_c = \frac{1 - fw}{w}, \quad (14)$$

and assume that the population is monogynous and highly polyandrous with balanced sex-ratio (i.e. in their notation, $f = 1/2$; $g_f = 1/4$; $g_m = 1/2$; $v_f = 2$; $v_m = 1$), then we find that eq. 3 of Reuter & Keller (2001) is proportional to our selection gradient $s_{\omega}(\mathbf{z})$ (eq. 1) with $\eta = 0$. In line with this, both yield the convergence stable equilibrium $w^* = 1/3$.

Extensions

We now consider several extensions to our baseline model.

Effect of finite matings

First, we relax our assumption that queens mate with an infinite number of mates (i.e. $m < \infty$).

Selection gradient. Working from eq. (8) with $c = 0$, we find that the selection gradient vector on caste determination ω and hybridization η under finite matings reads as,

$$\begin{aligned} \mathbf{s}(\mathbf{z}) &= \begin{pmatrix} s_\omega(\mathbf{z}) \\ s_\eta(\mathbf{z}) \end{pmatrix} \\ &= \begin{pmatrix} \frac{1}{6} \left(\frac{1-\eta}{\eta e + (1-\eta)\omega} - \frac{2}{1-\omega} + \frac{3e\eta + 2(1-\eta)\omega}{2[\eta e + (1-\eta)\omega][\eta e(m-1) + (1-\eta)\omega m + \eta\omega]} \right) \\ \frac{1}{1-\eta} \left(\frac{e}{3[\eta e + (1-\eta)\omega]} - \frac{1}{2} \right) + \frac{\omega}{6\eta} \left(\frac{1}{\eta e + (1-\eta)\omega} - \frac{m}{\eta e(m-1) + (1-\eta)\omega m + \eta\omega} \right) \end{pmatrix}. \end{aligned} \quad (15)$$

These gradients are complicated but we can extract relevant information by starting our analysis on the two boundaries of the trait space along which evolutionary dynamics may end up ($\omega = 0$ or $\eta = 0$). Using eq. (15), we ask first when is worker-loss ($\omega = 0$) stable? And second when is hybridization avoidance ($\eta = 0$) stable?

Stability of worker-loss. Worker-loss is stable only if: (1) selection maintains ω at zero (i.e. $s_\omega(\mathbf{z}) \leq 0$ when $\omega = 0$); and (2) selection on hybridization settles for an equilibrium η^* (i.e. $s_\eta(\mathbf{z}) = 0$ for some η^* when $\omega = 0$). From eq. (15), these two conditions reduce to

$$e \geq \frac{1}{4} + \frac{9}{8(m-1)} \quad (16)$$

(region above dashed line in fig. 4A) and

$$\eta^* = 2/3. \quad (17)$$

Note that condition (16) becomes impossible as $m \rightarrow 1$. This indicates that worker-loss cannot evolve under monandry in this model. For $m > 1$, it is straightforward to show that when condition (16) is true, the strategy $\eta = 2/3$ is both convergence stable and evolutionary stable when $\omega = 0$ (eqs. 9 and 10 for e.g. of the type of argument used).

Stability of hybridization avoidance. Conversely, hybridization avoidance is stable only if: (1) selection on hybridization maintains η at zero (i.e. $s_\eta(\mathbf{z}) \leq 0$ when $\eta = 0$); and (2) selection

on caste determination in absence of hybridization settles for an equilibrium ω^* (i.e. $s_\omega(\mathbf{z}) = 0$ for some ω^* when $\eta = 0$). From eq. (15), these two conditions reduce to

$$e \leq \frac{1}{2} + \frac{1}{2} \frac{5m - 1}{6m^2 - m - 1} \quad (18)$$

(region below plain line in fig. 4A) and

$$\omega^* = \frac{1}{3} + \frac{2}{3(1 + 3m)}. \quad (19)$$

Again, it is straightforward to show that when condition (18) holds, the strategy given by eq. (19) is both convergence stable and evolutionary stable when $\eta = 0$ (eqs. 3 and 4 for e.g. of argument).

Together, conditions (16) and (18) split the parameter space into 4 areas where both, none, or only one of the conditions are met (fig. 4A). Where condition (18) is met but (16) is not (grey region of fig. 4A), hybridization cannot evolve when rare and worker-loss cannot be maintained. We therefore focus on the three remaining cases where worker loss can emerge. Doing so, we find that there are four possible types of evolutionary dynamics.

Type 1: Evolution towards worker-loss. Where condition (16) is met but (18) is not (dark green region of fig. 4A), selection favours the emergence of hybridization and maintenance of worker-loss. In addition, it can be shown that under these conditions, there exists no singular strategy within the trait space (i.e., there exists no $\mathbf{z}^* = (\omega^*, \eta^*)$ such that $0 < \omega^*, \eta^* < 1$ and $\mathbf{s}(\mathbf{z}^*) = (0, 0)$, e.g. using the function `Reduce[]` in Mathematica, see notebook). This means that the phase portrait of evolutionary dynamics is qualitatively the same as in fig. 3D: worker-loss always evolves.

Type 2: Evolution towards worker-loss or hybridization avoidance depending on initial conditions. Where conditions (16) and (18) are met simultaneously, both worker-loss and hybridization avoidance are stable so either strategy is maintained when common (when $m \geq 5$, light green region of fig. 4A). Under these conditions, we find that there exists a singular strategy within the trait space (top row, columns $m = 5$ and $m = 6$ in fig. S1 for numerical values, see Mathematica notebook for analytical expression). When we compute numerically the leading eigenvalue of the system's Jacobian matrix, we find that it is positive (fig. S1, second row, columns $m = 5$ and $m = 6$, dashed line), revealing that the singularity is an evolutionary repeller. Therefore the phase portrait of evolutionary dynamics is qualitatively the same as in fig. 3C: depending on initial conditions, evolutionary dynamics will lead to worker-loss or hybridization avoidance.

Type 3: Convergence stable and uninvadable intermediate strategy. Where neither condition (16) nor (18) are met, neither worker-loss nor hybridization avoidance are stable (when $m \leq 4$, blue region of fig. 4A). In this case, a singular strategy within the trait space also exists ($0 < \omega^*, \eta^* < 1$; fig. S1, top row, columns $m \in \{1, 2, 3, 4\}$ for numerical values; Mathematica notebook for analytical expression). But now, this intermediate strategy is (strongly) convergence stable as indicated by a negative leading eigenvalue of both the Jacobian matrix and its symmetric part (fig. S1, second row, columns $m \in \{1, 2, 3, 4\}$, dashed and dotted lines). When $m \in \{2, 3, 4\}$, this intermediate strategy is also uninvadable as shown by a negative leading eigenvalue of the Hessian matrix (fig. S1, second row, columns $m \in \{2, 3, 4\}$, full line). Thus, when the number of mates is between two and four ($m \in \{2, 3, 4\}$) and neither conditions (16) and (18) are met, the population converges and remains monomorphic for an intermediate strategy $0 < \omega^*, \eta^* < 1$.

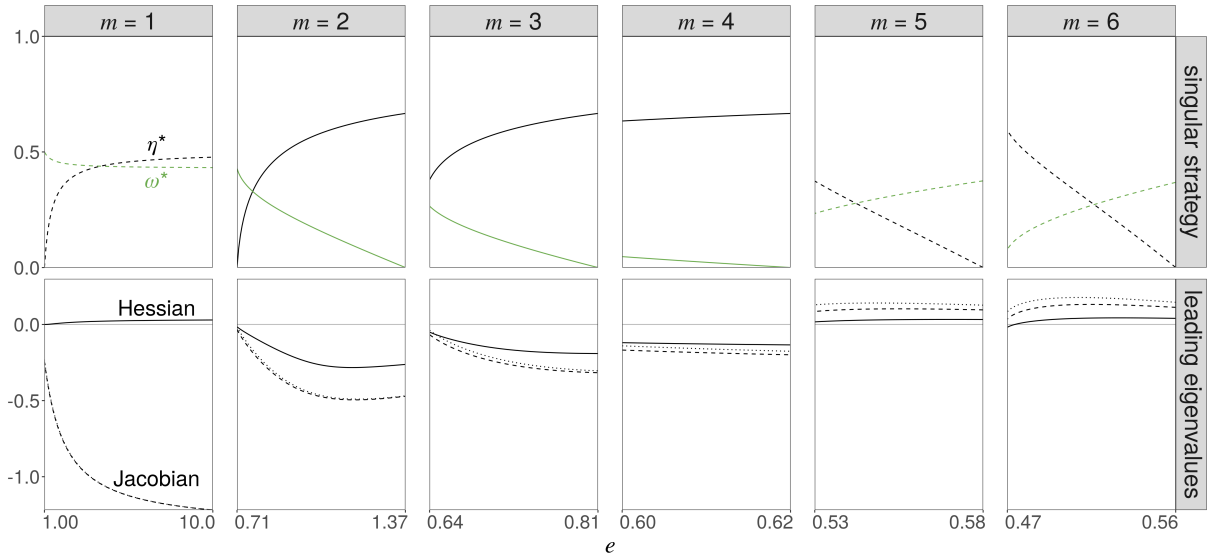


Figure S1: Properties of the internal singular strategy under monoandry and low polyandry. Each column describes the unique internal singular strategy for a specific value of m . **Top row:** value of the singular strategy (ω^* in green, η^* in black) within the range of e for which an internal strategy exists (range given by eqs. 16 and 18; Mathematica notebook for value of singular strategy). **Bottom row:** leading eigenvalues of the Jacobian (dashed line; for convergence stability), symmetric part of the Jacobian (dotted line; for strong convergence stability) and Hessian (full line; for evolutionary stability) matrices at the singular strategy (Mathematica notebook for calculations).

Type 4: Emergence of polymorphism under monandry. When neither condition (16) nor (18) are met and $m = 1$, the convergence stable intermediate strategy is invadable (i.e., the Hessian has a positive leading eigenvalue; fig. S1, second row, column $m = 1$, dashed line). This means that once the population has converged to this intermediate strategy, it experiences frequency-dependent disruptive selection leading to polymorphism (Geritz et al., 1998; Geritz & Gyllenberg, 2005; Geritz et al., 2016). Inspection of the entries of the Hessian matrix reveals

that

$$h_{\omega\eta}(\mathbf{z}^*)^2 - h_{\omega\omega}(\mathbf{z}^*)h_{\eta\eta}(\mathbf{z}^*) > 0 \quad (20)$$

(fig. S2A, black line) and that $h_{\omega\omega}(\mathbf{z}^*) \leq 0$ and $h_{\eta\eta}(\mathbf{z}^*) \leq 0$ (fig. S2A, green and grey lines). This says that disruptive selection in our model is due to correlational selection between caste determination and hybridization (i.e. the selection that associates caste determination and hybridization, Phillips & Arnold, 1989) and only occurs because both traits are coevolving (i.e. if either trait evolves while the other is fixed, the population remains monomorphic, e.g. Mullon et al., 2018). We also find that

$$h_{\omega\eta}(\mathbf{z}^*) > 0 \quad (21)$$

(fig. S2A, blue line), which tells us that correlational selection is positive (i.e. selection favours a positive correlation between caste determination and hybridization within individuals, Phillips & Arnold, 1989). This is confirmed by individual based simulations, in which we observe the emergence of a polymorphism characterised by a positive correlation between ω and η within haplotypes (fig. 4C and fig. S2B-D).

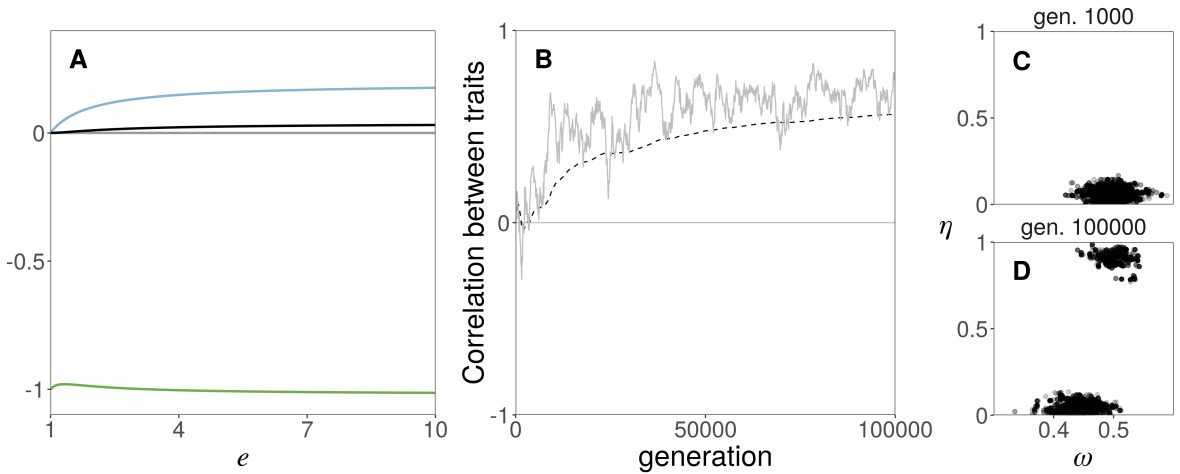


Figure S2: Polymorphism under monandry is due to positive correlational selection. **A.** Characteristics of the Hessian matrix at the internal singular strategy as a function of e for $m = 1$ (first column of fig. S1 for singular value): quadratic selection coefficient on ω ($h_{\omega\omega}(\mathbf{z}^*)$, in green) and on η ($h_{\eta\eta}(\mathbf{z}^*)$, in grey); correlational selection ($h_{\omega\eta}(\mathbf{z}^*)$, in blue) and its relative strength ($h_{\omega\eta}(\mathbf{z}^*)^2 - h_{\omega\omega}(\mathbf{z}^*)h_{\eta\eta}(\mathbf{z}^*)$, in black, Mathematica notebook for calculations). **B.** Correlation between genetic values of each trait within haplotypes in a simulated population (in gray, 4000 haplotypes sampled every 100 generations to compute Pearson's correlation coefficient, same replicate as fig. 4C; cumulative mean in black dashed). **C & D** Distribution of genetic values of all haplotypes after 1000 generations (panel C) and after 100000 generations (panel D, same replicate as panel B and fig. 4C).

Effect of thelytokous parthenogenesis

When we allow for a fraction c of a queens brood to be produce parthenogenetically, the selection gradient (obtained from eq. 8) is too complicated to be displayed or for singular strategies to be found analytically. We therefore go through an invasion analysis similar to above (Appendix 4.4 and 4.4) and again ask: (1) under which conditions and values of ω is hybridization avoidance ($\eta = 0$) stable? and (2) under which conditions and values of η is worker-loss ($\omega = 0$) stable?

Stability of hybridization avoidance. Hybridization avoidance is stable if selection on caste determination settles for an equilibrium ω^* in the absence of hybridization (i.e. $s_\omega(\mathbf{z}) = 0$ for some ω^* when $\eta = 0$), and if selection on hybridization at this equilibrium maintains η at zero (i.e. $s_\eta(\mathbf{z}) \leq 0$ when $\eta = 0$ and $\omega = \omega^*$). These two conditions respectively reduce to,

$$\omega^* = \frac{1+c}{3+c} \left(1 + \frac{2(1-c)^2}{(c+1)[(1-c)^2 + (c+3)m]} \right), \quad (22)$$

and

$$e \leq \frac{3(1+c)}{2(3+c)} + \frac{(1-c)(3-c)}{2(5-c)(c+2m-1)} + \frac{4(3-c)(1-c)^2}{(5-c)(3+c)[(1-c)^2 + (c+3)m]}. \quad (23)$$

Condition eq. (23) corresponds to the area of the graph below the plain line in fig. 5A-B, where hybridization avoidance is stable. Conversely, the area above the plain line in fig. 5A-B (in blue) is where avoidance is not stable and thus where hybridization evolves.

Stability of worker-loss. Similarly, worker-loss is stable if selection on hybridization settles for an equilibrium η^* in the absence of developmental plasticity (i.e. $s_\eta(\mathbf{z}) = 0$ for some $0 < \eta^* < 1$ when $\omega = 0$). We find that this equilibrium reads as

$$\eta^* = \frac{2}{3} \frac{1}{1-c} \left(1 - \frac{c}{1-m} \right) \quad (24)$$

(fig. 5D). The equilibrium eq. (24) is between 0 and 1 ($0 < \eta^* < 1$) and selection at this equilibrium maintains worker-loss (i.e. $s_\omega(\mathbf{z}) \leq 0$ when $\omega = 0$ and $\eta = \eta^*$) when

$$e \geq \frac{1}{4} + \frac{3c}{4} + \frac{3[3-c(12-c)]}{8(c+m-1)} - \frac{9(3-c)(1-c)c}{8(c+m-1)^2} \quad \text{and} \quad c < \frac{m-1}{3m-1}. \quad (25)$$

Note that condition eq. (25) is only possible when $m \geq 2$. It therefore does not appear in fig. 5A (which is for the case $m = 1$) but corresponds to the area above the dotted line in fig. 5B (which has $m = 2$).

Worker-loss coupled with complete hybridization. In principle, it is also possible with parthenogenesis for a population to evolve worker-loss ($\omega = 0$) with complete hybridization ($\eta = 1$) (as parthenogenesis allows the production of queens in the absence of intraspecific

matings). We therefore further need to determine whether worker-loss can also be stable in the case where $\eta = 1$ (rather than for some $0 < \eta^* < 1$). We find that selection under worker-loss ($\omega = 0$) and complete hybridization ($\eta = 1$) maintains both worker-loss and complete hybridization (i.e. $s_\omega(\mathbf{z}) \leq 0$ and $s_\eta(\mathbf{z}) \geq 0$ where $\mathbf{z} = (\omega, \eta) = (0, 1)$) when

$$e \geq \frac{c}{1-c} \quad \text{and} \quad c \geq \frac{m-1}{3m-1}. \quad (26)$$

Condition eq. (26) corresponds to the area above the dashed line in fig. 5A-B. While condition eq. (25) can only be met only under polyandry ($m > 1$), condition eq. (26) can be met for any number of mates m . This means that the evolution of worker-loss under monandry and thelytokous parthenogenesis is always associated with complete hybridization in our model.

Effect of non-linear workforce productivity

Our analyses so far have assumed a linear effect of worker number on colony fitness ($\alpha = 1$ in eq. 2b). Here we investigate how non-linear effects of the number of workers on the pre-mating survival of virgin queens and males influence our results. We restrict our exploration to the case where queens mate with an infinite number of males and do not reproduce via parthenogenesis for simplicity ($m \rightarrow \infty$ and $c = 0$). With α in eq (2b) as a variable, we find from eq. (8) that the selection gradient vector now reads as,

$$\mathbf{s}(\mathbf{z}) = \begin{pmatrix} s_\omega(\mathbf{z}) \\ s_\eta(\mathbf{z}) \end{pmatrix} = \begin{pmatrix} \frac{1}{6} \left(\frac{\alpha(1-\eta)}{\eta e + (1-\eta)\omega} - \frac{2}{1-\omega} \right) \\ \frac{1}{1-\eta} \left(\frac{\alpha e}{3[\eta e + (1-\eta)\omega]} - \frac{1+2\alpha}{6} \right) \end{pmatrix}. \quad (27)$$

Solving for both of these gradients to vanish simultaneously, we find that there exists a unique singular strategy,

$$\begin{cases} \omega^* = e + \frac{e-1}{3} \\ \eta^* = 1 + \frac{3e}{(e-1)(1+2\alpha)} \end{cases} \quad (28)$$

(fig. S3). The Jacobian matrix (eq. 10) of the system eq. (27) at this singular value eq. (28) reads as

$$\mathbf{J}(\mathbf{z}^*) = \begin{pmatrix} -\frac{3(2+\alpha)}{16(e-1)^2\alpha} & -\frac{(1+2\alpha)^2}{24e\alpha} \\ -\frac{(1+2\alpha)^2}{12e\alpha} & -\frac{(e-1)^2(1+2\alpha)^3}{108e^2\alpha} \end{pmatrix}. \quad (29)$$

It is straightforward to show from eq. (29) that the singular strategy eq. (28) is a repellor, just as under linear effects ($\alpha = 1$, eq. 7). This indicates that as illustrated in fig. 3, the coevolution of caste determination and hybridization under non-linear effects also lead to either hybridization avoidance or worker-loss depending on parameters and initial conditions.

We can gain further insights into the influence of non-linear effects by determining when the singular strategy eq. (28) is within the trait space (i.e., when $0 < \omega^*, \eta^* < 1$). We find that this is the case when

$$\frac{1}{4} < e < \frac{1 + 2\alpha}{4 + 2\alpha} \quad (30)$$

(light green region in fig. S3). This means that the threshold value for worker efficiency e above which worker-loss can evolve is $1/4$ (as under linear effects $\alpha = 1$). Condition (30) further shows that the threshold for e above which worker-loss always evolves (i.e. independently from initial conditions, fig. 3D for e.g.) increases with α (dark green region in fig. S3). In other words, the evolution of worker loss is facilitated under diminishing ($\alpha < 1$, fig. S3A) and impaired under increasing returns ($\alpha > 1$, fig. S3C).

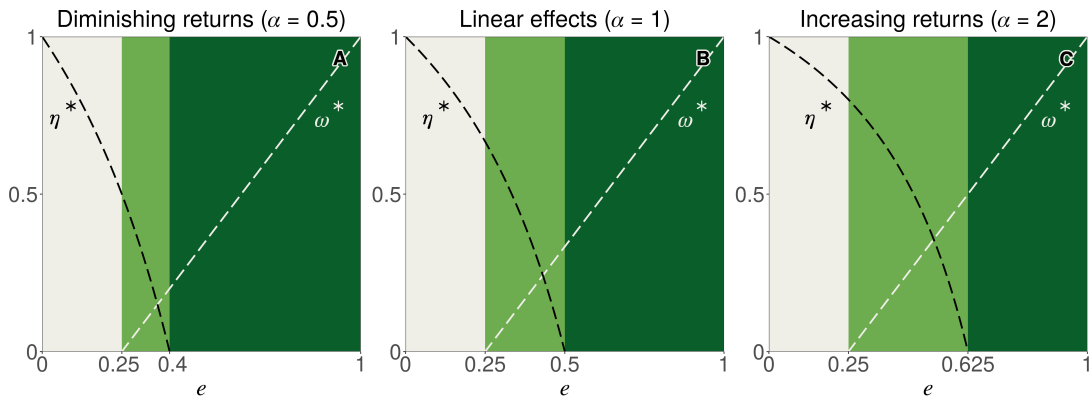


Figure S3: Non-linear effects of investment in workers. Singular values for η (in black) and ω (in white) as a function of hybrid worker efficiency e (given by eq. 28).

Chapter 2

Genomic evidence for the prevalence of social hybridogenesis in ants

Arthur Weyna, Lucille Bourouina, Nicolas Galtier & Jonathan Romiguier



Detection of F1 hybrids from single-genome data reveals frequent hybridization in Hymenoptera and particularly ants

Arthur Weyna¹, Lucille Bourouina¹, Nicolas Galtier^{1,*} & Jonathan Romiguier^{1,*}. Under revision in *Molecular Biology and Evolution*.

¹ Institut des Sciences de l'Evolution (UMR 5554), University of Montpellier, CNRS

*These authors share senior authorship.

Corresponding author: arthur.weyna@umontpellier.fr

Statement of authorship: AW and JR conceived the study. AW and NG developed statistical methods. AW, LB and JR performed preliminary analyses. AW performed the final analysis and wrote the first draft of the manuscript under the guidance of JR and NG. All authors contributed to the final version.

Data accessibility: Supplementary tables containing all results produced in this work (tables S1, S2 and S3), as well as scripts and files necessary to apply our statistical procedure, are available here: <https://zenodo.org/record/5415947>.

Keywords: Hybridization, Coalescent, F1-hybrids detection, Arthropods, Hymenoptera, Ants

Abstract

Hybridization occupies a central role in many fundamental evolutionary processes, such as speciation or adaptation. Yet, despite its pivotal importance in evolution, little is known about the actual prevalence and distribution of hybridization across the tree of life. Here we develop and implement a new statistical method enabling the detection of F1 hybrids from single-individual genome sequencing data. Using simulations and sequencing data from known hybrid systems, we first demonstrate the specificity of the method, and identify its statistical limits. Next, we showcase the method by applying it to available sequencing data from more than 1500 species of Arthropods, including Hymenoptera, Hemiptera, Coleoptera, Diptera and Archnida. Among these taxa, we find Hymenoptera, and especially ants, to display the highest number of candidate F1 hybrids, suggesting higher rates of recent hybridization in these groups. The prevalence of F1 hybrids was heterogeneously distributed across ants, with taxa including many candidates tending to harbor specific ecological and life history traits. This work shows how large-scale genomic comparative studies of recent hybridization can be implemented, uncovering the determinants of hybridization frequency across whole taxa.

Introduction

Hybridization, whereby members of genetically distinct populations mate and produce offspring of mixed ancestry (Abbott et al., 2013; Barton & Hewitt, 1985), has received much attention since the early days of evolutionary biology. From the onset, Darwin and his contemporaries spent a great deal of time studying hybrids and their fitness, which they recognized as a challenge to a discrete definition of species (Roberts, 1919). But the crucial importance of hybridization to biological evolution was fully realized only with the development of genetics in the following century. Formal studies of hybridization genetics led to the formulation of the biological species concept, and to the fundamental insight that speciation is generally driven by the evolution of isolating mechanisms in response to hybridization (Abbott et al., 2013; Dobzhansky, 1940; Mayr, 1942; Smadja & Butlin, 2011). The advent of genetic data also revealed the role of hybridization and introgression as important contributors to genetic variation and adaptation in many existing species (Anderson, 1953; Harrison & Larson, 2014), especially in the contexts of changing environments (Hamilton & Miller, 2016) and biological invasion (Prentis et al., 2008). Additionally, while hybridization was thought by many biologists to be relevant only for a few taxa such as plants (Barton, 2001), the accumulation of molecular data has continuously revealed its presence in many groups, including mammals, birds, fish, fungi, and insects (Taylor & Larson, 2019), with Mallet (2005) estimating that at least 10% of animal species frequently hybridize. These findings have further underlined the importance of hybridization in understanding many micro- and macro-evolutionary patterns across the tree of life (Abbott et al., 2013).

The same findings, however, also corroborated the old intuition that taxa can differ greatly in their susceptibility to hybridize, fueling discussions about the determinants of such heterogeneity (see Mallet, 2005 for a useful review). It was first understood that groups displaying a high number of sympatric species with low divergence, where the contact between compatible species is maximized, should be the most likely to hybridize (Edmands, 2002; Price & Bouvier, 2002). But sympatry and divergence are by themselves incomplete predictors of hybridization frequency, as strong reproductive barriers can arise from discrete evolutionary events (e.g., chromosome rearrangements or cytoplasmic incompatibilities; Bordenstein et al., 2001; Fishman et al., 2013), and can be rapidly selected for (i.e., reinforcement) or against depending on the relative fitness of hybrids (Smadja & Butlin, 2011). To understand heterogeneity in hybridization rates, it is thus important to also consider these ecological and phenotypic features of species that influence hybrid fitness, and more generally that influence the costs or gains in producing hybrids (Mallet, 2005). For instance, hybridization has been found to be more frequent in populations of spadefoot toads inhabiting ephemeral environments where hybrids outperform (Pfennig, 2007), or in rare species of birds where allospecific mates are easier to come by (Randler, 2002). A similar point was made by Mayr (1963), who suggested that polygamous species of birds should be the most likely to hybridize, because males with low parental investment should be more likely to accept interspecific mates. This early hypothesis is particularly significant in that it emphasizes on the idea that among characteristics of species relevant to hybridization, their life-history and mating system are of central importance.

One specific taxon in which relations between hybridization, mating systems and life-history have been extensively discussed is ants (Formicidae). Some ant genera are known to display unusually high rates of hybridization, based on both morphological and molecular data (Feldhaar et al., 2008; Nonacs, 2006; Umphrey, 2006). The first key trait of ants invoked to explain this pattern is haplodiploidy, a trait common to all Hymenoptera. Because males of Hymenoptera are haploids produced without fecundation, it is likely that hybrid sterility does not nullify the fitness of female Hymenoptera, which can still produce males after hybridizing (Feldhaar et al., 2008; Nonacs, 2006). This particularity of haplodiploids would hinder selection against hybridization and limit the formation of strict barriers to inter-specific mating. A second important ancestral trait of ants is eusociality, whereby reproductive females (i.e., queens) produce a large number of sterile helper individuals (i.e., workers) to form colonies. It was hypothesized that selection against hybridization is weaker in eusocial species because the fitness cost of hybrid sterility should be minimal in species producing a large majority of sterile individuals (Nonacs, 2006; Umphrey, 2006). This is especially likely in species in which queens mate multiply, and can combine inter- and intra-specific matings to ensure the production of a fraction of non-hybrid daughters (Cordonnier et al., 2020). Such interplay between hybridization, mating systems and life-history culminates in a handful of ant species that display unique hybridization-dependent reproductive systems, such as social hybridogenesis (Anderson et al., 2006; Fournier et al., 2005; Helms Cahan et al., 2002; Helms Cahan & Vinson, 2003; Kuhn et al., 2020; Lacy et al., 2019; Ohkawara et al., 2006; Pearcy et al., 2011; Romiguier et al., 2017). In these species, the cost of hybrid sterility is fully avoided because strong genetic caste determination constrains the development of hybrids towards the worker caste, while reproductive females can only be produced through intra-specific mating or parthenogenesis. The prevalence of hybridization-dependent systems within ants is virtually unknown (Anderson et al., 2008), but because they maintain large cohorts of F1-hybrid workers, they may help explain observations of high hybridization rates in ants.

While several hypotheses have been proposed to explain variation in hybridization rates across taxa, empirical comparative studies are still lacking, impeding any further understanding of its determinants. This is mainly due to the difficulties in evaluating the prevalence of hybridization at the group level. Methods to detect recent hybridization typically rely either on ambiguous morphological identification (which can lead to important ascertainment bias; Mallet, 2005), or on the use of large population-scale genetic samples including data for potential parental species (Anderson & Thompson, 2002; Payseur & Rieseberg, 2016; Schubert et al., 2017). These methods are sensitive and reliable in inferring hybrid status, but require large investments in time and money to produce results. To allow for comparative studies of hybridization at the level of entire taxa, it is necessary to implement methods that can be applied to many non-model species in parallel. In particular, methods applicable to the large volume of already published phylogenomic data (i.e., with one sequenced genome per species) would be especially desirable and cost-effective. For instance, phylogenomic data is available for more than 900 species of ants (223 represented genera), as the result of an extensive effort of Branstetter et al.

(2017), who set a goal to sequence a large part of the diversity of Formicidae using standardized protocols (Faircloth et al., 2012). The same type of data has also been produced for many other Hymenoptera, and for other groups of Arthropods (including Hemiptera, Coleoptera, Diptera and Arachnida), paving the way for a comparative study of hybridization across these taxa of interest.

In this study, we implement a coalescent-based statistical method that allows for the detection of F1-hybrids using single diploid genomes. We first test this method and assess its efficiency using simulations and real data from identified F1 hybrid and non-hybrid individuals. We then apply the method to phylogenomic data, assessing the prevalence of F1 hybrids among five groups of Arthropods.

Materials and methods

Model

In this section we present the coalescent-based model of divergence which forms the basis of our F1 hybrid detection procedure. A F1 hybrid is the result of a cross between individuals from two different species. The heterozygosity of a such hybrid therefore reflects the divergence between its parental species, and can be modeled as shown in Figure 1. This model describes the expected distribution of the number of differences between two alleles found in a F1 hybrid in terms of two main parameters: the divergence time between the two parental species t_s and the ancestral population size in their common ancestor Ne (figure 1a). Briefly, if no migration occurred between the two parental lineages after their separation, and if t_s is large enough for lineage sorting to be complete, the total coalescence time of the two alleles is the sum of the divergence time t_s and the coalescence time in the ancestral population t_i . It is known from standard coalescence theory that the distribution of t_i is well approximated by an exponential distribution with mean $2Ne$ (Wakeley, 2008). Consider a locus i of sequence length l_i at which the two alleles of an F1 hybrid individual have been sequenced. Assuming an infinite-site mutation model with constant per-site mutation rate μ , the number n_i of observed allelic differences follows a Poisson distribution with mean $2l_i\mu(t_i + t_s)$, that is

$$n_i \sim P(2l_i\mu(t_i + t_s)) \quad \text{with} \quad t_i \sim E\left(\frac{1}{2Ne}\right). \quad (1)$$

where P and E denote the Poisson and exponential distributions, respectively. Equation (1) leads to an expression for the probability to observe a number k of allelic differences between alleles at any given locus i in a F1 hybrid (see Appendix for a complete derivation),

$$Pr(n_i = k) = \frac{(l_i\theta)^k e^{(\gamma/\theta)}}{k!(l_i\theta + 1)^{k+1}} \int_{(l_i\gamma + \frac{\gamma}{\theta})}^{\infty} t^k e^{-t} dt \quad \text{with} \quad \begin{cases} \theta = 4Ne\mu \\ \gamma = 2t_s\mu \end{cases} \quad (2)$$

where θ is the ancestral population mutation rate, and γ is a measure of the heterozygosity acquired during the divergence process. Under the assumptions that μ , t_s and N_e are constant across a set of j independent loci in a given diploid individual, each locus can be considered as a replicate of the same divergence scenario. In this case, the likelihood function of the set of observed numbers of differences between alleles is obtained by multiplying equation (2) across loci, and can be used to jointly estimate of θ and γ . To our knowledge this model was first introduced by Takahata et al. (1995), and later refined by Yang (1997), in the context of phylogenomics and ancestral population size estimation, with equation (2) being the continuous equivalent to equation (8) given in Yang (1997). Figure 1b illustrates the signal that is intended

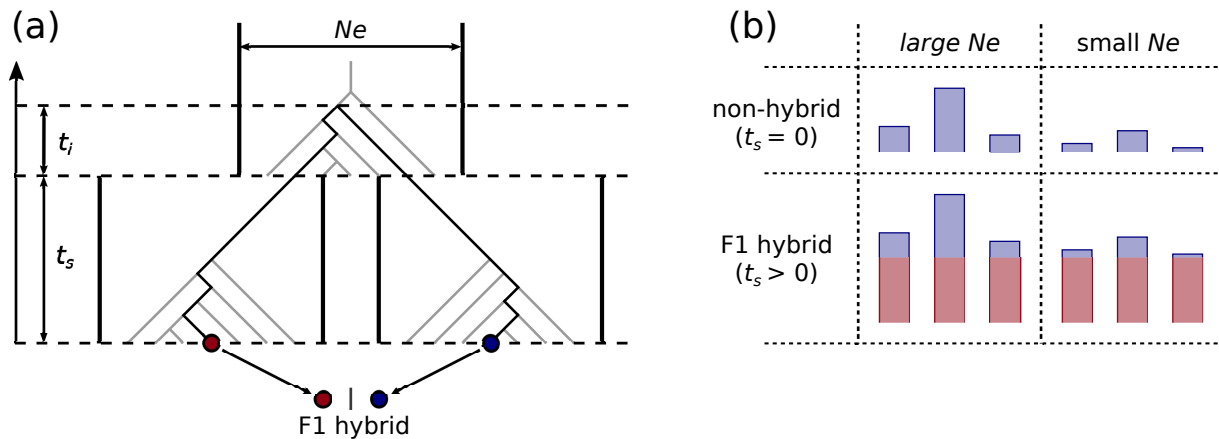


Figure 1: Coalescent-based model of divergence. (a) The population history assumed in the model of divergence described in the main text (eq. (1)). The darkened path represents the coalescence history of the two alleles (red and blue dots) that make up one locus in a diploid F1 hybrid. (b) Expected distribution of coalescence times for different values of N_e and t_s . Blue bars represent the components of coalescence time linked to coalescence in the ancestral population. Red bars represent the uniform increase in coalescence times brought by divergence between parental populations.

to be captured when estimating γ and θ . In a non-hybrid individual (i.e., whose parents belong to the same panmictic population), coalescence times between allele pairs are expected to follow an exponential distribution with mean and variance both determined by N_e (figure 1b; top). In F1 hybrids, coalescence times are further increased by a fixed amount, which corresponds to the number of generations of divergence between the parental populations (1b; bottom, red bars). This uniform increase in coalescence times brought by divergence logically leads to an increased average coalescence time. This effect, however, is not by itself diagnostic of hybridization as it could be produced by an increase in N_e . Instead, what constitutes a unique signature of F1 hybrids is a decrease in the variance of coalescence times relative to the mean (figure 1b, compare bottom to top). The relative variance in coalescence times is expected to be highest in non-hybrids, and to approach zero in F1 hybrids as the divergence between parental populations increases. The γ parameter captures this effect, whereas both γ and θ monitor the mean coalescence time. In other words, a non-zero estimate of γ means that the observed divergence between alleles is more similar across loci than expected under the standard coalescent.

Because the proposed statistical procedure partitions observed heterozygosity between γ and θ , it is expected that estimates of both parameters will be positively correlated with the genetic diversity of samples. For instance, a sample with low heterozygosity can only yield low estimates of γ and θ . For this reason, we mostly relied on the ratio γ/θ , which is not directly related to sample heterozygosity. This ratio is expected to be close to zero in non-hybrids, and non-zero in F1 hybrids. Furthermore, a γ/θ ratio above one implies that the divergence time between parental populations is longer than $2Ne$ generations, which is the expected time for complete lineage sorting. Such a high value is very unlikely to be reached by non-hybrid individuals.

Simulated test loci sets

To start evaluating our ability to detect F1 hybrids amongst diploid individuals, we simulated F1 hybrid, non-hybrid and 1st generation backcross hybrid samples in the following manner. Individual diploid loci were simulated by using *ms v2014.03.04* (Hudson, 2002) to sample pairs of alleles, together with the corresponding two-alleles gene trees, under the demographic scenario described in figure 1a. To span across realistic values of both parameters of interest, values of θ and γ in simulations were set to be $\{10^{-4}, 10^{-3}, 10^{-2}\}$ and $\{0, 10^{-4}, 10^{-3}, 10^{-2}\}$, respectively. Once obtained, gene trees were converted to explicit nucleotide sequences pairs through the application of a HKY mutation model using *seq-gen v1.3* (Rambaut & Grassly, 1997). The length of simulated sequences was set to be normally distributed with mean 1000bp and standard deviation 300bp. At this point, simulated F1 hybrid and non-hybrid individuals were constructed by putting together independent collections of sequences pairs simulated under $\gamma > 0$ and $\gamma = 0$, respectively. First generation backcross individuals were constructed by putting together both types of sequences pairs in random proportions following a binomial distribution with $p = 0.5$, (i.e., as expected from a backcross with random meiosis and no linkage). Ten individuals of each type were constructed for each possible combination of parameter values, and for two possible loci set sizes (200 or 500 loci). Finally, simulated individuals (i.e., loci sets) were sequenced in-silico using *art_illumina v2.5.8* (Huang et al., 2012). We emulated standard PE150 sequencing on HiSeq 2500 with 10X coverage, using a standard normally distributed fragment size with mean 400bp and standard deviation 20bp.

UCE datasets

In all applications to real data, we used ultra-conserved elements (UCEs) and their variable flanking regions as loci sets. UCEs are short (around 100bp on average) independent genomic regions that are conserved without duplication across large phylogenetic groups (Faircloth et al., 2012). These regions are usually sequenced through hybridization capture protocols (Faircloth, 2017; Miles Zhang et al., 2019), but subsets of UCEs that correspond to transcribed genomic regions can also be retrieved from transcriptomic data (Bossert et al., 2019; Miles Zhang et al., 2019). This last fact is convenient in the context of this study, because transcriptome sequencing data is available for known hybrid systems, featuring *a priori* identified F1 hybrids and non-hybrid individuals, and can be used to further test our procedure using real data. We retrieved

transcriptome sequencing data published on *genbank* from two types of well-characterized F1 hybrids: 12 hybrid workers from the harvester ant *Messor barbarus* (Romiguier et al., 2017), and 18 *Equus caballus x asinus* hybrids (9 mules and 9 hinnies; Wang et al., 2019). Data from the same sources for 7 haploid males and 5 non-hybrid queens of *M. barbarus*, as well as for 5 donkeys, were added for comparison. Genbank identifiers and metadata for *Messor* and *Equus* samples are available in supplementary tables S1 and S2, respectively.

Sequencing data obtained through UCE-capture protocols has been published for a large number of non-model species, especially in Hymenoptera (Faircloth et al., 2012; Miles Zhang et al., 2019), thus allowing for a large scale search for F1 hybrids in these groups. We retrieved from *genbank* UCE-capture sequencing data from diploid samples belonging to groups of Arthropods for which specific capture probe sets were available : Formicidae (“*Insect Hymenoptera 2.5K version 2, Ant-Specific*” probe set; Branstetter et al., 2017), non-Formicidae Hymenoptera (“*Insect Hymenoptera 2.5K version 2, Principal*” probe set; Branstetter et al., 2017), Hemiptera (“*Insect Hemiptera 2.7K version 1*” probe set; Branstetter et al., 2017 and Kieran et al., 2018), Coleoptera (“*Insect Coleoptera 1.1K version 1*” probe set; Faircloth, 2017), Diptera (“*Insect Diptera 2.7K version 1*” probe set; Faircloth, 2017), and Arachnida (“*Arachnida 1.1K version 1*” probe set; Faircloth, 2017 and Starrett et al., 2016). To minimize the statistical weight of multiply sampled species, while maximizing statistical power at the group level, we kept only one sample per identified species (choosing samples with highest file size) and all samples lacking a complete identification (identified only to the genus level). Hymenoptera samples reported as males were considered as haploid and discarded. All remaining data files were downloaded from *genbank* using the *fasterq-dump* program from *SRA Toolkit v2.10.9*. Genbank identifiers and metadata for these samples are available in supplementary table S3.

Parameters estimation

To obtain estimates of γ and θ from simulated and real sequencing data, we systematically applied the following procedure. Raw read files were cleaned with *fastp v0.20.0* (Chen et al., 2018) to remove adapters, reads shorter than 40 bp, and reads with less than 70 percent of bases with a phred score below 20. Cleaned reads were then assembled using *megahit v1.1.3* (Li et al., 2015) with k-mer size spanning from 31 to 101 by steps of 10. The *phyluce v1.6* (Faircloth, 2016) tool suite was used to identify and isolate UCE loci from de-novo assemblies, by blasting contigs against UCE probe sets with the *phyluce_assembly_match_contigs_to_probes* function. In this step, assemblies obtained from test samples of *M. barbarus* and *Equus* were blasted against the “*Insect Hymenoptera 2.5K version 2, Ant-Specific*” (Branstetter et al., 2017) and the “*Tetrapods 5K version 1*” (Faircloth et al., 2012) UCE probe sets, respectively. Likewise, assemblies obtained from UCE-capture samples were blasted against the probe set associated to their phylogenetic group. As no probe set exists for simulated loci, these were blasted against custom probe sets constructed from their true sequence (i.e., as output by *seqgen*). Following this step, cleaned sequencing reads were realigned to isolated loci using *bwa v0.7.17* (Li & Durbin, 2009) with default settings, and *angsd v0.921* (Korneliussen et al., 2014) was used to obtain

allelic substitutions counts from read alignment files. Finally, we obtained estimates of θ and γ through bayesian estimations, using the *R* package *rstan v2.21.2* (Stan Development Team, 2019; Stan Development Team, 2020) and uninformative priors spanning all realistic values for both parameters (i.e., uniform priors constrained between 0 and 0.2). The mean of the posterior distribution of each parameter was used as a point estimate, while credibility intervals were constructed from its 2.5% and 97.5% quantiles. *R* scripts and the *stan* file necessary to run statistical estimations on a given set of observed allelic differences counts are available as supplementary documents (<https://zenodo.org/record/5415947>).

Results

Simulations

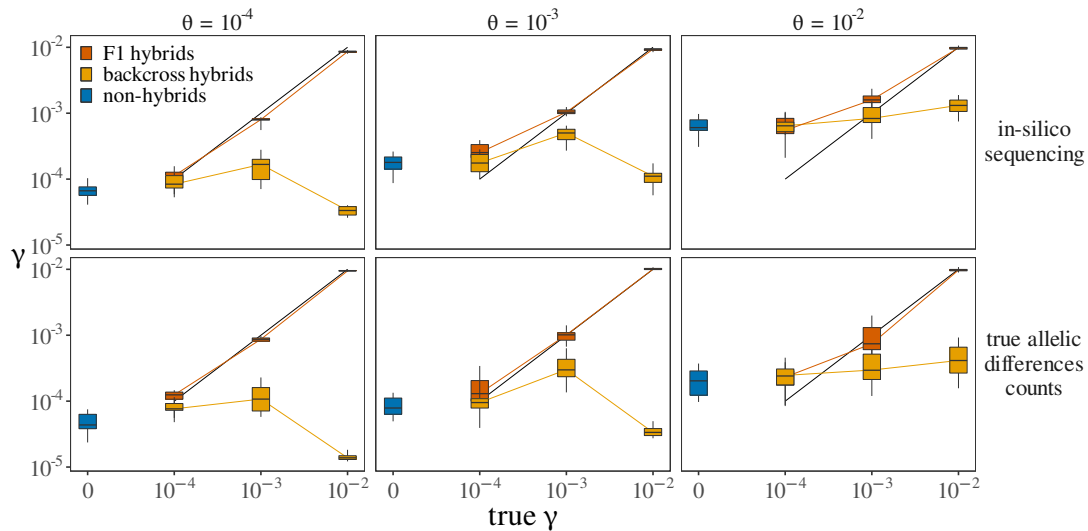


Figure 2: Estimates of divergence in simulated individuals. Each box represents the distribution of estimated γ values across 10 simulated individuals. Every individual consists of a collection of 200 loci simulated under a given combination of true θ (given in headers) and γ (given in x axis) values. In non-hybrid individuals γ is always zero. In backcross hybrids, the true value of γ is that given in the header, but only for a binomial proportion of loci (as described in the main text). The top row represents values obtained when estimating γ on loci sets obtained through the complete simulation procedure (including in-silico sequencing, read assembly and re-alignment, and substitutions counts estimation). The bottom row represents values obtained when estimating γ on sets of true counts data as output by *ms* (i.e., skipping subsequent simulation steps).

Applying our estimation procedure on simulated data, we find that our method can be used to efficiently discriminate F1 hybrids from non-hybrids and first generation backcross hybrids. Accurate divergence estimates can be obtained in simulated F1 hybrids using as little as 200 loci (figure 2), provided that γ is in the same order of magnitude as the ancestral population mutation rate θ or higher (i.e., consistent with the model’s requirement of complete lineage

sorting). Under the same condition, estimates of γ in non-hybrids and backcross hybrids are lower and do not exceed values one order of magnitude below estimated ancestral population size θ (which are themselves accurate; see figure S1). Across all simulations, 61.1% of simulated F1 hybrids yielded both estimates of γ higher than 10^{-3} and estimates of γ/θ higher 1, while no backcross hybrids or non-hybrids did, demonstrating the specificity of the method. Furthermore, we find that increasing the number of sequenced loci from 200 to 500 does not increase our ability to identify F1 hybrids (see figure S2), which suggests that 200 loci is a good minimal requirement in applications to real data.

Simulations also revealed the statistical limits of our approach, which tends to overestimate the divergence parameter γ whenever the true ancestral population mutation rate θ is high (figure 2, top row). This translates into estimates of γ departing from zero in non-hybrids with high overall polymorphism. Interestingly, this overestimation can be shown to arise in part from error in genome assembly, reads alignments, and estimations of allelic differences counts. When estimating parameters using sets of true allelic differences counts as first output by *ms* (figure 2, bottom row), divergence overestimation is less important in hybrids and non-hybrids (figure S2). This suggests that in real data, a positive correlation will be expected between divergence estimates and overall sample quality.

Accurate identification of F1 hybrids in two known hybrid systems

To further quantify our ability to distinguish between non-hybrids and typical F1 hybrid individuals, we applied our estimation procedure to sequencing data from two types of well-characterized F1 hybrids, hybrid workers from the harvester ant *Messor barbarus* (Romiguier et al., 2017), and *Equus caballus x asinus* hybrids (mules and hinnies) (Wang et al., 2019). Sequencing data from the same sources for males and non-hybrid queens of *M. barbarus*, as well as for donkeys, were added to the analysis for comparison. This analysis confirmed that F1 hybrids and non-hybrid individuals can be discriminated without ambiguity (figure 3; parameters estimates are given in table S1 and S2). Estimates of divergence (γ) in F1 hybrids always strongly departed from 0 and showed little variation across samples ($3.39 \times 10^{-3} \pm 2.05 \times 10^{-4}$ sd in *M. barbarus* workers; $1.47 \times 10^{-3} \pm 1.46 \times 10^{-4}$ sd in mules and hinnies). By contrast, estimated values of γ in non-hybrid samples were always much closer to 0 in non-hybrid individuals ($2.34 \times 10^{-5} \pm 3.29 \times 10^{-5}$ sd in *M. barbarus* males and queens; $1.63 \times 10^{-5} \pm 3.31 \times 10^{-6}$ sd in donkeys). The ratio γ/θ reached the critical value of one in *M. barbarus* workers (1.067 ± 0.190 sd) while being two orders of magnitude lower in males and queens (0.012 ± 0.010 sd). This confirms that such a threshold value is reliable for discriminating true F1 hybrids. Ratios obtained in mules and hinnies are lower than 1 however (0.418 ± 0.061 sd), further suggesting that $\gamma/\theta > 1$ is a conservative requirement likely not to be reached by many true F1 hybrid. Interestingly, UCE-capture data for a single worker of *M. barbarus* (figure 3a) led to slightly higher parameter estimates than transcriptomic data, but to a similar γ/θ ratio (1.131). This suggests that UCEs which could be retrieved from transcriptomes of *M. barbarus* are less polymorphic on average, but contain the same information regarding relative divergence and hybrid status.

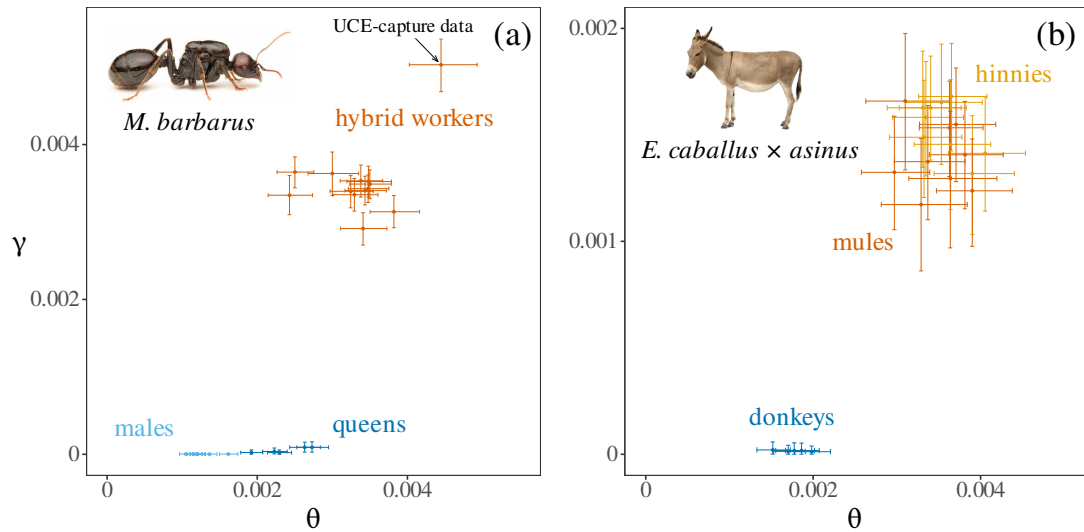


Figure 3: Discrimination of F1 hybrids in transcriptomes of *M. barbarus* and *Equus*. Estimated values for the divergence parameter γ and the ancestral population mutation rate θ are represented for *M. barbarus* (a) and *Equus* (b). Colored points and lines represent point estimates and confidence intervals, respectively. Values obtained using UCE-capture data for a single worker of *M. barbarus* (genbank:SRR5437981) were added for comparison (arrow in panel a).

High prevalence of F1 hybrids in Hymenoptera and Formicidae

The application of our procedure to UCE-capture data, comprised of many samples of heterogeneous quality, led to the observation of the quality bias predicted from simulations. Specifically, we noted that older samples yielded slightly higher γ/θ estimates on average than recent ones, resulting in a significant correlation between the later ratio and specimen collection date ($\rho = -0.275$, p-value $< 2.2 \times 10^{16}$). This bias is most likely due to lower sequence quality and increased data treatment error in old specimen, which leads to an overestimation of γ as mentioned in the previous section. To take this effect into account, we excluded samples collected before 1980 and specimen with unknown collection date from subsequent analyses. This does not eliminate the mentioned correlation which remains significant ($\rho = -0.163$, p-value $= 3.43 \times 10^{-11}$), but ensures that no old, highly degraded sample is wrongly interpreted as a hybrid. This choice of a threshold date does not affect our subsequent statistical results (see table S4). We also discarded samples for which less than 200 UCE loci could be retrieved to ensure sufficient statistical power. After application of these filters, we could obtain parameter estimates (figure 4) for 850 Formicidae (223 represented genera), 472 other Hymenoptera (288 genera), 177 Hemiptera (121 genera), 51 Coleoptera (45 genera), 25 Diptera (5 genera) and 65 Arachnida (56 genera). All parameter estimates can be found in supplementary table S3. Our results revealed important differences between phylogenetic groups regarding the prevalence of F1 hybrids. We found several candidate F1 hybrids ($\gamma/\theta > 1$) in Formicidae (29 candidates; figure 4a) and other Hymenoptera (15 candidates; figure 4b), while none were found in Hemiptera, Coleoptera, Diptera (figure 4c) or Arachnida (figure 4d). This result can not be explained by the larger number of Hymenoptera available, as under the observed frequency of candidates in this

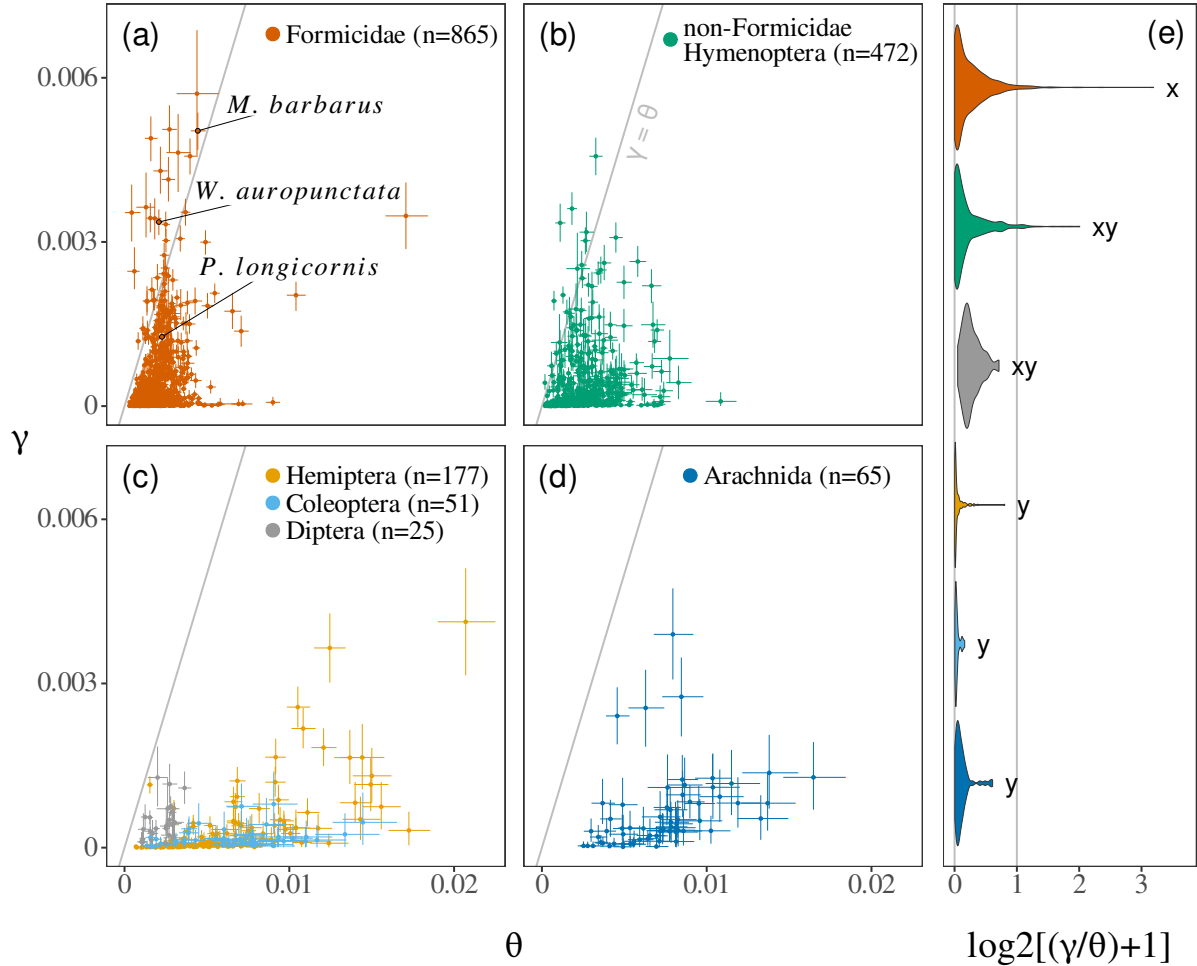


Figure 4: Genomic scans for hybridization in six groups of arthropodes.

Estimates of the divergence parameter γ and the ancestral population mutation rate θ are represented for Formicidae (a), Non-Formicidae Hymenoptera (b), other insects (c) and Arachnida (d). Colored points and lines represent bayesian point estimates and credibility intervals (see main text), respectively. (e) Distribution of the ratio γ/θ in each group. A one-shifted \log_2 -scale, under which the critical value of $\gamma/\theta = 1$ is unchanged, was used for visual convenience. Letters summarize the result of a post-hoc Tukey honest significance test, carried out using the *HSD.test* function of the *R* package *agricolae* (CIT). Groups with no letters in common have significantly different means (with $\alpha = 0.05$). All results were obtained using only dated and recent samples (see main text).

group (0.033), the probability to observe no candidates in other groups would be 8.36×10^{-5} . Species names, divergence estimates and metadata for all candidate F1 hybrids can be found in table 1. In Formicidae, two samples originating from species known to produce F1 hybrid workers (*M. barbarus* and *Wasmannia Auropunctata*) were identified as candidate F1 hybrids, further validating our method. Interestingly, a third known F1 hybrid (*Paratrechina longicornis*) was found to fall below the required value of $\gamma/\theta > 1$, again showing that this value is conservative and likely to produce many false negatives. Beyond individual candidates, Formicidae also displayed a significantly higher mean γ/θ ratio than non-Hymenoptera insects, as evidence by a post-hoc Tukey honest significance test (figure 4e). This suggests that, on average, successful interspecific mating is more frequent in ants than in other groups. Finally, candidate F1 hybrids displayed higher average divergence γ in Formicidae than in other Hymenoptera (T = 2.24, p-value = 0.0324), suggesting that hybridization events in this group tend to occur between more divergent individuals. Note that these two last results are mostly unchanged under other reasonable choices of threshold dates (see table S4).

Samples for roughly two thirds (223 represented genera) of the diversity of ants (about 300 genera, Bolton) were available for this study. This allowed us to evaluate whether the distribution of hybridization within ants genera is random. Positioning candidate F1 hybrids on a phylogeny of ants genera (figure 5) and the application of Abouheif’s test (Abouheif, 1999) revealed a significant positive phylogenetic correlation in mean γ/θ across genera (C = 0.1758; p-value = 0.007). This can be explained by the absence of candidate F1 hybrids from widely sampled groups, such as the Crematogastrini tribe (171 species from 59 genera), and by their high prevalence in other groups, such as the Attini tribe (10 candidates representing 9.4% of the tribe’s sampled species). Genera *Cyphomyrmex*, *Polyrhachis* and *Myrmecocystus* also displayed several distinct candidate F1 hybrids.

Discussion

F1 hybrid detection from single genomes

In this article we implement and showcase a fast and flexible statistical method for F1 hybrids detection. This method only relies on the distribution of heterozygosity across a set of diploid loci, and is thus theoretically applicable to any type of polymorphic loci set such as UCE loci, coding genes or even RAD tags. Note however that chosen loci should ideally be 1-1 orthologs, in order to limit the risk of paralogy inflating observed substitutions counts and facilitate intra-group estimate comparisons. Besides its applicability to a large range of data types, the method is also flexible in that it does not rely on the use of parental genomes, unlike population-centered hybrid detection approaches (Anderson & Thompson, 2002; Payseur & Rieseberg, 2016; Schubert et al., 2017). It is thus especially suited for preliminary hybrid status assessment in single-species datasets composed of many non-model species (i.e., most phylogenomic datasets). In addition to applications in the study of hybridization prevalence across taxa (i.e., as done in this study),

F1 hybrid detection could help preventing the use of error-inducing hybrids nuclear genomes in reconstructing species trees (McDade, 1992).

Naturally, the presented method also has some shortcomings, which stem in the limited statistical power provided by single individual genomes. Perhaps the most important limitation of the method is that it is restricted to the discrimination of F1 hybrids, and cannot reliably be used to identify backcross hybrids. This restricts the use of the method to the study of present hybridization and suggests that many hybrids can be missed, given the rarity of true F1 hybrids in natural populations. We have also shown that statistical error inherent to data treatment can inflate divergence estimates and lead to false identification of F1 hybrids. This is because our method relies on the assumption that divergence is characterized by a uniform increase in heterozygosity across loci. As sequencing, assembly and gene identification errors are likely to produce such an increase, their effect is mostly indistinguishable from true divergence using single genomes. This limits the application of our method to samples of good quality and limits its ability to identify F1 hybrids with low overall polymorphism. The sensitivity of the method is also hindered by any violation of the hypothesis of constant mutation rate in time and across loci. In fact, Yang (1997) has shown that variation in mutation rates generally reduces estimates of divergence by eroding any uniform component of heterozygosity. The limited sensitivity of the method might be problematic in other settings, but acts as a safeguard in our case by making F1 hybrids detection more conservative.

High prevalence of F1 hybrids in Hymenoptera and particularly in ants

F1 hybrids detection in 850 Formicidae, 472 non-Formicidae Hymenoptera, 177 Hemiptera, 51 Coleoptera, 25 Diptera and 65 Arachnida revealed a heterogeneous distribution of F1 hybrids prevalence across these groups. We identified 29 and 15 candidate F1 hybrids in Formicidae and other Hymenoptera, respectively, and none in other groups, a result that cannot be explained by uneven group sampling. High hybridization rates in Hymenoptera have been predicted by other authors (Feldhaar et al., 2008; Nonacs, 2006) under the rationale that haplodiploidy could mitigate the potential costs of out-breeding. More specifically, it was proposed that because haplodiploid females produce part of their descendants asexually, they should retain positive fitness even when engaging in non-viable inter-specific mating, leading to a weaker long-term selection against such behavior. While our results are compatible with this hypothesis, similar analyses on haplodiploid groups other than Hymenoptera will be necessary to confirm that haplodiploidy is the only factor explaining this pattern.

Within Hymenoptera, our analyses also revealed a significantly higher prevalence of F1 hybrids in Formicidae than in other Hymenoptera. High hybridization rates were previously described in a several ant genera (e.g. in some North American *Solenopsis* or European *Temnothorax*, Feldhaar et al., 2008), and have been suspected to be frequent in ants in general on the basis of several arguments. Some authors have hypothesized that hybrid sterility has a minimal fitness cost in eusocial species because they produce a large majority of normally sterile individuals (i.e.,

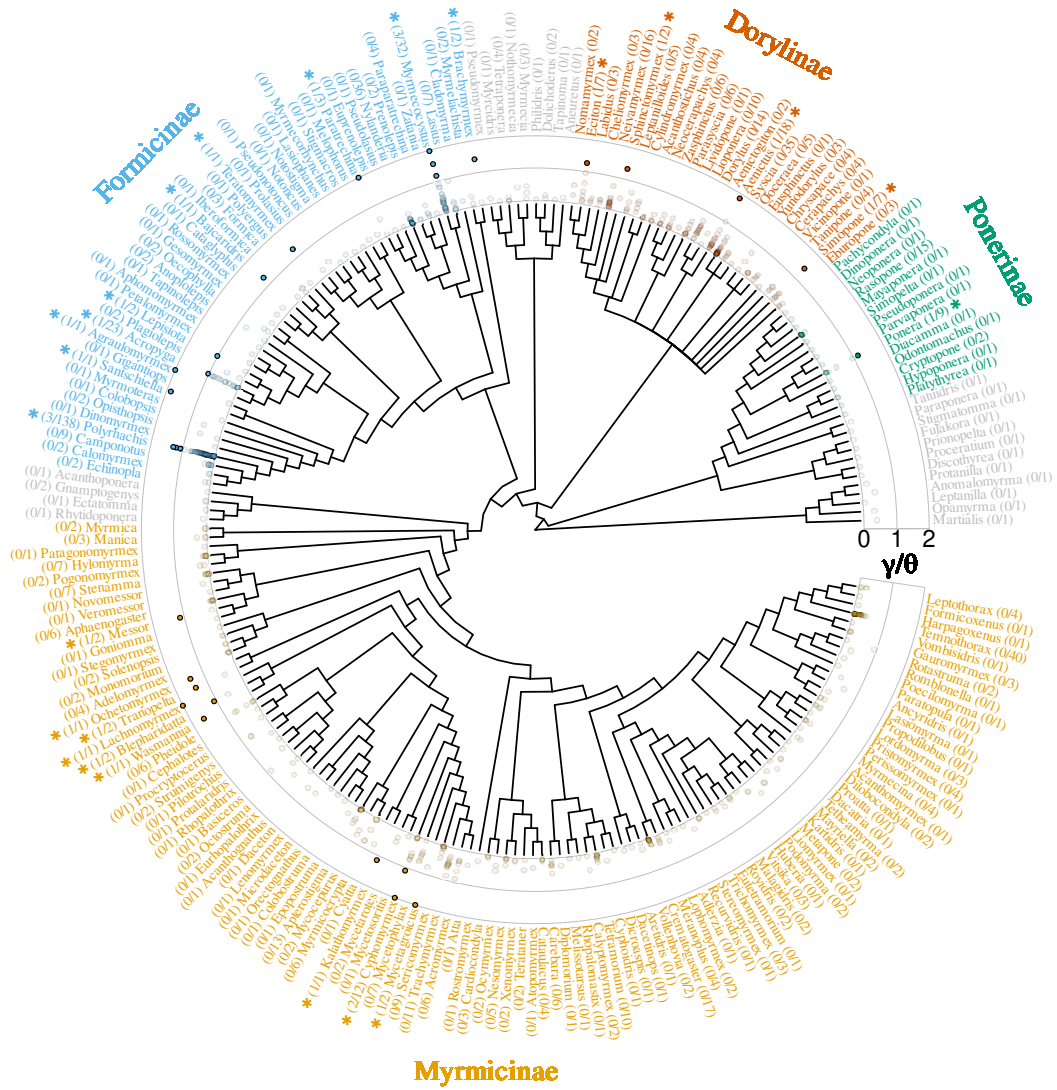


Figure 5: Occurrence of F1 hybrids across genera of Formicidae. Estimates of the ratio γ/θ obtained in Formicidae are represented against the topology of genera in this group (retrieved from Antwiki). Genera counting at least one species with $\gamma/\theta > 1$ (i.e., probable F1 hybrid) are highlighted by a star. The number of such species per genera, as well as the total number of species per genera are given for each genus. γ/θ ratios higher than 2 were truncated to 2 for readability. Three genera with no candidate F1 hybrids (*Cryptopone*, *Pseudoatta* and *Strongylognathus*), present in UCE capture data but not in the present topology, were not integrated in this representation or in statistical test for phylogenetic correlation.

workers), leading to weaker selection against hybridization (Nonacs, 2006; Umphrey, 2006). The same authors also proposed that eusocial queens could use inter-specific mating as a "best of a bad situation" strategy allowing for the production of a workforce and the successful rearing of haploid sons in the absence of conspecific mates (e.g. in locally rare species). Such strategy, sometimes referred to as "sperm parasitism", would be especially likely to arise if hybrid workers outperform regular ones, a hypothesis for which empirical evidence is still lacking (Feldhaar et al., 2008; Julian & Cahan, 2006; Ross & Robertson, 1990 but see James et al., 2002). Interestingly, the idea that eusociality facilitates or promotes hybridization is not clearly supported by the present analysis, as no candidate F1 hybrids were identified amongst 66 available non-Formicidae eusocial species (22 represented genera). While this might be because most of these species display relatively simple forms of eusociality as compared to ants (with 44 species belonging to either *Lasioglossum* or *Bombus*), it could also indicate that ants possess other traits relevant to frequent hybridization. Among characteristics unique to ants, the extreme functional simplification of workers (Peeters & Ito, 2015) could have favored hybridization by making hybrid individuals less affected by inherent developmental defects (e.g., fluctuating asymmetry). Additionally, the typically low morphological and behavioral divergence observed between males of related ant species has been proposed to reduce pre-mating barriers to hybridization in this group (Feldhaar et al., 2008).

Phylogenetic and ecological characteristics of F1 hybrids in ants

Beyond the higher prevalence of candidate F1 hybrids in ants, our analysis reveals that their phylogenetic distribution in the group follows a non-random pattern, hinting towards a potential connection with variation in ecological and life-history characteristics of species. One peculiar characteristic of some ants that is especially relevant to our findings is their display of hybridization-dependent reproductive systems. In these systems, strong genetic caste determination enforces that all workers are F1 hybrids developing from eggs fertilized by allospecific males (i.e., social hybridogenesis, as in *Messor*, *Pogonomyrmex*, *Solenopsis* or *Cataglyphis*; Anderson et al., 2006; Helms Cahan et al., 2002; Helms Cahan & Vinson, 2003; Kuhn et al., 2020; Lacy et al., 2019; Romiguier et al., 2017) or by males from a divergent lineage of the same species (i.e., as in *Wasmannia auropunctata*, *Vollenhovia emeyri* or *Paratrechina longicornis*; Fournier et al., 2005; Ohkawara et al., 2006; Percy et al., 2011), while queens are produced through regular intra-lineage mating or thelytokous parthenogenesis. In genera where it has been described, strong genetic caste determination has typically evolved independently multiple times (Anderson et al., 2006; Kuhn et al., 2020; Romiguier et al., 2017), indicating that phylogenetic correlation in this trait is expected. Furthermore, out of the three available species known to display such system (*M. barbarus* and *W. auropunctata*), two clearly stand out as F1 hybrids, indicating that our method is able to detect the divergence signal present in individual genomes of their workers. Overall, this suggests that other candidate F1 hybrids identified in this work might belong to species with similar reproductive systems, which would help explain why we detected a larger proportion of F1-hybrids in ants. This possibility echoes the prediction of some authors that the prevalence of strong genetic caste determination in Formicidae might

have been largely underestimated (Anderson et al., 2008). Note for instance the case of the *Paratrechina zanzensis*, which displays the highest divergence signal within the analyzed data (table 1) and belongs to the same genus as *P. longicornis*, a species known to produce hybrid workers (Pearcy et al., 2011). Further investigation of the population genetics of *P. zanzensis* might reveal a system similar to that found in *P. longicornis*, but with a longer history of divergence. If detected candidates correspond to undetected cases of strong genetic caste determination, our results might help shed new light on the conditions that drive the evolution of such systems. For instance, it has been hypothesized that genetic caste determination evolves more frequently in taxa with a highly specialized diet (such as granivory), as a reduced dietary spectrum would impede the use of differential larval feeding as a mean to drive caste determination (Romiguier et al., 2017). Interestingly, we found significantly higher γ/θ ratios in genera listed as strictly herbivorous (fungus-growing, granivorous or specialized aphid-rearing diets; Blanchard & Moreau, 2016) than in omnivorous or carnivorous genera (one-sided Welch t-test; $t = 3.3292$, $df = 154.75$, $p\text{-value} = 0.00054$). This may suggest that highly specialized diets do favor the evolution of genetic caste determination. This remains highly speculative however without an extended study on more genera and clear confirmation that γ/θ variations are mainly due to unusual reproductive systems across ants. While the exact proportion of detected F1-hybrids that are due to such reproductive systems is unknown at this stage, species with γ/θ ratios superior to known cases (*M. barbarus*, *W. auropunctata*, *P. longicornis*, see Fig 4) would be good first candidates for future studies.

Besides unusual reproductive systems, high hybridization rates in Dorylinae and in Attini could be linked to the unusually high polyandry observed in these group (Keller & Reeve, 1994; Strassmann, 2001). Queens that mate multiply are less likely to mate only with interspecific males (Umphrey, 2006), and are therefore expected to display lower pre-mating barriers to hybridization. Such effect of polyandry is especially likely when both types of males are easily accessible, as in species with massive mating flights that are synchronized with other sympatric species. Such a pattern is more frequent in species inhabiting temperate and arid climates, where mating flights are often triggered by heavy rainfall (Dunn et al., 2007). In favor of such connection, we find that the previously unsuspected xerophile genus *Myrmecocystus* counts several candidate F1 hybrids. As a final remark, we note that some ant groups display a high proportion of candidate F1 hybrids, while presenting no obvious life-history or ecological features likely to produce such a pattern. This is especially true of the paraphyletic group of attines composed of *Ochetomyrmex*, *Tranopelta*, *Lachnomyrmex*, *Blepharidatta* and *Wasmannia*. This suggests the existence of other unknown factors in species predisposition to hybridization, and new biological models for the study of such factors.

	Family/subfamily	Species	Collection	Origin	γ	γ/θ
Non-Formicidae Hymenoptera	Crabronidae	<i>Sphecius hogardii</i>	2010	unknown	0.0033	3.0241
	Cephidae	<i>Hartigia trimaculata</i>	2013	unknown	0.0019	2.6289
	Braconidae	<i>Pentatermus striatus</i>	2016	Thailand	0.0004	2.3057
	Crabronidae	<i>Microbembex cubana</i>	2011	unknown	0.0036	1.9806
	Sierolomorphidae	<i>Sierolomorpha sp.</i>	2006	unknown	0.002	1.5881
	Crabronidae	<i>Oxybelus analis</i>	2011	unknown	0.0046	1.3963
	Braconidae	<i>Macrostomion sumatranum</i>	1999	Japan	0.0007	1.2737
	Argidae	<i>Arge humeralis</i>	2013	unknown	0.0032	1.1781
	Braconidae	<i>Xenolobus sp.</i>	2009	Malawi	0.0025	1.1694
	Crabronidae	<i>Cerceris hatuey</i>	2011	unknown	0.003	1.1464
	Argidae	<i>Atomacera decepta</i>	2013	unknown	0.0017	1.1371
	Braconidae	<i>Cystomastax sp.</i>	1989	Costa Rica	0.001	1.1018
	Apidae	<i>Neolarra californica</i>	2005	Mexico	0.0012	1.0878
	Dryinidae	<i>Deinodryinus atriventris</i>	2013	unknown	0.0026	1.0677
	Braconidae	<i>Aleiodes coronopus</i>	2003	Thailand	0.0017	1.0152
Formicidae	Formicinae	<i>Paratrechina zanzensis</i>	2011	Tanzania	0.0035	8.1506
	Myrmicinae	<i>Lachnomyrmex scrobiculatus</i>	2008	Guatemala	0.0025	4.1156
	Formicinae	<i>Agraulomyrmex sp.</i>	2008	Tanzania	0.0049	3.0644
	Myrmicinae	<i>Cyphomyrmex sp.</i>	1992	Brazil	0.0036	2.7854
	Myrmicinae	<i>Mycetagroicus triangularis</i>	1992	Brazil	0.0034	2.1968
	Formicinae	<i>Myrmecocystus creightoni</i>	1997	USA	0.0043	1.9746
	Formicinae	<i>Santschiella kohli</i>	2000	Gabon	0.0034	1.8713
	Dorylinae	<i>Aenictus hoelldobleri</i>	2013	China	0.0051	1.855
	Myrmicinae	<i>Wasmannia auropunctata</i>	2001	Cuba	0.0034	1.6147
	Formicinae	<i>Myrmecocystus cf. navajo</i>	2003	Mexico	0.0041	1.555
	Myrmicinae	<i>Ochetomyrmex sp.</i>	2002	Guyana	0.0012	1.4361
	Formicinae	<i>Brachymyrmex sp.</i>	2009	Brazil	0.0046	1.4243
	Dorylinae	<i>Simopone marleyi</i>	1986	South Africa	0.0019	1.4099
	Myrmicinae	<i>Tranopelta gilva</i>	2006	Costa Rica	0.0019	1.3953
	Dorylinae	<i>Sphinctomyrmex stali</i>	2013	Brazil	0.0033	1.3282
	Formicinae	<i>Polyrhachis hector</i>	2010	Indonesia	0.0057	1.2988
	Formicinae	<i>Teratomyrmex greavesi</i>	2007	Australia	0.0021	1.2818
	Formicinae	<i>Bajcaridris theryi</i>	2010	Morocco	0.0014	1.2765
	Dorylinae	<i>Eciton mexicanum</i>	2013	Costa Rica	0.0014	1.2643
	Formicinae	<i>Polyrhachis mellita</i>	2008	Indonesia	0.003	1.2046
	Formicinae	<i>Myrmecocystus cf. mendax</i>	2014	USA	0.0023	1.1768
	Ponerinae	<i>Ponera coarctata</i>	1990	Italy	0.0046	1.1492
	Myrmicinae	<i>Kalathomyrmex emeryi</i>	2012	Brazil	0.0028	1.1466
	Myrmicinae	<i>Messor barbarus</i>	2008	Spain	0.005	1.1311
	Myrmicinae	<i>Cyphomyrmex costatus</i>	1996	Panama	0.0019	1.0993
	Myrmicinae	<i>Blepharidatta brasiliensis</i>	2000	Brazil	0.0019	1.0743
	Formicinae	<i>Polyrhachis taylori</i>	2008	Papua NG	0.0013	1.0721
	Formicinae	<i>Lepisiota sp.</i>	2011	South Africa	0.0024	1.0187
	Formicinae	<i>Acropyga stenotes</i>	2002	Guyana	0.0025	1.0181

Table 1: Candidate F1 hybrids. The table gives metadata and point parameter estimates for each candidate F1 hybrid (i.e. $\gamma/\theta > 1$) in our analysis.

Conclusion

Hybridization is a widespread and fundamental phenomenon that carries implications for many central processes of biological evolution, including speciation and adaptation. Here we present the first large-scale comparative study of hybridization prevalence in Arthropods, analyzing genomic data for more than 1500 non-model species obtained from public repositories. We report high rates of recent hybridization in Hymenoptera, and especially in ants, confirming previous predictions found in the literature. We also find the prevalence of F1 hybrids to be heterogeneously distributed within ants, with probable links with ecological and life-history features. These results were produced through the implementation of a scalable F1 hybrids detection method, which is applicable to virtually any modern sequencing data. Further applications of this method should help better assessing the frequency of hybridization across the tree of life, and understanding its determinants.

References

- Abbott, R., D. Albach, S. Ansell, J. W. Arntzen, S. J. Baird, N. Bierne, et al. (2013). Hybridization and speciation. *J. Evol. Biol.*, 26, 229–246.
- Abouheif, E. (1999). A method for testing the assumption of phylogenetic independence in comparative data. *Evol. Ecol. Res.*, 1, 895–909.
- Anderson, E. C. and E. A. Thompson (2002). A model-based method for identifying species hybrids using multilocus genetic data. *Genetics*, 160, 1217–1229.
- Anderson, K. E., J. Gadau, B. M. Mott, R. A. Johnson, A. Altamirano, C. Strehl, et al. (2006). Distribution and evolution of genetic caste determination in *Pogonomyrmex* seed-harvester ants. *Ecology*, 87, 2171–2184.
- Anderson, K. E., T. A. Linksvayer, and C. R. Smith (2008). The causes and consequences of genetic caste determination in ants (Hymenoptera : Formicidae). *Myrmecol. News*, 11, 119–132.
- Anderson, E. (1953). Introgressive hybridization. *Biol. Rev.*, 28, 280–307.
- Barton, N. H. and G. M. Hewitt (1985). Analysis of hybrid zones. *Annu. Rev. Ecol. Syst.*, 16, 113–148.
- Barton, N. H. (2001). The role of hybridization in evolution. *Mol. Ecol.*, 10, 551–568.
- Blanchard, B. D. and C. S. Moreau (2016). Defensive traits exhibit an evolutionary trade-off and drive diversification in ants. *Evolution (N. Y.)*, 71, 315–328.
- Bordenstein, S. R., F. P. O’hara, and J. H. Werren (2001). *Wolbachia*-induced incompatibility precedes other hybrid incompatibilities in *Nasonia*. *Nature*, 409, 707–710.
- Bossert, S., E. A. Murray, E. A. Almeida, S. G. Brady, B. B. Blaimer, and B. N. Danforth (2019). Combining transcriptomes and ultraconserved elements to illuminate the phylogeny of Apidae. *Mol. Phylogenet. Evol.*, 130, 121–131.
- Branstetter, M. G., J. T. Longino, P. S. Ward, and B. C. Faircloth (2017). Enriching the ant tree of life: enhanced UCE bait set for genome-scale phylogenetics of ants and other Hymenoptera. *Methods Ecol. Evol.*, 8, 768–776.
- Chen, S., Y. Zhou, Y. Chen, and J. Gu (2018). Fastp: An ultra-fast all-in-one FASTQ preprocessor. *Bioinformatics*, 34, i884–i890.
- Cordonnier, M., G. Escarguel, A. Dumet, and B. Kaufmann (2020). Multiple mating in the context of interspecific hybridization between two *Tetramorium* ant species. *Heredity*, 124, 675–684.
- Dobzhansky, T. (1940). Speciation as a stage in evolutionary divergence. *Am. Nat.*, 74, 312–321.
- Dunn, R. R., C. R. Parker, M. Geraghty, and N. J. Sanders (2007). Reproductive phenologies in a diverse temperate ant fauna. *Ecol. Entomol.*, 32, 135–142.
- Edmunds, S. (2002). Does parental divergence predict reproductive compatibility? *Trends Ecol. Evol.*, 17, 520–527.
- Faircloth, B. C., J. E. McCormack, N. G. Crawford, M. G. Harvey, R. T. Brumfield, and T. C. Glenn (2012). Ultraconserved elements anchor thousands of genetic markers spanning multiple evolutionary timescales. *Syst. Biol.*, 61, 717–726.
- Faircloth, B. C. (2016). PHYLUCES is a software package for the analysis of conserved genomic loci. *Bioinformatics*, 32, 786–788.
- Faircloth, B. C. (2017). Identifying conserved genomic elements and designing universal bait sets to enrich them. *Methods Ecol. Evol.*, 8, 1103–1112.
- Feldhaar, H., S. Foitzik, and J. Heinze (2008). Lifelong commitment to the wrong partner: Hybridization in ants. *Philos. Trans. R. Soc. B Biol. Sci.*, 363, 2891–2899.

- Fishman, L., A. Stathos, P. M. Beardsley, C. F. Williams, and J. P. Hill (2013). Chromosomal rearrangements and the genetics of reproductive barriers in *Mimulus* (monkey flowers). *Evolution (N. Y.)*, 67, 2547–2560.
- Fournier, D., A. Estoup, J. Orivel, J. Foucaud, H. Jourdan, J. Le Breton, et al. (2005). Clonal reproduction by males and females in the little fire ant. *Nature*, 435, 1230–1234.
- Hamilton, J. A. and J. M. Miller (2016). Adaptive introgression as a resource for management and genetic conservation in a changing climate. *Conserv. Biol.*, 30, 33–41.
- Harrison, R. G. and E. L. Larson (2014). Hybridization, introgression, and the nature of species boundaries. *J. Hered.*, 105, 795–809.
- Helms Cahan, S., J. D. Parker, S. W. Rissing, R. A. Johnson, T. S. Polony, M. D. Weiser, et al. (2002). Extreme genetic differences between queens and workers in hybridizing *Pogonomyrmex* harvester ants. *Proc. R. Soc. B Biol. Sci.*, 269, 1871–1877.
- Helms Cahan, S. and S. B. Vinson (2003). Reproductive division of labor between hybrid and nonhybrid offspring in a fire ant hybrid zone. *Evolution (N. Y.)*, 57, 1562–1570.
- Huang, W., L. Li, J. R. Myers, and G. T. Marth (2012). ART: A next-generation sequencing read simulator. *Bioinformatics*, 28, 593–594.
- Hudson, R. R. (2002). Generating samples under a Wright-Fisher neutral model of genetic variation. *Bioinformatics*, 18, 337–338.
- James, S. S., R. M. Pereira, K. M. Vail, and B. H. Ownley (2002). Survival of imported fire Ant (Hymenoptera: Formicidae) species subjected to freezing and near-freezing temperatures. *Environ. Entomol.*, 31, 127–133.
- Julian, G. E. and S. H. Cahan (2006). Behavioral differences between *Pogonomyrmex rugosus* and dependent lineages (H1/H2) harvester ants. *Ecology*, 87, 2207–2214.
- Keller, L. and H. K. Reeve (1994). Genetic variability, queen number, and polyandry in social Hymenoptera. *Evolution (N. Y.)*, 48, 694–704.
- Kieran, T. J., E. R. Gordon, M. Forthman, R. Hoey-Chamberlain, R. T. Kimball, B. C. Faircloth, et al. (2018). Insight from an ultraconserved element bait set designed for hemipteran phylogenetics integrated with genomic resources. *Mol. Phylogenet. Evol.*, 130, 297–303.
- Korneliussen, T. S., A. Albrechtsen, and R. Nielsen (2014). ANGSD: Analysis of Next Generation Sequencing Data. *BMC Bioinformatics*, 15, 1–13.
- Kuhn, A., H. Darras, O. Paknia, and S. Aron (2020). Repeated evolution of queen parthenogenesis and social hybridogenesis in *Cataglyphis* desert ants. *Mol. Ecol.*, 29, 549–564.
- Lacy, K. D., D. Shoemaker, and K. G. Ross (2019). Joint evolution of asexuality and queen number in an ant. *Curr. Biol.*, 29, 1394–1400.
- Li, H. and R. Durbin (2009). Fast and accurate short read alignment with Burrows-Wheeler transform. *Bioinformatics*, 25, 1754–1760.
- Li, D., C. M. Liu, R. Luo, K. Sadakane, and T. W. Lam (2015). MEGAHIT: An ultra-fast single-node solution for large and complex metagenomics assembly via succinct de Bruijn graph. *Bioinformatics*, 31, 1674–1676.
- Mallet, J. (2005). Hybridization as an invasion of the genome. *Trends Ecol. Evol.*, 20, 229–237.
- Mayr, E. (1942). Systematics and the origin of species. Columbia University Press, New York.
- Mayr, E. (1963). Animal species and evolution. Harvard Univ. Press, Cambridge, Massachusetts.
- McDade, L. A. (1992). Hybrids and phylogenetic systematics II. The impact of hybrids on cladistic analysis. *Evolution (N. Y.)*, 46, 1329.
- Miles Zhang, Y., J. L. Williams, and A. Lucky (2019). Understanding UCEs: A comprehensive primer on using ultraconserved elements for Arthropod phylogenomics. *Insect Syst. Divers.*, 3, 1–12.

- Nonacs, P. (2006). Interspecific hybridization in ants: At the intersection of ecology, evolution, and behavior. *Ecology*, 87, 2143–2147.
- Ohkawara, K., M. Nakayama, A. Satoh, A. Trindl, and J. Heinze (2006). Clonal reproduction and genetic caste differences in a queen-polymorphic ant, *Vollenhovia emeryi*. *Biol. Lett.*, 5, 359–363.
- Payseur, B. A. and L. H. Rieseberg (2016). A genomic perspective on hybridization and speciation. *Mol. Ecol.*, 25, 2337–2360.
- Pearcy, M., M. A. D. Goodisman, and L. Keller (2011). Sib mating without inbreeding in the longhorn crazy ant. *Proc. R. Soc.*, 278, 2677–2681.
- Peeters, C. and F. Ito (2015). Wingless and dwarf workers underlie the ecological success of ants (Hymenoptera: Formicidae). *Myrmecol. News*, 21, 117–130.
- Pfennig, K. S. (2007). Facultative mate choice drives adaptive hybridization. *Science*, 318, 965–967.
- Prentis, P. J., J. R. Wilson, E. E. Dormontt, D. M. Richardson, and A. J. Lowe (2008). Adaptive evolution in invasive species. *Trends Plant Sci.*, 13, 288–294.
- Price, T. D. and M. M. Bouvier (2002). The evolution of F1 postzygotic incompatibilities in birds. *Evolution (N. Y.)*, 56, 2083–2089.
- Rambaut, A. and N. C. Grassly (1997). Seq-gen: An application for the monte carlo simulation of DNA sequence evolution along phylogenetic trees. *Bioinformatics*, 13, 235–238.
- Randler, C. (2002). Avian hybridization, mixed pairing and female choice. *Anim. Behav.*, 63, 103–119.
- Roberts, H. F. (1919). Darwin’s contribution to the knowledge of hybridization. *Am. Nat.*, 53, 535–554.
- Romiguier, J., A. Fournier, S. H. Yek, and L. Keller (2017). Convergent evolution of social hybridogenesis in *Messor* harvester ants. *Mol. Ecol.*, 26, 1108–1117.
- Ross, K. G. and J. L. Robertson (1990). Developmental stability, heterozygosity, and fitness in two introduced fire ants (*Solenopsis invicta* and *S. richteri*) and their hybrid. *Heredity*, 64, 93–103.
- Schubert, M., M. Mashkour, C. Gaunitz, A. Fages, A. Seguin-Orlando, S. Sheikhi, et al. (2017). Zonkey: A simple, accurate and sensitive pipeline to genetically identify equine F1-hybrids in archaeological assemblages. *J. Archaeol. Sci.*, 78, 147–157.
- Smadja, C. M. and R. K. Butlin (2011). A framework for comparing processes of speciation in the presence of gene flow. *Mol. Ecol.*, 20, 5123–5140.
- Stan Development Team (2019). Stan Modeling Language Users Guide and Reference Manual, 2.17.
- Stan Development Team (2020). RStan: the R interface to Stan. R package version 2.21.2.
- Starrett, J., S. Derkarabetian, M. Hedin, R. W. Bryson, J. E. McCormack, and B. C. Faircloth (2016). High phylogenetic utility of an ultraconserved element probe set designed for Arachnida. *Mol. Ecol. Resour.*, 17, 812–823.
- Strassmann, J. (2001). The rarity of multiple mating by females in the social Hymenoptera. *Insectes Soc.*, 48, 1–13.
- Takahata, N., Y. Satta, and J. Klein (1995). Divergence time and population size in the lineage leading to modern humans. *Theor. Popul. Biol.*, 48, 198–221.
- Taylor, S. A. and E. L. Larson (2019). Insights from genomes into the evolutionary importance and prevalence of hybridization in nature. *Nat. Ecol. Evol.*, 3, 170–177.
- Umphrey, G. J. (2006). Sperm parasitism in ants: Selection for interspecific mating and hybridization. *Ecology*, 87, 2148–2159.
- Wakeley, J. (2008). Coalescent theory: An introduction. Roberts and Company Publishers.

- Wang, Y., S. Gao, Y. Zhao, W. H. Chen, J. J. Shao, N. N. Wang, et al. (2019). Allele-specific expression and alternative splicing in horse \times donkey and cattle \times yak hybrids. *Zool. Res.*, 40, 293–304.
- Yang, Z. (1997). On the estimation of ancestral population sizes of modern humans. *Genet. Res.*, 69, 111–116.

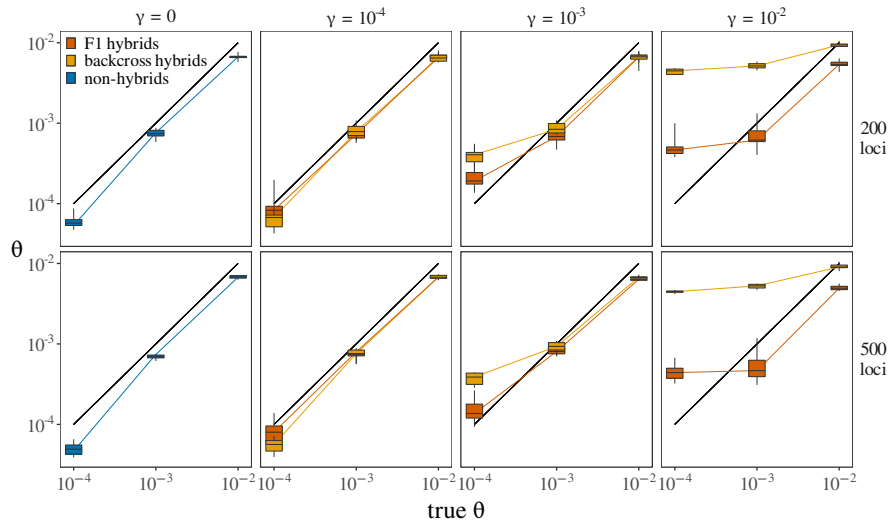


Figure S1: Ancestral population mutation rate estimation with varying number of loci. Each box represents the distribution of estimated γ values across 10 simulated individuals. Every individual consists of a collection of loci simulated under a given combination of true θ (given in x axis) and γ (given in headers) values. In non-hybrid individuals γ is always zero. In backcross hybrids, the true value of γ is that given in the header, but only for a binomial proportion of loci (as described in the main text). Rows give results obtained when varying loci set size.

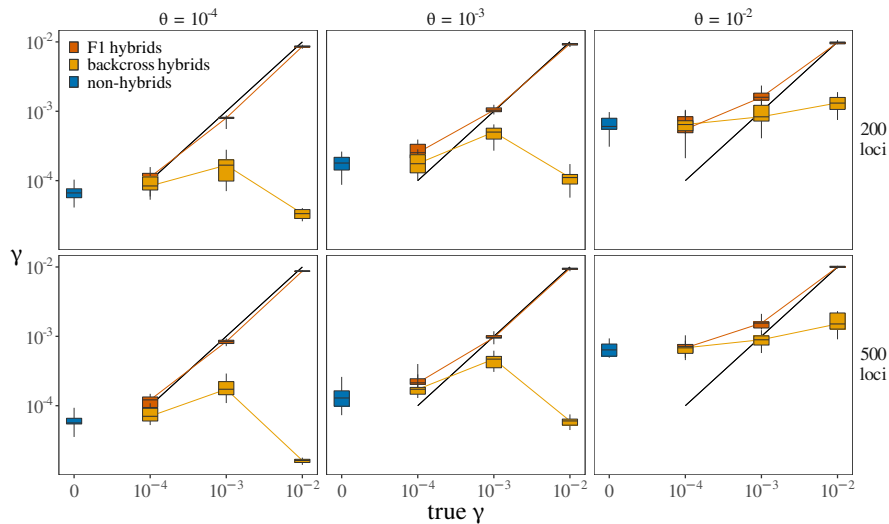


Figure S2: Divergence estimation with varying number of loci. Each box represents the distribution of estimated γ values across 10 simulated individuals. Every individual consists of a collection of loci simulated under a given combination of true θ (given in headers) and γ (given in x axis) values. In non-hybrid individuals γ is always zero. In backcross hybrids, the true value of γ is that given in the header, but only for a binomial proportion of loci (as described in the main text). Rows give results obtained when varying loci set size. The middle row is the same as the first row from figure 2 in main text.

difference in γ
between F1 hybrids
of Formicidae and
other Hymenoptera

correlation between
 γ/θ and collection date

Grouping from Tukey honest significance test

date	samples	Arachnida	Coleoptera	Hemiptera	Diptera	Hymenoptera	Formicidae	ρ	p-value	T	p-value
1960	97.874	yz	z	z	xyz	x	xy	-2.86e-01	8.72e-34	1.68e+00	9.89e-02
1962	97.402	yz	z	z	xyz	x	xy	-2.83e-01	4.48e-33	1.77e+00	8.26e-02
1964	96.552	y	y	y	xy	x	x	-2.45e-01	1.37e-24	2.61e+00	1.20e-02
1966	95.796	yz	z	z	xyz	xy	x	-2.24e-01	1.24e-20	2.47e+00	1.81e-02
1968	95.418	y	y	y	xy	xy	x	-2.10e-01	4.25e-18	2.51e+00	1.70e-02
1970	95.04	y	y	y	xy	xy	x	-1.95e-01	9.52e-16	2.33e+00	2.55e-02
1972	94.898	y	y	y	xy	xy	x	-1.89e-01	6.68e-15	2.33e+00	2.55e-02
1974	94.615	y	y	y	xy	xy	x	-1.88e-01	1.10e-14	2.33e+00	2.55e-02
1976	94.521	y	y	y	xy	xy	x	-1.88e-01	1.38e-14	2.33e+00	2.55e-02
1978	94.237	y	y	y	xy	xy	x	-1.82e-01	9.79e-14	2.33e+00	2.55e-02
1980	93.859	y	y	y	xy	xy	x	-1.63e-01	3.43e-11	2.24e+00	3.24e-02
1982	93.718	y	y	y	xy	xy	x	-1.63e-01	2.88e-11	2.24e+00	3.24e-02
1984	93.67	y	y	y	xy	xy	x	-1.62e-01	4.19e-11	2.24e+00	3.24e-02
1986	93.387	y	y	y	xy	xy	x	-1.66e-01	1.66e-11	2.24e+00	3.24e-02
1988	93.103	y	y	y	xy	xy	x	-1.63e-01	4.31e-11	2.33e+00	2.64e-02
1990	92.348	y	y	y	xy	xy	x	-1.56e-01	3.53e-10	2.07e+00	4.80e-02
1992	91.592	y	y	y	xy	xy	x	-1.47e-01	3.48e-09	1.92e+00	6.45e-02
1994	90.978	y	y	y	xy	xy	x	-1.14e-01	5.26e-06	1.78e+00	8.55e-02
1996	90.128	y	y	y	xy	xy	x	-1.15e-01	5.56e-06	1.78e+00	8.55e-02
1998	89.041	y	y	y	xy	xy	x	-9.88e-02	1.03e-04	1.73e+00	9.46e-02
2000	86.915	y	y	y	xy	xy	x	-1.00e-01	1.07e-04	1.44e+00	1.61e-01
2002	84.601	xy	y	y	xy	xy	x	-8.81e-02	8.00e-04	1.40e+00	1.72e-01
2004	78.035	xy	y	y	xy	xy	x	-9.29e-02	7.68e-04	1.33e+00	1.96e-01
2006	71.705	xy	y	y	xy	x	x	-9.60e-02	9.99e-04	1.06e+00	2.99e-01
2008	64.478	xy	y	y	xy	x	x	-1.09e-01	4.74e-04	1.15e+00	2.63e-01
2010	54.606	xy	y	y	xy	x	x	-1.32e-01	1.55e-04	6.25e-01	5.41e-01

Table S4: Main statistical results with varying maximum collection date.

The table gives statistical results obtained when discarding all non-dated samples and all dated samples collected before a given threshold date (first column). Letters in columns 2 to 7 summarize the result of a post-hoc Tukey honest significance test, carried out on γ/θ values across phylogenetic groups. The next column pair gives the pearson correlation coefficient between γ/θ and collection date. The last column pair summarizes results obtained when assessing the difference in mean γ between F1 hybrids (i.e., samples with $\gamma/\theta > 1$) of Formicidae and non-Formicidae Hymenoptera with Student's t-tests.

Appendix : Complete model derivation

With $T = t_s + t_i$ the total coalescence time between two divergent alleles (see figure 1), the probability to observe a number k of differences between them is

$$Pr(n_i = k) = \int_0^\infty Pr(T = t)Pr(n_i = k|T = t)dt. \quad (1)$$

As the total coalescence time between two divergent alleles has to be greater than or equal to the divergence time t_s , and as t_i is exponentially distributed with mean $2Ne$, we can write

$$\begin{aligned} Pr(T = t) &= 0 && \text{if } t < t_s \\ Pr(T = t) &= \frac{1}{2Ne} e^{-\left(\frac{t-t_s}{2Ne}\right)} && \text{if } t \geq t_s. \end{aligned} \quad (2)$$

Assuming a infinite-site mutation model with constant per-site mutation rate μ , the number n_i of expected substitutions between two alleles that diverged for t generations follows a Poisson distribution with mean $2l_i\mu t$, that is

$$Pr(n_i = k|T = t) = \frac{(2l_i\mu t)^k e^{-2l_i\mu t}}{k!}. \quad (3)$$

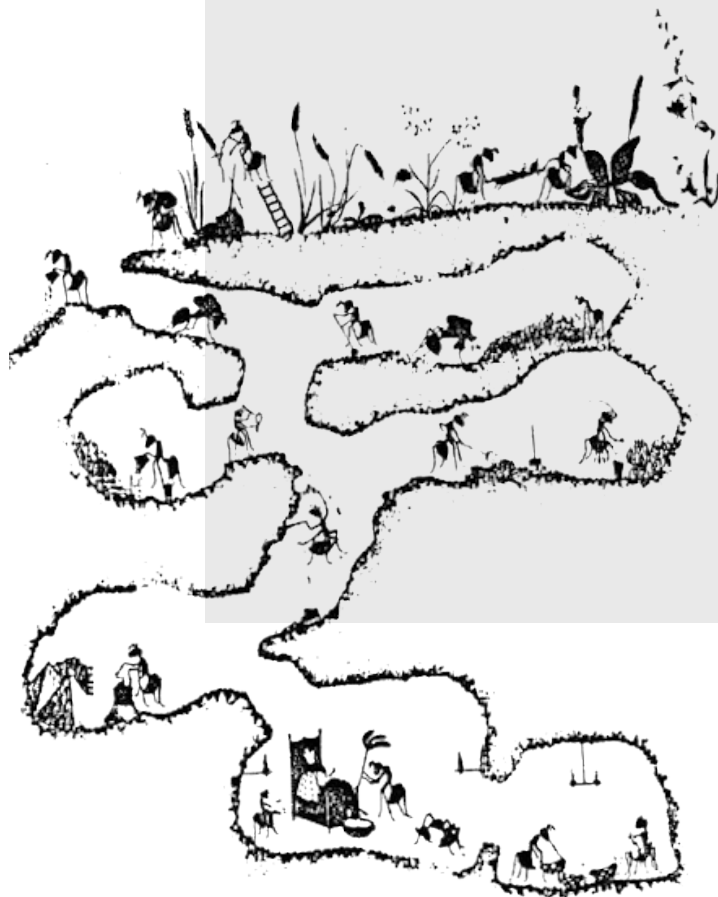
Plugging equations 2 and 3 into equation 1 leads to equation 2 presented in the main text.

$$\begin{aligned} Pr(n_i = k) &= \int_{t_s}^\infty \frac{1}{2Ne} e^{-\left(\frac{t-t_s}{2Ne}\right)} \frac{(2l_i\mu t)^k e^{-2l_i\mu t}}{k!} dt \\ &= \frac{(2l_i\mu)^k e^{\left(\frac{t_s}{2Ne}\right)}}{(2Ne)k!} \int_{t_s}^\infty t^k e^{-(2l_i\mu + \frac{1}{2Ne})t} dt \\ &= \frac{(2l_i\mu)^k e^{\left(\frac{t_s}{2Ne}\right)}}{(2Ne)k!(2l_i\mu + \frac{1}{2Ne})^{k+1}} \int_{t_s(2l_i\mu + \frac{1}{2Ne})}^\infty t^k e^{-t} dt \\ &= \frac{(4Ne l_i \mu)^k e^{\left(\frac{2t_s\mu}{4Ne\mu}\right)}}{k!(4Ne l_i \mu + 1)^{k+1}} \int_{(2t_s l_i \mu + \frac{2t_s\mu}{4Ne\mu})}^\infty t^k e^{-t} dt \\ &= \frac{(l_i\theta)^k e^{(\gamma/\theta)}}{k!(l_i\theta + 1)^{k+1}} \int_{(l_i\gamma + \frac{\gamma}{\theta})}^\infty t^k e^{-t} dt \quad \text{with} \quad \begin{cases} \theta = 4Ne\mu \\ \gamma = 2t_s\mu \end{cases} \end{aligned} \quad (4)$$

Chapter 3

Social hybridogenesis in *Messor* harvester ants

Arthur Weyna, Astrid Cruaud, Jean-Yves Rasplus, Elodie Lauroua, Sabine Nidelet, Bernard Kaufmann, Florian M. Steiner, Birgit C. Schlick-Steiner & Jonathan Romiguier



drawing by B. and R. DARCHEN

A phylogenetic study of *Messor* harvester ants from museum specimens: implications for the study of social hybridogenesis

Arthur Weyna¹, Astrid Cruaud², Jean-Yves Rasplus², Elodie Lauroua^{1,*}, Sabine Nidelet² and Jonathan Romiguier^{1,*}. *Unpublished*.

¹ Institut des Sciences de l'Evolution (UMR 5554), University of Montpellier, CNRS

² Centre de Biologie pour la Gestion des Populations, Université de Montpellier, INRAE, CIRAD, IRD, Montpellier SupAgro

Corresponding author: arthur.weyna@umontpellier.fr

Statement of authorship: JR and AW conceived the study. EL performed laboratory work under the supervision of SN, AC, JYR and AW. SN, AC and JYR provided key technical competences thorough all analyses. AW performed analyses and wrote the first draft of the manuscript under the supervision of JR.

Keywords: *Messor* harvester ants, Museum specimen, Ultra-Conserved Elements, Molecular phylogeny, Social hybridogenesis.

Abstract

Messor harvester ants are important biological models that provide key ecological services and display some of the most intriguing reproductive systems found amongst eusocial organisms. Yet, the phylogeny of this genus is mostly unknown, partly due to difficulties in sampling this widespread and speciose genus. In this study, we fill part of this knowledge gap by making use of museum material, which records more than one century of *Messor* sampling across the Old World. Applying non-destructive DNA extraction on museum specimens, we produce the first large scale genomic dataset of the genus, and reconstruct its phylogeny. We also use this data to scout out previously unidentified cases of unusual reproductive systems within *Messor*, laying the foundations for upcoming studies.

Introduction

Messor is a diverse genus (126 valid species; Bolton, 2021) of harvester ants distributed across the Palearctic region, from Western Europe to China, and across Africa, from the Maghreb to South Africa. The ecological success of these ants mostly stems in their ability to colonize arid and semi-arid environments as the result of a key innovation, granivory (Branstetter et al., 2016). Exploiting seed resources, *Messor* species can make the most of short burst of plant productivity during favorable periods, storing large amounts of grain underground to consume year-round (Plowes et al., 2013). This particular lifestyle is associated to a wide array of morphological and behavioral adaptations, such as subcaste polymorphism (i.e. with large major workers improving seed processing; Plowes et al., 2013), specialized seed-handling hair (i.e., *psammophores*; Porter & Jorgensen, 1990), or even the production of larvae-destined "bread" (Hölldobler & Wilson, 1990). This lifestyle also makes *Messor* species important ecosystem engineers (De Almeida et al., 2020; Plowes et al., 2013). Harvester ants influence the composition of local plants community through seed predation, storing and dispersal (Detrain & Tasse, 2000), making them key actors in plant succession (Wolff & Debussche, 1999). Furthermore, larger colonies of harvester have been reported to affect soil physical and chemical properties in their vicinity (De Almeida et al., 2020; Ginzburg et al., 2008), increasing nutrient content and fertility. Due to their central role in shaping their biotic and abiotic environments, *Messor* species bear importance for conservation and ecological restoration programs (Bulot et al., 2014).

Adding to their ecological significance, some *Messor* species also stand out in that they display intriguing reproductive systems. Recent studies have reported the convergent evolution of social hybridogenesis in three species of harvester ants, *M. barbarus*, *structor* and *ebeninus* (Norman et al., 2016; Romiguier et al., 2017). In these species, environmental caste determination (i.e., where female larvae differentiate into queens or workers depending on environmental conditions) has been replaced by genetic caste determination, whereby larvae are determined to develop into either caste depending on their genetic makeup. More specifically, what determines caste in these systems is the hybrid status of individuals. Workers can only arise from F1 hybrid larvae resulting from interspecific mating, while queens are always produced through intra-specific mating. This makes species with social hybridogenesis dependent on a second species for worker production, forcing queens to mate with both con- and inter-specific males. As such, cases of social hybridogenesis as found in *Messor* represent fascinating models for evolutionary biology, bringing together the study of eusociality, reproductive systems, hybridization, ecology and genomics.

Yet, despite the ecological role of *Messor* across the Old World, and despite its importance for evolutionary biology, relatively little is known about the genus. Some authors have pointed out that the taxonomic situation of *Messor* remains unsatisfactory (Schlick-Steiner et al., 2006; Steiner et al., 2018), despite a series of taxonomic revision (Bolton, 1984; Bolton, 1995; Santschi, 1917; Santschi, 1923; Santschi, 1927), and suggested that much cryptic diversity remains to be described. Other authors have begun to study the history and biogeography of *Messor* (Branstetter et al., 2016). This work seems to suggest that *Messor* originated in the Palearctic region around 14-17 Ma, and that one lineage dispersed into Africa approximately 9-6 Ma. However, due to a very limited sample size in this study (only six species), it remains mostly unknown how this genus diversified and dispersed across Eurasia and Africa. This lack of knowledge in turn impedes the comparative study of social hybridogenesis in *Messor*. While it is known that the three identified cases of such systems have evolved independently (Romiguier et al., 2017), the exact position of the associated species within *Messor* remains elusive. It is also unknown whether other previously undetected cases of social hybridogenesis occur in *Messor*. Because three cases of social hybridogenesis were discovered by probing only nine species, it is likely that a large scale search

will yield new occurrences.

In this study, we aim at filling some of the above-described knowledge gaps about *Messor*. We apply non-destructive DNA extraction and Ultra-Conserved Elements capture to museum specimens of *Messor* to produce a large-scale phylogenomic dataset of the genus. Using this data, we produce the first phylogenetic tree of *Messor*. We also apply a previously developed F1 hybrid detection method (Weyna et al., 2021) to identify potential new cases of social hybridogenesis.

Material and methods

Sampling and specimen handling

Because *Messor* is a very widespread genus with many species inhabiting secluded regions or politically unstable countries, we mainly relied on museum specimens collected through the last century. We retrieved all available specimens of *Messor* from the London Natural History Museum (MHN). We also retrieved specimens of *Veromessor*, a new-world genus from the same tribe as *Messor* and with similar ecology. The phylogeny of the less diverse (nine valid species) *Veromessor* ants is already known (Branstetter et al., 2016), but this provided us with an opportunity to evaluate the robustness of our results by comparison with previous results based on non-museum samples, and to detect additional convergences towards social hybridogenesis outside *Messor*. We analyzed dried pinned specimens from 54 distinct identified *Messor* species or subspecies (see table 1), as well as 9 identified *Veromessor* species and 24 unidentified *Messor* species (see table 2). Some key species such as *M. barbarus* or *M. structor* were represented by several distinct samples from different localities. Most species were represented by several workers, often belonging to different subcastes (i.e., minors, majors and media). Specimens included paratypes for *M. collingwoodi* (Bolton, 1982) and *M. testaceus* (Donisthorpe, 1950). The age and condition of samples ranged from recent complete specimen (figure1B), sampled as late as 2003, to very old and degraded specimen with many missing parts (figure1C), sampled as early as 1918.

From available samples, we chose one individual per unique species (or subspecies, treating unidentified samples as unique species) and per locality for sequencing. Individuals were chosen based on their characteristics, favoring bigger (i.e., majors) and more complete (i.e., more recent) individuals. The one available queen sample, identified as *M. barbarus mediosanguineus*, was also selected. This was done to provide a museum reference for *M. barbarus* queens, which, as non-hybrid representents of their species, are important regarding the study of social hybridogenesis. The 94 chosen specimen were first isolated from their respective pin. Specimen were then carefully separated from their paper mount using distilled water and sterilized minuten pins. The abdomen sternites of bigger specimens with harder cuticle were slightly punctured to facilitate DNA release during extraction.

DNA extraction

Non-destructive extraction consists in digesting and lysing soft tissues without destruction of specimens' external sclerotized structures. This allows for the preservation of important morphological characteristics relevant to identification and classification. Non-destructive extraction was achieved using the Qiagen (Valencia, CA) DNeasy Blood and Tissue kit, following the manufacturer's protocol with a few modifications, as detailed in (Cruaud et al., 2019) and summarized hereafter. Specimens were incubated overnight in an Eppendorf thermomixer (temperature = 56°C, mixing frequency = 300 rpm). Following incubation, specimens were removed, dried, and re-mounted using standard water-soluble and non-toxic



Figure 1: Museum specimens of *Messor* and *Veromessor*. **A.** Overview of samples as obtained from the London Natural History Museum. **B.** An example of recent and well-preserved specimens from *M. sp. 9*, sampled in Morocco in 1995. **C.** An example of less well-preserved specimens from *M. testaceus*, paratypes sampled in Turkey in 1947.

transparent glue. Any detached appendages were carefully retrieved and glued alongside corresponding specimen. The remaining buffer was treated with ethanol to precipitate DNA and filtered using binding columns. To increase DNA yield, two successive elutions (50 μ L each) were performed with heated AE buffer (56°C) and an incubation step of 15 minutes followed by centrifugation (8000 rpm for 1 minutes at room temperature). Eppendorf microtubes LoBind 1,5ml were used for elution and stored at -20°C until library preparation. DNA was quantified with a Qubit®2.0 Fluorometer (Invitrogen).

Library preparation and UCE capture

Sequencing library were prepared following the initial protocol of (Faircloth et al., 2012; Faircloth et al., 2015) for Ultra-Conserved Elements capture, with modifications as described in details in Cruaud et al. (2019). DNA was sheared to a size of 400 bp using the Bioruptor® Pico (Diagenode). End repair, 3'-end adenylation, adapters ligation and PCR enrichment were then performed with the NEBNext Ultra II DNA Library prep kit for Illumina (NEB). We used pairs of barcoded adapters that contained amplification and Illumina sequencing primer sites, as well as a nucleotide barcode of 5 or 6 bp long for sample identification. Pools of 16 samples were made at equimolar ratio. UCE capture was achieved by enriching each pool using the (“*Insect Hymenoptera 2.5K version 2, Ant-Specific*” probe set; Branstetter et al., 2017) and MYbaits kits (MYcroarray, Inc.). We followed the manufacturer’s protocol (MYbaits, user manual version 3, <http://www.mycroarray.com/pdf/MYbaits-manual-v3.pdf>). The hybridization reaction was run for 24h at 65°C. Post enrichment amplification was performed on beads with the KAPA Hifi HotStart ReadyMix. Enriched libraries were quantified with Qubit, an Agilent Bioanalyzer and qPCR with the Library Quantification Kit Illumina/Universal from KAPA (KK4824). They were then pooled at equimolar ratio. Paired-end sequencing (2*300bp) was performed on an Illumina Miseq platform at UMR AGAP (Montpellier, France).

Additional sequencing data

To anchor the produced species tree in previous knowledge about phylogenetic relationships within *Messor* (Branstetter et al., 2016; Romiguier et al., 2017; Steiner et al., 2018), the produced museum sequencing dataset was supplemented with available recent whole-genome and transcriptome sequencing data from several *Messor* species (*minor*, *wasmanni*, *aegyptiacus*, *arenarius*, *decipiens*, *capitatus*, *oertzeni*, *nodentatus*, *aciculatus*). Adding transcriptome sequencing data to otherwise genomic data was possible because while UCE are usually sequenced through hybridization capture protocols (as done in this study), subsets of UCEs that correspond to transcribed genomic regions can also be retrieved from transcriptomic data (Bossert et al., 2019; Miles Zhang et al., 2019). These data were obtained from previous studies (Romiguier et al., 2017) and parallel projects of this thesis (see next part of this chapter; DNA extraction and sequencing was performed by Novogene on Hiseq-PE150). Data from the same sources for the three species of *Messor* known to display social hybridogenesis (*barbarus*, *structor* and *ebeninus*; Romiguier et al., 2017) was also added, making sure that used individuals were not hybrids but pure representatives of their lineage (i.e., queens). Within these species, *M. structor* has a special status, because a recent taxonomic revision (Steiner et al., 2018) proposed to split it into five distinct species, *M. ibericus*, *ponticus*, *structor*, *muticus* and *mcarthuri*. We added sequencing data from recent specimens of these five species, kindly provided by the authors of this revision (see next part of this chapter). Thereafter, we refer to this whole group of species as *M. structor s.l.*, and use *M. structor s.s.* to designate the newly described “true” *M. structor*. Finally, we also added to the dataset a unique sample of *Pheidole longispinosa* obtained from genbank (id:SRR7248513; Branstetter et al., 2017) to act as an outgroup. *Pheidole* belongs to the same subfamily as *Messor* and *Veromessor*, and this particular sample was known from previous

analyses to be of particularly good quality (Weyna et al., 2021).

Phylogenetic analysis

Sequencing data from museum samples was demultiplexed using *Cutadapt v3.4* (Martin, 2011). Demultiplexed and added read files were cleaned with *fastp v0.20.0* (Chen et al., 2018) to remove adapters, reads shorter than 40 bp, and reads with less than 70 percent of bases with a phred score below 20. Cleaned reads were then assembled using *MEGAHIT v1.1.3* (Li et al., 2015) with k-mer size spanning from 31 to 101 by steps of 10. The *phyluce v1.6* (Faircloth, 2016) tool suite was used to identify and isolate UCE loci from de-novo assemblies, by blasting contigs against the “*Insect Hymenoptera 2.5K version 2, Ant-Specific*” probe set; Branstetter et al., 2017) using the *phyluce_assembly_match_contigs_to_probes* function. Contigs identified as UCEs were aligned using *mafft v7.407* (Katoh et al., 2002) in auto mode. Alignments were then cleaned using *trimAl v1.4* (Capella-Gutiérrez et al., 2009), removing 5bp windows with less than 50% representation or with average similarity less than 0.8. Cleaned alignment’s were concatenated into a matrix using a custom python script. The final matrix was further cleaned using *spruceup v2020.2.19* (Borowiec, 2019), removing for each species the 5% of most badly aligned 50bp sequence windows. Phylogenetic reconstruction was achieved using *IQ-TREE* (Nguyen et al., 2015) with nucleotide substitution model GTR+I+F+G4. Node support was evaluated using 1000 iterations of ultra-fast bootstrap.

Detection of F1 hybrids

The produced phylogenomic data was finally used as part of an analysis aiming at identifying potential F1 hybrids in both *Messor* and *Veromessor*. F1 hybrid detection was performed using a statistical method developed in a previous study (Weyna et al., 2021), extending on work by Takahata et al. (1995) and Yang (1997), which relies on the distribution of heterozygosity across loci of a given sample. Briefly, this method partitions the heterozygosity of a F1 hybrid individual between two estimated parameters: heterozygosity due to divergence between the populations of origin of the focal individual’s parents γ , and the population mutation rate of the population ancestral to both parents θ . This is achieved essentially by comparing the observed distribution of heterozygosity across loci to an expected distribution assuming no divergence between the individual’s parental populations. This method is known to yield close-to-zero estimates of divergence γ when applied on non-hybrid individuals, and perceptibly higher estimates when applied on true F1 hybrids. However, because estimates of both parameters correlate with the heterozygosity of samples, it is best to rely on the ratio γ/θ which is not directly related to sample heterozygosity and is more comparable across samples. This ratio, similarly to γ , is expected to be close to zero in non-hybrids, and non-zero in F1 hybrids. Furthermore, a γ/θ ratio above one implies that the divergence time between parental populations is sufficient for complete lineage sorting. Such a high value is very unlikely to be reached by non-hybrid individuals.

To obtain estimates of γ and θ , we applied the following procedure on each sample (described in more details in Weyna et al., 2021). Cleaned sequencing reads were first realigned to UCE loci using *bwa v0.7.17* (Li & Durbin, 2009) with default settings. Following this step, *angsd v0.921* (Korneliussen et al., 2014) was used to obtain allelic substitutions counts from read alignment files. Finally, we obtained estimates of θ and γ through bayesian estimations, using the *R* package *rstan v2.21.2* (Stan Development Team, 2019; Stan Development Team, 2020) and uninformative priors spanning all realistic values for both parameters (i.e., uniform priors constrained between 0 and 0.2). The mean of the posterior distribution of each parameter was used as a point estimate, while credibility intervals were constructed from its

2.5% and 97.5% quantiles.

Results

UCE capture from museum specimen

Non-destructive DNA extraction was found to be efficient overall when applied to dried workers of harvester ants. High cuticle sclerotization in these relatively big ants ensured that little to no specimen deformation occurred during incubation and re-mounting. Many appendages however, became detached from specimen during the separation from their original mounts. This was difficult to avoid especially in small or slender individuals, but should not have led to any loss of morphological features, as every detached piece was carefully retrieved.

In terms of produced data, only approximately 10% of museum specimen yielded less than a hundred valid reconstructed UCE sequences, limiting their use in phylogenetic reconstruction. As predictable, a majority of these specimens were among the oldest and less well-preserved individuals, leading to a strong negative correlation between the number of obtained UCE sequences and specimen age ($\rho = -0.517$, $t = 5.44$, p-value = 5.32×10^{-7}). But old age of not always synonymous to reduced data, as the five oldest specimen (all collected before 1936) yielded sufficient DNA and more than 400 reconstructed UCE sequences (see table 1. Old age was more detrimental in that it was positively correlated with samples heterozygosity ($\rho = 0.504$, $t = -5.50$, p-value = 3.47×10^{-7}), due to increased error and, perhaps, increased post-mortem DNA damage (Brotherton et al., 2007; Rowe et al., 2011; Staats et al., 2013). This suggests that heterozygosity-based estimations of divergence might be biased in older specimens.

A molecular phylogeny of *Messor*

Using UCE sequences obtained from museum samples, we produce the first molecular phylogeny of *Messor*, including approximately half of its species richness (Bolton, 1995). The reconstructed tree (figure 2) also comprises all nine species of *Veromessor*, with phylogenetic relationships within this group exactly matching those previously reported by Branstetter et al. (2016). Within *Messor*, the topology reported here divides species into three well supported but unequally represented clades. The first of these clades contains only *M. rufotestaceus* from Israel and four unidentified specimens from the middle-east and Tunisia. The second clade is formed by museum and recent samples of *M. aciculatus*, an Asian species which seems to have undergone isolation very early in the evolution of the group. The third clade contains all other species of *Messor*. At the basis of this large group are found three specimens from central Asia with slightly ambiguous positions, *M. lamellicornis*, *variabilis* and *sp. 4*. The rest of the group is itself distributed into three well-supported clades that were already recognized before (Romiguier et al., 2017), each harboring one known case of social hybridogenesis. Hereafter, we use this coincidental fact and, for convenience, call these three groups the *structor* group, the *barbarus* group and the *ebeninus* group.

The *structor* group contains all species of *M. structor s.l.* described by Steiner et al. (2018), with reconstructed relationships within *M. structor s.l.* closely matching that reported by these previous authors using mitochondrial DNA. Our analysis however also includes *M. structor s.l.* samples from the middle-east, a region that was not surveyed in previous studies. Middle-east samples grouped together and outside the rest of *M. structor s.l.*, suggesting that this region harbors yet undescribed lineages. These lineages might include *M. orientalis* from Syria, which was found to belong to *M. structor s.l.*

Species	Origin	Date	DNA (ng)	UCE loci	He	γ/θ
<i>M. luebberti</i>	Namibia	1967	0	445	0.0135	1.6824
<i>M. striatifrons</i>	Namibia	1982	NA	732	0.0027	1.3971
<i>M. cephalotes</i>	Kenya	1983	30.33	246	0.0119	1.305
<i>M. semoni</i>	Morocco	1987	67.32	464	0.0114	1.1518
<i>M. aegyptiacus</i>	Tunisia	1989	NA	722	0.002	0.9852
<i>M. instabilis</i>	Pakistan	1989	79.83	2036	0.0065	0.9434
<i>M. oertzeni</i>	Yugoslavia	1979	6.3	221	0.0106	0.8944
<i>M. collingwoodi</i>	Niger	1979	71.82	2028	0.0052	0.8589
<i>M. sanctus</i>	Tunisia	1978	0	169	0.0065	0.8514
<i>M. capitatus</i>	Yugoslavia	1979	20.07	76	0.0096	0.8362
<i>M. bernardi</i>	Morocco	1967	0	81	0.009	0.6917
<i>M. dentatus</i>	Syria	1989	131.4	2011	0.0054	0.6303
<i>M. testaceus</i>	Turkey	1947	7.2	25	0.0292	0.5839
<i>M. intermedius</i>	Israel	1966	0	133	0.005	0.5798
<i>M. structor</i>	Sicilia	1985	0	174	0.0126	0.5102
<i>M. structor</i>	Yugoslavia	1982	51.66	1999	0.0049	0.5068
<i>M. lamellicornis</i>	Uzbekistan	1935	6.21	404	0.0183	0.5053
<i>M. picturatus</i>	Morocco	1989	237.6	2211	0.0026	0.4722
<i>M. barbarus</i>	Morocco	1983	77.67	1452	0.0069	0.4545
<i>M. lobicornis</i>	NA	1934	111.6	293	0.0142	0.4436
<i>M. vaucheri</i>	Morocco	1961	18.63	457	0.0085	0.4311
<i>M. striativentris</i>	Algeria	NA	207.9	867	0.0038	0.418
<i>M. denticornis</i>	Namibia	1985	186.3	2031	0.0037	0.4038
<i>M. arenarius</i>	Tunisia	1989	190.8	1787	0.0068	0.4027
<i>M. minor</i>	Morocco	1987	7.74	303	0.0054	0.391
<i>M. semirufus</i>	Syria	1989	68.31	2039	0.004	0.3788
<i>M. structor</i>	Irak	1971	74.25	1596	0.0095	0.3697
<i>M. barbarus</i>	Tunisia	1978	NA	3	0.0007	0.368
<i>M. striatulus</i>	Morocco	1995	355.5	1584	0.013	0.3257
<i>M. antennatus</i>	Morocco	1961	18.27	145	0.0231	0.3061
<i>M. capensis</i>	South africa	1980	166.5	1934	0.0039	0.2793
<i>M. regalis</i>	Nigeria	1974	99.9	2172	0.0023	0.2722
<i>M. decipiens</i>	South africa	1986	98.1	2078	0.0028	0.2673
<i>M. striaticeps</i>	Morocco	1989	450.9	2241	0.0022	0.2282
<i>M. reticuliventris</i>	Pakistan	1988	123.3	2127	0.002	0.2277
<i>M. tropicorum</i>	Namibia	1916	NA	2	0.0048	0.2174
<i>M. barbarus mediosanguineus</i>	Syria	1990	1998	650	0.0044	0.2128
<i>M. structor</i>	Syria	1989	50.85	2163	0.0015	0.2107
<i>M. aciculatus</i>	China	1980	20.25	2113	0.0033	0.205
<i>M. variabilis</i>	Turkmenistan	1935	17.19	1002	0.0168	0.1966
<i>M. meridionalis</i>	Yugoslavia	1986	223.2	2300	0.0011	0.1928
<i>M. maroccanus</i>	Morocco	1976	NA	808	0.0013	0.191
<i>M. foreli</i>	Morocco	1995	219.6	1166	0.0067	0.1907
<i>M. hispanicus</i>	Spain	1976	55.08	1167	0.014	0.1769
<i>M. orientalis</i>	Syria	1989	76.68	2117	0.0031	0.1742
<i>M. himalayanus</i>	India	1986	659.7	2066	0.0015	0.1703
<i>M. rufotestaceus</i>	Israel	1982	22.05	1403	0.0086	0.1646
<i>M. structor</i>	Greece	1997	114.3	2159	0.0014	0.1607
<i>M. tropicorum</i>	Namibia	1987	82.71	2087	0.0044	0.1544
<i>M. lusitanicus</i>	Spain	1979	268.2	1918	0.0025	0.1424
<i>M. structor</i>	Iran	1960	10.8	1479	0.0031	0.1421
<i>M. minor calabricus</i>	Italy	1979	245.7	2248	0.0014	0.1085
<i>M. piceus</i>	South africa	1986	192.6	2241	0.0039	0.1025
<i>M. galla</i>	Kenya	1979	156.6	1754	0.0036	0.1002
<i>M. minor maurus</i>	Canary Islands	1988	283.5	2279	0.0028	0.0994
<i>M. angularis</i>	Kenya	1983	520.2	2294	0.0021	0.0959
<i>M. bowvieri</i>	Majorca	1978	61.92	2104	0.0023	0.0947
<i>M. rugosus</i>	Israel	1983	0	232	0.0084	0.0863
<i>M. barbarus mediosanguineus</i>	Iran	1979	222.3	2316	0.0015	0.0794

Table 1: Identified *Messor* specimens and associated results. The table gives the species name, country of origin, reported collection date, extracted DNA amount, number of obtained UCE loci, estimated mean heterozygosity and estimated γ/θ for every identified *Messor* sample in the dataset.

Species	Origin	Date	DNA (ng)	UCE loci	He	γ/θ
<i>M. sp. 4</i>	Pakistan	1988	76.23	2017	0.0186	1.3387
<i>M. sp. 24</i>	Israel	1984	0	41	0.0142	1.152
<i>M. sp. 8</i>	Tunisia	1978	0	79	0.0018	1.0833
<i>M. sp. 10</i>	Libya	2002	180.9	2195	0.0048	0.9686
<i>M. sp. 22</i>	Pakistan	1988	85.05	2102	0.0057	0.7392
<i>M. sp. 11</i>	Tunisia	1948	5.31	56	0.0199	0.7266
<i>M. sp. 19</i>	Turkey	1967	72.27	2074	0.0047	0.6177
<i>V. andrei</i>	California	1994	NA	671	0.0013	0.6165
<i>M. sp. 9</i>	Morocco	1995	81.45	2027	0.0033	0.4988
<i>M. sp. 14</i>	Algeria	1931	12.78	582	0.0126	0.4404
<i>V. lariversi</i>	Nevada	1994	41.49	1856	0.0025	0.4322
<i>V. chicoensis</i>	California	1995	NA	849	0.0006	0.3762
<i>M. sp. 2</i>	Irak	1990	203.4	1658	0.0009	0.3679
<i>M. sp. 18</i>	Israel	1983	83.16	2007	0.0024	0.3196
<i>M. sp. 7</i>	Morocco	1995	106.2	1997	0.0033	0.3045
<i>V. lobognathus</i>	Nevada	1994	NA	763	0.0008	0.281
<i>M. sp. 13</i>	Libya	2002	99.9	2316	0.0033	0.2651
<i>M. sp. 15</i>	Yemen	1937	9	36	0.0089	0.2596
<i>M. sp. 12</i>	Tunisia	1989	153.9	2272	0.0023	0.2426
<i>M. sp. 5</i>	Libya	1935	131.4	2048	0.0023	0.2337
<i>M. sp. 6</i>	Morocco	1995	87.3	2239	0.002	0.229
<i>M. sp. 23</i>	NA	1986	68.13	605	0.0044	0.2216
<i>M. sp. 16</i>	Oman	1976	62.55	55	0.0064	0.2198
<i>M. sp. 21</i>	Irak	1990	151.2	2234	0.0021	0.1795
<i>M. sp. 3</i>	Syria	1989	33.84	2148	0.0024	0.17
<i>M. sp. 1</i>	Pakistan	1988	38.43	2261	0.003	0.1659
<i>V. pergandei</i>	California	1970	28.62	1420	0.0065	0.1336
<i>V. smithi</i>	Canada	1994	178.2	1986	0.002	0.1258
<i>V. julianus</i>	Mexico	1975	91.8	1806	0.0043	0.1067
<i>M. sp. 20</i>	Spain	2003	277.2	2226	0.0029	0.0644
<i>V. stoddardi</i>	Mexico	1994	66.06	2314	0.0016	0.0541
<i>M. sp. 17</i>	Irak	1990	207	1936	0.0027	0.0385
<i>V. chamberlini</i>	California	1994	151.2	2174	0.0037	0.02

Table 2: Unidentified *Messor* specimens, *Veromessor* specimens, and associated results. The table gives the species name, country of origin, reported collection date, extracted DNA amount, number of obtained UCE loci, estimated mean heterozygosity and estimated γ/θ for every unidentified *Messor* and *Veromessor* sample in the dataset.

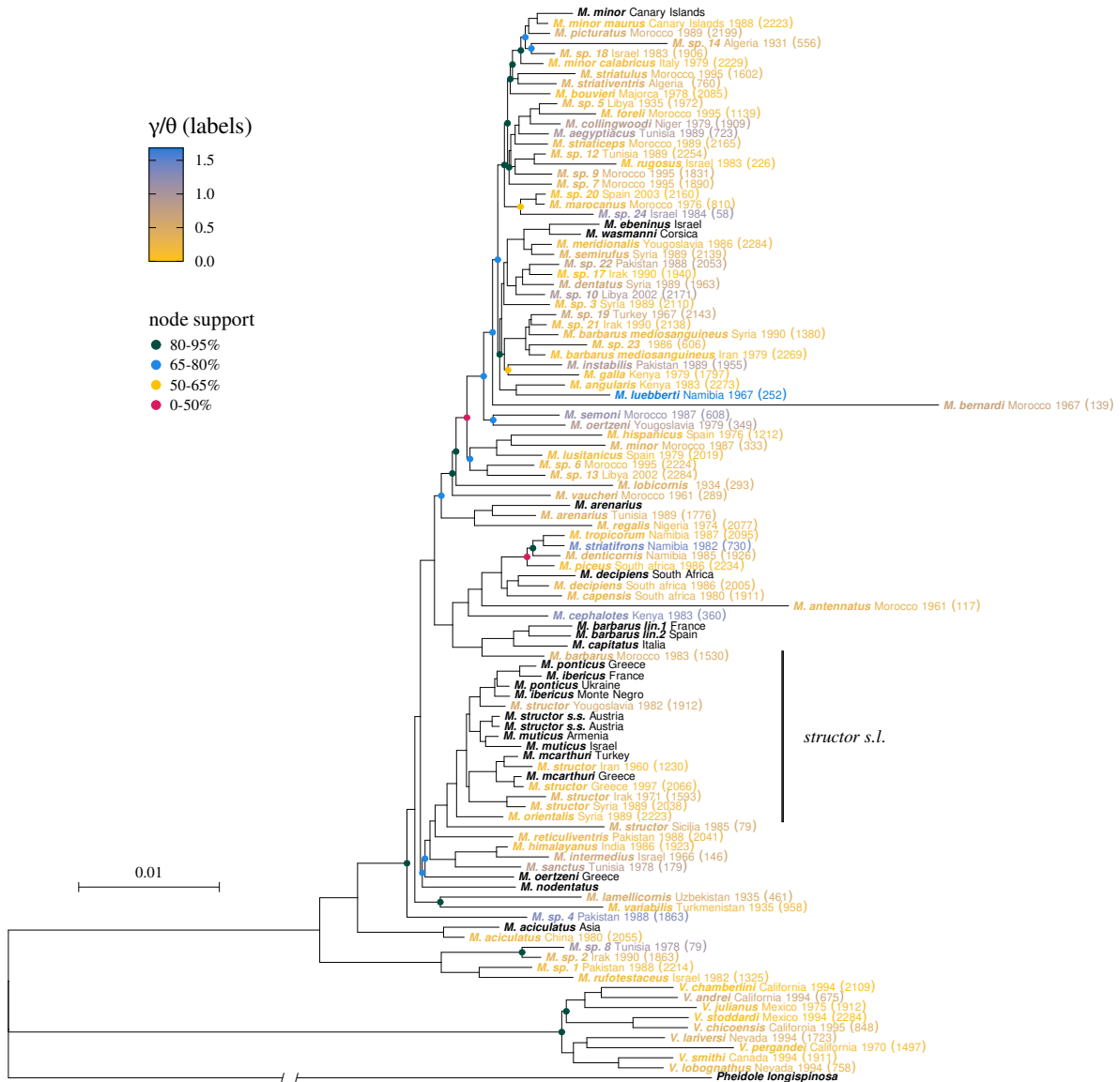


Figure 2: Inferred phylogenetic tree of *Messor* and *Veromessor*. Black labels indicate recent added samples, that were obtained outside of museum sampling. Colored labels correspond to museum samples, with color corresponding to estimates of γ/θ for each individual. Bluer labels indicate a stronger probability for the associated individual to be a F1 hybrid. Node support (percentage of bootstrap iterations where one node is found) is given by points at each node. The absence of point indicates that a node was strongly supported ($> 95\%$).

This finding however is not well supported as it relies only on the external position of one *M. structor* from Sicilia which yielded as few as 79 loci.

The *barbarus* group is divided into two groups, one mainly European group consisting of *M. barbarus* and *M. capitatus*, and one strictly African group featuring almost all *Messor* species from central and southern Africa. Interestingly, while the relationships between European *M. barbarus* and *M. capitatus* are thought to be known without ambiguity (Romiguier et al., 2017), we find one museum sample of *M. barbarus* from Morocco to be external to the the *barbarus/capitatus* pair of recent samples. This might be due to errors in phylogenetic reconstruction or identification, but also indicates that knowledge about the biogeography of this group will remain incomplete until more North African specimens of *M. barbarus* are integrated into analyses. One other surprise regarding *M. barbarus* is that two museum *M. barbarus mediosanguineus* samples (including a queen) from the Middle East grouped far from the true *M. barbarus* samples, and together with three other unidentified samples. This suggests that *M. barbarus mediosanguineus* is in fact a very distinct, unidentified species distributed from Turkey to Iran.

The *ebeninus* group is by far the richer group in the dataset, featuring European, African and Middle-East species. It is also the group in which the proposed internal topology has the worst support, with most of its older nodes being found in less than 95% of bootstrap iterations. In particular, a group consisting of Spanish and North African species including *M. hispanicus* and *lusitanicus* is found to have very little support (less than 50% of iterations). Despite limited confidence, the *ebeninus* group seems to consist mainly of two groups, a group of mostly African and Middle East species, and group of mostly North African species. Among this last group, samples of the west-Mediterranean species *M. minor*, including *M. minor calabricus* from Italy and *M. minor maurus* from the Canary Islands, are found to form a monophyletic group together with *M. picturatus* from Morocco. We also find one *M. minor* from Morocco to branch far from the rest of *M. minor* samples and together with *M. hispanicus* from Spain, suggesting identification errors.

F1 hybrids detection

F1 hybrids detection in museum samples allowed for the production of a first set of evidence regarding the frequency of social hybridogenesis in *Messor*. We found museum specimens belonging to species *M. striatifrons*, *cephalotes*, *luebberti*, *semoni* and *sp. 4* to be plausible candidate F1 hybrids, characterized by values γ/θ superior to one. Unluckily, confirmation of this status is impeded by two factors. First, most of these specimens are represented by a relatively low number of UCE loci. While a low number of loci was not always accompanied by strong hybridization signal in this study, it is known from previous work that statistical error may inflate false positive rates in our F1 hybrid detection method. Second, this analysis lacks examples of true F1 hybrid museum samples, which would have been useful as comparison points. This is because museum samples of *M. barbarus* and *M. structor s.l.*, which we hoped would provide good references, all behaved in unexpected ways or displayed little signal of hybridization. As mentioned before, *M. barbarus* samples either belonged to another species altogether, or were less similar to European *M. barbarus* than *M. capitatus*, casting doubt on their hybrid status. *M. structor s.l.* samples, on the other hand, all belonged to lineages that are not known to display social hybridogenesis (see second part of this chapter).

Discussion

A first glimpse into the phylogeny of *Messor*

The phylogeny and history of diversification of *Messor* are still poorly known, despite its ecological importance, and despite its central role in the study of social hybridogenesis. With this study we produce the first semi-exhaustive species tree of the genus, including roughly half of the world's *Messor* species. While this tree is an intermediate result that still contains ambiguities (e.g., some long terminal branches and poorly supported nodes), its present form nevertheless yields important insights about the history of the group, and about the distribution of social hybridogenesis within it.

Messor is known from the study of Branstetter et al. (2016) to have originated in the Palearctic region around 14-17 Ma, before dispersing into the Afrotropics 9-6 Ma. However, this study accounted for only 6 species of *Messor*, with 5 of these belonging to the *barbarus* group. Phylogenetic relationships within the more furnished tree of *Messor* presented here may provide additional details. First, we observe that most species of *Messor*, including most basal lineages, do occur in the Palearctic region, and especially in the middle-east and Maghreb. While this result might be due to incomplete sampling, it supports the hypothesis that this is the ancestral range of the genus. Our results however, also suggest that the subsequent history of dispersion within *Messor* might be more complicated than previously envisioned. We find that at least two independent groups of *Messor* dispersed into the Afrotropics, as *M. galla*, *angularis* and *luebberti* are not related to other African species from the *barbarus* group. We also note that dispersion into Europe likely occurred several times independently, both through the Middle East (e.g. European species from the *structor* group) and through the strait of Gibraltar (e.g., *M. lusitanicus* and *minor*). Finally, we find that Central and East Asian species such as *M. aciculatus*, *himalayanus*, *reticuliventris* and *instabilis*, do not form a monophyletic groups, and thus likely originated from several independent events of eastward migration. Altogether, these results suggest that a full understanding of the history and biogeography of the successful and very mobile *Messor* genus will require more detailed studies.

Perhaps an important step in this understanding will be to engage in a revision of the group's taxonomy. While several revisions of the group were undertaken in the last century (Schlick-Steiner et al., 2006), a consensus is still to be reached, as evidenced by recent developments in *M. structor s.l.* (Steiner et al., 2018). Some of the results presented here might help correct or complete taxonomic relationships within *Messor*. First, we report two possible synonyms. We find it plausible that *M. picturatus* and *M. minor* are synonyms, based on the internal position of *M. picturatus* within a group consisting of *M. minor* and other unidentified samples. We also suggest that *M. orientalis* might belong to *M. structor s.l.*, although the position of *M. orientalis* remains ambiguous. More generally, *M. structor s.l.* appears to be composed of more lineages than described by Steiner et al. (2018), as evidenced by the phylogenetic position of Middle East specimens. Besides synonymy and incompleteness in taxonomic descriptions, our results can also help guiding the identification of yet unidentified specimens, such as *M. sp. 19, 21* and *23*, which likely belong to the same unknown species as *M. barbarus mediosanguineus*. This exemplifies the potential power of non-destructive sequencing of museum specimens, when coupled to Ultra-Conserved Elements capture. Such methods allow for the production of insightful molecular phylogenies, making use of the large amount of biological material kept in museums, without the loss of original specimens, and despite their old age. These approach can thus result in fruitful synergies, where molecular data obtained from rare and taxonomically important specimens (i.e. such as types) helps refining taxonomy, in turn paving the way for more specialized downstream analysis.

Potential new cases of social hybridogenesis in *Messor*

In this analysis we use museum sequencing data in an attempt to identify new cases of social hybridogenesis. Social hybridogenesis is known to have evolved at least three times independently, in *M. barbarus*, *M. structor s.l.* and *M. ebeninus*. Outside *Messor*, multiple independent evolutions towards social hybridogenesis were also observed in the genera *Pogonomyrmex* (at least two times; Anderson et al., 2006), *Solenopsis* (at least two times; Helms Cahan & Vinson, 2003; Lacy et al., 2019), and *Cataglyphis* (at least 4 times; Kuhn et al., 2020). This pattern suggests that some groups of ants may have special ecological or genetic predispositions to evolve such reproductive systems. *Messor* is one example of such a group, and may display many unknown cases of social hybridogenesis. In particular, it is especially likely that these candidates will be found in the most understudied parts of the range of *Messor*, that is Africa and Asia. As expected, we report candidate F1 hybrids in these two regions, in *M. striatifrons*, *cephalotes*, *luebberti*, *semoni* from Africa and in *M. sp. 4* from Pakistan. While F1 hybrids could be produced through punctual hybridization (Feldhaar et al., 2008), or in a context of sperm parasitism (Umphrey, 2006), we argue instead that they are very likely indicators that these species evolved social hybridogenesis, given previous cases of such systems in *Messor*, and given the rarity of true F1 hybrids in other settings.

These species, of course, only represent the most likely candidates and other specimens displayed mild to intermediate signatures of hybridization. Unluckily, a more precise discrimination of true F1 hybrids within museum specimen has not been achieved so far. The limited quality of museum DNA is likely to have led to increased error rates in all parts of our analysis (i.e. sequencing, assembly, UCE identification, heterozygosity estimations), and these effect have not been accounted for yet. This is particularly important because such error is known to produce false positives in F1 hybrid detection (Weyna et al., 2021). In essence, this is because random error is expected to increase heterozygosity homogeneously across sequenced genomes, while a homogeneous increase in genome-wide heterozygosity is precisely the pattern that our method identifies as a signal for hybridization. Future potential solutions to this problem include phylogenetic-signal-based filtering of error-prone loci (Klopfstein et al., 2017), or even post-assembly correction of post-mortem DNA damage (Jónsson et al., 2013). Better confidence in our results will also be attained when including (preferably old) reference museum specimens of known true F1 hybrids. Such references points will allow to account for any bias in the method linked to the particularities of museum samples.

While our results are yet to be refined, and might change in the future, a few insights regarding the evolution of social hybridogenesis can still be gained. We report several candidate F1 hybrids within *Messor*, but none within the 9 new-world species of *Veromessor*. Although *Veromessor* is significantly less diverse than *Messor*, this might indicate that *Veromessor* lacks some ecological or genetic features relevant to the evolution of social hybridogenesis. In particular, *Veromessor* species are known to be more omnivorous than the almost strictly granivorous species of *Messor* (Branstetter et al., 2016). It has been hypothesized before that taxa with a highly specialized diet (such as granivory) could be more likely to evolve social hybridogenesis. The rationale behind this hypothesis is that a reduced dietary spectrum would impede the use of differential larval feeding as a mean to drive caste determination (Romiguier et al., 2017), thus favoring transitions towards genetic caste determination and social hybridogenesis. This remains highly speculative however and testing this hypothesis will require to include other genera from the same tribe as *Messor* and *Veromessor*, which display various levels of diet specialization (Branstetter et al., 2016).

Conclusion

The ecological significance and peculiar reproduction systems of *Messor* harvester ants make them particularly important, yet understudied, biological models. Here we produce the first large scale genomic dataset of the genus, gaining new insights about its phylogeny, dispersion history and about the distribution of social hybridogenesis within it. While additional sampling and methodological refining will be required to fully grasp these aspects and to resolve some remaining ambiguities in our results, this work lays the foundations of future studies of *Messor*. This was made possible through the use of museum material, and through the application of non-destructive DNA extraction, coupled with UCE capture. Such methods are gaining popularity, and we hope that this work will participate in advertising their great power as tools for taxonomy, and as providers of invaluable genetic data.

References

- Anderson, K. E., J. Gadau, B. M. Mott, R. A. Johnson, A. Altamirano, C. Strehl, et al. (2006). Distribution and evolution of genetic caste determination in *Pogonomyrmex* seed-harvester ants. *Ecology*, 87, 2171–2184.
- Bolton, B. (1984). Afrotropical species of the myrmicine ant genera *Cardiocondyla*, *Leptothorax*, *Melissotarsus*, *Messor* and *Cataulacus* (Formicidae). *Bul. Br. Mus. Nat. Hist.*, 45, 307–370.
- Bolton, B. (1995). A new general catalogue of the ants of the world. The Belknap Press of Harvard University Press, Cambridge, MA.
- Bolton, B. (2021). An online catalog of the ants of the world. <https://antcat.org>. Accessed 15 october 2021.
- Borowiec, M. (2019). Spruceup: fast and flexible identification, visualization, and removal of outliers from large multiple sequence alignments. *J. Open Source Softw.*, 4, 1635.
- Bossert, S., E. A. Murray, E. A. Almeida, S. G. Brady, B. B. Blaimer, and B. N. Danforth (2019). Combining transcriptomes and ultraconserved elements to illuminate the phylogeny of Apidae. *Mol. Phylogenet. Evol.*, 130, 121–131.
- Branstetter, M. G., J. T. Longino, J. Reyes-López, T. R. Schultz, and S. G. Brady (2016). Into the tropics: Phylogenomics and evolutionary dynamics of a contrarian clade of ants. *Preprint Biorxiv*, 102–107.
- Branstetter, M. G., J. T. Longino, P. S. Ward, and B. C. Faircloth (2017). Enriching the ant tree of life: enhanced UCE bait set for genome-scale phylogenetics of ants and other Hymenoptera. *Methods Ecol. Evol.*, 8, 768–776.
- Brotherton, P., P. Endicott, J. J. Sanchez, M. Beaumont, R. Barnett, J. Austin, et al. (2007). Novel high-resolution characterization of ancient DNA reveals C - U-type base modification events as the sole cause of post mortem miscoding lesions. *Nucleic Acids Res.*, 35, 5717–5728.
- Bulot, A., T. Dutoit, M. Renucci, and E. Provost (2014). A new transplantation protocol for harvester ant queens *Messor barbarus* (Hymenoptera: Formicidae) to improve the restoration of species-rich plant communities. *Myrmecol. News*, 20, 43–52.
- Capella-Gutiérrez, S., J. M. Silla-Martínez, and T. Gabaldón (2009). trimAl: A tool for automated alignment trimming in large-scale phylogenetic analyses. *Bioinformatics*, 25, 1972–1973.
- Chen, S., Y. Zhou, Y. Chen, and J. Gu (2018). Fastp: An ultra-fast all-in-one FASTQ preprocessor. *Bioinformatics*, 34, i884–i890.
- Cruaud, A., S. Nidelet, P. Arnal, A. Weber, L. Fusu, J. H. Gumovsky, et al. (2019). Optimised DNA extraction and library preparation for minute arthropods: application to target enrichment in chalcid wasps used for biocontrol. *Mol. Ecol. Resour.*, 19, 702–710.
- De Almeida, T., O. Blight, F. Mesléard, A. Bulot, E. Provost, and T. Dutoit (2020). Harvester ants as ecological engineers for Mediterranean grassland restoration: Impacts on soil and vegetation. *Biol. Conserv.*, 245, 108547.
- Detrain, C. and O. Tasse (2000). Seed drops and caches by the harvester ant *Messor barbarus*: Do they contribute to seed dispersal in Mediterranean grasslands? *Naturwissenschaften*, 87, 373–376.
- Faircloth, B. C., J. E. McCormack, N. G. Crawford, M. G. Harvey, R. T. Brumfield, and T. C. Glenn (2012). Ultraconserved elements anchor thousands of genetic markers spanning multiple evolutionary timescales. *Syst. Biol.*, 61, 717–726.
- Faircloth, B. C., M. G. Branstetter, N. D. White, and S. G. Brady (2015). Target enrichment of ultraconserved elements from arthropods provides a genomic perspective on relationships among hymenoptera. *Mol. Ecol. Resour.*, 15, 489–501.
- Faircloth, B. C. (2016). PHYLUCE is a software package for the analysis of conserved genomic loci. *Bioinformatics*, 32, 786–788.

- Feldhaar, H., S. Foitzik, and J. Heinze (2008). Lifelong commitment to the wrong partner: Hybridization in ants. *Philos. Trans. R. Soc. B Biol. Sci.*, 363, 2891–2899.
- Ginzburg, O., W. G. Whitford, and Y. Steinberger (2008). Effects of harvester ant (*Messor spp.*) activity on soil properties and microbial communities in a Negev Desert ecosystem. *Biol. Fertil. Soils*, 45, 165–173.
- Helms Cahan, S. and S. B. Vinson (2003). Reproductive division of labor between hybrid and nonhybrid offspring in a fire ant hybrid zone. *Evolution*, 57, 1562–1570.
- Hölldobler, B. and E. O. Wilson (1990). *The Ants*. Ed. by M. Harvard Univ. Press, Cambridge.
- Jónsson, H., A. Ginolhac, M. Schubert, P. L. Johnson, and L. Orlando (2013). MapDamage2.0: Fast approximate Bayesian estimates of ancient DNA damage parameters. *Bioinformatics*, 29, 1682–1684.
- Katoh, K., K. Misawa, K. I. Kuma, and T. Miyata (2002). MAFFT: A novel method for rapid multiple sequence alignment based on fast Fourier transform. *Nucleic Acids Res.*, 30, 3059–3066.
- Klopfstein, S., T. Massingham, and N. Goldman (2017). More on the best evolutionary rate for phylogenetic analysis. *Syst. Biol.*, 66, 769–785.
- Korneliussen, T. S., A. Albrechtsen, and R. Nielsen (2014). ANGSD: Analysis of Next Generation Sequencing Data. *BMC Bioinformatics*, 15, 1–13.
- Kuhn, A., H. Darras, O. Paknia, and S. Aron (2020). Repeated evolution of queen parthenogenesis and social hybridogenesis in *Cataglyphis* desert ants. *Mol. Ecol.*, 29, 549–564.
- Lacy, K. D., D. Shoemaker, and K. G. Ross (2019). Joint evolution of asexuality and queen number in an ant. *Curr. Biol.*, 29, 1394–1400.
- Li, H. and R. Durbin (2009). Fast and accurate short read alignment with Burrows-Wheeler transform. *Bioinformatics*, 25, 1754–1760.
- Li, D., C. M. Liu, R. Luo, K. Sadakane, and T. W. Lam (2015). MEGAHIT: An ultra-fast single-node solution for large and complex metagenomics assembly via succinct de Bruijn graph. *Bioinformatics*, 31, 1674–1676.
- Martin, M. (2011). Cutadapt removes adapter sequences from high-throughput sequencing reads. *EMBnet.journal*, 17, 10–12.
- Miles Zhang, Y., J. L. Williams, and A. Lucky (2019). Understanding UCEs: A comprehensive primer on using ultraconserved elements for arthropod phylogenomics. *Insect Syst. Divers.*, 3, 1–12.
- Nguyen, L. T., H. A. Schmidt, A. Von Haeseler, and B. Q. Minh (2015). IQ-TREE: A fast and effective stochastic algorithm for estimating maximum-likelihood phylogenies. *Mol. Biol. Evol.*, 32, 268–274.
- Norman, V., H. Darras, C. Tranter, S. Aron, and W. O. H. Hughes (2016). Cryptic lineages hybridize for worker production in the harvester ant *Messor barbarus*. *Biol. Lett.*, 12, 1–5.
- Plowes, N. J., R. A. Johnson, and B. Hölldobler (2013). Foraging behavior in the ant genus *Messor* (Hymenoptera: Formicidae: Myrmicinae). *Myrmecol. News*, 18, 33–49.
- Porter, S. D. and C. D. Jorgensen (1990). Psammophores: Do harvester ants (Hymenoptera : Formicidae) use these pouches to transport seeds? *J. Kansas Entomol. Soc.*, 63, 138–149.
- Romiguier, J., A. Fournier, S. H. Yek, and L. Keller (2017). Convergent evolution of social hybridogenesis in *Messor* harvester ants. *Mol. Ecol.*, 26, 1108–1117.
- Rowe, K. C., S. Singhal, M. D. Macmanes, J. F. Ayroles, T. L. Morelli, E. M. Rubidge, et al. (2011). Museum genomics: Low-cost and high-accuracy genetic data from historical specimens. *Mol. Ecol. Resour.*, 11, 1082–1092.
- Santschi, F. (1917). Races et variétés nouvelles du *Messor barbarus* L. *Bull. Soc. Hist. Nat. Afr. Nord*, 8, 89–94.
- Santschi, F. (1923). *Messor* et autres fourmis paléarctiques. *Rev. Suisse Zool.*

- Santschi, F. (1927). Revision des *Messor* du groupe *instabilis* Sm. *Bol. R. Soc. Esp. Hist. Nat.*, 27, 225–250.
- Schlick-Steiner, B. C., F. M. Steiner, H. Konrad, B. Markó, S. Csoz, G. Heller, et al. (2006). More than one species of *Messor* harvester ants (Hymenoptera: Formicidae) in Central Europe. *Eur. J. Entomol.*, 103, 469–476.
- Staats, M., R. H. Erkens, B. van de Vossenberg, J. J. Wieringa, K. Kraaijeveld, B. Stielow, et al. (2013). Genomic treasure troves: Complete genome sequencing of herbarium and Insect museum specimens. *PLoS One*, 8.
- Stan Development Team (2019). Stan Modeling Language Users Guide and Reference Manual, 2.17.
- Stan Development Team (2020). RStan: the R interface to Stan. R package version 2.21.2.
- Steiner, F. M., S. Csősz, B. Markó, A. Gamisch, L. Rinnhofer, C. Folterbauer, et al. (2018). Turning one into five: Integrative taxonomy uncovers complex evolution of cryptic species in the harvester ant *Messor* “*structor*”. *Mol. Phylogenet. Evol.*, 127, 387–404.
- Takahata, N., Y. Satta, and J. Klein (1995). Divergence time and population size in the lineage leading to modern humans. *Theor. Popul. Biol.*, 48, 198–221.
- Umphrey, G. J. (2006). Sperm parasitism in ants: Selection for interspecific mating and hybridization. *Ecology*, 87, 2148–2159.
- Weyna, A., L. Bourouina, N. Galtier, and J. Romiguier (2021). Detection of F1 hybrids from single-genome data reveals frequent hybridization in Hymenoptera and particularly ants. *submitted to Molecular Biology and Ecology*.
- Wolff, A. and M. Debussche (1999). Ants as seed dispersers in a Mediterranean old-field succession. *Oikos*, 84, 443.
- Yang, Z. (1997). On the estimation of ancestral population sizes of modern humans. *Genet. Res.*, 69, 111–116.

Distribution and characteristics of social hybridogenesis within the *Messor structor* species group

Arthur Weyna¹, Bernard Kaufmann², Florian M. Steiner³, Birgit C. Schlick-Steiner³ and Jonathan Romiguier^{1,*}. *Unpublished*.

¹ Institut des Sciences de l'Evolution (UMR 5554), University of Montpellier, CNRS, France

² Ecologie des Hydrosystèmes Naturels et Anthropisés (UMR 5023) , Université Lyon 1, ENTPE, CNRS, Villeurbanne, France

³ Molecular Ecology Group, Department of Ecology, University of Innsbruck, Austria

Corresponding author: arthur.weyna@umontpellier.fr

Statement of authorship: JR and AW conceived the study. AW performed analyses and wrote the first draft of the manuscript under the supervision of JR. BK provided samples and vital supervision during field work. FS and BS provided key samples.

Keywords: *Messor* harvester ants, Molecular phylogeny, Social hybridogenesis.

Abstract

In 2017, a population genetics study has reported that some French populations of *M. structor* displayed F1 hybrid workers and non-hybrid queens. This was interpreted as evidence for social hybridogenesis, a hybridization-dependent reproductive system that was also found in other species of *Messor*. Yet, a more recent taxonomic revision of this species that proposed to split *M. structor* into five distinct species has not addressed the presence of social hybridogenesis. In this study, we assemble a large-scale genomic dataset of the *M. structor* species group, and use it to determine which of the newly described species display this reproductive system. We report that social hybridogenesis is restricted to *M. ibericus*, a species inhabiting Southern Europe and that was found to produce F1 hybrid workers across its entire range. Using the same data, we also investigate the reproductive biology of *M. ibericus*. While many grey area remain in our understanding, our results strongly suggest that social hybridogenesis in this species involves some form of male clonality, as was previously described in species such as the little fire ant *Wasmannia auropunctata*. If this is confirmed by future analyses, it would make *Messor* the only known genus where separate forms of social hybridogenesis have evolved, thus reinforcing its value as a model for the study of these fascinating reproductive systems.

Introduction

Messor harvester ants are specialized granivores that thrive in arid and semi-arid environments of the Old World by taking advantage of seasonally abundant seed resources. In Europe, the large size, diurnal activities and mass foraging abilities of *Messor* ants has long captured the attention of naturalists. Yet, despite much attention and a series of taxonomic revisions conducted in the last century (Bolton, 1984; Bolton, 1995; Santschi, 1917; Santschi, 1923; Santschi, 1927), recent developments have suggested that our knowledge about the taxonomy and general biology of European *Messor* ants remains incomplete.

The first of these developments was the discovery of unusual reproductive systems within two species of *Messor* found in Europe, *M. barbarus* and *M. structor* (Norman et al., 2016; Romiguier et al., 2017). Population genetics analyses have revealed that these two species engage in social hybridogenesis, a hybridization-dependent reproductive system that was first described in the American harvester ants genus *Pogonomyrmex* (Helms Cahan et al., 2002). In social hybridogenesis, environmental caste determination (i.e., where female larvae differentiate into queens or workers depending on environmental conditions) is replaced by genetic caste determination, whereby larvae are determined to develop into either caste depending on their genetic makeup. More specifically, workers can only arise from F1 hybrid larvae, produced via sex with another species or lineage, while queens are always produced through intra-specific mating or parthenogenesis. Social hybridogenesis is relevant for taxonomy because ant species are often classified using worker morphology only. In cases where workers are F1 hybrids, this can lead to significant misunderstandings or omissions, as exemplified by the case of *M. barbarus*. This species is in fact composed of two divergent and genetically isolated lineages that share the same range and interact through *symmetrical* social hybridogenesis (Norman et al., 2016; Romiguier et al., 2017). Queens of each of these two lineages mate with males of the other lineage for worker production, and with males of their own lineage for queen production. Despite the existence of these two lineages, *M. barbarus* is still described as a single species, because workers produced by queens of both lineages have identical nuclear genomes (i.e., with one haplome from each lineage) and the same morphology. This demonstrates that a full taxonomic treatment of species with social hybridogenesis requires some understanding of their reproductive biology, and some knowledge about the biogeography of interacting genetic lineages. While substantial knowledge has been obtained for *M. barbarus* (Norman et al., 2016; Romiguier et al., 2017), *M. structor* remains understudied in this respect. Beyond the detection of social hybridogenesis in a few french specimens of *M. structor* (Romiguier et al., 2017), its distribution in the species is virtually unknown.

In addition to this lack of knowledge, the taxonomic situation of *M. structor* has recently evolved. Sampling and characterizing *M. structor* workers across Europe and Southwestern Asia, Steiner et al. (2018) have proposed to split *M. structor* into no less than 5 separate species with partially overlapping ranges. Following their proposition, we will from this point on refer to this whole group of species as *M. structor sensu lato*, and use the appropriate species names to refer to each of the five new species. These species are *M. ibericus* (found mostly in Southern Europe, from Spain to Greece), *M. ponticus* (found in the Balkans and on the west coast of the Black Sea), *M. structor* (which we will refer to as *M. structor sensu stricto*; found across all central Europe), *M. muticus* (found in Armenia and on the north coast of the Black Sea), and *M. macarthuri* (found in Greece and Turkey). While this new split is supported by several independent approaches including mitochondrial DNA phylogenetics, amplified fragment length polymorphism, morphometrics and niche modeling, previous reports of social hybridogenesis within *M. structor s.l.* were not addressed by Steiner et al. (2018). It is thus mostly unknown which of these five species display social hybridogenesis. In the worst case scenario, some of these species could even

be explained by regional variation in the reproductive system of one lineage (i.e., leading to variation in the hybrid status and phenotype of workers), as observed in *Pogonomyrmex* (Anderson et al., 2006). To characterize *M. structor s.l.* species accurately, it is necessary to link the results and descriptions of Steiner et al. (2018) with additional genomic data and information about the distribution of social hybridogenesis within the group.

In this study, we make a first attempt at drawing such a link. We collect as many *M. structor s.l.* specimens as possible (including specimens from Steiner et al., 2018) and produce the first genomic dataset of this group. With these data, we first produce a mitochondrial phylogeny of *M. structor s.l.*, identifying the species of origin of each new sample using reference samples from Steiner et al. (2018). Then, we use a F1 hybrid detection method developed in previous work (Weyna et al., 2021) to describe the phylogenetic distribution of social hybridogenesis within *M. structor s.l.*. Finally, we produce a draft phylogeny of non-hybrid members of the dataset using nuclear genes, and discuss our preliminary results in the context of social hybridogenesis.

Material and methods

Sampling and sequencing

We gathered specimens identified as *M. structor s.l.* from several sources (see table 1). Reference specimens for all five new species of *M. structor s.l.* (*M. ibericus*: 4 workers; *M. ponticus*: 2 workers; *M. structor s.s.*: 5 workers and 4 queens; *M. muticus*: 3 workers and 1 queen; *M. mearthuri*: 3 workers) were provided by the authors of their description. To these data were added non-identified *M. structor s.l.* specimens collected around Europe by several myrmecologists. Rumsaix Blatrix provided 1 male, 1 worker and 1 queen sampled in one colony from St-Gely-du-Fesc, France. Yannick Juvé provided 5 workers from 5 different colonies around Montpellier, France. Sergeï Yanov provided 6 workers from different locations in Bulgaria. Claude Lebas provided 2 queens and 3 workers from Greece, as well as 7 males, 6 workers and 13 queens from several locations of Pyrénées-Orientales in the south of France. Finally, Arthur Weyna, Jonathan Romiguier and Bernard Kaufmann collected 4 males 4 queens and 24 workers from several locations around Lyon, France, during a field mission. In most instance were queens could be collected on the field, they were sampled together with a worker of their own colony to insure that colony structure could be investigated. Finally, the resulting specimens were supplemented with 3 queens-and-daughter-worker pairs from Eastern Europe purchased online. DNA extraction and sequencing was performed for all specimens by Novogene on Hiseq-PE150 with high coverage (>50X). To the resulting sequencing data were added transcriptome sequencing data for 6 workers and 6 queens of *M. structor s.l.*, produced in the study that first reported social hybridogenesis in this group (Romiguier et al., 2017), and for 12 queens and 31 workers from France, produced in another study by the same authors (*not published*)

Mitochondrial and nuclear phylogenies

Raw sequencing reads were cleaned with *fastp v0.20.0* (Chen et al., 2018) to remove adapters, reads shorter than 40 bp, and reads with less than 70 percent of bases with a phred score below 20. Cleaned reads were then assembled using *MEGAHIT v1.1.3* (Li et al., 2015) with k-mer size spanning from 31 to 101 by steps of 10.

Nucleotidic sequences for 15 mitochondrial genes (including ATP6, ATP8, COX1, COX2, COX3, CYTB,

ND1, ND2, ND3, ND4, ND4L, ND5, ND6, rrnL and rrnS) were retrieved for each sample using *mitofinder v1.4* (Allio et al., 2020), following the tool’s authors guideline. Mitochondrial contigs were identified by blasting de-novo assemblies against the reference mitochondrial genomes of *Myrmica scabrinodis*, *Cardiocondyla obscurior*, *Solenopsis invicta*, *S. geminata*, *S. richteri*, *Atta laevigata* and *Wasmannia auropunctata*. tRNA annotation was performed on identified mitochondrial contigs using *MiTFI v0.1* (Jühling et al., 2012). After gene identification, multiple hits corresponding to different versions of the same gene within the same sample (i.e., contamination of NUMTs) were sorted manually to identified the “true” mitochondrial gene of each given sample. This was done by producing gene-wise draft phylogenies and removing outlying sequences.

Nucleotidic sequences for 5991 nuclear coding genes were retrieved for each sample using *BUSCO v5.1.2* (Manni et al., 2021). These genes correspond to 1-1 orthologs found across all Hymenoptera, as compiled in the *OrthoDB v10* database (Kriventseva et al., 2019). Within *BUSCO*, *Augustus v3.4.0* (Stanke & Waack, 2003) was used for gene prediction with a model pre-trained on the genome of *Acromyrmex echinator*. The resulting nuclear genes sequences, as well as mitochondrial genes sequences were concatenated into separate matrices using a custom python script. Phylogenetic reconstructions were achieved using *IQ-TREE* (Nguyen et al., 2015) with nucleotide substitution model GTR+I+F+G4. Node support was evaluated using 1000 iterations of ultra-fast bootstrap.

Detection of F1 hybrids

F1 hybrid detection was performed using a statistical method developed in a previous study (Weyna et al., 2021), extending on work by Takahata et al. (1995) and Yang (1997), which relies on the the distribution of heterozygosity across loci of a given sample. Briefly, this method partitions the heterozygosity of a F1 hybrid individual between two estimated parameters: heterozygosity due to divergence between the populations of origin of the focal individual’s parents γ , and the population mutation rate of the population ancestral to both parents θ . This is achieved essentially by comparing the observed distribution of heterozygosity across loci to an expected distribution assuming no divergence between the individual’s parental populations. This method is known to yield close-to-zero estimates of divergence γ when applied on non-hybrid individuals, and perceptibly higher estimates when applied on true F1 hybrids. However, because estimates of both parameters correlate with the heterozygosity of samples, it is best to rely on the ratio γ/θ which is not directly related to sample heterozygosity and is more comparable across samples. This ratio, similarly to γ , is expected to be close to zero in non-hybrids, and non-zero in F1 hybrids.

To obtain estimates of γ and θ , we applied the following procedure on each sample (described in more details in Weyna et al., 2021). Cleaned sequencing reads were first realigned to nuclear genes using *bwa v0.7.17* (Li & Durbin, 2009) with default settings. Following this step, *angsd v0.921* (Korneliussen et al., 2014) was used to obtain allelic substitutions counts from read alignment files. Finally, we obtained estimates of θ and γ through bayesian estimations, using the *R* package *rstan v2.21.2* (Stan Development Team, 2019; Stan Development Team, 2020) and uninformative priors spanning all realistic values for both parameters (i.e., uniform priors constrained between 0 and 0.2). The mean of the posterior distribution of each parameter was used as a point estimate, while credibility intervals where constructed from its 2.5% and 97.5% quantiles.

Unlike in previous uses of this F1 hybrids detection method (in Weyna et al., 2021 and first part of this chapter), the data treated here is both homogeneous and of good quality, as it was produced through deep sequencing of fresh samples from closely related species. This allowed for a more precise use of the method, using a more sensitive threshold in F1 hybrid detection. While a value of $\gamma/\theta > 1$ was employed

as a conservative decision threshold in previous work, here an inspection of the distribution of this ratio across all samples clearly showed that a value of $\gamma/\theta > 0.5$ separates clear-cut hybrids from non-hybrids (see figure 1A).

Results

Mitochondrial phylogeny and social hybridogenesis

Sequences for more than five mitochondrial genes could be retrieved for most samples, with 78 out of 164 samples counting all 15 genes (see table 1; one exception is a queen from Greece with only one COX1 sequence). This allowed for the reconstruction of a well supported mitochondrial phylogeny (figure 1), featuring all five species described by Steiner et al. (2018). Clades corresponding to these five species could readily be identified as the almost all samples were closely related to some of the reference specimens. Only two samples shared no recent ancestry with reference specimens. Specifically, one worker and one queen from the same Greek colony were found to form a sister group to all *M. structor s.s.*. Besides this unidentified lineage, the only qualitative difference between the mitochondrial phylogeny presented here and the COX1 phylogeny of Steiner et al. (2018) is the position of *M. mcarthuri*. While this species was previously found to be an outgroup to all other species of *M. structor s.l.*, our results suggest instead that it is more closely related to *M. ibericus* and *M. ponticus*. This alternative position is also found when constructing a phylogeny using only COX1 sequences (figure S1).

Besides relationships between species, this new sampling also confirms, and sometimes extends, the species ranges described by Steiner et al. (2018). *M. ibericus* was described to occur across Southern Europe, from Spain to Ukraine, with some populations being found as far north as Germany. New samples seem to confirm this distribution, and further suggest that it is the only species found in the deeply sampled South of France. *M. ponticus* was described as having a relatively small range, restricted to the Eastern Balkans and to the west coast of the Black Sea. One new sample collected in Ukraine slightly extends this range north. *M. structor s.s.* was already known to occur across all Central Europe, and we do not find any new samples outside this region. Likewise, new samples of *M. mcarthuri* all originated from regions (Greece and Crete) this species was already known to inhabit. Finally, *M. muticus* was previously found only in Armenia and in the North coast of the Black Sea. Two new samples seem to indicate that its range extends as far south as Israel. Even more unexpectedly, two samples purchased online, supposedly sampled in China, were found to share the same mitochondria as all other *M. muticus*. While misinformation by online retailers might explain this result, it could also represent our first available glimpse into the identity of East Asian *M. structor s.l.*

Using this new consistent phylogeny of *M. structor s.l.* together with F1 hybrids detection, we next positioned F1 hybrids in the group. F1 hybrid detection revealed very efficient in this settings, clearly separating F1 hybrids from other individuals (see figure 1A). With the exception of one *M. ponticus* worker from Bulgaria, all identified F1 hybrids belonged to *M. ibericus* (figure 1B). In fact, nearly all *M. ibericus* workers (72 out of 73), sampled from Spain to Montenegro, were F1 hybrids. As typically found in social hybridogenesis, all queens found alongside these F1 hybrid workers were not hybrids.

Nuclear phylogeny

Using sequences for 5991 genes, we next reconstructed the nuclear phylogeny of all non-hybrid samples in the dataset. Overall, this nuclear tree supported the same phylogenetic relationships between *M.*

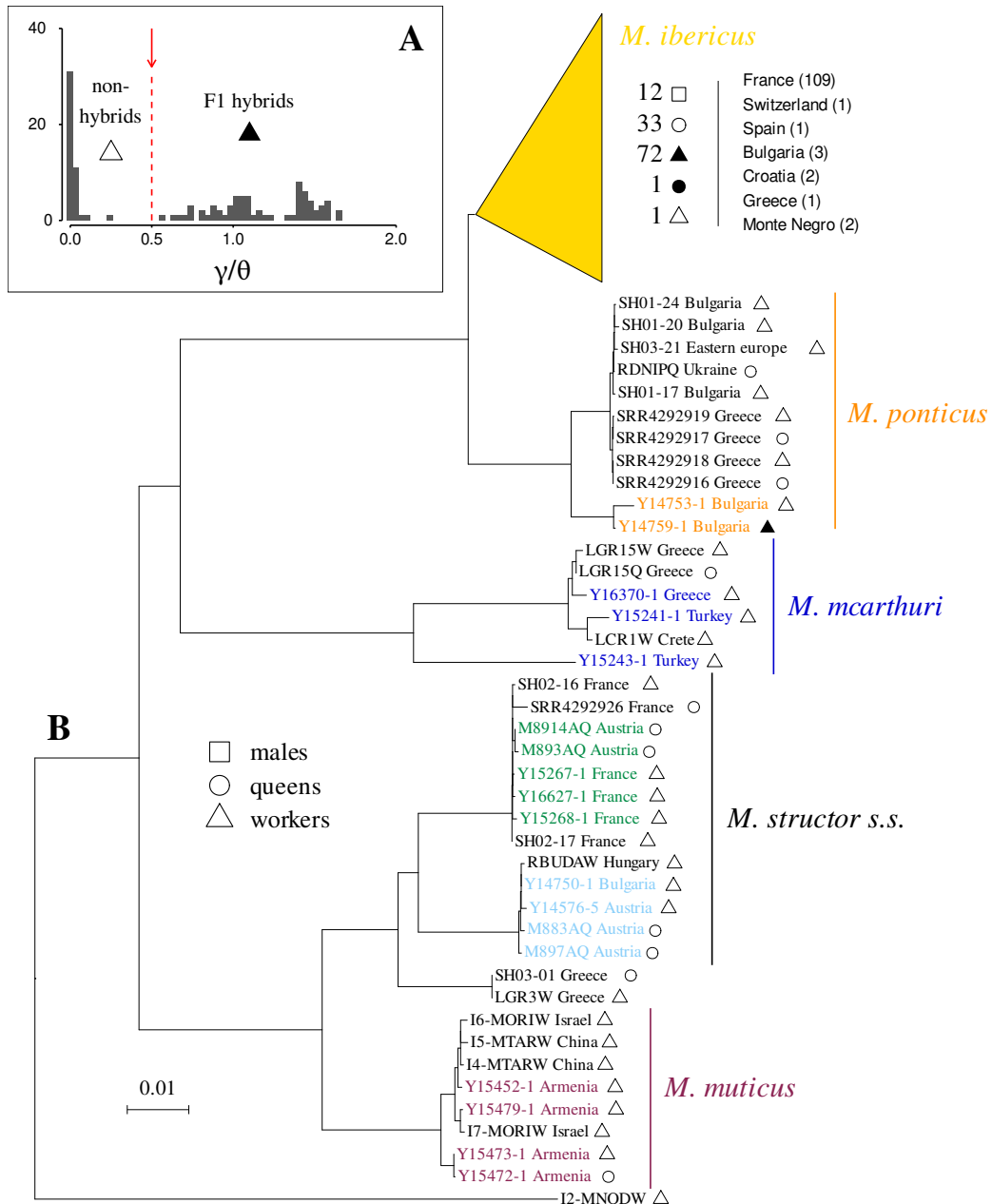


Figure 1: Distribution of social hybridogenesis in a mitochondrial phylogeny of *M. structor s.l.* **A.** Distribution of γ/θ across samples. The red arrow represents the chosen threshold (see methods) above which an individual is considered a F1 hybrid (filled symbol). **B.** Mitochondrial phylogeny reconstructed from 15 mitochondrial genes. Colored labels indicate reference samples from Steiner et al. (2018), used to identify clades as species. Green and light blue labels indicate samples from two lineages of *M. structor s.s.* described in the original study (i.e., lineage 3 and 4). The yellow triangle represent a clade composed of 119 very similar (i.e., median patristic distance in the group is 0.00063) individuals from Southern Europe (including 3 reference samples of *M. ibericus*). Symbols at the end of labels represent caste. All nodes between species have a support of 100%.

structor s.l. species as the previous mitochondrial tree. Yet a few individuals were found to display small to large mismatches between their nuclear and mitochondrial genomes. A queen from Montenegro and its daughter worker, which both possess *M. ibericus* mitochondria, grouped together as an outgroup to all other *M. ibericus* samples. Perhaps not so coincidentally, the daughter worker in this pair (RPODGW) was the only non-hybrid worker found that carried *M. ibericus* mitochondria. Two *M. structor s.s.* queens (M8914AQ and M893AQ) were found to have nuclear genomes of *M. structor s.s.* lineage 4 (light blue labels in fig 1), while having mitochondria of *M. structor s.s.* lineage 3 (green labels). Such mismatch was not unexpected as these two queens were sampled in a hybrid zone between the two lineages (as reported by Steiner et al., 2018). The last and most important mismatch observed between mitochondrial and nuclear genomes was found in 7 (out of 12) samples of French *M. ibericus* males. These males were sampled in populations and colonies where only *M. ibericus* queens could be found (based on both mitochondrial and nuclear data). They displayed typical *M. ibericus* mitochondria, but had completely different nuclear genomes, more closely related to *M. structor s.s.*

Discussion

Social hybridogenesis in *M. structor s.l.*

The present study produced key insights regarding the distribution of social hybridogenesis with *M. structor s.l.* Combining a mitochondrial phylogeny with F1 hybrids detection revealed that this reproductive system occurs exclusively in *M. ibericus* and across its entire range, from Spain to Bulgaria and as far north as Switzerland. This is evidence by the hallmark combination of F1 hybrid workers and non-hybrid queens occurring in the same populations, and in the same nests. The same pattern was not found in other species. While one F1 hybrid worker found in Bulgarian *M. ponticus* might suggest that some populations of this species engage in social hybridogenesis, a more exhaustive sampling will be necessary to reach any conclusions in this respect.

The observation that social hybridogenesis occurs across the whole range of *M. ibericus* helps explaining why this biological particularity could be overlooked in previous taxonomic descriptions. In the absence of contrasting non-hybrid workers, hybrid workers could not be identified without the adequate nuclear genomic data. In addition, because all *M. ibericus* workers are F1 hybrids, and all queens are non hybrids from the same lineage, morphological descriptions of both caste could be obtained without inconsistencies (Steiner et al., 2018). But social hybridogenesis should not be ignored in future taxonomic studies. We report that non-hybrid workers do occur in at least one population related to *M. ibericus*, found in the Balkans. These workers might display different morphological characteristics that, to our knowledge, still lack a description. Likewise, rare variation in the hybrid status of queens also seems to exist, as one F1 hybrid queen was sampled in France. F1 hybrids queens have been described before in *M. barbarus* (Norman et al., 2016). While their significance for social hybridogenesis is still debated (Darras & Aron, 2015; Kuhn et al., 2020), their occurrence might complicate taxonomic comprehension.

Reproductive biology of *M. ibericus*

Besides taxonomic implications, our results also raise several new questions regarding the reproductive biology of *M. ibericus*. In contrast to *M. barbarus* (Romiguier et al., 2017), populations of *M. ibericus* do not harbor two easily identifiable maternal lineages that interact through symmetrical social hybridogenesis. Instead, all sampled queens belonged to the same lineage, as evidence by both mitochondrial and

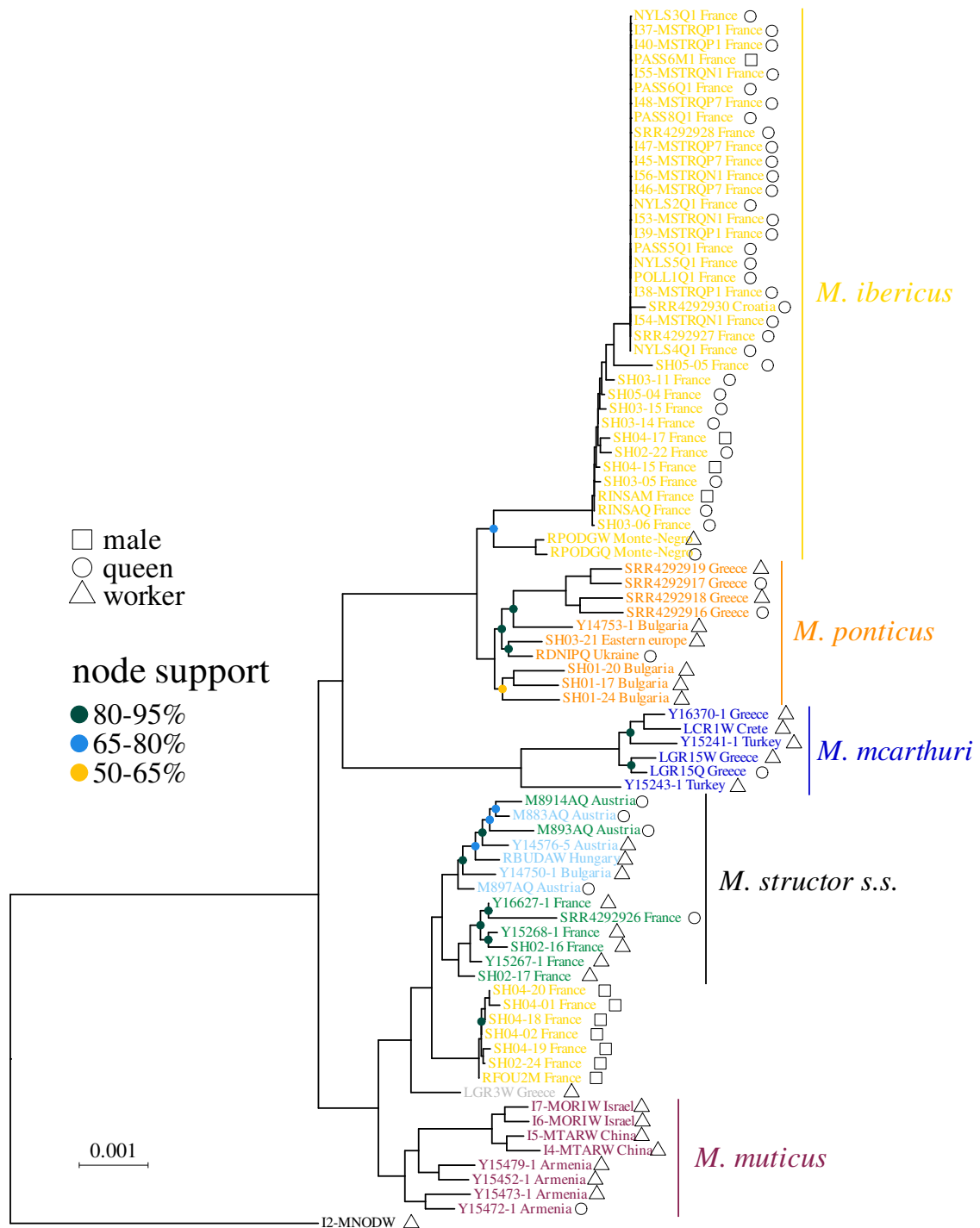


Figure 2: Nuclear phylogeny of *M. structor s.l.* Nuclear phylogeny reconstructed from 5991 genes. Colors in labels indicate species as identified from mitochondrial data (figure 1). Green and light blue labels indicate samples from two lineages of *M. structor s.s.* described in the original study (i.e., lineage 3 and 4).

nuclear phylogenies. In this respect, *M. ibericus* appears more similar to cases of *asymmetrical* social hybridogenesis, such as those found in two species of *Solenopsis* fire ants (Helms Cahan & Vinson, 2003; Lacy et al., 2019). As in these species, *M. ibericus* queens would mate with males of their own species (which were found in this study, see figure 2) for queen production, and with males of another “regular” (i.e., that does not engage in social hybridogenesis) species for worker production. Yet, as opposed to other known cases of asymmetrical social hybridogenesis, *M. ibericus* in a large part of its range does not co-occur with colonies of another male-providing species. In Mediterranean environments from Spain to Italy, only colonies of *M. ibericus* were found so far despite repeated field searches (which explains the very large sampling of Southern French populations). This initially appears as a conundrum, because the presence of a second species is strongly evidenced by large cohorts of F1 hybrid workers.

As a partial key to this puzzle, seven males were sampled in Southern France that could be representatives of the missing lineage. These males were found inside *M. ibericus* nests (i.e., with F1 hybrid workers and *M. ibericus* queens), had *M. ibericus* mitochondria, but had genomes more similar to that of *M. structor s.s.* While a formal proof is still lacking, the absence of alternative explanations make us believe that such males are in fact the fathers of *M. ibericus* workers. If this is the case, the next step in our comprehension of the reproductive biology of *M. ibericus* will be to understand how these males are produced. Because they possess *M. ibericus* mitochondria, and were recurrently found inside *M. ibericus* nests (where they were not attacked by workers), it is most probable that they were unmated males produced on site. We propose three competing hypotheses regarding their production.

First, it is possible that queens from a second lineage do exist in small proportion within *M. ibericus* nests (which are in fact polygynic), and were simply missed during sampling. We find this very unlikely, given that a total of 34 queens were sampled from different nests across the range of *M. ibericus*. Furthermore, such hypothesis would also require that these queens have acquired *M. ibericus* mitochondria through mitochondrial introgression. While mitochondrial introgression has been observed before in the context of social hybridogenesis (e.g., in *Cataglyphis*; Darras & Aron, 2015), it was never found in the more closely related *M. barbarus* (Norman et al., 2016; Romiguier et al., 2017). A second, more convoluted hypothesis would be that these haploid males are in fact produced by F1 hybrid workers, that in theory should possess the corresponding haplome. Male production by workers has been proven possible in *M. barbarus* (Romiguier et al., 2017). But for such system to maintain true F1 hybrid cohorts on the long term, as is observed, it would be required that workers somehow produce males without meiotic recombination, ensuring that males remain “pure” representatives of their lineage. Because this would probably require complex cytological mechanisms that to our knowledge have never been observed in ants, we do not favor this hypothesis.

Our last, preferred, hypothesis is that the reproductive system of *M. ibericus* resembles that of other species such as *Wasmannia auropunctata* (Fournier et al., 2005), *Vollenhovia emeyri* (Ohkawara et al., 2006) or *Paratrechina longicornis* (Pearcy et al., 2011). As in social hybridogenesis, queens of these species produce F1 hybrid workers via sex with genetically distant males. In contrast to social hybridogenesis however, these males belong to a divergent all-male lineage maintained by male clonality (i.e., *androgenesis*). Androgenesis, at least in *W. auropunctata*, is achieved through the exclusion of maternal genetic material from some ovules, which after fecundation only contain the male haplome (Rey et al., 2013). Because in this mechanism ovules still retain maternal mitochondria, we find it compatible with our finding of divergent males with *M. ibericus* mitochondria. Yet, androgenesis has also been suggested to be a by-product of female parthenogenesis in *W. auropunctata*, due to shared cytological mechanisms (Rey et al., 2013). It is not evident from our data that *M. ibericus* queens are able to reproduce through

female parthenogenesis. It could be argued that *M. ibericus* queens and males do display very low genetic diversity (as evidence by high genetic similarity across the whole species range; see figure 2 and figure S1), a traditional hallmark of clonality, but we also found several *M. ibericus* males, which suggest that this species does engage in intra-specific sexual reproduction.

Perspectives

Because the only potential fathers of F1 hybrid *M. ibericus* workers were found to belong to an evasive and potentially all-male lineage, we favor the hypothesis that social hybridogenesis in *M. ibericus* involves some form of androgenesis. Complementary analyses will be needed however to test this hypothesis, and to obtain a complete understanding of the reproductive biology of *M. ibericus*. First, it will be necessary to confirm that the presumed all-male lineage we described is also the one found in F1 hybrid workers. This will be possible through the implementation of phylogenetic analyses that account for worker haplotypes separately, using phased worker genomes. Such analyses are underway and will yield results in the near future. Next, it will be required to prove that androgenesis does occur in *M. ibericus*. We believe that this will be possible only through experimental rearing of *M. ibericus* colonies, controlling for queen identity and worker reproduction, as was done for *W. auropunctata* (Rey et al., 2013). Potential experimental designs are being discussed, but their implementation will certainly require long-term endeavor given the slow life cycle of *Messor* ants. Finally, it will be necessary to integrate all obtained results into a more fine-grain biogeographic analyses of *M. structor s.l.*, accounting for variable reproductive systems and potential inter-species gene flow. The multiplicity of species and genetic lineages in this group, together with their large overlapping ranges and variable reproductive systems, makes their study promising, but also very challenging.

Conclusion

This study represents a first attempt at describing the distribution and characteristics of social hybridogenesis within the *M. structor s.l.* species group. By producing the first large-scale genomic dataset for this group, we show that social hybridogenesis is found exclusively in *M. ibericus*, and across its entire range. This result carries some implications for taxonomy, but above all, opens the door for future studies of this still poorly understood hybridogenetic system. Such future studies have the potential to deliver new key insights into the evolution and maintenance of social hybridogenesis, because our results suggest that it takes a form that is quite distinct from what is known in the better understood *M. barbarus* system. In contrast to *M. barbarus*, social hybridogenesis in *M. ibericus* seems asymmetrical, and is likely to involve some form of male clonality. If this is confirmed, it would make *Messor* the first known genus where distinct forms of social hybridogenesis have evolved independently. In turn, this would make *Messor* a critical model for the understanding of the evolution of social hybridogenesis, and of the links between its many forms.

Id	Species	Caste	Country	Source	Mito. genes	Nuclear genes	He	γ/θ
PASS6M1	<i>ibericus</i>	male	France	C. Lebas	12	4097	0.0002	0.001
SH04-17	<i>ibericus</i>	male	France	C. Lebas	15	667	0.001	0.032
SH04-20	<i>ibericus</i>	male	France	C. Lebas	15	2645	0.0011	0.046
SH04-19	<i>ibericus</i>	male	France	C. Lebas	15	1507	0.0012	0.041
SH04-18	<i>ibericus</i>	male	France	C. Lebas	15	1485	0.0013	0.022
SH04-15	<i>ibericus</i>	male	France	C. Lebas	15	1981	0.001	0.016
SH04-16	<i>ibericus</i>	male	France	C. Lebas	15	58	0.0001	0.684
SH04-01	<i>ibericus</i>	male	France	Field mission	15	1269	0.0009	0.041
SH04-02	<i>ibericus</i>	male	France	Field mission	15	1972	0.0011	0.092
SH02-24	<i>ibericus</i>	male	France	R. Blatrix	15	2415	0.001	0.049
RINSAM	<i>ibericus</i>	male	France	Field mission	15	4954	0.0007	0.000
RFOU2M	<i>ibericus</i>	male	France	Field mission	14	4817	0.0007	0.000
I54-MSTRQN1	<i>ibericus</i>	queen	France	Romiguier <i>not pub.</i>	9	4073	0.0004	0.005
PASS5Q1	<i>ibericus</i>	queen	France	C. Lebas	12	4308	0.0003	0.001
I40-MSTRQP1	<i>ibericus</i>	queen	France	Romiguier <i>not pub.</i>	12	3850	0.0005	0.017
I46-MSTRQP7	<i>ibericus</i>	queen	France	Romiguier <i>not pub.</i>	11	4225	0.0004	0.005
I56-MSTRQN1	<i>ibericus</i>	queen	France	Romiguier <i>not pub.</i>	12	4055	0.0004	0.003
NYLS5Q1	<i>ibericus</i>	queen	France	C. Lebas	13	4328	0.0003	0.001
I48-MSTRQP7	<i>ibericus</i>	queen	France	Romiguier <i>not pub.</i>	9	4110	0.0004	0.007
I55-MSTRQN1	<i>ibericus</i>	queen	France	Romiguier <i>not pub.</i>	11	3901	0.0004	0.011
NYLS2Q1	<i>ibericus</i>	queen	France	C. Lebas	13	4325	0.0003	0.001
PASS6Q1	<i>ibericus</i>	queen	France	C. Lebas	14	4281	0.0002	0.001
PASS8Q1	<i>ibericus</i>	queen	France	C. Lebas	12	4359	0.0003	0.001
I37-MSTRQP1	<i>ibericus</i>	queen	France	Romiguier <i>not pub.</i>	13	4100	0.0005	0.004
I53-MSTRQN1	<i>ibericus</i>	queen	France	Romiguier <i>not pub.</i>	11	4140	0.0004	0.002
I39-MSTRQP1	<i>ibericus</i>	queen	France	Romiguier <i>not pub.</i>	13	4196	0.0004	0.002
I45-MSTRQP7	<i>ibericus</i>	queen	France	Romiguier <i>not pub.</i>	10	4149	0.0004	0.004
I38-MSTRQP1	<i>ibericus</i>	queen	France	Romiguier <i>not pub.</i>	12	4134	0.0004	0.005
I47-MSTRQP7	<i>ibericus</i>	queen	France	Romiguier <i>not pub.</i>	10	4093	0.0004	0.003
POLL1Q1	<i>ibericus</i>	queen	France	C. Lebas	11	4323	0.0003	0.001
NYLS3Q1	<i>ibericus</i>	queen	France	C. Lebas	12	4281	0.0003	0.001
SH03-08	<i>ibericus</i>	queen	France	C. Lebas	15	2367	0.0054	1.172
SH03-06	<i>ibericus</i>	queen	France	C. Lebas	15	2226	0.0011	0.038
SH03-15	<i>ibericus</i>	queen	France	C. Lebas	15	1325	0.0018	0.046
SH03-11	<i>ibericus</i>	queen	France	C. Lebas	15	1430	0.0015	0.015
SH03-05	<i>ibericus</i>	queen	France	C. Lebas	15	1142	0.0012	0.049
SRR4292930	<i>ibericus</i>	queen	Croatia	Romiguier et al. (2017)	13	4121	0.0003	0.002
SH03-14	<i>ibericus</i>	queen	France	Field mission	15	377	0.0018	0.052
SH02-22	<i>ibericus</i>	queen	France	R. Blatrix	15	841	0.001	0.035
RINSAQ	<i>ibericus</i>	queen	France	Field mission	15	4934	0.0007	0.001
SRR4292927	<i>ibericus</i>	queen	France	Romiguier et al. (2017)	14	3971	0.0003	0.001
SRR4292928	<i>ibericus</i>	queen	France	Romiguier et al. (2017)	13	4105	0.0002	0.001
SH05-04	<i>ibericus</i>	queen	France	Field mission	15	508	0.0015	0.044
SH05-05	<i>ibericus</i>	queen	France	Field mission	15	451	0.0016	0.076
NYLS4Q1	<i>ibericus</i>	queen	France	C. Lebas	10	4301	0.0003	0.001
RPODGQ	<i>ibericus</i>	queen	Montenegro	online purchase	14	4852	0.0012	0.001
I49-MSTRWN1	<i>ibericus</i>	worker	France	Romiguier <i>not pub.</i>	9	3523	0.0051	1.459
I59-MSTRWP8	<i>ibericus</i>	worker	France	Romiguier <i>not pub.</i>	9	3587	0.0051	1.565
I60-MSTRWN2	<i>ibericus</i>	worker	France	Romiguier <i>not pub.</i>	12	3613	0.0051	1.458
I58-MSTRWP6	<i>ibericus</i>	worker	France	Romiguier <i>not pub.</i>	13	3571	0.005	1.653
I25-MSTRWC1	<i>ibericus</i>	worker	France	Romiguier <i>not pub.</i>	12	3805	0.0052	1.451
I34-MSTRWP1	<i>ibericus</i>	worker	France	Romiguier <i>not pub.</i>	10	3506	0.0052	1.398
SRR4292924	<i>ibericus</i>	worker	France	Romiguier et al. (2017)	9	4668	0.0051	1.348
I29-MSTRWV	<i>ibericus</i>	worker	France	Romiguier <i>not pub.</i>	13	4132	0.0052	1.386
I63-MSTRWN5	<i>ibericus</i>	worker	France	Romiguier <i>not pub.</i>	9	3469	0.0051	1.463
I41-MSTRWP7	<i>ibericus</i>	worker	France	Romiguier <i>not pub.</i>	12	3376	0.0051	1.508
I33-MSTRWP1	<i>ibericus</i>	worker	France	Romiguier <i>not pub.</i>	14	3581	0.0051	1.448
I51-MSTRWN1	<i>ibericus</i>	worker	France	Romiguier <i>not pub.</i>	12	3696	0.0052	1.427
I57-MSTRWP5	<i>ibericus</i>	worker	France	Romiguier <i>not pub.</i>	10	3384	0.005	1.635
I36-MSTRWP1	<i>ibericus</i>	worker	France	Romiguier <i>not pub.</i>	13	3750	0.0052	1.395
I50-MSTRWN1	<i>ibericus</i>	worker	France	Romiguier <i>not pub.</i>	12	3545	0.0051	1.44
I44-MSTRWP7	<i>ibericus</i>	worker	France	Romiguier <i>not pub.</i>	14	3176	0.0052	1.527
I43-MSTRWP7	<i>ibericus</i>	worker	France	Romiguier <i>not pub.</i>	10	3795	0.0051	1.57
I42-MSTRWP7	<i>ibericus</i>	worker	France	Romiguier <i>not pub.</i>	10	3276	0.0051	1.531
I52-MSTRWN1	<i>ibericus</i>	worker	France	Romiguier <i>not pub.</i>	11	3819	0.0051	1.575
I35-MSTRWP1	<i>ibericus</i>	worker	France	Romiguier <i>not pub.</i>	12	3831	0.0052	1.401
SH05-03	<i>ibericus</i>	worker	France	C. Lebas	15	803	0.0045	0.575
I64-MSTRWPO	<i>ibericus</i>	worker	France	Romiguier <i>not pub.</i>	11	3614	0.0051	1.42
SRR4292923	<i>ibericus</i>	worker	France	Romiguier et al. (2017)	5	3924	0.0051	1.489
I30-MSTRWT	<i>ibericus</i>	worker	France	Romiguier <i>not pub.</i>	11	3712	0.0051	1.447
SRR4292925	<i>ibericus</i>	worker	France	Romiguier et al. (2017)	5	3925	0.0052	1.406
SH01-16	<i>ibericus</i>	worker	Bulgaria	Y. Yanov	14	1330	0.0051	1.06
I28-MSTRWF2	<i>ibericus</i>	worker	France	Romiguier <i>not pub.</i>	13	4252	0.0051	1.376

Table 1: Samples summary.

Id	Species	Caste	Country	Source	Mito. genes	Nuclear genes	He	γ/θ
I61-MSTRWN3	<i>ibericus</i>	worker	France	Romiguiier <i>not pub.</i>	12	3436	0.005	1.446
I27-MSTRWC3	<i>ibericus</i>	worker	France	Romiguiier <i>not pub.</i>	13	3841	0.0051	1.507
SH01-18	<i>ibericus</i>	worker	Bulgaria	Y. Yanov	14	2620	0.0053	1.059
SH03-09	<i>ibericus</i>	worker	France	C. Lebas	15	2604	0.0053	1.064
Y15609-1	<i>ibericus</i>	worker	Spain	Steiner et al. 2018	15	3926	0.0058	0.753
Y17671-1	<i>ibericus</i>	worker	Switzerland	Steiner et al. 2018	15	3988	0.0054	0.977
SH03-13	<i>ibericus</i>	worker	France	C. Lebas	15	2158	0.0049	1.003
SH03-12	<i>ibericus</i>	worker	France	C. Lebas	15	1874	0.0051	0.824
SH03-16	<i>ibericus</i>	worker	France	C. Lebas	15	1060	0.0044	0.707
SH03-07	<i>ibericus</i>	worker	France	C. Lebas	15	1531	0.0044	1.045
Y14133-1	<i>ibericus</i>	worker	Croatia	Steiner et al. 2018	15	3985	0.0055	0.914
SH01-19	<i>ibericus</i>	worker	Bulgaria	Y. Yanov	15	1317	0.0049	0.988
SH02-07	<i>ibericus</i>	worker	France	Field mission	15	2960	0.0051	1.213
SH02-14	<i>ibericus</i>	worker	France	Field mission	15	3094	0.0055	1.099
SH02-12	<i>ibericus</i>	worker	France	Field mission	15	3293	0.0054	1.051
SH01-13	<i>ibericus</i>	worker	France	Y. Juvé	15	2662	0.0047	1.034
SH02-13	<i>ibericus</i>	worker	France	Field mission	15	2154	0.0053	0.869
SH01-05	<i>ibericus</i>	worker	France	Field mission	15	1230	0.0045	0.65
SH01-11	<i>ibericus</i>	worker	France	Y. Juvé	15	2955	0.005	1.081
SH02-15	<i>ibericus</i>	worker	France	Field mission	15	3045	0.0055	1.205
SH01-04	<i>ibericus</i>	worker	France	Field mission	15	1668	0.005	0.803
SH02-11	<i>ibericus</i>	worker	France	Field mission	15	2837	0.0056	1.072
SH01-10	<i>ibericus</i>	worker	France	Y. Juvé	15	2175	0.0047	0.895
RMUR1W	<i>ibericus</i>	worker	France	Field mission	15	4046	0.0055	1.007
SH01-09	<i>ibericus</i>	worker	France	Y. Juvé	15	1015	0.0046	0.633
SH01-06	<i>ibericus</i>	worker	France	Field mission	15	3323	0.0057	1.143
SH01-03	<i>ibericus</i>	worker	France	Field mission	15	427	0.0041	0.707
SH01-02	<i>ibericus</i>	worker	France	Field mission	15	3550	0.0054	1.097
SH02-21	<i>ibericus</i>	worker	France	Field mission	15	1463	0.005	0.936
SH02-19	<i>ibericus</i>	worker	France	Field mission	15	1773	0.0051	0.861
SH05-01	<i>ibericus</i>	worker	France	Field mission	15	1495	0.0051	0.728
SH02-18	<i>ibericus</i>	worker	France	Field mission	15	605	0.0061	0.24
I14-MSTRW	<i>ibericus</i>	worker	France	Romiguiier <i>not pub.</i>	14	3706	0.0051	1.39
SH02-23	<i>ibericus</i>	worker	France	R. Blatrix	15	1673	0.0048	0.869
SH01-07	<i>ibericus</i>	worker	France	Field mission	15	2762	0.005	1.002
RINSAW	<i>ibericus</i>	worker	France	Field mission	14	4060	0.0055	1.015
SH02-08	<i>ibericus</i>	worker	France	Field mission	14	3488	0.0056	1.116
SRR4292929	<i>ibericus</i>	worker	France	Romiguiier et al. (2017)	14	3762	0.005	1.386
SH01-12	<i>ibericus</i>	worker	France	Y. Juvé	14	179	0.0044	0.588
SH02-09	<i>ibericus</i>	worker	France	Field mission	15	851	0.0048	0.751
SH01-01	<i>ibericus</i>	worker	France	Field mission	15	1639	0.005	0.842
SH02-10	<i>ibericus</i>	worker	France	Field mission	15	3311	0.0055	1.09
I26-MSTRWC2	<i>ibericus</i>	worker	France	Romiguiier <i>not pub.</i>	11	3864	0.0054	1.552
I62-MSTRWN4	<i>ibericus</i>	worker	France	Romiguiier <i>not pub.</i>	11	3133	0.005	1.581
RPODGW	<i>ibericus</i>	worker	Montenegro	online purchase	14	4800	0.0013	0.001
Y15420-1	<i>ibericus</i>	worker	Greece	Steiner et al. 2018	15	4002	0.0054	0.988
RDNIPQ	<i>ponticus</i>	queen	Ukraine	online purchase	15	4805	0.0015	0.001
SRR4292916	<i>ponticus</i>	queen	Greece	Romiguiier et al. (2017)	14	3566	0.0017	0.159
SRR4292917	<i>ponticus</i>	queen	Greece	Romiguiier et al. (2017)	12	4411	0.0017	0.224
Y14759-1	<i>ponticus</i>	worker	Bulgaria	Steiner et al. 2018	15	3993	0.0054	1.022
Y14753-1	<i>ponticus</i>	worker	Bulgaria	Steiner et al. 2018	15	4737	0.0018	0.003
SH01-20	<i>ponticus</i>	worker	Bulgaria	Y. Yanov	10	432	0.0024	0.054
SH01-24	<i>ponticus</i>	worker	Bulgaria	Y. Yanov	15	1589	0.0021	0.164
SH03-21	<i>ponticus</i>	worker	East Europe	online purchase	15	2332	0.0018	0.146
SH01-17	<i>ponticus</i>	worker	Bulgaria	Y. Yanov	15	2197	0.0026	0.223
SRR4292918	<i>ponticus</i>	worker	Greece	Romiguiier et al. (2017)	14	3723	0.0017	0.152
SRR4292919	<i>ponticus</i>	worker	Greece	Romiguiier et al. (2017)	13	4298	0.0017	0.206
LGR15Q	<i>mcarthuri</i>	queen	Greece	C. Lebas	15	4884	0.0008	0.001
LGR15W	<i>mcarthuri</i>	worker	Greece	C. Lebas	14	4792	0.0015	0.001
Y16370-1	<i>mcarthuri</i>	worker	Greece	Steiner et al. 2018	14	4880	0.0014	0.001
LCR1W	<i>mcarthuri</i>	worker	Crete	C. Lebas	15	4809	0.0018	0.077
Y15241-1	<i>mcarthuri</i>	worker	Turkey	Steiner et al. 2018	15	4842	0.0018	0.001
Y15243-1	<i>mcarthuri</i>	worker	Turkey	Steiner et al. 2018	15	4791	0.0019	0.001
M883AQ	<i>structor s.s.</i>	queen	Austria	Steiner et al. 2018	14	4689	0.0015	0.002
M897AQ	<i>structor s.s.</i>	queen	Austria	Steiner et al. 2018	14	4573	0.0016	0.003
M893AQ	<i>structor s.s.</i>	queen	Austria	Steiner et al. 2018	14	4685	0.0018	0.025
M8914AQ	<i>structor s.s.</i>	queen	Austria	Steiner et al. 2018	14	4495	0.0018	0.047
SRR4292926	<i>structor s.s.</i>	queen	France	Romiguiier et al. (2017)	14	4183	0.0005	0.002
Y14750-1	<i>structor s.s.</i>	worker	Bulgaria	Steiner et al. 2018	15	4625	0.0016	0.001
RBUDAW	<i>structor s.s.</i>	worker	Hungary	online purchase	14	4670	0.0017	0.004
Y14576-5	<i>structor s.s.</i>	worker	Austria	Steiner et al. 2018	15	4569	0.0017	0.003
SH02-16	<i>structor s.s.</i>	worker	France	Field mission	15	882	0.0014	0.023
Y16627-1	<i>structor s.s.</i>	worker	France	Steiner et al. 2018	15	4851	0.0009	0.000

Table 1: Samples summary.

Id	Species	Caste	Country	Source	Mito. genes	Nuclear genes	He	γ/θ
Y15267-1	<i>structor s.s.</i>	worker	France	Steiner et al. 2018	15	4831	0.001	0.000
Y15268-1	<i>structor s.s.</i>	worker	France	Steiner et al. 2018	15	4801	0.0011	0.000
SH02-17	<i>structor s.s.</i>	worker	France	Field mission	15	3823	0.0012	0.042
SH03-01	<i>structor ?</i>	queen	Greece	C. Lebas	1	52	0.000	0.944
LGR3W	<i>structor ?</i>	worker	Greece	C. Lebas	15	1295	0.0016	0.217
Y15472-1	<i>muticus</i>	queen	Armenia	Steiner et al. 2018	14	4497	0.0025	0.112
I7-MORIW	<i>muticus</i>	worker	Israel	Romiguier <i>not pub.</i>	9	3838	0.0011	0.111
Y15479-1	<i>muticus</i>	worker	Armenia	Steiner et al. 2018	15	4671	0.0018	0.002
I4-MTARW	<i>muticus</i>	worker	China	Romiguier <i>not pub.</i>	9	4036	0.0012	0.103
I5-MTARW	<i>muticus</i>	worker	China	Romiguier <i>not pub.</i>	8	3431	0.0013	0.225
I6-MORIW	<i>muticus</i>	worker	Israel	Romiguier <i>not pub.</i>	10	3669	0.0012	0.181
Y15452-1	<i>muticus</i>	worker	Armenia	Steiner et al. 2018	15	4627	0.0019	0.006
Y15473-1	<i>muticus</i>	worker	Armenia	Steiner et al. 2018	15	4589	0.0022	0.007

Table 1: Samples summary. The table summarizes sample information, including species, caste, country of origin and source (i.e., collector or original study). The last four columns give the number of mitochondrial and nuclear genes obtained for each sample, the mean observed heterozygosity across nuclear genes, and the estimated γ/θ ratio. Bold values are greater than 0.5, indicating F1 hybrids (see methods).

References

- Allio, R., A. Schomaker-Bastos, J. Romiguier, F. Prosdocimi, B. Nabholz, and F. Delsuc (2020). MitoFinder: Efficient automated large-scale extraction of mitogenomic data in target enrichment phylogenomics. *Mol. Ecol. Resour.*, 20, 892–905.
- Anderson, K. E., J. Gadau, B. M. Mott, R. A. Johnson, A. Altamirano, C. Strehl, et al. (2006). Distribution and evolution of genetic caste determination in *Pogonomyrmex* seed-harvester ants. *Ecology*, 87, 2171–2184.
- Bolton, B. (1984). Afrotropical species of the myrmicine ant genera *Cardiocondyla*, *Leptothorax*, *Melissotarsus*, *Messor* and *Cataulacus* (Formicidae). *Bul. Br. Mus. Nat. Hist. (Entomol.)*, 45, 307–370.
- Bolton, B. (1995). A new general catalogue of the ants of the world. The Belknap Press of Harvard University Press, Cambridge, MA, p. 504.
- Chen, S., Y. Zhou, Y. Chen, and J. Gu (2018). Fastp: An ultra-fast all-in-one FASTQ preprocessor. *Bioinformatics*, 34, i884–i890.
- Darras, H. and S. Aron (2015). Introgression of mitochondrial DNA among lineages in a hybridogenetic ant. *Biol. Lett.*, 11, 1–4.
- Fournier, D., A. Estoup, J. Orivel, J. Foucaud, H. Jourdan, J. Le Breton, et al. (2005). Clonal reproduction by males and females in the little fire ant. *Nature*, 435, 1230–1234.
- Helms Cahan, S., J. D. Parker, S. W. Rissing, R. A. Johnson, T. S. Polony, M. D. Weiser, et al. (2002). Extreme genetic differences between queens and workers in hybridizing *Pogonomyrmex* harvester ants. *Proc. R. Soc. B Biol. Sci.*, 269, 1871–1877.
- Helms Cahan, S. and S. B. Vinson (2003). Reproductive division of labor between hybrid and nonhybrid offspring in a fire ant hybrid zone. *Evolution (N. Y.)*, 57, 1562–1570.
- Jühling, F., J. Pütz, M. Bernt, A. Donath, M. Middendorf, C. Florentz, et al. (2012). Improved systematic tRNA gene annotation allows new insights into the evolution of mitochondrial tRNA structures and into the mechanisms of mitochondrial genome rearrangements. *Nucleic Acids Res.*, 40, 2833–2845.
- Korneliussen, T. S., A. Albrechtsen, and R. Nielsen (2014). ANGSD: Analysis of Next Generation Sequencing Data. *BMC Bioinformatics*, 15, 1–13.
- Kriventseva, E. V., D. Kuznetsov, F. Tegenfeldt, M. Manni, R. Dias, F. A. Simão, et al. (2019). OrthoDB v10: Sampling the diversity of animal, plant, fungal, protist, bacterial and viral genomes for evolutionary and functional annotations of orthologs. *Nucleic Acids Res.*, 47, D807–D811.
- Kuhn, A., H. Darras, O. Paknia, and S. Aron (2020). Repeated evolution of queen parthenogenesis and social hybridogenesis in *Cataglyphis* desert ants. *Mol. Ecol.*, 29, 549–564.
- Lacy, K. D., D. Shoemaker, and K. G. Ross (2019). Joint evolution of asexuality and queen number in an ant. *Curr. Biol.*, 29, 1394–1400.
- Li, H. and R. Durbin (2009). Fast and accurate short read alignment with Burrows-Wheeler transform. *Bioinformatics*, 25, 1754–1760.
- Li, D., C. M. Liu, R. Luo, K. Sadakane, and T. W. Lam (2015). MEGAHIT: An ultra-fast single-node solution for large and complex metagenomics assembly via succinct de Bruijn graph. *Bioinformatics*, 31, 1674–1676.
- Manni, M., M. R. Berkeley, M. Seppey, F. A. Simão, and E. M. Zdobnov (2021). BUSCO update: Novel and streamlined workflows along with broader and deeper phylogenetic coverage for scoring of eukaryotic, prokaryotic, and viral genomes. *Mol. Biol. Evol.*, 1–8.
- Nguyen, L. T., H. A. Schmidt, A. Von Haeseler, and B. Q. Minh (2015). IQ-TREE: A fast and effective stochastic algorithm for estimating maximum-likelihood phylogenies. *Mol. Biol. Evol.*, 32, 268–274.

- Norman, V., H. Darras, C. Tranter, S. Aron, and W. O. H. Hughes (2016). Cryptic lineages hybridize for worker production in the harvester ant *Messor barbarus*. *Biol. Lett.*, 12, 1–5.
- Ohkawara, K., M. Nakayama, A. Satoh, A. Trindl, and J. Heinze (2006). Clonal reproduction and genetic caste differences in a queen-polymorphic ant, *Vollenhovia emeryi*. *Biol. Lett.*, 5, 359–363.
- Pearcy, M., M. A. D. Goodisman, and L. Keller (2011). Sib mating without inbreeding in the longhorn crazy ant. *Proc. R. Soc.*, 278, 2677–2681.
- Rey, O., B. Facon, J. Foucaud, A. Loiseau, and A. Estoup (2013). Androgenesis is a maternal trait in the invasive ant *Wasmannia auropunctata*. *Proc. R. Soc. B Biol. Sci.*, 280, 1–7.
- Romiguier, J., A. Fournier, S. H. Yek, and L. Keller (2017). Convergent evolution of social hybridogenesis in *Messor* harvester ants. *Mol. Ecol.*, 26, 1108–1117.
- Santschi, F. (1917). Races et variétés nouvelles du *Messor barbarus* L. *Bull. Soc. Hist. Nat. Afr. Nord*, 8, 89–94.
- Santschi, F. (1923). *Messor* et autres fourmis paléarctiques. *Rev. Suisse Zool.*
- Santschi, F. (1927). Revision des *Messor* du groupe *instabilis* Sm. *Bol. R. Soc. Esp. Hist. Nat.*, 27, 225–250.
- Stanke, M. and S. Waack (2003). Gene prediction with a hidden Markov model and a new intron submodel. *Bioinformatics*, 19, 215–225.
- Stan Development Team (2019). Stan Modeling Language Users Guide and Reference Manual, 2.17.
- Stan Development Team (2020). RStan: the R interface to Stan. R package version 2.21.2.
- Steiner, F. M., S. Csősz, B. Markó, A. Gamisch, L. Rinnhofer, C. Folterbauer, et al. (2018). Turning one into five: Integrative taxonomy uncovers complex evolution of cryptic species in the harvester ant *Messor* “*structor*”. *Mol. Phylogenet. Evol.*, 127, 387–404.
- Takahata, N., Y. Satta, and J. Klein (1995). Divergence time and population size in the lineage leading to modern humans. *Theor. Popul. Biol.*, 48, 198–221.
- Weyna, A., L. Bourouina, N. Galtier, and J. Romiguier (2021). Detection of F1 hybrids from single-genome data reveals frequent hybridization in Hymenoptera and particularly ants. *submitted to Molecular Biology and Ecology*.
- Yang, Z. (1997). On the estimation of ancestral population sizes of modern humans. *Genet. Res.*, 69, 111–116.

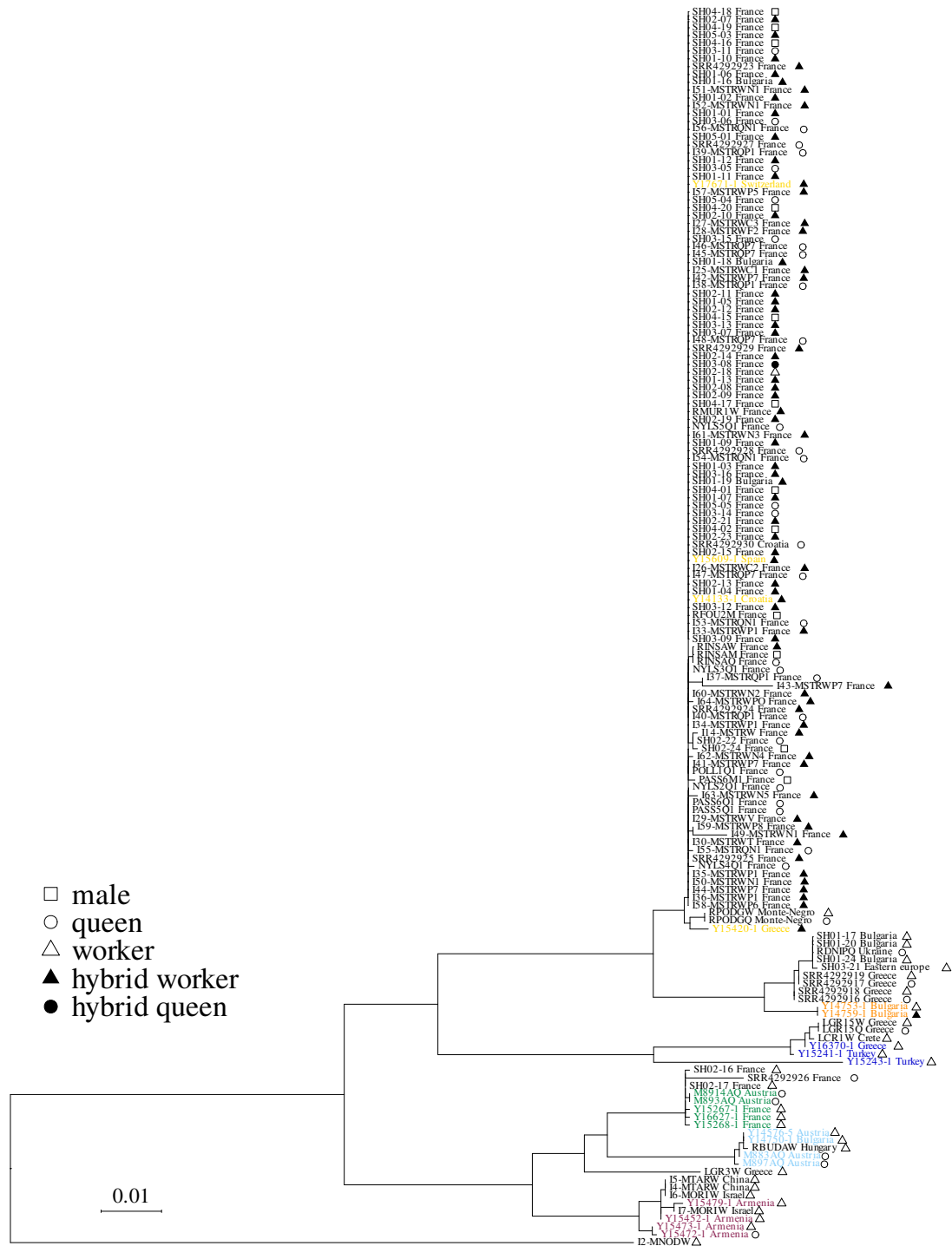


Figure S1: Phylogeny of *M. structor s.l.* using mitochondrial gene COX1. Colored labels indicate reference samples from Steiner et al. (2018), used to identify clades as species. Green and light blue labels indicate samples from two lineages of *M. structor s.s.* described in the original study (i.e., lineage 3 and 4). Symbols at the end of labels represent caste. All nodes between species have a support of 100%.

Discussion

A general evolutionary path towards social hybridogenesis ?

In chapter 1 of this thesis, we have shown that a combination of strong genetic caste determination (GCD) and hybridization by queens for worker production (i.e., social hybridogenesis) can arise from ancestral environmental caste determination (ECD) in a deterministic manner, even if hybridization is costly. In this section, I summarize the rationale behind this result and discuss its generality and limits.

The uncovered mechanism for social hybridogenesis evolution is an arms race, fueled by a very general and mostly inevitable conflict between developing larvae and their queen mother over the fraction of new workers and queens produced across the lifetime of a colony. In eusocial colonies, the realized worker-queen caste-ratio (similarly to the much more studied sex-ratio) is typically at the center of a multi-party conflicts involving the laying queens, adult workers and developing larvae (Bourke & Chan, 1999; Bourke & Ratnieks, 1999; Dobata, 2012; Ratnieks & Wenseleers, 2008; Reuter & Keller, 2011). Because these different actors do not share the same relatedness with a given, yet undifferentiated female larvae, they have conflicting interests regarding the proportion of larvae that access the reproductive and helping castes. In particular, developing larvae are predicted to prefer a lower worker-queen caste-ratio (i.e., more queens) because there are most related to themselves, and thus profit the most from accessing to the reproductive caste (Reuter & Keller, 2011). If larvae can control at least part of their development (i.e., in the absence of complete coercion by adults; Dobata, 2012; Ratnieks & Wenseleers, 2008), this is predicted to drive the realized caste-ratio downward and away from the queen-wise optimum. In the eventuality where queens can hybridize, and if F1 hybrid larvae have a higher probability to develop as workers (i.e., due to hybrid incompatibilities), then a likely response by queens will be to hybridize in order to realign caste-ratio to their own interest. This new supply of worker-destined individuals however will only further reduce the needs for regular larvae to develop into workers, as these are less and less needed to maintain colonies. On the long term, this conflict can lead to social hybridogenesis, where all workers are produced via hybridization, and all non-hybrid larvae develop into queens.

We have shown that the proposed mechanism is expected even in cases where hybridization and strong GCD come at a high cost for colonial fitness, which is consistent with the lack of evidence for heterosis in hybridizing ants (Feldhaar et al., 2008; James et al., 2002; Julian & Cahan, 2006; Ross & Robertson, 1990). In such situations, social hybridogenesis could be interpreted as a tragedy of the commons, that is as an inevitable evolutionary ending-point that is detrimental to all involved parties (Rankin et al., 2007). This mechanism might thus help explain why many convergences towards this reproductive system have occurred in ants, despite the variety of obvious costs it entails. In our analysis, such costs to hybridization can be of various origins. First, and perhaps most importantly, costs to hybridization can arise from hybrid depression in workers and reduced colony productivity, due to hybrid incompatibilities. In principle, incompatibilities can affect any component of phenotype and fitness. For instance,

incompatibilities could be expressed in larvae in the form of increased fluctuating asymmetry (Ross & Robertson, 1990), decreased ability to differentiate into sub-castes (Lillico-Ouachour & Abouheif, 2017), or decreased ability to communicate with adult members of the colony (leading to sub-optimal larval nutrition; Kaptein et al., 2005). Alternatively, hybrid incompatibilities may be expressed during adult life, in the form of reduced communication abilities (Julian & Cahan, 2006) or impaired metabolism (James et al., 2002). Besides hybrid incompatibilities, costs to hybridization and strong GCD may arise from various life-history constraints. In cases where queen cannot reproduce through thelytokous parthenogenesis, strong GCD forces queens to mate with both con- and inter-specific males. This is expected to increase the cost of mate searching for queens, especially if dependent lineages do not fully share phenological parameters, or if the local abundance of suitable inter-specific mates is limited by male-male competition (Davidson, 1982) or local population structure (Kuhn et al., 2017). In natural populations, many queens may fail to mate appropriately and never found colonies (Helms Cahan et al., 2004), leading to further fitness costs. Finally, strong GCD and the loss of developmental plasticity creates net costs in the form of increased rates of larval abortion. Because queens cannot directly control the proportion of hybrid and non-hybrid eggs they lay, queen-destined non-hybrid eggs are constantly produced even outside periods of sexual brood production. This may be seen as marginal in productive mature colonies, but was shown to impose significant energetic constraints on founding queens (Schwander et al., 2006).

Another important argument in favor of the generality of the proposed mechanism is that its principle is compatible to all known cases and forms of social hybridogenesis. At its core, the analyzed model is asymmetric, and considers only the evolution of one lineage, without making assumption about the evolution of the second male-providing lineage. For this reason, it is mostly compatible with asymmetrical social hybridogenesis. But there are no fundamental reasons to believe that such evolutionary path could not be walked in parallel by two lineages that have come in contact. In fact, it could be argued that in most instances where conditions allow for the evolution of strong GCD in one lineage, there is a great probability that these conditions are also met within the second. In particular, the phenological, morphological and behavioral compatibility between sexuals of two lineages should in general go both ways. According to our model, symmetrical social hybridogenesis would thus be the result of the independent evolution of two hybridogenetic systems in mirror. Known cases of asymmetrical social hybridogenesis, for their part, would correspond to situations where initial contacts between sexuals was in fact asymmetrical (see Purcell et al., 2016 for an example of asymmetrical hybridization in *Formica* ants). Alternatively, the existence of symmetrical social hybridogenesis may be explained by additional mechanisms that promote the tandem evolution of strong GCD in lineage pairs. As suggested in early models, gene flow within lineage pairs may lead to the introgression of caste biasing alleles from one lineage to another (Anderson et al., 2006; Volny & Gordon, 2002). In such scenario, strong GCD would be initiated in one lineage, before quickly spreading to the other. As was also envisioned in previous literature, hybridization within a species group and the transmission of caste-biasing alleles may even lead to the birth on entirely new hybridogenetic

systems (Anderson et al., 2006). Such a spread of strong GCD across species could help explain multiple convergences towards social hybridogenesis in *Cataglyphis*, *Pogonomyrmex* and *Messor*. In the course of this thesis, we have conducted analyses that aimed at detecting gene-flow within and across *Messor* hybridogenetic lineages, using an approximate bayesian computation approach (Fraïsse et al., 2021) and the data presented in part 2 of chapter 3. These analyses (conducted by François Monnet, an intern under the supervision of J. Romiguier and myself), produced intriguing preliminary results suggesting an absence of gene flow between *M. barbarus* dependent lineages, but high probability for ancestral gene flow between both *M. barbarus* lineages and *M. ibericus*. These results might suggest that the evolution of social hybridogenesis in these species is not so independent after all. These results however, also suffered from technical limitations and will have to be replicated and refined before any conclusion can be reached. Overall, whether gene flow is generally involved in the evolution of social hybridogenesis is still to be determined.

The last argument in favor of the generality of the proposed evolutionary path is that it can be triggered even in the absence of initial hybridization. As long as larvae drive worker-queen caste-ratio downwards, queens are expected to be under selective pressure to hybridize. Under this argument, hybridization could thus be seen as a secondary queen adaptation in response to intra-colonial conflicts, and does not require any introgression event between interacting species. I believe that this makes the proposed mechanism significantly more parsimonious than the epistasis-based evolutionary scenarii found in the literature, which assume complicated histories of ancestral hybridization and introgression (Helms Cahan & Keller, 2003; Linksvayer et al., 2006). But this also raises questions regarding the evolution and maintenance of social hybridogenesis when genetic material is exchanged between dependent lineages, as documented in *Cataglyphis* (Darras & Aron, 2015; Eyer et al., 2016). One important limit to our model is that it relies on the assumption that F1 hybrids are more likely to develop into workers, and cannot develop into fertile queens due to hybrid incompatibilities. In the eventuality of gene flow, genetic introgression may lead to the break-up of such incompatibilities, both promoting further gene flow and reducing the reliability of hybridization as source of workers. Moreover, it remains largely unclear how gene flow would act on intra-colonial conflicts and larval development, and if it would allow for social hybridogenesis to evolve under our proposed scenario. It is unlikely that these questions will be answered until a better understanding of the genetic basis of caste developmental plasticity is obtained. Beyond social hybridogenesis, it is interesting to note that the described incentive for queen to hybridize does not always lead to full-on social hybridogenesis in our model. Under some conditions (e.g., low polyandry, which seems to be the norm in ants; Hughes et al., 2008; Strassmann, 2001), hybridization can be employed as part of a stable mixed strategy, where non-hybrid larvae still retain some level of developmental plasticity. This may help in explaining the high frequency of hybridization in ants, reported in both previous literature (Feldhaar et al., 2008) and chapter 2 of this thesis.

Insights into the determinants of social hybridogenesis

If, as proposed in this work, social hybridogenesis often reduces average fitness within population but is nonetheless expected to evolve in many configurations, it is important to understand which characteristics of species favour such evolution or, conversely, shield species from it. In this section, I discuss the insights gained via modeling and empirical results regarding such characteristics.

Perhaps the most important facilitator for the evolution of social hybridogenesis is polyandry. When queens cannot reproduce via thelytokous parthenogenesis, polyandry is obviously essential due to the necessity for queens to mate with at least two males. A high level of polyandry should also reduce the risk for hybridogenetic queens to mate with only one type of male. But the facilitating effect of polyandry is probably even more general. As discovered in chapter 1 of this thesis, high polyandry rates may be predicted to further facilitate transitions towards strong GCD because it increases the relative advantage of caste biasing alleles by reducing relatedness between developing larvae. In accordance with these predictions, several known cases of social hybridogenesis occur in highly polyandric ants, such as *Pogonomyrmex* or *Messor*. In chapter 2 of this thesis, we also found several candidate F1 hybrids in other ant groups that are notorious for their high level of polyandry, such as leaf-cutting ants (tribe Attini; Keller & Reeve, 1994; Strassmann, 2001) and army ants (Dorylinae; Barth et al., 2014). This finding adds support to the idea that polyandry plays a key role in the evolution of hybridization and social hybridogenesis. One remaining question however, that was not addressed in our modeling work, is that of the evolution of polyandry following transition towards social hybridogenesis. It could be predicted that hybridogenesis produces additional selective pressure in favor of high polyandry rates, as it would further buffer the risks associated with dependence to hybridization. Polyandry however has its own costs, such as increased energetic expenditure by mating queens or increased vulnerability to predators and pathogens (Strassmann, 2001). Increased contact with pathogens, in particular, was shown to induce elevated immune responses in founding queen, which may impact the viability of stored sperm (Castella et al., 2009; Chérasse & Aron, 2018). In addition, high polyandry rates can be predicted to promote male-male competition (Pearcy et al., 2014), which could affect kinship structure within nests in unknown ways. Overall, it thus remains largely unknown how realized mating frequency would respond to the evolution of hybridogenesis. Another related question, also unaccounted for in our model, is that of the possible role of polygyny. As evidenced by empirical observations in *Solenopsis* (Helms Cahan & Vinson, 2003), polygyny makes social hybridogenesis possible under monandry, by allowing for colony co-founding by inter- and intra-specifically mated queens. On a more theoretical point of view, polyandry should also have the same risk-reducing and relatedness-reducing effect as polyandry. But polygyny may also have more drastic and unknown consequences, because polygynous nests can display much looser kinship structures than monogynous nests (i.e., workers in the latter are always at least half-sisters, but not in the former; see Pamilo, 1982 for an example). In addition, polygyny in the context of hybridogenesis may be expected to introduce new complex queen-queen conflicts over reproduction, because inter- and intra-specifically mated queens have

asymmetrical reproductive abilities (i.e., without clonality, the former will produce all worker and the latter all queens). In general, the two-way relationship between eusocial life-history strategies and hybridogenesis is obviously a very complex and still poorly understood topic. Adapting our model to explore its various facets is one possible research avenue for future studies.

Besides life-history constraints, one obvious ecological prerequisite for the evolution of social hybridogenesis is the availability of inter-specific males. Contact between species is most probable in diverse genus that contain many species with overlapping range and similar phenology (Kaspari et al., 2001). It is also expected to be facilitated in taxa that produce massive mating swarms, synchronized between species due to their dependence on rare climatic events. Such reproductive strategy is typical from species inhabiting dry environments, where mating flights are often dependent on rare and heavy rains that protect against desiccation and facilitate digging by founding queens. This has been proposed as a possible reason why most described hybridogenetic systems have been found in xerophile species (i.e., *Solenopsis*, *Pogonomyrmex*, *Cataglyphis* and *Messor* all share this trait; Boulay et al., 2017; Romiguier et al., 2017). Interestingly, in chapter 2 of this thesis we have found three separate candidate F1 hybrids in the iconic desert-dwelling *Myrmecocystus* honeypot ants. A confirmation that social hybridogenesis exists in these ants would be a strong argument in favor of an ecological component to social hybridogenesis. Another, less obvious, possible ecological factor for social hybridogenesis is diet. Inspired by the fact that *Pogonomyrmex* and *Messor* (and *Solenopsis*, to a lesser extent) ants are specialized granivores, Romiguier et al. (2017) has proposed that a specialized diet could facilitate the evolution of strong GCD, because it would reduce opportunities for adult workers to control larval development via differential feeding. In the language of the model presented in chapter 1, a specialized diet would limit opportunities for coercion by workers and facilitate larval control over their own caste, thus promoting the evolution of social hybridogenesis. Perhaps providing some support to this hypothesis, we find in chapter 2 of this thesis that several candidate F1 hybrids occur among species with at least some level of diet specialization, such as *Myrmecocystus* honeypot ants, basal fungus-growing Attini (i.e., which feed essentially on fungus), or mealybug-rearing *Acropyga* (i.e., which are thought to feed exclusively on honeydew).

One final and very speculative hypothesis can be formulated regarding the possible evolution of social hybridogenesis in basal Attini and *Acropyga*. These two ant groups share one uncommon feature: they live in obligate symbiosis with an organism (i.e., fungus or mealy-bug) that provides most, if not all, of their food. In both cases, the relationship between ants and their symbiont is so intimate that the latter can easily be seen as a full member of colonial units. As such, these symbionts must be, and have been, recognized as potential participant to intra-colonial conflicts (Ivens, 2015; Mueller, 2002). In particular, because these symbiont are usually vertically transmitted by queens (i.e., queens carry them when dispersing to found new nests), they could be predicted to evolve traits that increase colonial investment in new reproductive females. It is thus possible to imagine that maternally transmitted symbionts participate in skewing realized worker-queen caste-ratio downward, possibly triggering evolution

towards GCD and social hybridogenesis (i.e., just as developing larvae in our model). Because these symbionts are heavily involved in larval nutrition, they certainly occupy a place of choice as potential manipulators of developmental parameters. While I could not find any mention of the participation of multicellular ant symbionts in conflicts over caste-ratio (but see Mueller, 2002 for sex-ratio), it must be noted that the exact same argument has been made repeatedly for unicellular endosymbionts, such as *Wolbachia*, that share the same transmission pathway (see Treanor et al., 2018 for a review). The presence of *Wolbachia* has been documented in some species of ants (e.g., Tolley et al., 2019; Wenseleers et al., 1998), but to my knowledge has never been specifically investigated in the context of social hybridogenesis. Steiner et al. (2018) have shown that among all five species of *Messor structor s.l.*, the only species lacking a *Wolbachia* strain is also the only one displaying social hybridogenesis, *Messor ibericus*. Intrigued by this counter-intuitive result, we have searched for *Wolbachia* and other endosymbionts using transcriptome sequencing data for several *Messor* species (including *M. ibericus*, *M. barbarus* and *M. ebeninus*) during this thesis (this work was done by Yannick Juvé, an intern under the supervision of Jonathan Romiguier and myself). While we could confirm the result of Steiner et al. (2018), we found no other pattern linking social hybridogenesis to detected endosymbionts.

Are Hybridogenetic systems doomed to disappear ?

Overall, the number of candidate F1 hybrids reported in chapter 2 may be argued to be “low”, when compared to the generality of the deterministic evolutionary path proposed in this thesis. This claim is obviously quite precipitate, given that there is no actual proof that such mechanism can be credited for the evolution of hybridogenetic systems. Yet, it can still be useful to explore reasons that may account for the relative rarity of hybridogenesis. Perhaps the most obvious of these reasons could be the absence, in most ants, of the required characteristics (discussed in the previous section). In this section, I present and discuss other potential causes.

One potential explanation for the relative rarity of social hybridogenesis could be that such systems are in fact only transitional states, that quickly disappear. The question of the long-term stability of hybridogenetic systems has often been raised (Anderson et al., 2008; Darras & Aron, 2015; Romiguier et al., 2017; Schwander et al., 2006) but remains largely open, in most part because the exact age of hybridogenetic systems is difficult to assess. This difficulty arises from the fact that the divergence time between dependent lineages would only reflect the age of the corresponding system if they evolved from monophyletic and very closely related lineages or species. However such scenario is unlikely to be general. As evidenced by the parphyly of some dependent lineages in *Messor ebeninus* (Romiguier et al., 2017) and *Cataglyphis italica* (Kuhn et al., 2020), social hybridogenesis can arise after the contact of already divergent lineages. This is consistent with all existing models for the evolution of strong GCD including ours, that all assume some level of divergence between interacting lineages. The idea that divergence in hybridogenetic system is not correlated with their age is especially supported by the special case of *Messor ibericus*. In part 2 of chapter 3, we have produced results suggesting that this genetically homogeneous but widely distributed species reproduces via a combination of social

hybridogenesis and androgenesis, but also that the involved putative clonal male lineage is more related to *M. structor s.s.* than *M. ibericus*. If confirmed by future work, this would imply that such reproductive systems can in fact quickly appear and spread, following the “domestication” of males from another lineage. In any case, the phylogenetic resolution available in *Messor structor s.l.* makes this group a key model to answer remaining questions about the first steps of the evolution of social hybridogenesis. As for now, it remains a possibility that all known hybridogenetic systems are in fact quite young, which would entail that older systems have disappeared somehow.

A first possible mechanism to explain the putative disappearance of social hybridogenesis is reversion back to more standard modes of reproduction. According to epistasis-based models, such reversion could be possible if genetic introgression between dependent lineages restores the once-lost worker-inducing allele combinations. Under direct genetic effects models (i.e., the one-locus model and ours), reversion to ECD would be possible only if radical changes in the ecology of dependent lineages (e.g., a sudden dissipation of opportunities to hybridize) lead to the purge of caste-biasing alleles responsible for strong GCD. In all cases however, a successful reversion to ancestral ECD would require that both worker and queen developmental pathways (which are likely to involve many genes and developmental cascades; Tribble & Kronauer, 2017) are still fully available to non-hybrid genotypes. In *Pogonomyrmex* and *Cataglyphis*, experimental rearing has shown that non-hybrid larvae almost never develop as workers, but that a few exceptions still can be found (Kuhn et al., 2018; Schwander et al., 2006). This suggests that successive generations of exclusive queen development in non-hybrids have not yet led, via the relaxation of selection, to the irreversible loss of the worker developmental pathway. If this is true, reversions to ECD from strong GCD may be possible.

It is perhaps more easily conceivable that hybridogenetic systems may eventually lead to population collapse and extinction. As discussed in the previous section and chapter 1, our theoretical work suggest that social hybridogenesis can evolve and fix within populations even if leading to reduced overall fitness. In turn, this may lead hybridogenetic systems to be outcompeted by other sympatric species that have retained standard ECD. But even if social hybridogenesis initially evolves without significant fitness costs, it remains unclear how such costs can be avoided on the long-term. It was pointed out that dependent lineages should mechanically accumulate divergence (Anderson et al., 2008). In turn, increasing divergence should eventually lead to the gradual accumulation of hybrid incompatibilities in workers and, eventually, to reduced colonial fitness and extinction. Two alternative mechanisms can be invoked to salvage hybridogenetic lineages from such inevitable extinction, at least for a time. First, is a possibility that hybrid incompatibilities will be under strong purifying selection, as hybrid genomes are very frequent and systematically exposed to selection. Interestingly, this would lead to an overall reduction in evolutionary rates at key locus, which may be detected in future research. Alternatively, genetic introgression may help against the build up of hybrid incompatibilities. This would explain the number and apparent stability of social hybridogenesis in *Cataglyphis*, were sporadic gene flow was evidenced (Darras & Aron, 2015; Eyer et al., 2016). It is however more difficult to invoke

introgression to explain the stability and success of social hybridogenesis in *Messor*, where there is no such evidence for gene flow (Romiguier et al., 2017). It is perhaps more probable that in this species, social hybridogenesis does initially come with increased fitness.

The case of *M. barbarus* is also particularly interesting in that it highlights another poorly known aspect of the evolution of social hybridogenesis. Specifically, it remains mostly unknown how some hybridogenetic lineages have colonized large geographical ranges starting from an initial, presumably quite narrow, hybrid zone (Darras et al., 2014b). It is possible that range expansion in dependent lineage pairs strictly requires that hybridogenesis comes with an ecological advantage, in which case dependent lineages would experience a coupled range expansion, gradually replacing their parental species. This simple hypothesis would have the advantage to explain why some hybridogenetic systems remain confined to hybrid zones (e.g., *Solenopsis* and *Pogonomyrmex*). It could also help to explain the relative rarity of F1 hybrids in the data analyzed in chapter 2, which would follow from the restricted range of many hybridogenetic systems. Another, more speculative, hypothesis that does not involve ecological arguments is that the evolution of social hybridogenesis within hybrid zones leads to population decline in neighboring populations (i.e., outside the hybrid zone) via gene transfer. In this hypothesis, caste-biasing alleles whose frequency increased within a given hybrid zone would diffuse in neighboring populations, and lead to a net loss of fitness in the absence of opportunities to hybridize. In turn, this may eventually lead to their replacement by hybridogenetic lineages. To evaluate the likelihood of this last hypothesis will require to integrate a spacial dimension to further modeling studies. Alternatively, population genetic studies of hybrid zones where hybridogenesis has evolved may yield insights about genetic exchanges between these zones and neighboring populations.

Conclusion and perspectives

Social hybridogenesis is a fascinating mode of reproduction that is gradually revealing its many forms through intensive work by many research teams around the world. Since the first insights, more than forty years ago, that ant colonies can contain puzzling mixtures of divergent genetic material, this reproductive system has continuously yielded invaluable insights into the evolution of eusocial organizations. Yet, many challenges remain to be addressed before a complete understanding of all evolutionary facets of social hybridogenesis can be obtained.

In this thesis, my main focus has been on the evolutionary mechanisms that are responsible for the emergence of social hybridogenesis. I have proposed that an arms-race between queens and their larvae, instead of historical contingencies or heterosis, may be at the core of the evolution of this mode of reproduction. According to this new view, social hybridogenesis could be regarded in most cases as a detrimental evolutionary fate, as a tragedy of the commons. But empirical support for this hypothesis remains to be obtained before such a view can be fully adopted. I believe that the analyses that are most likely to yield answers in this regard will involve genomic and transcriptomic data. In particular, if an arms race is responsible for social hybridogenesis, it

is expected that this race has left specific patterns or rapid evolution in the genome of involved species. Tool specifically designed to detect selective sweeps may detect this putative signature of social hybridogenesis. Depending on the particular position of potential selective sweeps, transcriptomic data may then help drawing links with actual functions involved in development and caste differentiation. Therefore, such analyses may also work backward and yield important insight into the genomics of caste plasticity.

If specific loci can be identified that are involved in the evolution of social hybridogenesis, it will also become possible to ask whether the same genetic mechanisms are involved in related hybridogenetic systems. In particular, it will become possible to ask whether alleles present in hybridogenetic species from the same genus have been exchanged. Answering such questions will help a great deal in explaining why some groups seem to have such affinities with social hybridogenesis. In this particular endeavor, the *Messor* genus may reveal particularly important, because it seem to harbor different forms of social hybridogenesis, with possibly more to be discovered. As such, this genus may be key in uncovering the possible functional and evolutionary links between the various forms of social hybridogenesis.

Beyond the particular case of *Messor* harvester ants, a better understanding of the fundamental determinants of social hybridogenesis (both genetic and ecological) will require that large scale comparative studies are undertaken. For such studies to have enough power, it will be necessary that many systems are included. I hope that the methods and preliminary results presented in this thesis will help in this regard. In particular, the list of reported candidate F1 hybrids uncovered in chapter 2 may represent a good starting point for the discovery of new valuable models of study. Some groups, such as honeypot ants, basal leaf-cutting ant or army ants, clearly stand out in our analyses and possess traits that are expected to facilitate the evolution of hybridization-dependent reproductive systems. Investigating these groups may lead to new insights about the possible consequences of the interplay between life-history, ecology, and genetic conflicts in eusocial organisms.

References

- Abbott, R., D. Albach, S. Ansell, J. W. Arntzen, S. J. Baird, N. Bierne, et al. (2013). Hybridization and speciation. *J. Evol. Biol.*, 26, 229–246.
- Anderson, K. E., J. Gadau, B. M. Mott, R. A. Johnson, A. Altamirano, C. Strehl, et al. (2006). Distribution and evolution of genetic caste determination in *Pogonomyrmex* seed-harvester ants. *Ecology*, 87, 2171–2184.
- Anderson, K. E., T. A. Linksvayer, and C. R. Smith (2008). The causes and consequences of genetic caste determination in ants (Hymenoptera : Formicidae). *Myrmecol. News*, 11, 119–132.
- Anderson, E. (1949). *Introgressive Hybridization*. Chapman & Hall, London.
- Aron, S., P. Mardulyn, and L. Leniaud (2016). Evolution of reproductive traits in *Cataglyphis* desert ants: mating frequency, queen number, and thelytoky. *Behav. Ecol. Sociobiol.*, 70, 1367–1379.
- Barton, N. H. and G. M. Hewitt (1985). Analysis of hybrid zones. *Annu. Rev. Ecol. Syst.*, 16, 113–148.
- Barth, M. B., R. F. A. Moritz, and F. B. Kraus (2014). The evolution of extreme polyandry in social insects: Insights from army ants. *PLoS One*, 9.
- Barton, N. H. (2001). The role of hybridization in evolution. *Mol. Ecol.*, 10, 551–568.
- Barton, N. H. (2020). On the completion of speciation. *Philos. Trans. R. Soc. B*, 375, 1–10.
- Bateson, W. (1909). *Heredity and variation in modern lights*. Darwin Mod. Cambridge University Press, Cambridge, UK.
- Beukeboom, L. W. and R. C. Vrijenhoek (1998). Evolutionary genetics and ecology of sperm-dependent parthenogenesis. *J. Evol. Biol.*, 11, 755–782.
- Bhattacharyya, T., S. Gregorova, O. Mihola, M. Anger, J. Sebestova, P. Denny, et al. (2013). Mechanistic basis of infertility of mouse intersubspecific hybrids. *Proc. Natl. Acad. Sci. U. S. A.*, 110, E468–E477.
- Birchler, J. A., H. Yao, S. Chudalayandi, D. Vaiman, and R. A. Veitia (2010). Heterosis. *Plant Cell*, 22, 2105–2112.
- Birch, J. and S. Okasha (2015). Kin selection and its critics. *Bioscience*, 65, 22–32.
- Bolton, B. (2021). An online catalog of the ants of the world. <https://antcat.org>. Accessed 15 october 2021.
- Bombliès, K., J. Lempe, P. Epple, N. Warthmann, C. Lanz, J. L. Dangel, et al. (2007). Autoimmune response as a mechanism for a Dobzhansky-Muller-type incompatibility syndrome in plants. *PLoS Biol.*, 5, 1962–1972.
- Bordenstein, S. R., F. P. O’hara, and J. H. Werren (2001). *Wolbachia*-induced incompatibility precedes other hybrid incompatibilities in *Nasonia*. *Nature*, 409, 707–710.
- Boulay, R., S. Aron, X. Cerdá, C. Doums, P. Graham, A. Hefetz, et al. (2017). Social life in arid environments: The case study of *Cataglyphis* ants. *Annu. Rev. Entomol.*, 62, 305–321.
- Bourke, A. F. G. and G. L. Chan (1999). Queen-worker conflict over sexual production and colony maintenance in perennial social insects. *Am. Nat.*, 154, 417–426.
- Bourke, A. F. G. and F. L. W. Ratnieks (1999). Kin conflict over caste determination in social Hymenoptera. *Behav. Ecol. Sociobiol.*, 46, 287–297.
- Branstetter, M. G., J. T. Longino, J. Reyes-López, T. R. Schultz, and S. G. Brady (2016). Into the tropics: Phylogenomics and evolutionary dynamics of a contrarian clade of ants. *Preprint Biorxiv*, 1–52.
- Branstetter, M. G., J. T. Longino, P. S. Ward, and B. C. Faircloth (2017). Enriching the ant tree of life: enhanced UCE bait set for genome-scale phylogenetics of ants and other Hymenoptera. *Methods Ecol. Evol.*, 8, 768–776.

- Cachuela-Palacio, M. (2006). Towards an index of all known species: the Catalogue of Life, its rationale, design and use. *Integr. Zool.*, 1, 18–21.
- Castella, G., P. Christe, and M. Chapuisat (2009). Mating triggers dynamic immune regulations in wood ant queens. *J. Evol. Biol.*, 22, 564–570.
- Charlesworth, D. and J. H. Willis (2009). The genetics of inbreeding depression. *Nat. Rev. Genet.*, 10, 783–796.
- Chérasse, S. and S. Aron (2018). Impact of immune activation on stored sperm viability in ant queens. *Proc. R. Soc. B Biol. Sci.*, 285.
- Cordonnier, M., T. Gayet, G. Escarguel, and B. Kaufmann (2019). From hybridization to introgression between two closely related sympatric ant species. *J. Zool. Syst. Evol. Res.*, 57, 778–788.
- Cordonnier, M., G. Escarguel, A. Dumet, and B. Kaufmann (2020). Multiple mating in the context of interspecific hybridization between two *Tetramorium* ant species. *Heredity*, 124, 675–684.
- Darras, H., A. Kuhn, and S. Aron (2014a). Genetic determination of female castes in a hybridogenetic desert ant. *J. Evol. Biol.*, 27, 2265–2271.
- Darras, H., L. Leniaud, and S. Aron (2014b). Large-scale distribution of hybridogenetic lineages in a Spanish desert ant. *Proc. R. Soc. B Biol. Sci.*, 281, 1–8.
- Darras, H. and S. Aron (2015). Introgression of mitochondrial DNA among lineages in a hybridogenetic ant. *Biol. Lett.*, 11, 1–4.
- Darras, H., A. Kuhn, and S. Aron (2019). Evolution of hybridogenetic lineages in *Cataglyphis* ants. *Mol. Ecol.*, 28, 3073–3088.
- Davidson, D. W. (1982). Sexual selection in harvester ants (Hymenoptera: Formicidae: *Pogonomyrmex*). *Behav. Ecol. Sociobiol.*, 10, 245–250.
- Dion-Coté, A. M., R. Symonová, P. Ráb, and L. Bernatchez (2015). Reproductive isolation in a nascent species pair is associated with aneuploidy in hybrid offspring. *Proc. R. Soc. B Biol. Sci.*, 282.
- Dobata, S. (2012). Arms race between selfishness and policing: two-trait quantitative genetic model for caste fate conflict in eusocial hymenoptera. *Evolution*, 66, 3754–3764.
- Dobzhansky, T. (1940). Speciation as a stage in evolutionary divergence. *Am. Nat.*, 74, 312–321.
- Doums, C., A. L. Cronin, C. Ruel, P. Fédérici, C. Haussy, C. Tirard, et al. (2013a). Facultative use of thelytokous parthenogenesis for queen production in the polyandrous ant *Cataglyphis cursor*. *J. Evol. Biol.*, 26, 1431–1444.
- Doums, C., C. Ruel, J. Clémencet, P. Fédérici, L. Cournault, and S. Aron (2013b). Fertile diploid males in the ant *Cataglyphis cursor*: A potential cost of thelytoky? *Behav. Ecol. Sociobiol.*, 67, 1983–1993.
- Doums, C. and T. Monnin (2020). To have and not to have sex: When multiple evolutions of conditional use of sex elegantly solve the question in the ant genus *Cataglyphis*. *Mol. Ecol.*, 445–447.
- Douwes, P. and B. Stille (1991). Hybridization and variation in the *Leptothorax tuberum* group (Hymenoptera: Formicidae). *Z. Zool. Syst. Evol.*, 29, 165–175.
- Edmands, S. (2002). Does parental divergence predict reproductive compatibility? *Trends Ecol. Evol.*, 17, 520–527.
- Eyer, P. A., L. Leniaud, A. Tinaut, and S. Aron (2016). Combined hybridization and mitochondrial capture shape complex phylogeographic patterns in hybridogenetic *Cataglyphis* desert ants. *Mol. Phylogenet. Evol.*, 105, 251–262.
- Faircloth, B. C., J. E. McCormack, N. G. Crawford, M. G. Harvey, R. T. Brumfield, and T. C. Glenn (2012). Ultraconserved elements anchor thousands of genetic markers spanning multiple evolutionary timescales. *Syst. Biol.*, 61, 717–726.

- Feder, J. L., S. P. Egan, and P. Nosil (2012). The genomics of speciation-with-gene-flow. *Trends Genet.*, 28, 342–350.
- Feldhaar, H., S. Foitzik, and J. Heinze (2008). Lifelong commitment to the wrong partner: Hybridization in ants. *Philos. Trans. R. Soc. B Biol. Sci.*, 363, 2891–2899.
- Foucaud, J., D. Fournier, J. Orivel, J. H. Delabie, A. Loiseau, J. Le Breton, et al. (2007). Sex and clonality in the little fire ant. *Mol. Biol. Evol.*, 24, 2465–2473.
- Fournier, D., A. Estoup, J. Orivel, J. Foucaud, H. Jourdan, J. Le Breton, et al. (2005). Clonal reproduction by males and females in the little fire ant. *Nature*, 435, 1230–1234.
- Fournier, D. and S. Aron (2021). Hybridization and invasiveness in social insects — The good, the bad and the hybrid. *Curr. Opin. Insect Sci.*, 46, 1–9.
- Fraïsse, C., I. Popovic, C. Mazoyer, B. Spataro, S. Delmotte, J. Romiguier, et al. (2021). DILS: Demographic inferences with linked selection by using ABC. *Mol. Ecol. Resour.*, 1–16.
- Frank, S. A. (2013). Natural selection. VII. History and interpretation of kin selection theory. *J. Evol. Biol.*, 26, 1151–1184.
- Fu, H. and H. K. Dooner (2002). Intraspecific violation of genetic colinearity and its implications in maize. *Proc. Natl. Acad. Sci. U. S. A.*, 99, 9573–9578.
- Haldane, J. (1924). A mathematical theory of natural and artificial selection - I. *Bull. Math. Biol.*, 52, 209–240.
- Hamilton, W. D. (1964). The genetical evolution of social behaviour . I. *J. Theor. Biol.*, 7, 1–16.
- Helms Cahan, S., J. D. Parker, S. W. Rissing, R. A. Johnson, T. S. Polony, M. D. Weiser, et al. (2002). Extreme genetic differences between queens and workers in hybridizing *Pogonomyrmex* harvester ants. *Proc. R. Soc. B Biol. Sci.*, 269, 1871–1877.
- Helms Cahan, S. and L. Keller (2003). Complex hybrid origin of genetic caste determination in harvester ants. *Nature*, 424, 306–309.
- Helms Cahan, S. and S. B. Vinson (2003). Reproductive division of labor between hybrid and nonhybrid offspring in a fire ant hybrid zone. *Evolution*, 57, 1562–1570.
- Helms Cahan, S., J. E. Glennis, S. W. Rissing, T. Schwander, J. D. Parker, and L. Keller (2004). Loss of phenotypic plasticity generates genotype-caste association in harvester ants. *Curr. Biol.*, 14, 2277–2282.
- Helms Cahan, S. and G. E. Julian (2010). Shift in frequency-dependent selection across the life-cycle in obligately interbreeding harvester ant lineages. *Evol. Ecol.*, 24, 359–374.
- Herrmann, M. and S. H. Cahan (2014). Inter-genomic sexual conflict drives antagonistic coevolution in harvester ants. *Proc. R. Soc. B Biol. Sci.*, 281.
- Hughes, W. O. H., B. P. Oldroyd, M. Beekman, and F. L. W. Ratnieks (2008). Ancestral monogamy shows kin selection is key to the evolution of eusociality. *Science*, 320, 1213–1216.
- Hung, A. C. and S. B. Vinson (1977). Interspecific hybridization and caste specificity of protein in fire ant. *Science*, 196, 1458–1460.
- Ivens, A. B. (2015). Cooperation and conflict in ant (Hymenoptera: Formicidae) farming mutualisms - A review. *Myrmecol. News*, 21, 19–36.
- James, S. S., R. M. Pereira, K. M. Vail, and B. H. Ownley (2002). Survival of imported fire ant (Hymenoptera: Formicidae) species subjected to freezing and near-freezing temperatures. *Environ. Entomol.*, 31, 127–133.
- Julian, G. E. and S. H. Cahan (2006). Behavioral differences between *Pogonomyrmex rugosus* and dependent lineages (H1/H2) harvester ants. *Ecology*, 87, 2207–2214.
- Kaptein, N., J. Billen, and B. Gobin (2005). Larval begging for food enhances reproductive options in the ponerine ant *Gnamptogenys striatula*. *Anim. Behav.*, 69, 293–299.

- Kaspari, M., J. Pickering, J. T. Longino, and D. Windsor (2001). The phenology of a neotropical ant assemblage: Evidence for continuous and overlapping reproduction. *Behav. Ecol. Sociobiol.*, 50, 382–390.
- Keller, L. and H. K. Reeve (1994). Genetic variability, queen number, and polyandry in social Hymenoptera. *Evolution*, 48, 694–704.
- Kronauer, D. J., M. K. Peters, C. Schöning, and J. J. Boomsma (2011). Hybridization in East African swarm-raiding army ants. *Front. Zool.*, 8, 1–13.
- Kuhn, A., D. Bauman, H. Darras, and S. Aron (2017). Sex-biased dispersal creates spatial genetic structure in a parthenogenetic ant with a dependent-lineage reproductive system. *Heredity*, 119, 207–213.
- Kuhn, A., H. Darras, and S. Aron (2018). Phenotypic plasticity in an ant with strong caste-genotype association. *Biol. Lett.*, 14.
- Kuhn, A., H. Darras, O. Paknia, and S. Aron (2020). Repeated evolution of queen parthenogenesis and social hybridogenesis in *Cataglyphis* desert ants. *Mol. Ecol.*, 29, 549–564.
- Kulmuni, J., B. Seifert, and P. Pamilo (2010). Segregation distortion causes large-scale differences between male and female genomes in hybrid ants. *Proc. Natl. Acad. Sci. U. S. A.*, 107, 7371–7376.
- Kulmuni, J. and P. Pamilo (2014). Introgression in hybrid ants is favored in females but selected against in males. *Proc. Natl. Acad. Sci. U. S. A.*, 111, 12805–12810.
- Lacy, K. D., D. Shoemaker, and K. G. Ross (2019). Joint evolution of asexuality and queen number in an ant. *Curr. Biol.*, 29, 1394–1400.
- Lavanchy, G. and T. Schwander (2019). Hybridogenesis. *Curr. Biol.*, 29, R9–R11.
- Leniaud, L., H. Darras, R. Boulay, and S. Aron (2012). Social hybridogenesis in the clonal ant *Cataglyphis hispanica*. *Curr. Biol.*, 22, 1188–1193.
- Levin, D. A., J. Francisco-Ortega, and R. K. Jansen (1996). Hybridization and the extinction of rare plant species. *Conserv. Biol.*, 10, 10–16.
- Libbrecht, R., T. Schwander, and L. Keller (2011). Genetic components to caste allocation in a multiple-queen ant species. *Evolution*, 65, 2907–2915.
- Lillico-Ouachour, A. and E. Abouheif (2017). Regulation, development, and evolution of caste ratios in the hyperdiverse ant genus *Pheidole*. *Curr. Opin. Insect Sci.*, 19, 43–51.
- Linksvayer, T. A., M. J. Wade, and D. M. Gordon (2006). Genetic caste determination in harvester ants: Possible origin and maintenance by cyto-nuclear epistasis. *Ecology*, 87, 2185–2193.
- Linksvayer, T. A. (2006). Direct, maternal and sibsocial genetic effects on individual and colony traits in an ant. *Evolution*, 60, 2552–2561.
- Löfstedt, C., W. M. Herre, and S. B. Menken (1991). Sex pheromones and their potential role in the evolution of reproductive isolation in small ermine moths (Yponomeutidae). *Chemoecology*, 2, 20–28.
- Lynch, M. and A. G. Force (2000). The origin of interspecific genomic incompatibility via gene duplication. *Am. Nat.*, 156, 590–605.
- Mallet, J. (1995). A species definition for the Modern Synthesis. *Trends Ecol. Evol.*, 10, 294–299.
- Mallet, J. (2005). Hybridization as an invasion of the genome. *Trends Ecol. Evol.*, 20, 229–237.
- Mallet, J. (2007). Hybrid speciation. *Nature*, 446, 279–283.
- Martin, S. H. and C. D. Jiggins (2017). Interpreting the genomic landscape of introgression. *Curr. Opin. Genet. Dev.*, 47, 69–74.
- Maynard Smith, J. and E. Szathmáry (1995). The major transitions in evolution. Oxford University Press.
- Mayr, E. (1942). Systematics and the origin of species. Columbia University Press, New York.

- Moran, B. M., C. Payne, Q. Langdon, D. L. Powell, Y. Brandvain, and M. Schumer (2021). The genomic consequences of hybridization. *Elife*, 10, 1–33.
- Mott, B. M., J. Gadau, and K. E. Anderson (2015). Phylogeography of *Pogonomyrmex barbatus* and *P. rugosus* harvester ants with genetic and environmental caste determination. *Ecol. Evol.*, 5, 2798–2826.
- Mueller, U. G. (2002). Ant versus fungus versus mutualism: Ant-cultivar conflict and the deconstruction of the attine ant-fungus symbiosis. *Am. Nat.*, 160, 67–98.
- Muller, H. J. (1942). Isolating mechanisms, evolution, and temperature. *Biol. Symp.*, 6, 71–125.
- Nonacs, P. (2006). Interspecific hybridization in ants: At the intersection of ecology, evolution, and behavior. *Ecology*, 87, 2143–2147.
- Norman, V., H. Darras, C. Tranter, S. Aron, and W. O. H. Hughes (2016). Cryptic lineages hybridize for worker production in the harvester ant *Messor barbarus*. *Biol. Lett.*, 12, 1–5.
- Nowak, M. A. (2010). Evolution of eusociality. *Nature*, 466, 1057–1062.
- Ohkawara, K., M. Nakayama, A. Satoh, A. Trindl, and J. Heinze (2006). Clonal reproduction and genetic caste differences in a queen-polymorphic ant, *Vollenhovia emeryi*. *Biol. Lett.*, 5, 359–363.
- Okita, I. and K. Tsuchida (2016). Clonal reproduction with androgenesis and somatic recombination: The case of the ant *Cardiocondyla kagutsuchi*. *Sci. Nat.*, 103, 1–6.
- Otto, S. P. and J. Whitton (2000). Polyploid incidence and evolution. *Annu. Rev. Genet.*, 34, 401–437.
- Pamilo, P. (1982). Genetic population structure in polygynous *Formica* ants. *Heredity*, 48, 95–106.
- Pearcy, M., M. A. D. Goodisman, and L. Keller (2011). Sib mating without inbreeding in the longhorn crazy ant. *Proc. R. Soc.*, 278, 2677–2681.
- Pearcy, M., N. Delescaille, P. Lybaert, and S. Aron (2014). Team swimming in ant spermatozoa. *Biol. Lett.*, 10, 10–14.
- Pearson, B. (1983). Hybridisation between the ant species *Lasius niger* and *Lasius alienus*: The genetic evidence. *Insectes Soc.*, 30, 402–411.
- Peeters, C. and F. Ito (2015). Wingless and dwarf workers underlie the ecological success of ants (Hymenoptera: Formicidae). *Myrmecol. News*, 21, 117–130.
- Pfennig, K. S. (2007). Facultative mate choice drives adaptive hybridization. *Science*, 318, 965–967.
- Pfennig, K. S. (2021). Biased hybridization and its impact on adaptive introgression. *Trends Ecol. Evol.*, 36, 488–497.
- Pickersgill, B. (2009). Domestication of plants revisited - Darwin to the present day. *Bot. J. Linn. Soc.*, 161, 203–212.
- Pinho, C. and J. Hey (2010). Divergence with gene flow: Models and data. *Annu. Rev. Ecol. Evol. Syst.*, 41, 215–230.
- Purcell, J., S. Zahnd, A. Athanasiades, R. Türler, M. Chapuisat, and A. Brelsford (Aug. 2016). Ants exhibit asymmetric hybridization in a mosaic hybrid zone. *Mol. Ecol.*, 25, 4866–4874.
- Queller, D. C. and J. E. Strassmann (1998). Selection and social insects provide the most surprising predictions and satisfying. *Am. Inst. Biol. Sci.*, 48, 165–175.
- Racimo, F., S. Sankararaman, R. Nielsen, and E. Huerta-Sánchez (2015). Evidence for archaic adaptive introgression in humans. *Nat. Rev. Genet.*, 16, 359–371.
- Rankin, D. J., K. Bargum, and H. Kokko (2007). The tragedy of the commons in evolutionary biology. *Trends Ecol. Evol.*, 22, 643–651.
- Ratnieks, F. L. and T. Wenseleers (2008). Altruism in insect societies and beyond: voluntary or enforced? *Trends Ecol. Evol.*, 23, 45–52.

- Raychoudhury, R., L. Baldo, D. C. Oliveira, and J. H. Werren (2009). Modes of acquisition of *Wolbachia*: Horizontal transfer, hybrid introgression, and codivergence in the *Nasonia* species complex. *Evolution*, 63, 165–183.
- Reuter, M. and L. Keller (2011). Sex ratio conflict and worker production in eusocial Hymenoptera. *Am. Nat.*, 158, 166–177.
- Rey, O., B. Facon, J. Foucaud, A. Loiseau, and A. Estoup (2013). Androgenesis is a maternal trait in the invasive ant *Wasmannia auropunctata*. *Proc. R. Soc. B Biol. Sci.*, 280, 1–7.
- Rheindt, F. E., J. Gadau, C.-P. Strehl, and B. Hölldobler (2004). Extremely high mating frequency in the Florida harvester ant (*Pogonomyrmex badius*). *Behav. Ecol. Sociobiol.*, 56, 472–481.
- Roberts, H. F. (1919). Darwin’s contribution to the knowledge of hybridization. *Am. Nat.*, 53, 535–554.
- Romiguier, J., J. Lourenco, P. Gayral, N. Faivre, L. A. Weinert, S. Ravel, et al. (2014). Population genomics of eusocial insects: The costs of a vertebrate-like effective population size. *J. Evol. Biol.*, 27, 593–603.
- Romiguier, J., A. Fournier, S. H. Yek, and L. Keller (2017). Convergent evolution of social hybridogenesis in *Messor* harvester ants. *Mol. Ecol.*, 26, 1108–1117.
- Ross, K. G. and J. L. Robertson (1990). Developmental stability, heterozygosity, and fitness in two introduced fire ants (*Solenopsis invicta* and *S. richteri*) and their hybrid. *Heredity*, 64, 93–103.
- Safran, R. J., E. S. Scordato, L. B. Symes, R. L. Rodríguez, and T. C. Mendelson (2013). Contributions of natural and sexual selection to the evolution of premating reproductive isolation: A research agenda. *Trends Ecol. Evol.*, 28, 643–650.
- Schön, I., P. Van Dijk, and K. Martens (2009). Lost sex: The evolutionary biology of parthenogenesis. Springer.
- Schultz, R. J. (1969). Hybridization, unisexuality, and polyploidy in the teleost *Poeciliopsis* (Poeciliidae) and other Vertebrates. *Am. Nat.*, 103, 605–619.
- Schwander, T., S. H. Cahan, and L. Keller (2006). Genetic caste determination in *Pogonomyrmex* harvester ants imposes costs during colony founding. *J. Evol. Biol.*, 19, 402–409.
- Schwander, T., S. H. Cahan, and L. Keller (2007). Characterization and distribution of *Pogonomyrmex* harvester ant lineages with genetic caste determination. *Mol. Ecol.*, 16, 367–387.
- Schwander, T. and L. Keller (2008). Genetic compatibility affects queen and worker caste determination. *Science*, 322, 552.
- Schwander, T., N. Lo, M. Beekman, B. P. Oldroyd, and L. Keller (2010). Nature versus nurture in social insect caste differentiation. *Trends Ecol. Evol.*, 25, 275–282.
- Schwander, T. and L. Keller (2012). Evolution: Sociality as a driver of unorthodox reproduction. *Curr. Biol.*, 22, R525–R527.
- Schwander, T. and B. P. Oldroyd (2016). Androgenesis: Where males hijack eggs to clone themselves. *Philos. Trans. R. Soc. B Biol. Sci.*, 371.
- Seifert, B. and A. V. Goropashnaya (2004). Ideal phenotypes and mismatching haplotypes - Errors of mtDNA treeing in ants (Hymenoptera: Formicidae) detected by standardized morphometry. *Org. Divers. Evol.*, 4, 295–305.
- Seifert, B. (1999). Interspecific hybridisations in natural populations of ants by example of a regional fauna (Hymenoptera, Formicidae). *Insectes Soc.*, 46, 45–52.
- Seifert, B. (2021). A taxonomic revision of the Palaearctic members of the *Formica rufa* group (Hymenoptera: Formicidae) – the famous mound-building red wood ants. *Myrmecol. News*, 31, 133–179.
- Seixas, F. A., P. Boursot, and J. Melo-Ferreira (2018). The genomic impact of historical hybridization with massive mitochondrial DNA introgression. *Genome Biol.*, 19, 1–20.

- Semel, Y., J. Nissenbaum, N. Menda, M. Zinder, U. Krieger, N. Issman, et al. (2006). Overdominant quantitative trait loci for yield and fitness in tomato. *Proc. Natl. Acad. Sci. U. S. A.*, 103, 12981–12986.
- Sirviö, A., P. Pamilo, R. A. Johnson, R. E. Page, and J. Gadau (2011). Origin and evolution of the dependent lineages in the genetic caste determination system of *Pogonomyrmex* ants. *Evolution*, 65, 869–884.
- Smadja, C. M. and R. K. Butlin (2011). A framework for comparing processes of speciation in the presence of gene flow. *Mol. Ecol.*, 20, 5123–5140.
- Smith, A. L., T. R. Hodkinson, J. Villellas, J. A. Catford, A. M. Csergő, S. P. Blomberg, et al. (2020). Global gene flow releases invasive plants from environmental constraints on genetic diversity. *Proc. Natl. Acad. Sci. U. S. A.*, 117, 4218–4227.
- Stebbins, G. L. (1959). The role of hybridization in evolution. *Proc. Am. Philos. Soc.*, 103, 231–251.
- Steiner, F. M., B. Seifert, D. A. Grasso, F. Le Moli, W. Arthofer, C. Stauffer, et al. (2011). Mixed colonies and hybridisation of *Messor* harvester ant species (Hymenoptera: Formicidae). *Org. Divers. Evol.*, 11, 107–134.
- Steiner, F. M., S. Csősz, B. Markó, A. Gamisch, L. Rinnhofer, C. Folterbauer, et al. (2018). Turning one into five: Integrative taxonomy uncovers complex evolution of cryptic species in the harvester ant *Messor* “*structor*”. *Mol. Phylogenet. Evol.*, 127, 387–404.
- Strassmann, J. (2001). The rarity of multiple mating by females in the social Hymenoptera. *Insectes Soc.*, 48, 1–13.
- Toews, D. P., H. M. Streby, L. Burket, and S. A. Taylor (2018). A wood-warbler produced through both interspecific and intergeneric hybridization. *Biol. Lett.*, 14.
- Tolley, S. J., P. Nonacs, and P. Sapountzis (2019). *Wolbachia* horizontal transmission events in ants: What do we know and what can we learn? *Front. Microbiol.*, 10, 1–9.
- Treanor, D., T. Paminger, and W. O. Hughes (2018). The evolution of caste-biasing symbionts in the social hymenoptera. *Insectes Soc.*, 65, 513–519.
- Trible, W. and D. J. C. Kronauer (2017). Caste development and evolution in ants : it’s all about size. *Co. Biol.*, 53, 53–62.
- Turelli, M. (1998). The causes of Haldane’s rule. *Science*, 282, 889–891.
- Umphrey, G. J. and R. G. Danzmann (1998). Electrophoretic evidence for hybridization in the ant genus *Acanthomyops* (Hymenoptera: Formicidae). *Biochem. Syst. Ecol.*, 26, 431–440.
- Umphrey, G. J. (2006). Sperm parasitism in ants: Selection for interspecific mating and hybridization. *Ecology*, 87, 2148–2159.
- Van Der Have, T. M., J. S. Pedersen, and J. J. Boomsma (2011). Mating, hybridisation and introgression in *Lasius* ants (Hymenoptera: Formicidae). *Myrmecol. News*, 15, 109–115.
- Volny, V. P. and D. M. Gordon (2002). Genetic basis for queen-worker dimorphism in a social insect. *Proc. Natl. Acad. Sci. U. S. A.*, 99, 6108–6111.
- Vrana, P. B., J. A. Fossella, P. Matteson, T. Del Rio, M. J. O’Neill, and S. M. Tilghman (2000). Genetic and epigenetic incompatibilities underlie hybrid dysgenesis in *Peromyscus*. *Nat. Genet.*, 25, 120–124.
- Welch, J. J. (2004). Accumulating Dobzhansky-Muller incompatibilities: Reconciling theory and data. *Evolution*, 58, 1145–1156.
- Wenseleers, T., F. Ito, S. Van Borm, R. Huybrechts, F. Volckaert, and J. Billen (1998). Widespread occurrence of the micro-organism *Wolbachia* in ants. *Proc. R. Soc. B Biol. Sci.*, 265, 1447–1452.
- West, R. J. and A. Kodric-Brown (2015). Mate choice by both sexes maintains reproductive isolation in a species flock of pupfish (*Cyprinodon spp*) in the Bahamas. *Ethology*, 121, 793–800.
- Wheeler, W. M. (1911). The ant-colony as an organism. *J. Morphol.*, 22, 307–325.

- Wing, M. W. (1968). Taxonomic revision of the Nearctic genus *Acanthomyops* (Hymenoptera: Formicidae). Mem. 405. Cornell Univ. Agric. Exp. Station. Ithaca, New York, USA.
- Wojcieszek, J. M. and L. W. Simmons (2013). Divergence in genital morphology may contribute to mechanical reproductive isolation in a millipede. *Ecol. Evol.*, 3, 334–343.
- Yamauchi, A. and N. Yamamura (2006). Persistence conditions of symmetric social hybridogenesis in haplo-diploid Hymenoptera. *J. Theor. Biol.*, 240, 24–31.

Appendices

Other Scientific projects

Relaxation of purifying selection suggests low effective population size in eusocial Hymenoptera and solitary pollinating bees. 132

Weyna & Romiguier (2021). *Peer Community In Evolutionary Biology*.

This is my first scientific article as a first author. It contains results obtained during my second master internship, but was written and reviewed while I was a PhD student. In this work, we used an available phylogenomic dataset to ask whether the convergent evolution of eusociality in bees, wasps and ants was accompanied by reductions in long-term effective population size.

Mitochondrial genomics reveals the evolutionary history of the porpoises (Phocoenidae) across the speciation continuum. 154

Chehida et al. (2020). *Scientific Reports*.

This is the work of another PhD student (Yacine Ben Chehida). My participation was to run estimations of synonymous and non-synonymous substitution rates on the dataset assembled by the author.

Habitats shape taxonomic and functional composition of Neotropical ant assemblages. 172

Fichaux et al. (2020). *Oecologia*.

This article was written by Mélanie Fichaux, who supervised me (together with Jérôme Orivel), during a three-month internship in Kuru (French Guyana) while I was a third year bachelor student. I spent most of this internship measuring functional traits on pinned ant specimens she collected, and running preliminary analyses of functional composition. This was my first contact with research on ants, and has done much to determine my future interests.

How do invasion syndromes evolve? An experimental evolution approach using the ladybird *Harmonia axyridis*. 185

Foucaud et al. (2020). *Peer Community In Evolutionary Biology*.

This article is the result of a long-term project conducted by Julien Foucaud and others at the Centre de Biologie pour la Gestion des Populations, Montferrier-sur-Lez (near Montpellier). I participated to the project as an intern during the first year of my bachelor. While I could not grasp most of the theory behind this work at the time, my participation in the experimental breeding program was my first real contact with research.



RESEARCH ARTICLE



Open Access



Open Peer-Review

Relaxation of purifying selection suggests low effective population size in eusocial Hymenoptera and solitary pollinating bees

Arthur Weyna¹, Jonathan Romiguier¹

¹ Institut des Sciences de l'Evolution (UMR 5554), University of Montpellier, CNRS – Montpellier, France

Cite as: Weyna A, Romiguier J (2021) Relaxation of purifying selection suggests low effective population size in eusocial Hymenoptera and solitary pollinating bees. *bioRxiv*, 2020.04.14.038893, ver. 5 peer-reviewed and recommended by PCI Evol Biol. doi: <https://doi.org/10.1101/2020.04.14.038893>

This article has been peer-reviewed and recommended by

Peer Community in Evolutionary Biology

<https://doi.org/10.24072/pci.evolbiol.100120>

ABSTRACT

With one of the highest number of parasitic, eusocial and pollinator species among all insect orders, Hymenoptera features a great diversity of lifestyles. At the population genetic level, such life-history strategies are expected to decrease effective population size and the efficiency of purifying selection. In this study, we tested this hypothesis by estimating the relative rate of non-synonymous substitution in 169 species to investigate the variation in natural selection efficiency throughout the hymenopteran tree of life. We found no effect of parasitism, but we show that relaxed selection is associated with eusociality, suggesting that the division of reproductive labour decreases effective population size in ants, bees and wasps. Unexpectedly, the effect of eusociality is marginal compared to a striking and widespread relaxation of selection in both social and non social bees, which indicates that these keystone pollinator species generally feature low effective population sizes. This widespread pattern suggests specific constraints in pollinating bees potentially linked to limited resource availability and high parental investment. The particularly high load of deleterious mutations we report in the genome of these crucial ecosystem engineer species also raises new concerns about their ongoing population decline.

Keywords: *population size, selection efficiency, bees, Hymenoptera, eusociality, parasitism*

Posted: XXXXthe date of deposit in the preprint server dd mm yyy

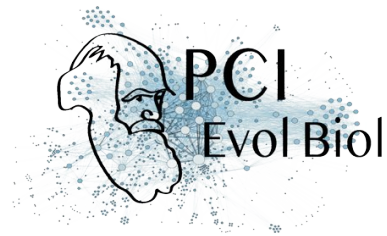
Recommender: Bertanne Visser

Reviewers: Michael Lattorff and an anonymous reviewer

Correspondence:
jonathan.romiguier@umontpellier.fr

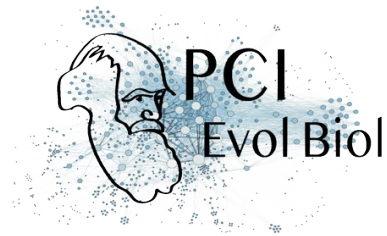
Introduction

The intensity of genetic drift experienced by a population depends on its effective population size, N_e (Wright 1931). Deleterious mutations reach fixation with a higher



probability in small populations, that undergo more drift, than in large populations where purifying selection is more efficient. N_e is usually defined for any observed population as the theoretical census size an ideal Wright-Fisher population should have to show the level of drift displayed by the observed population (Wang et al. 2016). While different definitions of N_e exist depending on the field, it generally correlates negatively with any process breaking the assumption of panmixia, which underlies the Wright-Fisher model (i.e., population structure, homogamy, inbreeding...). Building on this knowledge, it has been proposed that basic traits influencing the reproductive output and mating choices of organisms, such as life-history traits, should correlate with their genome-wide deleterious substitutions rates. Several examples confirming these predictions have been uncovered in the last two decades: species generation time, longevity or body mass were found to be positively correlated with the genome-wide dN/dS (i.e., the ratio of the non-synonymous substitution rate to the synonymous substitution rate) (Nikolaev et al. 2007; Romiguier et al. 2014; Popadin et al. 2007; Figueet et al. 2016; Botero-Castro et al. 2017; Rolland et al. 2020). However, most known examples are clustered within a few vertebrate taxa: mainly mammals, birds or reptiles. To date, only few examples of such patterns have been found in invertebrates, which casts doubt on the existence of a general relationship between life history strategies and the efficiency of natural selection in Metazoa. Various reasons might explain the difficulty to demonstrate such relationships in invertebrates: There is relatively fewer genomic data available than in mammals or birds, and gathering life-history data in a large number of non-model invertebrates can be difficult as they have generally received less attention than vertebrates. Effective population size comparisons among invertebrate clades can also be particularly difficult, as the existence of reproductive systems such as haplo-diploidy, where the male is haploid, affect N_e estimations (Wang et al. 2016).

Among invertebrates, all Hymenoptera conveniently share the same haplo-diploid system, while displaying a particularly wide diversity of life-history strategies. Notably, they exhibit extreme lifestyles that can be predicted to strongly influence their reproductive output, and thus their long-term N_e . First, many species within this clade are parasites of plants (phytophagous) or parasitoids of other arthropods (Mayhew 2016), which could shape their demography, as population structure and size of the host can restrict that of the parasite or, especially, of the parasitoid (Mazé-Guilmo et al. 2016). Second, the hymenopteran order contains a large number of pollinators, such as bees, that are involved in keystone insect-plant mutualisms and strictly depend on a limited floral resource generally scattered in time and space. Because of the limited availability of resources required for their brood, pollinating bees have to invest a lot of time and energy in terms of foraging, nesting and food processing for their offsprings (Zayed et al. 2005; Zayed and Packer 2007), which should limit their reproductive output and population size. Supporting this hypothesis, high parental investment has been previously identified as a general proxy for low N_e in animals (Romiguier et al. 2014a). Third, eusociality, which is a rare lifestyle in animals, is relatively common in Hymenoptera with at least 9 independent appearances (Hughes et al. 2008). Because reproduction is typically monopolized by few long-lived reproductive individuals (Keller and Genoud 1997), a decrease in long-term N_e and the efficiency of natural selection is often thought to be a general consequence of eusociality (Bromham and Leys 2005; Romiguier et al. 2014; Settepani et al. 2016). Maintenance of high relatedness within low- N_e inbred groups has also been proposed as a prerequisite to the evolution of eusociality because it favors altruistic behaviors



through kin-selection (Hamilton 1964; Husseneder et al. 1999; Hughes et al. 2008; Tabadkani et al. 2012). Ancestral population bottlenecks could thus be a typical feature of taxa in which eusociality frequently evolves, which is the case for several independent clades in Hymenoptera. Alternatively, it has been hypothesized that important population bottlenecks may be rare in Hymenoptera, because the associated loss of genetic diversity on single locus sex determination would lead to the costly production of sterile diploid males (Asplen et al. 2009; Rabeling and Kronauer 2013).

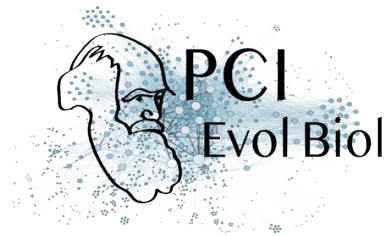
So far, few studies have investigated how N_e varies among Hymenoptera, and all were restricted to the effect of eusociality alone (Owen 1985; Berkelhamer 1983; Reeve et al. 1985; Bromham and Leys 2005; Romiguier et al. 2014; Imrit et al. 2020). Only recent studies with genome-wide datasets have detected associations between eusociality and decreases in N_e (Romiguier et al. 2014; Imrit et al. 2020), but these studies are typically restricted to few taxa compared to studies that rejected any significant effect (Bromham and Leys 2005). Disregarding the joint effect of other potential N_e determinants (e.g., body-size, parasitism, pollen-feeding, haplo-diploidy) may bias results and explain the discrepancy among studies with low vs high number of species comparisons.

Here, we tried to better assess the respective effects of potential N_e determinants in Hymenoptera. We used a phylogenomic dataset of 3256 genes in 169 species of Hymenoptera (Peters et al. 2017), including 10 eusocial species distributed among 4 independent origins of eusociality (Formicidae: 3 species; Polistinae/Vespinae wasps: 3 species; Stenogastrinae wasps: 1 species; Corbiculate bees: 3 species), 112 parasitic species and 32 solitary pollinating bees. We estimated mean genomic dN/dS for each species and compared these estimations between solitary and eusocial taxa, as well as between free and parasitic taxa (see figure S3). We also correlated these to body size, life-history descriptor variables of parasitoids (see table S1 for details) and geographical range descriptors (see table S5 for details). We further confirmed that detected increases in dN/dS do correspond to relaxed purifying selection (and thus to drops in N_e) via specialized analyses that differentiate positive selection from relaxed purifying selection. Unexpectedly, we found that, instead of large species, parasites or eusocial taxa, pollinating bees display by far the lowest long-term N_e among Hymenoptera.

Results

dN/dS distribution across the Hymenoptera phylogeny

We estimated dN/dS in 3241 gene alignments of 169 species of Hymenoptera using the mapNH program (Romiguier et al. 2012; <https://github.com/BioPP/testnh>) from the testnh program suite (Dutheil and Boussau 2008; Guéguen and Duret 2017). We used the tree obtained by Peters et al. (2017) and its topology through all analyses to correct for phylogenetic inertia. As eusocial Hymenoptera are known to have high recombination rates (Wilfert et al. 2007; Sirviö et al. 2011; Wallberg et al. 2015; Jones et al. 2019), which in turn are known to inflate dN/dS when associated to biased gene conversion in vertebrates (Duret and Galtier 2009; Lartillot 2012; Galtier et al. 2018), we estimated dN/dS considering GC-conservative substitutions only.



Estimated rates should, therefore, be impervious to the effects of biased gene conversion (Galtier et al. 2018). Average corrected genomic dN/dS values are displayed along the hymenopteran tree on figure 1 (see the distribution of uncorrected dN/dS values in figure S1). The largest and smallest mean ratios were inferred for *Eucera nigrescens* (0.1901) and *Cimbex rubida* (0.0684), respectively. As expected for conserved coding regions, the distribution of genomic dN/dS ratios is close to 0 (overall average of $0.0947 \pm 0.003sd$), indicative of the large prevalence of purifying selection. We observed above average dN/dS ratios in 3 of the 4 available eusocial clades: Formicidae ($0.1068 \pm 0.0093sd$, 3 species), Polistinae/Vespinae wasps ($0.1033 \pm 0.0088sd$, 3 species), and the *Apis/Bombus/Tetragonula* clade ($0.1086 \pm 0.0352sd$). This last clade of bees does not clearly stand out however, as most bees in the dataset (Anthophila, species characterized by pollen feeding of larvae: Apidae, Megachilidae, Halictidae, Colettidae, Andrenidae, and Melittidae) show high dN/dS ratios ($0.1190 \pm 0.0302sd$, 41 species) with no dependence on their social organization. Finally, only two purely solitary taxa displayed comparable dN/dS ratios: Siricoidea ($0.1025 \pm 0.0251sd$, 3 species) and Cynipoidea ($0.1005 \pm 0.0175sd$, 5 species).

We further used simple linear modeling to try and relate variation in dN/dS ratios to life history traits and geographical range descriptors. Phylogenetic independent contrasts were used to transform the data and account for phylogenetic relationships (Felsenstein 1985). We also used terminal branch length as a covariable in all models. This is because short terminal branches are known to bias dN/dS estimations upward as they yield more inaccurate estimations of this parameter, whose real value is often close to its zero boundary at a genomic scale. There is strong association between dN/dS ratios and branch length in this study (table 1). Variation in dN/dS estimation accuracy can also stem from variation in the number of genes available for each species. For example, four of the 10 available eusocial Hymenoptera (*Apis mellifera* and the three available ants), are species with published and annotated genomes (Consortium and The Honeybee Genome Sequencing Consortium 2006; Bonasio et al. 2010; Nygaard et al. 2011), and were used by Peters et al. (2017) as reference species for the identification of 1-1 orthologous genes, along with only one solitary reference species, *Nasonia vitripennis* (Werren et al. 2010). This translated into a relatively better power for gene prediction by Peters et al. (2017) in eusocial species, and thus into a significant ($T=3.0567$, $df=9.3549$, $p\text{-value}=0.01305$) over-representation of these eusocial species in alignments (mean number of alignments available per species: $2732.40 \pm 88.09sd$) compared to solitary species ($2276.7 \pm 90.74sd$). To control for potential biases originating from varying precision in estimations, we replicated all the analyses of this study using a balanced subsampled dataset containing 134 alignments, each of them containing data for the same 88 species (most represented half of the species, referred later as the 88-species dataset). Unless specified otherwise, presented results were obtained with the full dataset. Average corrected genomic dN/dS estimated using the 88-species subsampled dataset are displayed along the Hymenoptera tree in figure S2.

No effect of body size, parasitism and geographical range on relative protein evolution rates

Unlike findings in birds and mammals (Figuat et al. 2016; Botero-Castro et al. 2017), we found no significant effect of body size on dN/dS ratio in Hymenoptera (table 1). When testing for a difference in dN/dS ratios between parasitic (parasitoid or parasites) and free-living Hymenoptera (see table S3), we found a significant effect ($df=167$, $F=46.327$, $p\text{-val}=1.715e-10$, $R^2=0.217$), but which completely disappeared when taking

phylogeny into account ($df=166$, $F=1.211$, $p\text{-val}=0.272$, $R^2=0.007$). We thus interpret this as being a confounding effect of sampling disequilibrium, as groups with elevated ratios completely lack parasites (with the exception of the cuckoo bumblebee *Bombus rupestris* and *Sphecodes albilabris*), and discarded this grouping from our models. We further tried to test for an association between dN/dS ratios of reproductive strategy and diet specialization within parasitoids using life-history and host range descriptors found in the literature (Traynor and Mayhew 2005a; Traynor and Mayhew 2005b; Jervis et al. 2003; Mayhew 2016), and summarized in table S1. However these descriptors were very seldom available for the species contained in the present phylogenomic dataset, forcing us to use genus-level averaging for both traits and dN/dS ratios. We detected no significant associations between average dN/dS ratios and life-history in parasitoids at the genus-level. We also tested for an association between dN/dS ratios and four proxies of species geographical range obtained using occurrence data available on the GBIF database. dN/dS ratios showed no significant correlation with mean latitude of occurrences, maximal distance between occurrences, or two additional estimators of species range (table S5).

Anthophila bees and eusocial taxa reveal relaxed selection at the genomic scale

High dN/dS ratios in *Anthophila* bees is by far the strongest pattern observed in our results. Treating *Anthophila* as a covariable allows to significantly explain ($df=167$; $F=175.84$; $p\text{-val} < 2.2 \cdot 10^{-16}$) more than half the observed variation ($R^2=0.512$). Despite *Anthophila* being only one monophyletic group, this effect is still present when accounting for phylogeny (table 1), and when accounting for sampling effort variation by using the 88-species subsampled dataset (table S3). This effect is strong enough to completely mask the effect of eusociality when using the full dataset. Indeed, the social status of a terminal branch significantly explains dN/dS variations in the dataset only if removing all *Anthophila* samples from the analysis. This is because eusocial corbiculate bees do not show any increase in dN/dS values when compared to other *Anthophila*. The increase of dN/dS in ants and eusocial wasps, remains significant when accounting for sampling effort variation by using the 88-species subsampled dataset (table S3).

To ensure that previous results stem from a relaxation of selection and not from strong positive selection, we applied the Hyphy RELAX procedure (Pond et al. 2005; Wertheim et al. 2014) on each available alignment separately. This procedure allows to formally test for selection relaxation by modelling the distribution of dN/dS ratios along the branches a phylogeny and by comparing the distribution fitted on a focal group of branches (eusocial taxa and *Anthophila*, alternatively) to the distribution fitted for the rest of the tree. Out of 3236 realized tests, 1743 (53.9%) detected relaxed selection on eusocial branches (including eusocial bees) and 184 (5.7%) detected intensified selection. Genes under relaxation of selection thus represent 90% of the genes for which a difference of selection efficiency between eusocial branches and focal branches could be detected. Results of a gene ontology enrichment analysis conducted with genes under intensified selection in eusocial species as focal genes are presented in table S4, but revealed no clear pattern. Using a conservative bonferroni correction for multiple testing in this procedure still leads to the detection of selection relaxation in 751 genes and of selection intensification in 28 genes. These results also hold if the more balanced 88-species subsampled dataset is used, as out of 134 alignments, 68 genes supported a relaxation of selection and 16 genes supported an intensification of selection. Moreover, the detected effect of eusociality does not

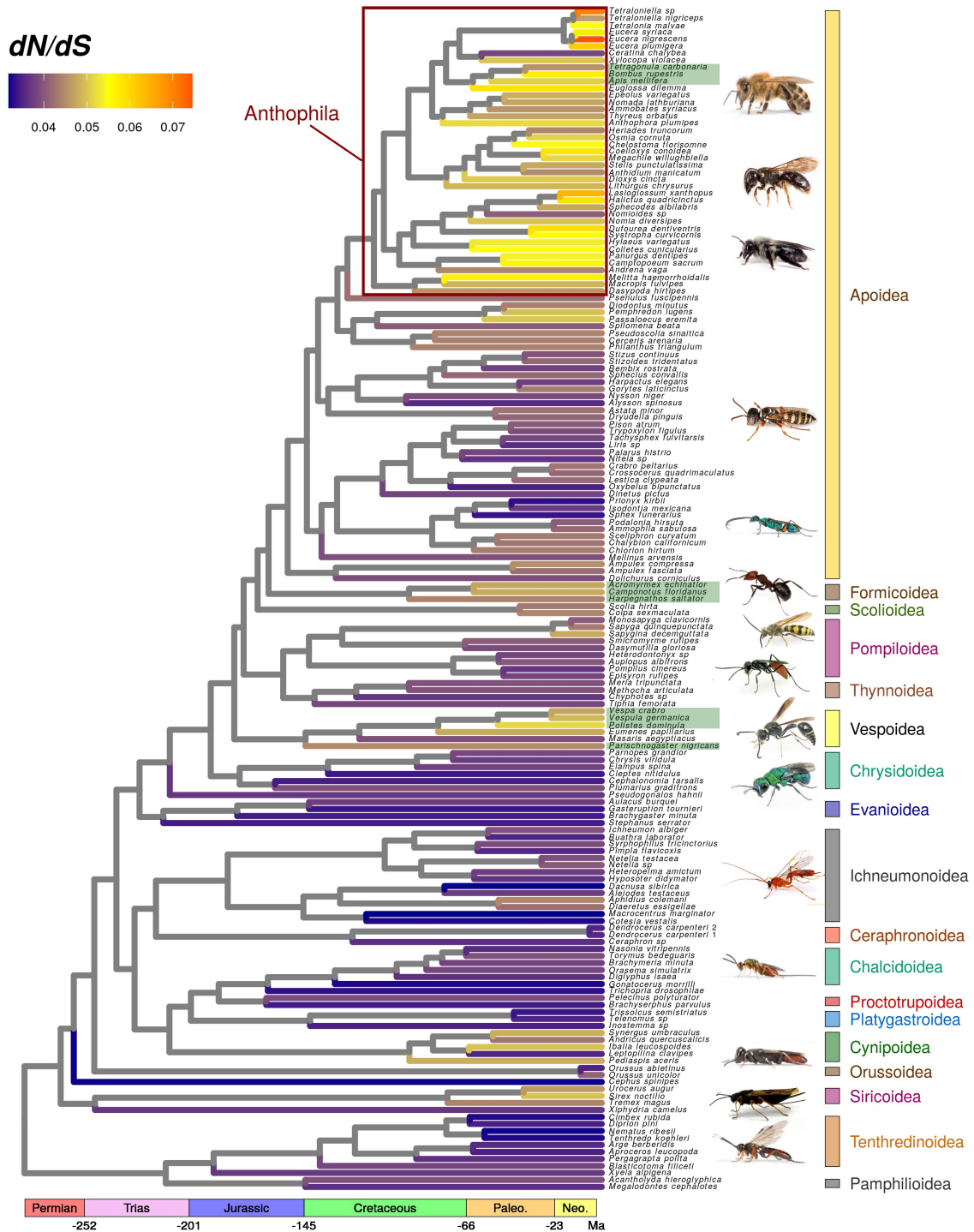


Figure 1. Corrected genomic dN/dS ratios for 169 species of Hymenoptera. dN/dS ratios estimated on terminal branches using 3241 genes are represented on the chronogram inferred by Peters et al. (2017). Green rectangles around labels indicate eusocial taxa.

seem to be driven by any over-representation of bees within eusocial species. The average number of eusocial bee sequences available for genes with relaxed selection ($2.427 \pm 0.018sd$) is not different than within genes without relaxed selection ($2.463 \pm 0.024sd$) ($F=2.11$; $pval=0.146$). These verifications are needed as bees experience an even stronger relaxation of selection. If this was apparent from simple modelling of genomic dN/dS ratios, it is made even more obvious by the application of the RELAX procedure with Anthophila branches as focal branches. Out of 3239 realized tests, 2000 (61.74%) detected relaxed selection on eusocial branches, while 294 detected an intensification of selection (9.07%). Using a conservative bonferroni correction for multiple testing in this procedure still leads to the detection of selection relaxation in 1210 genes and of selection intensification in 66 genes.

covariables	All samples residual df = 127; $R^2=0.082$			Non-Anthophila samples residual df = 97; $R^2=0.117$		
	R^2	F	p-value	R^2	F	p-value
branch length	0.0347	4.8040	0.0302	0.0751	8.2422	0.0051
adult size	0.0085	1.1793	0.2795	0.0048	0.5363	0.4657
Anthophila	0.0381	5.2677	0.0233	-	-	-
Eusociality	0.0008	0.1232	0.7261	0.0372	4.0915	0.0458

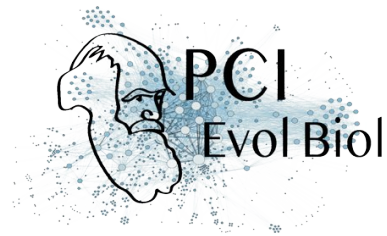
Table 1. Linear modelling of corrected dN/dS ratios. Corrected dN/dS are obtained using 3241 genes and GC-conservative substitutions. Displayed results are obtained when simultaneously using all covariables inside a multiple linear model. Phylogenetic independent contrasts are used for all variables so as to account for phylogenetic autocorrelation.

Discussion

Molecular consequences of body-size, parasitism and eusociality

Contrary to observed patterns in vertebrates (Nikolaev et al. 2007; Romiguier et al. 2014; Popadin et al. 2007; Figuet et al. 2016; Botero-Castro et al. 2017; Rolland et al. 2020), we did not detect any significant effect of body size on dN/dS in Hymenoptera. This suggests that the general association between body size and N_e observed in vertebrates is not universal in Metazoa, particularly in Hymenoptera. Parasitism is also not significantly associated to N_e decreases, which is surprising given the theoretical constraints imposed by the host (Papkou et al. 2016). This surprising negative result might be partly explained by the fact that Hymenoptera parasitoids lifecycle mostly requires a single insect host, a resource that might be not as limiting as parasites of vertebrates with complex lifecycles (Strobel et al. 2019).

We observed a significantly higher accumulation of non-synonymous substitutions in eusocial genomes, although the effect is relatively modest compared to the global pattern of increased dN/dS in pollinating bees (Anthophila). This increase can not be imputed to biased gene conversion, which is known to increase dN/dS by promoting the fixation of any G/C alleles (including deleterious alleles) (Rousselle et al. 2019), because our



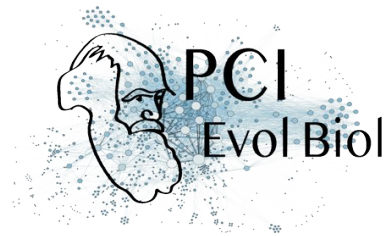
results are obtained using dN/dS ratios accounting only for GC-conservative substitutions. This result can not be imputed to positive selection either, as RELAX analyses detected relaxed selection on eusocial branches for more than half of the available alignments. This result supports the hypothesis of a relaxation of selection associated with eusociality through demographic effects. Long-lived reproductive female with delayed sexual maturity, as well as a biased sex-ratio and monopolization of the reproductive labor by few individuals, are typical features of eusocial species, which are bound to reduce effective population size. The hypothesis of a life-history effect matches well with the observation of a higher dN/dS in the highly eusocial formicoids ants *Acromyrmex echinatio* and *Camponotus floridanus* than in *Harpegnatos saltator*, which possesses a less complex social organization (Hölldobler and Wilson 1990) .

These results are however to be taken with care, as the number of eusocial species in the dataset is low, and as no significant increase in dN/dS due to eusociality has been detected within bees. In this study, a choice was made not to increment the original dataset with additional eusocial species, because this addition would have introduced heterogeneity in sample treatment, and translated into new bias in the estimation of dN/dS ratios. It might be necessary to replicate our analyses using a separate, tailor-made and more exhaustive dataset in terms of eusocial species number in order to confirm the effect of eusociality on demography. Another exciting prospect will be to study N_e variation within eusocial groups. Ants, which display a variety of complexity levels in their social organisation, could represent an ideal model for a more quantitative approach (Bourke 1999), allowing to test for an effect of variation in eusocial characteristics of species on selection efficiency.

Ecological and molecular predisposition to eusociality in bees

High genomic dN/dS ratios in all social and solitary bees unexpectedly appears as the major pattern of our results. Besides many independent transitions toward eusociality, Anthophila are characterized by their pollen-collecting behaviors which might explain our results. This dependence to large amounts of pollen to feed larvae is indeed believed to be a potential constraint on N_e , particularly in specialist species (Zayed et al. 2005; Zayed and Packer 2007). Pollen is a resource which is scattered in space and time and require a large energetic investment to come by and exploit (through progressive provisioning), thus constraining the very fecundity of females, which invest a lot of time and energy in their descent. Parental investment has already been highlighted as the major determinant of genetic diversity and long-term N_e in animal species (Romiguier et al. 2014). We suggest that high parental investment in pollinating bees might be a major factor limiting their N_e . This could in turn provide an explanation for the absence of differences between dN/dS ratios in social and solitary pollen-collecting species. Group-living might indeed represent a way to enhance the productivity of pollen collecting and metabolizing, thus compensating the decrease of N_e linked to eusociality in Anthophila.

Contrary to the general pattern in animals, pollinating bees appears as an exception and display higher species richness at high latitudes compared to tropics (Orr et al. 2020). This suggests that the diversification and origin of a pollinating bee lifestyle stems to environments with strong seasonality and important long-term climatic oscillations, which might have led to frequent bottlenecks in their population history. One previous study in Teleost fishes has shown that species of temperate regions display lower N_e than species of



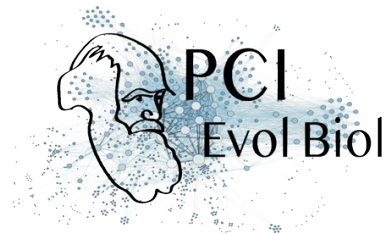
tropical regions (Rolland et al. 2020), while another found no such link across Metazoans (Romiguier et al. 2014b). Similarly to the latter, we found no associations between mean latitude (or other range descriptors) and dN/dS ratios in Anthophila (see table S5). However this result might be simply due to the massive over-representation of species from temperate regions in our dataset, and more thorough studies focusing on more tropical species will be necessary to draw any conclusions. In any case, specialized feeding on flowers appears here as a specialization to ecosystems with relatively low carrying capacity (Orr et al. 2020) requiring high parental investment for a scarce resource. Pollinating bees thus represent an ideal model to study the links between long-term demographics and seasonal variation in resource availability in temperate or arid environments. Anthophila could be also used to formally test whether the degree of specialization of a species towards one or a few plant species constrains N_e at the genomic scale in the general case (Zayed et al. 2005). Finally, bees might represent an opportunity to gain novel insights about the links between long-term demographics and characteristics more specific to Hymenoptera, such as nest parasite load (Wcislo 1987).

Interestingly, besides pollen-collecting, Anthophila (bees) is also the taxa with the highest number of independent origins of eusociality in the tree of life (Hughes et al. 2008). This suggests that low N_e is not only a consequence of group-living, but might also facilitate evolution toward eusociality. Supporting this hypothesis, low N_e due to intense inbreeding has been associated to communal behaviors in nesting and high parental care, two classical pre-requisites to an eusocial lifestyle (Hamilton 1964; Hussedener et al. 1999; Tabadkani et al. 2012; Wilson et al. 2008). Inbreeding also tends to increase within-group relatedness, which theoretically increases the benefit of kin selection, potentially favouring the emergence of eusociality (Hamilton 1964; Hussedener et al. 1999; Tabadkani et al. 2012; Kay et al. 2020; but see Nowak et al. 2010). Few genomic evidences supporting such a link have been observed so far. By showing a striking increase in dN/dS ratio in all Anthophila bees - the taxa concentrating more than half of the origins of eusociality in the tree of life - our results are the first genomic insight supporting the idea that low- N_e might have preceded and/or favoured evolution towards eusociality. As suggested previously in the literature, the evolution towards eusociality might have been favoured by the emergence of small groups of inbred individuals, despite the cost associated to genetic diversity loss at the sex determination single locus (Rabeling and Kronauer 2013).

Besides their implication regarding the evolution of eusociality, our results have important consequences for the conservation field. Pollination has been found to rely heavily on wild and domesticated bees, which ensure the majority of animal-mediated pollination of wild and domesticated plants in most ecosystems (Winfree 2010). Our finding of particularly high deleterious substitution rates within this group raises the additional concern that bee species might be especially sensitive to any further population decline, which are already known as particularly alarming (Murray et al. 2009; Arbetman et al. 2017; Powney et al. 2019).

Conclusion

This study brings supplemental genomic evidence supporting an association between eusociality and reduced effective population size. We thus bring further support to the hypothesis that the extreme life-



history traits of eusocial species constrain their molecular evolution. More interestingly, the surprisingly massive and widespread reduction of selection efficiency in both eusocial and solitary bees suggests unexpectedly high constraints of a pollinator lifestyle, potentially linked to limiting resource and high parental investment. This also brings genomic support to the hypothesis that some ecological characteristics associated with low N_e might have facilitated evolution towards eusociality. Altogether, this study suggests that, conversely to vertebrates, purifying selection efficiency in invertebrates is more constrained by lifestyle and ecology than simple body size.

Data accessibility

The original dataset of Peters et al. (2017), with alignments and trees, is provided by the its authors at <http://dx.doi.org/10.17632/trbj94zm2n.2>. Detailed tables containing data used for this paper as well as obtained results are available at Zenodo.org : <https://zenodo.org/record/3999857#.XOU5BBk6-it>.

Acknowledgements

We thanks Nicolas Galtier for advices during the writing of the manuscript and Laurent Keller for useful discussions. Version 5 of this preprint has been peer-reviewed and recommended by Peer Community In Evolutionary Biology (<https://doi.org/10.24072/pci.evolbiol.100120>)

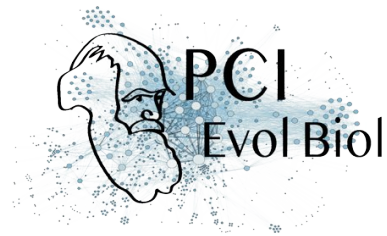
Conflict of interest disclosure

The authors of this preprint declare that they have no financial conflict of interest with the content of this article.

Materials and Methods

Genetic data

Data was downloaded from the authors' online repository (<http://dx.doi.org/10.17632/trbj94zm2n.2>). It originally contained nucleotide and amino-acids multi-sample alignments for 3256 protein coding genes predicted to be 1-1 orthologs in 174 species (see Peters et al. 2017 for details about the production of these alignments), 5 of which are outgroups to the Hymenoptera (2 Coleoptera, 1 Megaloptera, 1 Neuroptera and 1 Raphidioptera), and 10 of which are eusocial species. The latter belong to 5 independent eusocial clades: corbiculate bees (*Tetragonula carbonaria*, *Bombus rupestris* and *Apis mellifera*), ants (*Acromyrmex echinator*, *Camponotus floridanus* and *Harpegnathos saltator*), Polistinae/Vespinae wasps (*Vespa crabro*, *Vespula germanica* and *Polistes dominula*), Stenogastrinae wasps (*Parischnogaster nigricans*). (Cardinal and Danforth 2011). The data also contained the trees inferred using this data by the original authors. We used



the dated chronogram inferred by the authors using amino-acid data throughout this study. This tree corresponds to their main results and is contained in the file `dated_tree_aa_inde_2_used_in_Fig1.tre` available on the authors' online repository.

Data cleaning

Each amino-acid alignment was first checked for potential false homology using HmmCleaner (Di Franco et al. 2019; Philippe et al. 2017) with default settings. The resulting maskings were then reported on corresponding nucleotide sequences using the `reportMaskAA2NT` program from the MASCE program suite (Ranwez et al. 2011). At this point, we discarded individual sequences containing less than 50% of informative site within one alignment.

dN/dS ratios estimation

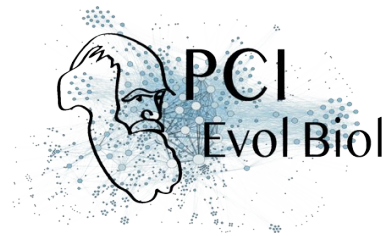
Cleaned alignments were then used, along with the tree topology inferred by Peters et al. (2017) and the mapNH binary (Romiguier et al 2012; <https://github.com/BioPP/testnh>), to estimate synonymous and non-synonymous substitution rates along the branches of the Hymenoptera tree. MapNH allows a fast estimation of those rates by using tree-wide parameters obtained a priori by fitting a homogeneous model (YN98) to the data with the help of `bppml` (Dutheil and Boussau 2008), to parsimoniously map observed substitutions to the supplied topology. Estimated substitution counts for specific branches, obtained separately for each alignments, can then be summed to obtain genome-wide substitution rates. We used this method to obtain dN/dS ratios of terminal branches, susceptible to carry information about the long-term drift regime of extant lineages. 15 alignments did not contain enough data to allow correct convergence of the homogeneous model needed by mapNH.

Controlling for biased gene conversion

We produced a corrected dN/dS using only GC conservative substitutions to estimate dN/dS. This was achieved using a custom version of mapNH developed in our lab (Rousselle et al. 2019) which categorizes mapped substitutions into GC-conservative (GC->GC or AT->AT) and GC-modifying (AT->GC or GC->AT) substitutions, and uses only the former to compute dN/dS ratios. Ratios obtained this way show more sampling variance, as they are obtained from smaller substitution counts. This translates in higher genomic dN/dS, as this parameter is usually close to its zero bound in exons. These rates are however supposedly impervious to gBGC.

Controlling for sampling bias

Four Hymenoptera (*Apis mellifera* and the three ants), which represent nearly half the eusocial species considered, are species with published genomes. This translates into a better power for gene prediction and thus, into an over-representation of these species in the dataset. Imprecisions in dN/dS ratios estimations are in turn known to yield higher values, because the real value of this ratio in functional sequences is often close to its zero boundary. We thus applied an additional sub-sampling procedure, designed to correct for any potential bias in our estimations that could stem from variation in the quantity of information available for each species. We applied every analysis mentioned before to a reduced but complete dataset containing



data only for the most represented half of the species (88 species), and only alignments containing information for each of these species (135 alignments).

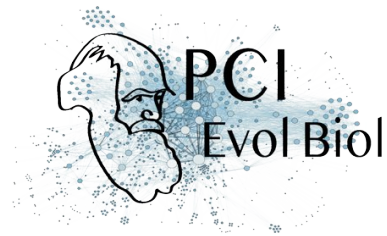
Linear modelling of dN/dS ratios

Estimated rates, corrected rates and rates obtained from the 88-species subsampled dataset were then modelled through simple linear models using the R software environment, using adult size, social status (eusocial or solitary) and membership to Anthophila as covariables. We also used this statistical setting to evaluate the effect of branch length. Short branches are known to bias dN/dS estimations upward because they yield more inaccurate and thus generally higher estimations of this parameter. The phylogenetic setting was taken into account by using phylogenetic independent contrast (Felsenstein 1981) for each variable. This was done using the `pic()` function in the R package `ape`. To try and further uncover the potential links between dN/dS ratios and life-history within Hymenoptera, we also attempted to correlate dN/dS ratios with major descriptors of parasitic type within parasitoid Hymenoptera. These descriptors were gathered from databases designed to describe the reproductive strategy of parasitoids (Traynor & Mayhew 2005a; Traynor & Mayhew 2005b, Jervis & Ferns 2011; Mayhew 2016) and are summarized in table S1. We conducted the analysis at the genus level using genus-averaged dN/dS ratios and descriptors. This was necessary because the species-level concordance between databases was too low (only 6 species in common between the genomic database and the parasitoid life-history database). We used Pearson's linear correlation coefficient for continuous descriptors and Kruskal-Wallis tests for discrete descriptors.

Finally, we tested the correlation of dN/dS ratios with four proxies of species range. For each species (and for all known synonyms) in the sample, we queried all available occurrence points from the GBIF database, using the R package `rgbif`. Occurrence data was then used to calculate for classical proxies of species range. The mean latitude was calculated as a simple unweighted mean between occurrences. The maximum distance between two occurrences was calculated taking all occurrences into account, even when the species occurred on more than one continent. The circular area around occurrence was calculated by casting 100km-radius circles around each occurrence, and estimating the total land surface contained in at least one circle. The convex hull area around occurrence was calculated by estimating the total land surface contained in the smallest convex hull containing all occurrences. When a species occurred on more than one continent, a separate convex hull was used per continent.

RELAX analyses

We used the RELAX procedure (Wertheim et al. 2014) from the HyPhy program suite (Pond, Frost, and Muse 2005) to test for the presence of a systematic relaxation of selection on branches belonging to eusocial groups (thereafter called "eusocial branches"), that is all branches descending from the ancestral node of one of the eusocial clade present in the dataset. HyPhy allows, for a specific sequence alignment, to model the distribution of dN/dS ratios along the branches of a tree. The RELAX procedure consists first in defining focal and background branches, associated with one focal and one background distribution of dN/dS ratios. It then consists in comparing a model where the two mentioned distribution are identical (null model, no differences between branch sets) to a model where the focal distribution is a power transform of the

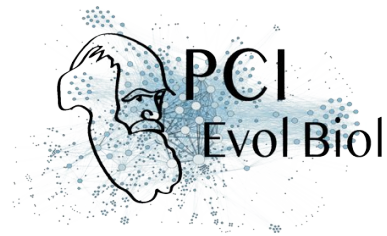


background distribution ($\omega_f = \omega_{bk}$). Relaxation of selection is inferred when the second model appears superior based on a log-ratio test (differences between branch sets), and when the focal distribution is narrower than the background distribution (k parameter estimated to be less than 1). Indeed, strong selection is thought to produce both low (close to 0) and high (greater than 1) dN/dS ratios, while neutrality should produce rates close to 1. This test thus correctly takes into account the fundamental two-sided nature of dN/dS ratios. 20 (0.61%) of the original alignments did not contain enough data to allow models necessary to the HyPhy RELAX procedure to be fitted with eusocial branches as background branches, and 17 (0.52%) of the original alignments didn't allow the procedure with Anthophila branches as background branches.

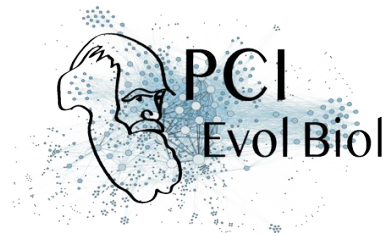
References

- Arbetman, M. P., G. Gleiser, C. L. Morales, P. Williams, and M. A. Aizen (2017). Global decline of bumblebees is phylogenetically structured and inversely related to species range size and pathogen incidence. *Proc. R. Soc. B Biol. Sci.*, 284, 1–8.
- Asplen, M. K., J. B. Whitfield, J. G. D. E. Boer, and G. E. Heimpel (2009). Ancestral state reconstruction analysis of hymenopteran sex determination mechanisms. *J. Evol. Biol.*, 22, 1762–1769.
- Berkelhamer, R. C. (1983). Intraspecific genetic variation and haplodiploidy, eusociality, and polygyny in the Hymenoptera. *Evolution*, 37, 540–545.
- Bonasio, R., G. Zhang, C. Ye, N. Mutti, X. Fang, N. Qin, et al. (2010). Genome sequencing and comparison of the socially distinct ant species *Harpegnathos saltator* and *Camponotus floridanus*. *Science*, 329, 1068–1071.
- Botero-Castro, F., E. Figuet, M.-k. Tilak, B. Nabholz, and N. Galtier (2017). Avian genomes revisited: hidden genes uncovered and the rates versus traits paradox in birds. *Mol. Biol. Evol.*, 32, 1–9.
- Bromham, L. and R. Leys (2005). Sociality and the rate of molecular evolution. *Mol. Biol. Evol.*, 22, 1393–1402.
- Cardinal, S. and B. N. Danforth (2011). The antiquity and evolutionary history of social behavior in bees. *PLoS One*, 6.
- Crespi, B. J. and D. Yanega (1995). The definition of eusociality. *Behav. Ecol.*, 6, 109–115.
- Di Franco, A., R. Poujol, D. Baurain, and H. Philippe (2019). Evaluating the usefulness of alignment filtering methods to reduce the impact of errors on evolutionary inferences. *BMC Evol. Biol.*, 19, 1–17.
- Duret, L. and N. Galtier (2009). Biased gene conversion and the evolution of mammalian genomic landscapes. *Annu. Rev. Genomics Hum. Genet.*, 10, 285–311.
- Dutheil, J. and B. Boussau (2008). Non-homogeneous models of sequence evolution in the Bio++ suite of libraries and programs. *BMC Evol. Biol.*, 8, 1–12.
- Felsenstein, J. (1985). Phylogenies and the comparative method. *Am. Nat.*, 125, 1–15.
- Figuet, E., B. Nabholz, M. Bonneau, E. Mas Carrio, K. Nadachowska-Brzyska, H. Ellegren, et al. (2016). Life history traits, protein evolution, and the nearly neutral theory in amniotes. *Mol. Biol. Evol.*, 33, 1517–1527.

- Galtier, N., C. Roux, M. Rousselle, J. Romiguier, E. Figuet, N. Bierne, et al. (2018). Codon usage bias in animals : disentangling the effects of natural selection, effective population size, and GC-biased gene conversion. *Mol. Biol. Evol.*, 35, 1092–1103.
- Guéguen, L. and L. Duret (2017). Unbiased Estimate of Synonymous and Nonsynonymous Substitution Rates with Nonstationary Base Composition. *Mol. Biol. Evol.*, 35, 734–742.
- Hamilton, W. D. (1964). The genetical evolution of social behaviour . I. *J. Theor. Biol.*, 7, 1–16.
- Hölldobler, B. and E. O. Wilson (1990). *The ants*. Harvard Univ. Press, Cambridge, Massachusetts, pp. 1–732.
- Hughes, W. O. H., B. P. Oldroyd, M. Beekman, and F. L. W. Ratnieks (2008). Ancestral monogamy shows kin selection is key to the evolution of eusociality. *Science*, 320, 1213–1216.
- Husseneder, C., R. Brandl, C. Epplen, J. T. Epplen, and M. Kaib (1999). Within-colony relatedness in a termite species : genetic roads to eusociality ? *Behaviour*, 136, 1045–1063.
- Imrit, M. A., K. A. Dogantzis, B. A. Harpur, and A. Zayed (2020). Eusociality influences the strength of negative selection on insect genomes. *Proc. R. Soc. B Biol. Sci.*, 287, 1–7.
- Jervis, M. A., P. N. Ferns, and G. E. Heimpel (2003). Body size and the timing of egg production in parasitoid wasps : a comparative analysis. *Funct. Ecol.*, 17, 375–383.
- Jervis, M. A. and P. Ferns (2011). Towards a general perspective on life-history evolution and diversification in parasitoid wasps. *Biol. J. Linn. Soc.*, 104, 443–461.
- Jones, J. C., A. Wallberg, M. J. Christmas, K. M. Kapheim, and M. T. Webster (2019). Extreme differences in recombination rate between the genomes of a solitary and a social bee. *Mol. Biol. Evol.*, 36, 2277–2291.
- Keller, L. and M. Genoud (1997). Extraordinary lifespans in ants: a test of evolutionary theories of ageing. *Nature*, 389, 958–960.
- Lartillot, N. (2012). Phylogenetic patterns of GC-biased gene conversion in placental mammals and the evolutionary dynamics of recombination landscapes. *Mol. Biol. Evol.*, 30, 489–502.
- Lynch, M. (2007). The frailty of adaptive hypotheses for the origins of organismal complexity. *Proc. Natl. Acad. Sci.*, 104, 8597–8604.
- Lynch, M. and J. S. Conery (2003). The origins of genome complexity. *Science*, 302, 1401–1404.
- Mayhew, P. J. (2016). Comparing parasitoid life histories. *Entomol. Exp. Appl.*, 159, 147–162.
- Mazé-Guilmo, E., S. Blanchet, K. D. McCoy, and G. Loot (2016). Host dispersal as the driver of parasite genetic structure: A paradigm lost? *Ecol. Lett.*, 19, 336–347.
- Murray, T. E., M. Kuhlmann, and S. G. Potts (2009). Conservation ecology of bees : populations , species and communities. *Apidologie*, 40, 211–236.
- Nikolaev, S. I., J. I. Montoya-Burgos, K. Popadin, L. Parand, E. H. Margulies, and S. E. Antonarakis (2007). Life-history traits drive the evolutionary rates of mammalian coding and noncoding genomic elements. *Proc. Natl. Acad. Sci.*, 104, 20443–20448.



- Nygaard, S., G. Zhang, M. Schiøtt, C. Li, Y. Wurm, H. Hu, et al. (2011). The genome of the leaf-cutting ant *Acromyrmex echinatior* suggests key adaptations to advanced social life and fungus farming. *Genome Res.*, 21, 1–10.
- Orr, M. C., A. C. Hughes, D. Chesters, J. Pickering, C.-d. Zhu, and J. S. Ascher (2020). Global patterns and drivers of bee distribution. *Curr. Biol.*, In Press, 1–8.
- Owen, R. E. (1985). Difficulties with the interpretation of patterns of genetic variation in the eusocial Hymenoptera. *Evolution*, 39, 205–210.
- Peters, R. S., L. Krogmann, C. Mayer, A. Donath, S. Gunkel, K. Meusemann, et al. (2017). Evolutionary History of the Hymenoptera. *Curr. Biol.*, 27, 1013–1018.
- Philippe, H., D. M. de Vienne, V. Ranwez, B. Roure, D. Baurain, and F. Delsuc (2017). Pitfalls in supermatrix phylogenomics. *Eur. J. Taxon.*, 283, 1–25.
- Pond, S. L. K., S. D. W. Frost, and S. V. Muse (2005). HyPhy : hypothesis testing using phylogenies. *Bioinformatics*, 21, 676–679.
- Popadin, K., L. V. Polishchuk, L. Mamirova, D. Knorre, and K. Gunbin (2007). Accumulation of slightly deleterious mutations in mitochondrial protein-coding genes of large versus small mammals. *Proc. Natl. Acad. Sci.*, 104, 13390–13395.
- Powney, G. D., C. Carvell, M. Edwards, R. K. A. Morris, H. E. Roy, B. A. Woodcock, et al. (2019). Widespread losses of pollinating insects in Britain. *Nat. Commun.*, 10, 1–7.
- Rabeling, C. and D. J. C. Kronauer (2013). Thelytokous parthenogenesis in eusocial hymenoptera. *Annu. Rev. Entomol.*, 58, 273–292.
- Rahnenfuhrer, J. and A. Alexa (2019). topGO: Enrichment Analysis for Gene Ontology (version 2.38.1.)
- Ranwez, V., S. Harispe, F. Delsuc, and E. J. Douzery (2011). MACSE: Multiple alignment of coding SEquences accounting for frameshifts and stop codons. *PLoS One*, 6, 1–10.
- Reeve, H. K., J. S. Reeve, and D. W. Pfennig (1985). Eusociality and genetic variability: a re-evaluation. *Evolution*, 39, 200–201.
- Rolland, J., D. Schluter, and J. Romiguier (2020). Vulnerability to fishing and life history traits correlate with the load of deleterious mutations in teleosts. *Mol. Biol. Evol.*, 37, 2192–2196.
- Romiguier, J., P. Gayral, M. Ballenghien, A. Bernard, V. Cahais, A. Chenuil, et al. (2014a). Comparative population genomics in animals uncovers the determinants of genetic diversity. *Nature*, 515, 261–263.
- Romiguier, J., J. Lourenco, P. Gayral, N. Faivre, L. A. Weinert, S. Ravel, et al. (2014b). Population genomics of eusocial insects: The costs of a vertebrate-like effective population size. *J. Evol. Biol.*, 27, 593–603.
- Rousselle, M., A. Laverré, E. Figuet, B. Nabholz, and N. Galtier (2018). Influence of Recombination and GC-biased Gene Conversion on the Adaptive and Nonadaptive Substitution Rate in Mammals versus Birds. *Mol. Biol. Evol.*, 36, 458–471.



- Settepani, V., J. Bechsgaard, and T. Bilde (2016). Phylogenetic analysis suggests that sociality is associated with reduced effectiveness of selection. *Ecol. Evol.*, 6, 469–477.
- Sirviö, A., J. S. Johnston, T. Wenseleers, and P. Pamilo (2011). A high recombination rate in eusocial Hymenoptera: evidence from the common wasp *Vespula vulgaris*. *BMC Genet.*, 12, 1–7.
- Tabadkani, S. M., J. Nozari, and M. Lihoreau (2012). Inbreeding and the evolution of sociality in arthropods. *Naturwissenschaften*, 99, 779–788.
- The Honeybee Genome Sequencing Consortium, T. H. G. S. (2006). Insights into social insects from the genome of the honeybee *Apis mellifera*. *Nature*, 443, 931–949.
- Traynor, R. E. and P. J. Mayhew (2005a). A comparative study of body size and clutch size across the parasitoid Hymenoptera. *Oikos*, 109, 305–316.
- (2005b). Host range in solitary versus gregarious parasitoids: A laboratory experiment. *Entomol. Exp. Appl.*, 117, 41–49.
- Wallberg, A., S. Glémin, and M. T. Webster (2015). Extreme recombination frequencies shape genome variation and evolution in the honeybee, *Apis mellifera*. *PLoS Genet.*, 11, 1–27.
- Wang, J., E. Santiago, and A. Caballero (2016). Prediction and estimation of effective population size. *Heredity*, 117, 193–206.
- Wcislo, W. T. (1987). The role of seasonality, host synchrony, and behaviour in the evolutions and distributions of nest parasites in Hymenoptera (Insecta) with special reference to bees (Apoidea). *Biol. Rev.*, 62, 515–543.
- Werren, J. H., S. Richards, C. A. Desjardins, O. Niehuis, J. Gadau, J. K. Colbourne, et al. (2010). Corrected 26 march 2010; see last page. *Science*, 327, 343–348.
- Wertheim, J. O., B. Murrell, M. D. Smith, S. L. K. Pond, and K. Scheffler (2014). RELAX : Detecting relaxed selection in a phylogenetic framework. *Mol. Biol. Evol.*, 32, 820–832.
- Wilfert, L., J. Gadau, and P. Schmid-Hempel (2007). Variation in genomic recombination rates among animal taxa and the case of social insects. *Heredity*, 98, 189–197.
- Wilson, E. O. (2008). One giant leap : How insects achieved altruism and colonial life. *Bioscience*, 58, 17–25.
- Winfree, R. (2010). The conservation and restoration of wild bees. *Ann. New York Acad. Sci.*, 1195, 169–197.
- Wright, S. (1931). Evolution in mendelian populations. *Genetics*, 16, 97–159.
- Yang, Z. (1997). PAML : a program package for phylogenetic analysis by maximum likelihood. *Bioinformatics*, 13, 555–556.
- Zayed, A. and L. Packer (2007). The population genetics of a solitary oligolectic sweat bee , *Lasioglossum (Sphecodogastra) oenotherae* (Hymenoptera : Halictidae). *Heredity*, 99, 397–405.
- Zayed, A., L. Packer, J. C. Grixti, L. Ruz, R. E. Owen, and H. Toro (2005). Increased genetic differentiation in a specialist versus a generalist bee : implications for conservation. *Conserv. Genet.*, 6, 1017–1026.

Supplementary

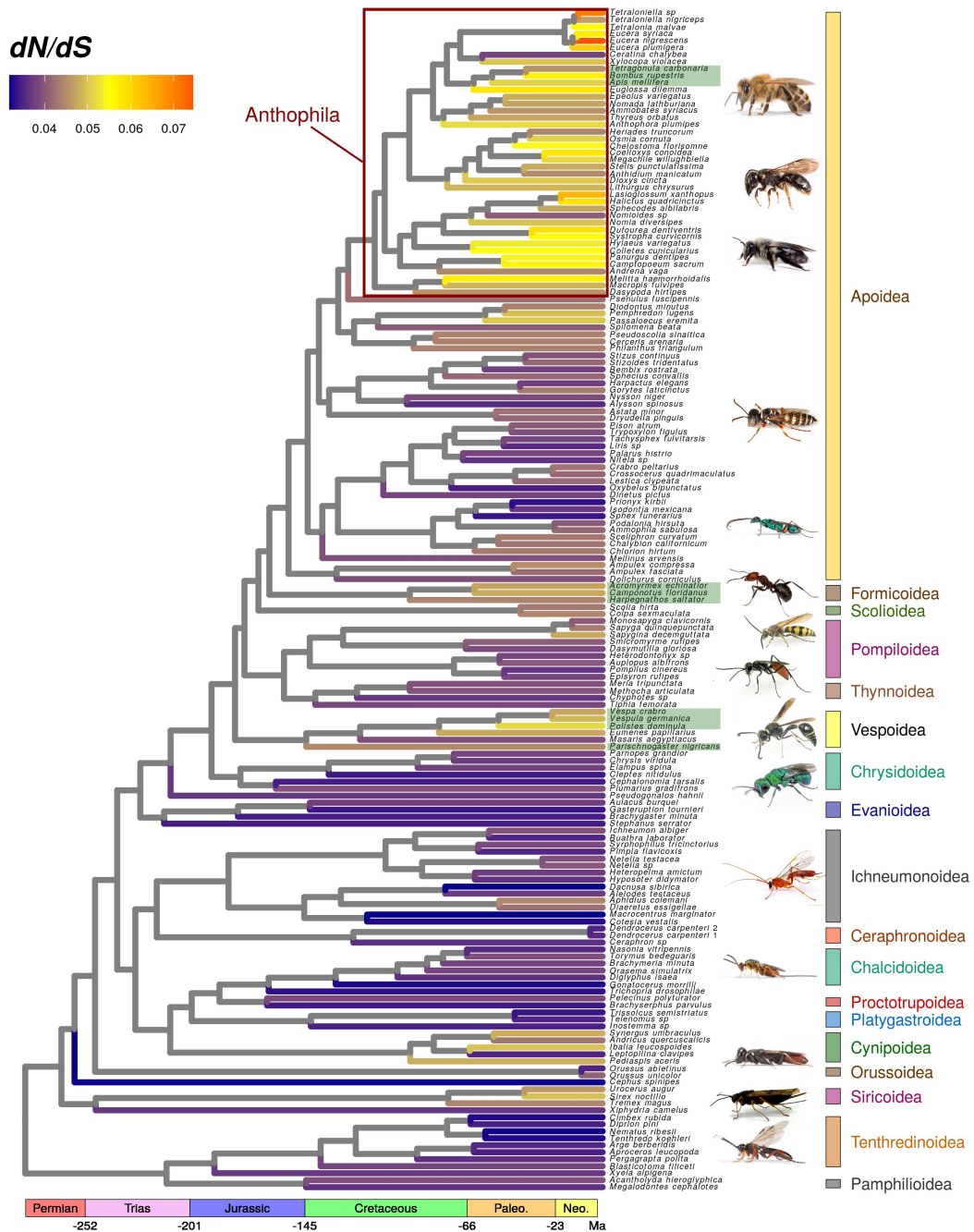


Figure S1. Uncorrected genomic dN/dS ratios for 169 species of Hymenoptera. dN/dS ratios estimated on terminal branches using 3241 genes and GC conservative substitutions are represented on the chronogram inferred by Peters et al. (2017). Green rectangles around labels indicate eusocial taxa.

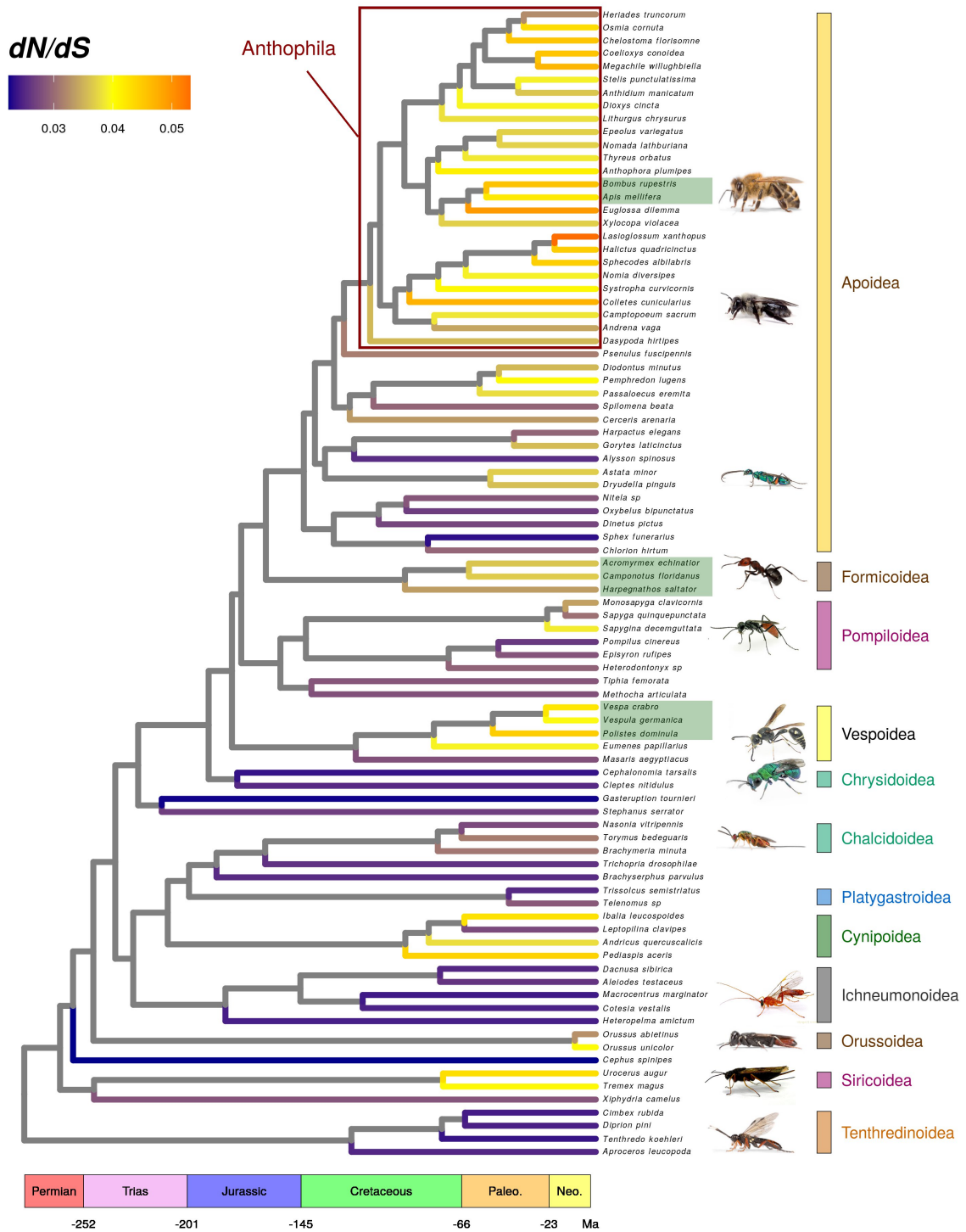


Figure S2. Genomic dN/dS ratios for 88 species of Hymenoptera. dN/dS ratios estimated on terminal branches using 134 genes with data for each of the displayed species are represented on the chronogram inferred by Peters et al. (2017). Green rectangles around labels indicate eusocial

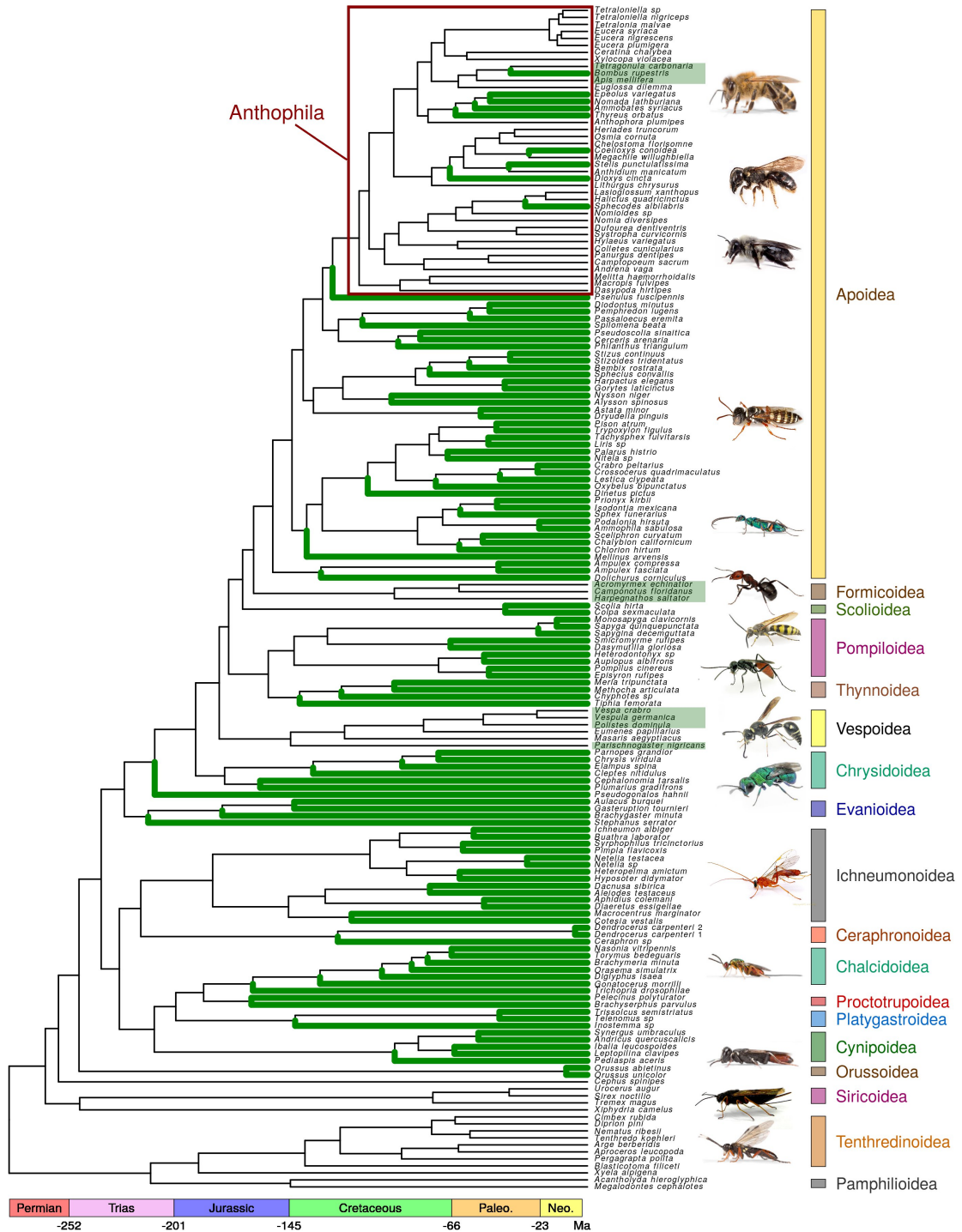


Figure S3. Parasitic species in the dataset. Parasitic species (parasitoids, parasites of plants and social parasites) are indicated by green terminal branches. Green rectangles around labels indicate eusocial taxa.

Variable	Description	Genera with information	correlation	p-val	source
continuous	Number of mature eggs at emergence	11	-0.048	0.889	Jervis & Ferns (2011) Mayhew (2016)
	Maximal number of mature eggs	10	0.146	0.688	Jervis & Ferns (2011) Mayhew (2016)
	Ovigenic index	10	0.114	0.711	Jervis & Ferns (2011) Mayhew (2016)
	Oviposition rate	10	0.176	0.627	Jervis & Ferns (2011)
	Egg length	3	-0.5	0.667	Traynor & Mayhew (2005a)
	Clutch size	5	-0.707	0.182	Traynor & Mayhew (2005a)
	Fecundity	14	0.415	0.14	Jervis & Ferns (2011) Traynor & Mayhew (2005a)
	Developpement time : egg -> adult	11	-0.2	0.55	Jervis & Ferns (2011)
	Time as an egg	4	0.2	0.8	Traynor & Mayhew (2005a)
	Time as a pupa	5	-0.3	0.624	Jervis & Ferns (2011) Traynor & Mayhew (2005a)
	Time as an adult	14	0.226	0.436	Jervis & Ferns (2011) Traynor & Mayhew (2005a)
	Host body length	8	0.119	0.779	Traynor & Mayhew (2005b)
	Number of potential host species	10	-0.234	0.515	Traynor & Mayhew (2005b)
discrete	Egg hydropisy	11	0.375	0.54	Jervis & Ferns (2011)
	Gregarious behavior	12	1.444	0.229	Jervis & Ferns (2011)
	Idiobiont/Koinobiont	13	1.371	0.242	Jervis & Ferns (2011)
	Ecto/Endoparasitism	18	0.022	0.882	Jervis & Ferns (2011) Traynor & Mayhew (2005b)
	Hyperparasitism	12	0.185	0.667	Jervis & Ferns (2011)
	Host-feeding behavior	12	0.26	0.61	Jervis & Ferns (2011)
	Host developpement stage during oviposition	10	3.836	0.28	Traynor & Mayhew (2005b)
	Host concealment	7	2.4	0.121	Traynor & Mayhew (2005b)

Table S1. Life-history and specialisation descriptors for parasitoids. Tested variables and their description are displayed along with the value of the statistic obtained for each correlation test with corrected dN/dS ratios. Correlation tests are Spearman tests for continuous variables and Kruskal-Wallis tests for discrete variables.

covariables	All samples residual df = 127; R ² =0.082			Non-Antophila samples residual df = 97; R ² =0.117		
	R ²	F	p-value	R ²	F	p-value
branch length	0.0389	5.5767	0.0197	0.0813	9.3867	0.0028
adult size	0.0269	3.8587	0.0516	0.0275	3.1808	0.0776
Antophila	0.0459	6.5762	0.0115	-	-	-
Eusociality	0.0011	0.1598	0.6900	0.0501	5.7797	0.0181

Table S2. Linear modelling of uncorrected dN/dS ratios. Displayed results are obtained when simultaneously using all covariables inside a multiple linear model. Phylogenetic independent contrasts are used for all variables so as to account for phylogenetic autocorrelation.

covariables	All samples residual df = 127; R ² =0.082			Non-Antophila samples residual df = 97; R ² =0.117		
	R ²	F	p-value	R ²	F	p-value
branch length	0.0281	2.2860	0.1351	0.0677	3.9381	0.0530
adult size	0.0283	2.2963	0.1342	0.0524	3.0525	0.0871
Antophila	0.0691	5.6131	0.0206	-	-	-
Eusociality	0.0237	1.9294	0.1692	0.0714	4.1567	0.0471

Table S3. Linear modelling of uncorrected dN/dS ratios in the 88-species subsampled dataset. Corrected dN/dS are obtained using GC-conservative substitutions only. Displayed results are obtained when simultaneously using all covariables inside a multiple linear model. Phylogenetic independent contrasts were used for all variables so as to account for phylogenetic autocorrelation.

domain	GO ID	Term	p-val
biological process	GO:0043623	cellular protein complex assembly	0.00011
	GO:0016043	cellular component organization	0.00011
	GO:0043604	amide biosynthetic process	0.00012
molecular function	GO:0003723	RNA binding	0.00018
	GO:0008092	cytoskeletal protein binding	0.00030
	GO:0003735	structural constituent of ribosome	0.00083
	GO:0005488	binding	0.00109
	GO:0051020	GTPase binding	0.00113
	GO:0005085	guanyl-nucleotide exchange factor activity	0.00350
	GO:0017069	snRNA binding	0.00376
	GO:0019899	enzyme binding	0.00491
	GO:0005198	structural molecule activity	0.00500
	GO:0030246	carbohydrate binding	0.01089
	GO:0019904	protein domain specific binding	0.01286
	GO:0008536	Ran GTPase binding	0.02269
	GO:0003924	GTPase activity	0.02838
	GO:0017016	Ras GTPase binding	0.03243
	GO:0031267	small GTPase binding	0.03243

Table S4. Go terms enriched in genes supporting an intensification of selection in eusocial Hymenoptera. P-values are those of a Fisher hypergeometric test used for significance in the GO enrichment analysis, as implemented in the R package topGO (Rahnenfuhrer and Alexa 2019)



OPEN

Mitochondrial genomics reveals the evolutionary history of the porpoises (Phocoenidae) across the speciation continuum

Yacine Ben Chehida¹, Julie Thumloup¹, Cassie Schumacher², Timothy Harkins², Alex Aguilar³, Asunción Borrell³, Marisa Ferreira^{4,5}, Lorenzo Rojas-Bracho⁶, Kelly M. Robertson⁷, Barbara L. Taylor⁷, Gísli A. Víkingsson⁸, Arthur Weyna⁹, Jonathan Romiguier⁹, Phillip A. Morin⁷ & Michael C. Fontaine^{1,10}✉

Historical variation in food resources is expected to be a major driver of cetacean evolution, especially for the smallest species like porpoises. Despite major conservation issues among porpoise species (e.g., vaquita and finless), their evolutionary history remains understudied. Here, we reconstructed their evolutionary history across the speciation continuum. Phylogenetic analyses of 63 mitochondrial genomes suggest that porpoises radiated during the deep environmental changes of the Pliocene. However, all intra-specific subdivisions were shaped during the Quaternary glaciations. We observed analogous evolutionary patterns in both hemispheres associated with convergent evolution to coastal versus oceanic environments. This suggests that similar mechanisms are driving species diversification in northern (harbor and Dall's) and southern species (spectacled and Burmeister's). In contrast to previous studies, spectacled and Burmeister's porpoises shared a more recent common ancestor than with the vaquita that diverged from southern species during the Pliocene. The low genetic diversity observed in the vaquita carried signatures of a very low population size since the last 5,000 years. Cryptic lineages within Dall's, spectacled and Pacific harbor porpoises suggest a richer evolutionary history than previously suspected. These results provide a new perspective on the mechanisms driving diversification in porpoises and an evolutionary framework for their conservation.

Most cetaceans possess a tremendous potential for dispersal in an environment that is relatively unobstructed by geographical barriers. This observation begs the question of how do populations of such highly mobile pelagic species in such an open environment split and become reproductively isolated from each other and evolve into new species. Recent micro- and macro-evolutionary studies showed that changes in environmental conditions¹⁻⁶, development of matrilineally transmitted cultures⁷, and resource specialization⁸⁻¹⁰ are major drivers of population

¹Groningen Institute for Evolutionary Life Sciences (GELIFES), University of Groningen, PO Box 11103 CC, Groningen, The Netherlands. ²Swift Biosciences, 674 S. Wagner Rd., Suite 100, Ann Arbor, MI 48103, USA. ³IRBIO and Department of Evolutionary Biology, Ecology and Environmental Sciences, Faculty of Biology, University of Barcelona, Diagonal 643, 08071 Barcelona, Spain. ⁴MATB-Sociedade Portuguesa de Vida Selvagem, Estação de Campo de Quiaios, Apartado EC Quiaios, 3080-530 Figueira da Foz, Portugal. ⁵CPRAM-Ecomare, Estrada Do Porto de Pesca Costeira, 3830-565 Gafanha da Nazaré, Portugal. ⁶Comisión Nacional de Áreas Naturales Protegidas (CONANP), C/o Centro de Investigación Científica y de Educación Superior de Ensenada, Carretera Ensenada-Tijuana 3918, Fraccionamiento Zona Playitas, 22860 Ensenada, BC, Mexico. ⁷Southwest Fisheries Science Center, National Marine Fisheries Service, NOAA, 8901 La Jolla Shores Dr., La Jolla, CA 92037, USA. ⁸Marine and Freshwater Research Institute, Fornubúðum 5, 220 Hafnarfjörður, Iceland. ⁹Institut Des Sciences de L'Évolution (Université de Montpellier, CNRS UMR 5554), Montpellier, France. ¹⁰Laboratoire MIVEGEC (Université de Montpellier, CNRS 5290, IRD 229) et Centre de Recherche en Écologie et Évolution de la Santé (CREES), Institut de Recherche Pour Le Développement (IRD), 911 Avenue Agropolis, BP 64501, 34394 Montpellier Cedex 5, France. ✉email: michael.fontaine@cnrs.fr

differentiation and speciation in cetacean species. Yet, the processes that link these two evolutionary timescales are still not fully understood and empirical examples are limited^{1,10}.

Several cetacean taxa display an antitropical distribution where the distribution of closely related taxa occurs on either side of the equator but are absent from the tropics^{11–13}. Multiple mechanisms have been proposed to explain such a peculiar distribution¹⁴. In cetaceans, the predominant hypothesis implies dispersal and vicariance of temperate species enabled by oceanographic, climatic and geologic fluctuations during the Miocene, Pliocene and early Pleistocene epochs^{1,12,15,16}. It has been hypothesized that during cold periods, cold adapted taxa extended their range into the tropics and possibly crossed the equator. In the subsequent warmer interglacial periods, these taxa would shift their range to higher latitudes. This geographic isolation in both hemispheres promoted allopatric divergence of conspecific taxa, resulting in their antitropical distribution. A closely related scenario suggests that the rise of the overall sea temperature during interglacial periods would have altered the wind's direction and upwelling strength, leading to a redistribution of feeding areas for cetaceans toward higher latitudes, which in turn promoted their antitropical distribution¹². Another plausible hypothesis implies that broadly distributed species, such as several cetacean species, were outperformed in the tropics by more competitive species¹⁴. A combination of these different mechanisms is also possible.

The porpoises family (Phocoenidae) displays one of the best known examples of antitropical distribution¹³. Porpoises are among the smallest cetaceans and represent an interesting evolutionary lineage within the Delphinoidea, splitting from the Monodontidae during the Miocene (~15 Myr)^{1,17}. Gaskin¹⁸ suggested that porpoises originated from a tropical environment and then radiated into temperate zones in both hemispheres. In contrast, based on the location of the oldest fossils, Barnes¹³ suggested that they arose in a more temperate environment of the North Pacific Ocean and subsequently colonized the southern hemisphere, the Indian and Atlantic Oceans. Porpoises consist of seven extant species that occur in both hemispheres in pelagic, coastal, and riverine habitats (Fig. 1a). The family includes primarily cold-water tolerant species, but two sister species of finless porpoises (*Neophocoena phocaenoides*, *N. asiaorientalis*)¹⁹ inhabit the tropical waters of the Indo-Pacific preferring mangrove zones. They are also found in the Yellow Sea, East China Sea, Sea of Japan and in estuaries and large river systems of the Indus, Ganges, and Yangtze rivers. The long pectoral fins of these porpoises represent a potential adaptation to warm water²⁰. The remaining species are considered cold-water tolerant. They are antitropically distributed and the short body appendices of most of these species are believed to represent an adaptation that limits thermal exchanges in colder environment²⁰. In the Northern Hemisphere, the harbor porpoise (*Phocoena phocoena*) inhabits the coastal waters of the North Pacific and North Atlantic, while the Dall's porpoise (*Phocoenoides dalli*) occupies the oceanic waters of the North Pacific. The large heart and high blood-oxygen of the Dall's porpoises suggest that this species is adapted to deep diving and so probably to the oceanic environment²¹. This neritic-oceanic habitat segregation is mirrored in the southern hemisphere with the Burmeister's porpoise (*Phocoena spinipinnis*), occupying the coastal waters of South America and the poorly known spectacled porpoise (*Phocoena dioptrica*) occupying the circum-Antarctic oceanic waters. The vaquita departs from the other species with an extremely localized geographical distribution in the upper Gulf of California and is now critically endangered²².

With the exception of vaquitas, all species of porpoises exhibit a relatively broad distribution range that appear fairly continuous at a global scale. Nevertheless, despite having the ability to disperse over vast distances in an open environment, many include distinct sub-species, ecotypes, or morphs. For example, the finless porpoises not only include two recognized species, but also an incipient species within the Yangtze River^{19,25}; the harbor porpoise also displays a disjunct distribution with three sub-species officially recognized and an additional one suggested by Fontaine et al.⁸; at least two forms of Dall's porpoise have been described²⁶; and the Burmeister's porpoise also shows evidence of deep population structure²⁷. Many of these subgroups show specific ecological²⁸, physiological¹⁹ and morphological²⁹ adaptations to their respective environments. For instance, Zhou et al.¹⁹ identified several genes under selection in the Yangtze finless porpoise associated with the renal function and urea cycle, reflecting adaptations to the freshwater environment. Likewise, morphological, stomach content and stable isotopes differences exclusive to Mauritanian and Iberian harbor porpoises are likely adaptations to the upwelling related environment³⁰. Such intraspecific subdivisions, also observed in killer whales (*Orcinus orca*)¹⁰ and bottlenose dolphins (*Tursiops truncatus*)³¹, illustrate the evolutionary processes in action, and can, in some cases, eventually lead to new species. Porpoises are thus an interesting model to investigate the evolutionary processes at both micro- and macroevolutionary time scale to better understand present and historical mechanisms driving population structure, adaptation to different niches, and speciation.

From a conservation perspective, the coastal habitat of many porpoise species largely overlaps with areas where human activities are the most intense. These have dramatic impacts on natural populations. For example, the vaquita lost 90% of its population between 2011 and 2016 leaving about 30 individuals in 2017³², and less than 19 in 2019³³. This species is on the brink of extinction and currently represents the most endangered marine mammal. Finless porpoises also face major conservation issues, especially the lineage within the Yangtze River (*N. a. asiaorientalis*) in China, also critically endangered due to human activities^{34,35}. Similarly, several populations of harbor porpoises are highly threatened^{36,37}. Little information about the spectacled and Burmeister's porpoises is available. While anthropogenic activities are an undeniable driver of the current threats to biodiversity, the evolutionary context can be also informative when assessing their vulnerability³⁸. For example, knowledge on population or species evolutionary history is useful to characterize population dynamics, identify evolutionary significant units relevant for conservation, recent or historical split related to environmental variation, evolutionary or demographic trends, and evolutionary processes that could explain, enhance, or mitigate the current threats experienced by a species^{39,40}.

To date, porpoise evolutionary history and biogeography remains contentious and superficial⁴¹. Previous phylogenetic studies led to incongruent results, as there are disagreements regarding some of their relationships, in particular about the position of the vaquita, Dall's, Burmeister's and spectacled porpoises^{13,41,42}. So far,

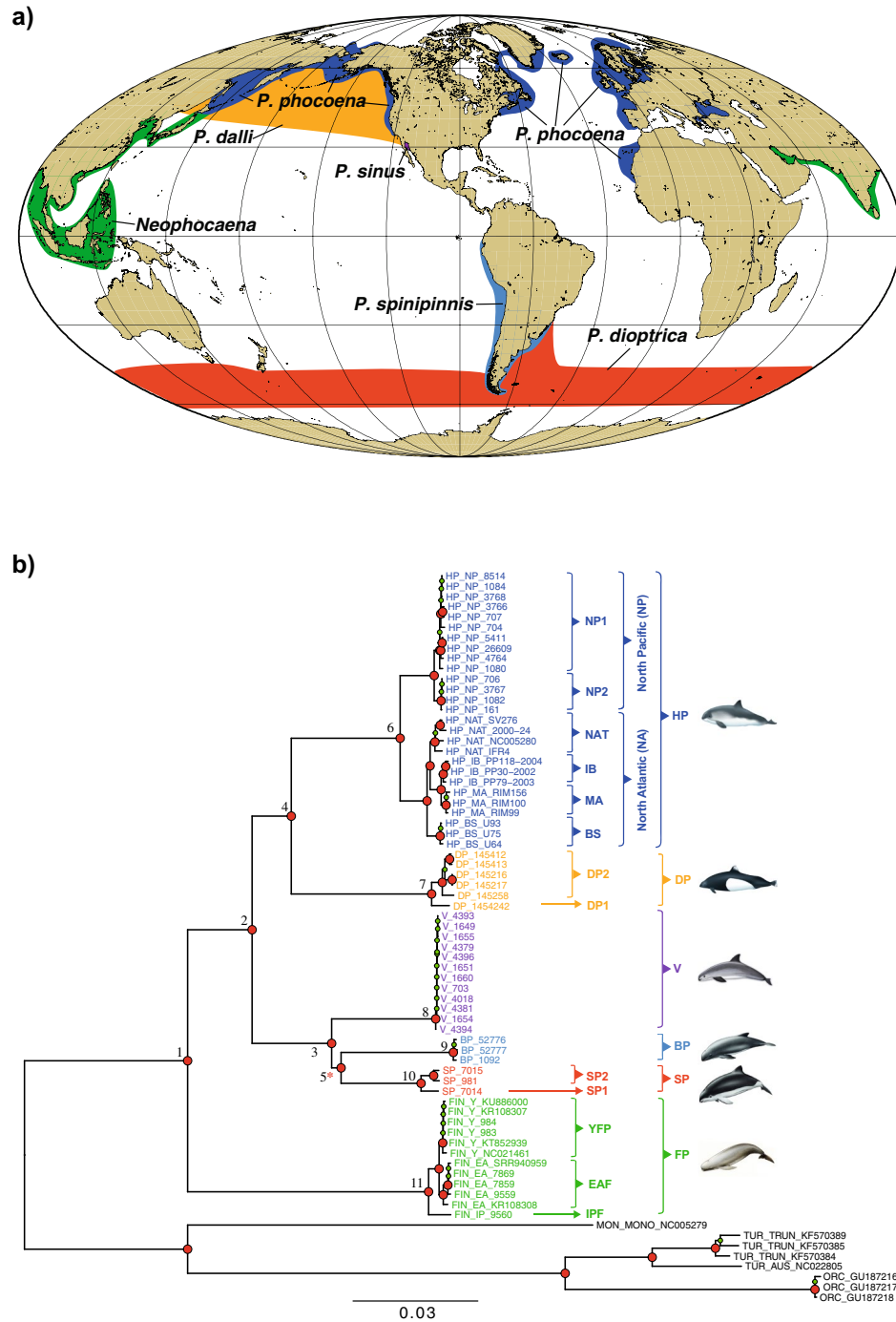


Figure 1. (a) Geographical range of each species in the Phocoenidae family. Map generated using ArcGIS 10.3 software using the open source data from the ETOPO1 Global Relief Model²³ (<https://www.ngdc.noaa.gov/mgg/global/>) and adapted from Gaskin¹⁸ and Berta et al.²⁴. (b) Maximum-likelihood mitochondrial phylogeny. The external branches and the tip labels are colored by species. The tree is rooted with eight sequences from four closely related *Odontoceti* species (in black). Numbers at the nodes are discussed in the text. The nodes indicated in red and green represent nodes with bootstrap support $\geq 90\%$ and $\geq 70\%$, respectively. The red star indicates a node with a 63% bootstrap support in the Neighbor-joining tree (Fig. S1b). The lineage code includes the vaquita (*P. sinus*, V), Burmeister's porpoise (*P. spinipinnis*, BP), spectacled porpoise (*P. dioptrica*, SP), Dall's porpoise (*P. dalli*, DP), harbor porpoise (*P. phocoena*, HP) and finless porpoise (*N. phocaenoides* + *N. asiakorialis*, FP). Some species have been also further subdivided into distinct groups: harbor porpoises are divided into North Pacific (NP) and North Atlantic (NA), and within each of these groups, further subdivisions are recognized. Four groups are recognized within NA: NAT (North Atlantic), IB (Iberian), MA (Mauritanian), BS (Black Sea). NP is divided into two subgroups: NP1 and NP2. Three sub-species or species are also recognized among the finless porpoises: Indo-Pacific (IPF), Yangtze finless (YFP) and East Asia finless (EAF). Spectacled porpoise subgroups are designated as SP1 and SP2. Dall's porpoise subgroups are designated as DP1 and DP2. The scale bar unit is in substitution per site.

Lineage	n	R _b	R _a	Depth	Assembly size	% GC
Harbor porpoise (HP)	27	30.8 ± 28.3	28.5 ± 25.9	1,323.9 ± 1,800.0	16,383.8 ± 0.8	40.6 ± 0.1
North Pacific 1 (NP1)	10	5.1 ± 1.8	5.0 ± 1.7	99.6 ± 92.6	16,384.3 ± 0.5	40.7 ± 0.0
North Pacific 2 (NP2)	4	5.9 ± 1.3	5.6 ± 1.2	97.2 ± 119.8	16,384.0 ± 0.0	40.7 ± 0.0
North Atlantic (NAT)	4	56.9 ± 3.4	52.2 ± 2.9	1656.3 ± 1,058.9	16,383.3 ± 0.6	40.6 ± 0.0
Mauritania (MA)	3	59.8 ± 5.4	54.9 ± 5.2	1,431.0 ± 648.1	16,384.0 ± 0.0	40.6 ± 0.0
Iberia (IB)	3	65.2 ± 8.2	60.5 ± 7.6	3,169.7 ± 1882.6	16,384.0 ± 0.0	40.5 ± 0.0
Black Sea (BS)	3	60.0 ± 2.2	54.8 ± 1.3	4,755.3 ± 1,376.9	16,382.0 ± 0.0	40.6 ± 0.0
Dall's porpoise (DP)	6	2.8 ± 0.9	2.7 ± 0.9	49.5 ± 14.5	16,367.5 ± 0.8	40.5 ± 0.1
Dall's porpoise 1 (DP1)	1	4.5 ± 0.0	4.4 ± 0.0	74.0 ± 0.0	16,369.0 ± 0.0	40.6 ± 0.0
Dall's porpoise 2 (DP2)	5	2.5 ± 0.5	2.4 ± 0.5	44.6 ± 9.0	16,367.2 ± 0.4	40.5 ± 0.0
Vaquita (V)	12	5.8 ± 5.7	5.7 ± 5.5	113.3 ± 108.6	16,370.0 ± 0.0	39.8 ± 0.0
Burmeister's porpoise (BP)	3	2.3 ± 0.3	2.3 ± 0.3	125.0 ± 121.2	16,378.7 ± 8.1	40.1 ± 0.0
Spectacled porpoise (SP)	3	2.4 ± 0.2	2.3 ± 0.2	55.0 ± 30.5	16,371.0 ± 0.0	39.7 ± 0.1
Spectacled porpoise 1 (SP1)	1	2.2 ± 0.0	2.1 ± 0.0	41.0 ± 0.0	16,371.0 ± 0.0	39.6 ± 0.0
Spectacled porpoise 2 (SP2)	2	2.5 ± 0.0	2.4 ± 0.0	62.0 ± 39.6	16,371.0 ± 0.0	39.7 ± 0.1
Finless porpoises (FP)	12	2.7 ± 1.1	2.6 ± 1.1	92.9 ± 74.9	16,383.1 ± 5.8	40.8 ± 0.0
Indo-Pacific (IPF)	1	2.3 ± 0.0	2.2 ± 0.0	77.0 ± 0.0	16,385.0 ± 0.0	40.8 ± 0.0
East Asian (EAF)	5	3.0 ± 1.5	2.9 ± 1.4	53.2 ± 22.8	16,381.2 ± 7.5	40.0 ± 0.0
Yangtze (YF)	6	2.3 ± 0.3	2.2 ± 0.3	180.0 ± 101.8	16,386.0 ± 0.0	40.8 ± 0.0

Table 1. Taxon sample size (n) and descriptive statistics for the shotgun sequencing and mitochondrial assembly per species and mitochondrial lineage. The statistics include the total number of reads before and after filtering (R_b and R_a), the sequencing coverage depth, the size of the mitochondrial assembly (in base-pairs), and the GC content in percent (%GC). The mean value and the standard deviation are shown.

molecular phylogenetic relationships among porpoises have been estimated using short sequences of the *D-loop* and cytochrome *b*^{17,42}. However, the *D-loop* can be impacted by high levels of homoplasy that blurs the resolution of the tree⁴³ and the *Cyt-b* may have limited power to differentiate closely related taxa⁴⁴.

In this study, we sequenced and assembled the whole mitogenome from all extant porpoise species, including most of the known lineages within species to resolve their phylogenetic relationships and reconstruct their evolutionary history. More specifically, (1) we assessed the phylogenetic and phylogeographic history of the porpoise family based on the whole mitogenomes including the timing and tempo of evolution among lineages; (2) we assessed the genetic diversity among species and lineages and (3) reconstructed the demographic history for some lineages for which the sample size was suitable. (4) We placed the evolutionary profile drawn for each lineage and species into the framework of past environmental changes to extend our understanding of porpoise biogeography. Finally, (5) we interpreted the IUCN conservation status of each taxa in the light of their evolutionary history.

Material and methods

Taxon sampling and data collection. Porpoise tissue samples from 56 live-biopsies, bycaught, or stranded animals (Table 1 and Table S1) were stored in salt-saturated 20% DMSO or 95% Ethanol and stored at −20 °C until analyses. All samples were collected under appropriate Marine Mammal Protection Act permits within the US, or appropriate permits elsewhere, following the relevant guidelines and regulations, and transferred internationally under CITES permit. Genomic DNA was extracted from tissues using the *PureGene* or *DNeasy* Tissue kits (Qiagen), following the manufacturer's recommendations. DNA quality and quantity were assessed on an agarose gel stained with ethidium bromide, as well as using a Qubit-v3 fluorometer. Genomic libraries for 44 porpoise samples including three spectacled porpoises, three Burmeister's porpoises, 12 vaquita, six Dall's porpoises, three East Asian finless porpoises, two Yangtze finless, one Indo-Pacific finless and 14 North Pacific harbor porpoises. Libraries were prepared by Swift Biosciences Inc. using either the Swift Biosciences Accel-NGS double-strand 2S (harbor porpoises) or single-strand 1S Plus DNA Library Kit (all other species), following the user protocol and targeting an insert-size of ~350 base-pairs (bps). The libraries were indexed and pooled in groups of 2–12 for paired-end 100 bps sequencing in five batches on an Illumina MiSeq sequencer at Swift Biosciences. Additional libraries for 12 samples of North Atlantic harbor porpoises were prepared at BGI Inc. using their proprietary protocol, indexed and pooled for paired-end 150 bps sequencing on one lane of HiSeq-4000 at BGI Inc. The total sequencing effort produced reads for 56 individuals (Table S2). Previously published reads from one additional finless porpoise sequenced with a HiSeq-2000 were retrieved from NCBI (Table S2). For this individual, we down-sampled the raw FASTQ files to extract 0.5% of the total reads and used the 5,214,672 first reads to assemble the mitogenome. The subsequent data cleaning and mitogenome assemblies were thus performed for a total of 57 individuals.

Data cleaning. The quality of the reads was first evaluated for each sample using *FastQC* v.0.11.5⁴⁵. *Trim-momatic* v.0.36⁴⁶ was used to remove low quality regions, overrepresented sequences and Illumina adapters. Dif-

ferent filters were applied according to the type of Illumina platform used (see Text S1 for details). Only mated reads that passed *Trimmomatic* quality filters were used for the subsequent analyses.

Mitogenome assembly. Porpoises mitogenome assemblies were reconstructed using two different approaches. First, we used *Geneious* v.8.1.8⁴⁷ to perform a direct read mapping to the reference mitogenome of the harbor porpoise (accession number AJ554063⁴⁸). We used default settings except the minimum mapping quality set to 20 and the number of iterations set to 5. This step was followed by a reconstruction of the consensus sequences (Table S2). The second approach implemented in *MITOBIM*⁴⁹ is a hybrid approach combining a baiting and iterative elongation procedure to perform a de-novo assembly of the mitogenome (see details in Text S2). We visually compared the assemblies provided by the two methods in *Geneious* to assess and resolve inconsistencies (Text S2 and Table S2).

In addition to the 57 assembled individuals, we retrieved six porpoise mitogenomes from Genbank (Table S2). We also added eight complete mitogenomes from four outgroup species: one narwhal (*Monodon monoceros*)⁴⁸, three bottlenose dolphins⁶, one Burrunan dolphin (*Tursiops australis*)⁶ and three orcas⁵⁰.

Sequences alignments. We performed the alignment of the 71 mitogenomes with *MUSCLE*⁵¹ using default settings in *Geneious*. A highly repetitive region of 226 bps in the *D-loop* was excluded from the final alignment (from position 15,508 to 15,734) because it was poorly assembled, and included many gaps and ambiguities. We manually annotated the protein-coding genes (CDS), tRNA and rRNA of the final alignment based on a published harbor porpoise mitogenome⁴⁸. Contrary to the remaining CDSs, *ND6* is transcribed from the opposite strand⁵². Therefore, to assign the codon positions in this gene, we wrote a custom script to reverse complement *ND6* in the inputs of all the analyses that separates coding and non-coding regions of the mitogenomes. This led to a 17 bps longer alignment due to the overlapping position of *ND5* and *ND6*.

Phylogenetic relationships. We estimated the phylogenetic relationships among the assembled mtDNA sequences using three approaches: a maximum-likelihood method (ML) in *PHYML* v3.0⁵³; a distance based method using the Neighbour-Joining algorithm (NJ) in *Geneious*; and an unconstrained branch length Bayesian phylogenetic tree (BI) in *MrBayes* v3.2.6⁵⁴. We used the Bayesian information criterion (*BIC*) to select the substitution model that best fits the data in *jModelTest2* v2.1.10⁵⁵. The best substitution model and parameters were used in the ML, NJ and BI approaches. For the ML approach, we fixed the proportion of invariable sites and the gamma distribution parameters to the values estimated by *jModelTest2*. The robustness of the ML and NJ tree at each node was assessed using 10,000 bootstrap replicates. For the Bayesian inference, a total of 1×10^6 MCMC iterations was run after a burn-in of 1×10^5 steps, recording values with a thinning of 2,000. We performed ten independent replicates and checked the consistency of the results. Runs were considered to have properly explored the parameter space if the effective sample sizes (ESS) for each parameter were greater than 200 and by visually inspecting the trace plot for each parameter using *Tracer* v1.6⁵⁶. We assessed the statistical robustness and the reliability of the Bayesian tree topology using the posterior probability at each node.

Finally, the four phylogenetic trees were rooted with the eight outgroup sequences and plotted using the R package *ggtree* v1.4⁵⁷.

Divergence time estimate. We estimated the divergence time of the different lineages using a time-calibrated Bayesian phylogenetic analysis implemented in *BEAST* v2.4.3⁵⁸. We assumed two calibration points in the tree: (1) the split between the Monodontidae and Phocoenidae, node calibrated with a lognormal mean age at 2.74 Myr¹⁷ (sd = 0.15) as a prior and (2) the split between the Pacific and Atlantic harbor porpoise lineages, node calibrated with a uniform distribution between 0.7 and 0.9 Myr as a prior².

Divergence times were estimated using a relaxed log-normal molecular clock model for which we set the parameters *uclMean* and *uclStdev* to exponential distributions with a mean of 1 and 0.3337, respectively. We used a Yule speciation tree model and fixed the mean of the speciation rate parameter to 1. The *BIC* was used in *jModelTest2* to identify the substitution model best fitting to the data, using the empirical base frequencies. We assumed a substitution rate of 5×10^{-8} substitutions per-site and per-year. This mutation rate was estimated by Nabholz et al.⁵⁹ for cetacean mitogenomes and was previously used on harbor porpoise^{8,60}. A total of 1.2×10^9 MCMC iterations were run after a burn-in length of 1.2×10^8 iterations, with a thinning of 5,000 iterations. We performed eight independent replicates and checked for the consistency of the results among replicates. A run was considered as having converged if the ESS values were greater than 200, and if they produced consistent trace plots using *Tracer* v1.6. Subsequently, we combined all runs together after a burn-in of 98% using *LogCombiner*⁵⁸. The best supported tree topology was the one with the highest product of clade posterior probabilities across all nodes (maximum clade credibility tree), estimated using *TreeAnnotator*⁵⁸. We also calculated the 95% highest posterior density for the node ages using *TreeAnnotator*. The final chronogram was rooted with the eight outgroups sequences and plotted using *FigTree* v1.4.3⁶¹.

Genetic diversity within species and sub-species. We subdivided each species into their distinct lineages in order to compare their genetic diversity at the different taxonomic level. Specifically, we divided the harbor porpoise into five subgroups, North Pacific (*P. p. vomerina*), Black Sea (*P. p. relicta*), Mauritanian—Iberian (*P. p. meridionalis*) and North Atlantic (*P. p. phocaena*) in accordance with the subdivisions proposed for this species in the literature³⁰. Finless porpoise was split into Indo-Pacific finless (*N. phocaenoides*; IPF), East Asian finless (*N. a. sunameri*; EAF) and Yangtze finless porpoises (*N. a. asiaorientalis*; YFP). For simplicity, we refer here to finless porpoises as a single group of species and IPF, EAF and YFP as the distinct lineages throughout this paper. Additionally, we subdivided the other groups into lineages that were as divergent or more divergent than

the sub-species that were described in the literature. This includes splitting the North Pacific harbor porpoises into NP1 and NP2, Dall's porpoises into DP1 and DP2 and spectacled porpoises into SP1 and SP2 to reflect the deep divergence observed in the phylogenetic tree within these three lineages (Fig. 1b and Fig. S1).

For each species and subgroup, several statistics capturing different aspects of the genetic diversity were calculated for different partitions of the mitogenome, including the whole mitogenomes, the non-coding regions (i.e. inter-gene regions and *D-loop*) and the 13 protein coding genes (e.g. CDS) excluding tRNAs and rRNA. The number of polymorphic sites, nucleotide diversity (π), number of singletons, number of shared polymorphisms, number of haplotypes, haplotype diversity and Watterson estimator of θ were calculated. For CDSs, we also estimated the number of synonymous ($\#Syn$) and non-synonymous mutations ($\#NSyn$), π based on synonymous (π_S) and non-synonymous mutations (π_N), and the ratio π_N/π_S . All these statistics were computed in *DnaSP* v.5.10.01⁶². Since we only have a unique sample for IPF, DP1 and SP1 we did not estimate these statistics for these lineages.

Differences in sample sizes can influence some of these statistics. As our sample size ranged from three to 26 individuals per group, we used a rarefaction technique⁶³ to account for the differences in sample size. We assumed a sample size of three individuals in order to compare the genetic diversity among lineages that have different sample sizes. For each lineage, we randomly subsampled 2,500 times a pool of three sequences and estimated the median, mean and 95% confidence interval for π .

Test for selective neutrality. We tested for evidence of natural selection acting on the mitogenomes using a McDonald–Kreitman test⁶⁴ (MK-tests). This test infers deviation from the neutral theory by comparing the ratio of divergence between species (d_N/d_S) versus polymorphism within species (π_N/π_S) at synonymous (silent) and non-synonymous (amino acid-changing) sites in protein coding regions using the so-called neutrality index (*NI*). *NI* is 1 when evolution is neutral, greater than 1 under purifying selection, and less than 1 in the case of positive selection. MK-tests were conducted on the 13 CDS regions of the mitogenome using *DnaSP*. We conducted this test in two different ways: first comparing all the interspecific lineages to a same outgroup, the killer whale for which multiple mitogenome sequences were available, and second comparing all interspecific lineages to each other in order to assess how the MK-tests were affected by the outgroup choice. The significance of the *NI* values was evaluated using a G-tests in *DnaSP*. Furthermore, the distribution of *NI* values for each lineage were compared among each other using a PERMANOVA with the R package *RVAideMemoire* v.0.9-77⁶⁵. Pairwise comparisons were assessed with a permutation tests and were adjusted for multiple comparisons using the false rate discovery method⁶⁶. The PERMANOVA and pairwise comparisons were conducted using 9,999 permutations. The neutral theory predicts that the efficacy of purifying selection increases with Ne ⁶⁷. Under these assumptions, Ne is expected to be proportional to NI ^{68,69}. To test this hypothesis, we assessed the correlation between values of *NI*s and π derived by rarefaction as a proxy of Ne . However, MK-test is also known to be impacted by demographic changes in some specific cases. For instance, an increase in Ne could mimic the effect of positive selection⁷⁰ while recent reduction in Ne could prevent the detection of positive selection and lead to an artefactual signal of purifying selection⁷¹. This problem is exacerbated in species with very low Ne and the results of MK-tests should be interpreted accordingly.

In addition to the MK-tests, we quantified the branch-specific non-synonymous to synonymous substitution ratios (d_N/d_S) to infer direction and magnitude of natural selection along the phylogenetic tree. To estimate the branch-specific ratio we first counted the number of synonymous ($\#S$) and non-synonymous ($\#NS$) substitutions for the 13 CDSs. Then $\#S$ and $\#NS$ were mapped onto a tree using the mapping procedure of Romiguier et al.⁷². Next, we divided $\#S$ and $\#NS$ by the number of synonymous and nonsynonymous sites to obtain an approximation of d_S and d_N , respectively. More specifically, we first fitted the YN98 codon model using the *BPPML* program⁷³, then we mapped the estimated d_N/d_S values onto the branches of the ML tree using the program *MAPNH* of the *TESTNH* package v1.3.0⁷⁴. Extreme d_N/d_S ratio (> 3) are often due to branches with very few substitution (d_N or d_S)⁷² and were discarded. We compared the distribution of d_N/d_S among species (i.e., across all the branches) using a PERMANOVA. Finally, the estimated ratios were correlated with π values obtained by rarefaction using a Pearson's correlation tests in R⁷⁵. To do so, we pooled the signal from each lineage as a single data point as suggested by Figuet et al.⁷⁶. We considered the intraspecific and interspecific lineages, except for those where no non-synonymous substitutions were observed (ex. NP2). Within a lineage, π was summarized as the mean of the \log_{10} -transformed value of its representatives and the d_N/d_S was obtained by summing the non-synonymous and synonymous substitution counts across its branches and calculating the ratio⁷⁶.

Inference of demographic changes. We investigated changes in effective population size (Ne) through time for the lineages that included a sample size ≥ 10 to conduct reliable demographic inferences. This includes the vaquitas and North Pacific NP1 harbor porpoise lineage. We first tested for deviations from neutral model expectations using three statistics indicative of historical population size changes: Tajima's D ⁷⁷, Fu and Li's D^* and F^* ⁷⁸ in *DnaSP*. The p -values were assessed using coalescent simulations in *DnaSP* using a two tailed test as described in Tajima⁷⁷. We then reconstructed the mismatch distributions indicative of population size changes using *Arlequin* v.3.5.2.2⁷⁹. Mismatch distributions were generated under a constant population size model and a sudden growth/decline population model⁸⁰. This later model is based on three parameters: the population genetic diversity before the population size change (θ_i); the population genetic diversity after the population size change (θ_j), and the date of the change in population size in mutational units ($\tau = 2\mu t$, where μ is the mutation rate per sequence and generation and t is the time in generations). These parameters were estimated in *Arlequin* using a generalized non-linear least-square approach. The 95% confidence interval was obtained using 10,000 parametric bootstraps⁸⁰. Finally, we used the coalescence based Bayesian Skyline Plot (BSP)⁸¹ to estimate demographic changes in Ne back to the T_{MRCA} . BSP analysis was performed in *BEAST* v2.4.3 using the empirical base frequencies and a strict molecular clock. We applied *jModelTest2* separately to both lineages to

evaluate the best substitution models. We assumed a substitution rate of 5×10^{-8} substitutions per site and per year⁵⁹ in order to obtain the time estimates in years. We conducted a total of ten independent runs of 10^8 MCMC iterations following a burn-in of 1×10^7 iterations, logging every 3,000 iterations. We constrained N_e between 0 and 150,000 individuals and between 0 and 380,000 individuals for the vaquita and the NP1 harbor porpoise lineage, respectively. This upper boundary on N_e was empirically set to encompass the entire marginal posterior distribution. All other parameters were kept at default values. The convergence of the analysis was assessed by checking the consistency of the results over ten independent runs. For each run, we also used *Tracer* to inspect the trace plots for each parameter to assess the mixing properties of the MCMCs and estimate the *ESS* value for each parameter. Runs were considered as having converged if they displayed good mixing properties and if the *ESS* values for all parameters were greater than 200. We discarded the first 10% of the MCMC steps as a burn-in and obtained the marginal posterior parameter distributions from the remaining steps using *Tracer*. N_e values were obtained by assuming a generation time of 10 years³⁶. To test whether the inferred changes in N_e over time were significantly different from a constant population size null hypothesis, we compared the BSP of both lineages with the 'Coalescent Constant Population' model (CONST)^{58,82} implemented in *BEAST* v2.4.3 using Bayes Factors⁸³. We thus conducted ten independent CONST runs using 10^8 MCMC iterations after a burn-in of 10%, logging every 3,000 iterations. We assessed the proper mixing of the MCMC and ensured *ESS* were greater than 200. We then used the Path sampler package in *BEAST* v2.4.3 to compute the log of marginal likelihood (*logML*) of each run for both BSP and CONST. We set the number of steps to 100 and used 10^8 MCMC iterations after a burn-in of 10%. Bayes Factors were computed as twice the difference between the log of the marginal likelihoods (i.e. $2[\text{LogML}_{\text{BSP}} - \text{LogML}_{\text{CONST}}]$) and were performed for pairwise comparisons between BSP and CONST runs. As recommended, Bayes Factors greater than 6 were considered as a strong evidence to reject the null hypothesis (i.e. CONST)⁸³.

Results

Porpoise mitogenomes assemblies. A total of 57 mitogenomes of the seven species of porpoise (Table S1) were newly sequenced and assembled using Illumina sequencing. After read quality check, trimming, and filtering (Table 1 and Table S2), between 1,726,422 and 67,442,586 cleaned reads per sample were used to assemble the whole mitogenomes. The two methods used to assemble the mitogenomes delivered consistent assemblies with an average sequencing depth coverage ranging from 15 to 4,371X for *Geneious* and 17 to 4,360X for *MITOBIM* (Table 1 and Table S2). In total, 35 of the 57 mitogenome assemblies were strictly identical with both methods. The 22 remaining assemblies included between 1 and 4 inconsistencies which were visually inspected and resolved (Text S2 and Table S2). Augmented with the 14 previously published mitogenome sequences, the final alignment counted 71 mitogenome sequences of 16,302 bps and included less than 0.2% of missing data. The alignment was composed of 627 singletons and 3,937 parsimony informative sites defining 68 haplotypes (including the outgroup sequences). Within the 63 ingroup porpoise sequences, we observed 2,947 segregating sites, including 242 singletons and 2,705 shared polymorphisms defining 58 distinct haplotypes with a haplotype diversity of 99.6% (Table 2, Tables S3 and S4).

Phylogenetic history of the porpoises. A Hasegawa–Kishino–Yano (HKY + G, Gamma = 0.19) model was selected as the best-fitting nucleotide substitution model. Phylogenetic inferences using a maximum-likelihood (ML) approach (Fig. 1b and Fig. S1a), a distance-based neighbor-joining method (Fig. S1b), and a Bayesian approach (Fig. S1c) all produced concordant phylogenies (i.e., similar topologies and statistical supports). All phylogenies were fully resolved with high statistical support at the inter- and intra-specific levels (bootstrap supports $\geq 93\%$ or node posterior probability of one). One exception was the node 5 grouping the Burmeister's and spectacled porpoises in the neighbor-joining tree (Fig. S1b) as it displayed a slightly lower bootstrap support of 61% (red star in Fig. 1b and Fig. S1b), but it was fully supported by the ML and Bayesian approaches (Fig. 1b and Fig. S1).

The resulting phylogenetic reconstruction (Fig. 1b) showed that all porpoises formed a monophyletic group (node 1). The most basal divergence in the tree split the more tropical finless porpoises from the other temperate to subpolar porpoises. Then, the temperate species split into two clades (node 2) composed of two reciprocally monophyletic groups. The first is composed of the southern hemisphere species (spectacled and Burmeister's porpoises) and vaquitas (node 3). The second is composed of the porpoises from the northern hemisphere (harbor and Dall's porpoises, node 4). In contrast with a previous phylogenetic study based on control region sequences⁴², the phylogenetic tree based on the whole mitogenome suggested that vaquitas split from a common ancestor to the spectacled and Burmeister's porpoises (node 3), and thus that the two species from the southern hemisphere are more closely related to each other (node 5) than they are to vaquitas. Finally, the mitogenome tree supported the monophyly of each recognized species (nodes 6–11).

Intraspecific subdivisions were also evident from the mitogenome phylogeny in some species, such as in the harbor and finless porpoises (Fig. 1b). In the harbor porpoises, the split between the North Atlantic and North Pacific sub-species constituted the deepest divergence of all intraspecific subdivisions across all species. Within the North Atlantic harbor porpoises, further subdivisions were also observed and corresponded to the three previously described ecotypes or sub-species³⁰. These included the relict population in the Black Sea, the harbor porpoises from the upwelling waters with two closely related but distinct lineages in Iberia and Mauritania, and the continental shelf porpoises further north in the North Atlantic. Finally, within the North Pacific, two cryptic subgroups were also observed (NP1 and NP2; Fig. 1b). Among the finless porpoises, the three taxonomic groups currently recognized¹⁹, including IPF and the two closely related species of narrow-ridged finless porpoises, were clearly distinct from each other on the mitogenome phylogenetic tree (node 11). Finally, despite a limited

	N	MD	S	Singl	Shared P	θ_w (%)	π (%)	SD_π (%)	H	H_d (%)	SD_{HD} (%)
Species											
All porpoises	63	51	2,947	242	2,705	4.28	5.35	0.23	58	99.6	0.04
Finless porpoise ^a	12	36	229	173	56	0.47	0.35	0.00	12	100.0	3.40
Burmeister's porpoise ^b	3	31	33	33	0	0.13	0.13	0.04	3	100.0	27.20
Vaquita ^b	12	32	16	13	3	0.03	0.02	0.00	8	89.4	7.80
Spectacled Porpoise ^a	3	30	145	145	0	0.59	0.59	0.21	3	100.0	27.20
Dall's Porpoise ^a	6	34	208	152	56	0.56	0.49	0.13	5	93.3	14.80
Harbor Porpoise ^a	27	37	602	158	444	0.98	1.11	0.06	26	99.7	1.10
Harbor porpoise											
North Atlantic ^b	4	36	102	85	17	0.34	0.33	0.07	4	100.0	3.12
Iberia ^b	3	32	31	31	0	0.12	0.12	0.04	3	100.0	27.20
Mauritania ^b	3	32	28	28	0	0.11	0.11	0.03	3	100.0	27.20
Black Sea ^b	3	34	18	18	0	0.07	0.07	0.02	3	100.0	27.20
North Pacific 1 ^b	10	31	76	53	23	0.16	0.12	0.01	10	100.0	4.50
North Pacific 2 ^b	4	31	6	4	2	0.02	0.02	0.00	3	83.3	4.94
Finless porpoise											
Yangtze ^b	6	34	33	30	3	0.09	0.07	0.01	6	100.0	0.93
East Asian ^b	5	33	58	55	3	0.17	0.15	0.04	5	100.0	16.00
Dall's porpoise											
Dall's porpoise 2 ^b	5	33	107	61	46	0.32	0.32	0.07	4	90.0	16.10
Spectacled porpoise											
Spectacled porpoise 2	2	29	39	39	0	0.24	0.24	0.12	2	100.0	50.00

Table 2. Summary statistics describing the genetic diversity of the mitochondrial genomes among porpoise species and their distinct lineages. The statistics includes the sample size (N), number of sites with missing data in number of gaps (MD), segregating sites (S), singletons ($Singl.$), shared polymorphism ($Shared P.$), Watterson's theta (θ_w), average nucleotide diversity per site (π) and its standard deviation (SD_π), number of haplotypes (H), haplotypic diversity (H_d) and its standard deviation (SD_{HD}). ^aSpecies including multiple distinct mitochondrial lineages. ^bSpecies with a single mitochondrial lineage.

sampling, Dall's (node 7) and spectacled porpoises (node 10) each also displayed distinct lineages (DP1/DP2 and SP1/SP2, respectively; Fig. 1b and Fig. S1) as divergent as those observed in the harbor and finless porpoises.

The time-calibrated Bayesian mitochondrial phylogeny (Fig. 2 and Table S5) suggested that all extant porpoises find their common ancestor ~5.42 M years ago (95% Highest Posterior Density, HPD, 4.24–6.89; node 1). This time corresponds to the split between the finless and the other porpoise species. Spectacled, vaquita and Burmeister's porpoises diverged from harbor and Dall's porpoise ~4.06 Myr ago (95% HPD, 3.15–5.12; node 2). The split between vaquitas, spectacled and Burmeister's porpoises was estimated at ~2.39 Myr (95% HPD, 1.74–3.19; node 3) and between spectacled and Burmeister's at ~2.14 Myr (95% HPD, 1.51–2.86; node 4). The Dall's and harbor porpoises split from each other ~3.12 Myr ago (95% HPD, 2.31–3.98; node 5). Finally, the common ancestor of the subdivisions observed within each species was dated within the last million years (nodes 6–11).

Genetic diversity of the mitogenome. Mitochondrial genetic diversity varied greatly among species and lineages within species (Table 2, Tables S3, S4 and Fig. 3). The highest values of π were observed in the harbor porpoises ($\pi = 1.15\%$), followed by the spectacled ($\pi = 0.60\%$), Dall's ($\pi = 0.50\%$), finless ($\pi = 0.35\%$), and Burmeister's porpoises ($\pi = 0.13\%$), while vaquitas displayed the lowest values ($\pi = 0.02\%$). The variation among species was strongly related to the occurrence of distinct mitochondrial lineages within species that corresponds to ecologically and genetically distinct sub-species or ecotypes (Table 2, Tables S3, S4 and Fig. 3). Once the lineages that included more than three sequences were compared to each other while accounting for the difference in sample size using a rarefaction procedure⁶³ (Fig. 3), π values were more homogeneous among lineages and species, with however some variation. The most diversified lineages included DP2 in Dall's porpoise ($\pi = 0.32\%$) and the North Atlantic (NAT) lineage in harbor porpoise ($\pi = 0.33\%$). In contrast, the vaquita lineage ($\pi = 0.02\%$), harbor porpoise North Pacific lineage NP2 ($\pi = 0.02\%$) and Black Sea lineage (BS) ($\pi = 0.07\%$), and the Yangtze finless porpoise YFP lineage ($\pi = 0.06\%$) displayed the lowest nucleotide diversity. The other lineages displayed intermediate π values.

Molecular evolution of the mitogenome. The nucleotide diversity also varied greatly along the mitogenome. It was lowest in the origin of replication, tRNA and rRNAs, intermediate in the coding regions and highest in non-coding regions (Fig. S2, Tables S3 and S4). This result indicates different levels of molecular constraints along the mitogenome.

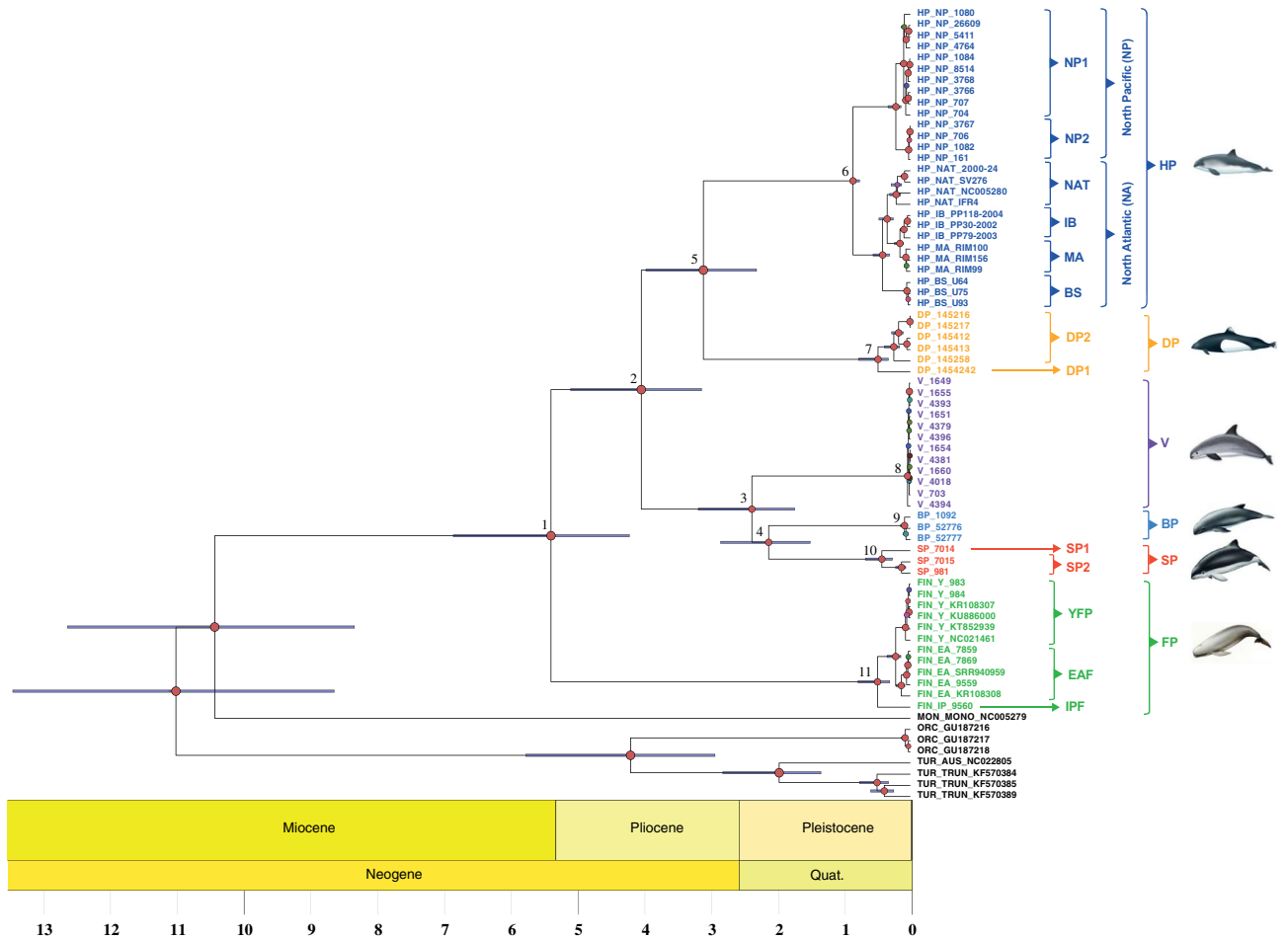


Figure 2. Bayesian chronogram of the porpoise family. The tree represents the maximum clade credibility tree. Red node labels indicate posterior probabilities of 1; node position indicates median node age estimates and the error bars around the node indicate the 95% highest posterior density of the estimated node age. Time is in millions of years. Numbers at the nodes are discussed in the text. The acronyms are provided in Fig. 1.

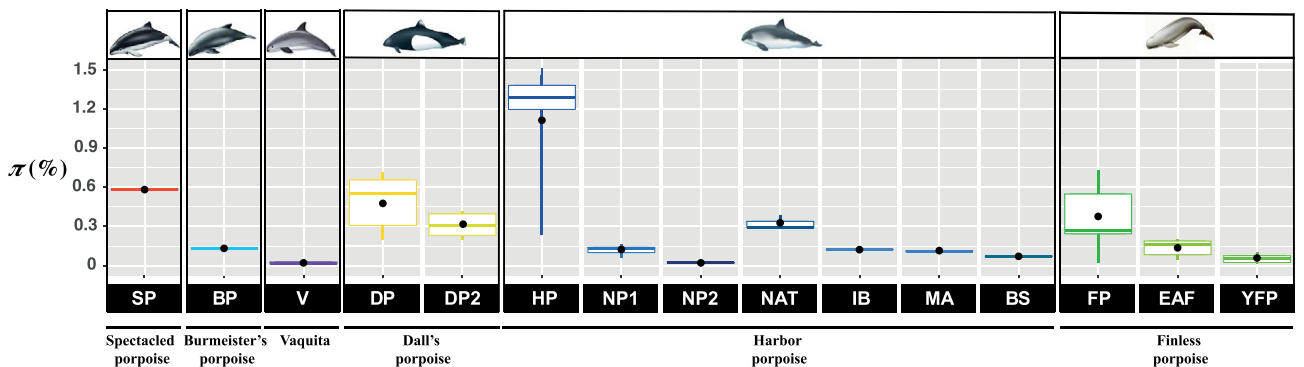


Figure 3. Nucleotide diversity (π) among species and lineages within species of porpoise. The median and mean π values are represented respectively by the colored line in the boxplot and the black dot. The whiskers represent the 95% confidence interval. The boxes represent the upper and lower quartile. No overlapping boxplots are significantly different. The species are represented by a pictogram on the top of the figure. The names of the distinct lineages are provided at the bottom of the plot in the black boxes. The acronyms are provided in Fig. 1 and Table 1.

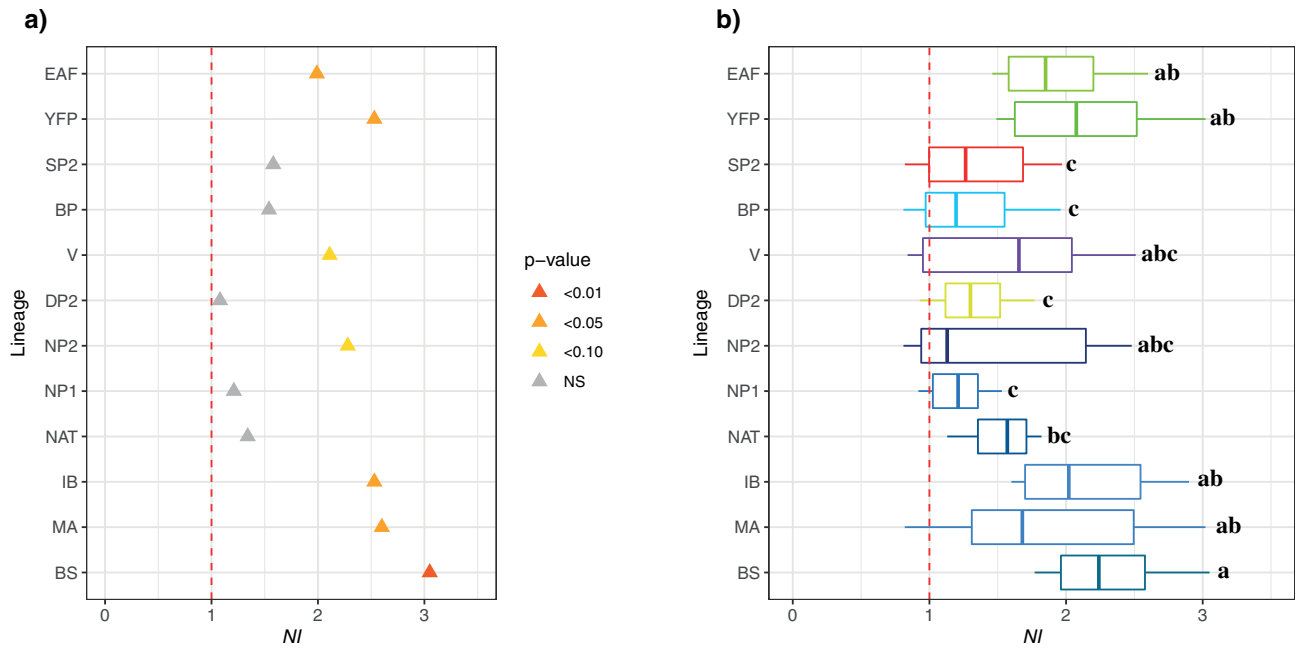


Figure 4. McDonald–Kreitman tests on the 13 protein coding regions of the mitogenome among porpoise subgroups. **(a)** Neutrality index (*NI*) estimated using the orca as outgroup. **(b)** *NI* distributions per mitochondrial lineages, calculated using various outgroups, including orca and all possible interspecific comparisons. The letters on the right of the boxplots indicate significant differences in the mean *NI* between the different lineages (i.e. boxplot with different letters are statistically different from one another). The red dashed lines represent the limit at which *NI* reflects positive ($NI < 1$), neutral ($NI = 1$), or purifying ($NI > 1$) selection. *NS* not significant. The acronyms are provided in Fig. 1.

The π_N/π_S ratio in the 13 CDSs, displaying the relative proportion of non-synonymous versus synonymous nucleotide diversity, was lower than one in all the lineages. This is consistent with purifying selection acting on the coding regions. At the species level, the ratio π_N/π_S ranged from 0.04 in Dall’s and spectacled to 0.10 in finless porpoises (Table S3). The vaquita displayed an intermediary value of 0.06. Within each species, π_N/π_S also varied markedly across lineages: in the harbor porpoise, π_N/π_S ratios ranged from 0 in the North Pacific NP2 lineage to 0.21 in the Black Sea BS lineage; in the finless porpoises from 0.14 in EAF to 0.17 in YFP; 0.05 in the DP2 Dall’s porpoise lineage; and 0.06 in SP2 spectacled porpoise lineage (Table S3).

The branch-specific non-synonymous to synonymous substitution rates (d_N/d_S , Fig. S3a) were fairly conserved across the phylogenetic tree and ranged from 0 in the finless porpoise to 1.08 in the harbor porpoise, with a median value at 0.12. A d_N/d_S lower than one implies purifying selection. Thus, similar to π_N/π_S , the branch-specific d_N/d_S suggested that the porpoise mitogenomes were mostly influenced by purifying selection. Furthermore, the d_N/d_S ratios did not differ significantly among species (PERMANOVA, p -value = 0.49). Interestingly, the d_N/d_S ratio was negatively correlated with the nucleotide diversity (Fig. S3b; Pearson’s $r = -0.64$, p -value = 0.01) suggesting that purifying selection removes deleterious mutations more effectively in genetically more diversified lineages.

The McDonald–Kreitman (MK) tests using first the orca as an outgroup showed that all the lineages for each species had neutrality index (*NI*) values greater or equal to one (Fig. 4a). In particular, some lineages displayed *NI* values significantly higher than one (G-tests, p -value < 0.05), consistent with a signal of purifying selection. These included the EAF and YFP lineages in the finless porpoises and the MA, IB and BS in the harbor porpoises (Fig. 4a). Vaquitas and NP2 harbor porpoises also displayed marginally significant *NI* values ($NI > 2$, p -value ≤ 0.10 ; Fig. 4a). The remaining lineages showed *NI*s close to one suggestive of selective neutrality. The MK tests applied to all pairs of interspecific lineages showed *NI* values often higher than one (Fig. 4b and Fig. S4a). The values were especially high (Fig. S4a) and significant (Fig. S4b) when comparing the harbor porpoise lineages (MA, IB, and BS) with the finless porpoise lineages (YFP and EAF). The variation in the distribution of *NI* among interspecific lineages (Fig. 4b) showed that these same lineages displayed significantly larger *NI* values compared to spectacled SP2 and Dall’s DP2 porpoise lineages (PERMANOVA, p -value < 0.001 and all pairwise comparisons have a p -value < 0.04 after False Rate discovery adjustment). We observed a significant negative correlation between π and *NI* (Pearson’s $r = -0.28$, p -value = 0.003), suggesting that purifying selection could be stronger in lineages with small N_e or that demographic events impacted the polymorphism of these lineages.

Demographic history. The vaquita displayed significant departure from neutral constant population size expectations with significant negative values for Fu and Li’s D^* and F^* , and Tajima’s D , even if this latter statistic was not significantly different from zero (Table 3). This result indicates a significant excess of singleton mutations compared to a neutral expectation, consistent with a bottleneck or a selective sweep. In contrast, the harbor

Lineage	D	D^*	F
Vaquita ($n = 12$)	-1.44 ^{NS}	-1.89*	-1.84*
North Pacific 1 ($n = 10$)	-1.18 ^{NS}	-1.27 ^{NS}	-1.28 ^{NS}

Table 3. Neutrality tests based on the site frequency spectrum. The neutrality tests were only applied to lineages where at the sample size (n) was at least 10. The statistics include the Tajima's D , Fu and Li's D^* , and Fu and Li's F . NS Not significant. * p -value < 0.05.

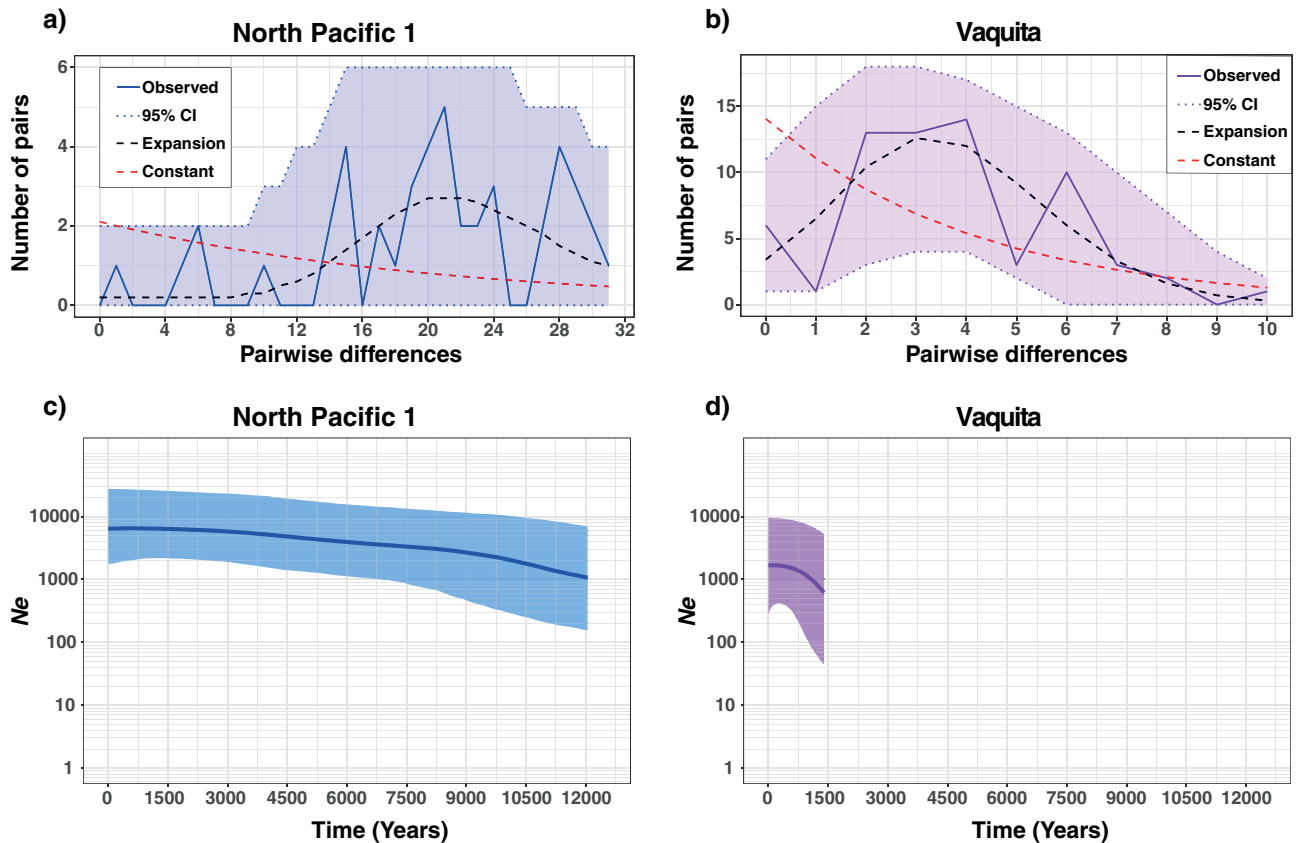


Figure 5. Mismatch distributions (a, b) and Bayesian Skyline Plots (BSPs) (c, d) for the North Pacific harbor porpoise 1 (NP1) lineage and the vaquita. The BSPs (c, d) show the temporal changes in mitochondrial diversity. The y-axis of the BSPs shows the genetic diversity expressed as the effective female population size (N_e). The bold line inside each BSPs represents the median value and thin lines the 95% HPD intervals. For both BSPs, the null hypothesis of a constant population size was rejected with a high confidence (Bayes Factors > 6).

porpoise NP1 lineage did not show any such significant deviation, even though all the statistics displayed negative values.

The mismatch distribution and the coalescent-based BSP also captured this contrast (Fig. 5). For the North Pacific harbor porpoise NP1 lineage, the mismatch distribution was consistent with an ancient population expansion (Fig. 5a) with a modal value close to 20 differences on average between pairs of sequences. Despite the ragged distribution and large 95% CI, the best fitted model suggested an ancient increase in genetic diversity ($\theta = 2 \cdot N_e \cdot \mu$) by a factor of 40 after a period ($\tau = 2 \cdot t \cdot \mu$) of 18 units of mutational time. This old expansion was also detected by the BSP analysis (Fig. 5c). Indeed, NP1 displayed an old steady increase in N_e with time since the most recent common ancestor (T_{MRCA}) 16,166 years before present (years BP) (95% CI 12,080–20,743), with a median N_e increasing from 1,660 to 6,436 (Fig. 5c). This model was strongly supported over the null hypothesis of a constant population size with all Bayes factors greater than 6.4. For the vaquita lineage, the mismatch distribution and the BSP analyses both supported a much more recent expansion than in NP1. The mismatch distribution (Fig. 5b) showed an increase of θ by a factor of 1,000 after a τ of four units of mutational time. The mode of the bell shape distribution for the best fitted model was around three differences among pairs of sequences, which is consistent with a recent population expansion. The BSP analysis (Fig. 5d) captured this expansion and explained the data significantly better than a constant population size model (Bayes factors > 8.7). This expansion was dated

back to 3,079 years BP (95% CI 1,409–5,225), with median N_e increasing from 613 (95% CI 45–5,319) to 1,665 (95% CI 276–9,611). Thus, the estimated current N_e was 3–6 times lower than in NP1 (Fig. 5d).

Discussion

The phylogeny of the Phocoenidae has been debated for decades, in part due to the lack of polymorphism and statistical power that came from the analyses of short fragments of the mitochondrial genome^{17,42}. Using massive parallel sequences technologies, the analyses of newly sequenced and assembled whole mitogenomes from all the species and sub-species of porpoises provide a robust comprehensive picture of the evolutionary history of the porpoises. The phylogenetic relationships estimated here delivered a fully resolved evolutionary tree (Fig. 1b and Fig. S1). While most of the phylogenetic relationships were suggested previously^{17,42}, the resolution and statistical support recovered here was maximal. Our results support the monophyly and branching of each species and sub-species. Moreover, the comparative view of the mitochondrial polymorphism within and among species provides one of the first attempts to bridge macro- to micro-evolutionary processes in a cetacean group (see also Ref.⁸⁴). This perspective across evolutionary time-scales can shed light on the isolation dynamics and their drivers across the speciation continuum of the Phocoenidae.

New insights into the biogeography of the Phocoenidae. The biogeographical history of cetacean species has been hypothesized to results of a succession of vicariant and dispersal events influenced by geological, oceanic, and climatic reorganization during the Late Miocene, Pliocene and early Pleistocene^{1,17}. Changes in climate, ocean structure, circulation, and marine productivity opened new ecological niches, enhanced individual dispersal and isolation, and fostered specialization to different food resources. All these factors promoted the adaptive radiation in cetaceans which led to the extant species diversity in the odontocete families⁸⁵. For example, the Monodontidae and Delphinidae are the closest relatives to the Phocoenidae. They originated during the Miocene and displayed an accelerated evolution marked with the succession of speciation events during 3 Myr, leading to the extant species diversity in these groups^{1,17}. The time calibrated phylogeny of the Phocoenidae (Fig. 2) suggests that porpoises also diversified following similar processes during the late Miocene until the early-Pleistocene (between 6 and 2 Myr). This timing is about 2–3 Myr more recent than those proposed by McGowen et al.¹⁷ and Steeman et al.¹. It is worth mentioning that recent estimates proposed by McGowen et al.⁸⁶ included four of the six porpoise species and were more in line with our estimates. The increase of the genetic information, node calibrations and number of sequences per species are known to influence phylogenetic inferences and divergence time estimates^{6,87,88}. The use of complete mitogenomes, two node calibrations (instead of one), and several sequences per species in our study likely explain the difference compared to previous studies.

Consistent with previous findings^{17,41,42}, the finless porpoises were the first species to split among the Phocoenidae. As the vast majority of the porpoise fossils found so far come from tropical or subtropical regions⁴¹, and considering their current predominant affinity for warm waters, the finless porpoises seem to be the last members of a group of porpoise species that adapted primarily to tropical waters. Interestingly, finless porpoises further diversified and colonized more temperate waters of the Yellow Sea and Sea of Japan (Fig. 1a). The five remaining porpoise species diverged ~4.0 Myr ago and all but the vaquita occupy temperate regions with an antitropical distribution (Fig. 1a). Harbor and Dall's porpoises inhabit the cold water of the Northern hemisphere whereas spectacled and Burmeister's porpoises are found in the Southern hemisphere. This result is consistent with the hypothesis that antitropically distributed cetaceans have evolved with the deep environmental changes that occurred during the late Pliocene and as a response to the fluctuations in surface water temperatures in the tropics, concomitant with the changes in oceanographic currents, marine productivity, and feeding areas^{1,12,15}. About 3.2 Myr ago, the formation of the Panama Isthmus altered the tropical currents and water temperatures in coastal regions of the Pacific, and throughout the world oceans. It promoted the dispersion of numerous taxa from the Northern to the Southern Hemisphere⁸⁹. This process is also a plausible driver that led to the antitropical distribution of the modern porpoises⁴¹.

During the porpoises' evolutionary history, a symmetric evolution took place approximatively at the same time in both hemispheres resulting in analogous ecological adaptations. In the Northern hemisphere, the split between Dall's and harbor porpoises ~3.1 Myr ago led to offshore versus coastal specialized species, respectively. This pattern was mirrored in the Southern hemisphere with the split between the spectacled and Burmeister's porpoises ~2.1 Myr ago which led also to the divergence between offshore versus coastal specialized species. Such a symmetric habitat specialization likely reflects similar ecological opportunities that opened in both hemispheres and triggered a convergent adaptation in the porpoises. Interestingly, this possible parallel offshore evolution observed in Dall's and spectacled porpoises would have been accompanied by a convergent highly contrasted countershading coloration pattern with a white ventral side and black dorsal back side in both species. This color pattern is thought to be an adaptation to the offshore environment serving as camouflage for prey and predators⁹⁰.

Resources and diet specializations are known to be a major driver of cetacean evolution as their radiation is linked to the colonization of new vacant ecological niches in response to past changes⁸⁵. As small endothermic predators with elevated energetic needs associated with their cold habitat and small size, limited energy storage capacity and a rapid reproductive cycle, porpoises are known for their strong dependency on food availability^{91,92}. These characteristics reinforce the hypothesis that their adaptive radiation has been strongly shaped by historical variation in food resources and should also be visible at the intraspecific level.

Porpoises phylogeography and microevolutionary processes. The processes shaping the evolution of porpoises at the macro-evolutionary time scale find their origins at the intraspecific level (micro-evolutionary scale), with the split of multiple lineages within species that may or may not evolve into fully distinct and reproductively isolated species. We showed that all lineages forming the intraspecific subdivisions (sub-species

or ecotypes) each formed a monophyletic group. All these distinct lineages found their most recent common ancestor within the last million years. These results corroborate previous phylogeographic studies suggesting that intraspecific subdivisions observed in many porpoise species were mediated by environmental changes during the last glacial cycles of the Quaternary^{19,25,26,30}. The Last Glacial Maximum (LGM) and the subsequent ice retreat have profoundly shaped the phylogeographic patterns of many organisms, leaving behind multiple divergent lineages in many cetacean taxa that are vestiges of past environmental variations^{2,6,9,10,25,27,30,93}. Adaptive evolution to different niches in response to past changes associated with variation in marine sea ice, primary production, and redistribution of feeding areas led to intraspecific divergence in many cetaceans in terms of genetics, behavior, morphology, and geographical distribution. For example, the specialization between coastal versus offshore ecotypes in bottlenose dolphins has been dated back to the LGM, and explains the observed patterns of genetic and morphological differentiation⁹. Likewise, the behavior, size, color patterns and genetic divergence among some different types of killer whales were attributed to specialization onto different food resources since the LGM¹⁰. The present study shows that analogous processes occurred in each porpoise species too.

The finless porpoises represent probably one of the best documented cases of incipient speciation related to habitat specializations among the porpoises. Consistent with the results of Zhou et al.¹⁹ based on whole genome sequencing, our mitogenome results dated the radiation of the finless porpoise species within the last ~0.5 Myr. This coincides with the profound environmental changes associated with the Quaternary glaciations. In particular, our results are congruent with the hypothesis suggesting that the diversification of the finless porpoises has been driven by the elimination of the Taiwan Strait associated with the sea-level drop during glacial periods⁹⁴. Indeed, at least three land bridges connected Taiwan to mainland China since the last 0.5 Myr and could have enhanced the separation between the Indo-Pacific and the narrow ridged finless porpoises⁹⁴. Likewise, we dated the emergence of the Yangtze finless porpoise to the last ~0.1 Myr, which is consistent with previous studies suggesting that the last glacial event have strongly determined the evolutionary history of this species^{19,25,95}.

Similar to the finless porpoises, the harbor porpoises are also divided into several lineages previously recognized as distinct sub-species. The deepest split is observed between the North Pacific (*P. p. vomerina*) and North Atlantic lineages, and is deeper than the genetic divergence observed between the two species of finless porpoises. The lack of shared haplotypes between Pacific and Atlantic porpoises confirm previous results supporting their total isolation⁹⁶. Their splitting time was estimated at ~0.86 Myr, which is consistent with the presumed time when the North Pacific porpoises colonized the North Atlantic basin². The two ocean basins were last in contact across the Arctic approximately 0.7–0.9 Myr. ago, with estimated sea surface temperatures of ca. 0.5 °C⁹⁷, which corresponds to the lowest temperature at which harbor porpoises are currently observed. Within the North Atlantic, the three known sub-species^{2,30} (i.e. *P. p. phocoena*; *P. p. meridionalis* and *P. p. relicta*) were also detected as distinct monophyletic groups based on the mitogenome (Fig. 1b and Fig. S1). Their evolutionary history has been strongly influenced by recent environmental changes during the Quaternary period² and particularly the LGM^{8,30,60}. For example, Tolley and Rosel² discussed in great detail how major climatic shifts during the Quaternary constantly reshaped the distribution of harbor porpoise in the North Atlantic and the Black Sea (through episodes of isolation, colonization, contraction and expansion of different habitats) leading to the current divergence among sub-species (see also³⁰). North Pacific harbor porpoises also showed cryptic subdivisions (i.e. NP1 and NP2 in Fig. 1b and Fig. S1). Although several studies observed genetic structure among Pacific porpoises^{4,98}, none captured the deep divergence highlighted here. NP1 and NP2 displayed a level of divergence deeper than the one observed between the Iberian and Mauritanian harbor porpoises or between the Yangtze and East Asian finless porpoises. These two clades (NP1 and NP2) may also represent lineages that split during the LGM, with NP1 showing a steady increase in genetic diversity since the end of the LGM period 12 kyrs ago (Fig. 5c). These results are consistent with those of Taguchi et al.⁴ suggesting that climatic fluctuation during the Pleistocene shaped the genetic structure of Pacific harbor porpoises.

Compared to the finless and harbor porpoises, little is known about the Dall's, Burmeister's and spectacled porpoises. This is in part due to the limited number of observations and access to biological data (but see Refs.^{26,27,99}), especially for the spectacled porpoise. Despite these limitations, our study revealed that the patterns and processes described for the finless porpoise and harbor porpoise may apply also to the majority of the other porpoise species. Previous studies identified multiple intraspecific subdivisions within the Dall's²⁶ and Burmeister's²⁷ porpoises. The long branches in the phylogenetic tree (Fig. 1b) for Dall's porpoise (DP1/DP2 lineages) and spectacled porpoises (SP1/SP2) imply that distinct evolutionary units may also exist in these species. Furthermore, their vast distribution (Fig. 1a) and divergence times among lineages (Tables S5) suggest that the different lineages in these species also split during the Quaternary glaciations. This is congruent with the study of Hayano et al.²⁶ indicating that different lineages of Dall's porpoises from the west Pacific diverged in response to multiple events of population isolation occurring between 40,000 and 10,000 years ago during the LGM.

The vaquita contrasts strikingly with the other species with its narrow distribution, the smallest of all marine mammals (see Fig. 1a and Ref.¹⁰⁰). Previous studies based on a short fragment of the mitochondrial *D-loop* and *Cyt-b* identified the Burmeister's porpoise as the closest relative to the vaquitas. However, the phylogenetic results reported here using the whole mitogenome support that the vaquita coalesce with the ancestor of the Burmeister's and spectacled porpoise with maximal support. The estimated split time of ~2.4 Myr ago between vaquita and the southern porpoises is consistent with the onset of the Quaternary glaciations, 2.6 Myr ago¹⁰¹. The fact that the vaquita is found in the northern hemisphere, while the Burmeister's and spectacled porpoises are in the southern hemisphere implies that some ancestors with cold-affinities from the southern species crossed the equator in the past and became isolated long enough to become the ancestors of the extant vaquita. The most parsimonious hypothesis is that the decrease in water temperature associated with a glacial maximum likely allowed vaquita's ancestor to cross the equator and disperse to the Northern Hemisphere¹⁰². The current vaquita representatives thus form a relic population of the temperate southern species' ancestor that crossed the intertropical zone. In contrast with previous mitochondrial studies that found no variation at the *D-loop*¹⁰³,

we observed 16 sites segregating along the entire mitogenome. Among them, 13 were singleton mutations. This extremely low nucleotide diversity was the lowest of all porpoise lineages, as illustrated by the extremely short branches in the phylogenetic tree (Figs. 1b and 2). The origin of the present mitochondrial diversity is also relatively recent, with a $T_{MRC A}$ estimated at ~20,000 to 70,000 years with the phylogenetic approach and ~1,500 to 5,000 years with coalescent approach. The main reason behind this discrepancy is called “time dependency of molecular rates”^{6,87}. Population genetics coalescent-based estimates reflect the spontaneous mutation rates, whereas phylogeny-based estimates reflect the substitution rates (i.e. mutations fixed among taxa). Contrasting with these recent estimates, the branch connecting to the ancestor of vaquitas and southern species dates back to ~2.4 Myr. This suggests that either additional lineages may have existed in the past and went extinct or that only a single lineage crossed the intertropical zone. Whole genome analyses may help enlightening the evolutionary history of this peculiar species.

Genetic diversity and conservation. Maintenance of genetic diversity has been considered as an important factor in conservation biology. Genetic factors can contribute to the “extinction vortex” by a mutual reinforcement with demographic processes speeding-up population decline and increasing their extinction risk¹⁰⁴. As a consequence, ideal conservation measures should be designed to maximize genetic diversity, especially through the management of evolutionary significant units (ESU)¹⁰⁵. However, conservation status does not explicitly take this parameter into account since the relationship between IUCN status and genetic diversity is not always straightforward¹⁰⁶. In this study, the genetic diversity of each porpoise species correlates well with its IUCN status, especially when we account for intraspecific subdivision. The *Critically Endangered* taxa, such as the vaquitas or the YPF finless porpoises displayed extremely low π suggesting a low N_e . The *Endangered* (EAF finless porpoise) and *Vulnerable* (Black Sea harbor porpoise) taxa displayed low to average π . *Least Concern* taxa (e.g. North Atlantic harbor porpoise and Dall’s porpoise DP2) exhibited higher π , suggesting larger N_e and/or the presence of internal subdivision. This link between π and the IUCN conservation status may thus provide a useful proxy to assess the conservation status of taxa for which an IUCN status has not been yet established, due to data deficiency. For example, the Iberian harbor porpoise population is among the marine mammals displaying the highest stranding and by-catch rates reported³⁷. The low genetic diversity reported in the present study represents thus an additional signal indicating how possibly vulnerable are these Iberian porpoises. On the other hand, spectacled porpoises represent currently one of the least known cetacean species. Their genetic diversity is comparable to the one observed in the Dall’s porpoise DP2 lineage or the North Atlantic (NAT) harbor porpoise lineage, suggesting these populations display large N_e .

Mitochondrial diversity may not always be a good proxy of population abundance. Other evolutionary processes than just demography may impact genetic diversity¹⁰⁷ (i.e., such as natural selection). The d_N/d_S and π_N/π_S lower than 1 highlighted in this study would be usually indicative of purifying selection acting on the mitochondrial genetic diversity. The negative relationships observed between π and d_N/d_S (Fig. S3b) lend further support to this hypothesis, suggesting that purifying selection is more effective in large populations as predicted by the neutral theory^{68,69}. Surprisingly, the MK-tests suggested that purifying selection was prevailing on the mitochondrial genomes of the endangered porpoises with NI values larger than 1. In contrast, selective neutrality could not be rejected for less threatened species. At first glance, this result for the endangered porpoises seems counter intuitive. Purifying selection is expected to be less effective in lineages where population size is very small, since genetic drift is expected to outperform selective forces⁶⁷. However, when a lineage harbors a low N_e , slightly deleterious variants are expected to increase in frequency and segregate for a longer time without being fixed. Parsch et al.⁷¹ showed in different populations of *Drosophila melanogaster* that this effect will increase the number of polymorphic nonsynonymous mutations compared to the divergent nonsynonymous mutations ($\pi_N \gg d_N$). Hence, despite the reported increase of d_N/d_S in endangered taxa, it induces a bias in the neutrality index toward positive values creating an artefactual signal of purifying selection. The higher values of π_N/π_S observed in the endangered porpoise taxa (Table S3) and the negative relationships reported between π and NI support this hypothesis. All these elements suggest that demographic processes rather than selective forces drive the genetic diversity of the mitochondrial genome, and lead to high values of NI or d_N/d_S in the endangered taxa.

Conclusions

Using complete mitochondrial genomes, we reconstructed a comprehensive picture of the evolutionary history of the Phocoenidae. Besides clarifying the debated phylogenetic relationships among porpoises, our results provided new insights into the process driving species diversification in the porpoises across the speciation continuum. Similar to the Delphinidae, the Phocoenidae recently radiated in response to past environmental variation, adapting to different environments, ecological niches, and food resources. Furthermore, our results suggested that the processes governing their divergence at the macro-evolutionary scale find their origins at the micro-evolutionary scale. We revealed cryptic genetic subdivision for several taxa suggesting that our knowledge about many species, especially the data deficient southern species, is still scarce. Finally, the level of mitochondrial genetic diversity within a species seems to be primarily driven by demographic processes, rather than natural selection and turned out to be a good proxy for the conservation issues reported in these groups (i.e. Yangtze finless porpoises or vaquita).

The phylogenetic inferences in this study rely only on the mitogenome. A single genetic marker may not be fully representative of the species evolutionary history because individual gene trees may sometimes differ from the species tree¹⁰⁸. Selection, incomplete lineage sorting and introgression can create discordance between gene trees and the species tree¹⁰⁸. This issue is expected to be especially problematic in closely related species where introgression can still occur¹⁰⁹, in group of species that rapidly radiated^{84,110}, or in species with large effective population sizes where genetic drift may be inefficient to sort out lineages among groups and where selection

can have a significant impact^{109,111}. The macroevolutionary timescale of divergence among porpoise species associated with their small population size, and their largely allopatric current distributions, imply that ILS, introgression, and selection should have a limited impact. We are thus confident in the phylogenetic inferences made from the mitogenome data. Nevertheless, it will be important in future studies to use genome scale data to validate and complement the phylogenetic inferences of the present study and provide finer resolution of the evolutionary processes within and among species.

Data availability

Mitochondrial genome assemblies and sequence reads were deposited on NCBI under the BioProject ID: PRJNA659918. Genbank accession numbers of mitochondrial sequence assemblies referring to individual specimens are listed in table S2. Alignment data and scripts are available via the IRD Porpoises genetics and genomics Dataverse (<https://doi.org/10.23708/QBIUMI>).

Received: 10 January 2020; Accepted: 17 August 2020

Published online: 16 September 2020

References

1. Steeman, M. E. *et al.* Radiation of extant cetaceans driven by restructuring of the oceans. *Syst. Biol.* **58**, 573–585 (2009).
2. Tolley, K. A. & Rosel, P. E. Population structure and historical demography of eastern North Atlantic harbour porpoises inferred through mtDNA sequences. *Mar. Ecol. Prog. Ser.* **327**, 297–308 (2006).
3. Banguera-Hinestroza, E., Bjørge, A., Reid, R. J., Jepson, P. & Hoelzel, A. R. The influence of glacial epochs and habitat dependence on the diversity and phylogeography of a coastal dolphin species: *Lagenorhynchus albirostris*. *Conserv. Genet.* **11**, 1823–1836 (2010).
4. Taguchi, M., Chivers, S. J., Rosel, P. E., Matsuishi, T. & Abe, S. Mitochondrial DNA phylogeography of the harbour porpoise *Phocoena phocoena* in the North Pacific. *Mar. Biol.* **157**, 1489–1498 (2010).
5. Amaral, A. R. *et al.* Influences of past climatic changes on historical population structure and demography of a cosmopolitan marine predator, the common dolphin (genus *Delphinus*). *Mol. Ecol.* **21**, 4854–4871 (2012).
6. Moura, A. E. *et al.* Recent diversification of a Marine Genus (*Tursiops* spp.) tracks habitat preference and environmental change. *Syst. Biol.* **62**, 865–877 (2013).
7. Whitehead, H. Cultural selection and genetic diversity in matrilineal whales. *Science* **282**, 1708–1711 (1998).
8. Fontaine, M. C. *et al.* Postglacial climate changes and rise of three ecotypes of harbour porpoises, *Phocoena phocoena*, in western Palearctic waters. *Mol. Ecol.* **23**, 3306–3321 (2014).
9. Louis, M. *et al.* Ecological opportunities and specializations shaped genetic divergence in a highly mobile marine top predator. *Proc. Biol. Sci.* **281**, 20141558–20141558 (2014).
10. Foote, A. D. *et al.* Genome-culture coevolution promotes rapid divergence of killer whale ecotypes. *Nat. Commun.* **7**, 11693 (2016).
11. Hare, M. P., Cipriano, F. & Palumbi, S. R. Genetic evidence on the demography of speciation in allopatric dolphin species. *Evolution* **56**, 804–816 (2002).
12. Pastene, L. A. *et al.* Radiation and speciation of pelagic organisms during periods of global warming: The case of the common minke whale, *Balaenoptera acutorostrata*. *Mol. Ecol.* **16**, 1481–1495 (2007).
13. Barnes, L. G. Evolution, taxonomy and antitropical distributions of the porpoises (Phocoenidae, Mammalia). *Mar. Mammal Sci.* **1**, 149–165 (1985).
14. Burrige, C. P. Antitropicality of Pacific fishes: Molecular insights. *Environ. Biol. Fishes* **65**, 151–164 (2002).
15. Banguera-Hinestroza, E., Hayano, A., Crespo, E. & Hoelzel, A. R. Delphinid systematics and biogeography with a focus on the current genus *Lagenorhynchus*: Multiple pathways for antitropical and trans-oceanic radiation. *Mol. Phylogenet. Evol.* **80**, 217–230 (2014).
16. Marx, F. G. & Uhen, M. D. Climate, critters, and cetaceans: Cenozoic drivers of the evolution of modern whales. *Science* **327**, 993–996 (2010).
17. McGowen, M. R., Spaulding, M. & Gates, J. Divergence date estimation and a comprehensive molecular tree of extant cetaceans. *Mol. Phylogenet. Evol.* **53**, 891–906 (2009).
18. Gaskin, D. E. *The ecology of whales and dolphins* (Heinemann, London, 1982).
19. Zhou, X. *et al.* Population genomics of finless porpoises reveal an incipient cetacean species adapted to freshwater. *Nat. Commun.* **9**, 1276 (2018).
20. Teilmann, J. & Sveegaard, S. Porpoises the World over: Diversity in behavior and ecology. in *Ethology and Behavioral Ecology of Odontocetes* (ed. Würsig, B). Vol. 54, 449–464 (Springer International Publishing, New York, 2019).
21. Ridgway, S. H. & Johnston, D. G. Blood oxygen and ecology of porpoises of three genera. *Science* **151**, 456–458 (1966).
22. Morell, V. World's most endangered marine mammal down to 30. *Science* **355**, 558–559 (2017).
23. Amante, C. & Eatkins, B. W. *ETOPO1 1 Arc-Minute Global Relief Model: Procedures, Data Sources and Analysis. NOAA Technical Memorandum NESDIS NGDC*. <https://doi.org/10.7289/V5C8276M>.
24. Berta, A., Sumich, J. L. & Kovacs, K. M. Chapter 6 - Evolution and geography. in *Marine Mammals: Evolutionary Biology* 131–166 (Elsevier, Amsterdam, 2015). <https://doi.org/10.1016/B978-0-12-397002-2.00006-5>.
25. Chen, M. *et al.* Genetic footprint of population fragmentation and contemporary collapse in a freshwater cetacean. *Sci. Rep.* **7**, 14449 (2017).
26. Hayano, A., Amano, M. & Miyazaki, N. Phylogeography and population structure of the Dall's porpoise, *Phocoenoides dalli*, in Japanese waters revealed by mitochondrial DNA. *Genes Genet. Syst.* **78**, 81–91 (2003).
27. Rosa, S. *et al.* Population structure of nuclear and mitochondrial DNA variation among South American Burmeister's porpoises (*Phocoena spinipinnis*). *Conserv. Genet.* **6**, 431–443 (2005).
28. Méndez-Fernández, P. *et al.* Ecological niche segregation among five toothed whale species off the NW Iberian Peninsula using ecological tracers as multi-approach. *Mar. Biol.* **160**, 2825–2840 (2013).
29. Galatius, A., Kinze, C. C. & Teilmann, J. Population structure of harbour porpoises in the Baltic region: Evidence of separation based on geometric morphometric comparisons. *J. Mar. Biol. Ass.* **92**, 1669–1676 (2012).
30. Fontaine, M. C. Harbour porpoises, *Phocoena phocoena*, in the Mediterranean Sea and adjacent regions: Biogeographic relicts of the Last Glacial Period. *Adv. Mar. Biol.* **75**, 333–358 (2016).
31. Tezanos-Pinto, G. *et al.* A worldwide perspective on the population structure and genetic diversity of bottlenose dolphins (*Tursiops truncatus*) in New Zealand. *J. Hered.* **100**, 11–24 (2009).
32. Thomas, L. *et al.* Last call: Passive acoustic monitoring shows continued rapid decline of critically endangered vaquita. *J. Acoust. Society Am.* **142**, EL512–EL517 (2017).

33. Jaramillo Legorreta, A. M. *et al.* Decline towards extinction of Mexico's vaquita porpoise (*Phocoena sinus*). *R. Soc. Open Sci.* **6**, 190598 (2019).
34. Wang, J. Y. & Reeves, R. R. *Neophocaena phocaenoides*. The IUCN Red List of Threatened Species. e.T198920A50386795. <https://doi.org/10.2305/IUCN.UK.2017-3.RLTS.T198920A50386795.en>. Downloaded on 04 April 2019 (2017).
35. Wang, D., Turvey, S. T., Zhao, X. & Mei, Z. *Neophocaena asiaorientalis ssp. asiaorientalis*. The IUCN Red List of Threatened Species. e.T43205774A45893487. <https://doi.org/10.2305/IUCN.UK.2013-1.RLTS.T43205774A45893487.en>. Downloaded on 04 April 2019. (2013).
36. Birkun, A. A., Jr & Frantzis, A. *Phocoena phocaena ssp. relicta*. The IUCN Red List of Threatened Species. e.T17030A6737111. <https://doi.org/10.2305/IUCN.UK.2008.RLTS.T17030A6737111.en>. Downloaded on 04 April 2019 (2008).
37. Read, F. L., Santos, M. B. & González, A. F. *Understanding Harbour Porpoise (Phocoena phocaena) and Fishery Interactions in the North-West Iberian Peninsula*. (Final report to ASCOBANS, 2012).
38. Dufresnes, C. *et al.* Conservation phylogeography: Does historical diversity contribute to regional vulnerability in European tree frogs (*Hyla arborea*)?. *Mol. Ecol.* **22**, 5669–5684 (2013).
39. Malaney, J. L. & Cook, J. A. Using biogeographical history to inform conservation: The case of Preble's meadow jumping mouse. *Mol. Ecol.* **22**, 6000–6017 (2013).
40. Moritz, C. C. & Potter, S. The importance of an evolutionary perspective in conservation policy planning. *Mol. Ecol.* **22**, 5969–5971 (2013).
41. Fajardo-Mellor, L. *et al.* The phylogenetic relationships and biogeography of true porpoises (Mammalia: Phocoenidae) based on morphological data. *Mar. Mammal Sci.* **22**, 910–932 (2006).
42. Rosel, P. E., Haygood, M. G. & Perrin, W. F. Phylogenetic relationships among the true porpoises (Cetacea: Phocoenidae). *Mol. Phylogenet. Evol.* **4**, 463–474 (1995).
43. Torroni, A., Achilli, A., Macaulay, V., Richards, M. & Bandelt, H.-J. Harvesting the fruit of the human mtDNA tree. *Trends Genet.* **22**, 339–345 (2006).
44. Viricel, A. & Rosel, P. E. Evaluating the utility of cox1 for cetacean species identification. *Mar. Mammal Sci.* **28**, 37–62 (2011).
45. Andrews, S. *FastQC: A quality control tool for high throughput sequence data*. <https://www.bioinformatics.babraham.ac.uk/projects/fastqc> (2010).
46. Bolger, A. M., Lohse, M. & Usadel, B. Trimmomatic: A flexible trimmer for Illumina sequence data. *Bioinformatics* **30**, 2114–2120 (2014).
47. Kears, M. *et al.* Geneious Basic: An integrated and extendable desktop software platform for the organization and analysis of sequence data. *Bioinformatics* **28**, 1647–1649 (2012).
48. Arnason, U., Gullberg, A. & Janke, A. Mitogenomic analyses provide new insights into cetacean origin and evolution. *Gene* **333**, 27–34 (2004).
49. Hahn, C., Bachmann, L. & Chevreaux, B. Reconstructing mitochondrial genomes directly from genomic next-generation sequencing reads—A baiting and iterative mapping approach. *Nucleic Acids Res.* **41**, e129–e129 (2013).
50. Morin, P. A. *et al.* Complete mitochondrial genome phylogeographic analysis of killer whales (*Orcinus orca*) indicates multiple species. *Genome Res.* **20**, 908–916 (2010).
51. Edgar, R. C. MUSCLE: Multiple sequence alignment with high accuracy and high throughput. *Nucleic Acids Res.* **32**, 1792–1797 (2004).
52. Clayton, D. A. Transcription and replication of mitochondrial DNA. *Hum. Reprod.* **15**(Suppl 2), 11–17 (2000).
53. Guindon, S. *et al.* New algorithms and methods to estimate maximum-likelihood phylogenies: Assessing the performance of PhyML 3.0. *Syst. Biol.* **59**, 307–321 (2010).
54. Ronquist, F. *et al.* MrBayes 3.2: Efficient Bayesian phylogenetic inference and model choice across a large model space. *Syst. Biol.* **61**, 539–542 (2012).
55. Darriba, D., Taboada, G. L., Doallo, R. & Posada, D. jModelTest 2: More models, new heuristics and parallel computing. *Nat. Methods* **9**, 772–772 (2012).
56. Rambaut, A., Suchard, M. A., Xie, D. & Drummond, A. J. Tracer v.1.6. (2014). <https://tree.bio.ed.ac.uk/software/tracer/>. Accessed 26 Feb 2017.
57. Yu, G., Lam, T.T.-Y., Zhu, H. & Guan, Y. Two methods for mapping and visualizing associated data on phylogeny using Ggtree. *Mol. Biol. Evol.* **35**, 3041–3043 (2018).
58. Bouckaert, R. *et al.* BEAST 2: A software platform for bayesian evolutionary analysis. *PLoS Comput. Biol.* **10**, e1003537–e1003546 (2014).
59. Nabholz, B., Glemin, S. & Galtier, N. Strong variations of mitochondrial mutation rate across mammals—The longevity hypothesis. *Mol. Biol. Evol.* **25**, 120–130 (2007).
60. Fontaine, M. C. *et al.* Genetic and historic evidence for climate-driven population fragmentation in a top cetacean predator: The harbour porpoises in European water. *Proc. Biol. Sci.* **277**, 2829–2837 (2010).
61. Rambaut, A. & Drummond, A. J. *FigTree version 1.4.3*. (tree.bio.ed.ac.uk/software/figtree, 2012).
62. Librado, P. & Rozas, J. DnaSP v5: A software for comprehensive analysis of DNA polymorphism data. *Bioinformatics* **25**, 1451–1452 (2009).
63. Sanders, H. L. Marine benthic diversity: A comparative study. *Am. Nat.* **102**, 243–282 (1968).
64. McDonald, J. H. & Kreitman, M. Adaptive protein evolution at the Adh locus in *Drosophila*. *Nature* **351**, 652–654 (1991).
65. Hervé, M. *RVAideMemoire*: Testing and plotting procedures for biostatistics. <https://cran.r-project.org/web/packages/RVAideMemoire/index.html> (2019).
66. Benjamini, Y. & Hochberg, Y. Controlling the false discovery rate: A practical and powerful approach to multiple testing. *J. Roy. Stat. Soc. Ser. B (Methodol.)* **57**, 289–300 (1995).
67. Kimura, M. *The Neutral Theory of Molecular Evolution* (Cambridge University Press, Cambridge, 1983). <https://doi.org/10.1017/CBO9780511623486>.
68. Hughes, A. L. Near neutrality: Leading edge of the neutral theory of molecular evolution. *Ann. N. Y. Acad. Sci.* **1133**, 162–179 (2008).
69. Phifer-Rixey, M. *et al.* Adaptive evolution and effective population size in wild house mice. *Mol. Biol. Evol.* **29**, 2949–2955 (2012).
70. Eyre-Walker, A. Changing effective population size and the McDonald–Kreitman test. *Genetics* **162**, 2017–2024 (2002).
71. Parsch, J., Zhang, Z. & Baines, J. F. The influence of demography and weak selection on the McDonald–Kreitman test: An empirical study in *Drosophila*. *Mol. Biol. Evol.* **26**, 691–698 (2009).
72. Romiguier, J. *et al.* Fast and robust characterization of time-heterogeneous sequence evolutionary processes using substitution mapping. *PLoS ONE* **7**, e33852 (2012).
73. Duthel, J. & Boussau, B. Non-homogeneous models of sequence evolution in the Bio++ suite of libraries and programs. *BMC Evol. Biol.* **8**, 255 (2008).
74. Duthel, J. Y. *et al.* Efficient selection of branch-specific models of sequence evolution. *Mol. Biol. Evol.* **29**, 1861–1874 (2012).
75. R Core Team. *R: A language and environment for statistical computing*. Vienna, Austria. <https://www.R-project.org/> (2018).
76. Figuet, E., Romiguier, J., Duthel, J. Y. & Galtier, N. Mitochondrial DNA as a tool for reconstructing past life-history traits in mammals. *J. Evol. Biol.* **27**, 899–910 (2014).
77. Tajima, F. Statistical method for testing the neutral mutation hypothesis by DNA polymorphism. *Genetics* **123**, 585–595 (1989).

78. Fu, Y. X. & Li, W. H. Statistical tests of neutrality of mutations. *Genetics* **133**, 693–709 (1993).
79. Excoffier, L. & Lischer, H. E. L. Arlequin suite ver 3.5: A new series of programs to perform population genetics analyses under Linux and Windows. *Mol. Ecol. Res.* **10**, 564–567 (2010).
80. Schneider, S. & Excoffier, L. Estimation of past demographic parameters from the distribution of pairwise differences when the mutation rates vary among sites: application to human mitochondrial DNA. *Genetics* **152**, 1079–1089 (1999).
81. Drummond, A. J., Rambaut, A., Shapiro, B. & Pybus, O. G. Bayesian coalescent inference of past population dynamics from molecular sequences. *Mol. Biol. Evol.* **22**, 1185–1192 (2005).
82. Kingman, J. F. C. The coalescent. *Stochastic Process. Appl.* **13**, 235–248 (1982).
83. Kass, R. E. & Raftery, A. E. Bayes factors. *J. Am. Stat. Assoc.* **90**, 773–795 (1995).
84. Moura, A. E. *et al.* Phylogenomics of the genus *Tursiops* and closely related Delphininae reveals extensive reticulation among lineages and provides inference about eco-evolutionary drivers. *Mol. Phylogenet. Evol.* **146**, 106756 (2020).
85. Slater, G. J., Price, S. A., Santini, F. & Alfaro, M. E. Diversity versus disparity and the radiation of modern cetaceans. *Proc. Biol. Sci.* **277**, 3097–3104 (2010).
86. McGowen, M. R. *et al.* Phylogenomic resolution of the cetacean tree of life using target sequence capture. *Syst. Biol.* **31**, 2553 (2019).
87. Ho, S. Y. W., Saarma, U., Barnett, R., Haile, J. & Shapiro, B. The effect of inappropriate calibration: Three case studies in molecular ecology. *PLoS ONE* **3**, e1615 (2008).
88. Zheng, Y. & Wiens, J. J. Do missing data influence the accuracy of divergence-time estimation with BEAST? *Mol. Phylogenet. Evol.* **85**, 41–49 (2015).
89. Lindberg, D. R. Marine biotic interchange between the northern and southern hemispheres. *Paleobiology* **17**, 308–324 (1991).
90. Perrin, W. F. Coloration. in *Encyclopedia of Marine Mammals* (eds Würsig, B., Perrin, W. & Thewissen, J. G. M.) 243–249 (Elsevier, 2009). <https://doi.org/10.1016/B978-0-12-373553-9.00061-4>.
91. Koopman, H. N., Pabst, D. A., McLellan, W. A., Dillaman, R. M. & Read, A. J. Changes in blubber distribution and morphology associated with starvation in the harbor porpoise (*Phocoena phocoena*): Evidence for regional differences in blubber structure and function. *Physiol. Biochem. Zool.* **75**, 498–512 (2002).
92. Hoekendijk, J. P. A., Spitz, J., Read, A. J., Leopold, M. F. & Fontaine, M. C. Resilience of harbor porpoises to anthropogenic disturbance: Must they really feed continuously? *Mar. Mammal Sci.* **34**, 258–264 (2018).
93. Escorza-Treviño, S. & Dizon, A. E. Phylogeography, intraspecific structure and sex-biased dispersal of Dall's porpoise, *Phocoenoides dalli*, revealed by mitochondrial and microsatellite DNA analyses. *Mol. Ecol.* **9**, 1049–1060 (2000).
94. Wang, J. Y., Frasier, T. R., Yang, S. C. & White, B. N. Detecting recent speciation events: The case of the finless porpoise (genus *Neophocaena*). *Heredity (Edinb)* **101**, 145–155 (2008).
95. Lin, W. *et al.* Phylogeography of the finless porpoise (genus *Neophocaena*): Testing the stepwise divergence hypothesis in the northwestern Pacific. *Sci. Rep.* **4**, 6572 (2014).
96. Rosel, P. E., Dizon, A. E. & Haygood, M. G. Variability of the mitochondrial control region in populations of the harbour porpoise, *Phocoena*, on interoceanic and regional scales. *Can. J. Fish. Aquat. Sci.* **52**, 1210–1219 (1995).
97. Harris, S. A. Thermal history of the Arctic Ocean environs adjacent to North America during the last 3.5 Ma and a possible mechanism for the cause of the cold events (major glaciations and permafrost events). *Progress Phys. Geogr. Earth Environ.* **29**, 218–237 (2005).
98. Chivers, S. J., Dizon, A. E. & Gearin, P. J. Small-scale population structure of eastern North Pacific harbour porpoises (*Phocoena phocoena*) indicated by molecular genetic analyses. *J. Cetacean Res. Manag.* **4**, 111–122 (2002).
99. Pimper, L. E., Goodall, R. N. P. & Remis, M. I. First mitochondrial DNA analysis of the spectacled porpoise (*Phocoena dioptrica*) from Tierra del Fuego, Argentina. *Mamm. Biol. Zeitschrift für Säugetierkunde* **77**, 459–462 (2012).
100. Lundmark, C. Science sings the blues: Other words for Nothin' left to lose. *Bioscience* **57**, 208–208 (2007).
101. Ehlers, J. R. & Gibbard, P. Quaternary glaciation. in *Encyclopedia of Snow, Ice and Glaciers* 873–882 (Springer, Dordrecht, 2014). https://doi.org/10.1007/978-90-481-2642-2_423
102. Norris, K. S. & McFarland, W. N. A new harbor porpoise of the genus *Phocoena* from the Gulf of California. *J. Mammal.* **39**, 22 (1958).
103. Rosel, P. E. & Rojas-Bracho, L. Mitochondrial DNA variation in the critically endangered Vaquita *Phocoena Sinus Norris* and Macfarland, 1958. *Mar. Mammal Sci.* **15**, 990–1003 (1999).
104. Allendorf, F. W., Luikart, G. H. & Aitken, S. N. *Conservation and the Genetics of Populations* (Wiley, New York, 2012).
105. Moritz, C. Defining 'Evolutionarily Significant Units' for conservation. *Trends Ecol. Evol.* **9**, 373–375 (1994).
106. Nabholz, B., Mauffrey, J.-F., Bazin, E., Galtier, N. & Glemin, S. Determination of mitochondrial genetic diversity in mammals. *Genetics* **178**, 351–361 (2008).
107. Bazin, E., Glemin, S. & Galtier, N. Population size does not influence mitochondrial genetic diversity in animals. *Science* **312**, 570–572 (2006).
108. Degnan, J. H. & Rosenberg, N. A. Gene tree discordance, phylogenetic inference and the multispecies coalescent. *Trends Ecol. Evol.* **24**, 332–340 (2009).
109. Fontaine, M. C. *et al.* Mosquito genomics. Extensive introgression in a malaria vector species complex revealed by phylogenomics. *Science* **347**, 1258524 (2015).
110. Heliconius Genome Consortium. Butterfly genome reveals promiscuous exchange of mimicry adaptations among species. *Nature* **487**, 94–98 (2012).
111. Miles, A. *et al.* Genetic diversity of the African malaria vector *Anopheles gambiae*. *Nature* **552**, 96–100 (2017).

Acknowledgements

The following persons deserve our special thanks for having collected and made the samples available for this study: Tom Jefferson, Carlos Olavarria, Jay Barlow, Robin Baird, Marilyn Dahlheim, Lorenzo Rojas-Bracho. All live biopsy, bycaught, or stranded samples were collected under appropriate Marine Mammal Protection Act permits within the U.S., or appropriate permits elsewhere, following the relevant guidelines and regulations, and transferred internationally under CITES permit. We thank Andrew D. Foote for his constructive feedback that greatly improved the manuscript. We are also grateful to Frédéric Labbé for his assistance with the preparation of the map in Fig. 1 and Jorge Eduardo Amaya Romero for helping with the MITOBIM pipeline. We would like also to thank the Center for Information Technology of the University of Groningen for their support and for providing access to the *Peregrine* high-performance computing cluster. This study benefitted from the funding of the University of Groningen (The Netherlands). YBC was supported by a PhD fellowship from the University of Groningen. MF was supported through a Portuguese Foundation for Science and Technology (FCT) Grant SFRH/BD/30240/2006.

Author contributions

M.C.F. designed the study with the contribution of P.A.M.; Y.B.C. analyzed the data under the supervision of M.C.F., with help from A.W. and J.R.; A.A., A.B., M.F., B.L.T., L.R.B., K.M.R., G.A.V., P.A.M. contributed with the biological materials; J.T., K.M.R. performed the DNA extractions; C.S. and T.H. constructed the genomic libraries at Swift Bioscience and performed part of the sequencing; Y.B.C. and M.C.F. wrote the manuscript with input and feedbacks from all the co-authors.

Competing interests

The authors declare no competing interests.

Additional information

Supplementary information is available for this paper at <https://doi.org/10.1038/s41598-020-71603-9>.

Correspondence and requests for materials should be addressed to M.C.F.

Reprints and permissions information is available at www.nature.com/reprints.

Publisher's note Springer Nature remains neutral with regard to jurisdictional claims in published maps and institutional affiliations.



Open Access This article is licensed under a Creative Commons Attribution 4.0 International License, which permits use, sharing, adaptation, distribution and reproduction in any medium or format, as long as you give appropriate credit to the original author(s) and the source, provide a link to the Creative Commons license, and indicate if changes were made. The images or other third party material in this article are included in the article's Creative Commons license, unless indicated otherwise in a credit line to the material. If material is not included in the article's Creative Commons license and your intended use is not permitted by statutory regulation or exceeds the permitted use, you will need to obtain permission directly from the copyright holder. To view a copy of this license, visit <http://creativecommons.org/licenses/by/4.0/>.

© The Author(s) 2020



Habitats shape taxonomic and functional composition of Neotropical ant assemblages

Mélanie Fichaux¹ · Benoît Béchade¹ · Julian Donald^{1,2} · Arthur Weyna¹ · Jacques Hubert Charles Delabie^{3,4} · Jérôme Murienne² · Christopher Baraloto⁵ · Jérôme Orivel¹

Received: 10 August 2017 / Accepted: 15 January 2019
© Springer-Verlag GmbH Germany, part of Springer Nature 2019

Abstract

Determining assembly rules of co-occurring species persists as a fundamental goal in community ecology. At local scales, the relative importance of environmental filtering vs. competitive exclusion remains a subject of debate. In this study, we assessed the relative importance of habitat filtering and competition in structuring understory ant communities in tropical forests of French Guiana. Leaf-litter ants were collected using pitfall and Winkler traps across swamp, slope and plateau forests near Saül, French Guiana. We used a combination of univariate and multivariate analyses to evaluate trait response of ants to habitat characteristics. Null model analyses were used to investigate the effects of habitat filtering and competitive interactions on community assembly at the scale of assemblages and sampling points, respectively. Swamp forests presented a much lower taxonomic and functional richness compared to slope and plateau forests. Furthermore, marked differences in taxonomic and functional composition were observed between swamp forests and slope or plateau forests. We found weak evidence for competitive exclusion based on null models. Nevertheless, the contrasting trait composition observed between habitats revealed differences in the ecological attributes of the species in the different forest habitats. Our analyses suggest that competitive interactions may not play an important role in structuring leaf-litter ant assemblages locally. Rather, habitats are responsible for driving both taxonomic and functional composition of ant communities.

Keywords Formicidae · Traits · Functional diversity · Habitat filtering · Rainforest

Communicated by Andreas Prinzing.

Electronic supplementary material The online version of this article (<https://doi.org/10.1007/s00442-019-04341-z>) contains supplementary material, which is available to authorized users.

✉ Mélanie Fichaux
fichaux.mel@gmail.com

¹ CNRS, UMR Ecologie des Forêts de Guyane (EcoFoG), AgroParisTech, CIRAD, INRA, Université de Guyane, Université des Antilles, Campus Agronomique, BP 316, 97379 Kourou Cedex, France

² Laboratoire EDB (UMR 5174: CNRS, Université Toulouse 3 Paul Sabatier, IRD), Université Paul Sabatier, bâtiment 4R1, 118, route de Narbonne, 31062 Toulouse Cedex 9, France

³ Laboratório de Mirmecologia, CEPEC, CEPLAC, Caixa Postal 7, Itabuna, BA 45600-970, Brazil

⁴ Departamento de Ciências Agrárias e Ambientais, Universidade Estadual de Santa Cruz, Rodovia Jorge Amado Km 16, Ilheus, BA 45662-900, Brazil

⁵ International Center for Tropical Botany, Department of Biological Sciences, Florida International University, Miami, FL 33199, USA

Introduction

Determining general assembly rules of species occurring in the same place at a given time persists as a key goal in community ecology (Weiher and Keddy 2001). Mechanisms that delimit diversity can be broadly classified as deterministic (i.e. “niche-related”) and non-deterministic (i.e. “neutral”). From the deterministic perspective, both biotic and abiotic factors influence the presence and coexistence of species (Weiher and Keddy 2001; Maire et al. 2012). Habitat filtering limits the establishment of species unable to tolerate abiotic conditions of a given habitat, resulting in co-occurring species with similar ecological attributes (Keddy 1992). Competitive interactions can reduce the coexistence of species sharing similar niches (MacArthur and Levins 1967) or reinforce competitive hierarchies of species (Chesson 2000; Kunstler et al. 2012), resulting in spatial and/or temporal partitioning of species with similar ecological attributes (Diamond 1975; Gotelli and McCabe 2002). Alternatively, communities can be controlled by non-deterministic

processes which are purely stochastic, such as ecological drift (Hubbell 2001).

Early studies investigating assembly rules of species across different ecosystems focused mainly on taxonomic diversity without examining character displacement (but see Hutchinson 1957). A more comprehensive functional trait-based approach has recently been formalized, which links taxonomic entities with the ecological functions they fulfill in their environment (McGill et al. 2006; Cadotte et al. 2011). A combination of taxonomic and functional approaches can provide complementary insights not only into the role of environmental filtering and competitive exclusion in community assembly but also into the spatial scales at which such processes play important roles.

Indeed, the patterns of both species and trait distributions are likely to depend on the spatial scale of analysis. The effect of competitive exclusion is generally assumed to be strongest at the scale of interactions among individuals, where they directly compete for resources (Weiher and Keddy 1995). In contrast, habitat filtering is expected to be strongest at larger scales than that for competition, since habitat features such as topography typically vary over greater distances than interactions between individuals (Swenson et al. 2007; Kraft and Ackerly 2010). This transition in the respective role of niche-based processes across spatial scales should translate into a pattern of overdispersion in the trait values of co-occurring species at small spatial scales (MacArthur and Levins 1967), shifting to an opposing pattern of clustering in the trait values of species at larger spatial scales (Swenson et al. 2007).

In tropical regions, arthropods represent a highly diverse group (Basset et al. 2012), yet the structure of arthropod communities across spatial scales remains poorly understood (but see Ellwood et al. 2009; Lessard et al. 2011; Lamarre et al. 2016). Vertical stratification, seasonality and host specificity have been put forward as main factors that explain variation in arthropod distribution (Novotny and Basset 2005; Basset et al. 2015). Among arthropods, ants (Hymenoptera: Formicidae) are an ideal model for studies on diversity and community assembly patterns since they are relatively sessile organisms, moderately diverse and highly dominant in terrestrial ecosystems (Hölldobler and Wilson 1990), and because they perform an important range of ecological functions such as predation, scavenging and seed dispersal (Folgarait 1998). Moreover, a wide range of ecological strategies employed by ants can be captured by morphological approaches (e.g. Weiser and Kaspari 2006; Bihn et al. 2010; Silva and Brandão 2010). However, most studies examining patterns of trait diversity in ant assemblages have been conducted across broad geographic gradients, and they have found strong associations between the environment and functional responses of ant assemblages along broad gradients (e.g. Arnan et al. 2014; Silva and

Brandão 2014). Determining how communities are structured at small spatial scales will help to infer the mechanisms that structure local communities (e.g. Bihn et al. 2010; Blaimer et al. 2015; Liu et al. 2016; Arnan et al. 2018; Martello et al. 2018). However, most of local-scale studies have been performed with the aim of examining responses of ant assemblages to anthropogenic disturbance, by comparing the functional and/or phylogenetic diversity of ant assemblages in natural and human-modified habitats (Bihn et al. 2010; Liu et al. 2016; Arnan et al. 2018; Martello et al. 2018). Patterns of functional diversity of tropical ant assemblages in natural habitats at local scale remain largely unexplored (but see Wiescher et al. (2012) in which strong associations were observed between traits of subtropical ants and their environment).

In this study, we evaluated differences in both taxonomic and functional diversity of ant assemblages in naturally contrasted habitats distributed over a restricted geographic area within the Neotropical rainforest of French Guiana. The forests of French Guiana are among the most species-rich in the world, with broad environmental gradients, and they provide an ideal place to investigate the ecological drivers of diversity. Due to differences in seasonal water stress of Neotropical habitats across a relatively small area, marked differences in floristic composition are observed at relatively small spatial scales (Baraloto et al. 2007). Such contrasted habitats should differ in terms of potential niches for ant species, leading to gaps in the functional traits of species occurring in the different habitats. Here we measured the taxonomic and functional diversity of ant assemblages to address the following questions:

1. How does the taxonomic and functional diversity of ant assemblages vary across habitats? If habitats are filtering species based on their tolerance to abiotic conditions, then ecological strategies of ant assemblages should differ across contrasted habitats. We predicted that contrasted habitats would differ in terms of niches for ant species from the regional species pool, which would be translated by compositional changes across assemblages from contrasted habitats. If habitat filtering is a contributing factor, ant assemblages should display lower functional diversity than expected by chance. We also tested the prediction that such dissimilarities between habitats would lead to shifts in trait values of species. For example, longer legs would enable ants occurring in seasonally flooded forests to move out rapidly from the litter during flooding periods. In contrast, ants in plateau and slope forests should have large ranges of trait values due to broader niche availability in these habitats.
2. Does the functional structure of ant assemblages express the signature of competitive exclusion? We investigated the role of competition by measuring the functional

diversity at the scale of the sampling point (i.e. the finest scale of the study). If interspecific competition plays an important role in structuring communities, coexisting species should display higher functional diversity than expected by chance.

Materials and methods

Study site

Sampling took place in the forests surrounding Crique Limonade, close to Saül (03°34'09"N, 53°11'58"W), French Guiana. The region experiences an equatorial humid climate affected by the Inter-Tropical Convergence Zone (ITCZ), with a mean annual temperature of around 26 °C, a mean humidity of 80% and annual rainfall ranging from 3600 mm in the north-east to 2000 mm in the south and the west. The study site was defined as an area of ca. 100 km² which includes three different forest habitats—seasonally flooded (here referred as swamp), plateau and slope forests. Specifically, these habitats were discriminated based on variation in soil fertility, seasonal soil waterlogging and slope angle. Plateau forests on clay-rich soils exhibit flat gradients in topography and high nutrient content. In slope forests, the angle of the slope may limit the accumulation of leaf-litter due to lateral and superficial soil drainage (Allié et al. 2015). Soil waterlogging of plateau and slope forests is rare, while soil surfaces in swamp forests are submerged for at least two consecutive months each year (Baraloto et al. 2007; Soares et al. 2013). The elevation varied from 176 to 278 m a.s.l. across the nine assemblages sampled (three replicates of three habitats).

Ant sampling

Collection of leaf-litter ant fauna took place during the dry season (October) in 2013. The three forest habitats (plateau, swamp and slope forests) were sampled along three transects (3 × 3 = 9 assemblages) set up within the study site. Each assemblage was sampled over an area of 30 m × 40 m, within which we established a grid system of 20 points separated by 10 m, according to the Ants of Leaf Litter Protocol (Agosti and Alonso 2000). At each sampling point, we collected ants using pitfall traps and the Winkler method (see Bestelmeyer et al. 2000). Pitfall traps consisted of 6 cm diameter containers placed in the ground with the opening at the surface level. They were partially filled with a solution of water, soap and salt, and left open for 72 h. Collections of 1 m² leaf litter samples were also performed at each sampling point and ants were extracted from these samples using mini-Winkler extractors. In this apparatus, the sifted litter is held in a mesh sack suspended inside a larger cotton enclosure.

A plastic cup containing 70% ethanol is placed at the bottom of the cotton sack to collect insects that drop from the mesh sack over a period of 48 h (Bestelmeyer et al. 2000). The combination of pitfall traps and Winkler extractors have proven to be an efficient method for collecting the majority of leaf-litter ant species in a locality (Delabie et al. 2000; Silva et al. 2013).

Specimen identification

For each sample, ant specimens were identified to morphospecies or species level whenever possible. Voucher specimens were deposited in the Laboratório de Mirmecologia, Cocoa Research Centre CEPEC/CEPLAC (Itabuna, BA, Brazil) under the references #5761 (mini-Winkler traps) and #5762 (pitfall traps). For genera for which morphological identification proved to be problematic (e.g. *Pheidole* and *Solenopsis*), the 16S rRNA gene was sequenced in up to four specimens per morphospecies, with a mean of three specimens per morphospecies (for more details about the protocol, see Kocher et al. 2016). This procedure enabled us to discriminate ant specimens previously grouped as the same morphospecies or, on the contrary, to cluster several morphospecies into a single one.

Morphological data

Nine morphological attributes were measured (Table 1) for 99% of all species collected (203 out of 206 species). We selected these traits based on their expected link with ecological strategies related to resource use. Four randomly selected workers by species were measured whenever possible (average = 3.2 specimens measured per species). For morphologically dimorphic or polymorphic species, only minor-caste workers were measured. Measurements were made using an ocular micrometer accurate to 0.01 mm mounted on a stereomicroscope Leica M80 (Leica Microsystems, Heerbrugg, Switzerland).

Data analysis

To avoid bias in measures of species abundances (Gotelli et al. 2011), only species occurrences were used (i.e. the number of sampling points per assemblage in which a species occurred). Since pitfall traps and mini-Winkler extractors were used as complementary traps, we pooled data from both methods in following analyses so that only a single occurrence was reported for a species that was collected in both traps at the same sampling point. All analyses were conducted using R 3.3.2 statistical software (R Core Team 2018).

Table 1 List of morphological traits measured and their hypothesized ecological functions

Traits	Hypothesized ecological functions
Weber's length	Proxy for body size, associated to habitat complexity (Weber 1938; Kaspari and Weiser 1999)
Head width	Indicator of mandibular musculature, associated to trophic position (Weiser and Kaspari 2006)
Head length	Indicator of body size (Kaspari and Weiser 1999) and body mass which determines the quantity of resources consumed
Pronotum width	Predictor of body mass (Kaspari and Weiser 1999)
Femur length	Indicator of foraging speed, associated to habitat complexity (Feener et al. 1988)
Scape length	Associated with sensory abilities (Weiser and Kaspari 2006), indicative of an ant's ability to navigate and move through its surroundings (Yates et al. 2014)
Eye length	Indicator of feeding behavior; hypogaecic ant species have smaller eyes compared to epigaecic ant species (Weiser and Kaspari 2006; Yates et al. 2014)
Clypeus length	Related to liquid absorption abilities (Davidson et al. 2004); clypeus length is here used as a surrogate for liquid feeding habits in ants
Mandible length	Longer mandibles are associated with larger prey consumption (Fowler et al. 1991). In some cases (i.e. trap-jaw ants), sublinear to linear and long mandibles are used as extremely rapid trap for hunting and killing fast preys (Gronenberg et al. 1993)

Taxonomic diversity metrics

Taxonomic diversity was represented by species richness (i.e. the number of species) and species evenness (using the Pielou index; Pielou 1975) in each of the nine assemblages. We also calculated Fisher's alpha, the Gini-Simpson index, and the Hill number translation of the Shannon index (Supplementary material 1). Since all of these indices correlated with species richness (Spearman rank correlation, all $p < 0.05$), we only used the latter index for further analyses. Variation in species composition among habitats was evaluated using correspondence analysis (CA). The significance of compositional differences among habitats was assessed by permutational multivariate analysis of variance (PERMANOVA) with Bray-Curtis distance, using "adonis" in the R package "vegan" (Oksanen et al. 2017). In order to evaluate the degree of association of ant species with habitats, we also calculated indicator taxa values for each ant species after Dufrêne and Legendre (1997), using "indval" in the R package "labdsv" (Roberts 2016). Here, we only report species with significant associations with the three habitats sampled.

Functional diversity metrics

Functional analyses only included species for which morphological measurements were performed. Because trait values were not normally distributed and some of them correlated, they were standardized and transformed prior to calculating functional diversity metrics. Such trait transformation and/or standardization is widely used in functional diversity studies (e.g. Díaz et al. 2016; Silva et al. 2016; Arnan et al. 2018; Céréghino et al. 2018; Chun and Lee 2018). To do so and for each species, all traits, except Weber's length, were divided by Weber's length to correct for individual body size (see Table 1). A principal

component analysis (PCA) was then performed on a matrix of the mean value of the log-transformed relative trait per species in order to summarize the trait data and eliminate trait redundancy. The resulting orthogonal axes represent the generated "traits" defined by the loading of trait values. The multivariate metrics were calculated based on the first three principal components (Supplementary material 2).

Functional diversity was measured using the multidimensional framework proposed by Mouillot et al. (2013) which includes functional richness (FRic, Villéger et al. 2008), functional evenness (FEve, Villéger et al. 2008), functional divergence (FDiv, Villéger et al. 2008), functional dispersion (FDis, Laliberté and Legendre 2010), functional specialization (FSpe, Bellwood et al. 2006) and functional originality (FOri, Mouillot et al. 2008). Functional richness (FRic) represents the volume of the minimum convex hull occupied by all species of the assemblage (Cornwell et al. 2006), expressed here as the proportion of functional space filled by species present in the assemblage. Functional evenness (FEve) represents the regularity of species distribution in the functional trait space, weighted by their occurrences. Functional divergence (FDiv) measures the occurrence-weighted deviation of species from the non-weighted center of gravity of the convex hull. Functional dispersion (FDis) quantifies the occurrence-weighted mean dispersion of species from the occurrence-weighted center of gravity of all the species. Functional specialization (FSpe) measures the global weighted mean distance to the centroid of the functional space of the community. Functional originality (FOri) measures the weighted mean distance to the nearest species in the functional space of the community; this index reveals the functional redundancy between species. All functional indices were computed using the "MultidimFD" function (Mouillot et al. 2013, <<http://www.ecolog.univ-montp2.fr/software>>). We used Spearman rank

correlations to investigate associations between species richness and functional diversity indices.

In addition to the multivariate measures, we calculated the community-weighted mean value (CWM) for each of the nine morphological traits in each of the nine assemblages using the “FD” package (Laliberté et al. 2014). The CWM is an indicator of functional composition, representing the average of trait values in a community, weighted by the relative abundance of species (Lavorel et al. 2008). Examining single-trait differences among assemblages of contrasted habitats can help to identify ecological strategies adopted by species as a result of the environment.

Differences in diversity indices (FRic, FEve, FDiv, FDis, FSpe, FOr and CWMs) among habitats were evaluated using generalized linear models (GLMs) with quasipoisson error family. The significance of the tests was determined by computing an analysis of deviance using the *F* test.

Beta diversity

We used the partitioning of beta diversity proposed by Baselga (2010) and the analogous partitioning proposed by Villéger et al. (2013) for functional beta diversity in order to evaluate changes in, respectively, species and functional composition between assemblages. The total compositional variation between assemblages was calculated using the Jaccard pair-wise dissimilarity index. The turnover-fraction of Jaccard pair-wise dissimilarity accounted for compositional changes as a result of species or functional turnover. The nestedness component of Jaccard pair-wise dissimilarity represented the difference in species or functional richness between the assemblages compared. All pairwise beta-diversity measures were calculated using the “betapart” package (Baselga and Orme 2012).

Null models

A null modelling approach was used to investigate whether environmental filtering and competitive interactions drive the observed patterns of diversity. We generated 999 null communities by randomizing species names in the species-by-traits matrix in order to conserve all combinations of the three PC axis scores of each species. The assemblage data matrix was maintained constant in the null models. The observed metrics of functional diversity were then compared with the distribution of those calculated on the 999 null matrices. The quantile values of the null distributions were calculated separately for each functional metric.

The “environmental filtering hypothesis” was tested by comparing the observed functional diversity metrics to the metrics generated with the null model at the assemblage level ($n=9$). A reduction of functional richness, divergence, dispersion, specialization and originality (observed value

lower than the 5th percentile of the simulated values) or an increase in functional evenness (observed value higher than the 95th percentile of the simulated values) within assemblages compared to the total range of values in the regional species pool (i.e. the entire community) was interpreted as a signature of environmental filtering. Additionally, a change (reduction or increase) of the observed metrics from the simulated ones in the CWM at the assemblage scale was also interpreted as an evidence of a role of environmental filtering. In this case, a significant difference was considered if the observed value fell outside the 95% confidence interval of the simulated values (two-tailed test).

The “competitive exclusion hypothesis” was tested by comparing the observed functional diversity metrics to the metrics generated with the null models for each sampling point of each assemblage separately ($n=20$ points per assemblage). Evidence for competition would be supported by a higher functional richness, divergence, dispersion, specialization and originality (observed value higher than the 95th percentile) or a lower functional evenness (observed value lower than the 5th percentile) in the observed value than expected with the null model within sampling points of each assemblage. We also calculated the kurtosis of individual traits at the scale of the sampling points for each assemblage separately. If a competitive exclusion occurred among species within assemblages, the kurtosis of the distribution of trait values would be lower than expected (Cornwell and Ackerly 2009) with an observed value lower than the 5th percentile of the simulated values.

Results

A total of 9849 individuals belonging to 206 species from 60 genera were collected by the combined use of pitfall traps and mini-Winkler extractors (Supplementary material 3). Species richness reached 155, 136, and 70 species in plateau, slope and swamp forests respectively, ranging from 34 to 100 species per assemblage.

Taxonomic and functional alpha diversity

We found significant differences in both the mean species richness (GLM: $F_{2,6}=51.83$, $p<0.001$) and the mean functional richness (GLM: $F_{2,6}=9.16$, $p<0.05$) among habitats, with much lower richness in swamp assemblages compared to slope and plateau assemblages (Fig. 1a; Supplementary material 4). These results were consistent with significant differences in functional dispersion (GLM: $F_{2,6}=6.27$, $p<0.05$; Fig. 1b), with lower values in swamp compared to slope and plateau assemblages (Supplementary material 4). In contrast, we found no difference in the mean functional originality (GLM: $F_{2,6}=2.05$, $p=0.21$; Fig. 1c),

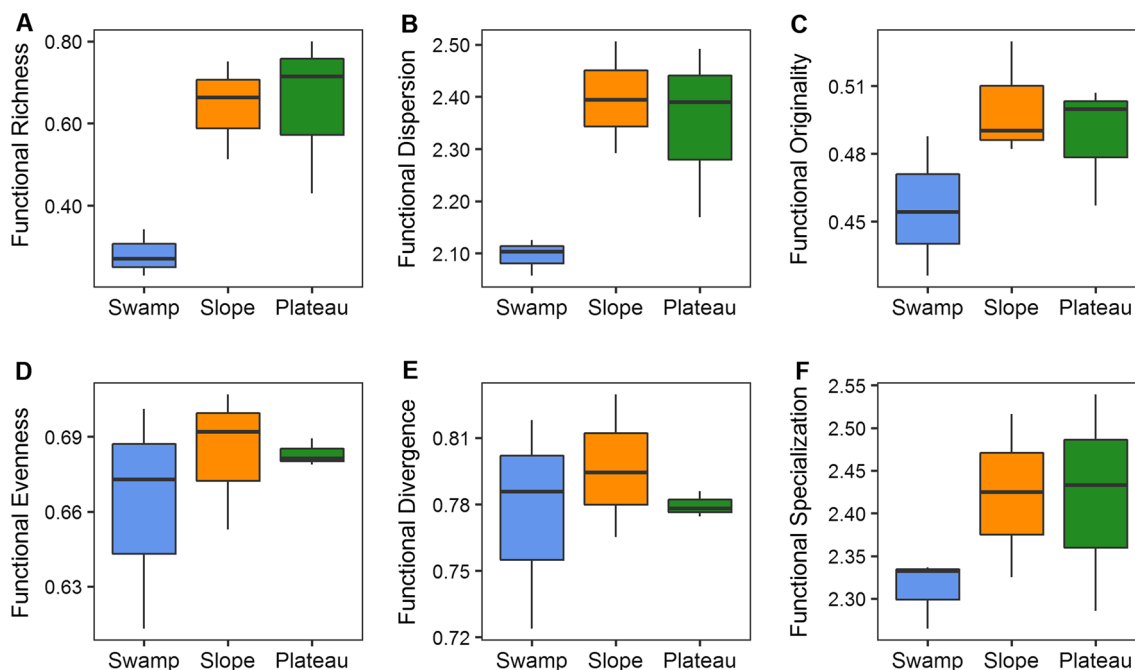


Fig. 1 Mean values of multi-trait diversity measures (**a** functional richness, **b** functional dispersion, **c** functional originality, **d** functional evenness, **e** functional divergence, **f** functional specialization) in the

three habitats (assemblages pooled per habitat). Error bars indicate standard error values

in the mean functional divergence (GLM: $F_{2,6} = 0.32$, $p = 0.74$; Fig. 1e) and in the mean functional specialization (GLM: $F_{2,6} = 1.36$, $p = 0.33$; Fig. 1f) among habitats. Species evenness significantly differed among habitats (GLM: $F_{2,6} = 68.26$, $p < 0.001$) whereas we found no difference in functional evenness among habitats (GLM: $F_{2,6} = 0.47$, $p = 0.65$; Fig. 1d). Regardless of the habitat, species richness was strongly positively correlated to functional richness (Spearman rank correlation: $\rho = 0.91$, $p < 0.001$) and moderately correlated to functional dispersion (Spearman rank correlation: $\rho = 0.76$, $p < 0.05$) and functional originality (Spearman rank correlation: $\rho = 0.78$, $p < 0.05$; Supplementary material 5).

At the habitat scale, the permutational multivariate analysis using Bray–Curtis distances on ant assemblages showed that an important and significant proportion of variance in species composition was explained by the habitats ($R^2 = 0.57$, $F_{2,6} = 3.96$, $p = 0.004$; Fig. 2a). Such separation of habitats was also highlighted from a functional perspective with swamp assemblages clearly separated from slope and plateau ones along the first axis of a principal component analysis computed on CWM scores for the nine traits (Dim1: 62.3%, Fig. 2b). A total of 13 species displayed significant habitat preference according to the indicator taxa value of Dufrene and Legendre (1997), with the highest number of indicator species found in plateau (six species), followed by swamp (five species) and slope (two species) forests (Table 2).

When comparing CWMs across habitats, no difference was found in CWMs for relative head length (GLM: $F_{2,6} = 1.51$, $p = 0.29$; Fig. 3a), relative head width (GLM: $F_{2,6} = 0.95$, $p = 0.44$; Fig. 3b) and Weber’s length (GLM: $F_{2,6} = 1.24$, $p = 0.35$; Fig. 3c). In contrast, CWM for relative scape length (GLM: $F_{2,6} = 39.22$, $p < 0.001$), relative eye length (GLM: $F_{2,6} = 71.50$, $p < 0.001$) and relative femur length (GLM: $F_{2,6} = 44.05$, $p < 0.001$) differed significantly among habitats, with ants from swamp forest having longer enumerated morphological attributes (Figs. 3d–f). CWM values for relative mandible length (GLM: $F_{2,6} = 8.47$, $p < 0.05$) and relative clypeus length (GLM: $F_{2,6} = 68.44$, $p < 0.001$) also differed among habitats, with ants having shorter relative mandibles (Fig. 3g) and longer relative clypeus (Fig. 3h) in swamp assemblages. Finally, we observed differences in CWM of relative pronotum width among habitats (GLM: $F_{2,6} = 7.48$, $p < 0.05$) with ants in slope forest having a narrower relative pronotum width (Fig. 3i).

Taxonomic and functional beta diversity

A high dissimilarity in species composition was observed among the assemblages of different habitats (Jaccard Dissimilarity Index, mean \pm SD = 0.71 ± 0.10 , range = $0.54–0.72$, Fig. 4). These differences in species composition among habitats were essentially due to species turnover (mean \pm SD = 0.57 ± 0.06), while the species

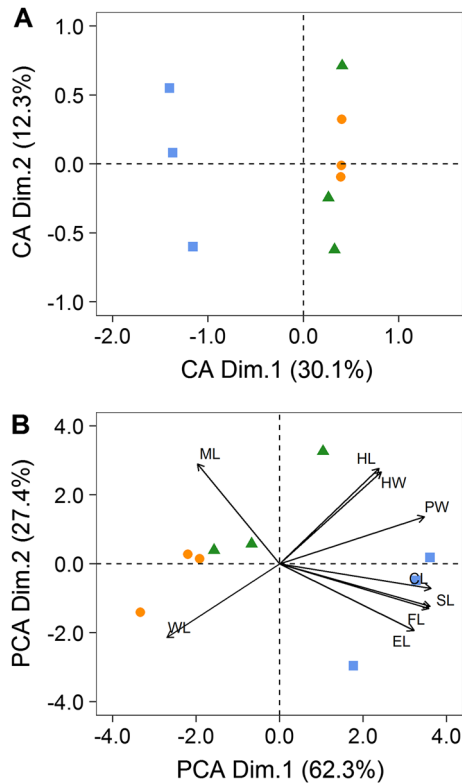


Fig. 2 Species and functional compositions of ant communities in each of the three forest habitats (squares = swamp, circles = slope, triangles = plateau). **a** Ordination of taxonomic composition on the first two axes of a correspondence analysis (CA). **b** Principal Component Analysis ordination (PCA) of functional composition (CWM) of the nine assemblages for each morphological trait. *HL* relative head length, *HW* relative head width, *ML* relative mandible length, *CL* relative clypeus length, *SL* relative scape length, *EL* relative eye length, *WL* Weber’s length, *FL* relative femur length, *PW* relative pronotum width

nestedness was relatively low across all pairs of habitats (mean ± SD = 0.15 ± 0.08).

Functional dissimilarity was moderately high across assemblages of all habitats (mean ± SD = 0.49 ± 0.16, range = 0.15–0.71, Fig. 4). A similar pattern was obtained with functional nestedness (mean ± SD = 0.39 ± 0.21), whereas functional turnover was relatively low across assemblages of all habitats (mean ± SD = 0.09 ± 0.08).

While we found a relatively high dissimilarity between swamp vs. plateau and slope assemblages (mean ± SD = 0.58 ± 0.11), this dissimilarity was relatively low between slope and plateau assemblages (mean ± SD = 0.31 ± 0.10, Fig. 4). Functional nestedness accounted for 86.3% of differences in functional composition between swamp vs. plateau and slope assemblages, and 60.7% of functional dissimilarity between slope and plateau assemblages.

Functional structure

We found only weak evidence of habitat filtering from multivariate metrics; we only detected a significant underdispersion in functional richness for one-third of the assemblages (two swamps and one plateau). Similarly, the competitive exclusion hypothesis assessed at the local scale for co-occurring species was rarely supported by multivariate indices. At the sampling point scale, we detected a deviation from the null expectation in 18.3% (33 out of 180, all metrics combined) of the samples (Table 3). Depending on the functional diversity metric, the proportion of samples in which we detected significant values ranged from 1.7% (for F_{Ori}) to 6.1% (for F_{Div}). A higher number of samples displayed overdispersion in functional metrics in slope assemblages (max. 11.6%, F_{Spe}) compared to plateau (max. 8.2%, F_{Div}) and swamp assemblages (max. 5%, F_{Div}).

Table 2 Species showing significant associations with the three forest habitats, following Dufrêne and Legendre (1997)

Species	Subfamily	Preferred habitat	Indicator value	<i>p</i>
<i>Lachnomyrmex pilosus</i> (Weber, 1950)	Myrmicinae	Swamp	1.000	0.036
<i>Pheidole</i> gp. <i>flavens</i> sp. D2	Myrmicinae	Swamp	0.912	0.049
<i>Pheidole alexeter</i> (Wilson, 2003)	Myrmicinae	Swamp	0.885	0.031
<i>Nylanderia</i> sp. 2	Formicinae	Swamp	0.792	0.041
<i>Pheidole</i> nr. <i>impressa</i>	Myrmicinae	Swamp	0.742	0.043
<i>Odontomachus scalptus</i> (Brown, 1978)	Ponerinae	Slope	1.000	0.032
<i>Crematogaster flavosensitiva</i> (Longino, 2003)	Myrmicinae	Slope	0.667	0.049
<i>Pheidole</i> gp. <i>fallax</i> sp. A2	Myrmicinae	Plateau	1.000	0.038
<i>Brachymyrmex heeri</i> (Forel, 1874)	Formicinae	Plateau	1.000	0.040
<i>Anochetus bispinosus</i> (Smith, 1858)	Ponerinae	Plateau	1.000	0.043
<i>Cyphomyrmex peltatus</i> (Kempf, 1966)	Myrmicinae	Plateau	0.813	0.036
<i>Solenopsis</i> sp. 22	Myrmicinae	Plateau	0.571	0.032
<i>Strumigenys denticulata</i> (Mayr, 1887)	Myrmicinae	Plateau	0.549	0.035

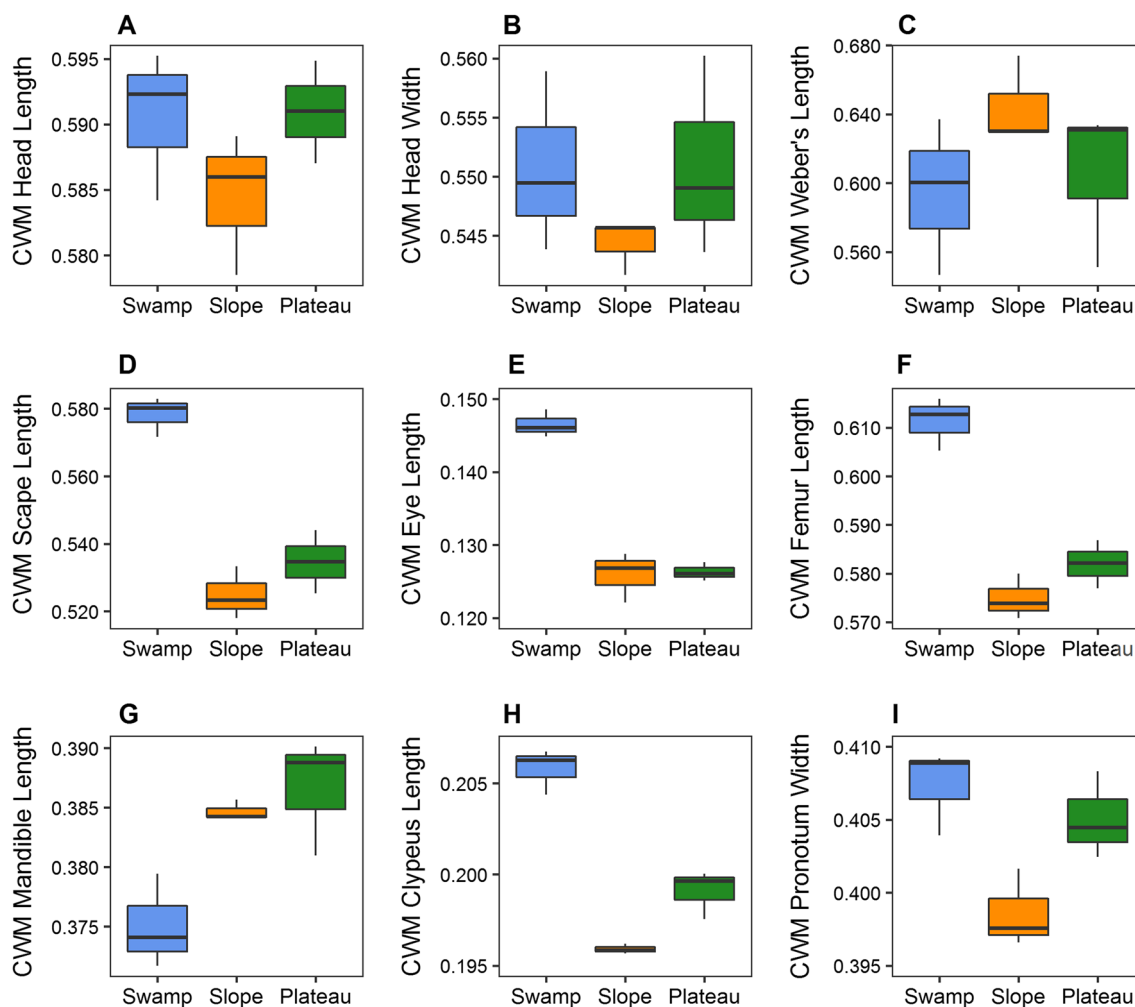


Fig. 3 Community-weighted mean values (CWM) of all species in the three sampled habitats for each trait (**a** head length, **b** head width, **c** Weber's length, **d** scape length, **e** eye length, **f** femur length, **g** mandible length, **h** clypeus length, **i** pronotum width). All traits except Weber's length are relative to body size (i.e. divided by Weber's length)

dible length, **h** clypeus length, **i** pronotum width). All traits except Weber's length are relative to body size (i.e. divided by Weber's length)

Compared to null communities, swamp assemblages were composed of ants with significantly longer scape (relative to body size) than expected given their number of species (Supplementary material 6). In contrast, mandibles tended to be relatively longer than expected in slope and plateau assemblages (Supplementary material 6). At the sampling point scale, the comparison between the observed trait values and the simulated values yielded a relatively low number of significant deviations, and the results were not consistent across samples from the same assemblage (Supplementary material 7). Depending on the trait, the proportion of samples in which we detected significant values ranged from 2.8% (for relative mandible length and Weber's length) to 11.7% (for relative clypeus length). A higher number of samples displayed a reduction in kurtosis of traits in slope assemblages (max. 20%, relative clypeus length) compared to plateau (max. 11.7%, relative clypeus length) and swamp assemblages (max. 8.3%, relative mandible length).

Discussion

In this study, we used a functional approach to determine the respective role of habitat filtering and competitive exclusion in structuring Neotropical ant assemblages. Our methodological design enabled us to evaluate the role of these two processes at the scale at which their signature should be the strongest. Thus, the role of habitat filtering was evaluated at the scale of assemblages while the role of competitive exclusion was tested at the scale of sampling points. This study shows that both the number of species and their functional roles vary across contrasted habitats over a relatively small spatial scale. However, we found weak evidence for competitive exclusion between co-occurring species at the scale of sampling points. The results of this study underline the key role played by distinct habitats in structuring leaf-litter ant communities

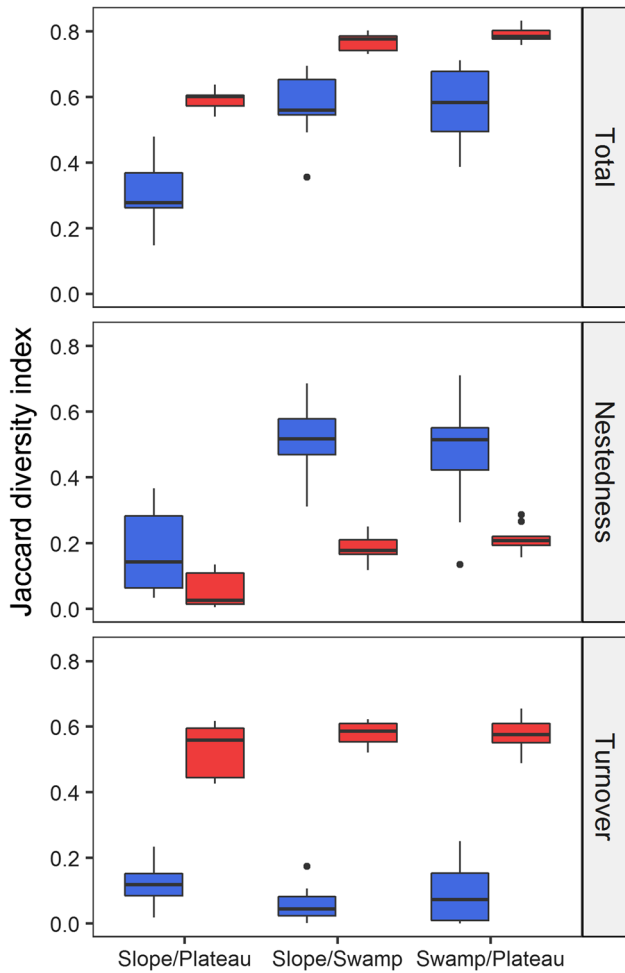


Fig. 4 Taxonomic (red boxplots) and functional (blue boxplots) Jaccard dissimilarity indices between assemblages of each habitat. For both dimensions of diversity, the value of total beta diversity corresponds to the sum of its nestedness and turnover components (top-down) (color figure online)

in tropical forests and how a complex mosaic of habitats could facilitate the maintenance of high levels of diversity.

Variation in ant diversity across contrasted habitats

Habitats contrasting in their topography or levels of perturbation are likely to differ in terms of potential niches for ant species from the regional species pool. Such dissimilarities among habitats should be reflected by either turnover or nestedness in species and/or trait composition, i.e. either habitats are composed of different sets of species or the less species-rich habitats represent subsets of the richest ones, respectively. Our results showed that ant communities found in the contrasted habitats differed in their species and functional composition. A high species turnover was observed among all habitats, joined by high levels of functional nestedness between swamp forests vs. slope and plateau forests. Given that swamp assemblages contained a lower number of species compared to slope and plateau assemblages, these results suggest that swamp forests are suitable for a limited set of species that have a range of functional traits which are not confined to this habitat; rather the traits of these species are ubiquitous for the three forest habitats. The differences in species and functional community composition in swamp forests compared to the two other habitats may be explained by disturbance caused by water-table fluctuation (Ellis et al. 2001; Baccaro et al. 2013; Soares et al. 2013). These differences may also be driven by distinct habitat characteristics such as vegetation structure (Chen et al. 2015), soil texture and fertility (Baraloto et al. 2011), which are likely to influence leaf-litter ant community composition. Such integration of environmental descriptions of habitats would benefit our understanding of ant community ecology, although this should be examined at larger spatial scales where environmental variables are likely to vary among the same habitats over space, which is unlikely at the limited spatial scale of our study.

In addition, we observed marked functional shifts in single traits of swamp assemblages when compared with slope

Table 3 Number of sampling points per assemblage ($n=20$ for each assemblage) significantly deviating from the null expectation based on multiple-trait metrics

	Plateau			Slope			Swamp			Total
	P4	P7	P10	P5	P8	P11	P6	P9	P12	
FRic	1/20	0	1/20	2/20	2/20	2/20	0	0	0	8/180
FEve	0	1/20	2/20	2/20	0	3/20	1/20	1/20	0	10/180
FDiv	0	5/20	0	0	0	3/20	2/20	1/20	0	11/180
FDis	1/20	0	1/20	2/20	0	4/20	0	0	0	8/180
FSpe	1/20	0	0	2/20	1/20	4/20	1/20	0	0	9/180
FOri	0	0	1/20	0	1/20	1/20	0	0	0	3/180

The total number of points indicate the number of points in each assemblage for which at least one metric significantly deviated from the null expectation. All the tests were one-tailed (expected $p \geq 0.95$ for FRic, FDiv, FDis, FSpe and FOri; expected $p \leq 0.05$ for FEve)

and plateau assemblages, with a higher abundance of ant species with longer body parts (relative to body size) related to sensory abilities (eyes and scapes) and liquid-feeding habits (clypeus). These morphological features are typical of generalist and omnivorous ant species that are commonly favored in habitats affected by flooding (Mertl et al. 2009; Baccaro et al. 2013). This result was further supported by the lower values of functional dispersion in swamp compared to slope and plateau assemblages, suggesting that swamps are composed of functionally more similar and generalist species. In contrast, the relatively smaller femur in the upslope habitats suggests that these assemblages are composed of a higher number of small hypogaecic species foraging and nesting inside the leaf-litter. The smaller eyes (relative to body size) of species occupying slope and plateau compared to swamp assemblages support this interpretation, given that hypogaecic ant species are characterized by reduced eye size (Brandão et al. 2012).

Moreover, ant species tended to have relatively longer mandibles in slope and plateau assemblages, supporting a role for a predatory food regime. This was supported by the clear preference displayed by the species *Strumigenys denticulata* and *Anochetus bispinosus* for plateau forest, and *Odontomachus scalptus* for slope forest. All these species have relatively long mandibles, especially *S. denticulata*, and are predatory species (Brandão et al. 2012). Taken together, the results of individual trait analyses reveal significant contrasts in the habitat use by ant species.

Structuring mechanisms of ant assemblages

We observed not only a reduction in species richness in swamp forests, but also a reduction in the morphological space occupied by species occurring in this habitat compared to the two other forest types. Because species in harsh environments are expected to be functionally similar (Swenson et al. 2012), we predicted some level of clustering of functional traits in leaf-litter ant communities from swamp forests. Furthermore, the lower dispersion of functional traits in swamp assemblages is consistent with the interpretation that species are more tightly packed in this habitat. Nevertheless, there was little evidence for a non-random pattern in multidimensional trait composition of ant assemblages based on our null models. A similar lack of evidence for the clustering of functional traits measured by multiple-trait metrics has already been reported in some plant and animal communities (e.g. Trisos et al. 2014); and this may be the result of opposing processes acting on different traits.

The use of single-trait metrics can help to disentangle the signature of contrasting assembly processes operating on functional traits (Kraft et al. 2008; Trisos et al. 2014). Indeed, we found contrasting patterns of community structure for the different traits. For instance, scape length was

clustered in our three swamp assemblages, supporting a role of trait-based habitat filtering in this morphological pattern. In contrast, clustering of mandible length was observed in slope and plateau assemblages, thus highlighting potential variations in the ecological attributes of the species in the different habitats. We may, therefore, conclude from our null model analyses that habitat filtering was operating on single traits rather than on overall trait dimensionality.

Finally, although competition is assumed to be a major factor influencing community assembly in the tropics (Wine-miller et al. 2015), we found very weak evidence for a role of this assembly process in structuring leaf-litter ant assemblages sampled in this study. An absence of functional overdispersion at a small spatial scale can be interpreted as either evidence for neutral assembly processes (Hubbell 2001) or alternatively for the cancelling-out effect of habitat filtering and competition (Helmus et al. 2007; Swenson and Enquist 2009) that precludes detection of competition. This latter explanation is unlikely here given that the analysis was performed at the sampling point scale for each assemblage separately, thus limiting variation in environmental filters acting on each community. According to contemporary coexistence theory, an absence of overdispersion at small spatial scales is not necessarily interpreted as an absence of competition acting between co-occurring species (Chesson 2000). Rather, competitive interactions among co-occurring species may lead species to converge in their traits but with an overall competitive hierarchy (Chesson 2000; Kunstler et al. 2012).

Acknowledgements Financial support for this study was provided by an *Investissement d'Avenir* grant of the *Agence Nationale de la Recherche* (CEBA: ANR-10-LABX-25-01) through a PhD fellowship to MF and the funding of the DIADEMA project (Dissecting Amazonian Diversity by Enhancing a Multiple taxonomic-groups approach), by the *Programme Convergence* 2007–2013, *Région Guyane* from the European community (BREGA, 757/2014/SGAR/DE/BSF) and by the *PO-FEDER* 2014–2020 *Région Guyane* (BING, GY0007194). JHCD acknowledges his research grant from CNPq.

Author contribution statement JO and CB designed protocol and methodology. JO and JD carried out the field sampling. MF and JD sorted specimen to morphospecies and JHCD supervised species identifications. JM performed the molecular analyses. BB and AW performed the morphological measurements. MF analysed the data and wrote the manuscript, with comments from all authors.

Compliance with ethical standards

Conflict of interest The authors declare that they have no conflict of interest.

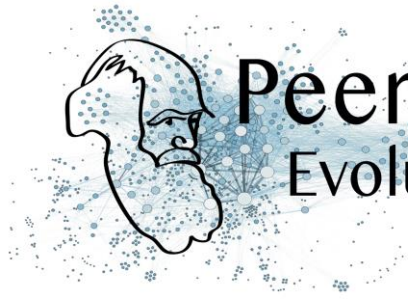
References

- Agosti D, Alonso LE (2000) The ALL protocol: a standard protocol for the collection of ground-dwelling ants. In: Agosti D, Majer J, Alonso LE, Schultz T (eds) *Ants: standard methods for measuring*

- and monitoring biodiversity. Smithsonian Institution Press, Washington, pp 204–206
- Allié E, Péliissier R, Engel J et al (2015) Pervasive local-scale tree-soil habitat association in a tropical forest community. *PLoS One* 10:e0141488. <https://doi.org/10.1371/journal.pone.0141488>
- Arnan X, Cerdá X, Retana J (2014) Ant functional responses along environmental gradients. *J Anim Ecol* 83:1398–1408. <https://doi.org/10.1111/1365-2656.12227>
- Arnan X, Arcoverde GB, Pie MR et al (2018) Increased anthropogenic disturbance and aridity reduce phylogenetic and functional diversity of ant communities in Caatinga dry forest. *Sci Total Environ* 631–632:429–438. <https://doi.org/10.1016/j.scitotenv.2018.03.037>
- Baccaro FB, Rocha IF, del Aguila BEG et al (2013) Changes in ground-dwelling ant functional diversity are correlated with water-table level in an Amazonian terra firme forest. *Biotropica* 45:755–763. <https://doi.org/10.1111/btp.12055>
- Baraloto C, Morneau F, Bonal D et al (2007) Seasonal water stress tolerance and habitat associations within four Neotropical tree genera. *Ecology* 88:478–489. [https://doi.org/10.1890/0012-9658\(2007\)88%5b478:SWSTAH%5d2.0.CO;2](https://doi.org/10.1890/0012-9658(2007)88%5b478:SWSTAH%5d2.0.CO;2)
- Baraloto C, Rabaud S, Molto Q et al (2011) Disentangling stand and environmental correlates of aboveground biomass in Amazonian forests. *Glob Change Biol* 17:2677–2688. <https://doi.org/10.1111/j.1365-2486.2011.02432.x>
- Baselga A (2010) Partitioning the turnover and nestedness components of beta diversity. *Glob Ecol Biogeogr* 19:134–143. <https://doi.org/10.1111/j.1466-8238.2009.00490.x>
- Baselga A, Orme CDL (2012) betapart: an R package for the study of beta diversity. *Methods Ecol Evol* 3:808–812. <https://doi.org/10.1111/j.2041-210X.2012.00224.x>
- Basset Y, Cizek L, Cuénoud P et al (2012) Arthropod diversity in a tropical forest. *Science* 338:1481–1484. <https://doi.org/10.1126/science.1226727>
- Basset Y, Cizek L, Cuénoud P et al (2015) Arthropod distribution in a tropical rainforest: tackling a four dimensional puzzle. *PLoS One*. <https://doi.org/10.1371/journal.pone.0144110>
- Bellwood DR, Wainwright PC, Fulton CJ, Hoey AS (2006) Functional versatility supports coral reef biodiversity. *Proc R Soc B Biol Sci* 273:101–107. <https://doi.org/10.1098/rspb.2005.3276>
- Bestelmeyer BT, Agosti D, Alonso LE et al (2000) Field techniques for the study of ground-dwelling ants: an overview, description, and evaluation. In: Agosti D, Majer J, Alonso LE, Schultz T (eds) *Ants: standard methods for measuring and monitoring biodiversity*. Smithsonian Institution Press, Washington, pp 122–144
- Bihn JH, Gebauer G, Brandl R (2010) Loss of functional diversity of ant assemblages in secondary tropical forests. *Ecology* 91:782–792. <https://doi.org/10.1890/08-1276.1>
- Blaimer BB, Brady SG, Schultz TR, Fisher BL (2015) Functional and phylogenetic approaches reveal the evolution of diversity in a hyper diverse biota. *Ecography* 38:901–912. <https://doi.org/10.1111/ecog.01370>
- Brandão CRF, Silva RR, Delabie JHC (2012) Neotropical ants (Hymenoptera) functional groups: nutritional and applied implications. In: Parra JRP (ed) *Insect bioecology and nutrition for integrated pest management*. CRC, Boca Raton, pp 213–236
- Cadotte MW, Carscadden K, Mirotchnick N (2011) Beyond species: functional diversity and the maintenance of ecological processes and services. *J Appl Ecol* 48:1079–1087. <https://doi.org/10.1111/j.1365-2664.2011.02048.x>
- Céréghino R, Pillar VD, Srivastava DS et al (2018) Constraints on the functional trait space of aquatic invertebrates in bromeliads. *Funct Ecol* 32:2435–2447. <https://doi.org/10.1111/1365-2435.13141>
- Chen X, Adams B, Bergeron C et al (2015) Ant community structure and response to disturbances on coastal dunes of Gulf of Mexico. *J Insect Conserv* 19:1–13. <https://doi.org/10.1007/s10841-014-9722-9>
- Chesson P (2000) Mechanisms of maintenance of species diversity. *Annu Rev Ecol Syst* 31:343–366. <https://doi.org/10.1146/annurev.ecolsys.31.1.343>
- Chun J-H, Lee C-B (2018) Partitioning the regional and local drivers of phylogenetic and functional diversity along temperate elevational gradients on an East Asian peninsula. *Sci Rep* 8:2853. <https://doi.org/10.1038/s41598-018-21266-4>
- Cornwell WK, Ackerly DD (2009) Community assembly and shifts in plant trait distributions across an environmental gradient in coastal California. *Ecol Monogr* 79:109–126. <https://doi.org/10.1890/07-1134.1>
- Cornwell WK, Schwilk DW, Ackerly DD (2006) A trait-based test for habitat filtering: convex hull volume. *Ecology* 87:1465–1471. [https://doi.org/10.1890/0012-9658\(2006\)87%5b1465:ATTFHF%5d2.0.CO;2](https://doi.org/10.1890/0012-9658(2006)87%5b1465:ATTFHF%5d2.0.CO;2)
- Davidson DW, Cook SC, Snelling RR (2004) Liquid-feeding performances of ants (Formicidae): ecological and evolutionary implications. *Oecologia* 139:255–266. <https://doi.org/10.1007/s00442-004-1508-4>
- Delabie JHC, Fisher BL, Majer JD, Wright IW (2000) Sampling effort and choice of method. In: Agosti D, Majer J, Alonso LE, Schultz T (eds) *Ants: standard methods for measuring and monitoring biodiversity*. Smithsonian Institution Press, Washington, pp 145–154
- Diamond JM (1975) Assembly of species communities. In: Cody ML, Diamond JM (eds) *Ecology and evolution of communities*. Harvard University Press, Cambridge, pp 342–444
- Díaz S, Kattge J, Cornelissen JHC et al (2016) The global spectrum of plant form and function. *Nature* 529:167–171. <https://doi.org/10.1038/nature16489>
- Dufrêne M, Legendre P (1997) Species assemblages and indicator species: the need for a flexible asymmetrical approach. *Ecol Monogr* 67:345–366. <https://doi.org/10.2307/2963459>
- Ellis LM, Crawford CS, Molles MC Jr (2001) Influence of annual flooding on terrestrial arthropod assemblages of a Rio Grande riparian forest. *Regul Rivers Res Manag* 17:1–20. [https://doi.org/10.1002/1099-1646\(200101/02\)17:1<1::AID-RRR603>3.0.CO;2-L](https://doi.org/10.1002/1099-1646(200101/02)17:1<1::AID-RRR603>3.0.CO;2-L)
- Ellwood MDF, Manica A, Foster WA (2009) Stochastic and deterministic processes jointly structure tropical arthropod communities. *Ecol Lett* 12:277–284. <https://doi.org/10.1111/j.1461-0248.2009.01284.x>
- Feener DH Jr, Lighton JRB, Bartholomew GA (1988) Curvilinear allometry, energetics and foraging ecology: a comparison of leaf-cutting ants and army ants. *Funct Ecol* 2:509–520. <https://doi.org/10.2307/2389394>
- Folgarait PJ (1998) Ant biodiversity and its relationship to ecosystem functioning: a review. *Biodivers Conserv* 7:1221–1244. <https://doi.org/10.1023/A:1008891901953>
- Fowler HG, Forti LC, Brandão CRF et al (1991) Ecologia nutricional de formigas. In: Panizzi AR, Parra JRP (eds) *Ecologia nutricional de insetos e suas implicações no manejo de pragas*. Editora Manole, São Paulo, pp 131–223
- Gotelli NJ, McCabe DJ (2002) Species co-occurrence: a meta-analysis of J. M. Diamond's assembly rules model. *Ecology* 83:2091–2096. <https://doi.org/10.2307/3072040>
- Gotelli NJ, Ellison AM, Dunn RR, Sanders NJ (2011) Counting ants (Hymenoptera: Formicidae): biodiversity sampling and statistical analysis for myrmecologists. *Myrmecol News* 15:13–19. <https://doi.org/10.1111/j.1461-0248.2007.01045.x>
- Gronenberg W, Tautz J, Hölldobler B (1993) Fast trap jaws and giant neurons in the ant *Odontomachus*. *Science* 262:561–563. <https://doi.org/10.1126/science.262.5133.561>
- Helmus MR, Bland TJ, Williams CK, Ives AR (2007) Phylogenetic measures of biodiversity. *Am Nat* 169:E68–E83. <https://doi.org/10.1086/511334>

- Hölldobler B, Wilson EO (1990) *The ants*. Harvard University Press, Cambridge
- Hubbell SP (2001) *The unified neutral theory of biodiversity and biogeography*. Princeton University Press, Princeton
- Hutchinson GE (1957) Concluding remarks. *Cold Spring Harb Symp Quant Biol* 22:415–427. <https://doi.org/10.1101/SQB.1957.022.01.039>
- Kaspari M, Weiser MD (1999) The size-grain hypothesis and interspecific scaling in ants. *Funct Ecol* 13:530–538. <https://doi.org/10.1046/j.1365-2435.1999.00343.x>
- Keddy PA (1992) Assembly and response rules: two goals for predictive community ecology. *J Veg Sci* 3:157–164. <https://doi.org/10.2307/3235676>
- Kocher A, Gantier J-C, Gaborit P et al (2016) Vector soup: high-throughput identification of Neotropical phlebotomine sand flies using metabarcoding. *Mol Ecol Resour* 17:172–182. <https://doi.org/10.1111/1755-0998.12556>
- Kraft NJB, Ackerly DD (2010) Functional trait and phylogenetic tests of community assembly across spatial scales in an Amazonian forest. *Ecol Monogr* 80:401–422. <https://doi.org/10.1890/09-1672.1>
- Kraft NJB, Valencia R, Ackerly DD (2008) Functional traits and niche-based tree community assembly in an Amazonian forest. *Science* 322:580–582. <https://doi.org/10.1126/science.1160662>
- Kunstler G, Lavergne S, Courbaud B et al (2012) Competitive interactions between forest trees are driven by species' trait hierarchy, not phylogenetic or functional similarity: implications for forest community assembly. *Ecol Lett* 15:831–840. <https://doi.org/10.1111/j.1461-0248.2012.01803.x>
- Laliberté E, Legendre P (2010) A distance-based framework for measuring functional diversity from multiple traits. *Ecology* 91:299–305. <https://doi.org/10.1890/08-2244.1>
- Laliberté E, Legendre P, Shipley B (2014) FD: measuring functional diversity from multiple traits, and other tools for functional ecology. R package version 1.0-12
- Lamarre GPA, Hérault B, Fine PVA et al (2016) Taxonomic and functional composition of arthropod assemblages across contrasting Amazonian forests. *J Anim Ecol* 85:227–239. <https://doi.org/10.1111/1365-2656.12445>
- Lavorel S, Grigulis K, McIntyre S et al (2008) Assessing functional diversity in the field—methodology matters! *Funct Ecol* 22:134–147. <https://doi.org/10.1111/j.1365-2435.2007.01339.x>
- Lessard J-P, Sackett TE, Reynolds WN et al (2011) Determinants of the detrital arthropod community structure: the effects of temperature and resources along an environmental gradient. *Oikos* 320:333–343. <https://doi.org/10.1111/j.1600-0706.2010.18772.x>
- Liu C, Guénard B, Blanchard B et al (2016) Reorganization of taxonomic, functional, and phylogenetic ant biodiversity after conversion to rubber plantation. *Ecol Monogr* 86:215–227. <https://doi.org/10.1890/15-1464.1>
- MacArthur R, Levins R (1967) The limiting similarity, convergence, and divergence of coexisting species. *Am Nat* 101:377–385. <https://doi.org/10.1086/282505>
- Maire V, Gross N, Börger L et al (2012) Habitat filtering and niche differentiation jointly explain species relative abundance within grassland communities along fertility and disturbance gradients. *New Phytol* 196:497–509. <https://doi.org/10.1111/j.1469-8137.2012.04287.x>
- Martello F, de Bello F, Santana M et al (2018) Homogenization and impoverishment of taxonomic and functional diversity of ants in *Eucalyptus* plantations. *Sci Rep* 8:3266. <https://doi.org/10.1038/s41598-018-20823-1>
- McGill BJ, Enquist BJ, Weiher E, Westoby M (2006) Rebuilding community ecology from functional traits. *Trends Ecol Evol* 21:178–185. <https://doi.org/10.1016/j.tree.2006.02.002>
- Mertl AL, Ryder Wilkie KT, Traniello JFA (2009) Impact of flooding on the species richness, density and composition of Amazonian litter-nesting ants. *Biotropica* 41:633–641. <https://doi.org/10.1111/j.1744-7429.2009.00520.x>
- Mouillot D, Culiolo JM, Pelletier D, Tomasini JA (2008) Do we protect biological originality in protected areas? A new index and an application to the Bonifacio Strait Natural Reserve. *Biol Conserv* 141:1569–1580. <https://doi.org/10.1016/j.biocn.2008.04.002>
- Mouillot D, Graham NAJ, Villéger S et al (2013) A functional approach reveals community responses to disturbances. *Trends Ecol Evol* 28:167–177. <https://doi.org/10.1016/j.tree.2012.10.004>
- Novotny V, Basset Y (2005) Host specificity of insect herbivores in tropical forests. *Proc R Soc B Biol Sci* 272:1083–1090. <https://doi.org/10.1098/rspb.2004.3023>
- Oksanen J, Blanchet FG, Friendly M, et al (2017) *vegan: community ecology package*. R package version 2.4-6
- Pielou EC (1975) *Ecological diversity*. Wiley, New York
- R Core Team (2018) *R: a language and environment for statistical computing*. R Foundation for Statistical Computing, Vienna, Austria
- Roberts DW (2016) *labdsv: ordination and multivariate analysis for ecology*. R package version 1.8-0
- Silva RR, Brandão CRF (2010) Morphological patterns and community organization in leaf-litter ant assemblages. *Ecol Monogr* 80:107–124. <https://doi.org/10.1890/08-1298.1>
- Silva RR, Brandão CRF (2014) Ecosystem-wide morphological structure of leaf-litter ant communities along a tropical latitudinal gradient. *PLoS One* 9:e93049. <https://doi.org/10.1371/journal.pone.0093049>
- Silva FHO, Delabie JHC, dos Santos GB et al (2013) Mini-Winkler extractor and pitfall trap as complementary methods to sample Formicidae. *Neotrop Entomol* 42:351–358. <https://doi.org/10.1007/s13744-013-0131-7>
- Silva RR, Del Toro I, Brandão CRF, Ellison AM (2016) Morphological structure of ant assemblages in tropical and temperate forests. *bioRxiv*. <https://doi.org/10.1101/065417>
- Soares SDA, Suarez YR, Fernandes WD et al (2013) Temporal variation in the composition of ant assemblages (Hymenoptera, Formicidae) on trees in the Pantanal floodplain, Mato Grosso do Sul, Brazil. *Rev Bras Entomol* 57:84–90. <https://doi.org/10.1590/S0085-56262013000100013>
- Swenson NG, Enquist BJ (2009) Opposing assembly mechanisms in a Neotropical dry forest: implications for phylogenetic and functional community ecology. *Ecology* 90:2161–2170. <https://doi.org/10.1890/08-1025.1>
- Swenson NG, Enquist BJ, Thompson J, Zimmerman JK (2007) The influence of spatial and size scale on phylogenetic relatedness in tropical forest communities. *Ecology* 88:1770–1780. <https://doi.org/10.1890/06-1499.1>
- Swenson NG, Enquist BJ, Pither J et al (2012) The biogeography and filtering of woody plant functional diversity in North and South America. *Glob Ecol Biogeogr* 21:798–808. <https://doi.org/10.1111/j.1466-8238.2011.00727.x>
- Trisos CH, Petchey OL, Tobias JA (2014) Unraveling the interplay of community assembly processes acting on multiple niche axes across spatial scales. *Am Nat* 184:593–608. <https://doi.org/10.1086/678233>
- Villéger S, Mason NWH, Mouillot D (2008) New multidimensional functional diversity indices for a multifaceted framework in functional ecology. *Ecology* 89:2290–2301. <https://doi.org/10.1890/07-1206.1>
- Villéger S, Grenouillet G, Brosse S (2013) Decomposing functional β -diversity reveals that low functional β -diversity is driven by low functional turnover in European fish assemblages. *Glob Ecol Biogeogr* 22:671–681. <https://doi.org/10.1111/geb.12021>
- Weber NA (1938) *The biology of the fungus-growing ants*. Part 4. Additional new forms. Part 5. The Attini of Bolivia. *Rev Entomol* 7:154–206

- Weihner E, Keddy PA (1995) Assembly rules, null models, and trait dispersion: new questions from old patterns. *Oikos* 74:159–164. <https://doi.org/10.2307/3545686>
- Weihner E, Keddy P (2001) *Ecological assembly rules: perspectives, advances, retreats*. Cambridge University Press, Cambridge
- Weiser MD, Kaspari M (2006) Ecological morphospace of New World ants. *Ecol Entomol* 31:131–142. <https://doi.org/10.1111/j.0307-6946.2006.00759.x>
- Wiescher PT, Pearce-Duvert JMC, Feener DH (2012) Assembling an ant community: species functional traits reflect environmental filtering. *Oecologia* 169:1063–1074. <https://doi.org/10.1007/s00442-012-2262-7>
- Winemiller KO, Fitzgerald DB, Bower LM, Pianka ER (2015) Functional traits, convergent evolution, and periodic tables of niches. *Ecol Lett* 18:737–751. <https://doi.org/10.1111/ele.12462>
- Yates ML, Andrew NR, Binns M, Gibb H (2014) Morphological traits: predictable responses to macrohabitats across a 300 km scale. *PeerJ* 2:e271. <https://doi.org/10.7717/peerj.271>



Peer Community In Evolutionary Biology

RESEARCH ARTICLE

 Open Access

 Open Data

 Open Code

 Open Peer-Review

Cite as: Foucaud J, Hufbauer RA, Ravigne V, Olazcuaga L, Loiseau A, Ausset A, Wang S, Zang LS, Leménager N, Tayeh A, Weyna A, Gneux P, Bonnet E, Dreuilhe V, Poutout B, Estoup A, and Facon B. How do invasion syndromes evolve? An experimental evolution approach using the ladybird *Harmonia axyridis*. bioRxiv 849968, ver. 3 peer-reviewed and recommended by PCI Evolutionary Biology (2020).

Posted: 21st April 2020

Recommender:

Inês Fragata and Ben Philipps

Reviewers:

Two anonymous reviewers

Correspondence:

benoit.facon@inrae.fr
julien.foucaud@inrae.fr

How do invasion syndromes evolve? An experimental evolution approach using the ladybird *Harmonia axyridis*

Julien Foucaud^{1,*}, Ruth A. Hufbauer^{1,2}, Virginie Ravigné³, Laure Olazcuaga¹, Anne Loiseau¹, Aurélien Ausset¹, Su Wang⁴, Lian-Sheng Zang⁵, Nicolas Leménager¹, Ashraf Tayeh¹, Arthur Weyna¹, Pauline Gneux¹, Elise Bonnet¹, Vincent Dreuilhe¹, Bastien Poutout¹, Arnaud Estoup¹, Benoît Facon^{6,*}

¹ UMR CBGP (INRA-IRD-CIRAD, Montpellier SupAgro), Campus International de Baillarguet, CS 30 016, 34988 Montferrier / Lez cedex, France

² Colorado State Univ, Dept Bioagr Sci & Pest Management, Graduate Degree Program in Ecology, Ft Collins, CO 80523 USA

³ CIRAD, UMR PVBMT, F-97410 Saint-Pierre, Réunion, France

⁴ Beijing Academy of Agriculture and Forestry Sciences, China

⁵ Institute of Biological Control, Jilin Agricultural University, Changchun, China

⁶ INRA, UMR PVBMT, F-97410 Saint-Pierre, Réunion, France

This article has been peer-reviewed and recommended by
Peer Community in Evolutionary Biology



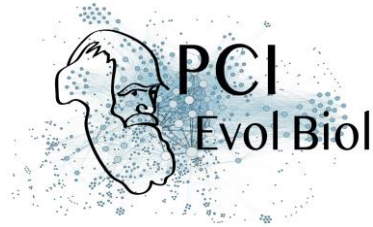
Peer Community In Evolutionary Biology

ABSTRACT

Experiments comparing native to introduced populations or distinct introduced populations to each other show that phenotypic evolution is common and often involves a suite of interacting phenotypic traits. We define such sets of traits that evolve in concert and contribute to the success of invasive populations as an ‘invasion syndrome’. The invasive Harlequin ladybird *Harmonia axyridis* displays such an invasion syndrome with, for instance, females from invasive populations being larger and heavier than individuals from native populations, allocating more resources to reproduction, and spreading reproduction over a longer lifespan. Invasion syndromes could emerge due to selection acting jointly and directly on a multitude of traits, or due to selection on one or a few key traits that drive correlated indirect responses in other traits. Here, we investigated the degree to which the *H. axyridis* invasion syndrome would emerge in response to artificial selection on either female body mass or on age at first reproduction, two traits involved in their invasion syndrome. To further explore the interaction between environmental context and evolutionary change in molding the phenotypic response, we phenotyped the individuals from the selection experiments in two environments, one with abundant food resources and one with limited resources. The two artificial selection experiments show that the number of traits showing a correlated response depends upon the trait undergoing direct selection. Artificial selection on female body mass resulted in few correlated responses and hence poorly reproduced the invasion syndrome. In contrast, artificial selection on age at first reproduction resulted in more widespread phenotypic changes, which nevertheless corresponded only partly to the invasion syndrome. The artificial selection experiments also revealed a large impact of diet on the traits, with effects dependent on the trait considered and the selection regime. Overall, our results indicate that direct selection on multiple traits was likely necessary in the evolution of the *H. axyridis* invasion syndrome. Furthermore, they show the strength of using artificial selection to identify the traits that are correlated in different selective contexts, which represents a crucial first step in understanding the evolution of complex phenotypic patterns, including invasion syndromes.

Introduction

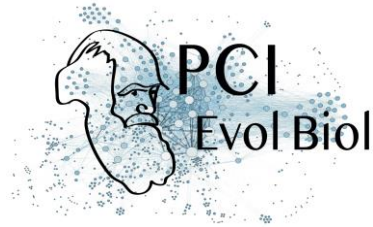
The field of biological invasions has its own quest for the Holy Grail: establishing a list of traits that can predict invasion success. Traits linked to invasion success and ecological or economic impact are already used in risk assessment to identify potentially harmful species, and then focus efforts to prevent introduction of those species (Kumschick & Richardson 2013). In plants, such risk assessment is commonly



based on the evaluation of five characteristics related to reproduction and habitat use (seed mass, chromosome number, native range size, wetland association and maximum height; Schmidt et al. 2012). Unfortunately, these trait-based approaches have met limited success, belying the existence of universal traits that predict invasiveness (Catford et al. 2009, Perkins et al. 2011). Clearly, further refining our understanding of the kinds of traits, and suites of traits, that predict invasion success will move us closer to being able to predict, and prevent, biological invasions. A first step in this process is acknowledging that traits do not exist in isolation from each other; organisms are physiologically integrated units (Ketterson et al. 2009), and organismal traits are constrained by physiological and genetic trade-offs.

Research focused on identifying traits that can predict biological invasions has been happening concurrently with a quickly growing body of research that has revealed biological invasions as crucibles for rapid evolution (Reznick & Ghalambor 2001, Lee et al. 2007, Keller & Taylor 2008, Phillips et al. 2010, Estoup et al. 2016). These studies have shown not only that evolutionary changes can be extremely fast, but that rapid evolution increases the success of invasive species (see for instance Blair & Wolfe 2004, Phillips et al. 2006, Colautti & Lau 2015), and thus likely their economic and ecological impacts as well. Thus, it is now obvious that accounting for evolutionary change is critical for developing robust predictive models of biological invasions as well as sound long-term approaches both for preventing future invasions and for managing existing ones (Estoup et al. 2016, Reznick et al. 2019).

These two bodies of work overlap with experiments that compare native to introduced populations or distinct introduced populations to each other, and show that phenotypic evolution is common (Bossdorf et al. 2005, Dlugosch & Parker 2008, Phillips et al. 2010, Colautti & Lau 2015, Chuang & Peterson 2016) and often involves changes in a suite of interacting phenotypic traits (such as growth, reproduction, dispersal and defense against enemies) rather than in a single trait, (Blair & Wolfe 2004, Phillips et al. 2006, Colautti et al. 2010). These suites of phenotypic changes could be crucial in the evolution of invasive populations, because interacting traits may form opportunities for or constraints to phenotypic change that are different from the evolution of a single trait. Here, we define the set of traits that evolve in concert and contribute to the success of invasive populations as an 'invasion syndrome'. Understanding how such invasion syndromes evolve within invasive populations is critical to assess the extent to which invasions might be repeatable or predictable, as well as the degree to which such suites of traits can be used in risk assessment and prevention of new invasions.

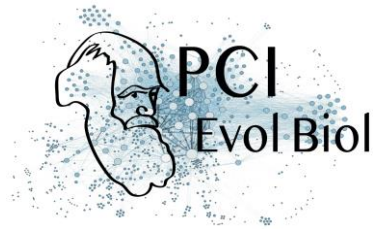


A powerful biological model for studying rapid evolution associated with invasions is provided by the invasive Harlequin ladybird *Harmonia axyridis* (Roy et al. 2016). Native to Asia, *H. axyridis* was intentionally introduced into many countries as a biological control agent of pest insects and is now considered invasive nearly worldwide (Lombaert et al. 2014). Population size in the invasive range can fluctuate dramatically (Brown et al. 2007), likely leading to strong differences in resource availability, and providing an ecologically relevant environmental axis for experimentally evaluating the evolution of traits involved in the invasion. Additionally, invasive *H. axyridis* exhibits a clear invasive syndrome, involving several evolutionary shifts (reviewed in Tayeh et al. 2012 and Roy et al. 2016). *Harmonia axyridis* females from invasive populations reproduce earlier, allocate more resources to reproduction, and spread reproduction over a longer lifespan. They are larger and heavier than individuals from native populations (Tayeh et al. 2015, and see Table 1).

Table 1: Phenotypic changes observed in invasive populations of *H. axyridis* that contribute to the invasion syndrome and the corresponding changes displayed by the experimental lines of the selection experiments achieved in the present study on female body mass (heavy lines) and age at first reproduction (fast lines) using an *ad libitum* nutritional environment for the phenotyping step. See Facon et al. 2011, Tayeh et al. 2012 and Tayeh et al. 2015 for additional details about phenotypic characteristics of invasive *H. axyridis* populations.

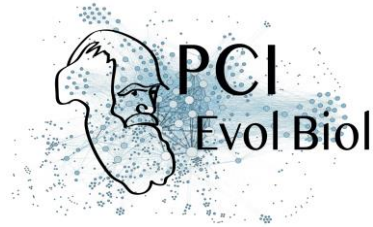
Trait	Natural invasive	Experimental selection	
	Populations	Heavy lines	Fast lines
Hatching rate	No change	No change	No change
Larval development	Faster	No change	Faster
Larval survival	No change	No change	No change
Female body mass	Heavier	Heavier	Heavier
Age at first reproduction	Earlier	No change	Earlier
Fecundity	Higher	No change	Lower
Survival	Longer	No change	Shorter

Additionally, invasive males mate more often and outperform native males in sperm competition (Laugier et al. 2013). Larvae show a higher propensity for cannibalism in invasive populations than in native ones (Tayeh et al. 2014). Finally, invasive populations experience almost none of the inbreeding depression for lifetime



performance and generation time suffered by native populations, likely because deleterious alleles were purged during the introduction and invasion process (Facon et al. 2011). Importantly, this suite of evolutionary shifts in morphological, behavioural and life-history traits has been consistently found in different invasive populations originating from distinct source populations, strongly suggesting that their evolution has played a role in the invasion process itself. These evolutionary changes constitute the invasion syndrome of *H. axyridis*. Three potential explanations for this invasion syndrome (see Tayeh et al. 2015 for details) are as follows. First, invasive individuals by chance might have a higher rate of resource acquisition than the native ones (Reznick et al. 2000), providing them with the resources needed to support the shifts in traits that have been observed. Second, possible trade-offs with other (unmeasured) traits could be large in the native area but smaller in the invasive area allowing invasive populations to reallocate resources to growth and reproduction. Third, deleterious mutations could have been purged from invasive *H. axyridis* populations during the course of the invasion. This could enable invasive individuals to exhibit higher fitness than native ones (Facon et al. 2011).

While the existence of an invasion syndrome, such as the one described above for *H. axyridis*, can be well-established, identifying the evolutionary forces that produced it is challenging. The evolution of a given invasion syndrome could be due to a simple selective process acting on a single trait that drives the evolution of other genetically-correlated traits (i.e. correlated responses to selection; e.g. Irwin & Carter 2014). In this case, the syndrome may stem from historical selection (i.e. past selective pressures that have favored integrated combinations of particular traits) or from pleiotropic effects (one or few genes that influence multiple phenotypic traits). If the syndrome relies on historical selection, the genetic correlations could be more easily broken and subsequent evolutionary changes would be relatively unconstrained (Roff 1997) compared to the case where the syndrome relies on pleiotropic effects (Schluter 1996). The evolution of an invasion syndrome could also be linked to complex selection pressures acting jointly and directly on multiple traits (Anderson et al. 2010). Indeed, selection on multiple traits could happen either during the introduction process or during the range expansion within the new range. First, the introduction events act as selective filters that can pick up individuals displaying particular suites of behaviors such as having higher foraging activity or being bolder and more aggressive (Blackburn & Duncan 2001, Chapple et al. 2012). Then, selective pressures experienced during expansion across the invaded region can drive the evolution of distinctive phenotypic traits. An excellent example of this occurs when individuals on an invasion front are assorted by dispersal ability and also experience a lower-density environment than individuals behind the front. This spatial dynamic leads to the evolution of increased

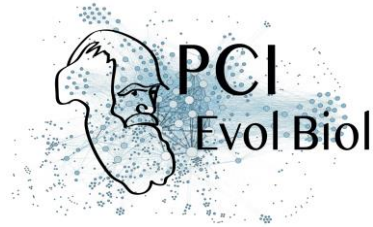


dispersal and reproductive rates, and can select for decreases in resources allocated to defense against specialized enemies (Phillips et al. 2010, Chuang & Peterson 2016).

Which of these processes underlies the evolution of invasion syndromes is difficult to infer from natural populations. This limits our ability to pinpoint the evolutionary forces and the genetic bases of the traits involved in the invasion syndromes (Keller & Taylor 2008). Approaches based on experimental evolution and selection provide a means of overcoming limitations inherent to studying wild populations as the evolutionary processes imposed are evident, and the underlying genetic basis of traits can be known (Kawecki et al. 2012, Bataillon et al. 2013). An outstanding example of the use of selection experiments to understand invasions is the study of the transition from saline to freshwater by the marine copepod *Eurytemora affinis* (Lee et al. 2011, Lee 2016). In replicate laboratory selection experiments, Lee et al. (2011) found that adaptation to freshwater was repeatedly accompanied by evolution of ion-motive enzyme activity and development rate (Lee et al. 2007, Lee 2016). Habitat transition in both natural and laboratory settings in this copepod predictively led to the evolution of a suite of interacting phenotypic traits contributing to invasion success (i.e. an ‘invasion syndrome’).

Importantly, invaders are likely to experience a variety of environments during invasions (including benign and stressful ones), but whether and how environment quality influences the expression of invasion syndromes remains an open question. More specifically, invasive species often initially experience abundant resources (Davis & Pelsor 2001, Tyler et al. 2007, Blumenthal et al. 2009) and escape from predation (Garvey et al. 1994, Roy et al. 2011). As population densities increase, intense intraspecific competition may lead to resource stress (Gioria & Osborne 2014). Resource availability may also change from generation to generation, particularly as densities become high in the introduced range, and thus diet may change with the shifting resource base (Tillberg et al. 2007). It has been shown that diet variation can have huge impacts on trait variances and covariances. For instance, diet reduction may generate trade-offs by prioritizing some physiological functions over others (Royauté et al. 2019).

The main aim of the present study is to understand the evolution of invasion syndromes, and how consistently they are expressed following different selection regimes and in different environmental contexts. More specifically, our goal was to better understand the invasion syndrome of *H. axyridis*. To achieve this goal, we performed two distinct artificial selection experiments, each focused on a phenotypic trait involved in the *H. axyridis* invasion syndrome and we examined the potential joint evolution on other life-history traits. The two focal traits, body mass and age at first

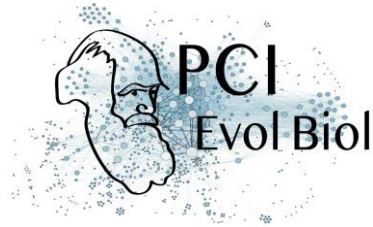


reproduction of females, show marked differences between native and invasive populations of *H. axyridis* (see Supplementary Figure 1). Both selection experiments started from individuals sampled in the native range of the species (China). After multiple generations of experimental selection, we measured the selected traits as well as other life-history traits, several of which are also part of the *H. axyridis* invasion syndrome (hatching rate, survival and fecundity). To explore the interaction between the environmental context and the evolutionary changes in molding the phenotypic response, we measured these traits in two environments: one with abundant food resources and one with limited resources (hereafter referred to as *ad libitum* and stress, respectively). Our study addressed the following specific questions: 1) Do body size and age at first reproduction respond to selection? 2) How does selection on these individual traits affect other traits in the invasion syndrome, specifically what are the directions and magnitudes of correlated responses to selection? 3) How are the relationships between phenotypic traits affected by selection on a single trait? And 4) to what extent does the environmental context, here food availability, modify the expression of the phenotypic syndrome that evolved through artificial selection?

Methods

Sampling and laboratory rearing conditions

Adult *H. axyridis* individuals were sampled in the native area of the Jilin province, China (43°58' N, 125°45' E) in October 2013 and 2015. This population was previously sampled and found to be a source of the first invasive population of *H. axyridis* established in Western North America (N-China3 population from Lombaert et al, 2011). The 2013 sampling was used for artificial selection on female body mass and the 2015 sampling was used for selection on age at first reproduction of females (the first time when females laid eggs). In 2013, collected individuals were first maintained in diapause at 4°C during the whole winter, before gradually breaking diapause in April 2014. Approximately 1,500 individuals were collected, of which approximately 900 survived the winter and were allowed to mate and lay eggs, constituting what we hereafter call base population 1. The individuals collected in October 2015 were not maintained in diapause for a long period, as they were immediately put in conditions to gradually break diapause in November 2015. Approximately 1,500 individuals were collected, of which approximately 1,000 survived, constituting what we hereafter call base population 2. As both populations experienced diapause and showed similar rates of mortality during their diapause, we assumed that different durations of diapause did not induce large differences between the 2013 and 2015 populations. All *H. axyridis* rearing took place at 25°C on 14L:10D light cycle. Unless otherwise stated, *H. axyridis* were fed *ad libitum* with *Ephestia kuhnellia* eggs.



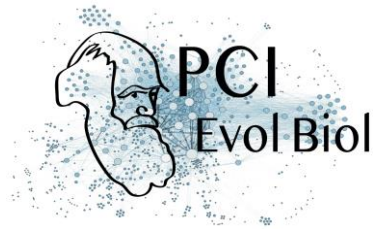
Heritability estimates of female body mass and age at first reproduction

A full-sib design was used to estimate simultaneously the broad-sense heritabilities of female body mass and age at first reproduction using base population 1. Forty third-generation couples were formed randomly and their eggs were allowed to develop. Of the 30 couples that had offspring, 24 produced 10 or more female offspring that survived to adulthood. These females were used to estimate heritability (total = 485 female offspring from 24 families). The remaining six families were not included because they had too few offspring, which would unnecessarily inflate the variance of our heritability estimations. Every adult female offspring was weighed two days after emergence. Each female was then paired with a male of the same age randomly chosen from base population 1. *Harmonia axyridis* is a multi-copulating species (i.e. males and females can mate multiple times with the same or different individuals during their lives; Laugier et al. 2013). Each female was presented a new male from base population 1 every day for 21 days, in order to limit the effect on reproduction that might be observed if only a single particularly poor or high quality male was used. Age at first reproduction of females was recorded as the number of days between hatching of the female as an adult and the day she first laid a clutch of eggs.

For each trait, broad-sense heritability was computed using intra-class (family) correlation and standard errors were estimated taking into account unequal family sizes using eq. 2.29 from Roff (1997). Because multiple paternity is likely in our experimental set-up, offspring could be full- or half-siblings. This design may thus systematically underestimate true broad-sense heritability, making our estimates of broad-sense heritability estimate conservative. The goal of these estimates of broad-sense heritability was to ensure that the phenotypic traits possessed sufficient additive genetic variance to respond to artificial selection. In addition, we also estimated narrow-sense heritabilities of the selected traits using the mean response to selection per generation, the intensity of selection (in both selection experiments, truncation is at $p = 0.25$ so $i = 1.27$) and the phenotypic variance available at the beginning of the selection experiments (Roff 1997).

Divergent selection on female body mass

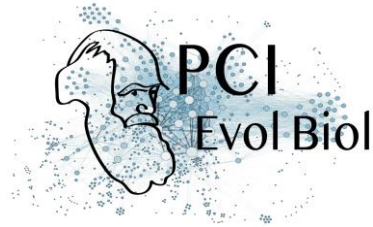
At the eighth generation of base population 1 (referred to as G0 hereafter), the selection experiment on female body mass was initiated. Selection on body mass was carried out in females only, because only female *H. axyridis* evolved larger size during the course of worldwide invasion. Two days after emergence, 700 females were weighed, and 14 experimental lines were established as follows (Supplementary Figure 2A). Four control lines were founded by randomly sampling 50 females across the entire body mass distribution for each line. Five light lines were founded by randomly



sampling 50 females from the 50% lower part of the female body mass distribution for each line. Five heavy lines were founded by randomly sampling 50 females from the 50% higher part of the body mass distribution for each line. Each of the 14 experimental lines was supplemented with 50 males randomly chosen from base population 1. Once founded, all lines were maintained independently for the rest of the experimental selection (there was no gene flow between lines; Supplementary Figure 2B). For each subsequent generation, 200 females were weighed two days after emergence for each line and 50 females were chosen to initiate the next generation. For the control lines, 50 random females were chosen, for the light lines, 50 females were chosen from the lightest quartile, and for the heavy lines, 50 females were chosen from the heaviest quartile. For each line, 10 days after emergence, 50 males were randomly chosen from the relevant line and added to the 50 females. Fourteen days after emergence, >70 clutches per line were collected to establish the next generation. While mating and egg-laying were carried out in a single arena per line containing all individuals, we are confident that most individuals of both sexes contributed to next generation because (i) number of collected clutches was generally very high (>200 clutches), (ii) repeated mating was confirmed visually to occur all four days. Collected clutches were distributed into several dozens of small boxes per line (diameter = 55mm; 2 clutches per box), to ensure a balanced contribution of all clutches to the next generation. After hatching, a minimum of 33 boxes per line, each containing 12 larvae from a single hatching box (i.e., minimum $n = 396$ individuals per line), was reared and fed by adding *E. kuhnellia* eggs *ad libitum* twice a week until emergence of adult individuals. The use of small boxes with a low density of larvae enabled us to limit cannibalism, which otherwise is common in this species (Tayeh et al. 2014) and to prevent an unbalanced contribution of clutches to the next generation. This selection scheme was continued for eight generations.

Directional selection on the age at first reproduction of females

At the second generation of base population 2, the distribution of the age at first reproduction was estimated for females using 128 couples isolated at emergence. Males were rotated between females each day to limit the effect of males on the timing of oviposition. From this distribution, we determined the numbers of days at which 25% and 75% of females had reproduced and laid their first clutch, respectively. Those numbers (25% quartile = 7 days, 75% quartile = 21 days) were used to determine the day on which eggs were to be collected to establish both selected and control experimental lines. At the third generation, ten experimental lines were established from 240 randomly chosen egg clutches as follows (Supplementary Figure 2C). Seven fast lines were founded by collecting egg clutches that were laid on days 5-7 (the 2 days before the 25% quartile of the distribution of age at first reproduction). Three control lines were founded by collecting eggs laid on days 19-21 (the two days before

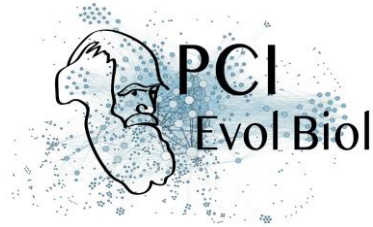


the 75% quartile). Note that these lines included eggs from the earliest reproducing females as well as eggs from later reproducing females and that all eggs laid prior to day 19 were removed every two days (and hence did not participate in the next generation). Those quartiles were chosen to: (i) ensure sufficient production of females and males to sustain the selection experiment in the fast lines, and (ii) provide a maximum number of individuals with the opportunity to participate in reproduction, while reasonably limiting generation time in the control lines. At each generation, selection proceeded as follows (Supplementary Figure 2D). Each of the egg clutches collected was maintained in a separate 5cm-diameter box and larvae were maintained at a maximal density of 12 individuals per box during their development. Upon emergence, adults of each line were moved into a single cage, and date of the peak of emergence of each experimental line was recorded. For fast lines, new egg clutches were counted and collected each day until 20 clutches were collected. For control lines, new egg clutches were counted but only collected during the 48-hrs period before the 75% quartiles of the distribution of ages (i.e., between days 19-21 after the peak of emergence), except at generation G2 for technical reasons. Each fast and control line was maintained at approximately 100 females and 100 males able to mate freely for the entire selection process. This selection scheme was continued for nine generations.

Phenotyping of experimental lines

At the end of the selection experiments, we phenotyped individuals of each experimental line using the same protocol for the following traits: hatching rate, larval survival rate, development time, female and male body mass, age at first reproduction of females, female fecundity and adult survival (Supplementary Figure 3). These traits span the life history of *H. axyridis* and five of them are involved in the *H. axyridis* invasion syndrome. Apart from hatching rate, all traits were measured on individuals reared in two environments: either with *ad libitum* food resources or with limited food resources (hereafter *ad libitum* and stressful conditions, respectively). Individuals from the female body mass experiment were phenotyped at G9 and those from the age at first reproduction experiment were phenotyped at G10.

Specifically, females from the generation just before phenotyping (G8 for body mass and G9 for age at first reproduction) were allowed to mate and lay eggs for 24h, 19 days after emergence as adults. For each line, 30 clutches were randomly chosen and their number of eggs were counted. The clutches were then placed in individual 8cm-diameter boxes. Hatching rate was recorded for each clutch three days after collection. For each line, we monitored larval development of groups of 10 larvae under an *ad libitum* food diet (1.5g of *E. kuhnellia* eggs per group, twice a week) and groups of 10 larvae under a stressful food diet (0.5g of *E. kuhnellia* eggs per group,



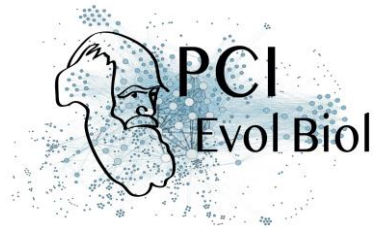
twice a week), maintained in 8cm-diameter boxes. For each of the 14 lines selected for female body mass, we monitored eight groups of 10 larvae fed *ad libitum* and 10 groups of 10 larvae under food stress (for a total of 2,520 larvae). For each of the 10 lines selected for age at first reproduction, we monitored 15 groups of 10 larvae fed *ad libitum* and 15 under food stress (for a total of 3,000 larvae). We recorded the number of surviving larvae, pupae and adults daily for the entire duration of development to adulthood. These data were used to compute development time from egg to adult and larval survival rate. Upon emergence, individuals were sexed and moved to individual boxes. All individuals that survived to adulthood (both males and females) were weighed two days after their emergence. When possible, couples were formed immediately after weighting (or the next day at the latest), by keeping one male and one female in a 5cm-diameter box together with the same diet they received as larvae (*ad libitum* diet: 0.35g of *E. kuhnellia* eggs per couple twice a week; stressful diet: 0.1g per couple twice a week). Twenty-four couples were formed per female body mass line per diet and 48 couples were formed per line selected for age at first reproduction (total of 672 and 960 monitored couples, respectively). Females were checked daily for eggs and males were rotated between females to limit the effect of individual males on female fecundity. When eggs were laid, age at first reproduction was recorded and both the female and its current male partner were placed in a large box (10 x 5 x 5cm) containing reproducing couples of the same line and diet, with a maximum of 48 individuals per box. Individuals from each line and diet were gathered in one box and two boxes for the female body mass and age at first reproduction selection experiments, respectively (total = 28 and 40 boxes, respectively). Adults that had already reproduced were fed twice a week, again following a diet that matched their larval and adult stages (*ad libitum* diet: 0.17g of *E. kuhnellia* eggs per individual twice a week; stressful diet: 0.05g per individual twice a week). Once a week, fecundity was measured by counting the number of clutches laid during the last 24h. Twice a week, adult survival was measured by counting and sexing live and dead adults. Fecundity and survival were monitored until the death of all individuals (1,344 and 1,920 individuals followed for body mass and age at first reproduction schemes, respectively).

Statistical treatments

All data and R code are available at:

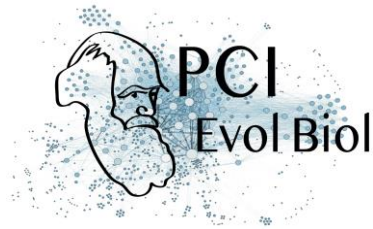
<https://data.inra.fr/dataset.xhtml?persistentId=doi:10.15454/V9XCA2>

For each variable (i.e. trait), we performed a Generalized Linear Mixed Model (GLMM) analysis with Laplace approximation (Bolker et al. 2009), using the *lme4* package (Bates et al. 2014) in the R statistical framework (R Core Team). Depending on variable distribution, we ran an LMM for Gaussian variables (i.e., female and male body mass), a binomial GLMM with a logit link for proportion variables (i.e., hatching rate,



larval survival rate) and a Poisson GLMM with a log link for Poisson distributed variables (i.e., development time, age at first reproduction, number of eggs laid and age at death of females and males). For all individual variables, we investigated the significance of the following explanatory factors: selection type (selected or control during the experimental selection assay), diet type (*ad libitum* or stressful diet during the phenotyping experiment) and line (the identity of replicate experimental lines during selection). Both selection and diet types were treated as fixed effects, while line was treated as a random effect. To account for over-dispersion in some variables, we added an observation-level random effect to the models when necessary, as recommended by Bolker et al. (2009). We followed a step-by-step procedure of model simplification from the full model (starting with random effects and then fixed effects) based on the Akaike Information Criterion (AIC), and tested the significance of the remaining effects via Likelihood Ratio Tests (LRT). Normality of residuals was checked using quantile-quantile plots. Adjusted means and confidence intervals for each significant fixed effect were calculated using a bootstrap resampling procedure (1,000 resampling of 500 observations each) with the *boot* package (Canty & Ripley 2015).

This univariate trait-by-trait analysis was complemented with a multivariate analysis. We include these analyses because no trait is truly independent from all others, and it provides an evaluation of joint responses to selection, acknowledging that the evolution of one trait may affect and be affected by the evolution of the others. Furthermore, the best way to measure the evolution of a syndrome, i.e. of multiple traits, is to account for the correlated nature of phenotypic traits (and the modification of these correlations due to selection). Specifically, we performed a Multiple Factor Analysis (MFA) using the *FactoMineR* package (Le et al. 2008). MFA is an extension of a principal component analysis (PCA) where variables can be grouped. For the analysis, we grouped traits by life-history stage. Similarly to a PCA, MFA provides an easy visualization of phenotypic similarities and differences as well as contributions of individual traits to these similarities and differences. Two independent and similar MFAs were conducted for female body mass and age at first reproduction selection schemes. For each selection scheme, each phenotyped trait was averaged over line and diet and included in a global table (except for hatching rate, because no diet was applied prior to hatching). The seven phenotyped traits were gathered into four groups: development (including larval survival rate, development time and age at first reproduction), body mass (including only female body mass), fecundity (including only the number of eggs laid) and survival (including age at death of males and females). Line, diet type, selection type and the interaction between diet type and selection type were added as supplementary qualitative variables and used to interpret the results of the MFA. Dimensions were retained for interpretation when their associated eigenvalue was greater than one. Relationships between variables and



between individuals were investigated graphically and using dimension descriptors. Additional graphical representations of trait values and correlations matrices were performed for illustrative purposes, but insufficient replication and high correlations between some trait combinations precluded thorough statistical testing of differences in correlation matrices. All figures were plotted using the *ggplot2* package (Wickham 2016).

Results

Direct responses to experimental selection

Female body mass was heritable, with a mean \pm s.e. of a broad-sense heritability, $H^2 = 0.46 \pm 0.13$, and the age at first reproduction was also heritable, with a mean broad-sense heritability $H^2 = 0.19 \pm 0.08$.

Both selection experiments led to phenotypic changes. Female body mass evolved in both directions during the course of the divergent selection experiment (Figure 1A). At generation 9, female body mass increased by 12% on average in the heavy lines and decreased by 4% in the light lines compared to the control lines (Figure 1B). Age at first reproduction evolved to be significantly earlier in response to selection ($\chi^2_2 = 15.650$, $p < 0.001$). At generation 10, age at first reproduction of the replicate lines were between three and 13 days earlier than that of control lines, representing development times that were 29% to 54% faster. These responses to selection led to estimates of narrow-sense heritabilities of $h^2 = 0.11 \pm 0.01$ for heavy lines and $h^2 = 0.04 \pm 0.01$ for light lines during selection on female body mass, and $h^2 = 0.10 \pm 0.007$ for fast lines during selection on the age at first reproduction.

Correlated responses to experimental selection

Experimental selection on female body mass did not trigger significant correlated response for most other investigated traits. Hatching rates did not differ among selection types (LRT: $\chi^2_2 = 3.510$, $p = 0.173$; Figure 2A). Similarly, larval survival rate was not influenced by selection on female body mass (LRT: $\chi^2_2 = 0.30$, $p = 0.86$; Figure 2B). Selection on female body mass altered neither development time (LRT: $\chi^2_2 = -1.858$, $p = 0.395$; Figure 2C), nor age at first reproduction (Figure 3A; LRT: $\chi^2_1 = -0.220$, $p = 0.896$). Fecundity did not shift overall with selection on female body mass (Figure 4A; LRT: $\chi^2_2 = 1.35$, $p = 0.51$), but it was influenced by an interaction between selection and diet (see below). While survival differed among sexes, with higher survival in females (LRT: $\chi^2_1 = 107.88$, $p < 0.0001$), it was not influenced by selection on female body mass

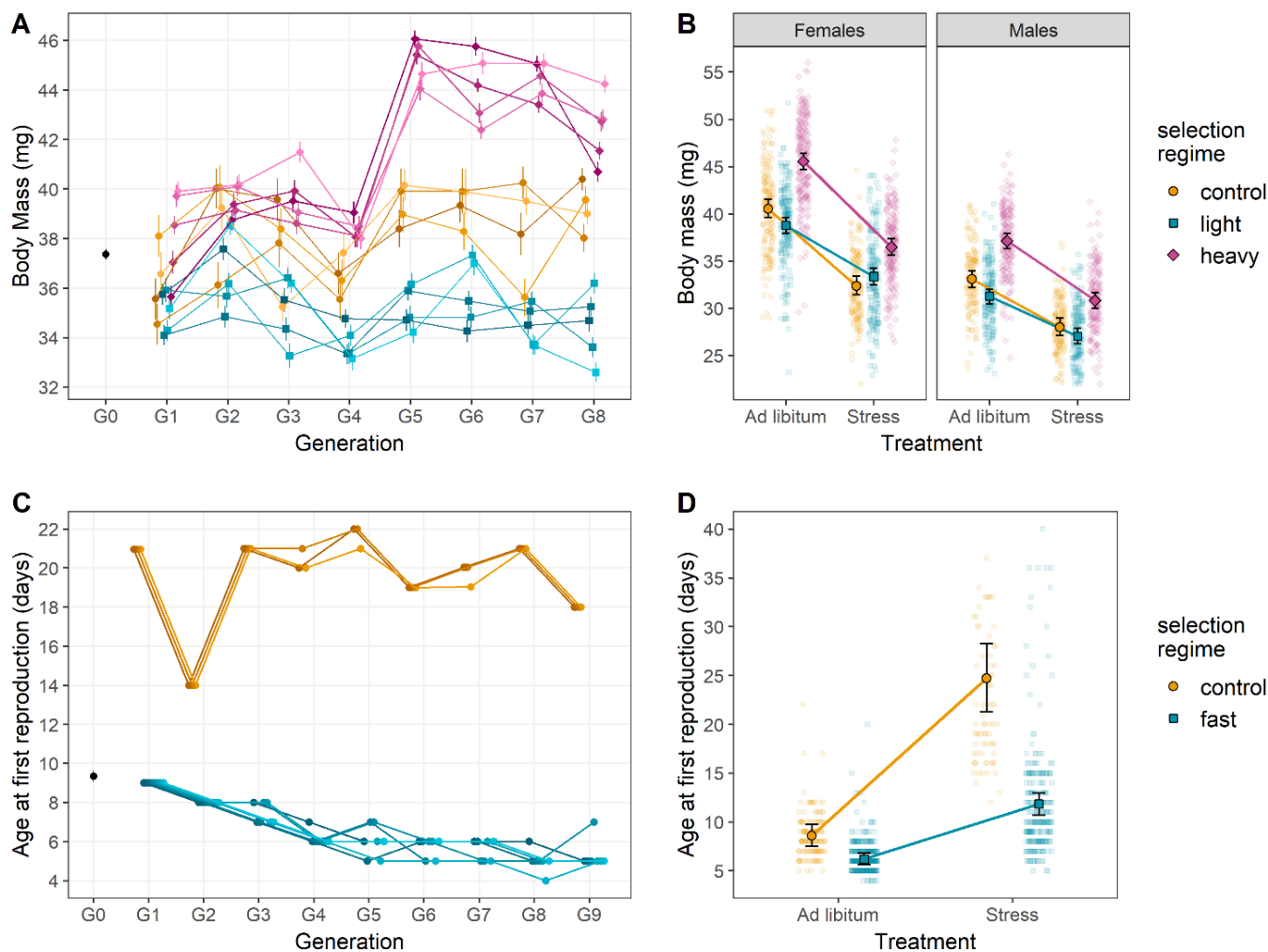
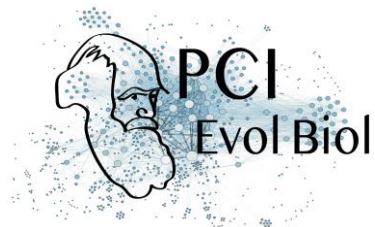


Figure 1: Responses to selection on female body mass and age at first reproduction.

(A) Evolution of female body mass for our 14 experimental lines throughout divergent selection on this trait. Heavy, control and light experimental lines are represented in purple, orange and blue, respectively. (B) Body mass of males and females of the G9 generation of female body mass selection. Body masses were measured in either *ad libitum* or stressful nutritional environments. The color code is similar to Fig. 1A. (C) Evolution of female age at first reproduction for our 10 experimental lines throughout directional selection on this trait. Control and selected (fast) lines are represented in orange and blue, respectively. (D) Age at first reproduction for females of the G10 generation of selection on the same trait. Age at first reproduction was measured in either an *ad libitum* or a stressful nutritional environment. The color code is similar to Fig. 1C. Error bars represent standard errors between replicates.

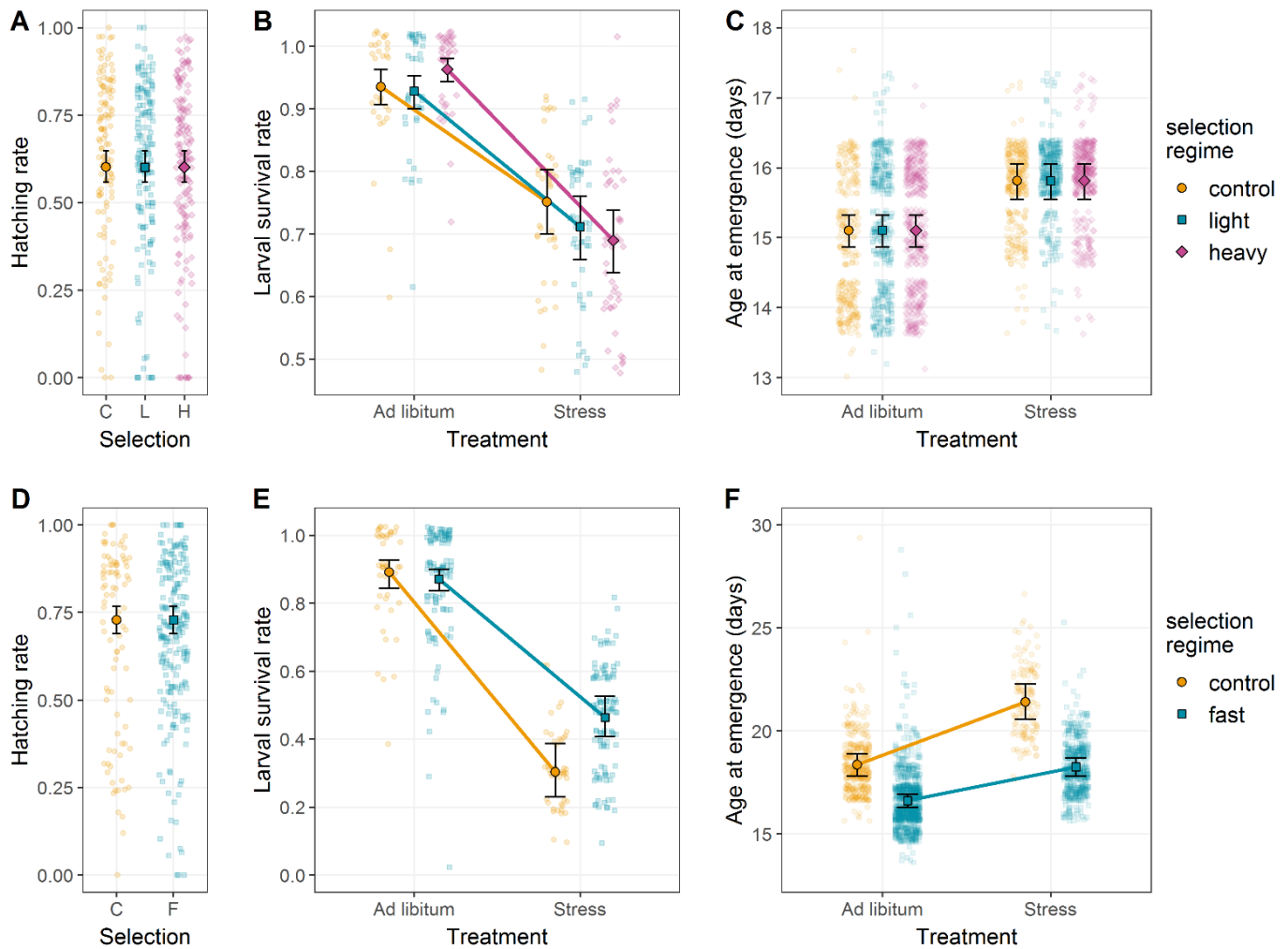
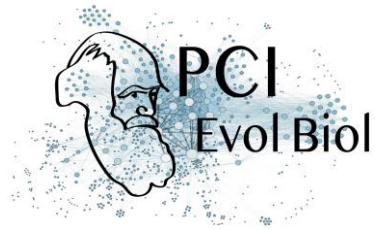


Figure 2: Juvenile phenotypic responses to selection on female body mass and age at first reproduction.

Juvenile responses to female body mass selection on (A) hatching rate, (B) larval survival rate and (C) development time. While hatching rate and developmental time were not affected by the selection regime, larval survival rate depended on the interaction between selection regime and developmental environment. In addition, developmental environment had a significant influence on development time. Juvenile responses to age at first reproduction selection on (D) hatching rate, (E) larval survival rate and (F) development time. Hatching rate was not influenced by selection regime, but both larval survival rate and development time were significantly affected by the interaction between selection regime and diet. Color code is similar to Figure 1. Error bars represent standard errors between replicates.

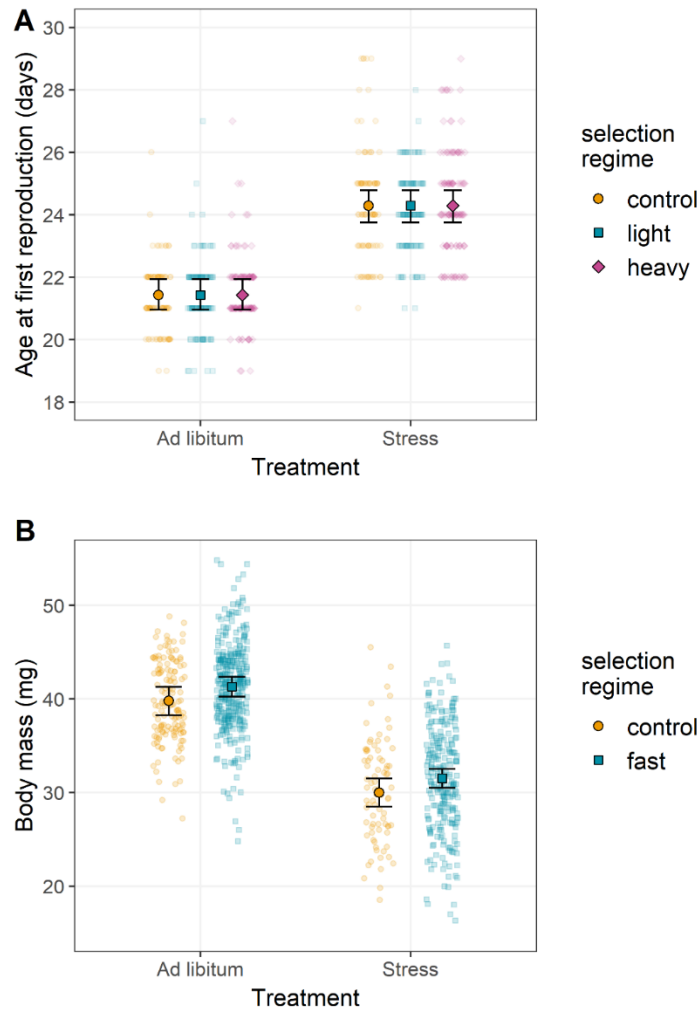
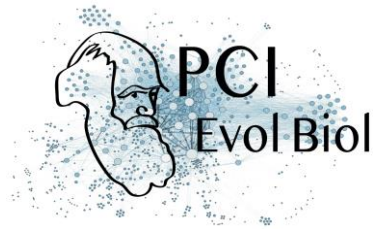


Figure 3: Reciprocal phenotypic responses to selection on female body mass and age at first reproduction.

(A) Age at first reproduction of G9 individuals from the selection on female body mass. Diet but not selection regime significantly affected age at first reproduction. (B) Female body mass of G10 individuals from the selection on age at first reproduction. Female body mass was significantly influenced by diet and marginally by selection regime. Color code is similar to Figure 1. Error bars represent standard errors between replicates.

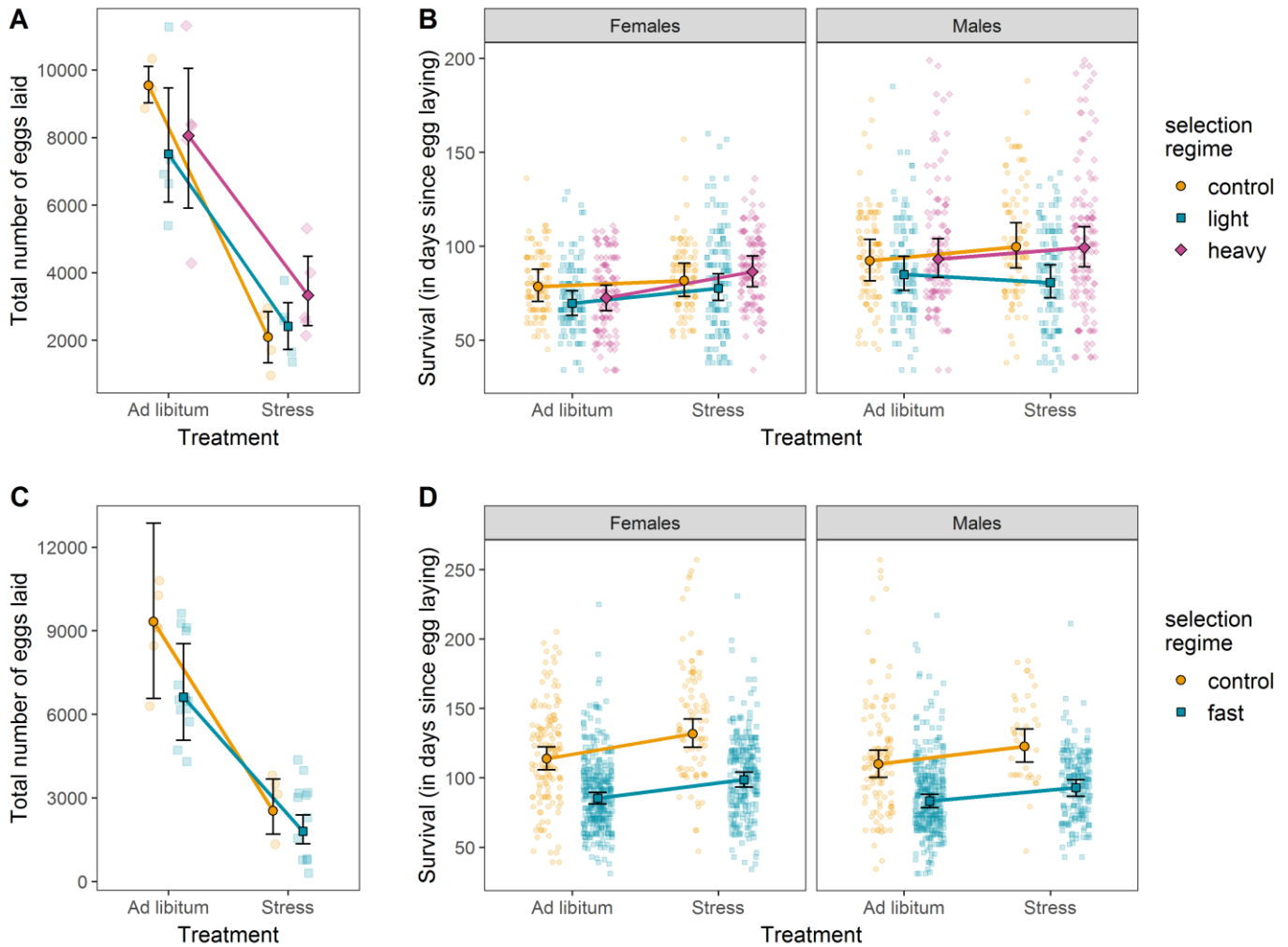
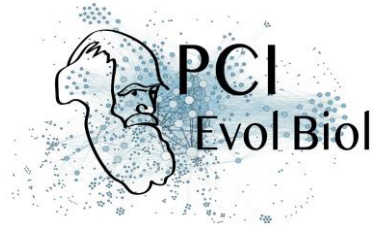
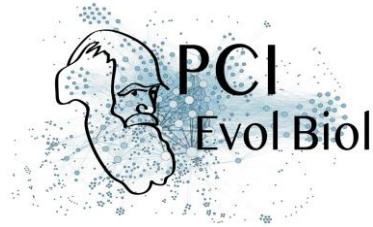


Figure 4: Adult phenotypic responses to selection on female body mass and age at first reproduction.

(A) Fecundity of G9 females from experimental lines of the female body mass selection. (B) Female and male survival of G9 individuals of the female body mass selection. (C) Fecundity of G10 females from lines of the age at first reproduction selection. (D) Female and male survival of G10 individuals of the age at first reproduction selection. Color code is similar to Figure 1. Error bars represent standard errors between replicates.



in females (Figure 4B; LRT: $\chi^2_2 = 1.87$, $p = 0.39$), or in males (LRT: $\chi^2_2 = 1.21$, $p = 0.27$). However, even though the truncation selection was only imposed on females, male mass displayed a correlated response to selection on female body mass with an average increase of 12% in the heavy lines and a decrease of 6% in light lines compared to the control lines in generation 9 (Figure 1B). Additionally, heavy lines seemed to have a higher larval survival rate than light lines (in the *ad libitum* treatment only: multiple comparison of means: $Z = 2.275$, $p = 0.047$).

In contrast, experimental selection on age at first reproduction triggered various correlated phenotypic responses, with the exception of hatching rates (LRT: $\chi^2_1 = 0.176$, $p = 0.675$; Figure 2D) and larval survival (approx. 90% survival for all lines; $Z = -0.777$, $p = 0.857$). Development time, fecundity and survival all responded to selection for fast (i.e. earlier) age at first reproduction, with adults emerging earlier (LRT: $\chi^2_1 = 19.56$, $p < 0.001$; Figure 2F), fecundity decreasing in selected females (LRT: $\chi^2_1 = 4.110$, $p = 0.043$; Figure 4C), and control lines surviving longer than lines selected to reproduce early ($Z = 7.280$, $p < 0.001$; Figure 4D). Notably, in contrast to selection on female body mass, which did not affect age at first reproduction, selection on age at first reproduction tended to increase female body mass (best AIC, but LRT only marginally significant: $\chi^2_1 = 2.933$, $p = 0.087$) when provided food *ad libitum* (Wilcoxon rank sum test with continuity correction: $p < 0.001$; Figure 3B).

Multivariate response to selection

The Multiple Factor Analyses (MFA) helped visualize the effects of selection (whether targeting female body mass or age at first reproduction) and environmental conditions on trait correlations. We here focus on the effect of selection and will treat the effect of diet in the next section. For both selection experiments, two MFA dimensions had eigenvalues greater than one, hence explaining more variance than any given phenotypic trait alone.

In the female body mass experiment, MFA dimension 1 explained a large proportion of the total variance (58.2%). Traits that contributed to the first dimension were larval survival rate, female body mass, number of eggs laid, development time and age at first reproduction (all correlation coefficients $|r| > 0.78$, all p -values < 0.001 ; Figure 5A). Dimension 1 separates lines with large females, producing many larvae with short development time and high survival rates (right hand side) from lines with smaller females producing fewer, low-quality larvae. Dimension 2 explained 22.3% of total variance and was mainly due to variance in adult survival (Figure 5A). Dimension 1 clearly separated diet groups ($r^2_{\text{diet}} = 0.927$, p -value < 0.001), a point that will be detailed in the next paragraph, with selection treatment interacting with diet group ($r^2_{\text{interaction}} = 0.965$, p -value < 0.001). Dimension 2 correlated weakly with

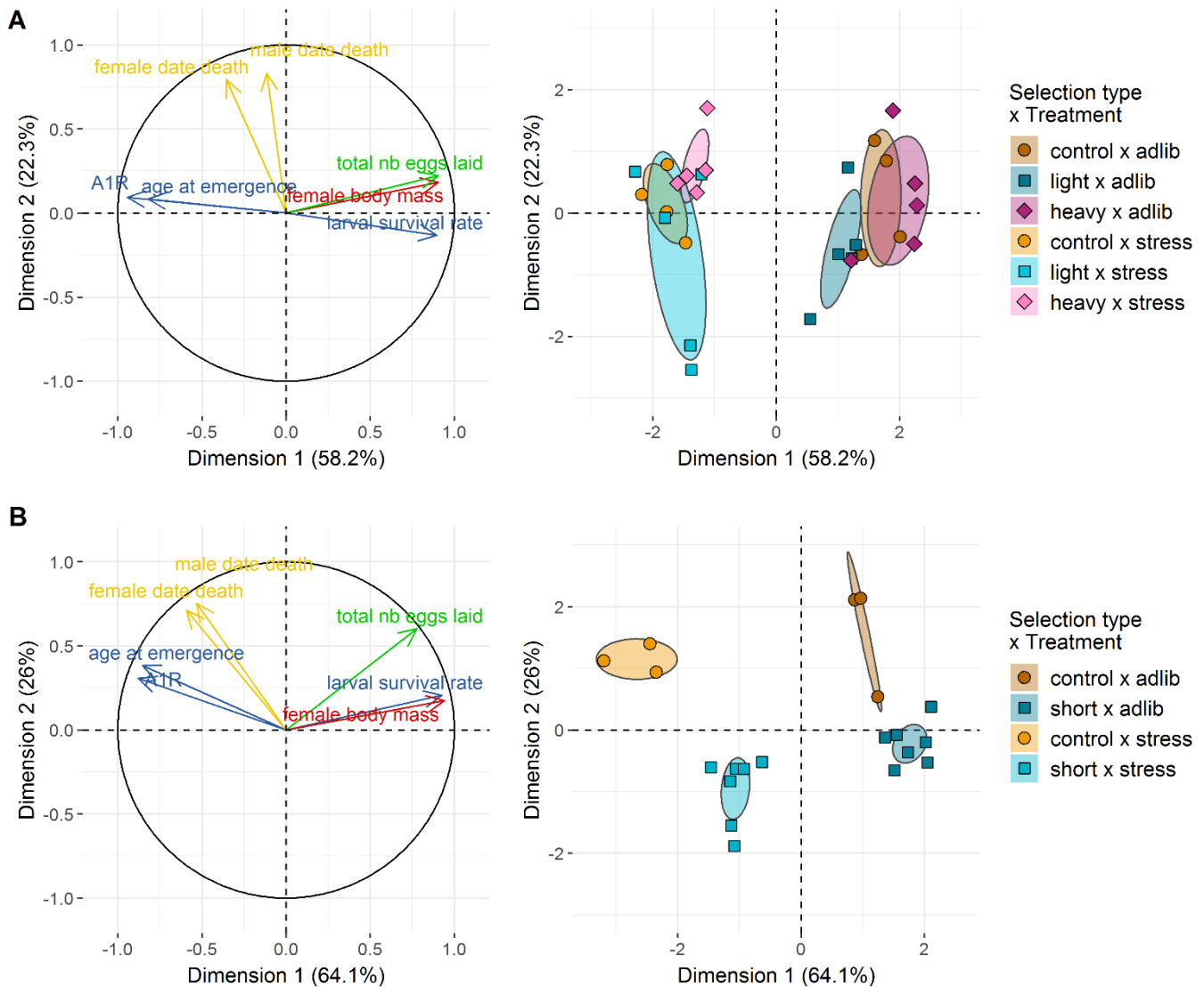
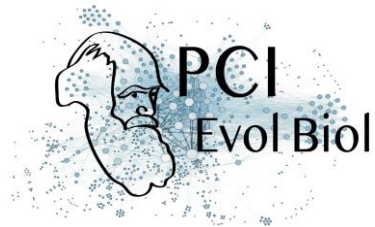
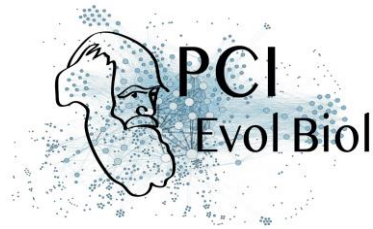


Figure 5: Organismal-level phenotypic responses to selection and diet.

(A) right: Projection of phenotypic traits into the first two dimensions of the Multiple Factor Analysis (MFA) on G9 individuals of the female body mass selection regime. A1R stands for age at first reproduction. (A) left: Projection of replicate experimental lines from selection on female body mass into the first two dimensions of the same MFA. Diet is a major factor separating global phenotypes while selection regime is a more modest one. (B) right: Projection of phenotypic traits into the first two dimensions of the MFA on G10 individuals of the age at first reproduction selection. When comparing (A) right and (B) right, it is worth noting that the relationships between phenotypic traits are mostly similar on Dimension 1 (i.e., related to diet treatment) but are more dissimilar on Dimension 2 (i.e., related to selection regime). (B) left: Projection of replicate lines from selection on age at first reproduction into the first two dimensions of the same MFA. Both the diet and selection regime are participating in the clear-cut clustering of individual lines' phenotypes, contrary to (B) where diet and the interaction between diet and selection regime are the main clustering factors.



selection treatments ($r^2_{\text{selection}} = 0.237$, $p = 0.034$) and strongly with replicate lines ($r^2_{\text{line}} = 0.830$, $p = 0.002$).

Overall this MFA showed that selection on female body mass only weakly influenced the distribution of trait values, with lines belonging to different selection treatments not completely separated in the MFA plane. The phenotypic correlation matrices (Supplementary Figure 4) corroborate this conclusion. Some selected lines had trait combinations close to those of control lines while other selected lines differed from the control lines. The lines that were the most distinct from control lines, tended to have either greater (heavy lines) or smaller (light lines) coordinates on MFA Dimension 2 compared to control lines, an indication that selection on female body mass might have altered other traits in these lines. Radar plots provide a visual confirmation that global phenotypic variation due to selection on body mass was low, except for body mass itself (Figure 6, top row), with marginal effects on adult survival in some selected lines.

In the age at first reproduction experiment, dimensions 1 and 2 explained 64.1% and 26% of the variance, respectively. The contributions of traits to both dimensions were relatively similar to the body mass selection experiment, with however looser correlations between dimension 2 and adult survival rates, and between dimension 1 and age at first emergence (Figure 5B). Here, male and female survival were also significantly negatively correlated with the MFA dimension 1 ($\rho = -0.53$, $p = 0.016$ and $\rho = -0.59$, $p = 0.006$, respectively; Figure 5B). In contrast to selection on female body mass, both dimensions clearly separated both diet and selection groups (Figure 5B). Dimension 1 strongly correlated with diet ($r^2_{\text{diet}} = 0.857$, $p\text{-value} < 0.001$) and the interaction between diet and selection ($r^2_{\text{interaction}} = 0.974$, $p\text{-value} < 0.001$), Dimension 2 correlated strongly with both selection treatment ($r^2_{\text{selection}} = 0.717$, $p < 0.001$) and line ($r^2_{\text{line}} = 0.813$, $p = 0.011$). Lines tended to group by diet and selection treatments revealing a strong effect of selection on the distribution of the other traits. Radar plots confirm that the global phenotypic variation due to selection on age at first reproduction was high (Figure 7, top row). Correlation matrices showed that selection on the age at first reproduction modified phenotypic correlations, with a noticeable relaxation of correlations between traits in the selected lines (Supplementary Figure 5, top row). These multivariate analyses show that correlations between traits has been profoundly been modified by selection on age at first reproduction, with some traits positively responding to the treatment (e.g., adult survival rates) and others not.

Environmental context and trait expression

In both selection experiments, we found that the environmental context, here expressed in the form of abundant versus reduced resources during the final

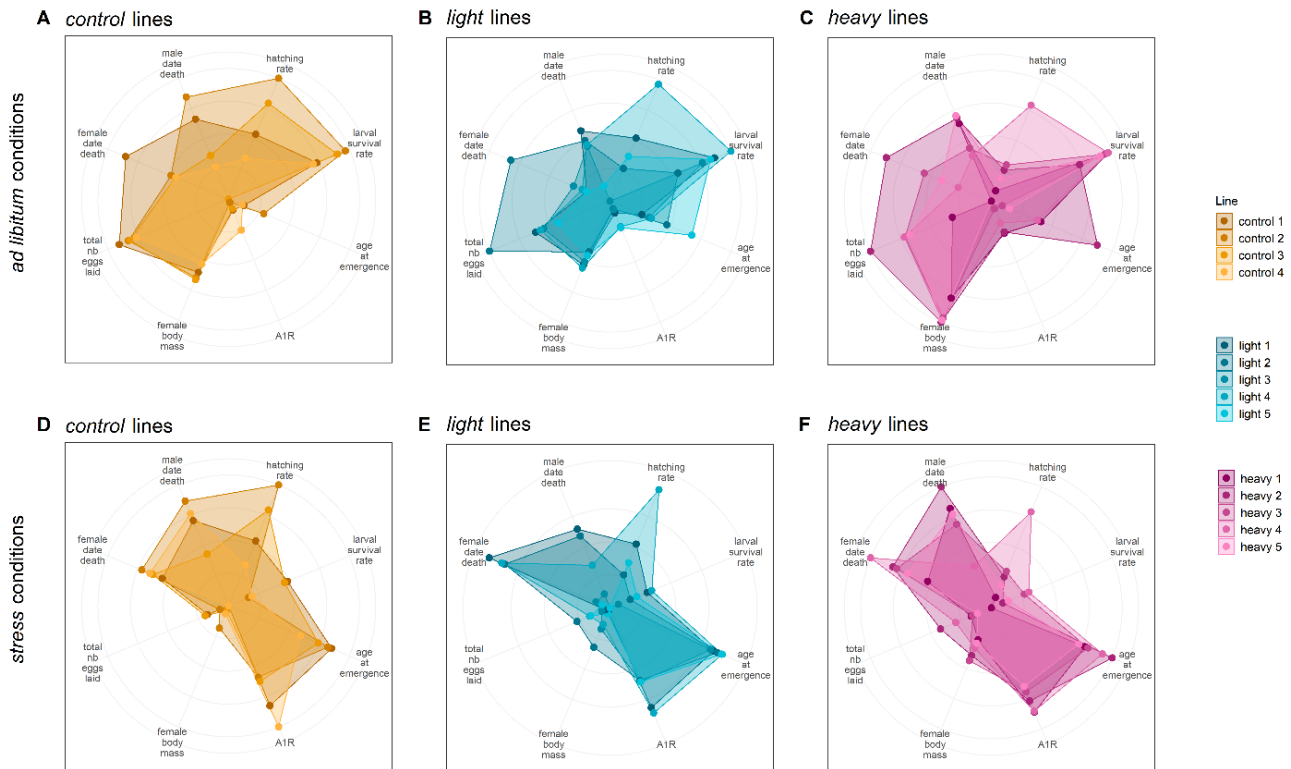
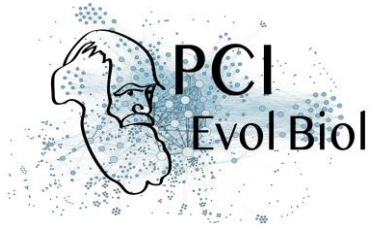


Figure 6: Multi-trait phenotypes of experimental lines of the female body mass selection scheme

(A-C) Radar plots of G9 control, light and heavy lines phenotyped under ad libitum conditions for eight traits. The lines display a strong phenotypic response on the selected trait (female body mass), while the rest of their phenotype remains similar. A1R stands for age at first reproduction. (D-F) Radar plots of G9 control, light and heavy lines phenotyped under stressful conditions for eight traits. The lines display a similar phenotypic response, which is strongly dissimilar to the phenotypic response obtained under ad libitum conditions. Color code is similar to Figure 1.

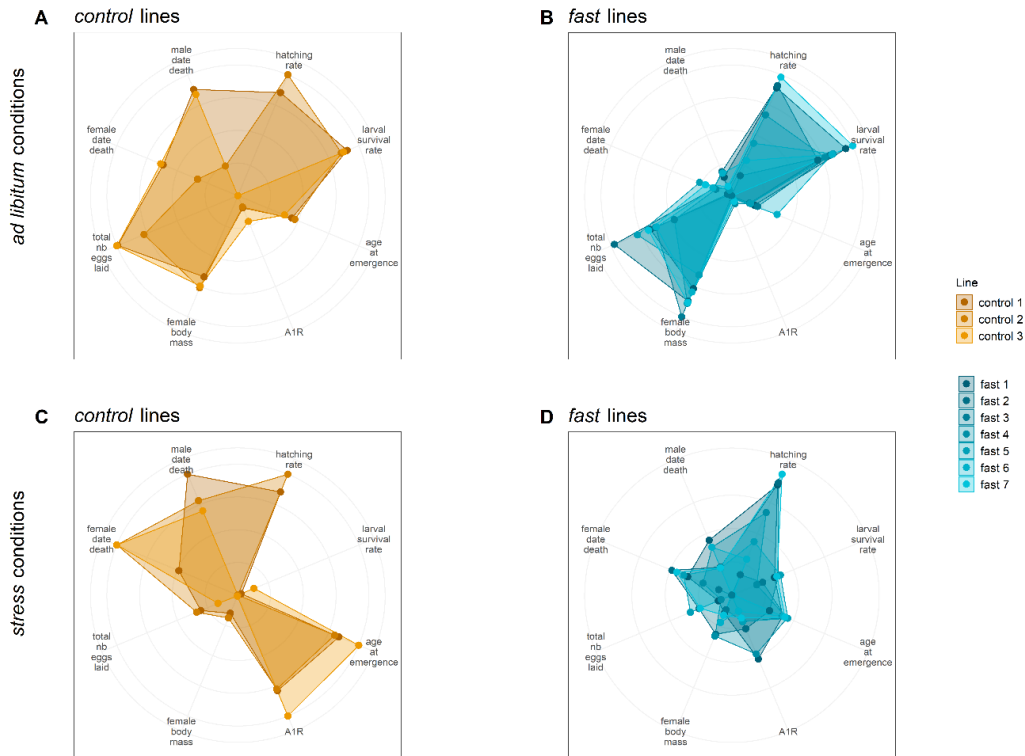
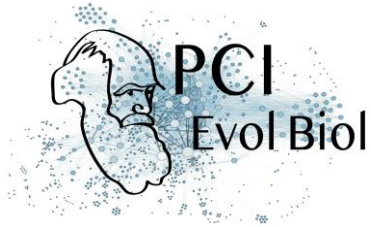
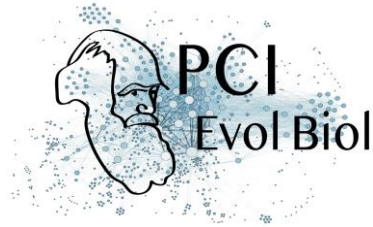


Figure 7: Multi-trait phenotypes of experimental lines of the age at first reproduction selection scheme

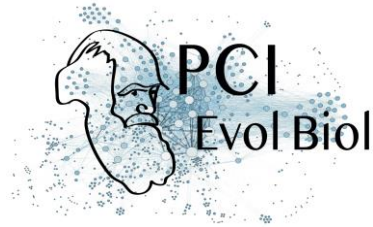
Radar plots of G10 control and fast lines phenotyped under ad libitum conditions (A-B, respectively) and stressful conditions (C-D, respectively) for eight traits. Each line displays a distinctive phenotypic response to selection x environment conditions. In contrast to the female body mass selection, selection on age at first reproduction modified most investigated traits. Color code is similar to Figure 1.



phenotyping step, played a major role in explaining the phenotypic syndromes, often in interaction with selection.

After experimental selection on female body mass, food stress reduced the mass of females and males as expected, with a significant interaction between the diet type and the direction of the selection (Figure 1A; females: $\chi^2_2 = 36.337$, $p < 0.001$; males: $\chi^2_2 = 15.288$, $p < 0.001$). The difference in mass between heavy and light lines was always more pronounced when fed *ad libitum* than under stress for both sexes (multiple comparisons of means: females: $Z = 5.875$, $p < 0.001$; males: $Z = 3.923$, $p < 0.001$). Larval survival was also influenced by the interaction between selection type and diet type (Figure 2B; $\chi^2_2 = 7.397$, $p = 0.025$). Heavy lines survived at a higher rate than light lines in the *ad libitum* but not in the stressful diet (multiple comparison of means: $Z = 2.275$, $p = 0.047$). On the other hand, heavy lines survived at a lower rate than control lines in the stress but not in the *ad libitum* diet ($Z = -2.364$, $p = 0.047$). The difference between control and light lines did not depend on diet ($Z = -0.264$, $p = 0.792$). Adults emerged earlier when they had abundant food than when under food stress (Figure 2C; LRT: $\chi^2_2 = -16.683$, $p < 0.001$), but no interaction with selection was present for this trait (LRT: $\chi^2_2 = -0.344$, $p = 0.842$). While selection on female body mass did not alter the age at first reproduction (Figure 3A), diet did (LRT: $\chi^2_1 = 59.23$, $p < 0.001$), with reproduction delayed for all lines under food stress, whether selected to be heavy or light (+2.86 days on average; no selection x diet interaction: $\chi^2_2 = -0.145$, $p = 0.930$). Fecundity was influenced by an interaction between selection on female body mass and diet (Figure 4A; LRT: $\chi^2_2 = 4.730$, $p = 0.030$). Specifically, control lines suffered a more severe drop in fecundity when food was limited than selected lines (control vs. heavy lines: $Z = 3.038$, $p = 0.007$; control vs. light lines: $Z = 1.855$, $p = 0.064$). The diet type affected heavy and light lines in a similar manner ($Z = -1.255$, $p = 0.210$). Survival was affected by a 3-way interaction between sex, selection and diet (Figure 4B; LRT: $\chi^2_2 = 6.378$, $p = 0.041$). We thus analyzed the survival results according to sex. For females, selection type interacted with diet (LRT: $\chi^2_2 = 6.378$, $p = 0.017$). This interaction was mostly driven by the increase in female survival in heavy lines under stress when compared to control females ($Z = 2.863$, $p = 0.012$). For males, the interaction between the selection type and the diet type was also statistically significant (LRT: $\chi^2_2 = 8.180$, $p = 0.020$), mostly driven by the drop in survival in males from light lines under stress in comparison to heavy and control lines (Figure 4A).

After experimental selection on the age at first reproduction, the earlier female reproduction we observed was magnified under the stressful diet (selection x diet interaction: $\chi^2_2 = 35.567$, $p < 0.001$), with fast lines laying their first eggs on average three days earlier than control lines under the *ad libitum* diet (fast lines = 6 days, control lines = 9 days), and as much as 13 days earlier in the stress diet (fast lines = 12

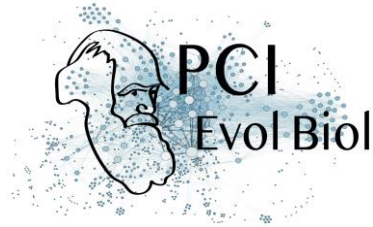


days, control lines = 25 days, Figure 1D). Food stress reduced larval survival overall (all comparisons: $p < 0.001$), with greater reductions in the fast lines than in the control lines (46% and 30% survival for fast and control lines, respectively; selection x diet interaction: $\chi^2_1 = 13.434$, $p < 0.001$; Figure 2E). Adults emerged earlier when they had abundant food (Figure 2F; LRT: $\chi^2_1 = 91.88$, $p < 0.001$). Development time was also influenced by an interaction between selection and diet (LRT: $\chi^2_1 = -5.709$, $p = 0.017$), with the control lines under food limitation taking the longest to emerge. Fecundity also responded to diet, with food stress strongly reducing fecundity (LRT: $\chi^2_1 = 51.200$, $p < 0.001$), but without interacting with selection (LRT: $\chi^2_1 = 0.188$, $p = 0.665$). Finally, survival increased with food stress (LRT: $\chi^2_1 = 14.14$, $p < 0.001$, Figure 4D), without any interaction between other significant factors (such as sex and selection; all $p > 0.12$).

Multivariate analyses of the responses to selection highlighted a strong effect of the diet type on phenotypes. As mentioned above, for both experimental selection schemes, MFA dimension 1 significantly correlated with diet and with the interaction between diet and selection (female body mass: $r^2_{\text{diet}} = 0.927$ and $r^2_{\text{interaction}} = 0.965$, both p -values < 0.001 ; age at first reproduction: $r^2_{\text{diet}} = 0.857$ and $r^2_{\text{interaction}} = 0.974$, both p -values < 0.001); Figure 5). In both experiments, within each selection treatment, stress and *ad libitum* lines tended to separate along the direction given by female body mass quasi-orthogonally to that of adult survival rates. Stressed lines therefore had trait combinations dominated by small females, few low-quality larvae with long development and late reproduction, with no major effect on adult survival. This MFA also revealed a large interaction effect with selection corresponding to different responses to diet according to the selection type. For instance, in Figure 5B heavy lines are distinct from control and light lines under food stress, while light lines are distinct from control and heavy lines when fed *ad libitum*. Diet and diet x selection effects were most obvious when comparing *ad libitum* and stress phenotypes in radar plot illustrations and correlation matrices (Figures 6-8, Supplementary Figures 4 and 5, top vs. bottom rows).

Discussion

We investigated the mechanisms underlying the emergence of the invasion syndrome occurring in invasive populations of *H. axyridis* using two distinct artificial selection experiments performed on two traits involved in this syndrome. This suite of experiments enabled us to assess whether (i) the selected traits evolved, (ii) other phenotypic traits evolved in concert, (iii) the new phenotypic syndromes resembled the invasion syndrome found in natural populations of *H. axyridis*, and (iv) environmental conditions impacted the expression of the evolved syndromes.



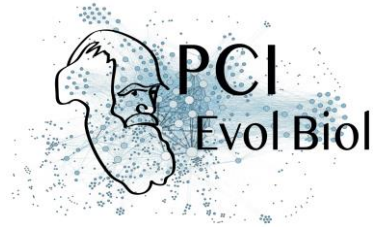
Rapid evolution of traits under direct selection

The two focal traits, female body mass and age at first reproduction, were heritable ($H^2 = 0.46$ and 0.19 for female body mass and age at first reproduction, respectively) and responded to selection. In less than ten generations, female body mass increased by 12% in the heavy lines and decreased 4% in the light lines compared to the control lines and the age at first reproduction declined by 33% in the fast lines compared to the control lines in *ad libitum* conditions. In contrast, control lines displayed no evolution of age at first reproduction and only a slight increase of female body mass compared to the initial generation, indicating no ongoing evolutionary response to rearing conditions. These results confirm several studies showing that in many species body mass or size and age at first reproduction are heritable and can rapidly evolve in artificial selection experiments (e.g. Teuschl et al. 2007, Miyatake 1997), as well as in natura especially in the context of biological invasion (e.g. Reznick et al. 1990, Huey et al. 2000, Diamantidis et al. 2009, Kingsolver et al. 2012). The fact that single traits linked to growth or reproduction can quickly respond to selection was expected, due to the phenotypic changes that we observed for this type of traits between native and invasive populations of *H. axyridis* (Supplementary Figure 1).

The evolution of a phenotypic syndrome highly depends on the selected trait

The main objective of our work was to assess whether other phenotypic traits evolved in response to selection on body mass or age at first reproduction, and to evaluate the extent to which such correlated shifts mimicked the invasion syndrome. Life-history theory has given keys to understand how different traits could interact to produce different life-history strategies (Stearns 1992). Faced with new selection pressures, it is quite common that a suite of traits will evolve rather than a single trait in isolation, whether in a context of experimental evolution or in natura (Reznick et al. 1990, Reznick & Ghalambor 2001, Teuschl et al. 2007). Here we found that the number of traits showing a correlated response is highly variable depending on the trait undergoing direct selection.

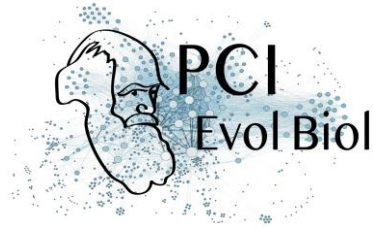
The impact of selection on female body mass on the other studied traits was weak when measured in *ad libitum* conditions. Male body mass showed a correlated response to selection, suggesting that genes determining weight are mostly on autosomal chromosomes. Larval survival rate also displayed a slight correlated response, with larvae from heavy lines surviving better than those from light lines. Finally, fecundity tended to decrease for both heavy and light lines compared to control lines. Overall, while selection on female body mass was highly efficient in both directions, it did not lead to the emergence of a complex phenotypic syndrome such



as the one observed in invasive populations of *H. axyridis*. At first glance, this result seems contradictory with the fact that most life-history traits often covary with size (Woodward et al. 2005). However, observing weak correlated responses of other traits to direct selection on a single focal trait is not uncommon in experimental selection assays (Spitze et al. 1991). A first potential explanation is related to the relatively short duration of our artificial selection experiments, which led to a female body mass increase of 12%. In comparison, Malerba et al. (2018) used 280 generations of artificial selection to evolve a 10-fold difference in mean body size between small- and large-selected lineages of the phytoplankton *Dunaliella tertiolecta*. In the Malbera et al. (2018) experiment, the intense selection on the size resulted in a shift in several traits involved in the ability of this species to cope with resource fluctuations. It is possible that *H. axyridis* would have exhibited such shifts over time. A second potential explanation relies on the fact that presumed trade-offs underlying the evolution of adaptive life histories often become visible only in stressful environments (Schluter et al. 1991). Finally, although metabolic theory explains the covariation between size and demography across species, this pattern does not seem to hold within a species and the link between size and other life-history traits within species could be less direct than commonly thought (Malerba et al. 2019).

In contrast, artificial selection on age at first reproduction resulted in a strong correlated response in most of the other traits that were studied. We observed a strong shift in four of the six traits (development time, body mass, fecundity and survival). Only the earliest developmental traits did not show a correlated response (i.e., hatching rate and larval survival). In *ad libitum* phenotyping conditions, individuals from fast lines developed faster and died earlier than control lines, and females from fast lines were bigger and laid fewer eggs than control lines. Thus, selection on a single trait (here age at first reproduction) resulted in the evolution of a clearly distinct multi-trait phenotypic syndrome.

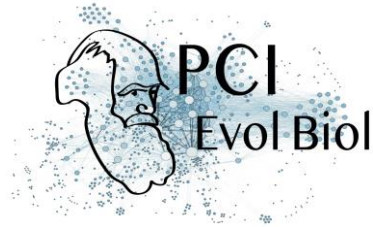
Overall, our results suggest that all traits are not equivalent and symmetric in building a genetic response to selection. It seems that selection on age at first reproduction drove the evolution of female body mass, but that the reverse was not true. Due to technical constraints, the two experiments had to be performed separately, and thus it is not impossible that the observed differences in the response to selection are due to other differences in the experiments. Most notably, the experiments started with different base populations. The base population for selection on female body mass experienced eight generations in the laboratory environment before the start of artificial selection process, while the base population for selection on age at first reproduction experienced only two generations in the lab. Since base populations were not lab adapted at the start, this may mean that during selection on



age at first reproduction, the populations, also could have been experiencing selection to the laboratory environment. To test this, we compared the G0 founding population with control lineages at the end of selection (G10). Both univariate and multivariate analyses indicate that most traits evolved only slightly or not at all between G0 to G10 in the absence of selection on age at first reproduction (results not shown, R code and data available in the online supplementary material). We tested a potential impact of differences between experiments by re-running all analyses using the difference between observed trait values and the means of controls lines rather than the raw trait data. These analyses yielded the same results as raw-value analyses, indicating a lack of influence of different experimental settings on the conclusion (results not shown, R code and data available in the online supplementary material, <https://data.inra.fr/dataset.xhtml?persistentId=doi:10.15454/V9XCA2>). In addition to the evolution of trait values, the relationships between the phenotypic traits were modified by the selection experiments. Multivariate analyses confirmed that selection for a faster age at first reproduction modified the phenotype more profoundly than selection for female body mass. Interestingly, we found that selection on the age at first reproduction (and to a lower extent on the body mass), resulted in a global relaxation of phenotypic correlations, and this was independent of the environmental context (i.e. the diet type during the phenotyping step). The correlated responses varied highly depending on the trait under direct selection. This indicates that selective pressures, even when transient like in our experiments, may have profound impacts on additive genetic variance-covariance matrices (G-matrices) and therefore on future evolutionary trajectories (Steppan et al. 2002; Arnold et al. 2008, Blows & Mcguigan 2015). Overall, our results show that the phenotypic matrices are far from rigid and can evolve rapidly due to both selective and environmental contexts, indicating that selection on different traits will have different consequences for the relationships between traits. Rapid evolution of correlated traits following introduction into a novel environment might be common, as illustrated by correlated morphological and behavioral traits evolution following colonization of a new habitat in the isopod *Asellus aquaticus* (Eroukhmanoff & Svensson 2011; Karlsson Green et al. 2016).

Experimental selection to study invasion syndromes

A key question of the present study was whether selection on one trait of the invasion syndrome observed in invasive populations of *H. axyridis* could lead to inducing the whole or at least a part of the syndrome in the laboratory. We have compiled the correlated responses observed in *ad libitum* phenotyping conditions for the two artificial selection experiments as well as the invasion syndrome observed *in natura* in Table 1. Regarding female body mass, artificial selection has clearly resulted in few correlated responses and hence poorly reproduced the invasion syndrome. In contrast, for age at first reproduction, artificial selection resulted in more widespread



phenotypic changes, which nevertheless corresponded only partly to the invasion syndrome. Similar to invasive populations, artificial selection on age at first reproduction triggered faster larval development, earlier age at reproduction and heavier body mass. However, we observed several trade-offs that were not found in invasive populations: individuals from fast lines exhibited a shorter lifespan and had a lower egg production than individuals from control lines.

The discrepancy between phenotypes of natural invasive populations and experimentally selected lines has several potential explanations. First selection *in natura* was longer than 10 generations of artificial selection in the lab. Second selective pressures are likely more complex during the course of the invasion as compared to the laboratory, probably involving a large set of biotic factors and biotic interactions (Reznick and Ghalambor 2001, Mitchell et al. 2006). Moreover selection pressures *in natura* can be variable through time (Sakai et al. 2001), which would greatly alter the phenotypic outcome of selection. Finally, the successful settlement of introduced propagules followed by demographic expansion leading to invasion is as a trial and error process (Laugier et al. 2016) from which we only see the winners (McKinney and Lockwood 1999). In the case of *H. axyridis*, multiple introductions for biological control occurred prior to invasion, and the groups that did finally invade may have been superior in some way that enabled them to escape the trade-offs we observed between time to first reproduction, lifespan and fecundity in our selection experiment. It remains unknown whether the invasion and its associated syndrome were successful due to such lottery effects or because of the purging of deleterious during the multiple introductions, creating individuals with overall higher fitness (Facon et al. 2011).

Environmental features strongly influence the expression of phenotypic syndromes

Our experiments revealed a large impact of diet on the evolutionary shifts observed for all measured traits. In agreement with the study of Sikkink et al. (2017), we found that the effect of diet was far from being homogeneous and was very dependent on the trait considered and the selection regime. The phenotypic differences between control and selected lines were magnified in stressful conditions for the fast reproduction lines. Differences between heavy lines and light and control lines were exacerbated under stressful diet. Interestingly, control lines displayed a positive relationship between growth and reproductive traits in *ad libitum* conditions and a negative relationship between the same traits in stressful conditions (Figure 8). These observations are reminiscent of the *Daphnia pulex* balance between ‘superfleas’ showing no phenotypic trade-offs in favorable environments, while stressful conditions reveal a cost of acquisition leading to allocation trade-offs (Reznick et al.

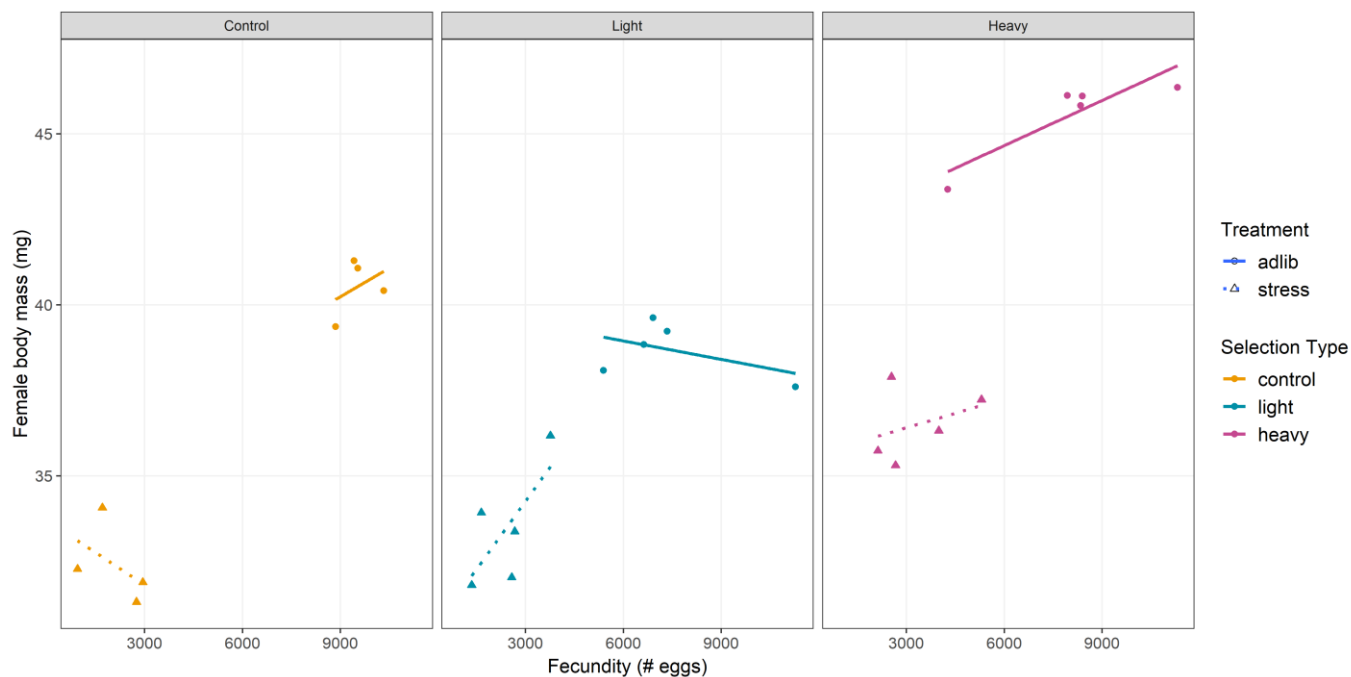
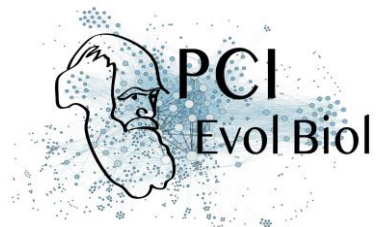
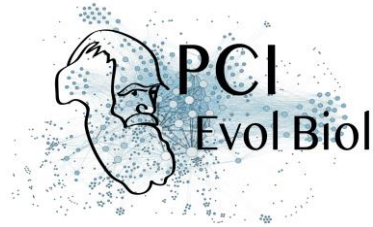


Figure 8: Relationship between reproductive and growth traits of experimental lines of the female body mass selection scheme

Each point refers to a replicate line in a given experimental condition. Dots and triangles indicate lines in ad libitum and stressful conditions, respectively. Solid and dashed lines represent linear regression for ad libitum and stressful conditions, respectively. Color code is similar to Figure 1.



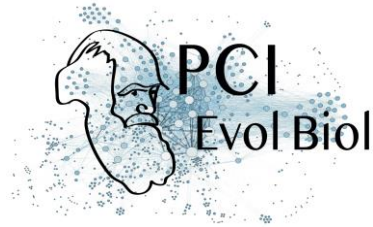
2000). Such dependence of trade-offs on environmental conditions is interpreted as revealing a cost of acquisition where ‘high acquisition-low allocation’ phenotypes are favored in situations where resources are abundant and ‘low acquisition-high allocation’ phenotypes are favored in low resources environments (Reznick et al. 2000).

Selection for lighter females seemed to have reversed this pattern, with light lines showing no trade-off between growth and reproduction in stressful phenotyping conditions, while a trade-off appeared in *ad libitum* conditions. Moreover, selection for heavier females might have triggered a ‘high acquisition’ phenotype that displays a lack of genetic variation in resource allocation (Reznick et al. 2000), a pattern particularly marked in stressful conditions (e.g., positive slope for heavy x stress lines in Figure 8). Different directions of selection thus seem to have triggered new responses in the allocation and acquisition of available diet resources. This pattern however deserves a dedicated experimental study to evaluate the influence of past selection on the balance between acquisition and allocation of diet resources.

By supporting that adaptation in one environment may induce benefits and costs in another environment (Dutilleul et al. 2017), our results underline the importance that $G \times E$ interactions could have for the studies of biological invasions. Indeed, native and invaded environments are likely to be different (Reznick and Ghalambor 2001) and the invaded environments may themselves undergo substantial changes during the course of the invasion (Sakai et al. 2001). In the case of *H. axyridis*, the agricultural habitats in which *H. axyridis* was introduced as a biocontrol agent are certainly different in terms of nutritional resources and habitat structures from the habitats encountered later during its geographical expansion. Moreover, the eco-evolutionary dynamics of spreading populations may also be constrained due to the balance between selective and stochastic processes (Williams et al. 2019). Overall, our results highlight the need to systematically examine the consequences of experimental evolution in a variety of environments (Amarillo-Suarez et al. 2011).

Conclusion

The adaptive challenges encountered by a species in its introduced habitat are complex. Manipulative field experiments imposing selection are difficult to impossible to implement, particularly with invasive species. Thus, artificial selection can be employed to mimic what could have happened during the course of invasion, evaluate correlated responses to selection for focal traits and estimate the extent to which those correlations shape the suite of traits specific of the invasive populations (Fuller et al. 2005). Our artificial selection experiments failed, however, to reproduce the complete invasion syndrome we documented in natural populations of *H. axyridis*. This



result underlines the limits of using laboratory experiments to study complex evolutionary trajectories in natural conditions. To go further in the evaluation of the common points and discrepancies between artificial selection lines and natural populations, it would be relevant to carry out whole-genome scans to compare the genomic regions showing signals of selection associated with invasive natural populations to the genomic regions showing signals of selection in our experimental lines. The laboratory experiments we carried out are nonetheless a mandatory step in identifying the traits that are correlated and those that are less so in various selective contexts, helping us understand the evolution of an invasion syndrome. Finally, the strong $G \times E$ interactions we observed indicate that trait values adaptive in one environment may no longer be advantageous following environmental change. This could explain, at least partly, why boom-bust dynamics – the rise of a population to outbreak levels, followed by a strong decline – have been frequently described in invasive populations (Lockwood et al. 2013; Strayer et al. 2017).

Data accessibility

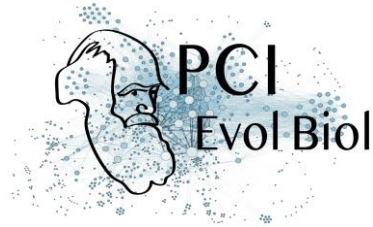
All data and R code are available online at:

<https://data.inra.fr/dataset.xhtml?persistentId=doi:10.15454/V9XCA2>

Supplementary material

Supplementary material is available online at:

<https://www.biorxiv.org/content/10.1101/849968v2.supplementary-material>

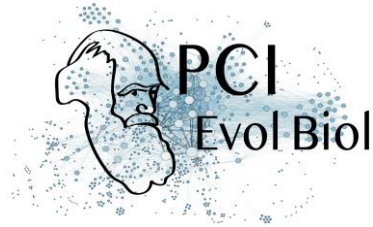


Acknowledgements

AE and BF acknowledge financial support by the national funder ANR (France) through the European Union program ERA-Net BiodivERsA (project EXOTIC), and the INRA scientific department SPE. AE and JF acknowledge the UMR CBGP from its internal grant support. VR acknowledges financial support by the European Union regional development fund (ERDF), the Conseil Départemental de la Réunion, the Région Réunion, and the French Agropolis Fondation (Labex Agro–Montpellier, E-SPACE project number 1504-004). RAH acknowledges support from USDA AFRI COLO-2016-09135, USDA NIFA Hatch project 1012868, the French Agropolis Fondation (LabEx Agro–Montpellier) through the AAP ‘International Mobility’ (CfP 2015-02), the French programme investissement d’avenir, and the LabEx CEMEB through the AAP ‘invited scientist 2016’. We are grateful to the SEPA technical platform of the CBGP laboratory for hosting all experiments presented in this study. JF would like to thank Pierre E. Sirius and Ariane N. Véga for their early support.

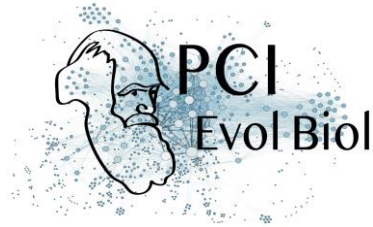
Conflict of interest disclosure

The authors of this preprint declare that they have no financial conflict of interest with the content of this article. RAH, VR, AE and BF are PCI Evol Biol recommenders.

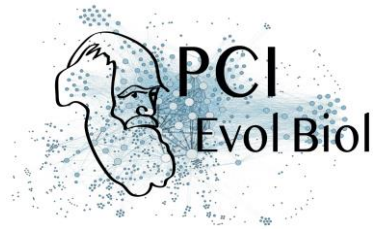


References

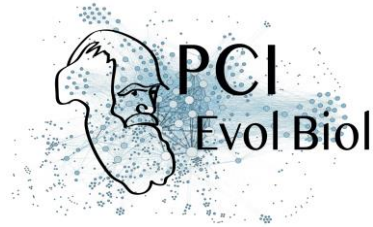
- Amarillo-Suarez A. R., Stillwell R. C., Fox C. W. (2011) Natural selection on body size is mediated by multiple interacting factors: a comparison of beetle populations varying naturally and experimentally in body size. *Ecology and Evolution*, 1: 1-14.
- Anderson J. H., Faulds P. L., Atlas W. I., Pess G. R., Quinn T. P. (2010) Selection on breeding date and body size in colonizing coho salmon, *Oncorhynchus kisutch*. *Molecular Ecology*, 19: 2562-2573.
- Arnold, S. J., Bürger, R., Hohenlohe, P. A., Ajie B. C., Jones A. G. (2008) Understanding the evolution and stability of the G-matrix. *Evolution*, 62: 2451-61.
- Bataillon T., Joyce P., Sniegowski P. (2013) As it happens: current directions in experimental evolution. *Biology Letters*, 9: 20120945.
- Bates D., Maechler M., Bolker B., Walker S. (2014) lme4: Linear mixed-effects models using Eigen and S4. Available: <http://CRAN.R-project.org/package=lme4>.
- Blackburn T. M., Duncan R. P. (2001) Establishment patterns of exotic birds are constrained by non-random patterns in introduction. *Journal of Biogeography*, 28: 927-939.
- Blair A. C., Wolfe L. M. (2004) The evolution of an invasive plant: An experimental study with *Silene latifolia*. *Ecology*, 85: 3035-3042.
- Blows M. W., Mcguigan K. (2015) The distribution of genetic variance across phenotypic space and the response to selection. *Molecular Ecology*, 24: 2056-2072.
- Blumenthal D., Mitchell C. E., Pysek P., Jarosik V. (2009) Synergy between pathogen release and resource availability in plant invasion. *Proceedings of the National Academy of Sciences of the United States of America*, 106: 7899-7904.
- Bolker B. M., Brooks M. E., Clark C. J., Geange S. W., Poulsen J. R., Stevens M. H. H., White J. S. (2009) Generalized linear mixed models: A practical guide for ecology and evolution. *Trends in Ecology and Evolution*, 24: 127-135.
- Bossdorf .O., Auge H., Lafuma L., Rogers W. E., Siemann E., Prati D. (2005) Phenotypic and genetic differentiation between native and introduced plant populations. *Oecologia*, 144: 1-11.
- Brown P. M. J., Adriaens T., Bathon H., Cuppen J., Goldarazena A., Hägg T., Kenis M., Klausnitzer B. E. M., Kovář I., Loomans A. J. M., Majerus M. E. N., Nedved O., Pedersen J., Rabitsch W., Roy H. E., Ternois V., Zakharov I. A., Roy D. B. (2007) *Harmonia axyridis* in Europe: spread and distribution of a non-native coccinellid. *BioControl*, 53: 5-21.



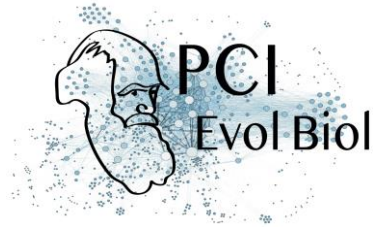
- Canty A., Ripley B. (2015) boot: Bootstrap R (S-Plus) functions. R package version 1.3-16.
- Catford J. A., Jansson R., Nilsson C. (2009) Reducing redundancy in invasion ecology by integrating hypotheses into a single theoretical framework. *Diversity and Distributions*, 15: 22-40.
- Chapple D. G., Simmonds S. M., Wong B. B. M. (2012) Can behavioral and personality traits influence the success of unintentional species introductions? *Trends in Ecology and Evolution*, 27: 57–64.
- Chuang A., Peterson C. R. (2016) Expanding population edges: theories, traits, and trade-offs. *Global Change Biology*, 22: 494-512.
- Colautti R. I., Lau J. A. (2015) Contemporary evolution during invasion: evidence for differentiation, natural selection, and local adaptation. *Molecular Ecology*, 24: 1999-2017.
- Colautti R. I., Eckert C. G., Barrett S. C. H. (2010) Evolutionary constraints on adaptive evolution during range expansion in an invasive plant. *Proceedings of the Royal Society B-Biological Sciences*, 277: 1799-1806.
- Davis M. A., Pelsor M. (2001) Experimental support for a resource-based mechanistic model of invisibility. *Ecology Letters*, 4: 421-428.
- Diamantidis A. D., Carey J. R., Papadopoulos N. T. (2009) Life-history evolution of an invasive tephritid. *Journal of Applied Entomology*, 132: 695-705.
- Dlugosch K. M., Parker I. M. (2008) Invading populations of an ornamental shrub show rapid life history evolution despite genetic bottlenecks. *Ecology Letters*, 11: 1-9.
- Dutilleul M., Réale D., Goussen B., Lecomte C., Galas S., Bonzom J.-M. (2017) Adaptation costs to constant and alternating polluted environments. *Evolutionary Applications*, 10: 839-851.
- Eroukhmanoff, F., Svensson E. I. (2011) Evolution and stability of the G-matrix during the colonization of a novel environment. *Journal of Evolutionary Biology*, 24: 1363-73.
- Estoup A., Ravigné V., Hufbauer R.A., Vitalis R., Gautier M., Facon B. (2016) Is there a genetic paradox of biological invasions. *Annual Review of Ecology, Evolution, and Systematics*, 47: 51-72.
- Facon B., Hufbauer R. A., Tayeh A., Loiseau A., Lombaert E., Vitalis R., Guillemaud T., Lundgren J. G., Estoup A. (2011). Inbreeding depression is purged in the invasive insect *Harmonia axyridis*. *Current Biology*, 21: 424-427.
- Fuller R. C., Baer C. F., Travis J. (2005) How and when selection experiments might actually be useful. *Integrative and Comparative Biology*, 45: 391-404.



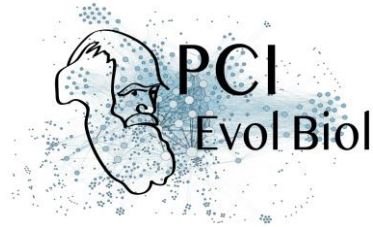
- Garvey J. E., Stein R. A., Thomas H. M. (1994) Assessing how fish predation and interspecific prey competition influence a crayfish assemblage. *Ecology*, 75:532-547.
- Gioria M., Osborne B. (2014) Resource competition in plant invasions: Emerging patterns and research needs. *Frontiers in Plant Science*, 5: 1-21.
- Huey R. B., Gilchrist G. W., Carlson M. L., Berrigan D., Serra L. (2000) Rapid evolution of a geographic cline in size in an introduced fly. *Science*, 287: 308-309.
- Irwin K. K., Carter P. A. (2014) Artificial selection on larval growth curves in *Tribolium*: correlated responses and constraints. *Journal of Evolutionary Biology*, 27: 2069-2079.
- Karlsson Green, K., Eroukhmanoff, F., Harris, S., Pettersson, L. B., Svensson E. I. (2016) Rapid changes in genetic architecture of behavioural syndromes following colonization of a novel environment. *Journal of Evolutionary Biology*, 29: 144-52.
- Kawecki T. J., Lenski R. E., Ebert D., Hollis B., Olivieri I., Whitlock M. C. (2012) Experimental evolution. *Trends in Ecology and Evolution*, 27: 547-560.
- Keller S. R., Taylor D. R. (2008) History, chance and adaptation during biological invasion: separating stochastic phenotypic evolution from response to selection. *Ecology Letters*, 11: 852-866.
- Ketterson E. D., Atwell J. W., Mcglothlin J. W. (2009) Phenotypic integration and independence: hormones, performance, and response to Environmental Change. *Integrative and Comparative Biology*, 49: 365-379.
- Kingsolver J. G., Diamond S. E., Seiter S. A., Higgins J. K. (2012) Direct and indirect phenotypic selection on developmental trajectories in *Manduca sexta*. *Functional Ecology*, 26: 598-607.
- Kumschick S., Richardson D. M. (2013) Species-based risk assessments for biological invasions: advances and challenges. *Diversity and Distributions*, 19: 1095-1105.
- Laugier G., Le Moguedec G., Tayeh A., Loiseau A., Osawa N., Estoup A., Facon B. (2013). Increase in male reproductive success and female reproductive investment in invasive populations of the harlequin ladybird *Harmonia axyridis*. *Plos One*, 8: e77083.
- Laugier G., Le Moguedec G., Su W., Ashraf T., Soldati L., Serrate B., Estoup A., Facon B. (2016). Reduced population size can induce quick evolution of inbreeding depression in the invasive ladybird *Harmonia axyridis*. *Biological Invasions*, 18: 2871-2881.
- Le S., Josse J., Husson F. (2008) FactoMineR: An R package for multivariate analysis. *Journal of Statistical Software*, 25: 1-18.



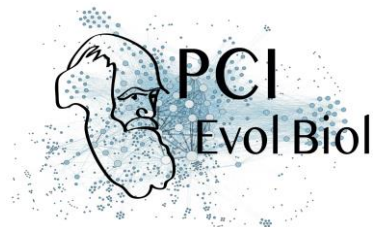
- Lee C. E. (2016) Evolutionary mechanisms of habitat invasions, using the copepod *Eurytemora affinis* as a model system. *Evolutionary Applications*, 9: 248-270.
- Lee C. E., Remfert J. L., Chang Y. M. (2007) Response to selection and evolvability of invasive populations. *Genetica*, 129:179-192.
- Lee C. E., Kiergaard M., Eads B. D., Gelembiuk G. W., Posavi M. (2011) Pumping ions: Rapid parallel evolution of ionic regulation following habitat invasions. *Evolution*, 65:2229-2244.
- Lockwood J. L., Hoopes M. F., Marchetti M. P. (2013). *Invasion Ecology*, 2nd ed. Wiley-Blackwell, Oxford, UK. 466 pp.
- Lombaert, E., Guillemaud, T., Thomas, C.E., Handley, L.J.L., Li, J., Wang, S., Pang, H., Goryacheva, I., Zakharov, I.A., Jusselin, E., Poland, R.L., Migeon, A., van Lenteren, J., De Clercq, P., Berkvens, N., Jones, W., Estoup, A. (2011). Inferring the origin of populations introduced from a genetically structured native range by approximate Bayesian computation: case study of the invasive ladybird *Harmonia axyridis*. *Molecular Ecology*, 20: 4654–4670.
- Lombaert E., Estoup A., Facon B., Joubard B., Gregoire J. C., Jannin A., Blin A., Guillemaud T. (2014). Rapid increase in dispersal during range expansion in the invasive ladybird *Harmonia axyridis*. *Journal of Evolutionary Biology*, 27: 508-517.
- Malerba M. E., Palacios M. M., Marshall D. J. (2018) Do larger individuals cope with resource fluctuations better? An artificial selection approach. *Proceedings of the Royal Society B-Biological Sciences*, 285: 20181347.
- Malerba M. E., Marshall D. J. (2019) Size-abundance rules? Evolution changes scaling relationships between size, metabolism and demography. *Ecology Letters*, 22: 1407-1416.
- Mitchell C.E., Agrawal A. A., Bever J. D., Gilbert G. S., Hufbauer R. A., Klironomos J. N., Maron J. L., Morris W. F., Parker I. M., Power A. G., Seabloom E. W., Torchin M. E., Vázquez D. P. (2006) Biotic interactions and plant invasions. *Ecology Letters*, 9: 726-740.
- Miyatake T. (1997) Correlated responses to selection for developmental period in *Bactrocera cucurbitae* (Diptera: Tephritidae): time of mating and daily activity rhythms. *Behavior Genetics*, 27: 489-498.
- Perkins L. B., Leger E. A., Nowak R. S. (2011) Invasion triangle: an organizational framework for species invasion. *Ecology and Evolution*, 1: 610-625.
- Phillips B. L., Brown G. P., Webb J. K., Shine R. (2010) Life-history evolution in range-shifting populations. *Ecology*, 91: 1617-1627.



- Phillips B. L., Brown G. P., Webb J. K., Shine R. (2006) Invasion and the evolution of speed in toads. *Nature*, 439: 803.
- Reznick D. A., Bryga H., Endler J. A. (1990) Experimentally induced life-history evolution in a natural population. *Nature*, 346; 357-359.
- Reznick D., Nunney L., Tessier A. (2000) Big houses, big cars, superfleas and the costs of reproduction. *Trends in Ecology & Evolution*, 15: 421-425.
- Reznick D. N., Ghalambor C. K. (2001) The population ecology of contemporary adaptations: what empirical studies reveal about the conditions that promote adaptive evolution. *Genetica*, 112-113: 183-198.
- Reznick D. N., Losos J., Travis J. (2019) From low to higher gear: there has been a paradigm shift in our understanding of evolution. *Ecology Letters*, 22: 233-244.
- Richardson D. M., Pyšek P. (2012) Naturalization of introduced plants: ecological drivers of biogeographical patterns. *New Phytologist*, 196: 383-396.
- Roff D. A. (1997) *Evolutionary Quantitative Genetic*. Chapman and Hall, New York.
- Roy H. E., Lawson Handley L.-J., Schönrogge K., Poland R. L., Purse B. V. (2011) Can the enemy release hypothesis explain the success of invasive alien predators and parasitoids? *Biocontrol*, 56: 451-468.
- Roy H. E., Brown P. M. J., Adriaens T., Berkvens N., Borges I., Clusella-Trullas S., Comont R. F., De Clercq P., Eschen R., Estoup A., Evans E. W., Facon B., Gardiner M. M., Gil A., Grez A. A., Guillemaud T., Haelewaters D., Herz A., Honek A., Howe A. G., Hui C., Hutchison W. D., Kenis M., Koch R. L., Kulfan J., Lawson Handley L., Lombaert E., Loomans A., Losey J., Lukashuk A. O., Maes D., Magro A., Murray K. M., Martin G. S., Martinkova Z., Minnaar I. A., Nedved O., Orlova-Bienkowskaja M. J., Osawa N., Rabitsch W., Ravn H. P., Rondoni G., Rorke S. L., Ryndevich S. K., Saethre M.-G., Sloggett J. J., Soares A. O., Stals R., Tinsley M. C., Vandereycken A., van Wielink P., Vigišová S., Zach P., Zakharov I. A., Zaviero T., Zhao Z. (2016). The harlequin ladybird, *Harmonia axyridis*: global perspectives on invasion history and ecology. *Biological Invasions*, 18: 997-1044.
- Royauté R., Garrison C., Dalos J., Berdal M. A., Dochtermann N. A. (2019) Current energy state interacts with the developmental environment to influence behavioural plasticity. *Animal Behavior*, 148: 39-51.
- Sakai A. K., Allendorf F. W., Holt J. S., Lodge D. M., Molofsky J., With K. A., Baughman S., Cabin R. J., Cohen J. E., Ellstrand N. C., McCauley D. E., O'Neil P., Parker I. M., Thompson J. N., Weller S. G. (2001) The population biology of invasive species. *Annual Review of Ecology and Systematics*, 32: 305-332.
- Schluter D. (1996) Adaptive radiation along genetic lines of least resistance. *Evolution*, 50:1766-1774.



- Schluter D., Price T. D., Rowe L. (1991) Conflicting selection pressures and life history trade-offs. *Proceedings of the Royal Society B: Biological Sciences*, 246: 11-17.
- Schmidt J. P., Springborn M., Drake J. M. (2012) Bioeconomic forecasting of invasive species by ecological syndrome. *Ecosphere*, 3: 46.
- Sikkink K. L., Reynolds R. M., Cresko W. A., Phillips P. C. (2017) Environmentally induced changes in correlated responses to selection reveal variable pleiotropy across a complex genetic network. *Evolution*, 69: 1128-1142.
- Spitze K., Burnson J., Lynch M. (1991) The covariance structure of life-history characters in *Daphnia pulex*. *Evolution*, 45: 1081-1090.
- Stearns S. C. (1992) *The evolution of life histories*. Oxford University Press, London.
- Steppan S. J., Phillips P. C., Houle D. (2002) Comparative Quantitative Genetics: Evolution of the G matrix. *Trends in Ecology & Evolution*, 17: 320-27.
- Strayer D.L., D'Antonio C.M., Essl F., Fowler M. S., Geist J., Hilt S., Jarić I., Jöhnk K., Jones C. G., Lambin X., Latzka A. W., Pergl J., Pyšek P., Robertson P., von Schmalensee M., Stefansson R. A., Wright J., Jeschke J. M. (2017) Boom-bust dynamics in biological invasions: towards an improved application of the concept. *Ecology Letters*, 20: 1337–1350.
- Tayeh A., Estoup A., Laugier G., Loiseau A., Turgeon J., Toepfer S., Facon B. (2012). Evolution in biocontrol strains: insight from the harlequin ladybird *Harmonia axyridis*. *Evolutionary Applications*, 5: 481-488.
- Tayeh A., Estoup A., Lombaert E., Guillemaud T., Kirichenko N., Lawson-Handley L., De Clercq P., Facon B. (2014). Cannibalism in invasive, native and biocontrol populations of the harlequin ladybird. *BMC Evolutionary Biology*, 14: 15.
- Tayeh A., Hufbauer R. A., Estoup A., Ravigné V., Frachon L., Facon B. (2015). Biological invasion and biological control select for different life histories. *Nature Communications*, 6: 7268.
- Teuschl Y., Reim C., Blanckenhorn W. U. (2007) Correlated responses to artificial body size selection in growth, development, phenotypic plasticity and juvenile viability in yellow dung flies. *Journal of Evolutionary Biology*, 20:87-103.
- Tillberg C. V., Holway D. A., LeBrun E. G., Suarez A. V. (2007) Trophic ecology of invasive Argentine ants in their native and introduced ranges. *Proceedings of the National Academy of Sciences of the United States of America*, 104: 20856-20861.
- Tyler A., Lambrinos J., Grosholz E. (2007) Nitrogen inputs promote the spread of an invasive marsh grass. *Ecological Applications*, 17: 1886– 1898.
- Wickham H. (2016) *ggplot2: Elegant graphics for data analysis*. Springer-Verlag New York.



Williams J. L., Hufbauer R. A., Miller T. E. X. (2019) How evolution modifies the variability of range expansion. *Trends in Ecology & Evolution*, 34: 903-913.

Woodward G., Ebenman B., Emmerson M., Montoya J. M., Olesen J. M., Valido A., Warren P. H. (2005) Body size in ecological networks. *Trends in Ecology & Evolution*, 20: 402-409.

Résumé détaillé

Introduction

L'hybridation peut-être définie comme un processus dans lequel des membres de populations génétiquement distinctes s'accouplent et produisent des descendants viables d'ascendance mixte. Ce processus a depuis longtemps fasciné les biologistes de l'évolution, qui ont très vite reconnu son potentiel en tant que modèle d'étude. Darwin et ses contemporains s'intéressaient déjà à l'hybridation, à la fois du fait de son intérêt pour l'agriculture, et car elle fournit une fenêtre de compréhension sur les mécanismes de l'hérédité. Les biologistes du siècle suivant, à l'aide des outils génétiques et moléculaires, démontrèrent la place centrale de l'hybridation dans plusieurs processus micro- et macro-évolutifs.

Il fut d'abord compris que selon la valeur sélective (i.e., fitness) des hybrides, l'hybridation peut participer à déterminer le rythme de la spéciation. Si les hybrides entre deux espèces peuvent survivre et se reproduire, les générations successives de croisements peuvent mener au mélange de leur matériel génétique et ralentir leur spéciation. Ceci est particulièrement probable dans l'éventualité où les hybrides montrent une meilleure fitness que leur parents non-hybrides (i.e., vigueur hybride). Dans de tel cas, l'hybridation représente une stratégie avantageuse qui peut être sélectionnée, ce qui favorisera d'autant plus les échanges de gènes entre populations. Une telle vigueur hybride peut être le résultat de plusieurs phénomènes. Dans certaines configurations, les hybrides peuvent montrer des phénotypes nouveaux ou intermédiaires, qui sont plus performants écologiquement. Les hybrides peuvent également profiter d'une plus forte hétérozygotie, de nouvelles combinaisons génétiques, de la complémentation d'allèles délétères fixés dans leurs populations parentales, ou même du cumul de gènes uniques à chacune de ces populations. Mais les effets de l'hybridation ne sont pas toujours bénéfiques, et les hybrides montrent souvent une fitness réduite en comparaison de leur parents (i.e., dépression hybride) ou une incapacité à se reproduire (i.e., stérilité hybride). Ceci est généralement le résultat d'incompatibilité intrinsèques entre les génomes mis en contact. En effet, les nouvelles combinaisons génétiques présentes dans les hybrides n'ont en principe jamais été soumises à la sélection, et sont donc dysfonctionnelles dans la majorité des cas. De telles incompatibilités hybrides résultent alors en un avantage pour les individus à éviter l'hybridation, ce qui peut mener à l'évolution rapide de phénotypes spécifiques qui empêchent les accouplements inter-spécifiques. Ces phénotypes, après leur installation dans les populations, favorise la spéciation en réduisant la quantité de matériel génétique échangé.

En plus de ses effets sur la spéciation, les outils génétiques ont également révélé que l'hybridation joue un rôle important en tant que source de variation génétique. Il existe dans la littérature de très nombreux exemples de gènes qui, après avoir sauté la barrière des espèces (i.e, introgression génétique), ont fourni de nouvelles fonctions et adaptations à leur nouveaux porteurs. Un exemple iconique de telles introgressions adaptatives est retrouvé chez les humains modernes. Il a en effet été démontré que certaines population humaines actuelles portent des gènes issus d'autres Homininés éteints (Néanderthaliens et Denisoviens), et qui fournissent des adaptations clefs en lien avec la pigmentation, l'immunité ou le métabolisme. Mais ce type de phénomènes est loin d'être restreint aux humains. De nombreux auteurs considèrent que l'hybridation et l'introgression génétiques sont une source majeure de nouveau matériel génétique chez de nombreuses organismes (e.g., certains estiment que 10% des animaux et 25% des plantes s'hybride régulièrement). En effet, la grande force de l'hybridation est quelle peut, contrairement à la mutation, mener à l'acquisition de gènes entièrement nouveaux, de combinaisons de ces gènes, ou même de nouvelles organelles et endosymbionte.

Parmi les groupes importants pour l'étude de l'hybridation, les fourmis occupent une place particulière. En effet, les fourmis sont connues depuis longtemps pour montrer des taux importants d'hybridation (plus de 20% des espèces de fourmis s'hybrident dans certains groupes). Historiquement, De tels taux ont souvent été expliqués à travers deux hypothèses non exclusives, qui reposent sur le système de reproduction et sur leur mode de vie des fourmis. Les fourmis possèdent un système de reproduction particulier nommé haplo-diploïdie, dans lequel les mâles sont des individus haploïdes (i.e., qui ne possèdent qu'une seule copie de chacun de leurs chromosomes) de développant à partir d'œufs non fécondés. Il est considéré que ce type de reproduction peut favoriser l'hybridation car même en cas de forte dépression hybride, les femelles s'étant accouplées en dehors de leur espèce peuvent toujours produire des mâles viables. Les fourmis vivent également au sein d'organisations coloniales, dans lesquelles une majorité des femelles (i.e. les ouvrières) sont stériles. Ce mode de vie, appelé eusocialité, pourrait favoriser l'hybridation car la présence inhérente de nombreux individus stériles limiterait les conséquences négative de la stérilité hybride.

Une autre explication pour la fréquence de l'hybridation chez les fourmis est l'existence, chez ces dernières, de systèmes de reproduction uniques qui intègrent l'hybridation en tant que part intégrante du cycle de vie, au point que celle-ci est devenu obligatoire au bon développement des colonies. En particulier, certaines espèces de fourmis possèdent un système de reproduction

nommé hybridogénèse sociale. Chez ces espèces, les ouvrières ne peuvent se développer qu'à partir de larves hybrides, tandis que les larves non-hybrides ne se développent qu'en reines. L'hybridogénèse sociale a d'importantes conséquences sur l'écologie des espèces qui la pratiquent, car ces dernières deviennent dépendantes de la présence de mâles d'une seconde espèce, sans lesquelles elle ne peuvent produire de colonies viables. L'hybridogénèse sociale est également un modèle d'étude important car elle correspond à une manière entièrement nouvelle d'organiser la vie en colonie, dans laquelle les mécanismes ancestraux de différenciations larvaires ont été entièrement réorganisés.

Objectifs et résultats

chapitre 1

L'évolution répétée de l'hybridogénèse sociale, au sein d'espèces de fourmis éloignées et montrant de nombreuses différences en termes d'écologie et d'histoire de vie, a alimenté de nombreux questionnements quant aux conditions de son évolution. Plusieurs hypothèses et modèles verbaux ont été développés afin d'expliquer comment de multiples transitions vers l'hybridogénèse ont pu être déclenchées, mais aucun consensus n'a pu être atteint. En particulier, il existe un débat quant à la part relative des processus sélectifs et des contingences historiques et démographiques dans l'évolution de l'hybridogénèse sociale. Ce système de reproduction évolue-t-il à la suite d'événements particuliers, ou du fait d'un mécanisme déterministe ? Dans le premier chapitre de cette thèse, mes collaborateurs et moi avons tenté d'apporter des réponses à ces questions en développant un modèle mathématique rigoureux pour l'évolution de l'hybridogénèse sociale. Ce modèle permet d'étudier les conditions qui peuvent mener une espèce eusociale standard (i.e., dans laquelle les larves peuvent se développer en reines ou en ouvrières) à perdre sa capacité à produire des ouvrières sans recourir à l'hybridation. Un soin particulier a été apporté à la description en détails de résultats mathématiques obtenus lors de ce projet, avec l'espoir que cette étude puisse servir de base aux travaux futurs.

Ce travail de modélisation a mené à des résultats semblant suggérer que l'hybridogénèse sociale peut évoluer de manière déterministe dans un éventail large de conditions initiales. Le mécanisme sous-jacent à cette évolution est une course aux armements entre les larves en développement, qui cherchent à accéder à la caste reproductive, et leur reine, qui utilise l'hybridation pour produire plus d'ouvrières. Les larves, qui sont initialement capables de se développer en ouvrières ou en reines, tendent à favoriser leur propre reproduction en préférant un développement en reine.

Bien qu'à ce stade de nombreuses larves continuent à se développer en ouvrières pour maintenir leur colonie, ceci mène tout de même à un déficit global en ouvrières dans les colonies, et donc à une baisse de leur productivité. Si les reines peuvent s'hybrider (i.e., si des mâles d'une autre espèce sont disponibles), et si les larves hybrides ont une probabilité moindre de se développer en reines due à une dépression hybride, l'hybridation peut alors être sélectionnée comme une contre-adaptation des reines au déficit en ouvrières créé par les larves. Seulement, le comblement du manque d'ouvrière par la production d'hybrides permet aussi à un plus grand nombre de larves de favoriser un développement en reines, ce qui maintient le déficit et encourage de plus en plus l'hybridation par les reines. Cet emballement évolutif peut alors graduellement mener à une situation dans laquelle la totalité des larves non-hybrides se développent en reines, et dans laquelle toutes les ouvrières sont issues de larves hybrides, l'hybridogénèse sociale.

L'intérêt du modèle mathématique développé, au-delà de montrer que le processus décrit ici est possible, a été d'étudier les facteurs qui permettent ou facilitent ce type d'évolution. En particulier, ce modèle a permis d'évaluer l'effet de plusieurs paramètres clés sur ce type de transition, comme le nombre d'accouplements effectués par les reines, leur éventuelle capacité à produire des larves par clonage, ou l'efficacité des ouvrières hybrides. Nous avons pu montrer que le nombre d'accouplements effectués par les reines est un paramètre important dans l'évolution de l'hybridogénèse sociale. Pour que l'hybridogénèse sociale puisse évoluer, il est tout d'abord nécessaire que les reines se reproduisent avec au moins deux mâles, un mâle de leur espèce (i.e., pour pouvoir produire de nouvelles reines), et un mâle d'une autre espèce (i.e., pour pouvoir produire des ouvrières hybrides). Quand les reines ne peuvent par directement choisir l'identité de leurs partenaires, les accouplements répétés leur permettent également de limiter les risques de ne se reproduire qu'avec un type de mâle, ce qui mènerait à l'impossibilité de produire soit des ouvrières, soit de nouvelles reines. Nous avons également pu montrer que cet effet du nombre d'accouplement est largement diminué chez les espèces capables de clonage, pour lesquelles la reproduction intra-spécifique n'est pas strictement nécessaire (i.e, les nouvelles reines peuvent alors être issues de clones de leur mère). Enfin, et surtout, nous avons pu montrer que le chemin évolutif proposé ici peut être emprunté même si les ouvrières hybrides sont moins performantes que les ouvrières non-hybrides, et même si l'hybridation crée des coûts supplémentaires (e.g., plus forte mortalité des reines ou plus grande exposition aux pathogènes). Ceci signifie que l'hybridogénèse sociale peut évoluer même si elle mène à une réduction globale de la fitness de tous les individus impliqués.

Chapitre 2

Selon les résultats obtenus dans le chapitre 1, l'hybridogénèse sociale peut évoluer de manière déterministe même si elle est désavantageuse, du fait de conflits intra-coloniaux propres à l'immense majorité des espèces eusociales. Une interprétation possible de ces résultats est alors que l'évolution vers l'hybridogénèse sociale est un phénomène relativement probable chez les fourmis, susceptible de s'être déclenché de nombreuses fois dans ce groupe. En d'autres termes, les cas connus d'hybridogénèse sociale pourraient n'être que la partie immergée de l'iceberg, et de nombreux autres cas toujours inconnus pourraient exister.

Dans le chapitre 2, nous avons suivi ce raisonnement et développé une méthodologie qui pourrait permettre de découvrir de nouveaux systèmes hybridogénétiques. Prouver la présence de l'hybridogénèse sociale dans une espèce est globalement difficile car cela requiert d'obtenir des données génétique pour de nombreux individus, notamment des reines. Ce type de données n'est disponible que pour un nombre réduit d'espèces modèles, et la grande majorité des espèces de fourmis (13 964 espèces valides) n'a jamais été séquencée. A ce jour, le jeu de données génétique le plus important concernant les fourmis est un jeu de données produit pour la phylogénie, qui contient des séquences pour plusieurs centaines d'espèces, mais où la majorité ne sont représentée que par un individu (i.e., une ouvrière dans la majorité des cas). Si ces données ne peuvent pas être utilisées pour prouver formellement la présence de l'hybridogénèse sociale dans ces espèces, nous avons montré dans ce chapitre qu'elles peuvent tout de même être exploitées afin de détecter l'une des caractéristiques de ce système de reproduction : les ouvrières hybrides de première génération. Les hybrides de première génération portent des paires de chromosomes d'origine différente, ce qui se manifeste par un patron caractéristique dans la distribution des différences génétiques observées lorsqu'ils sont séquencés. En développant une description statistique de ce patron attendu, et en la testant à l'aide d'hybrides connus, nous avons montré qu'il est possible d'identifier les individus qui y répondent. Nous avons ensuite appliqué cette méthode aux données mentionnées plus haut afin de produire une liste d'espèces candidates dont les représentants répondent à nos critères, et qui pourraient donc être impliquées dans des systèmes hybridogénétiques. En parallèle, en appliquant la même méthode sur d'autres groupes d'Arthropodes, nous produisons des preuves nouvelles de la grande fréquence de l'hybridation chez les fourmis.

La liste d'espèces candidates que nous avons produite dans ce chapitre est aussi intéressante car elle nous a permis d'identifier d'éventuelles caractéristiques sur-représentées parmi les candidats,

qui pourraient être impliqués dans l'évolution de l'hybridogénèse sociale. En particulier, elle nous a permis de recroiser les résultats théoriques obtenus dans le chapitre 1 avec des données réelles. Nous avons ainsi remarqué que plusieurs espèces candidates identifiées appartiennent à des groupes connus pour effectuer des accouplements multiples, comme les fourmis coupe-feuille (tribu des Attini) ou les fourmis légionnaires (sous-famille des Dorylinae). Ceci apporte un support empirique à l'idée selon laquelle le nombre de reproduction effectués par les reines est un paramètre clefs dans l'évolution de l'hybridation et de l'hybridogénèse sociale. Nous avons également relevé que plusieurs espèces candidates appartiennent à un groupe iconique de fourmis des milieux désertiques, les fourmis pot-de-miel du genre *Myrmecocystus*. Ceci est important car il a été suggéré que les fourmis des milieux arides soit plus susceptible de développer un système hybridogénétique, en raison de leur forte tendance à produire des vols nuptiaux massifs et synchronisés entre espèces qui favorisent les contacts inter-spécifiques.

Chapitre 3

La méthodologie développée dans le chapitre 2 à aussi été utile dans deux autre projets plus exploratoires. Cette méthode nous a permis de positionner les cas d'hybridogénèse sociale chez un groupe particulier, les fourmis moissonneuses du genre *Messor*, à deux échelles différentes. Le genre *Messor* était connu avant le début de cette thèse pour abriter trois cas indépendants d'hybridogénèse sociale, chez *M. barbarus*, *M. ebeninus* et *M. structor*. Cependant, ces trois systèmes hybridogénétiques ont été décrits dans une étude qui n'a inspecté que 9 espèces, quand le genre en compte 126 au total. Il est donc possible que ce groupe contiennent de nombreux autres systèmes hybridogénétiques. Si cela se vérifie, *Messor* pourrait alors permettre à terme la mise en place de puissantes analyses comparatives, avec le potentiel d'éclaircir les déterminants démographique, écologique et génétique de l'hybridogénèse sociale. Les deux projets présentés dans ce chapitre sont des projets toujours en cours, qui visent à produire des données et des résultats préliminaires concernant l'hybridogénèse sociale chez *Messor*, et à ouvrir la voie pour les études futures.

Dans la première partie du chapitre 3, nous nous sommes concentré sur l'ensemble du genre *Messor* avec un objectif double : produire la première phylogénie du genre (qui est toujours inconnue) contenant un maximum d'espèces nouvelles, et identifier des espèces candidates susceptible d'être hybridogénétique. Comme la répartition géographique du genre est très large, (de l'Afrique du Sud à la Chine en passant par l'Europe), l'échantillonnage sur le terrain n'était pas possible dans le cadre de cette thèse. Nous avons donc décidé d'utiliser des espèces disponibles

dans les musées, sous la forme de spécimens de collection. Nous avons pu obtenir des spécimens pour 54 espèces de *Messor*, prêtés par le National History Museum de Londres, que nous avons séquencé à l'aide de méthodes non-destructives. Les méthodes de séquençage non-destructives permettent de préserver les spécimens en évitant de les broyer lors des extractions d'ADN, ce qui est très utile pour les spécimens de collection car ils sont souvent important d'un point de vue historique et taxonomique. Ainsi, nous avons pu produire le premier jeu de données génétique d'envergure de *Messor*, et avons pu produire une première phylogénie du groupe. Nous avons également pu obtenir des résultats concernant la distribution de l'hybridogénèse dans le genre, qui concernerait au moins quatre nouvelles espèces, *M. luebberti* et *M. striatifrons* en Namibie, *M. cephalotes* au Kenya et *M. semoni* au Maroc. Plusieurs autre espèces pourrait constituer des candidats sérieux mais ont montré des patrons génétiques moins claires.

Dans la seconde partie du chapitre 3, nous nous sommes concentré sur le cas particulier de *M. structor*, un complexe d'espèces Européen dans lequel l'hybridogénèse sociale à été détectée, mais n'a jamais été décrite en détails. En particulier, il n'était pas su au début de cette thèse laquelle ou lesquelles des 5 espèces décrites dans ce groupe étaient hybridogénétiques. Dans ce projet, nous avons assemblé un jeu de données génétique important, comportant des reines et des ouvrières de chacune des 5 espèces de *M. structor*. Nous avons ensuite appliqué la méthode du chapitre 2, pour montrer qu'une seule de ces espèces, *M. ibericus*, possède l'hybridogénèse sociale. De manière inattendu, nous avons également obtenu des résultat qui sous-entendent que le système de reproduction de *M. ibericus* possède une caractéristique rare. Sur une large part de aire de distribution, cette espèce ne semble coexister avec aucune autre espèce capable de lui fournir des mâles, mais produit tout de même des ouvrières hybrides. Nous avons trouvés des mâles susceptibles d'être les pères de ces ouvrières, mais ceci ont été collectés vierge au sein même des colonies de *M. ibericus*, preuve qu'il ont été produits sur place. Nous interprétons ce résultat comme étant la preuve que l'hybridogénèse sociale chez *M. ibericus* fait intervenir un forme de clonalité mâle, un phénomène rare mais connu dans le cadre de trois autres espèce hybridogénétiques.

Discussion

Les résultats obtenus dans le chapitre 1 permettent de jeter un regard nouveau sur l'hybridogénèse sociale et son évolution. Ce système de reproduction est en effet souvent considéré comme profitable aux espèces qui le développent. Parmi les avantages souvent proposés, le plus important est

sûrement la vigueur hybride, qui augmenterait la productivité globale des colonies possédant des ouvrières hybrides. Si un tel avantage pourrait en effet être suffisant pour expliquer l'évolution de l'hybridogénèse sociale par sélection naturelle, l'idée d'une vigueur hybride chez les ouvrières des fourmis n'a dans les faits reçu que peu de support empirique. Dans le chapitre 1, nous avons montré qu'un autre mécanisme déterministe, dont le moteur est un conflit larve-reine, pourrait expliquer l'évolution de l'hybridogénèse social. Si cette voie évolutive s'avère être celle empruntée par les fourmis ayant développé ces systèmes, alors cela pourrait signifier qu'un avantage à l'hybridogénèse social, bien qu'éventuellement facilitant, n'est pas nécessaire à son émergence. Au delà même, il est possible de suggérer que l'hybridogénèse sociale puisse évoluer malgré les coûts qu'elle impose aux espèces concernés (e.g., dépression hybride, risques multiples pour les reines). Dans ce cas, l'hybridogénèse sociale se révélerait alors être un exemple de tragédie des biens communs, une situation dans laquelle une course aux armements entre des parties en conflits mène à une situation globalement défavorable.

La résilience du mécanisme évolutif face aux éventuels coûts de l'hybridogénèse social n'est pas le seul argument en faveur de sa généralité. En effet, ce mécanisme est également générale de par le fait qu'il est suffisant pour expliquer l'évolution des différentes formes existantes d'hybridogénèse sociale. Ce système de reproduction montre de nombreuses variations autour du même thème. Il existe parfois sous une forme asymétrique (i.e., une seule lignée hybridogénétique profite des mâles d'une espèce à système de reproduction classique), mais plus souvent sous une forme symétrique (i.e., deux lignées hybridogénétiques coexistent et utilisent les mâles l'une de l'autre). Notre modèle est compatible avec ces deux formes. L'hybridogénèse existe également combinée à la production de nouvelles reines par clonage. Nous avons montré que cela est également compatible avec notre modèle, et même que le clonage serait alors un facilitateur majeur de l'évolution de l'hybridogénèse sociale. Enfin, ce système existe combiné à une forme de clonalité mâle, dans laquelle les mâles utilisés pour la production d'hybride sont issue d'une lignée entièrement constitué de mâles, qui se clonent en détournant les oeufs pondus par les reines. Notre modèle ne prends pas directement en compte l'évolution de ce type de clonalité, mais si elle est admise peut expliquer l'évolution de l'hybridogénèse sociale. Un dernier argument en faveur de la généralité du mécanisme proposé est qu'il ne nécessite aucune hybridation initiale entre les lignées impliquées, mais seulement que le contact entre lignées soit possible (i.e., l'hybridation évoluera d'elle même en réponse au conflit larve-reine)

Si l'hybridogénèse sociale peut évoluer de manière générale et déterministe, et malgré les coûts

qu'elle impose, alors il est possible que de nombreux exemple de ce système de reproduction restent à être découverts. Toutefois, bien que plusieurs espèces candidates aient été relevées dans le second chapitre de cette thèse, leur fréquence reste relativement restreinte relativement à la généralité du mécanisme proposé. Ceci pourrait être expliqué par la rareté, chez les fourmis, de certaines caractéristiques nécessaires à l'évolution de l'hybridogénèse sociale. En particulier, la capacité pour une reine à se reproduire avec plusieurs mâles est un trait relativement rare, et qui semble partagé par la grande majorité des espèces hybridogénétiques connues. Alternativement, la rareté des ces systèmes pourrait s'expliquer par leur éventuel instabilité. Il est possible que l'hybridogénèse sociale soit un système de transition, voué dans la majorité des cas à disparaître. En fonction du modèle d'évolution considéré, il est tout d'abord envisageable que ces systèmes puissent rapidement subir une réversion vers des systèmes de reproduction plus standard. Cependant, il est peut-être plus probable que la disparition de ces systèmes soit due à une extinction directe des espèces impliqués. En effet, les coûts sous-jacents à l'hybridogénèse sociale pourraient rendre les espèces qui la développent moins compétitives écologiquement, et les mener à se faire remplacer par d'autres espèces. De plus, même si l'hybridogénèse évolue initialement sans coûts, il est difficile d'imaginer que ces coûts ne s'accumulent pas avec le temps, au fur et à mesure de la divergence entre les espèces hybridogénétiques et leur lignée fournisseuses de mâles.

Conclusion

L'hybridogénèse sociale est un mode de reproduction fascinant qui continue de révéler ses secrets à travers le travail intensifs de nombreux biologistes à travers le monde. Depuis sa première description, il y a plus de 40 ans, son étude n'a cessé de de fournir d'importants résultats concernant les différentes facettes de l'histoire de vie des espèces eusociales. Cependant, une compréhension complète de l'hybridogénèse sociale est loin d'avoir été atteinte, et de nombreuse questions restent en suspens.

Dans cette thèse, mon attention s'est porté tout particulièrement sur les déterminants de l'émergence de l'hybridogénèse sociale. J'ai proposé que des conflits intra-coloniaux, plutôt que des évènement aléatoires ou la vigueur hybride, soient à l'origine de ce système de reproduction. Selon cette vue nouvelle, l'hybridogénèse sociale pourrait être interprétée comme un phénomène délétère, qui pourrait accélérer l'extinction des espèces impliquées. Cependant, des

preuves empiriques doivent être fournies avant que ce point de vue puisse être adopté. Je pense que de telles preuves pourront être obtenues à travers l'étude des génomes des espèces hybridogénétiques. En particulier, il est très probable la course au armements décrite dans cette thèse se soit accompagnée d'une évolution rapide des gènes impliqués dans la détermination de la caste chez les larves en développement. Si de tels événements d'évolution rapide ont eut lieu, l'usage d'outils dédiés rendra possible leur identification. Ce type d'analyses, à terme, à le potentiel d'aider à la compréhension des mécanismes sous-jacents non-seulement à l'évolution de l'hybridogénèse social, mais aussi à la plasticité de caste elle-même.

Pour pouvoir mener de telles études et isoler les déterminants fondamentaux de l'évolution de l'hybridogénèse sociale, il sera crucial de pouvoir comparer de nombreuses espèces hybridogénétiques. J'espère que les méthodes et les études préliminaires de *Messor* présentées dans cette thèse participeront à la découverte de nouveaux modèles et à leur compréhension. En particulier, la liste d'espèce candidates à l'hybridogénèse présentée dans le second chapitre pourrait représenter un point de départ utile. Certain groupes, comme les fourmis pot-de-miel, les fourmis coupe-feuille ou les fourmis légionnaires, semblent particulièrement enclines à l'hybridation et présentent plusieurs caractéristiques clefs pour l'évolution de l'hybridogénèse sociale. Se pencher sur ces espèces pourrait révéler de nouveaux systèmes d'études, et pourrait mener à des résultats importants pour la compréhension des interactions entre conflits les intra-coloniaux, l'écologie et l'histoire de vie chez les organismes eusociaux.